UNIVERSITY OF CALIFORNIA SAN DIEGO

# Oxidative Atom Transfer Radical Strategies

A dissertation submitted in partial satisfaction of the requirements for the degree Doctor of Philosophy

in

Chemistry

by

Samuel William Lardy

Committee in charge:

Professor Valerie Schmidt, Chair
Professor Carlo Ballatore
Professor Guy Bertrand
Professor Simpson Joseph
Professor Joseph O'Connor

2021

The Dissertation of Samuel William Lardy is approved, and it is acceptable in quality and form for publication on microfilm and electronically.

University of California San Diego

2021

# DEDICATION

I would like to dedicate this dissertation to my wife, Sarah Roa. I have dreams of being with you forever and riding ponies and eating lots of eggs and whip cream.

TABLE OF CONTENTS

LIST OF ABBREVIATIONS

**AIBN:** 2,2'-azobis(2-methylpropionitrile)
**ATRA:** atom transfer radical addition
**BDE:** bond dissociation energy
**Bm:** benzyl
**BPO:** benzoyl peroxide
**Bu:** butyl
**DCE**: 1,2-dichloroethane
**DDQ:** dichloro-5,6-p-benzoquinone
**DLP:** dilauroyl peroxide
**DTBHN:** di-tertbutyl hyponitrite
**DTBP:** di-tertbutyl peroxide
**EtOAc:** ethyl acetate
**Equiv:** equivalents
**GC:** gas chromatography
**GC-MS:** gas chromatography-mass spectrometry
**GTRA:** group transfer radical addition
**$H_2NNH_2$:** hydrazine
**HAT:** hydrogen-atom transfer
**kcal:** kilocalorie
**M:** molar
**MeCN:** acetonitrile
**MeOH:** methanol
**MHz:** megahertz
**MOM:** methoxy methyl
**NBS:** N-bromosuccinimide
**NBVE:** n-butyl vinyl ether
**NHPI:** *N*-hydroxyphthalimide
**NMR:** nuclear magnetic resonance
**OAT:** oxygen-atom transfer
**PhCl:** chlorobenzene
**Phth:** phthalimidyl
**PINO:** phthalimide N-oxyl radical
**PMB:** p-methoxy benzyl
**$P(OEt)_3$:** triethyl phosphite
**$S_NAr$:** nucleophilic aromatic substitution
**TFA:** trifluoroacetic acid
**TLC:** thin layer chromatography

LIST OF FIGURES

LIST OF SCHEMES

LIST OF TABLES

ACKNOWLEDGEMENTS

I want to acknowledge everyone that helped me get to where I am now. My family, my friends, my educators, and my research advisors, Dr. Jeremy McCallum and Dr. Valerie Schmidt, both of whom have collectively taught me almost everything I know about chemistry.

Chapter 1 has been adapted from materials published in Lardy, S. W.; Schmidt, V. A. Intermolecular Radical Mediated Anti-Markovnikov Alkene Hydroamination Using *N*-Hydroxyphthalimide. *J. Am. Chem. Soc.* **2018**, 12318-12322. The dissertation author was the primary investigator of this publication.

Chapter 2 has been adapted from materials published in Lardy, S. W.; Schmidt, V. A. Regioselective Alkene Amination Strategies by Using Phosphite Mediated Deoxygenation, *Synlett*, **2019**, *30,* 2022, as well as Lardy, S. W.: Schmidt, V. A. Intermolecular Aminoallylation Using Allyl-oxyphthalimide Derivatives: A Case Study in Radical Polarity Effects, *Eur. J. Org. Chem.* **2019**, 6796. The dissertation author was the primary investigator of these publications.

Chapter 3 has been adapted from materials published in Lardy, S. W.; Luong, K. C.; Schmidt, V. A. Formal Aniline Synthesis from Phenols via Deoxygenative N-Centered Radical Substitution, *Chem. Eur. J.* **2019**, *25*, 15271. The dissertation author was the primary investigator of this publication.

Chapter 4 has been adapted from materials prepared to be published in Lardy, S. W.; Schmidt, V. A. Thiol Catalyzed Aerobic Debenzylation of Alcohols and Amines. The dissertation author was the primary investigator of this publication.

VITA

## Education

**Ph.D. in Chemistry** **2019-2021**
University of California San Diego (Prof. Valerie Schmidt)
**M.S. in Chemistry** **2017-2019**
University of California San Diego (Prof. Valerie Schmidt)
**B.S. in Chemistry with Summa Cum Laude Honors** **2014-2016**
Loyola Marymount University

## Publications

1. **Lardy, S. W.**; Schmidt, V. A. Intermolecular Radical Mediated Anti-Markovnikov Alkene Hydroamination Using N-Hydroxyphthalimide, *J. Am. Chem. Soc.* **2018**, *40* (39), 12318.

2. **Lardy, S. W.**; Schmidt, V. A. Regioselective Alkene Amination Strategies by Using Phosphite Mediated Deoxygenation, *Synlett*, **2019**, *30,* 2022.

3. **Lardy, S. W.**; Luong, K. C.; Schmidt, V. A. Formal Aniline Synthesis from Phenols via Deoxygenative N-Centered Radical Substitution, *Chem. Eur. J.* **2019**, *25*, 15271.

4. **Lardy, S. W.**: Schmidt, V. A. Intermolecular Aminoallylation Using Allyl-oxyphthalimide Derivatives: A Case Study in Radical Polarity Effects, *Eur. J. Org. Chem.* **2019**, 6796.

## Presentations

1. **Lardy, S. W.**; Schmidt, V. A. "Radical Amination Strategies Enabled by O-Atom Transfer." Genentech Graduate Student Symposium in Chemical Research, Zoom presentation, May 2021.

2. **Lardy, S. W.**; Schmidt, V. A. "Regioselective Radical Alkene Amination Strategies by Using Phosphite-Mediated Deoxygenation." ACS 258$^{th}$ National Conference, San Diego, CA, August, 2019, Oral Presentation.

3. **Lardy, S. W.**; Schmidt, V. A. "Radical Mediated O-Atom Transfer Amination Strategies." University of California Chemical Symposium, Lake Arrowhead, CA, March, 2019, Poster Presentation.

## Technical Capabilities

1. Expert at small molecule synthesis, purification, and analysis.

2. Operation of analytical instrumentation such as FTIR, multinuclear NMR, and GCMS.

**Honors and Awards**

1. Genentech Graduate Student Symposium Honoree

2. UCSD Teddy Traylor Award

3. UCSD Distinguished Graduate Student Research Fellowship

4. National Science Foundation GRFP Honorable Mention

5. ACS Undergraduate Award in Organic Chemistry

6. LMU Outstanding Graduating Senior in Chemistry Award

7. Rains Undergraduate Research Grant

8. Seaver College Summer Undergraduate Research Grant

9. DeMartini Endowed Scholarship

ABSTRACT OF THE DISSERTATION

Oxidative Atom Transfer Radical Strategies

by

Samuel William Lardy

Doctor of Philosophy in Chemistry

University of California San Diego, 2021

Professor Valerie Schmidt, Chair

The triphenylmethyl radical was first discovered and isolated by Moses Gomberg at the University of Michigan in the year 1900. The prospect of an isolable carbon-centered radical as described by Gomberg blew open the door to a whole new realm of chemistry and helped pave the way for modern organic synthesis. Now nearly 120 years past this initial discovery, radical reactions are common place in all areas of organic synthesis, and new methods are continuously being developed that utilize open shell species. Radical-mediated methods are complimentary to traditional, two-electron pathways in that they are uniquely tolerant of otherwise reactive polar functionalities.

The first chapter of this manuscript describes our development of a new method for the intermolecular hydroamination of alkenes using *N*-hydroxyphthalimide (NHPI). Owing to the impressive oxophilicity of trivalent phosphorus, we were able to generate reactive phthalimidyl radicals via phosphorus-mediated homolytic cleavage of the N-O bond in NHPI. The installation of the phtalimidyl moiety is highly advantageous, as it can be easily removed via simple hydrolysis to provide an overall, formal-ammonia hydroamination for the production of primary amines. During the course of our investigation, we determined that this process occurred through an atom-transfer radical addition (ATRA) type mechanism wherein NHPI was used to supply both the nitrogen and hydrogen atoms for the overall hydroamination.

The second chapter of this manuscript describes an extension of the ATRA capabilities of our hydroamination method in the form of an aminoallylation of alkenes using allyl-oxy phthalimides. By substituting the hydrogen atom of NHPI with an electron deficient allyl group, we took advantage of predictable radical polarity effects to invoke an overall alkene difunctionalization by way of a group transfer radical addition (GTRA). This provided further evidence for an ATRA-type mechanism for our hydroamination method, and similarly reinforced the guiding effects of proper radical polarity matching.

The third chapter of this manuscript discusses our development of a method for the formal conversion of phenols to anilines utilizing an intermediary hydroxamic scaffold. Again taking advantage of the oxophilicity of trivalent phosphorus, hydroxamic acids were unmasked to reveal reactive amidyl radicals capable of performing an intramolecular, ipso-substitution at the phenolic carbon of the hydroxamic acid substrate. In comparison to traditional $S_NAr$ processes, our method was not limited to electron deficient arenes, but tolerated electronically rich substrates as well.

The fourth and final chapter of this manuscript transitions away from radical amination strategies enabled by phosphorus(III)-mediated O-atom transfer, and instead describes our efforts to utilize thiyl radicals as cite-selective H-atom abstraction reagents. During the course of our investigation, we found that we could perform a thiol-catalyzed, aerobic debenzylation of amines and alcohols using pentafluorothiyl radical as the active abstracting species. This process uses only a substoichiometric quantity of thiol, air as the only oxidant, and operates in the presence of functional groups that would otherwise be intolerant of traditional benzyl-deprotection methods.

# Chapter 0: General Introduction

## 0.1 Radical-Mediated, Phosphorus-Enabled Deoxygenation

Phosphorous-oxygen bonds play vital roles in biochemistry, forming the phosphodiester linkages of nucleic acids and nucleotides that convey the genetic codes of life and provide the energetic driving force of biochemical processes.[1] The synthetic utility of phosphorus containing compounds is demonstrated by classic reactions such as the Wittig,[2] the Corey-Fuchs olefination,[3] the Mitsunobu,[4] the Appel,[5] and the Horner-Wadsworth-Emmons,[6] all of which take advantage of the oxophilicity of phosphorus to allow for chemical transformations to take place (Scheme 0.1). The Radosevich laboratory has similarly leveraged the O-atom transfer capabilities of trivalent phosphorus reagents toward the development of unique deoxygenative methods that rely on P(III)/P(V) redox cycling.[7] In all of these cases, the driving force for the conversion of starting material to product lies in the thermodynamic favorability of forming an exceptionally strong phosphorus-oxygen bond (P=O = 130 kcal/mol for $Ph_3PO$).[8] While many of the most well known of these transformations involve 2-electron, ionic pathways,[9] significant progress has been made on the development of single electron synthetic methods.[10]

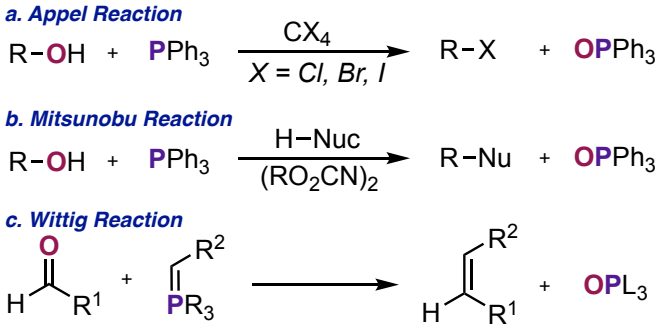


Scheme 0.1. Classic two-electron deoxygenation processes enabled by trivalent phosphorus.

Radical-mediated processes are attractive for use in chemical synthesis because they are generally tolerant of sensitive chemical functionalities that would otherwise not withstand polar

reactants. Because of this, processes involving phosphorus-based radical intermediates are particularly of interest for reaction development through oxygen atom transfer (OAT). The strength of P-O bonds can serve as a favorable driving force for these reactions and activate oxygen-carbon/hetero bonds in mechanistically distinct pathways compared to direct bond homolysis or through oxidative addition using a transition-metal.

The family of trivalent P-centered radicals involved in OAT processes can be broken up into two primary categories: phosphoranyl radicals ($L_3ZP\bullet$) and phosphoniumyl radical cations ($L_3P\bullet^+$), which are inevitably converted to phosphoranyl radicals following nucleophilic attack (Scheme 0.2).

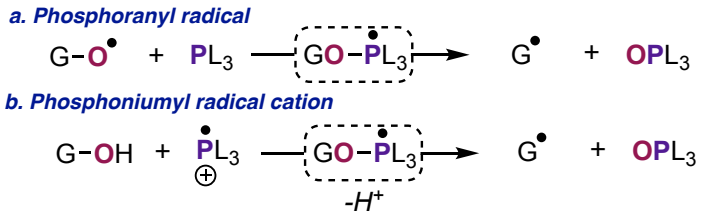


Scheme 0.2. P-centered radicals in deoxygenation reactions.

The chemical properties of phosphoranyl radicals ($L_3ZP\bullet$) were extensively investigated by Bentrude[11] and others[12] during the mid- to late-twentieth century, and have since been well reviewed.[13] Phosphoranyl intermediates are generated when an external radical ($Z\bullet$) forms a covalent bond with trivalent phosphorus ($PL_3$). Pioneering studies by Bentrude and coworkers served to lay the foundation and predictive power of reactivity of alkoxy radicals in the presence of $PL_3$. The phosphoranyl radical generated by addition of an alkoxy radical as shown in Scheme 0.3 generally has two reactive pathways. First, a displacement resulting from α-scission of a P-L bond is a major pathway when the O-R bond of the incoming alkoxy radical is relatively strong and α-scission is capable of producing a stabilized radical ($L\bullet$). This is most often observed when $PL_3$ is a trialkyl phosphine such as tri-*t*-butylphosphine or phosphite such as triphenylphosphite.

Similarly, α-scission may occur to regenerate the original alkoxy radical and $PL_3$ substrate if the O-P bond formed from initial addition is relatively weak compared to that of P-L, thereby producing no net reaction. The second common pathway results from a β-fragmentation that oxidizes the phosphorous center and releases a corresponding R•. Oxidation is the favored pathway when the P-L bonds are stronger than the R-O bond of the incoming alkoxy radical, commonly observed when alkyl phosphites are used as the trivalent phosphorous reagents. In this same vein, if the phosphorus reagent is a phosphite that contains a relatively weak β O-R bond associated with one of the ligands (L), a radical, Arbuzov-type substitution/oxidation may occur upon alkoxy radical addition. Productive reactivity for recently developed synthetic methods are typically encompassed by the second pathway wherein β-scission produces a carbon- or nitrogen-radical from an incoming alkoxy radical.

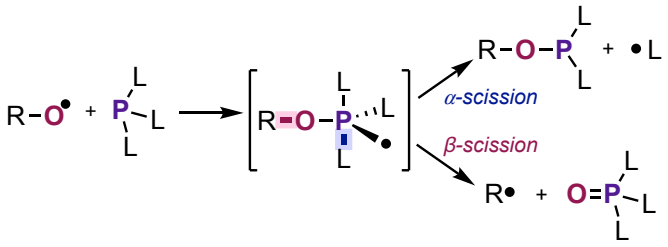


Scheme 0.3. Possible reaction pathways for phosphoranyl radicals.

While the OAT capability of trivalent phosphorus is well documented in cases concerning alkoxy and peroxy radicals, instances involving the addition of N-hydroxyl radicals to trivalent phosphorus to furnish N-centered radicals have only recently been developed. This is particularly interesting since the N-O and O-H bond strengths of these species are typically lower than the C-O and O-H bond strengths of alcohols, thereby favoring the oxidative, β-scission pathway. Owing to the prevalence of nitrogen-containing scaffolds in pharmaceuticals and agrochemicals, the

development of deoxygenative methodologies for harnessing reactive N-centered radicals from unsubstituted *N*-hydroxy amines is of great interest (Scheme 0.4).[14]

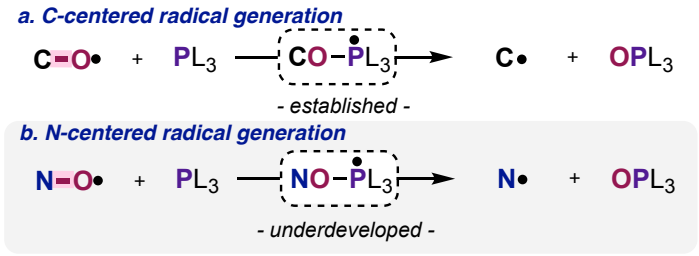


Scheme 0.4. Generation of C- and N-centered radicals via trivalent phosphorus OAT.

Interactions between trivalent phosphorus and N-hydroxy containing compounds have been documented since the 1970's,[15] but it is only recently that major synthetic advances have been made in this realm. An early example from Weinreb[16] in 2001 revealed that diethyl chlorophosphite could be used as an effective deoxygenation reagent for oximes and hydroxamic acids to produce N-centered radicals through thermolysis of the N-O bonds in the O-phosphino hydroxylamines[17] generated in situ (Scheme 0.5). While mechanistically this method does not conform to the Bentrude-type deoxygenation profile seen with peroxides and alcohols wherein an oxygen-centered radical adds to phosphorus to generate a phosphoranyl radical, it still relies on the use of a trivalent phosphorus O-atom acceptor reagent and provides excellent precedence for later developed OAT processes involving hydroxylamine functionality. O-phosphino hydroxylamines are well known to undergo thermolytic bond cleavage, and Weinreb succesfully leveraged this documented reactivity to achieve the intramolecular aminooxygenation, aminosulphination, and aminoselenation of oximes and hydroxamic acids in moderate to excellent yields.

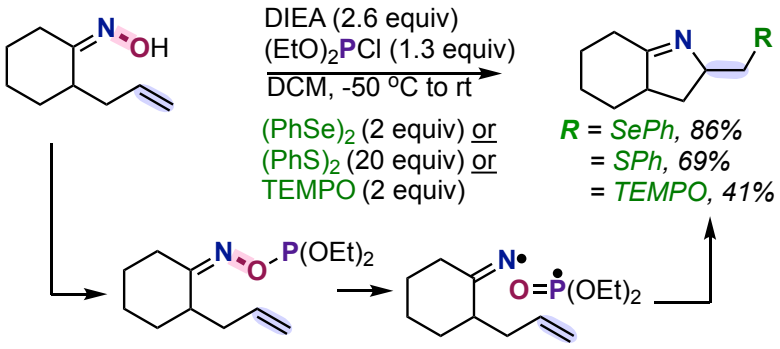


Scheme 0.5. Phosphorus mediated deoxygenation of oximes and hydroxamic acids (Weinreb, 2001).

The next three chapters of this manuscript describe our efforts at leveraging the impressive oxophilicity of trivalent phosphorus, as well as the known interactions of these compounds with alkoxy radicals to generate highly reactive, N-centered radicals from benchtop stable, easily synthesized hydroxylamine-based substrates.

## 0.2 Thiols as Hydrogen-Atom Abstraction Reagents

Traditionally, organic synthesis has relied on leveraging inherently reactive functional groups to invoke the desired transformations necessary to build complex molecular scaffolds (Scheme 0.6.a). Over the past several decades, there has been a great push towards the development of new synthetic methods that utilize C-H bond activation to invoke sophisticated chemical transformations at classically inert positions of a molecule (Scheme 0.6.b). Many of the newly developed methods in this realm are polar processes catalyzed by transition metals,[18] though a number of methods have emerged that invoke a radical pathway.[19]

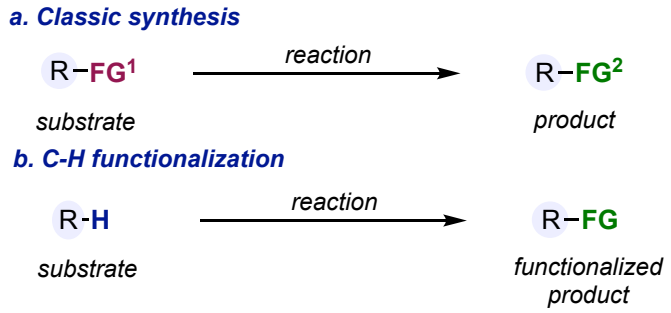


Scheme 0.6. C-H bond activation as a unique method for the synthesis of organic compounds.

One strategy for the development of radical-mediated C-H functionalization reactions is to perform a site-selective H-atom transfer to furnish a carbon-centered radical intermediate (Scheme 0.7).[20] This approach allows for otherwise inert C-H bonds to be homolytically cleaved and engage in productive reactivity toward the functionalization of the substrate. N-functionalized-amides,[21] alcohols,[22] and photo-active polyoxometalates[23] have all recently been realized as powerful HAT reagents for radical C-H functionalization reactions, to name but a few.

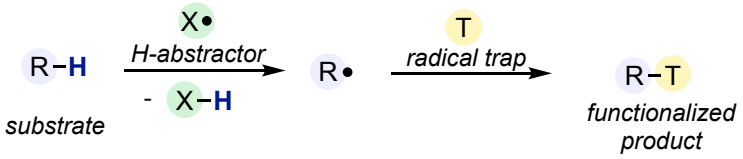


Scheme 0.7. Hydrogen atom abstraction as a radical-mediated strategy toward C-H functionalization.

Thiols have long been known to be excellent H-atom sources for carbon-centered radicals, and do so at near diffusion controlled rates for many substrates due to the thermodynamically favorable generation of the thiyl radical.[24] This H-atom transfer event between thiols and carbon radicals, while typically favoring the thiyl radical due to the relatively low bond dissociation energy (BDE) of S-H bonds as compared to most C-H bonds, exists in equilibrium. Consequently, thiyl radicals can act as C-H abstracting species toward the generation of C-centered radicals. Roberts pioneered the development of synthetic methods that utilize thiyl radicals as H-atom

transfer reagents in the late twentieth century and found that they could be used for the radical hydroacylation of alkenes,[25] reductive deoxygenation of MOM-protected alcohols,[26] and intramolecular cyclization of acetals (Scheme 0.8).[27]

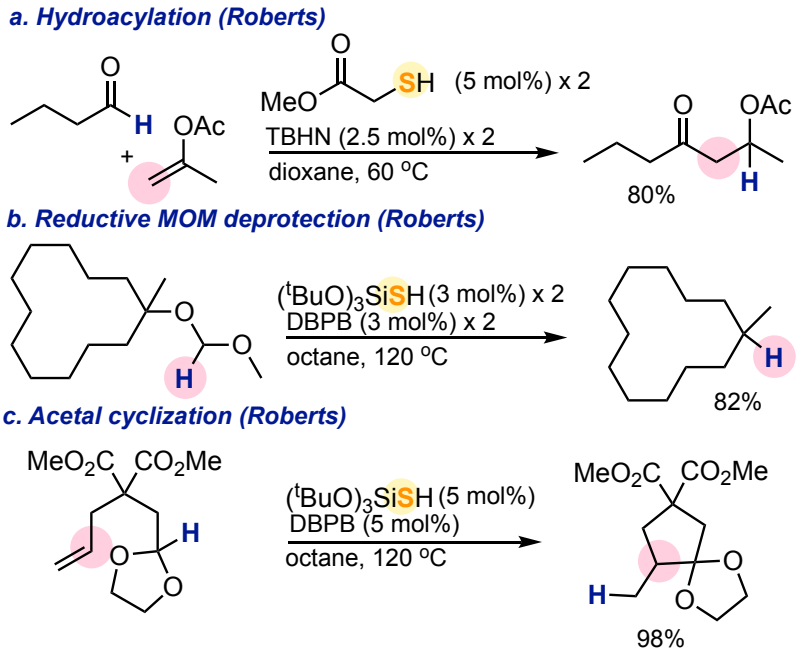


Scheme 0.8. Synthetic methods invoking the thiyl radical as an H-atom abstracting reagent.

The fourth chapter of this manuscript details our investigation of thiyl radicals as site-selective hydrogen atom transfer reagents toward the development of new synthetic methodologies.

## 0.3 References


[1] Nelson, D. L.; Cox, M. M. *Lehninger Principles of Biochemistry*; W. H. Freeman; Sixth Edition: New York, 2012.

[2] Wittig, G.; Schöllkopf, U. Über Triphenyl-phosphin-methylene als olefinbildende Reagenzien. *Chem. Ber.* **1954**, *87*, 1318-1330.

[3] Corey, E. J.; Fuchs, P. L. A Synthetic Method for Formayl to Ethynyl Conversion. *Tetrahedron Lett.* **1972**, *13*, 3769-3772.

[4] Mitsunobu, O.; Yamada, Y. Preparation of Esters of Carboxylic and Phosphoric acid via Quaternary Phosphonium Salts. *Bull. Chem. Soc. Jpn.* **1967**, *40*, 2380-2382.

[5] Appel, R. Tertiary Phosphane/Tetrachloromethane, a Versatile Reagent for Chlorination, Dehydration, and P-N Linkage. *Angew. Chem. Int. Ed.* **1975**, *14*, 801-811.

[6] (a) Boutagy, J.; Thomas, R. Olefin Synthesis with Organic Phosphonate Carbanions. *Chem. Rev.* **1974**, *74*, 87-99. (b) Wadsworth, W. S, Jr. Synthetic Applications of Phosphoryl-Stabilized Anions. *Org. React.* **1977**, *25*, 73-252. (c) Stec, W. J. Wadsworth-Emmons Reaction Revisited. *Acc. Chem. Res.* **1983**, *16*, 411-417.

[7] (a) Lecomte, M. Lipshultz, J. M.; Kim-Lee, S.-H.; Li, G.; Radosevich, A. T. Driving Recursive Dehydration by $P^{III}/P^{V}$ Catalysis: Annulation of Amines and Carboxylic Acids by Sequential C-N and C-C Bond Formation. *J. Am. Chem. Soc.* **2019**, ASAP. DOI: 10.1021/jacs.9b06277. (b) Ghosh, A.; Lecomte, M.; Kim-Lee, S.-H.; Radosevich, A. T. Organophosphorus-Catalyzed Deoxygenation of Sulfonyl Chlorides: Electrophilic (Fluoroalkyl)sulfenylation by $P^{III}/P^{V}$=O Redox Cycling. *Angew. Chem. Int. Ed.* **2019**, *58*, 2864-2869. (c) Nykaza, T. V.; Cooper, C. J.; Li, G.; Mahieu, N.; Ramirez, A.; Luzung, M. R.; Radosevich, A. T. Intermolecular Reductive C-N Cross Coupling of Nitroarenes and Boronic Acids by $P^{III}/P^{V}$-O Catalysis. *J. Am. Chem. Soc.* **2018**, *140*, 15200-15205. (d) Nykaza, T. V.; Harrison, T. S.; Ghosh, A.; Putnik, R. A.; Radosevich, A. T. A Biphilic Phosphetane Catalyzes N-N Bond-Forming Cadogan Heterocyclization via $P^{III}/P^{V}$=O Redox Cycling. *J. Am. Chem. Soc.* **2017**, *139* 6839-6842. (e) Zhao, W.; Yan, P. K.; Radosevich, A. T. A Phosphetane Catalyzes Deoxygenative Condensation of alpha-Keto Esters and Carboxylic Acids via P(III)/P(V)=O Redox Cycling. *J. Am. Chem. Soc.* **2015**, *137*, 616-619.

[8] Luo, Y.-R. *Handbook of Bond Dissociation Energies in Organic Compounds*; CRC Press: Boca Raton, 2003.

[9] For reviews on recent advances please see: (a) Karanam, P.; Reddy, G. M.; Koppolu, S. R.; Lin, W. Recent topics of phosphine-mediated reactions. *Tetrahedrom Letters*, **2018**, *59*, 59-76. (b) Guo, H.; Fan, Y. C.; Sun, Z.; Wu, Y.; Kwon, O. Phosphine Organocatalysis. *Chem. Rev.* **2018**, *118*, 10049-10293.

[10] For reviews on recent advances please see: (a) Marque, S.; Tordo, P. Reactivity of Phosphorus Centered Radicals. *Top. Curr. Chem.* **2005**, *250*, 43-76. (b) Leca, D.; Fensterbank, L.; Lacôte, E.; Malacria, M. Recent advances in the use of phosphorus-centered radicals in organic chemistry. *Chem. Soc. Rev.* **2005**, *34*, 858-865.

[11] For an overview please see: (a) Bentrude, W. G. Phosphoranyl Radicals: Their Structure, Formation, and Reactions. *Acc. Chem. Res.* **1982**, *15*, 117-125. For specific examples please see: (b) Bangwei, D.; Bentrude, W. G. Trimethyl Phosphite as a Trap for Alkoxy Radicals Formed from the Ring Opening of Oxiranylcarbinyl Radicals. Conversion to Alkenes. Mechanistic Applications to the Study of C-C versus C-O Ring Cleavage. *J. Am. Chem. Soc.* **2003**, *125*, 3248-3259. (c) Ganapathy, S.; Sekhar, B. B. V. S.; Cairns, M.; Akutagawa, K.; Bentrude, W. G. Photo-Arbozov Rearrangements of Dimethyl Benzyl and Dimethyl *p*-acetylbenzyl Phosphite. *J. Am. Chem. Soc.* **1999**, *121*, 2085-2096.

[12] (a) Walling, C.; Rabinowitz, R. The Reaction of Trialkyl Phosphites with Thiyl and Alkoxy Radicals. *J. Am. Chem. Soc*. **1959**, *81*, *5*, 1243-1249. (b) Kim, S.; Oh, D. H. Generation of 5- and 6-memebered Ring Radicals by Deoxygenation of Alkoxy Radicals. *Synlett*, **1998**, 525-527. (c) Burn, A. J.; Cadogan, J. I. G.; Bunyan, P. J. The Reactivity of Organophosphorus Compounds. Part XV. Reactions of Diaroyl Peroxides with Triethyl Phosphite. *J. Chem. Soc.* **1963**, 1527-1533

[13] (a) Bentrude, W. G. **1990**, in The chemistry of organo phosphorous compounds, vol 1. *Willey,* Sussex, pp. 531. (b) Bentrude, W. G. **1983,** in Reactive intermediates, vol 3. *Plenum,* London, pp. 199. (c) Roberts, B. P. **1980**, in Advances in free radical chemistry, vol 6. *Heyden*, London, pp. 225.

[14] For a review on the N-centered radical in synthesis please see Zard, S. Z. Recent Progress in the Generation and Use of Nitrogen-Centred Radicals. *Chem. Soc. Rev.* **2008**, *37*, 1603-1618.

[15] (a) Cadogan, J. I. G.; Rowley, A. G. The Reactivity of Organophosphorus Compounds. Part XXIX. Deoxygenation of Nitroxyl Radicals by Trialkyl Phosphites: a New Route to Nitrenium Ions *via* Electron Transfer Reactions of Aminyl Radicals. *J. Chem. Soc. Perkin Trans. 2*, **1974**, 1030-1033. (b) Ohmori, H.; Nakai, S.; Masui, M. Activation of N-Hydroxy Compounds by P-O Bond Formation through Anodic Oxidation of Triphenylphosphine. *Chem. Pharm. Bull.* **1980**, *28*, 2247-2250. (c) Cadogan, J. I. G.; Rowley, A. G. The Reactivity of Organophosphorus Compounds. Part XXIX. Deoxygenation of Nitroxyl Radicals by Trialkyl Phosphites: a New Route to Nitrenium Ions *via* Electron Transfer Reactions of Aminyl Radicals. *J. Chem. Soc. Perkin Trans. 2*, **1974**, 1030-1033. (d) Nesterov, V.; Qu, Z.-W.; Schnakenburg, G.; Grimme, S.; Streubel, R. Selective phosphanyl complex trapping using TEMPO. Synthesis and reactivity of P-functional P-nitroxyl phosphane complexes. *Chem. Commun.* **2014**, *50*, 12508-12511. (e) Ishida, S.; Hirakawa, F.; Iwamoto, T. Reactions of a Stable Phosphinyl Radical with Stable Aminoxyl Radicals. *Chem. Lett.* **2015**, *44*, 94-96. (f) Mar'in, A.; Damiani, E.; Canestrari, S.; Dubs, P.; Greci, L. Interaction Between Trialkyl Phosphites and Aminoxyl Radicals: A Model Study for Polymer Stabilization. *J. Chem. Soc., Perkin Trans. 2,* **1999**, 1363-1367.

[16] Lin, X.; Artman III, G. D.; Stien, D.; Weinreb, S. M. Development of Efficient New Methodology for Generation, Cyclization and Functional Trapping of Iminyl and Amidyl Radicals. *Tetrahedron*, **2001**, 8779-8791.

[17] For early examples of the thermolysis of O-phosphino hydroxylamines, please see (a) Banks, M. R.; Hudson, R. F. The Reaction Between N-methyl-p-toluohydroxamic Acid and Tervalent Phosphorus Compounds: a Thermal $P^{III}$ to $P^{V}$ Rearrangement Proceeding by a Radical Mechanism. *J. Chem. Soc. Perkin Trans. II* **1989**, 463-467. (b) Lopez, L.; Barrans, J. Phosphorus Derivatives of Amide Oximes. Part 1. Synthesis of $N^2$-[Bis(dimethylamino)phosphinoyl]amidines, 4,6-Disubstituted 2,5-dihydro-1,3,5,2-triazaphosphorine 2-Oxides, and 3-dialkylamino-1-dimethyl-amino-1H-2,1-benzaphosphole 2-Oxides. *J. Chem. Soc. Perkin Trans. I*, **1977**, 1806-1811. (c) Heurich, T.; Qu, Z.-W.; Nožinović, S.; Schnakenburg, G.; Matsuoka, H.; Grimme, S.; Schiemann, O.; Streubel, R. Synthesis and Rearrangement of P-nitroxyl-Substituted $P^{III}$ and $P^{V}$ Phosphanes: A Combined Experimental and Theoretical Case Study. *Chem. Eur. J.* **2016**, *22*, 10102-10110. (d) Alonso, C.; de los Santos, J. M.; Vicario, J.; Palacious, F. Phosphorus Substituted Hydroxylamine and Hydroxamic Acid Derivatives, Synthesis and Reactivity. *Arkivoc*, **2011**, 221-253.

[18] Wu, Y.; Wan, Y.; Zhang, F. Characteristics and Trends of C-H Activation Research: A Review of Literature. *Curr. Org. Synth.* **2018**, 781-792.

[19] Yi, H.; Zhang, G.; Wang, H.; Huang, Z.; Wang, J.; Sing, A. K.; Lei, A. Recent Advances in Radical C-H Activation/Radical Cross-Coupling. *Chem. Rev.* **2017**, 9016-9085.

[20] (a) Capaldo, L.; Ravelli, D.; Hydrogen Atom Transfer (HAT): A Versatile Strategy for Substrate Activation in Photocatalyzed Organic Synthesis. *Eur. J. Org. Chem.* **2017**, 2056-2071. (b) Sarkar, S.; Cheung, K. P. S.; Gevorgyan, V. C-H Functionalization Reactions Enabled by Hydrogen Atom Transfer to Carbon-Centered Radicals. *Chem Sci.* **2020**, 1297-12993.

[21] (a) Na, C. G.; Ravelli, D.; Alexanian, E. J. Direct Decarboxylative functionalization of Carboxylic Acids via O-H Hydrogen Atom Transfer. *J. Am. Chem. Soc.* **2020** 44-49. (b) Czaplyski, W. L.; Na, C. G.; Alexanian, E. J. C-H Xanthylation: A Synthetic Platform for Alkane Functionalization. *J. Am. Chem. Soc.* **2016**, 13854-13857. (c) Quinn, R.; Konst, Z.; Michalak, S.; Schmidt, Y.; Szklarski, A.; Flores, A.; Nam, S.; Horne, D.; Vanderwal, C.; Alexanian, E. Site-Selective Aliphatic CH Chlorination Using N-Chloroamides Enables a Synthesis of Chlorolissoclimide. *J. Am. Chem. Soc.* **2016**, 696-702.

[22] (a) An, Q.; Wang, Z.; Chen, Y.; Wang, X.; Zhang, K.; Pan, H.; Liu, W, Zuo, Z. Cerium-Catalyzed C-H Functionalizations of Alkanes Utilizing Alocohols as Hydrogen Atom Transfer Agents. *J. Am. Chem. Soc.* **2020**, 6216-6226. (b) Hu, A.; Guo, J.-J.; Zuo, Z. Selective Functionalization of Methane, Ethane, and Higher Alkanes by Cerium Photocatalysis. *Science*, **2018**, 668,672.

[23] Ravelli, D.; Fagnoni, M.; Fukuyama, T.; Nishikawa, T.; Ryu, I. Site-Selective C-H Functionalization by Decatungstate Anion Photocatalysis: Synergistic Control by Polar and Steric Effect Expands the Reaction Scope. *ACS Catal.* **2018**, 701-713.

[24] Denes, F.; Pichowicz, M.; Povie, G.; Renaud, P. Thiyl Radicals in Organic Synthesis. *Chem. Rev.* **2014***,* 2587-2693.

[25] Dang, H.-S.; Roberts, B. P. Radical-Chain Addition of Aldehydes to Alkenes Catalyzed by Thiols. *J. Chem. Soc. Perkin Trans 1.* **1998**, 67-76.

[26] Dang, H.-S.; Franchi, P.; Roberts, B. P. Radical -Chain Deoxygenation of Tertiary Alcohols, Protected as their Methoxymethyl (MOM) Ethers, Using Thiols as Polarity-Reversal Catalysts. *Chem. Commun.* **2000**, 499-500.

[27] Dang, H.-S.; Roberts, B. P. Radical-Chain Cyclization of Unsaturated Acetals and Thioacetals in the Presence of Thiols as Polarity-Reversal Catalysts. *Tet. Lett.* **1999**, 8929-8933.

# Chapter 1: Intermolecular Hydroamination of Alkenes using *N*-Hydroxypthalimide

## 1.1 Introduction

Nitrogen containing functionalities are vastly important and can be found in pharmaceuticals, agrochemicals, and natural products. As such, the construction of new carbon-nitrogen bonds is of great interest to synthetic and process chemists alike, and the development of new methodologies that allow for the facile formation of these bonds is an ongoing goal. The hydroamination of olefins is an attractive approach for the installation of nitrogen containing functionalities because alkene-containing substrates are a diverse class of molecules and are widely available. Furthermore, the prospect of adding a N-H bond across an alkene is a conceptionally simple method for the preparation of nitrogen-rich molecules.

Many of the traditional methods for alkene hydroamination proceed with Markovnikov regioselectivity, where the nitrogen atom is added at the more substituted carbon of the reacting alkene.[1] While methods that produce the anti-Markovnikov hydroamination regioisomer are more rare, significant advances have been made using transition metal[2] and photoredox catalysis (Scheme 1.1).[3]

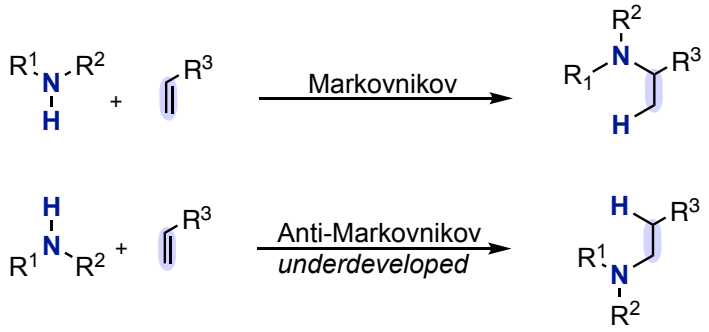


Scheme 1.1. Possible regioisomers for the hydroamination of an asymmetric alkene.

One strategy for obtaining the more elusive anti-Markovnikov hydroamination regioisomer is by using a radical mediated pathway, as a nitrogen-centered radical generated in situ would predictably add at the less substituted cite of an alkene.[4] Furthermore, radical driven processes are

conceptually attractive because of their compatibility with otherwise reactive polar functionalities.[5]

In addition to regioselectivity, yet another challenge in the realm of hydroamination is the ability to synthesize primary amines through hydroamination. Many successful methods use substituted amine substrates to preclude the possibility of the product, typically more nucleophilic than the initial starting material because of increased alkyl substitution, from engaging in further hydroamination (Scheme 1.2.a). Ammonia itself as a substrate is challenging because of its relatively poor nucleophilicity and the handling and storage of ammonia, a toxic and corrosive gas, can be prohibitive. As a result, recent attention has been directed toward the development of new methods that rely on the use of formal ammonia surrogates to achieve the synthesis of primary amines via hydroamination (Scheme 1.2.b).[6]

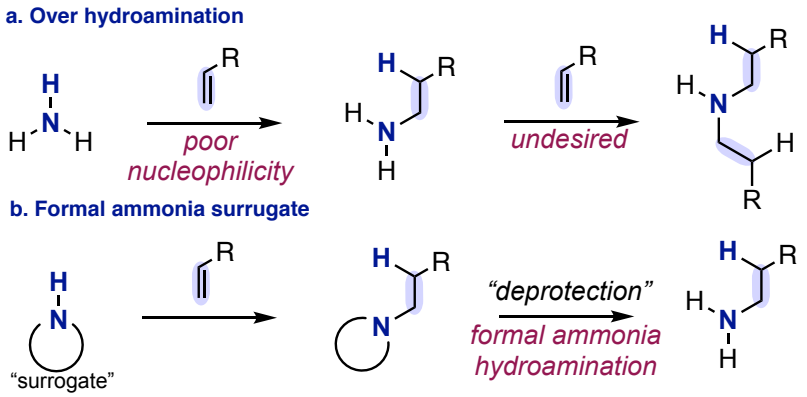


Scheme 1.2. Synthesis of primary amines through hydroamination.

We became interested in phthalimidyl radicals for use in alkene hydroamination because of the known propensity of these species to add into alkenes,[7] and this route would predictably furnish the anti-Markovnikov regioisomer. Furthermore, the phthalimidyl (Phth) group can be conveniently removed using a facile deprotection procedure to furnish the desired primary amine product.[8] Previous efforts include the use of phthalimidyl radicals for the amination of arenes[9] (Scheme 1.3.a) and the aminohalogenation of alkenes (Scheme 1.3.b),[10] relying on phthalimidyl

substrates bearing photochemically labile N-X bonds to generate the requisite N-centered radicals. Despite the interest in selective C-N bond formation via alkene hydroamination, phthalimidyl radicals have not previously been employed for this application. This is likely due to a lack of phalimidyl-radical precursors that possess a transferable H-atom, and the addition of a stoichiometric hydrogen-atom source would likely inhibit the desired reactivity.

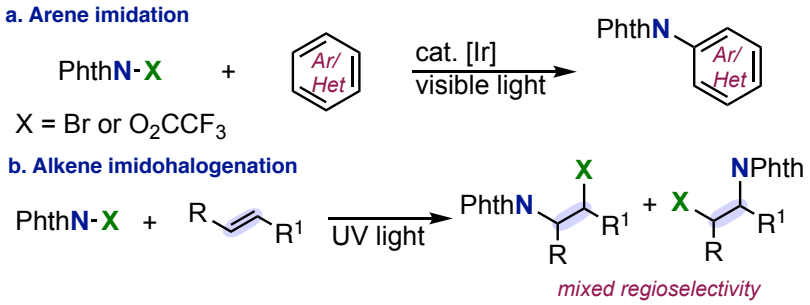


Scheme 1.3. Phthalimidy radicals in organic synthesis.

## 1.2 Reaction Development and Substrate Scope

*N*-Hydroxyphthalimide (NHPI) is an inexpensive, commercially available, and benchtop stable compound with well documented participation in radical mediated processes.[11] In spite of this, the use of NHPI is limited to that of an O-radical precursor in the form of the PINO radical (PhthNO·). We hypothesized that with a suitable oxygen-atom transfer type procedure, NHPI could be deoxygenated to provide the N-centered phthalimidyl radical.

We began this investigation by exploring the possibility of using a trivalent phosphorus reagent as an oxygen-atom abstraction reagent, owing to the known propensity of phosphines and phosphites to engaged in deoxygenative radical processes.[12] Furthermore, we hypothesized that the exchange of a weak N-O bond (~55-65 kcal/mol) for a strong phosphoryl unit (148 kcal/mol for **OP**$(OEt)_3$) would provide a favorable thermodynamic driving force for our desired transformation.[13] We attempted the hydroamination of electron rich *n*-butyl vinyl ether using NHPI in the presence of triethyl phosphite and thermal radical initiators (Table 1). *N*-butyl vinyl ether

was selected as a model substrate because its electron richness is well paired with the known electrophilicity of the phthalimidyl radical, and triethyl phosphite was selected as the trivalent phosphorus reagent because of its commercial availability and reasonable price point.

Table 1.1. Reaction optimization for the hydroamination of n-butyl vinyl ether. Reactions carried out with NHPI (1 equiv), *n*-butyl vinyl ether (5 equiv), triethyl phosphite (1.5 equiv), and radical initiator (0.25 equiv) in the specified solvent (0.04 M) at 90 °C. [a]Determined by gas chromatography using mesitylene as an internal standard. [b]Isolated yield of **1.1a** following purification on silica gel. [c]Reaction temperature 35 °C. [d]No triethyl phosphite added.

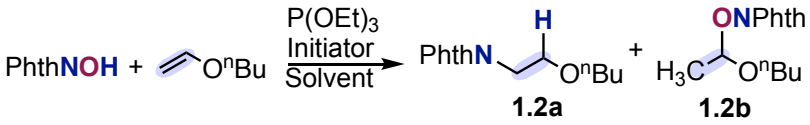


| Entry | Initiator | Solvent | Ratio 1.2a:1.2b[a] | Yield[b] |
|---|---|---|---|---|
| 1 | AIBN | Benzene | 23:77 | 9% + 30% **1.2b** |
| 2 | AIBN | MeCN | 93:7 | 67%[a] |
| 3 | AIBN | DCE | 75:25 | 79% |
| 4 | *None* | DCE | <2:98 | 81% **1.2b** |
| 5 | BPO | DCE | 38:62 | 30%[a] |
| 6 | DTBP | DCE | 7:93 | 8%[a] |
| 7 | DLP | DCE | 94:6 | 79% |
| 8[c] | DTBHN | DCE | 98:2 | 82% |
| 9[d,e] | DTBHN | DCE | <2:98 | 47% **1.2b** |

A first reaction involving NHPI (1 equiv), *n*-butyl vinyl ether (NBVE, 5 equiv), triethyl phosphite (1.5 equiv), and 2,2'-azobis(2-methylpropionitrile) (AIBN, 25 mol%) in 0.04M benzene at 90 °C resulted in the formation of the desired hydroamination product **1.2a** in 9% isolated yield (Table 1, entry 1). The major product isolated from this reaction was acetal **1.2b** in 30% yield. The formation of **1.2b** is a polar, non-radical process that can be easily explained, as its formation is analogous to the preparation of tetrahydropyran-acetal protected NHPI, which takes place by the

acid catalyzed addition of NHPI to 3,4-dihydro-2*H*-pyran, a vinyl ether.[14] In our reaction here, NHPI is likely sufficiently acidic to promote the formation of **1.2b** on its own.[15]

Switching the solvent from benzene to acetonitrile (MeCN) improved the reaction efficiency for the production of **1.2a** to 67%, with only a minimal amount of **1.2b** being formed (entry 2). Switching the solvent again to 1,2-dichloroethane (DCE) further improved the yield of the desired hydroamination product to 79%, although the ratio of **1.2a:1.2b** decreased from entry 2 (entry 3). The use of other common radical initiators such as benzoyl peroxide (BPO, entry 5) or di-tertbutyl peroxide (DTBP, entry 6) resulted in significantly decreased reaction efficiency. Conversely, the use of dilauroyl peroxide (DLP, entry 7) or di-tertbutly hyponitrite at 35 °C (DTBHN, entry 8) provided the desired hydroamination product in 79% and 82% yield, respectively, with only minimal quantities of the acetal **1.2b**. Control experiments that individually excluded either radical initiator (entry 4) or phosphite (entry 9) resulted in no production of **1.2a**, thereby indicating their necessity in the reaction.

We set out to explore the scope of alkenes amenable to this hydroamination protocol (Scheme 1.4) . In addition to NBVE, a variety of other vinyl ethers and similarly functionalized alkenes participated in this transformation in good to excellent yields as well (**1.2c-k**). As a general trend, we found that terminal vinyl ethers typically resulted in higher reaction efficiencies than internal vinyl ethers; we attribute this to a slower addition of phthalimidyl radical to an internal alkene substrate. Notably, product **1.2h** bearing a primary chloride was furnished in 49% yield, indicating that hydroamination was able to outcompete potential Arbuzov-type side reactivity involving the phosphite. Similarly electron rich alkenes including vinyl silanes (**1.2l-m)** and sulfides (**1.2n-q**) took place in this hydroamination transformation, albeit with slightly diminished yields as compared to the analogous vinyl ethers.

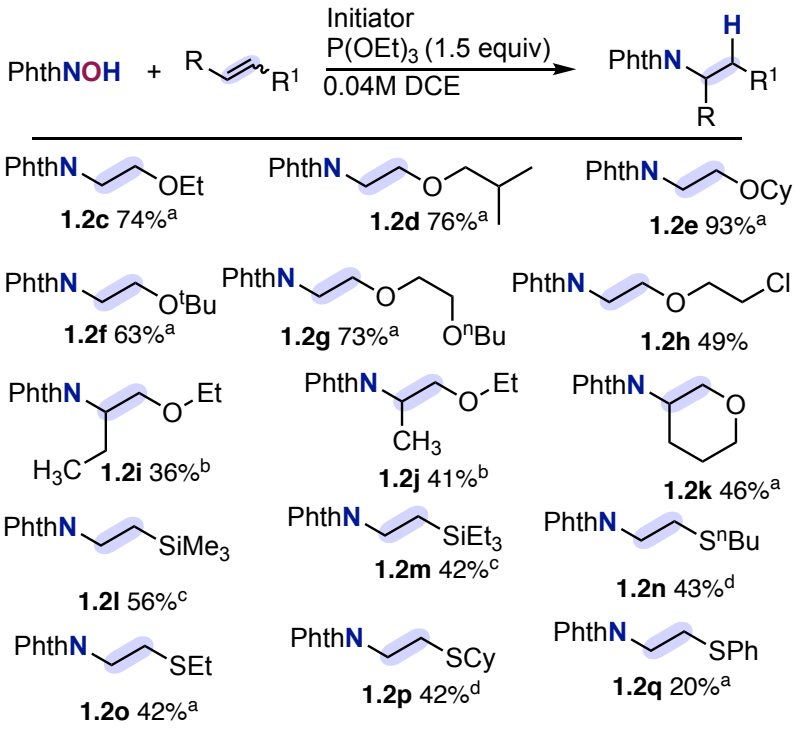


Scheme 1.4. Hydroamination reaction substrate scope with functionalized alkenes. All yields are for isolated material following chromatography on silica gel; >20:1 regioselectivity for isomer shown; 12 h reaction times. [a]Reactions carried out using $P(OEt)_3$ (1.5 equiv), DTBHN (0.25 equiv), alkene (10 equiv) in DCE (0.04M) at 50 °C. [b]Carried out using 5 equiv alkene, dilauroyl peroxide (0.5 equiv) at 90 °C. [c]Carried out using dilauroyl peroxide (1 equiv) at 110 °C. [d]5 equiv alkene used.

Further investigation indicated that along with functionalized alkenes such as vinyl ethers, silanes, and sulfides, unfunctionalized alkenes participated in this reaction as well (Scheme 1.5). Cyclic internal alkenes including cyclohexene, norbornene, cyclopentene, cycloheptene, and cyclooctene all participated in this transformation in good yield (**1.2r-1.2v**). The trisubstituted 1-methylcyclohexene similarly participated in this reaction, albeit with diminished yield (**1.2w**). Camphene, a common monoterpene bearing an exo-methylene was also able to take part in this hydroamination protocol in fair yield (**1.2y**). Other unactivated, linear alkenes such as tert-butyl ethylene (**1.2z**), 1-hexene (**1.2aa**), and 4-octene (**1.2ad**) similarly took part in this reaction in fair to good yield.

Notably, hydroamination product **1.2ab** bearing a primary bromide was isolated in 55% yield, again illustrating the ability of this hydroamination procedure to outcompete potential

Arbuzov-type side reactivity. Alkenes containing pivalate esters were also able to participate in this protocol (**1.2ac** and **1.2ae**). Dienes capable of cyclization similarly took part in this reaction such as allyl ether which solely provided the cyclized, tetrahydrofuranyl product **1.2af** in modest yield indicating that the rate of cyclization of the carbon centered radical produced after addition of phthalimidyl radical to the alkene ($\sim 9 \times 10^6\ s^{-1}$)[16] is faster than hydrogen atom transfer to that same C-radical. On the other hand, the reaction with 1,5-cycloctadiene produced a separable mixture of the cyclized, bicyclic amination product **1.2ag** as well as the singly hydroaminated, noncyclized product **1.2ah**, thereby indicating that this slower 5-*exo*-trig cyclization rate ($\sim 1 \times 10^5\ s^{-1}$) is competitive with the rate of hydrogen atom transfer necessary to produce product **1.2ah**. Finally, we found that in addition to a host of alkenyl substrates, 1-octyne participated in this reaction providing the vinyl phthalimide **1.2ai** exclusively as the E isomer, albeit in modest yield

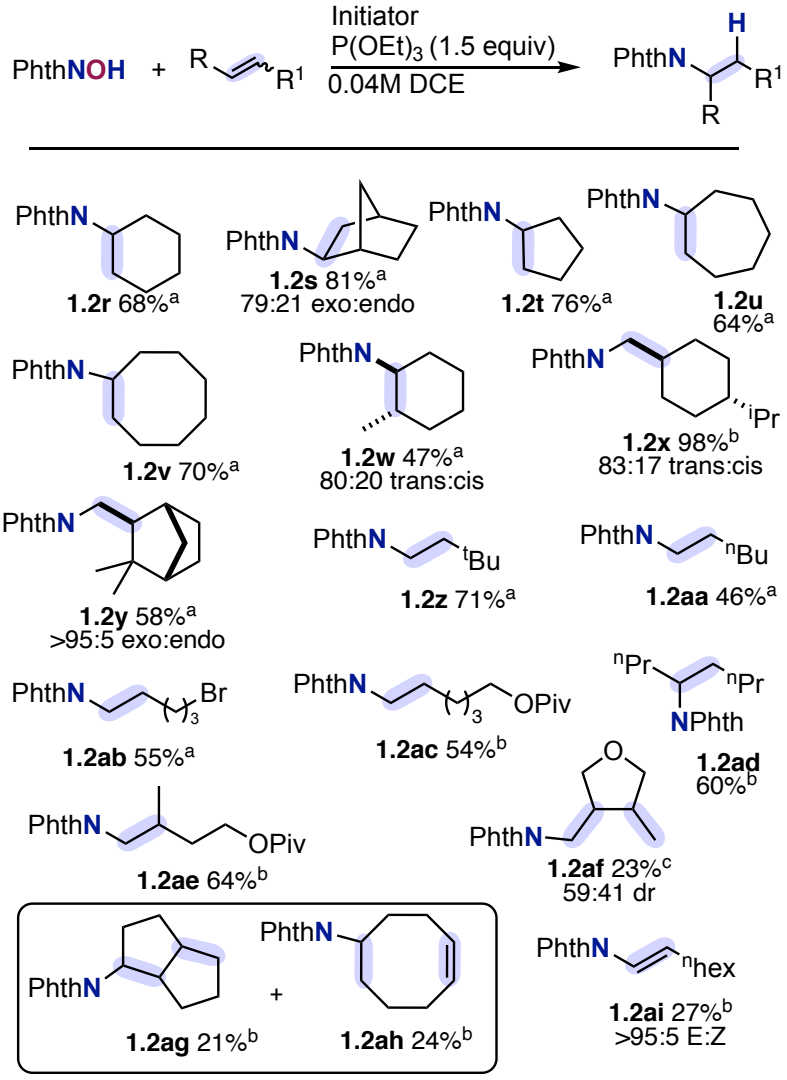


Scheme 1.5. Hydroamination reaction substrate scope with unactivated alkenes. All yields are for isolated material following chromatography on silica gel; >20:1 regioselectivity for isomer shown; 12 h reaction times. [a]Carried out using dilauroyl peroxide (1 equiv) at 110 °C. [b]Reactions carried out using $P(OEt)_3$ (1.5 equiv), DTBHN (0.25 equiv), alkene (10 equiv) in DCE (0.04M) at 50 °C. [c]Carried out using dilauroyl peroxide (0.20 equiv).

While a host of functionalized, electron-rich alkenes, as well as a variety of wholly unactivated alkenes performed well in this hydroamination procedure, a handful of olefins failed to partake. Alkenes bearing pendent phenyl groups did not result in any isolable quantities of hydroamination product. Even styrene, which would predictably generate a stabilized, benzylic radical following phthalimidyl addition, failed to undergo this transformation. In fact, the only substrate to produce any appreciable quantity of hydroamination product was phenyl vinyl sulfide,

which only resulted in a mere 20% isolated yield (**1.2q**). This lack of desired reactivity can likely be attributed to the tendency of the phthalimidyl radical to add into aromatic systems. We hypothesize that in the reactions involving this class of substrates, arene addition outcompetes alkene addition, and because these reactions are run under reductive conditions, there is a difficulty in oxidizing and subsequently rearomatizing the C-radical intermediate following addition. This inability to terminate likely results in accelerated decomposition of the starting material.

Likewise, vinyl acetate and similarly categorized vinyl esters failed to produce the desired hydroamination products in appreciable yields. In these instances, small quantities of the anticipated products were detected by proton NMR and gas chromatography-mass spectrometry (GC-MS), but could not be isolated. Electron deficient alkenes such as acrylates similarly failed to partake in this transformation, as did substrates bearing acetyl groups. Interestingly, acetyl-protected 5-hexen-1-ol did not result in the formation of the desired product, while the more sterically encumbered pivalate derivative was isolated in 54% yield (**1.2ac**).

A host of allylic substrates failed to undergo this reaction, likely due to the presence of highly abstractable hydrogen atoms present on these substrates that could shunt the desired reactivity pathway. Substrates containing amino functionalities similarly failed to undergo this transformation, and simply resulted in decomposition of the starting material. Even amino substrates analogous to allyl ether, which was used for the synthesis of compound **1.2af**, failed to produce any hydroamination products.

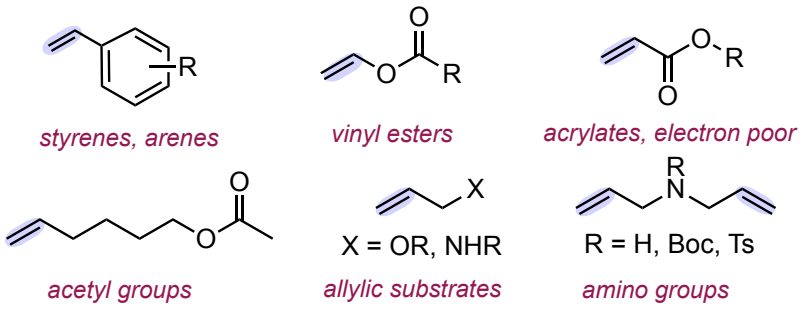


Scheme 1.6. Unsuccessful hydroamination substrates.

## 1.3 Phthalimidyl Deprotection and Synthetic Utility

In order to illustrate the applicability and synthetic utility of this hydroamination method, we performed the deprotection of product **1.2a** using aqueous hydrazine in methanol (MeOH). With gentle heating to 60 °C, the reaction was complete in a mere 30 minutes and the primary amine product was isolated in 89% yield (Scheme 1.7.a). Next, we performed the hydroamination of norbornene on a scaled-up gram scale and observed no decrease in reaction efficiency; followed by a facile deprotection to provide the primary amine in 76% total yield over 2 steps (Scheme 1.7.b/c). This protocol for the straight forward synthesis of 2-aminonorbornane from norbornene in great yield illustrates the synthetic utility of this hydroamination protocol and its practicality toward the synthesis of value-added chemicals.

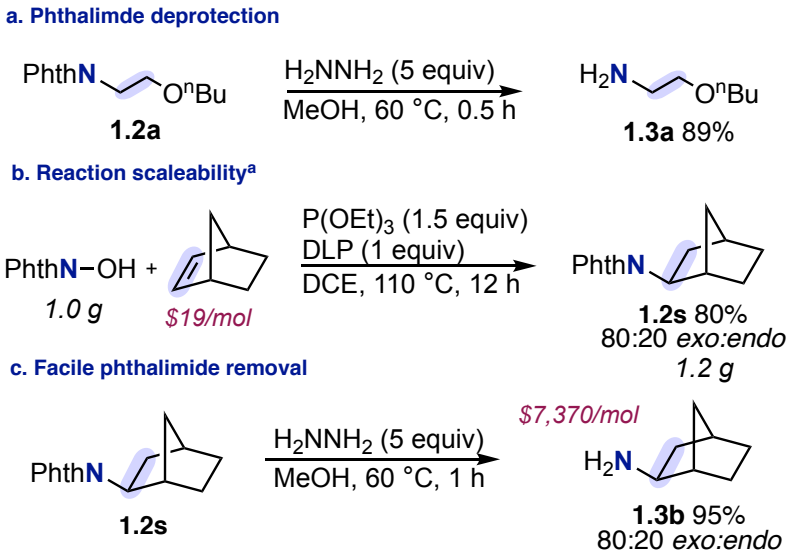


Scheme 1.7. Reaction synthetic utility. [a]5 equiv alkene used.

## 1.4 Mechanistic Investigation

A mechanistic hypothesis in line with our data is shown in Scheme 1.8. First, radical initiation generates the imidoxyl radical, PINO, which then engages with triethyl phosphite to form a phosphoranyl-radical intermediate. Subsequent ß-scission produces the phosphate byproduct and requisite phthalimidyl radical, now prone to add at the anti-Markovnikov position of the external alkene substrate. Finally, hydrogen atom abstraction from a second equivalent of NHPI delivers the final hydroaminated product and turns over the radical chain through regeneration of the PINO radical.

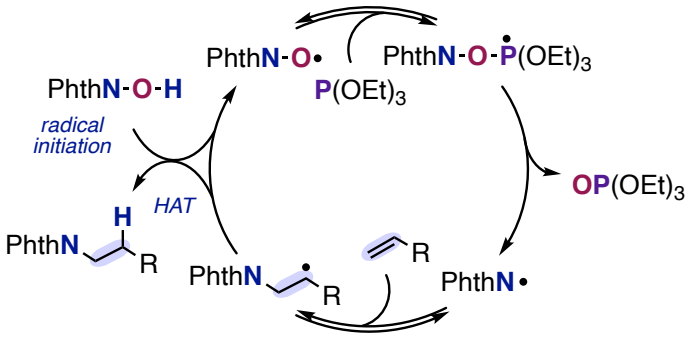


Scheme 1.8. Hydroamination mechanistic proposal.

As postulated in Scheme 1.8., this mechanism appears markedly similar to that of an atom transfer radical addition (ATRA) type strategy first explored by Kharasch in the 1940s wherein a single reagent is able to transfer multiple groups to a single substrate. For example, in Kharasch's seminal paper, he found that carbon tetrachloride in the presence of a radical initiator was capable of transferring both a chloro and a trichloromethyl group to a single alkene, providing an overall alkene difunctionalization.[17] In this protocol, NHPI is apparently supplying both the N- and H-atoms necessary for the overall hydroamination, thereby making the transformation similar to the ATRA processes pioneered by Kharasch.

In order to determine whether or not NHPI was indeed serving as the H-atom source for this reaction, we prepared NHPI-$d_1$ and subjected it to standard reaction conditions with *tert*-butyl ethylene (Scheme 1.9). As predicted, we were able to produce the deuterium enriched product **1.2z-*d*$_1$** in 58% yield, with exclusive deuteration at the carbon ß-to the phthalimide. This was confirmed by decreased integration in the proton NMR of **1.2z-*d*$_1$** (Figure 1.1.), the appearance of new peak at 1.439 ppm in the deuterium NMR (Figure 1.2.), the appearance of a triplet in the aliphatic region of the carbon NMR corresponding to the ß-position carbon of the deuterated product, as well as the doubling up of the other signals in the carbon NMR (Figure 1.3.). While deuterium incorporation at the ß-position was indeed observed, both the proton and the carbon NMRs of the product clearly show that the reaction resulted in relatively modest overall deuterium incorporation (33%), with the rest of the product being the natural abundance product that would be expected when using non-enriched NHPI.

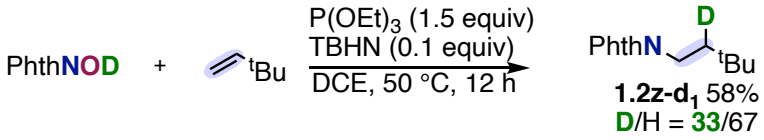


Scheme 1.9. Hydroamination deuterium labeling experiment using $d_1$-NHPI.

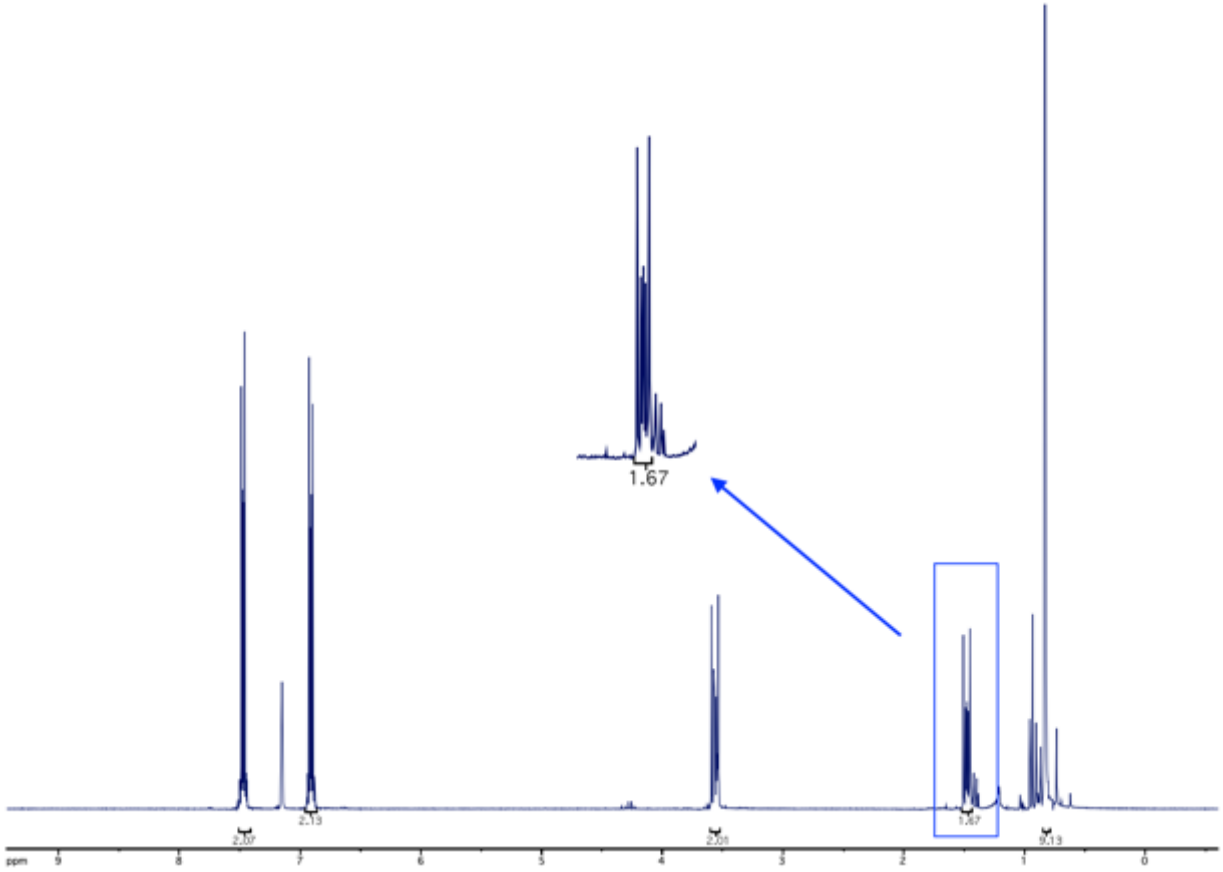


Figure 1.1. $^1$H-NMR of **1.2z-d$_1$**.

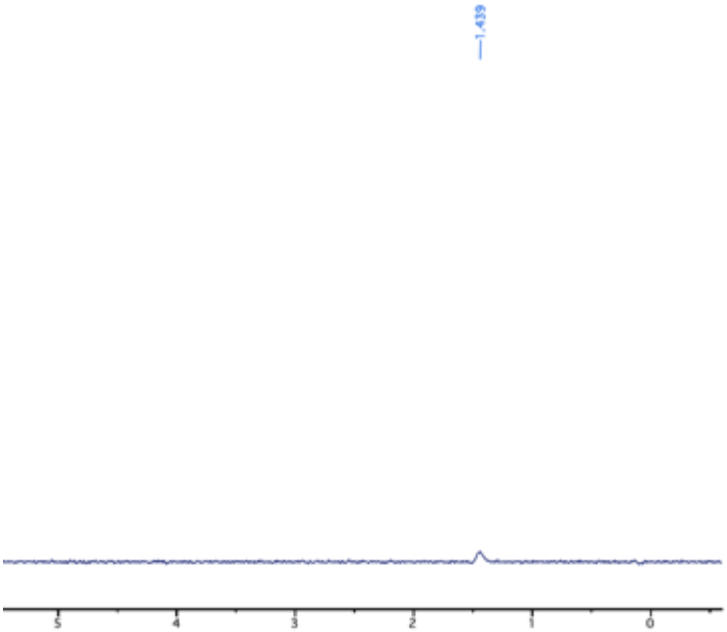


Figure 1.2. Deuterium NMR of **1.2z-d$_1$**.

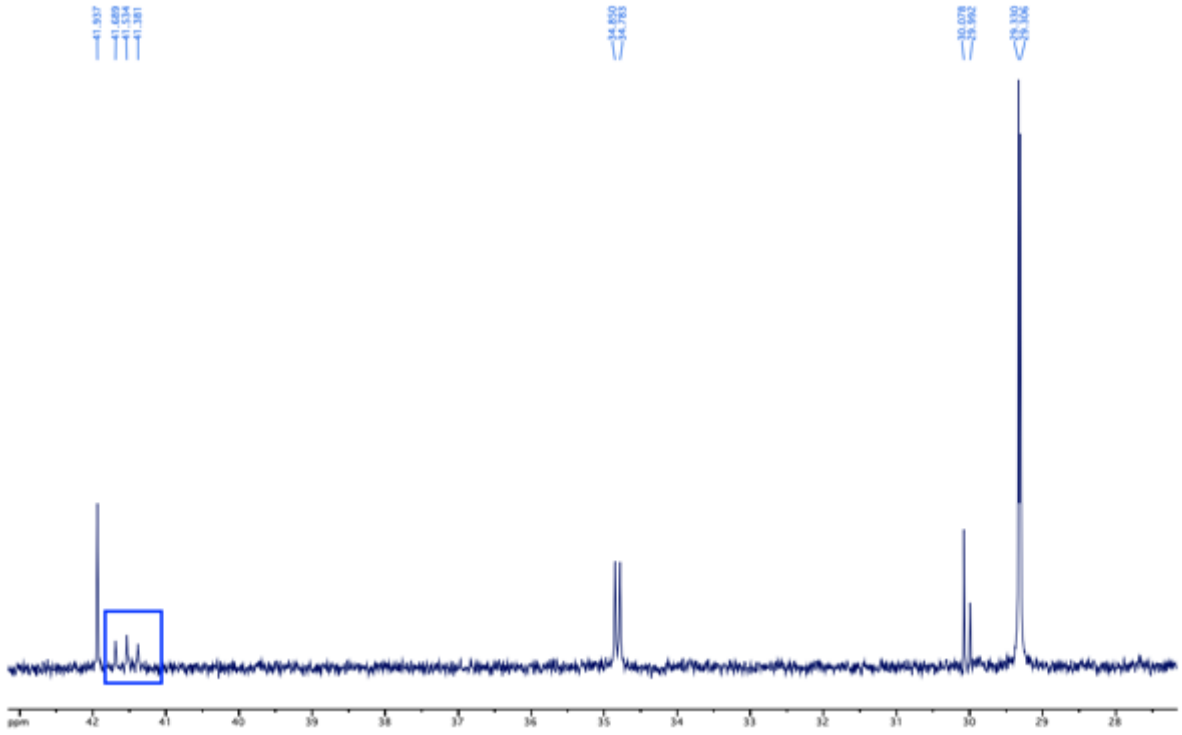


Figure 1.3. $^{13}$C-NMR of **1.2z-*d*$_1$**.

We hypothesized that perhaps this modest deuterium incorporation was a result of the acidic O-D of NHPI-$d_1$ ($pk_a$ = 7.0) rapidly exchanging with trace water found in the solvent, thereby decreasing the total deuterium available to transfer. To test this hypothesis, an experiment with added $D_2O$ was carried out. While the reaction efficiency decreased significantly to 5% yield, the product was further enriched in deuterium (up from 33% to 64%. Scheme 1.10.a). Furthermore, we conducted an analogous experiment with natural abundance NHPI and added $D_2O$ to support the claim that water diminishes the reaction efficiency, and found that this reaction did result in mild deuteration (34%), but was not as effective as using NHPI-$d_1$ and $D_2O$ combined (Scheme 1.10.b). Direct H-atom abstraction from water is not likely the final step in this transformation as this would be thermodynamically unfavorable because of the impressive bond dissociation energy of O-H in water (119 kcal/mol). As a result, we believe this collection of data is in support of our proposed mechanism as outlined in Scheme 1.8.

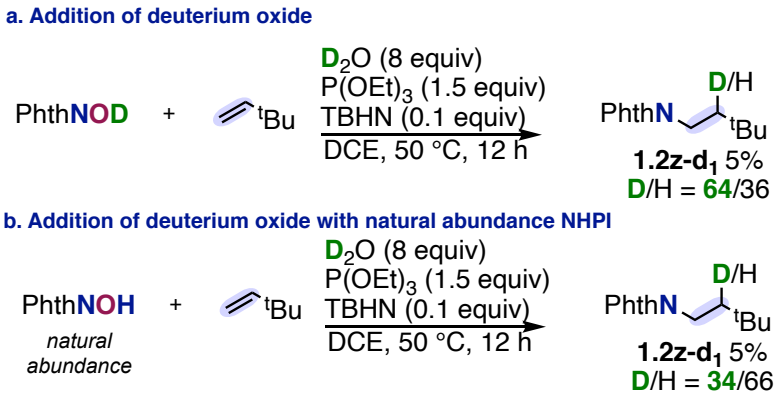


Scheme 1.10. Deuterium oxide addition experiments.

## 1.5 Conclusions

In summary, we have disclosed a new, radical-mediated hydroamination protocol using *N*-hydroxyphthalimide as both the N- and H-source for the overall transformation, and triethyl phosphite as an oxygen atom acceptor. This method allows for the hydroamination of wide variety of alkenes including vinyl ether, silanes, and sulfides, as well as a host of unactivated olefins in

good to excellent yields. In order to demonstrate the synthetic utility of this method, we performed this reaction on a gram scale without any diminishment in yield, as well as the facile deprotection of the phthalimide to provide the formal ammonia hydroamination product in excellent yield. Extensive mechanistic experiments were conducted in order to elucidate the exact process through which this transformation proceeds, ultimately revealing an ATRA-type pathway where NHPI is capable of supplying both the N- and H atoms for the overall hydroamination.

Chapter 1 has been adapted from materials published in Lardy, S. W.; Schmidt, V. A. Intermolecular Radical Mediated Anti-Markovnikov Alkene Hydroamination Using *N*-Hydroxyphthalimide. *J. Am. Chem. Soc.* **2018**, 12318-12322. The dissertation author was the primary investigator of this publication.

## 1.6 Appendix

### 1.6.1 General Considerations

All air- and moisture-sensitive manipulations were carried out using standard high vacuum line, Schlenk or cannula techniques or in an M. Braun inert atmosphere drybox containing an atmosphere of purified nitrogen. Solvents for air- and moisture-sensitive manipulations were dried and deoxygenated using literature procedures. *N*-hydroxyphthalimide was purchased from Sigma-Aldrich and was used as received without further purification. All reagents were purchased from commercial sources and were used as received without further purification. $^{1}$H and $^{13}$C NMR were recorded on Varian Mercury 400 MHz or Varian Unity/Inova 500 MHz spectrometers at 400 and 126 MHz, respectively. All chemical shifts are reported relative to $SiMe_4$ using $^{1}$H (residual) chemical shifts of the solvent as a secondary standard. GC analyses were performed using an Agilent Technologies 7890B gas chromatograph equipped with an Agilent 7693 autosampler and Agilent HP-5 capillary column (30 m x 0.320 mm x 250 μm). Standard method parameters: 1.2

mL/min flow rate with oven program 80 – 250 °C with a ramp rate of 25 °C/min and hold time of 8.7 minutes at 250 °C. Low-resolution mass spectra were measured using a Thermo LCQdeca APCI-MS. High-resolution mass spectra were measured using an Agilent 6230 ESI-TOFMS. IR spectra were recorded on an FT/IR-4100typeA spectrometer with a TGS detector.

****Caution: while preparing DTBHN we experienced no issues, care should be exercised when handling hyponitrites as they can be shock and heat sensitive. DTBHN should be stored under an inert atmosphere at -35 °C and be handled to avoid contact with metal surfaces****

****Caution: while no problems were encountered in this work, alkylhydroperoxides can undergo spontaneous and rapid exothermic decomposition and appropriate care should be taken in their handling****

### 1.6.2 Preparation of Substrates

Cyclohexyl vinyl sulfide,[18] *n*-butyl vinyl sulfide,[18] hex-5-enyl pivalate,[19] 1-isopropyl-4-methylenecyclohexane,[20] and di-*tert*butyl hyponitrite (DTBHN) were prepared as previously reported[21]

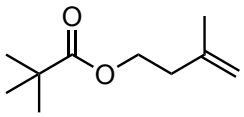

**3-Methylbut-3-enyl pivalate.** A solution of pivaloyl chloride (7.4 mL, 60 mmol, 1.3 equiv) in dichloromethane (10 mL) was added dropwise to a mixture of 3-methylbut-3- enol (4.7 mL, 46 mmol, 1 equiv) and triethylamine (8.4 ml, 60 mmol, 1.3 equiv) in dichloromethane (50 mL) at 0 °C. Following addition, the reaction mixture was allowed to warm to ambient temperature overnight. The reaction mixture was then diluted with diethyl ether (100 mL) and quenched with 1.0 M aqueous HCl (100 mL). The organic layer was separated and the aqueous layer was extracted with diethyl ether (3 x 50 mL). The combined organic layers were neutralized with

saturated aqueous $NaHCO_3$ (50 mL), dried over $Na_2SO_4$, filtered, and the solvent was evaporated to give **3-methylbut-3-enyl pivalate** in quantitative yield as a pale orange liquid. Analytical data for **3-methylbut-3-enyl pivalate:** **$^1$H-NMR** (400 MHz; $CDCl_3$): δ 4.79-4.79 (m, 1H), 4.73-4.72 (m, 1H), 4.17 (t, *J* = 6.7 Hz, 2H), 2.33 (t, *J* = 6.8 Hz, 2H), 1.76 (s, 3H), 1.18 (s, 9H). **$^{13}$C-NMR** (126 MHz; $CDCl_3$): δ 178.5, 141.7, 112.3, 62.4, 38.7, 36.8, 27.2, 22.4. **LRMS** (APCI) Calc. for $[C_{10}H_{18}O_2]^+$ = 170.13, Found = 170.92. **HRMS** (ESI-TOF) Calc. for $[C_{10}H_{18}O_2]^+$ = 170.1307, Found = 170.1307.

### 1.6.3 General Hydroamination Procedures

*Procedure A:* To a 1-dram vial charged with a magnetic stir bar was added *N*-hydroxyphthalimide (20 mg, 0.12 mmol), *tert*-butyl hyponitrite (5 mg, 0.03 mmol, 0.25 equiv), triethyl phosphite (32 μL, 0.18 mmol, 1.5 equiv), olefin (1.12 mmol, 10 equiv), and 1,2-dichloroethane (3 mL). The vial was capped and heated to 50 °C. Upon consumption of *N*-hydroxyphthalimide as judged by TLC (25% EtOAc in hexanes), the reaction mixture was concentrated under reduced pressure and purified by flash chromatography (8% dichloromethane and 8% diethyl ether in hexanes).

*Procedure B:* To a 1-dram vial charged with a magnetic stir bar was added *N*-hydroxyphthalimide (20 mg, 0.12 mmol), dilauroyl peroxide (49 mg, 0.12 mmol, 1.0 equiv), triethyl phosphite (32 μL, 0.18 mmol, 1.5 equiv), olefin (1.12 mmol, 10 equiv), and 1,2-dichloroethane (3 mL). The vial was capped and heated to 110 °C. Upon consumption of *N*-hydroxyphthalimide as judged by TLC (25% EtOAc in hexanes), the reaction mixture was concentrated under reduced pressure and purified by flash chromatography (10% EtOAc in hexanes).

### 1.6.4 Characterization of Products (1.1a – 1.2ai)

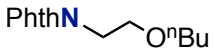


**1.2a** was synthesized via Procedure A in 82% yield as a colorless oil. Analytical data for **1.2a**: **$^{1}$H-NMR** (400 MHz; CDCl3): δ 7.84-7.82 (m, 2H), 7.71-7.69 (m, 2H), 3.89 (t, *J* = 5.9 Hz, 2H), 3.66 (t, *J* = 5.9 Hz, 2H), 3.45 (t, *J* = 6.6 Hz, 2H), 1.53-1.46 (m, 2H), 1.33-1.24 (m, 2H), 0.84 (t, *J* = 7.4 Hz, 3H). **$^{13}$C-NMR** (126 MHz; CDCl3): δ 168.5, 134.0, 132.2, 123.4, 70.8, 67.5, 37.6, 31.8, 19.3, 14.0. **LRMS** (APCI) Calc. for $[C_{14}H_{17}NO_3]^+$ = 247.12, Found = 247.99. **HRMS** (ESI-TOF) Calc. for $[C_{14}H_{17}NO_3+H^+]^+$ = 248.1281, Found = 248.1283. **Rf** (25% EtOAc in hexanes): 0.36.

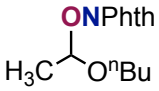


**1.2b** was obtained as a byproduct produced during reaction optimization. Analytical data for **1.2b**: **$^{1}$H-NMR** (500 MHz; $CDCl_3$): δ 7.83-7.82 (m, 2H), 7.74-7.73 (m, 2H), 5.28 (q, *J* = 4.89 Hz, 1H), 4.10 (q, *J* = 7.9, 1H), 3.73 (q, J = 7.8 Hz, 1H), 1.57 (quintet, *J* = 7.2 Hz, 2H), 1.51 (d, *J* = 5.3 Hz, 3H), 1.37 (dq, *J* = 14.9, 7.4 Hz, 2H), 0.91 (t, *J* = 7.4 Hz, 3H). **$^{13}$C-NMR** (126 MHz; $CDCl_3$): δ 164.5, 134.5, 129.2, 123.6, 106.9, 68.3, 31.7, 19.3, 19.1, 14.0. **HRMS** (ESI-TOF) Calc. for $[C_{14}H_{17}NO_4+Na^+]^+$ = 286.1050, Found = 286.1052. **Rf** (25% EtOAc in hexanes): 0.38.

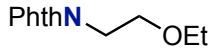


**1.2c** was synthesized via Procedure A in 74% yield as a colorless oil. Analytical data for **1.2c**: **$^{1}$H-NMR** (400 MHz; $CDCl_3$): δ 7.84-7.82 (m, 2H), 7.71-7.69 (m, 2H), 3.88 (t, *J* = 5.8 Hz, 2H), 3.66 (t, *J* = 5.8 Hz, 2H), 3.51 (q, *J* = 7.0 Hz, 2H), 1.13 (t, *J* = 7.0 Hz, 3H). **$^{13}$C-NMR** (126 MHz; $CDCl_3$): δ 168.3, 133.9, 132.1, 123.3, 67.2, 66.1, 37.4, 15.1. **LRMS** (APCI) Calc. for $[C_{12}H_{13}NO_3]^+$ = 219.09, Found = 219.97. **HRMS** (ESI-TOF) Calc. for $[C_{12}H_{13}NO_3+H^+]^+$ = 220.0968, Found = 220.0970. **Rf** (25% EtOAc in hexanes): 0.2.

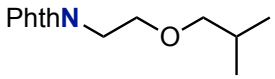


**1.2d** was synthesized via Procedure A in 76% yield as a colorless oil. Analytical data for **1.2d**: **$^{1}$H-NMR** (400 MHz; $CDCl_3$): δ 7.85-7.82 (m, 2H), 7.71-7.69 (m, 2H), 3.88 (t, J = 5.9 Hz, 2H), 3.65 (t, J = 5.9 Hz, 2H), 3.20 (d, J = 6.7 Hz, 2H), 1.81-1.73 (m, 1H), 0.81 (d, J = 6.7 Hz, 6H). **$^{13}$C-NMR** (126 MHz; $CDCl_3$): δ 168.4, 134.0, 132.2, 123.3, 77.9, 67.7, 37.6, 28.5, 19.3. **LRMS** (APCI) Calc. for $[C_{14}H_{17}NO_3]^+$ = 247.12, Found = 247.97. **HRMS** (ESI-TOF) Calc. for $[C_{14}H_{17}NO_3+H^+]^+$ = 248.1281, Found = 248.1283. **Rf** (25% EtOAc in hexanes): 0.36.

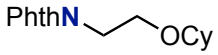


**1.2e** was synthesized via Procedure A in 93% yield as a colorless oil. Analytical data for **1.2e1.2d**: **$^{1}$H-NMR** (400 MHz; $CDCl_3$): δ 7.86-7.83 (m, 2H), 7.72-7.70 (m, 2H), 3.87 (t, *J* = 6.1 Hz, 2H), 3.68 (t, *J* = 6.1 Hz, 2H), 3.31-3.22 (m, 1H), 1.83-1.81 (m, 2H), 1.67-1.64 (m, 2H), 1.51-1.46 (m, 2H), 1.21-1.16 (m, 4H). **$^{13}$C-NMR** (126 MHz; $CDCl_3$): δ 168.5, 134.0, 132.2, 123.4, 77.61, 77.41, 38.1, 32.1, 25.8, 24.1. **LRMS** (APCI) Calc. for $[C_{16}H_{19}NO_3]^+$ = 273.14, Found = 273.94. **HRMS** (ESI-TOF) Calc. for $[C_{16}H_{19}NO_3+^+]^+$ = 274.1438, Found = 274.1441. **Rf** (25% EtOAc in hexanes): 0.33.

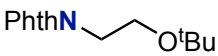


**1.2f** was synthesized via Procedure A in 63% yield as a colorless oil. Analytical data for **1.2f**: **$^{1}$H-NMR** (400 MHz; $CDCl_3$): δ 7.86-7.83 (m, 2H), 7.72-7.70 (m, 2H), 3.84 (t, J = 6.2 Hz, 2H), 3.59 (t, J = 6.6 Hz, 2H), 1.12 (s, 9H). **$^{13}$C-NMR** (126 MHz; $CDCl_3$): δ 168.5, 134.0, 132.2, 123.4, 73.5, 58.9, 38.9, 27.5. **LRMS** (APCI) Calc. for $[C_{14}H_{17}NO_3]^+$ = 247.12, Found = 247.84. **HRMS** (ESI-TOF) Calc. for $[C_{14}H_{17}NO_3+Na^+]^+$ = 270.1101, Found = 270.1104. **Rf** (25% EtOAc in hexanes): 0.33.

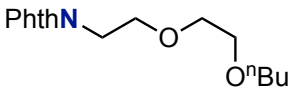


**1.2g** was synthesized via Procedure A in 73% yield as a colorless oil. Analytical data for **1.2g:** **$^{1}$H-NMR** (400 MHz; $CDCl_3$): δ 7.85-7.83 (m, 2H), 7.71-7.69 (m, 2H), 3.90 (t, *J* = 5.8 Hz, 2H), 3.74 (t, *J* = 5.8 Hz, 2H), 3.63 (t, *J* = 4.7 Hz, 2H), 3.52 (t, *J* = 4.7 Hz, 2H), 3.39 (t, *J* = 6.7 Hz, 2H), 1.52-1.44 (m, 2H), 1.28 (sextet, *J* = 7.6 Hz, 2H), 0.86 (t, *J* = 7.4 Hz, 3H). **$^{13}$C-NMR** (126 MHz; $CDCl_3$): δ 168.4, 134.0, 132.2, 123.3, 71.3, 70.2, 68.0, 37.3, 31.8, 29.8, 19.3, 14.0. **HRMS** (ESI-TOF) Calc. for $[C_{16}H_{21}NO_4+Na^+]^+$ = 314.1363, Found = 314.1363. **Rf** (25% EtOAc in hexanes): 0.2.

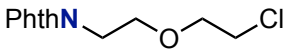


**1.2h** was synthesized via Procedure A in 49% yield as a colorless oil. Analytical data for **1.2h:** **$^{1}$H-NMR** (400 MHz; $CDCl_3$): δ 7.86-7.83 (m, 2H), 7.72-7.70 (m, 2H), 3.91 (t, *J* = 5.7 Hz, 2H), 3.77 (t, *J* = 5.7 Hz, 2H), 3.73 (t, *J* = 5.8 Hz, 2H), 3.56 (t, *J* = 5.8 Hz, 2H). **$^{13}$C-NMR** (126 MHz; $CDCl_3$): δ 168.4, 134.1, 132.2, 123.4, 70.7, 68.1, 42.9, 37.3. **HRMS** (ESI-TOF) Calc. for $[C_{12}H_{12}ClNO_3+Na^+]^+$ = 276.0398, Found = 276.0397. **Rf** (25% EtOAc in hexanes): 0.21.

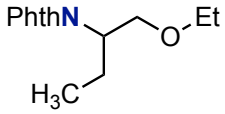


**1.2i** was synthesized via Procedure B using 0.25 equiv dilauroyl peroxide and 5 equiv olefin at 90 °C in 36% yield as a colorless oil. Analytical data for **1.2i**: **$^{1}$H-NMR** (400 MHz; $CDCl_3$): δ 7.84-7.82 (m, 2H), 7.73-7.69 (m, 2H), 4.38 (tdd, J = 9.9, 5.6, 4.4 Hz, 1H), 3.98 (dd, J = 12.4, 7.0 Hz, 1H), 3.64 (dd, J = 10.1, 5.4 Hz, 1H), 3.57- 3.49 (m, 1H), 3.42 (dq, J = 9.4, 7.0 Hz, 1H), 2.06-1.96 (m, 1H), 1.83-1.72 (m, 1H), 1.09 (t, J = 7.0 Hz, 3H), 0.91 (t, J = 7.5 Hz, 3H). **$^{13}$C-NMR** (126 MHz; $CDCl_3$): δ 168.9, 134.0, 132.0, 123.3, 70.0, 66.4, 53.0, 22.2, 15.2, 11.0. **LRMS** (APCI) Calc. for $[C_{14}H_{17}NO_3]^+$ = 247.12, Found = 247.98. **HRMS** (ESI-TOF) Calc. for $[C_{14}H_{17}NO_3+H^+]^+$ = 248.1281, Found = 248.1282. **Rf** (25% EtOAc in hexanes): 0.36.

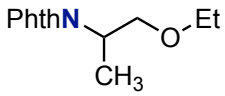


**1.2j** was synthesized via Procedure B using 0.25 equiv dilauroyl peroxide and 5 equiv olefin at 90 °C in 41% yield as a colorless oil. Analytical data for **1.2j: $^{1}$H-NMR** (400 MHz; $CDCl_3$): δ 7.84-7.81 (m, 2H), 7.71-7.69 (m, 2H), 4.59 (dddd, *J* = 9.0, 7.2, 5.6, 1.7 Hz, 1H), 3.97 (t, *J* = 9.6 Hz, 1H), 3.62-3.41 (m, 3H), 1.44 (d, *J* = 7.1 Hz, 3H), 1.10 (t, *J* = 7.0 Hz, 3H). **$^{13}$C-NMR** (126 MHz; $CDCl_3$): δ 168.7, 133.9, 132.2, 123.2, 70.0, 66.4, 46.6, 15.26, 15.22. **HRMS** (ESI-TOF) Calc for $[C_{13}H_{15}NO_3+H^+]^+$ = 234.1225, Found = 234.1226. **Rf** (25% EtOAc in hexanes): 0.33.

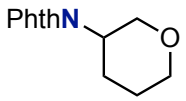


**1.2k** was synthesized via Procedure A in 46% yield as a colorless oil. Analytical data for **1.2k**: **$^{1}$H-NMR** (400 MHz; $CDCl_3$): δ 7.84-7.81 (m, 2H), 7.73-7.70 (m, 2H), 4.40-4.32 (m, 1H), 4.07-4.02 (m, 1H), 3.97-3.93 (m, 1H), 3.84-3.80 (m, 1H), 3.49-3.43 (m, 1H), 2.51-2.41 (m, 1H), 1.92-1.88 (m, 1H), 1.81-1.76 (m, 2H). **$^{13}$C-NMR** (126 MHz; $CDCl_3$): δ 168.3, 134.2, 131.9, 123.4, 68.1, 67.8, 47.9, 26.9, 26.2. **LRMS** (APCI) Calc. for $[C_{13}H_{13}NO_3+H^+]^+$ = 232.10, Found = 232.09. **HRMS** (ESI-TOF) Calc. for $[C_{13}H_{13}NO_3+H^+]^+$ = 232.0968, Found = 232.0968. **Rf** (25% EtOAc in hexanes): 0.26.

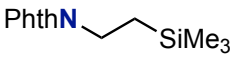


**1.2l** was synthesized via Procedure B in 56% yield as a colorless oil. Analytical data for **1.2l:** **$^{1}$H-NMR** (400 MHz; $CDCl_3$): δ 7.84-7.82 (m, 2H), 7.70-7.68 (m, 2H), 3.73-3.69 (m, 2H), 1.03-0.99 (m, 2H), 0.07 (s, 9H). **$^{13}$C-NMR** (126 MHz; $CDCl_3$): δ 168.4, 133.9, 132.4, 123.2, 34.6, 17.2, -1.6. **HRMS** (ESI-TOF) Calc. for $[C_{13}H_{17}NO_2Si\text{-}C_1H_3]^+$ = 232.0794, Found = 232.0792; under all MS conditions attempted, the major ion detected was a fragment via the loss of a methyl group from the trimethylsilane portion. **Rf** (25% EtOAc in hexanes): 0.47

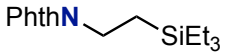


**1.2m** was synthesized via Procedure B in 42% yield as a colorless oil. Analytical data for **1.2m**: **$^{1}$H-NMR** (400 MHz; $CDCl_3$): δ 7.84-7.82 (m, 2H), 7.70-7.68 (m, 2H), 3.73-3.69 (m, 2H), 0.98 (t, J = 7.9 Hz, 11H), 0.59 (q, J = 7.9 Hz, 6H). **$^{13}$C-NMR** (126 MHz; $CDCl_3$): δ 168.4, 133.9, 132.5, 123.2, 34.6, 12.5, 7.5, 3.3. **LRMS** (APCI) Calc. for $[C_{16}H_{23}NO_2Si\text{-}C_2H_{15}]^+$ = 260.11, Found = 260.16; under all MS conditions attempted, the major ion detected was a fragment via the loss of an ethyl group from the triethylsilane portion. **HRMS** (ESI-TOF) Calc. for $[C_{16}H_{23}NO_2Si\text{-}C_2H_5]^+$ = 260.1107, Found = 260.1104; under all MS conditions attempted, the major ion detected was a fragment via the loss of an ethyl group from the triethylsilane portion. **Rf** (25% EtOAc in hexanes): 0.53.

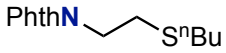


**1.2n** was synthesized via Procedure A using 5 equiv olefin at 35 °C in 43% yield as a yellow oil. Analytical data for **1.2n: $^{1}$H-NMR** (400 MHz; $CDCl_3$): δ 7.86-7.84 (m, 2H), 7.73-7.71 (m, 2H), 3.88 (t, *J* = 7.1 Hz, 2H), 2.81 (t, *J* = 7.1 Hz, 2H), 2.59 (t, *J* = 7.4 Hz, 2H), 1.59-1.53 (quintet, *J* = 7.2 Hz, 2H), 1.45-1.36 (sextet, *J* = 7.2 Hz, 2H), 0.91 (t, *J* = 7.3 Hz, 3H). **$^{13}$C-NMR** (126 MHz; $CDCl_3$): δ 168.3, 134.1, 132.1, 123.5, 37.2, 31.62, 31.48, 30.1, 22.1, 13.8. **LRMS** (APCI) Calc. for $[C_{14}H_{17}NO_2S]^+$ = 263.10, Found = 263.98. **HRMS** (ESI-TOF) Calc. for $[C_{14}H_{17}NO_2S+H^+]^+$ = 264.1053, Found = 264.1055. **Rf** (25% EtOAc in hexanes): 0.39.

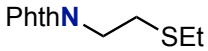


**1.2o** was synthesized via Procedure A in 42% yield as a yellow oil. Analytical data for **1.2o**: **$^1$H-NMR** (400 MHz; $CDCl_3$): δ 7.86-7.84 (m, 2H), 7.74-7.71 (m, 2H), 3.89 (t, J = 7.1 Hz, 2H), 2.83 (t, J = 7.1 Hz, 2H), 2.62 (q, J = 7.4 Hz, 2H), 1.27 (t, J = 7.4 Hz, 3H). **$^{13}$C-NMR** (126 MHz; $CDCl_3$): δ 168.3, 134.2, 132.1 123.51, 37.2, 29.6, 25.6, 14.7. **LRMS** (APCI) Calc. for $[C_{12}H_{13}NO_2S+H^+]^+$ = 236.07, Found = 236.00. **HRMS** (ESI-TOF) Calc. for $[C_{12}H_{13}NO_2S+H^+]^+$ = 236.0740, Found = 236.0740. **Rf** (25% EtOAc in hexanes): 0.34.

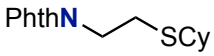


**1.2p** was synthesized via Procedure A using 5 equiv olefin at 35 °C in 42% yield as a yellow oil. Analytical data for **1.2p: $^1$H-NMR** (400 MHz; $CDCl_3$): δ 7.87-7.84 (m, 2H), 7.74-7.71 (m, 2H), 3.87 (t, *J* = 7.3 Hz, 2H), 2.83 (t, *J* = 7.3 Hz, 2H), 2.80-2.70 (m, 1H), 2.00-1.96 (m, 2H), 1.78-1.75 (m, 2H), 1.68-1.59 (m, 2H), 1.34-1.26 (m, 4H). **$^{13}$C-NMR** (126 MHz; $CDCl_3$): δ 168.3, 134.1, 132.1, 123.4, 43.2, 37.9, 33.6, 28.1, 26.2, 25.9**.** **LRMS** (APCI) Calc. for $[C_{16}H_{19}NO_2S]^+$ = 289.11, Found = 289.95. **HRMS** (ESI-TOF) Calc. for $[C_{16}H_{19}NO_2S+H^+]^+$ = 290.1209, Found = 290.1208. **Rf** (25% EtOAc in hexanes): 0.39.

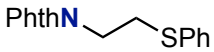


**1.2q** was synthesized via Procedure A in 20% yield as a yellow oil. Analytical data for **1.2q: $^1$H-NMR** (400 MHz; $CDCl_3$): δ 7.81-7.81 (m, 2H), 7.72-7.71 (m, 2H), 7.42 (d, *J* = 7.6 Hz, 2H), 7.23 (m, 2H), 7.14-7.10 (m, 1H), 3.94 (t, *J* = 6.9 Hz, 2H), 3.24 (t, *J* = 7.0 Hz, 2H). **$^{13}$C-NMR** (126 MHz; $CDCl_3$): δ 168.2, 134.9, 134.1, 132.1, 129.8, 129.1, 126.5, 123.4, 37.7, 31.8 . **HRMS** (ESI-TOF) Calc. for $[C_{16}H_{13}NO_2S+H^+]^+$ = 284.0740, Found = 284.0741. **Rf** (25% EtOAc in hexanes): 0.32.

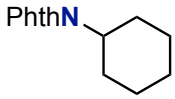


**1.2r** was synthesized via Procedure B in 68% yield as a white crystalline sold. Analytical data for **1.2r:** **$^{1}$H-NMR** (400 MHz; $CDCl_3$): δ 7.82-7.80 (m, 2H), 7.70-7.68 (m, 2H), 4.15-4.07 (m, 1H), 2.21 (q, *J* = 12.4 Hz, 2H), 1.87 (d, *J* = 13.0 Hz, 2H), 1.71 (t, *J* = 12.9 Hz, 2H), 1.42-1.25 (m, 4H). **$^{13}$C-NMR** (126 MHz; $CDCl_3$): δ 168.6, 133.9, 132.2, 123.1, 51.0, 30.0, 26.2, 25.2 **HRMS** (ESI-TOF) Calc. for $[C_{14}H_{15}NO_2+H^+]^+$ = 230.1176, Found = 230.1174. **Rf** (25% EtOAc in hexanes): 0.45.


**1.2s** was synthesized via Procedure B in 81% yield as a white crystalline solid and as a 79:21 *exo*:*endo* mixture of diastereomers as determined by gas chromatography. Diastereomers were identified by comparing chemicals shifts and coupling constants to those presented in the literature following deprotection of the phthalimide. Analytical data for **1.2s:** **$^{1}$H-NMR** (400 MHz; $CDCl_3$): δ 7.81-7.78 (m, 2H), 7.70-7.67 (m, 2H), 4.47-4.43 (m, 1H)*, 4.14 (dd, J = 8.7, 5.6 Hz, 1H), 2.56-2.52 (m, 1H), 2.42 (d, J = 13.0 Hz, 1H), 2.27-2.24 (m, 2H), 1.80-1.69 (m, 2H), 1.62-1.53 (m, 2H), 1.27-1.19 (m, 2H). **$^{13}$C-NMR** (126 MHz; $CDCl_3$): δ 169.9*, 169.1, 133.93*, 133.91, 132.1, 123.07, 123.03*, 55.5, 42.6*, 42.3, 38.1*, 37.6*, 37.3, 36.5, 36.2, 29.10, 29.08*, 28.2, 23.6*. (* indicates minor diastereomer). **LRMS** (APCI) Calc. for $[C_{15}H_{15}NO_2+H^+]^+$ = 242.12, Found = 242.09. **HRMS** (ESI-TOF) Calc. for $[C_{15}H_{15}NO_2+H^+]^+$ = 242.1176, Found = 242.1174 **Rf** (25% EtOAc in hexanes): 0.46.

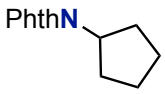


**1.2t** was synthesized via Procedure B in 76% yield as a white crystalline solid. Analytical data for **1.2t**: **$^{1}$H-NMR** (400 MHz; $CDCl_3$): δ 7.81-7.79 (m, 2H), 7.69-7.67 (m, 2H), 4.62 (quintet, *J* = 8.4 Hz, 1H), 2.12-2.06 (m, 2H), 1.98-1.89 (m, 4H), 1.67-1.61 (m, 2H). **$^{13}$C-NMR** (126 MHz; $CDCl_3$): δ 168.6, 133.9, 132.2, 123.1, 51.1, 29.7, 25.2. **HRMS** (ESI-TOF) Calc. for $[C_{13}H_{13}NO_2+H^+]^+$ = 216.1019, Found = 216.1020. **Rf** (25% EtOAc in hexanes): 0.45.

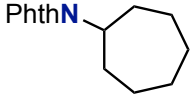


**1.2u** was synthesized via Procedure B in 64% yield as a white crystalline solid. Analytical data for **1.2u: $^{1}$H-NMR** (400 MHz; $CDCl_3$): δ 7.81-7.79 (m, 2H), 7.69-7.66 (m, 2H), 4.26 (tt, *J* = 10.9, 3.8 Hz, 1H), 2.26 (qd, *J* = 10.7, 5.9 Hz, 2H), 1.82-1.79 (m, 2H), 1.64-1.50 (m, 8H). **$^{13}$C-NMR** (126 MHz; $CDCl_3$): δ 168.4, 133.9, 132.2, 123.1, 52.9, 32.8, 27.7, 25.6 **HRMS** (ESI-TOF) Calc. for $[C_{15}H_{17}NO_2+H^+]^+$ = 244.1332, Found = 244.1332. **Rf** (25% EtOAc in hexanes): 0.47.

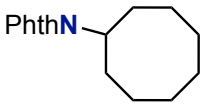


**1.2v:** was synthesized via Procedure B in 70% yield as a white crystalline solid. Analytical data for **1.2v**: **$^{1}$H-NMR** (400 MHz; $CDCl_3$): δ 7.82-7.79 (m, 2H), 7.69-7.67 (m, 2H), 4.40-4.33 (m, 1H), 2.36-2.27 (m, 2H), 1.83-1.69 (m, 6H), 1.63-1.55 (m, 6H). **$^{13}$C-NMR** (126 MHz; $CDCl_3$): δ 168.4, 133.9, 132.2, 123.1, 51.7, 31.8, 26.5, 26.0, 25.3. **LRMS** (APCI) Calc. for $[C_{16}H_{19}NO_2+H^+]^+$ = 258.15, Found = 258.07. **HRMS** (ESI-TOF) Calc. for $[C_{16}H_{19}NO_2+H^+]^+$ = 258.1489, Found = 258.1488. **Rf** (25% EtOAc in hexanes): 0.49.

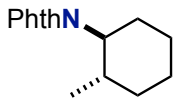


**1.2w** was synthesized via Procedure B in 47% yield as a white crystalline solid and as a 80:20 *trans*:*cis* mixture of diastereomers as determined by gas chromatography. Diastereomers were identified by comparing chemicals shifts and coupling constants to those presented in the literature. Analytical data for **1.2w**: **$^{1}$H -NMR** (500 MHz; $CDCl_3$): δ 7.82-7.81 (m, 2H), 7.70-7.69 (m, 2H), 4.27 (dt, *J* = 12.9, 4.1 Hz, 1H)*, 3.75 (td, *J* = 11.7, 3.6 Hz, 1H), 2.80 (dd, *J* = 13.0, 3.8 Hz, 1H)*, 2.34 (dd, *J* = 6.7, 4.0 Hz, 1H), 2.18 (ddd, *J* = 14.6, 10.4, 4.0 Hz, 2H), 1.90 (ddq, *J* = 12.5, 5.9, 2.9 Hz, 2H)*, 1.86-1.01 (m, 6H), 1.01 (d, *J* = 7.2 Hz, 3H)*, 0.79 (d, *J* = 6.6 Hz, 3H). **$^{13}$C-NMR** (126 MHz; $CDCl_3$): δ 169.2*, 168.7, 133.80, 133.76*, 131.91, 131.86*, 123.07, 122.98*, 57.1*, 55.5, 34.9, 33.9*, 33.5*, 32.2, 30.0, 26.7*, 26.1, 25.7*, 23.8, 19.8*, 19.0, 13.6*. (*indicates minor diastereomer) **HRMS** (ESI-TOF) Calc. for $[C_{15}H_{17}NO_2+H^+]^+$ = 244.1332, Found = 244.1334. **Rf** (25% EtOAc in hexanes): 0.46.

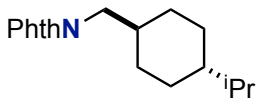


**1.2x** was synthesized via Procedure B in quantitative yield as a white crystalline solid and as a 83:17 *trans*:*cis* mixture of diastereomers as determined by gas chromatography. Diastereomers were identified by comparison to analogous compounds in the literature, specifically by taking into account the relative chemical shifts of the methylenes alpha to the heteroatom for both isomers. Analytical data for **1.2x:** **$^{1}$H -NMR** (400 MHz; $CDCl_3$): δ 7.84-7.82 (m, 2H), 7.72-7.68 (m, 2H) 3.64 (d, *J* = 7.8 Hz, 2H)*, 3.51 (d, *J* = 6.9 Hz, 2H), 1.73-1.67 (m, 5H), 1.48-1.42 (m, 2H), 0.99-0.93 (m, 4H), 0.87 (d, *J* = 6.7 Hz, 6H)*, 0.81 (d, *J* = 6.8 Hz, 6H). **$^{13}$C-NMR** (126 MHz; $CDCl_3$): δ 168.8, 168.8*, 134.0, 134.0*, 132.2, 132.2*, 123.3, 123.3*, 44.2, 44.2*, 43.9, 43.9*, 37.4, 37.4*, 32.9, 32.9*, 31.0, 29.1, 27.2*, 25.5*, 20.5*, 19.9. (* indicates minor diastereomer) **LRMS** (APCI) Calc. for $[C_{18}H_{23}NO_2+H^+]^+$ = 286.18, Found = 286.21. **HRMS** (ESI-TOF) Calc. for $[C_{18}H_{23}NO_2+H^+]^+$ = 286.1802, Found = 286.1799 **Rf** (25% EtOAc in hexanes): 0.43.

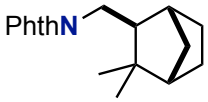


**1.2y** was synthesized via Procedure B in 58% yield as a single diastereomer and as a colorless oil. Analytical data for **1.2y**: **$^{1}$H-NMR** (400 MHz; $CDCl_3$): δ 7.83-7.80 (m, 2H), 7.70-7.68 (m, 2H), 3.78 (dd, J = 13.6, 11.7 Hz, 1H), 3.57 (dd, J = 13.6, 4.4 Hz, 1H), 1.94 (s, 1H), 1.89 (dd, J = 8.5, 3.0 Hz, 1H), 1.94 (s, 2H), 1.91-1.87 (m, 1H), 1.78-1.74 (m, 1H), 1.66-1.61 (m, 2H), 1.55-1.53 (m, 1H), 1.32-1.26 (s, 3H), 1.17-1.15 (s, 3H). **$^{13}$C-NMR** (126 MHz; $CDCl_3$): δ 168.6, 133.9, 132.3, 123.2, 49.19, 49.16, 40.2, 37.04, 36.92, 36.1, 32.2, 24.8, 21.4, 20.3. **LRMS** (APCI) Calc. for $[C_{18}H_{21}NO_2+H^+]^+$ = 284.16, Found = 284.15. S21 **HRMS** (ESI-TOF) Calc. for $[C_{18}H_{21}NO_2+Na^+ + MeOH]^+$ = 338.1727, Found = 338.1729. **Rf** (25% EtOAc in hexanes): 0.43.

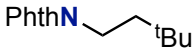


**1.2z** was synthesized via Procedure B in 71% yield as a white crystalline solid. Analytical data for **1.2z:** **$^{1}$H-NMR** (400 MHz; $CDCl_3$): δ 7.84-7.82 (m, 2H), 7.71-7.69 (m, 2H), 3.71-3.67 (m, 2H), 1.58-1.54 (m, 2H) 0.99 (s, 9H). **$^{13}$C-NMR** (126 MHz; $CDCl_3$): δ 168.5, 133.9, 132.4, 123.2, 41.9, 34.9, 30.1, 29.3 **HRMS** (ESI-TOF) Calc. for $[C_{14}H_{17}NO_2+Na^+ + MeOH]^+$ = 286.1414, Found = 286.1409. **Rf** (25% EtOAc in hexanes): 0.43.

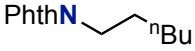


**1.2aa** was synthesized via Procedure B in 46% yield as a colorless oil. Analytical data for **1.2aa:** **$^{1}$H-NMR** (400 MHz; $CDCl_3$): δ 7.84-7.82 (m, 2H), 7.70-7.68 (m, 2H), 3.66 (t, $J$ = 7.4 Hz, 2H), 1.67-1.63 (m, 2H), 1.34-1.26 (m, 6H), 0.86 (t, $J$ = 7.1 Hz, 3H). **$^{13}$C-NMR** (126 MHz; $CDCl_3$): δ 168.6, 134.0, 132.3, 123.3, 38.2, 31.5, 28.7, 26.7, 22.7, 14.2. **HRMS** (ESI-TOF) Calc. for $[C_{14}H_{17}NO_2+Na^+ + MeOH]^+$ = 286.1414, Found = 286.1408. **Rf** (25% EtOAc in hexanes): 0.43.

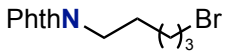


**1.2ab** was synthesized via Procedure B in 55% yield as a colorless oil. Analytical data for **1.2ab:** **$^{1}$H-NMR** (400 MHz; $CDCl_3$): δ 7.85-7.83 (m, 2H), 7.73-7.70 (m, 2H), 3.69 (t, $J$ = 7.2 Hz, 2H), 3.39 (t, $J$ = 6.7 Hz, 2H), 1.90 (quintet, $J$ = 7.6 Hz, 2H), 1.71 (quintet, $J$ = 7.5 Hz, 2H), 1.53-1.47 (m, 2H). **$^{13}$C-NMR** (126 MHz; $CDCl_3$): δ 168.6, 134.1, 132.2, 123.4, 37.8, 33.6, 32.3, 27.9, 25.5. **HRMS** (ESI-TOF) Calc. for $[C_{13}H_{14}NO_2+Na^+ + MeOH]^+$ = 350.0362, Found = 350.0365. **Rf** (25% EtOAc in hexanes): 0.3.

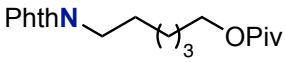


**1.2ac** was synthesized via Procedure B in 54% yield as a colorless oil. Analytical data for **1.2ac**: **$^{1}$H-NMR** (400 MHz; $CDCl_3$): δ 7.84-7.82 (m, 2H), 7.71-7.69 (m, 2H), 4.02 (t, *J* = 6.5 Hz, 2H), 3.67 (t, *J* = 7.3 Hz, 2H), 1.71-1.66 (m, 2H), 1.64-1.58 (m, 2H), 1.39-1.37 (m, 4H), 1.17 (s, 9H). **$^{13}$C-NMR** (126 MHz; $CDCl_3$): δ 178.7, 168.6, 134.0, 132.2, 123.3, 64.4, 38.8, 38.0, 28.66, 28.64, 27.3, 26.6, 25.7. **LRMS** (APCI) Calc. for $[C_{19}H_{25}NO_4+H^+]^+$ = 332.19, Found = 332.16. **HRMS** (ESI-TOF) Calc. for $[C_{19}H_{25}NO_4+Na^+]^+$ = 354.1676, Found = 354.1679. **Rf** (25% EtOAc in hexanes): 0.35.

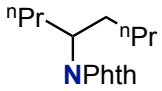


**1.2ad** was synthesized via Procedure B in 57% yield as a colorless oil. Analytical data for **1.2ad**: **$^{1}$H-NMR** (400 MHz; $CDCl_3$): δ 7.82-7.80 (m, 2H), 7.71-7.68 (m, 2H), 4.24-4.16 (m, 1H), 2.12-2.01 (m, 2H), 1.74-1.60 (m, 2H), 1.30-1.22 (m, 6H), 0.91-0.81 (m, *J* = 2.9 Hz, 6H). **$^{13}$C-NMR** (126 MHz; $CDCl_3$): δ 168.6, 133.9, 132.3, 123.2, 49.19, 40.2, 37.04, 36.1, 32.2, 24.8, 21.4, 20.3. **LRMS** (APCI) Calc. for $[C_{16}H_{21}NO_2+H^+]^+$ = 260.16, Found = 260.07. **HRMS** (ESI-TOF) Calc. for $[C_{16}H_{21}NO_2+Na^+$+MeOH$]^+$ = 314.1727, Found = 314.1731. **Rf** (25% EtOAc in hexanes): 0.49.

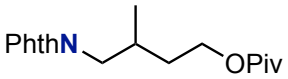


**1.2ae** was synthesized via Procedure B in 64% yield as a colorless oil. Analytical data for **1.2ae**: **$^{1}$H**-NMR (400 MHz; $CDCl_3$): δ 7.85-7.83 (m, 2H), 7.74-7.70 (m, 2H), 4.18-4.06 (m, 2H), 3.63-3.51 (m, 2H), 2.18-2.10 (m, 1H), 1.79-1.71 (m, 2H), 1.17 (s, 9H), 0.96 (d, J = 6.8 Hz, 3H). **$^{13}$C-NMR** (126 MHz; $CDCl_3$): δ 178.7, 168.7, 134.1, 132.1, 123.4, 62.3, 44.0, 38.8, 33.1, 30.0, 27.3, 17.4. **LRMS** (APCI) Calc. for $[C_{18}H_{23}NO_4+H^+]^+$ = 318.17, Found = 318.07. **HRMS** (ESI-TOF) Calc. for $[C_{18}H_{23}NO_4+Na^+]^+$ = 340.1519, Found = 340.1523. **Rf** (25% EtOAc in hexanes): 0.32.

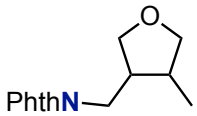


**1.2af** was synthesized via Procedure B using 0.25 equiv dilauroyl peroxide at 90 °C in 23% yield as a colorless oil and as a 59:41 *cis*:*trans* mixture of diastereomers as determined by gas chromatography. Diastereomers were identified by 2D-NMR and by comparison to the literature. Analytical data for **1.2af: $^{1}$H-NMR** (400 MHz; $CDCl_3$): δ 7.88-7.84 (m, 2H), 7.77-7.71 (m, 2H), 4.04 (t, *J* = 7.9 Hz, 1H)*, 3.94 (q, *J* = 7.8 Hz, 1H), 3.94 (q, *J* = 7.8 Hz, 1H)*, 3.86-3.61 (m, 2H), 3.86-3.61 (m, 3H)*, 3.54 (dd, *J* = 8.4, 5.0 Hz, 1H), 3.35-3.31 (m, 1H)*, 2.76-2.66 (m, 1H), 2.46-2.39 (m, 1H), 2.25 (q, *J* = 6.9 Hz, 1H)*, 2.10-2.03 (m, 1H)*, 1.15-1.10 (d, *J* = 7.2 Hz, 3H), 1.07- 1.04 (d, *J* = 6.8 Hz, 3H)*. **$^{13}$C-NMR** (126 MHz; $CDCl_3$): δ 168.66*, 168.54, 134.5, 134.2*, 132.06, 132.00*, 123.7, 123.5*, 75.13*, 75.11, 71.6*, 70.7, 46.6*, 41.7, 39.8, 37.7*, 37.0, 35.5*, 17.2*, 13.1. (* indicates minor diastereomer) **LRMS** (APCI) Calc. for $[C_{14}H_{15}NO_3]^+$ = 245.11, Found = 245.12. **HRMS** (ESI-TOF) Calc. for $[C_{14}H_{15}NO_3+H^+]^+$ = 246.1125, Found = 246. 1124 **Rf** (25% EtOAc in hexanes): 0.16.

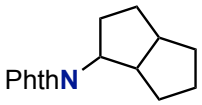


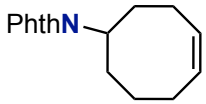


**1.2ag** and **1.2ah** were synthesized via Procedure B using 1,5-*cis*-*cis*-cyclooctadiene in 21% and 14% yield respectively, each as a white crystalline solid. Analytical data for **1.2ag**: **$^{1}$H-NMR** (400 MHz; $CDCl_3$): δ 7.82-7.80 (m, 2H), 7.71-7.68 (m, 2H), 4.13 (ddd, *J* = 11.3, 8.4, 6.4 Hz, 1H), 2.99-2.92 (m, 1H), 2.78-2.68 (m, 1H), 2.32 (qd, *J* = 11.9, 6.9 Hz, 1H), 2.07 (dddd, *J* = 12.9, 8.3, 6.9, 1.6 Hz, 1H), 1.81-1.75 (m, 1H), 1.63-1.54 (m, 3H), 1.53- 1.46 (m, 2H), 1.41 (td, *J* = 6.1, 3.1 Hz, 1H), 1.19 (tdd, *J* = 12.6, 8.9, 6.3 Hz, 1H). **$^{13}$C-NMR** (126 MHz; $CDCl_3$): δ 168.9, 133.9, 132.2, 123.1, 58.4, 45.8, 42.5, 33.4, 31.9, 31.6, 30.8, 24. **HRMS** (ESI-TOF) Calc. for $[C_{16}H_{17}NO_2+H^+]^+$ = 256.1332, Found = 256.1333. **Rf** (25% EtOAc in hexanes): 0.49. Analytical data **1.2ah: $^{1}$H-NMR** (400 MHz; $CDCl_3$): δ 7.81-7.79 (m, 2H), 7.69-7.67 (m, 2H), 5.81-5.67 (m, 2H), 4.34-4.28 (m, 1H), 2.49-2.14 (m, 7H), 1.87-1.81 (m, 1H), 1.73-1.63 (m, 1H), 1.54-1.47 (m, 1H). **$^{13}$C-NMR** (126 MHz; $CDCl_3$): δ 168.3, 133.9, 132.3, 130.8, 129.2, 123.1, 50.9, 33.9, 32.3, 27.1, 25.9, 23.7. **HRMS** (ESI-TOF) Calc. for $[C_{16}H_{17}NO_2+H^+]^+$ = 256.1332, Found = 256.1331. **Rf** (25% EtOAc in hexanes): 0.44.

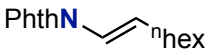


**1.2ai** was synthesized via Procedure B using 1-octyne in 27% yield as a yellow oil. Analytical data for **1.2ai: $^{1}$H-NMR** (400 MHz; $CDCl_3$): δ 7.86-7.84 (m, 2H), 7.73-7.71 (m, 2H), 6.63-6.58 (m, 2H), 2.19-2.14 (m, 2H), 1.50-1.43 (m, 2H), 1.36-1.27 (m, 6H), 0.89 (t, *J* = 6.7 Hz, 3H). **$^{13}$C-NMR** (126 MHz; $CDCl_3$): δ 166.9, 134.4, 131.8, 123.6, 123.2, 117.6, 31.8, 31.3, 29.5, 29.0, 22.8, 14.3. **HRMS** (ESI-TOF) Calc. for $[C_{16}H_{20}NO_2]^+$ = 258.1489, Found = 258.1488. **Rf** (25% EtOAc in hexanes): 0.53.

### 1.6.5 Phthalimidyl Deprotection Procedures

Phthalimidyl-2-butoxyehthylamine deprotection procedure: To a 50 mL roundbottom flask charged with a magnetic stir bar was added phthalimidyl- 2-butoxyethylamine (200 mg, 0.81 mmol), 35 wt% hydrazine aqueous solution (0.36 mL, 5.0 equiv), and methanol (20 mL). The reaction mixture was equipped with a reflux condenser and heated at 60 °C for 30 minutes. Upon complete consumption of phthalimidyl-2-butoxyethylamine as judged by TLC (25% EtOAc in hexanes), the reaction mixture was cooled to ambient temperature and made alkaline (pH 14) using 50 wt% KOH aqueous solution. The reaction mixture was then extracted with DCM (3x 100 mL), and the combined organic layers were washed with brine, dried over $Na_2SO_4$, and concentrated under reduced pressure to yield 2-butoxyethylamine in 89% yield as a pale yellow liquid. Physical and spectral data below (**1.3a**).

Phthalimidyl-aminonorbornane deprotection procedure: To a 50 mL roundbottom flask charged with a magnetic stir bar was added a 80:20 *exo*:*endo* mixture of phthalimidyl-aminonorbornane (500 mg, 2.07 mmol), 35 wt% hydrazine aqueous solution (0.93 mL, 5.0 equiv), and methanol (20 mL). The reaction mixture was equipped with a reflux condenser and heated at 60 °C for 30 minutes. Upon complete consumption of phthalimidyl-aminonorbornane as judged by TLC (25% EtOAc in hexanes), the reaction mixture was cooled to ambient temperature and acidified to a pH of 0 with concentrated HCl. The reaction was then heated to 60 °C and stirred for one additional hour, after which the mixture was allowed to cool to ambient temperature and was made alkaline (pH 14) using 50 wt% KOH aqueous solution. The reaction mixture was then extracted with DCM (3x 100 mL), and the combined organic layers were washed with brine, dried over $Na_2SO_4$, and concentrated under reduced pressure to yield a 80:20 *exo*:*endo* mixture of aminonorbornane in 95% yield as a pale yellow liquid. Diastereomer identification was determined

by comparing chemicals shifts and coupling constants to those presented in the literature. Physical and spectral data was in accordance with literature data (data below, **1.3b**)

### 1.6.6 Characterization of Products (1.3a and 1.3b)

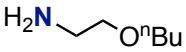

**1.3a** was synthesized via the procedure presented in section **1.6.5** in 89% yield as a pale yellow liquid. Analytical data for **1.3a**: **$^{1}$H-NMR** (300 MHz; $CDCl_3$): δ 3.46-3.41 (m, 4H), 2.87-2.85 (m, 2H), 1.70 (s, 3H), 1.56 (quintet, $J$ = 6.9 Hz, 2H), 1.37 (sextet, $J$ = 7.2 Hz, 2H), 0.91 (t, $J$ = 7.3 Hz, 3H). **$^{13}$C-NMR** (126 MHz; $CDCl_3$): δ 72.9, 71.1, 42.0, 31.9, 19.5, 14.1. **HRMS** (ESI-TOF) Calc. for $[C_6H_{15}NO+H^+]^+$ = 118.1226, Found = 118.1227. **Rf** (25% EtOAc in hexanes): 0.02.

**1.3b** was synthesized via the procedure presented in section **1.6.5** in 95% yield as a pale yellow oil. Analytical data for **1.3b**: **$^{1}$H-NMR** (400 MHz; $CDCl_3$): δ 3.26-3.23 (m, 1H)*, 2.79 (dd, $J$ = 7.4, 3.0 Hz, 1H), 2.19 (s, 1H), 2.13 (s, 1H), 2.08-2.02 (m, 1H)*, 1.91 (s, 1H)*, 1.65-0.55 (m, 10H). **$^{13}$C-NMR** (126 MHz; $CDCl_3$): δ 55.08, 55.00*, 53.1, 45.5, 42.3*, 40.4, 38.8*, 36.09, 36.04*, 34.3, 30.3*, 28.3, 26.8*, 20.4*(* indicates minor diastereomer). **HRMS** (ESI-TOF) Calc. for $[C_7H_{13}N+H^+]^+$= 112.1121, Found = 112.1121 **Rf** (25% EtOAc in hexanes): 0.02.

### 1.6.7 $^{1}$H, $^{13}$C, and 2-D NMR Spectra

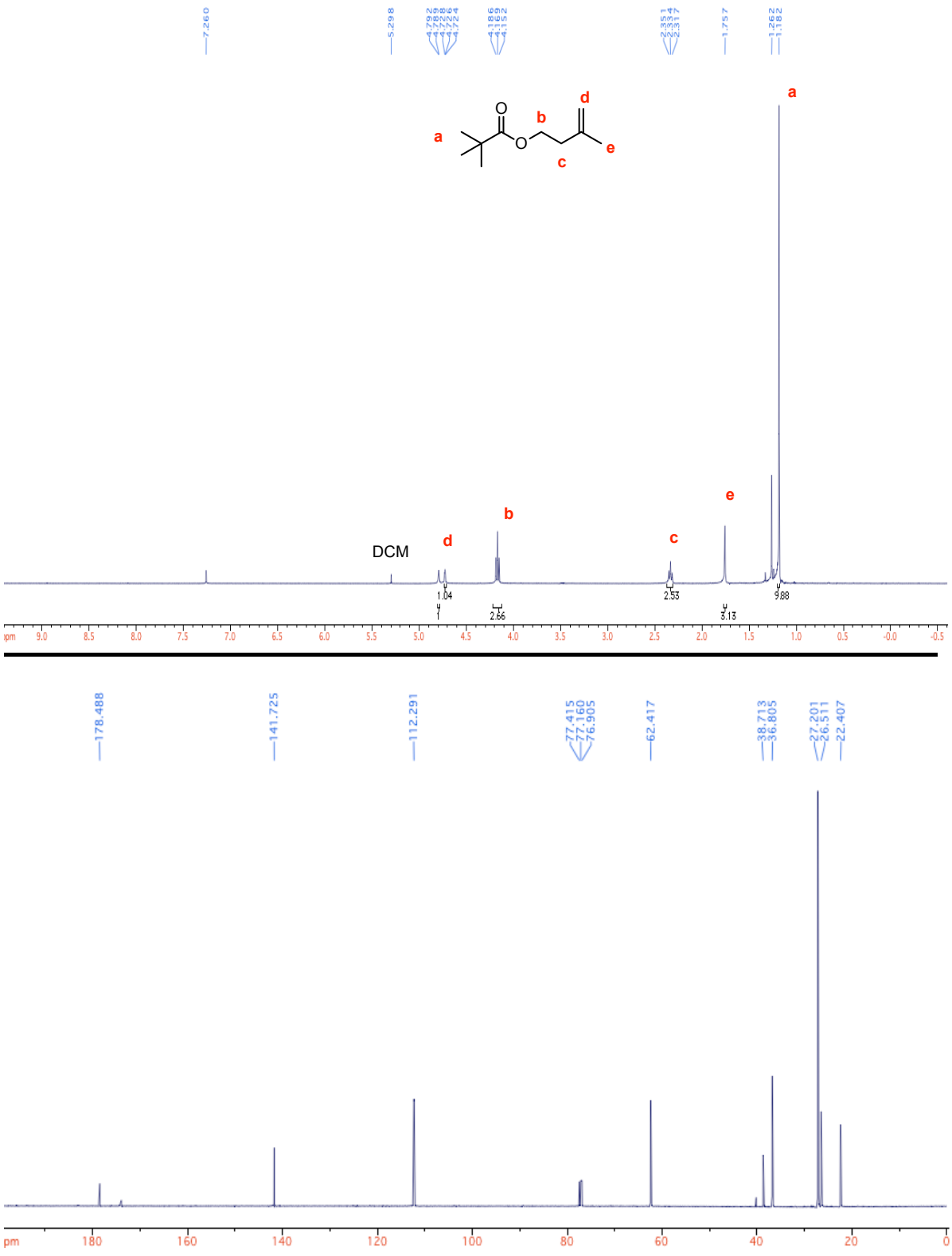
7.260
5.298
4.792
4.788
4.728
4.726
4.724
4.186
4.169
4.152
2.351
2.334
2.317
1.757
1.262
1.182
a
b
c
d
e
DCM
1.04
2.66
2.53
3.13
9.88
178.488
141.725
112.291
77.415
77.160
76.905
62.417
38.713
36.805
27.201
26.511
22.407

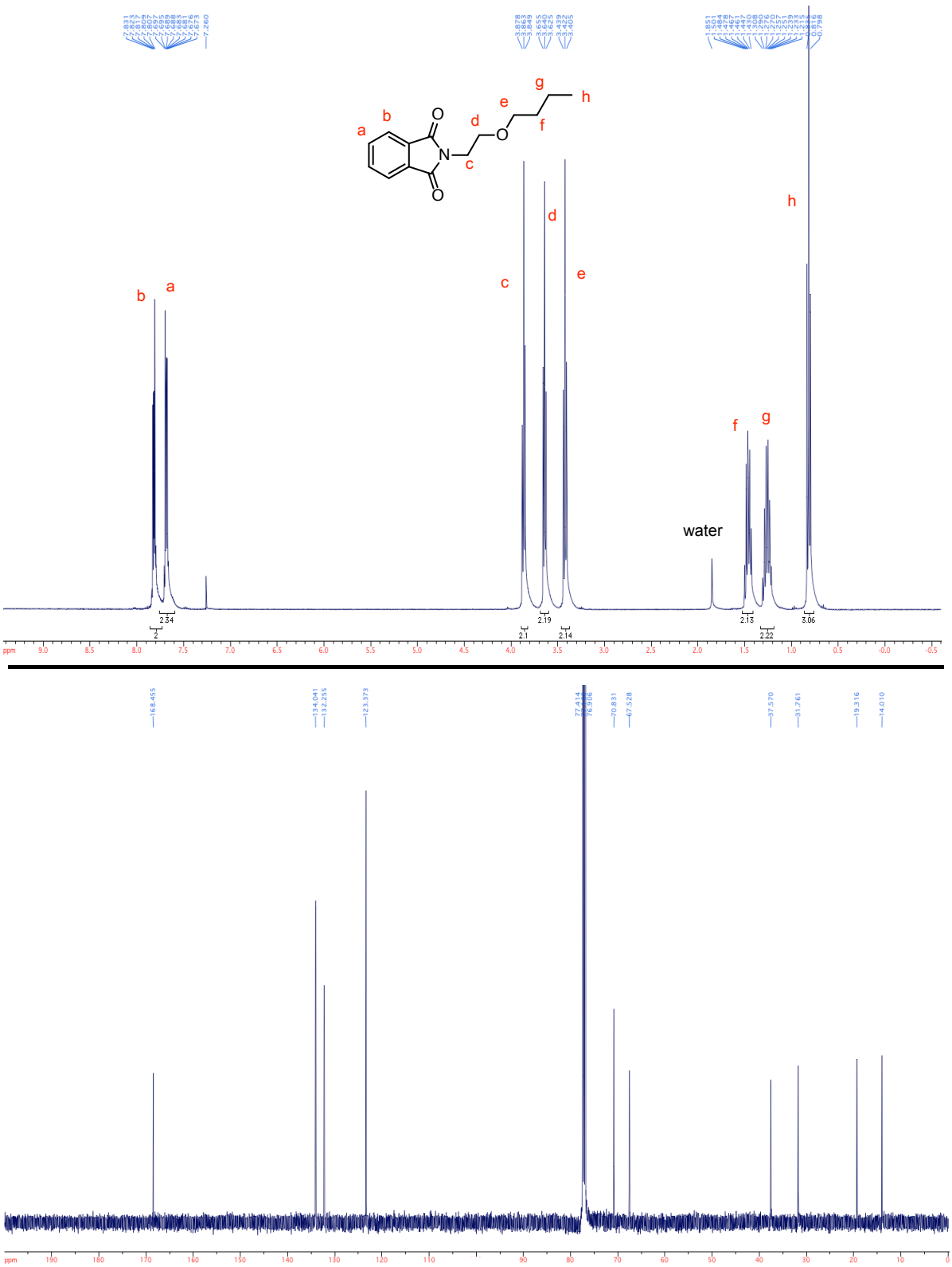
a
b
c
d
e
f
g
h
water

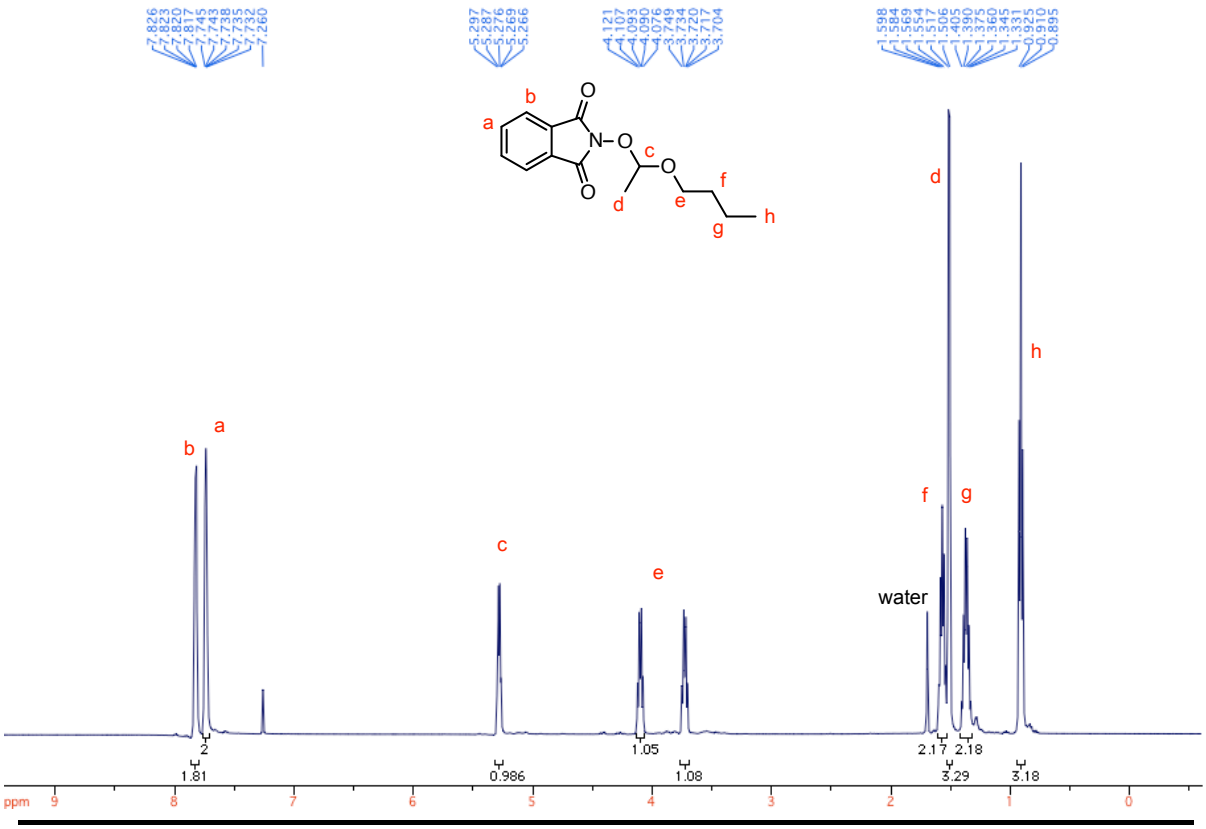
7.826
7.823
7.820
7.817
7.745
7.743
7.738
7.735
7.732
7.260
5.297
5.287
5.276
5.269
5.266
4.121
4.107
4.093
4.090
4.076
4.049
3.734
3.720
3.717
3.704
1.598
1.584
1.569
1.554
1.517
1.506
1.405
1.390
1.375
1.360
1.345
1.331
0.925
0.910
0.895
a
b
c
d
e
f
g
h
water
2
1.81
0.986
1.05
1.08
2.17
2.18
3.29
3.18
ppm

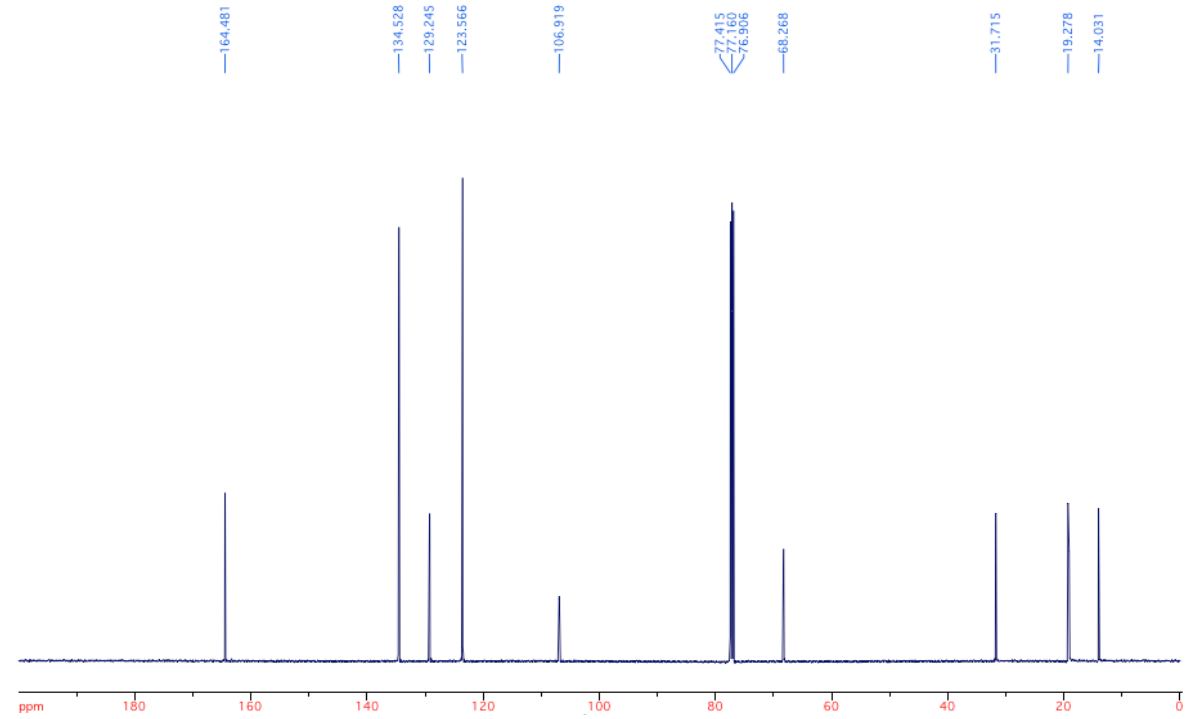
164.481
134.528
129.245
123.566
106.919
77.415
77.160
76.906
68.268
31.715
19.278
14.031
ppm

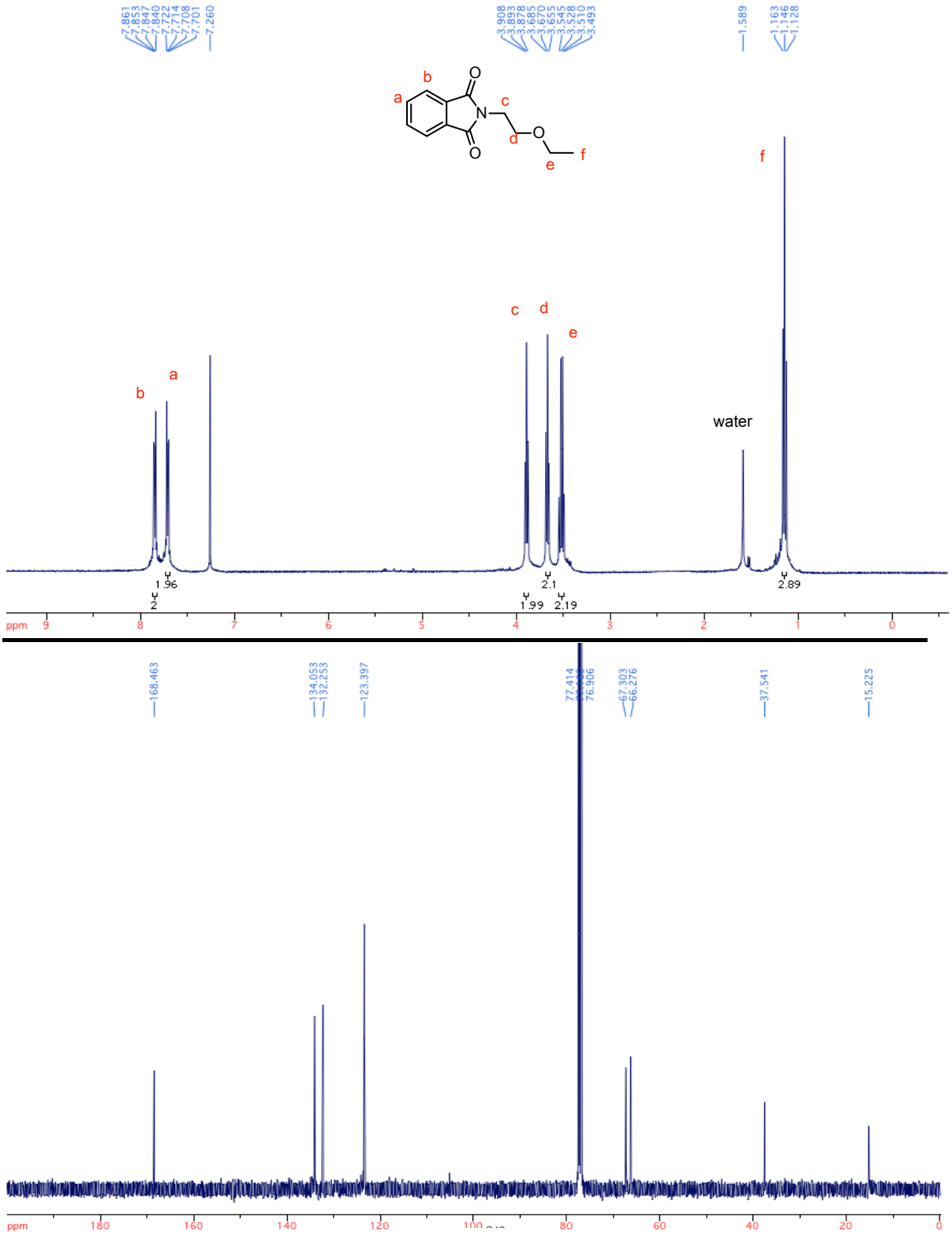
7.861
7.853
7.847
7.840
7.722
7.714
7.708
7.701
7.260
3.908
3.893
3.878
3.695
3.670
3.655
3.545
3.528
3.510
3.493
1.589
1.163
1.146
1.128
a
b
c
d
e
f
water
1.96
2
2.1
1.99
2.19
2.89
ppm
168.463
134.053
132.253
123.397
77.414
77.088
76.906
67.303
66.276
37.541
15.225

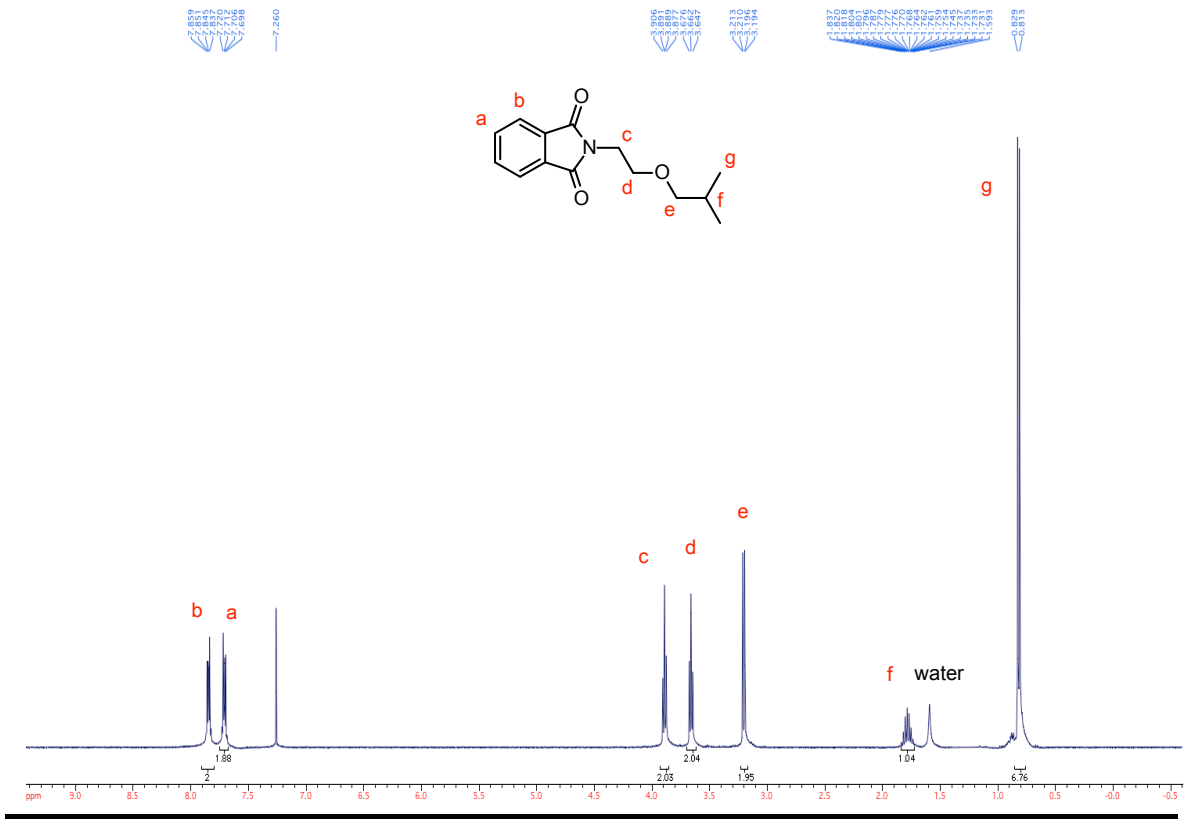
a
b
c
d
e
f
g
water
1.88
2
2.03
2.04
1.95
1.04
6.76
ppm

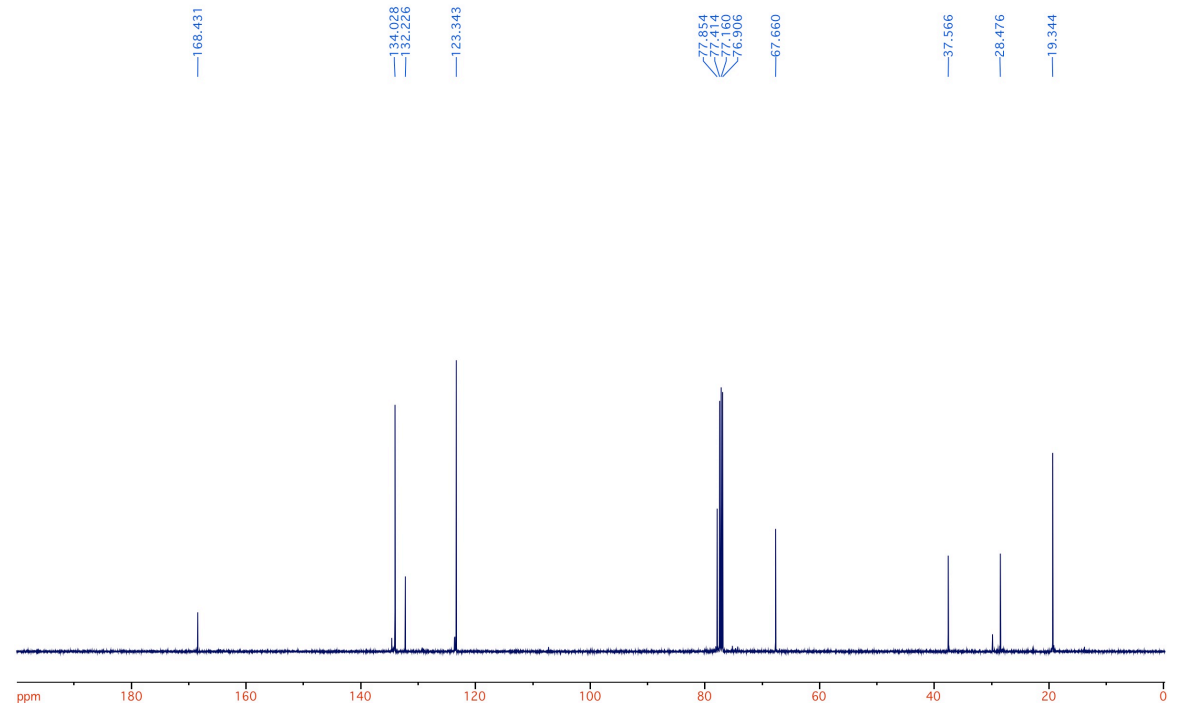
168.431
134.028
132.226
123.343
77.854
77.434
77.160
76.906
67.660
37.566
28.476
19.344
ppm

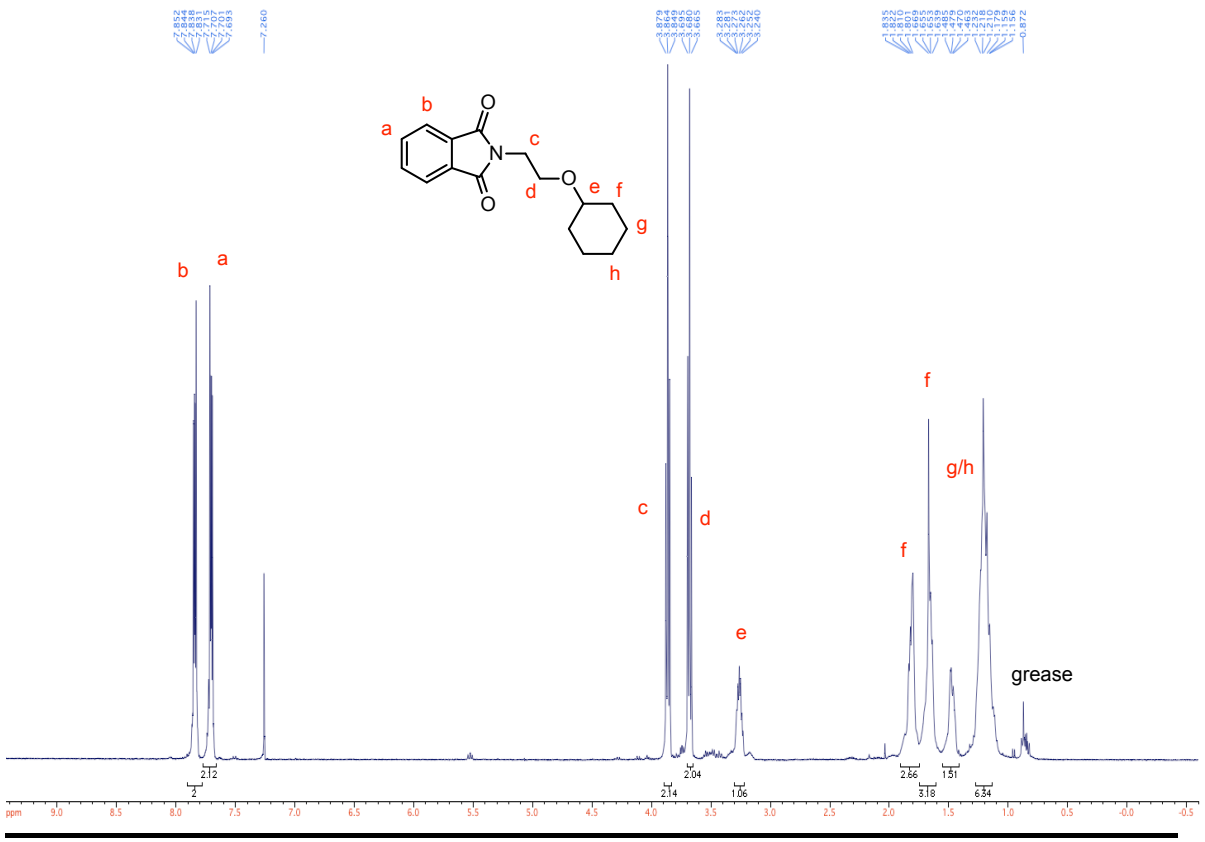
a
b
c
d
e
f
g
h
grease
2.12
2
2.14
2.04
1.06
2.66
3.18
1.51
6.34

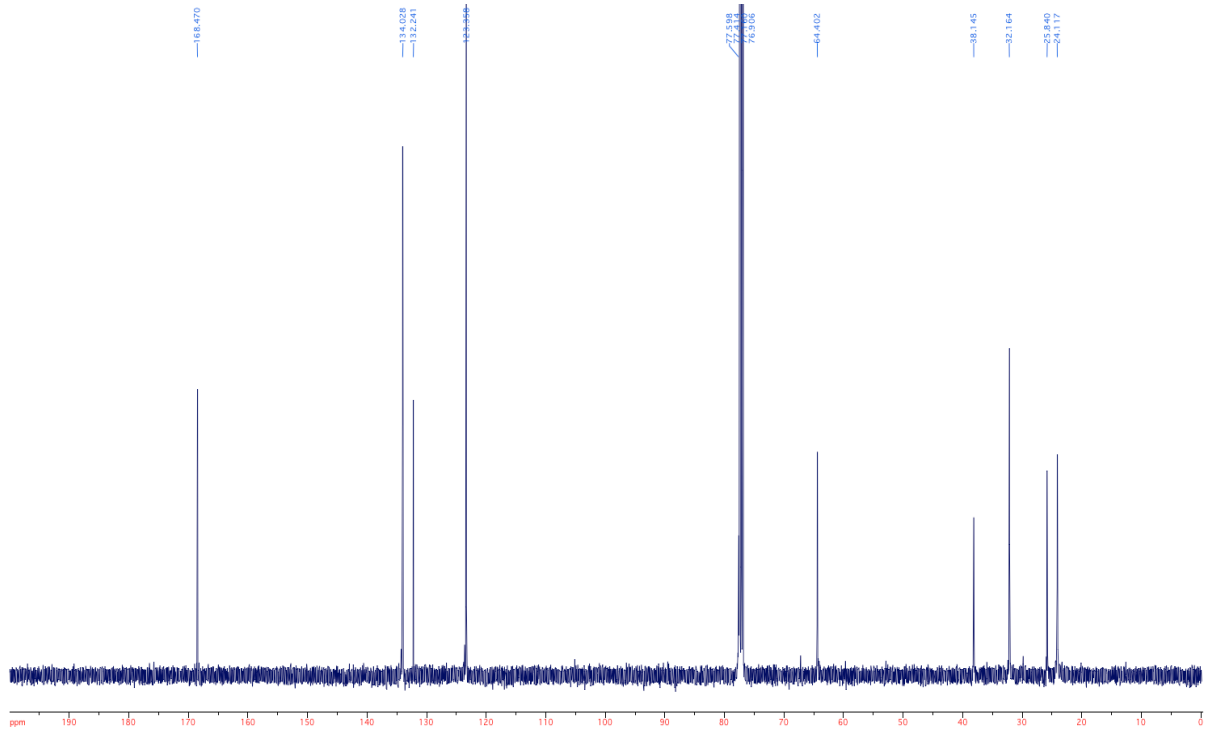

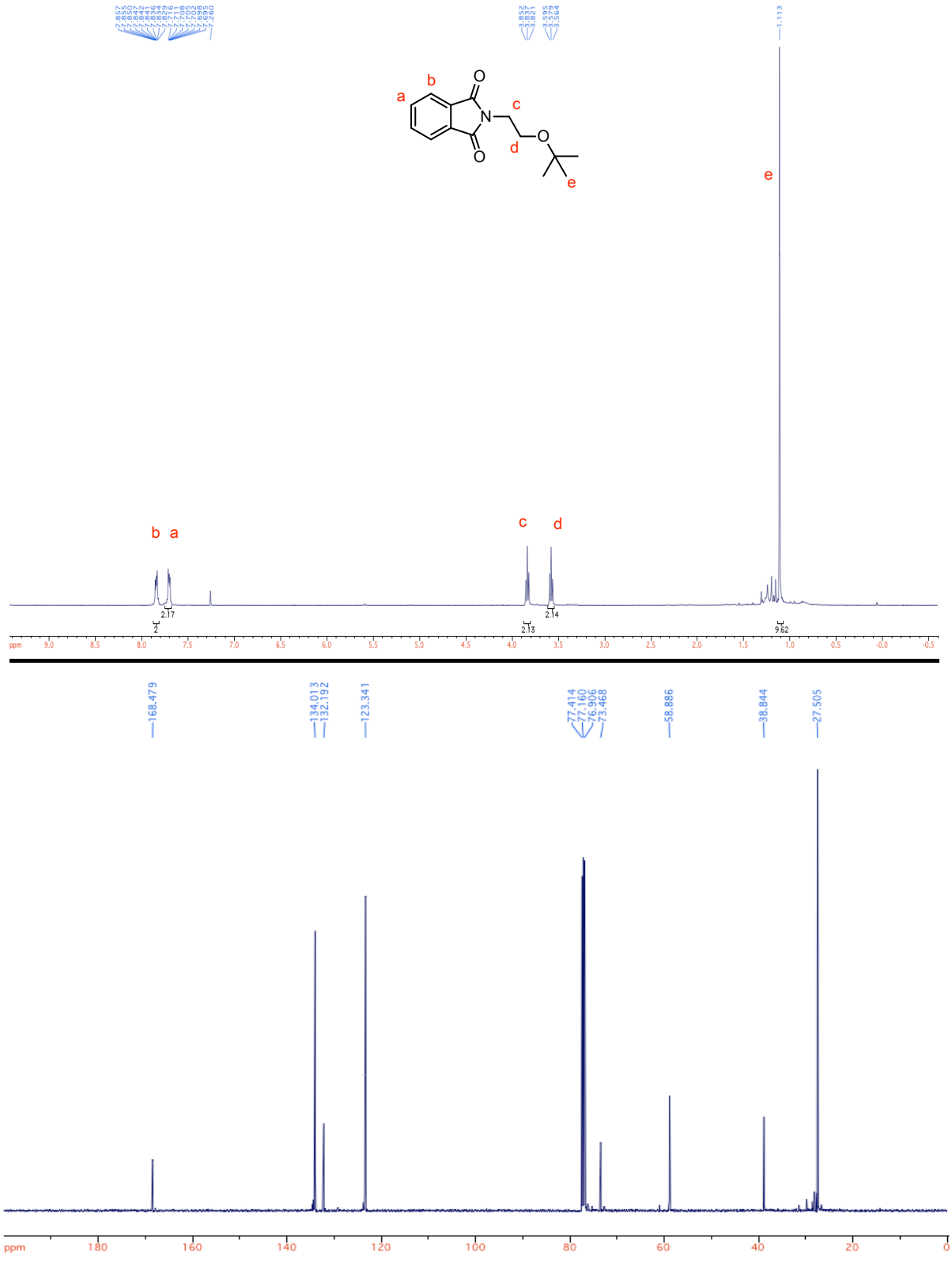
a
b
c
d
e
O
N
O
O
b a
c d
e
2.17
2.13
2.14
9.62
ppm
168.479
134.013
132.192
123.341
77.414
77.160
76.906
73.468
58.886
38.844
27.505
ppm

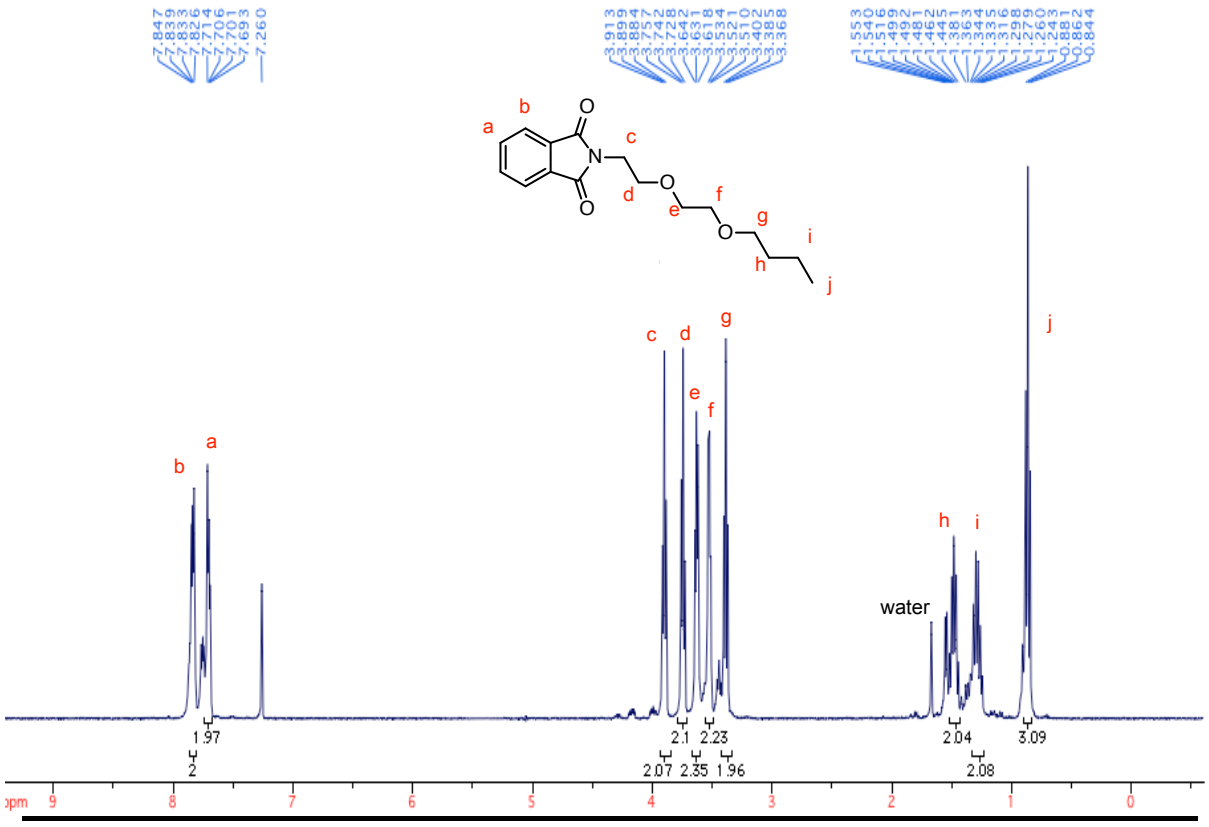
7.847
7.833
7.823
7.714
7.706
7.701
7.693
7.260
3.913
3.899
3.884
3.737
3.722
3.642
3.631
3.618
3.534
3.521
3.502
3.385
3.368
1.553
1.540
1.516
1.499
1.492
1.481
1.462
1.445
1.363
1.344
1.335
1.316
1.298
1.279
1.260
1.243
0.862
0.844
a
b
c
d
e
f
g
h
i
j
water
1.97
2
2.1
2.23
2.07
2.35
1.96
2.04
3.09
2.08
ppm
9
8
7
6
5
4
3
2
1
0

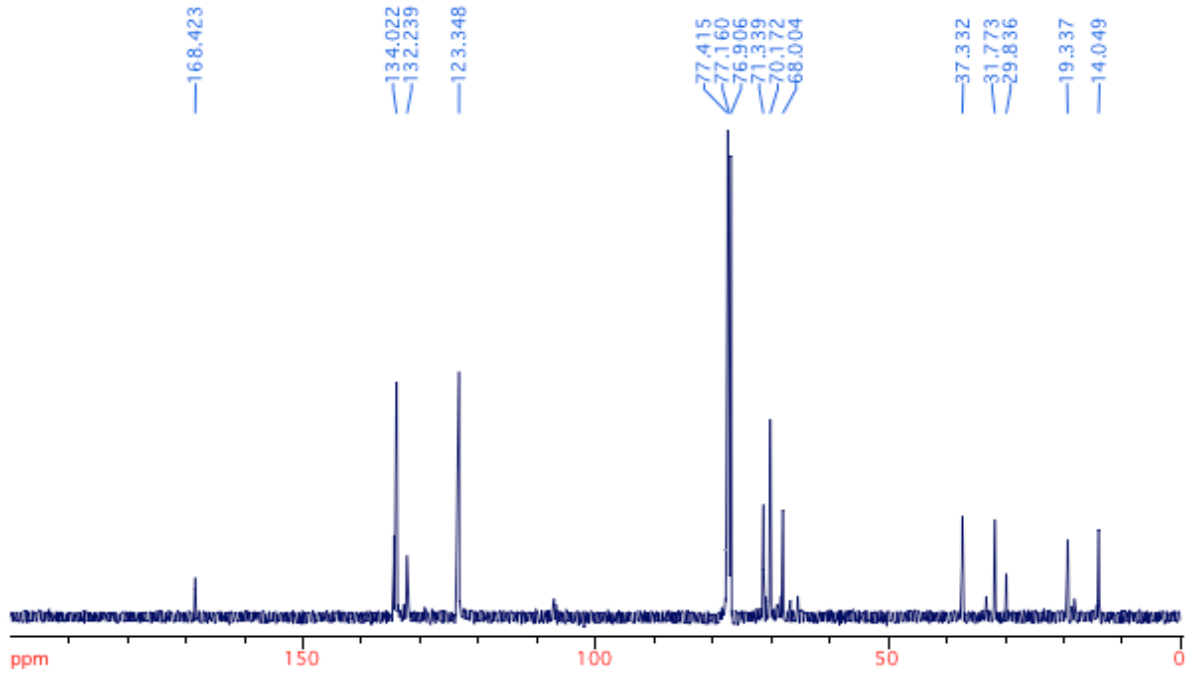
168.423
134.022
132.239
123.348
77.415
77.160
76.906
71.339
70.172
68.004
37.332
31.773
29.836
19.337
14.049
ppm
150
100
50
0

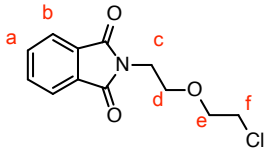
a
b
c
d
e
f
O
N
O
O
Cl

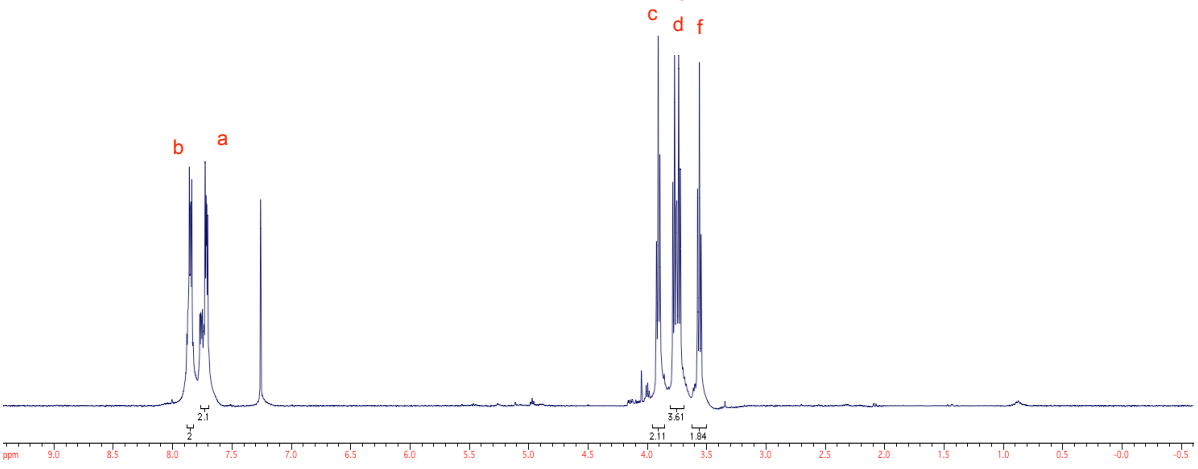
b
a
c
d
f
2.1
2.11
3.61
1.84
ppm

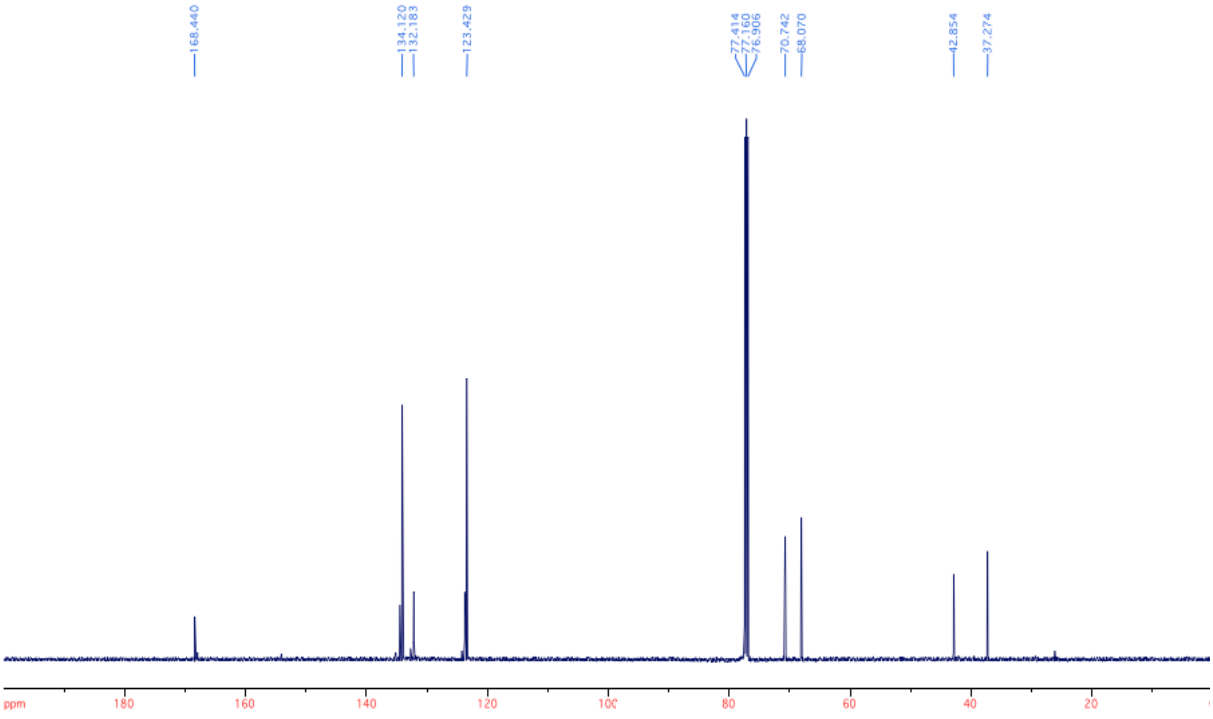
168.440
134.120
132.183
123.429
77.414
77.160
76.906
70.742
68.070
42.854
37.274
ppm

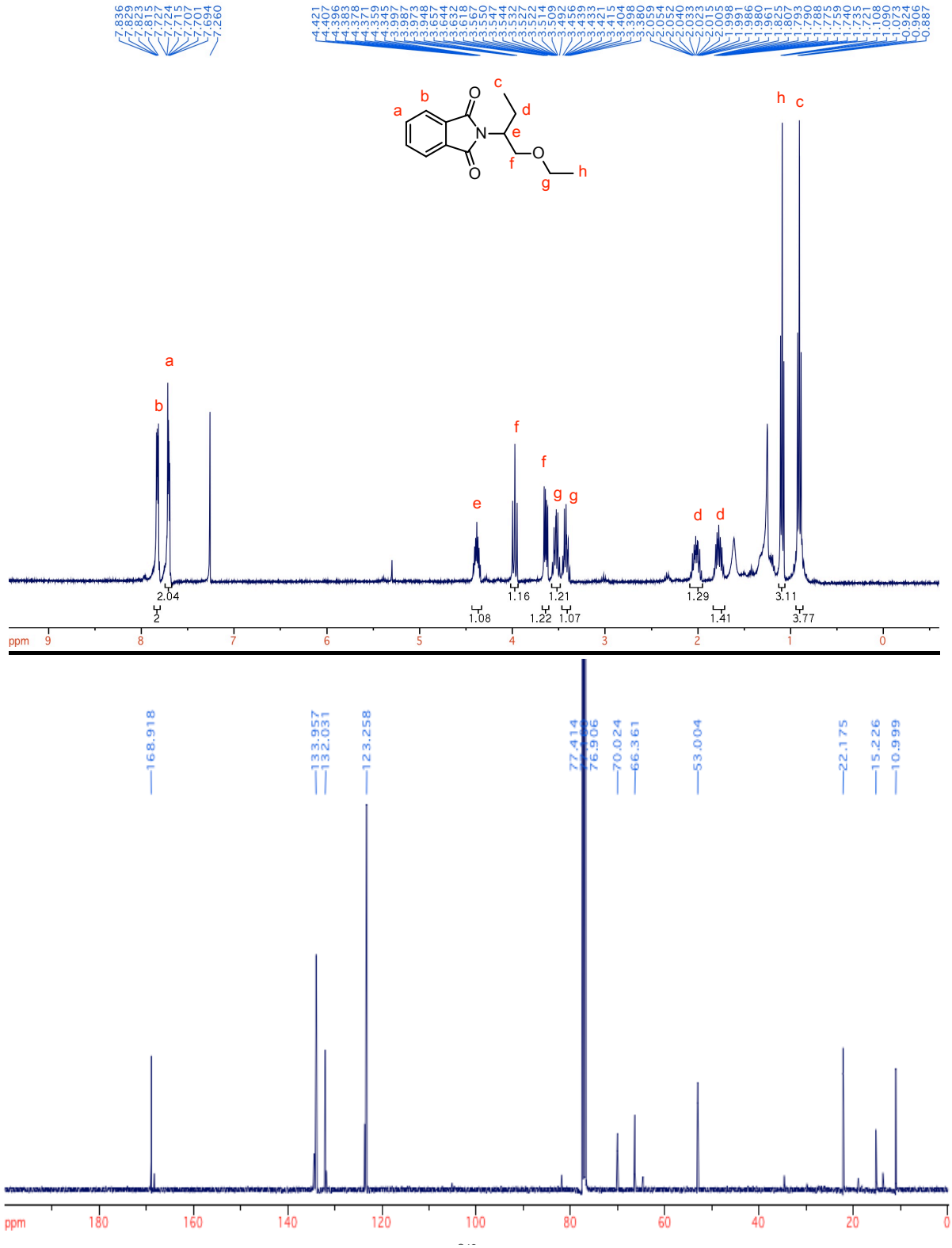
7.836
7.839
7.823
7.815
7.727
7.724
7.715
7.707
7.701
7.694
7.260
4.421
4.407
4.396
4.383
4.378
4.371
4.359
4.345
4.327
3.987
3.973
3.948
3.657
3.644
3.632
3.618
3.567
3.560
3.547
3.544
3.532
3.527
3.522
3.514
3.509
3.492
3.456
3.439
3.433
3.421
3.415
3.404
3.398
3.380
2.059
2.054
2.052
2.040
2.033
2.023
2.015
2.005
1.998
1.991
1.986
1.980
1.961
1.825
1.807
1.793
1.790
1.788
1.785
1.759
1.740
1.735
1.721
1.108
1.090
1.073
0.924
0.906
0.887
a
b
c
d
e
f
g
h
2.04
2
1.08
1.16
1.22
1.21
1.07
1.29
1.41
3.11
3.77
ppm
168.918
133.957
132.031
123.258
77.414
77.000
76.906
70.024
66.361
53.004
22.175
15.226
10.999
ppm

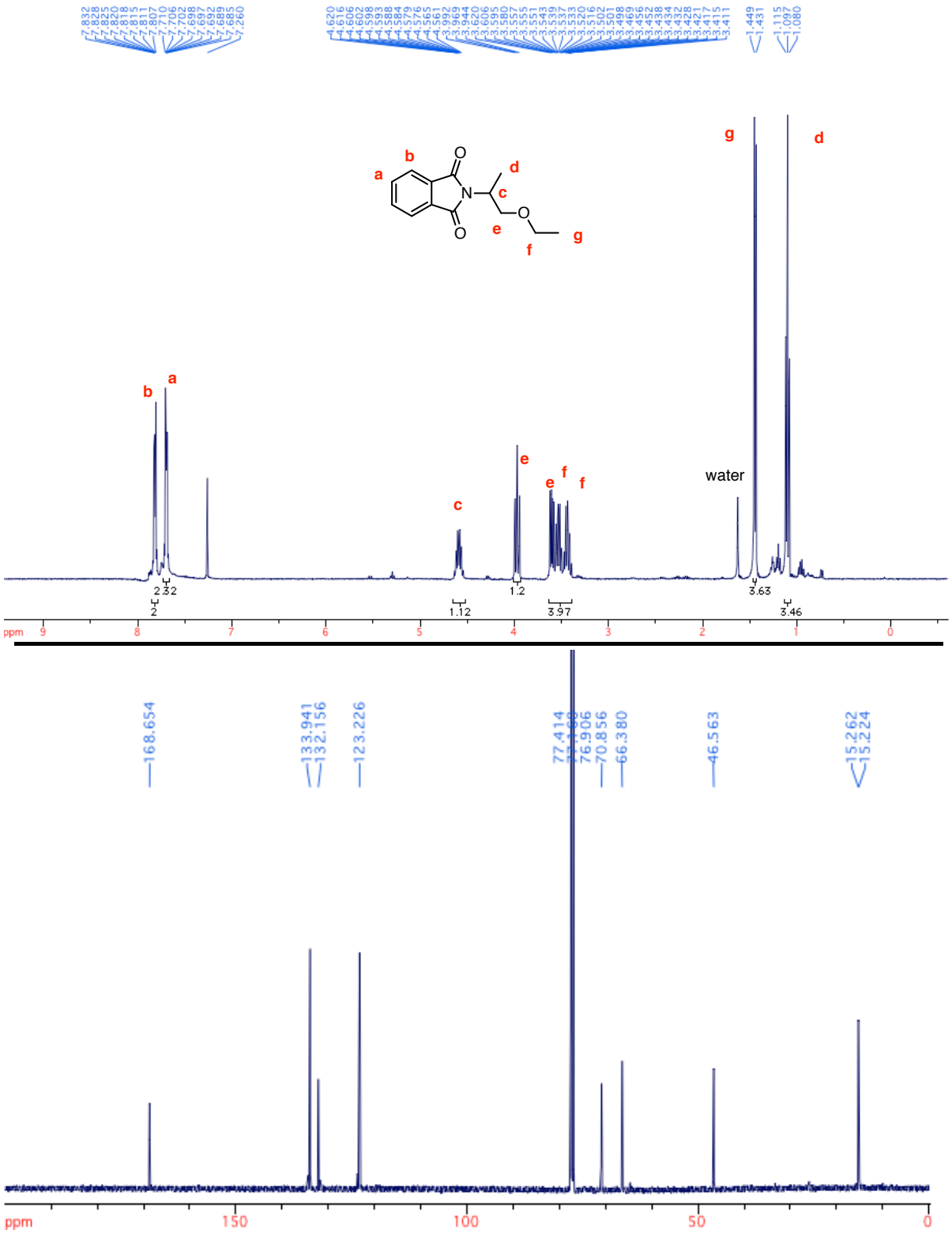
7.832
7.828
7.825
7.820
7.818
7.815
7.811
7.807
7.710
7.706
7.702
7.698
7.697
7.692
7.689
7.685
7.260
4.620
4.616
4.606
4.602
4.598
4.593
4.588
4.584
4.579
4.576
4.565
4.561
3.992
3.969
3.644
3.640
3.606
3.595
3.580
3.557
3.555
3.551
3.543
3.539
3.537
3.533
3.520
3.516
3.502
3.501
3.498
3.469
3.456
3.452
3.438
3.434
3.432
3.428
3.421
3.417
3.415
3.411
1.449
1.431
1.115
1.097
1.080
a
b
c
d
e
f
g
water
2.32
2
1.12
1.2
3.97
3.63
3.46
ppm
9
8
7
6
5
4
3
2
1
0
168.654
133.941
132.156
123.226
77.414
76.906
70.856
66.380
46.563
15.262
15.224
ppm
150
100
50
0

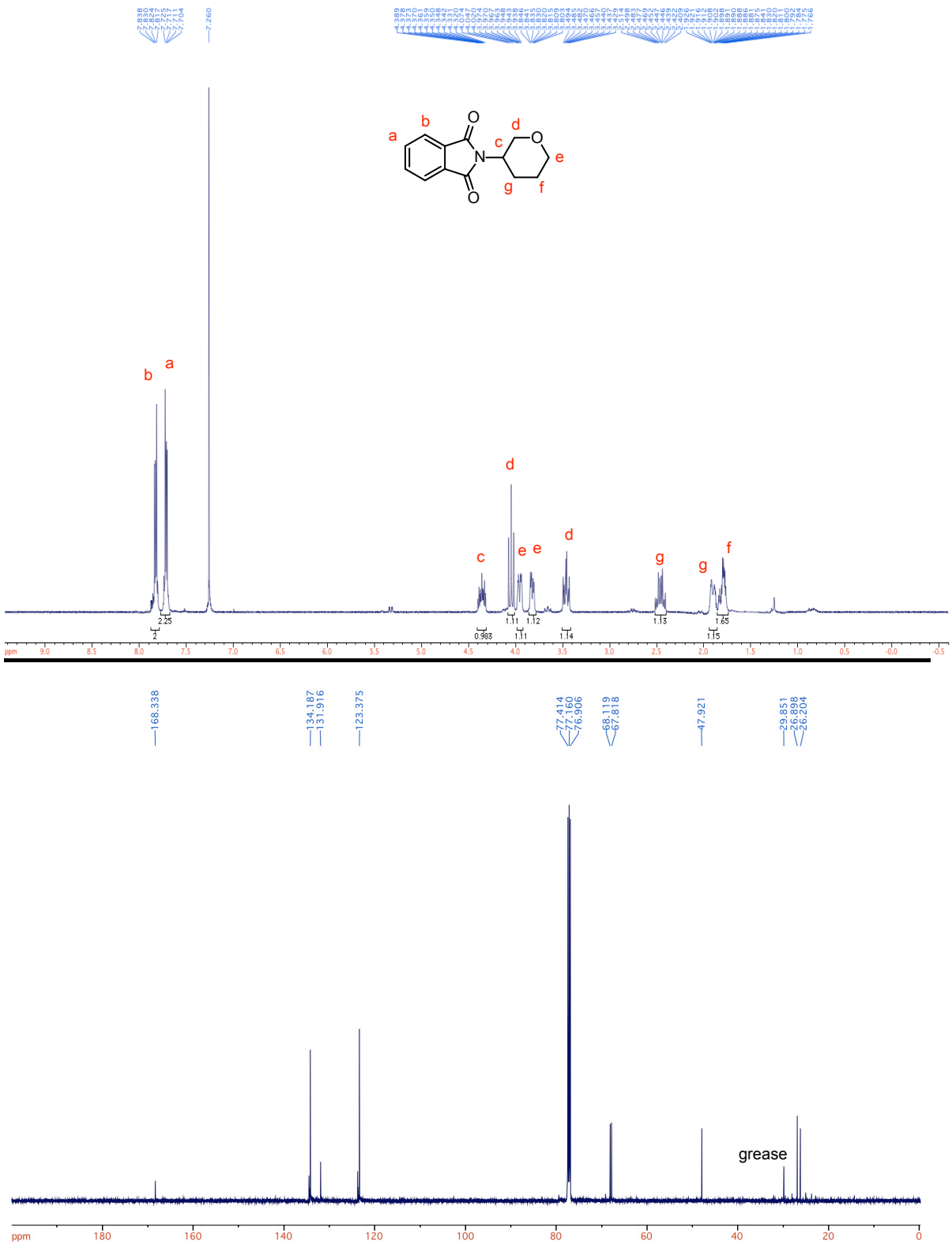
a
b
c
d
e
f
g
grease
ppm

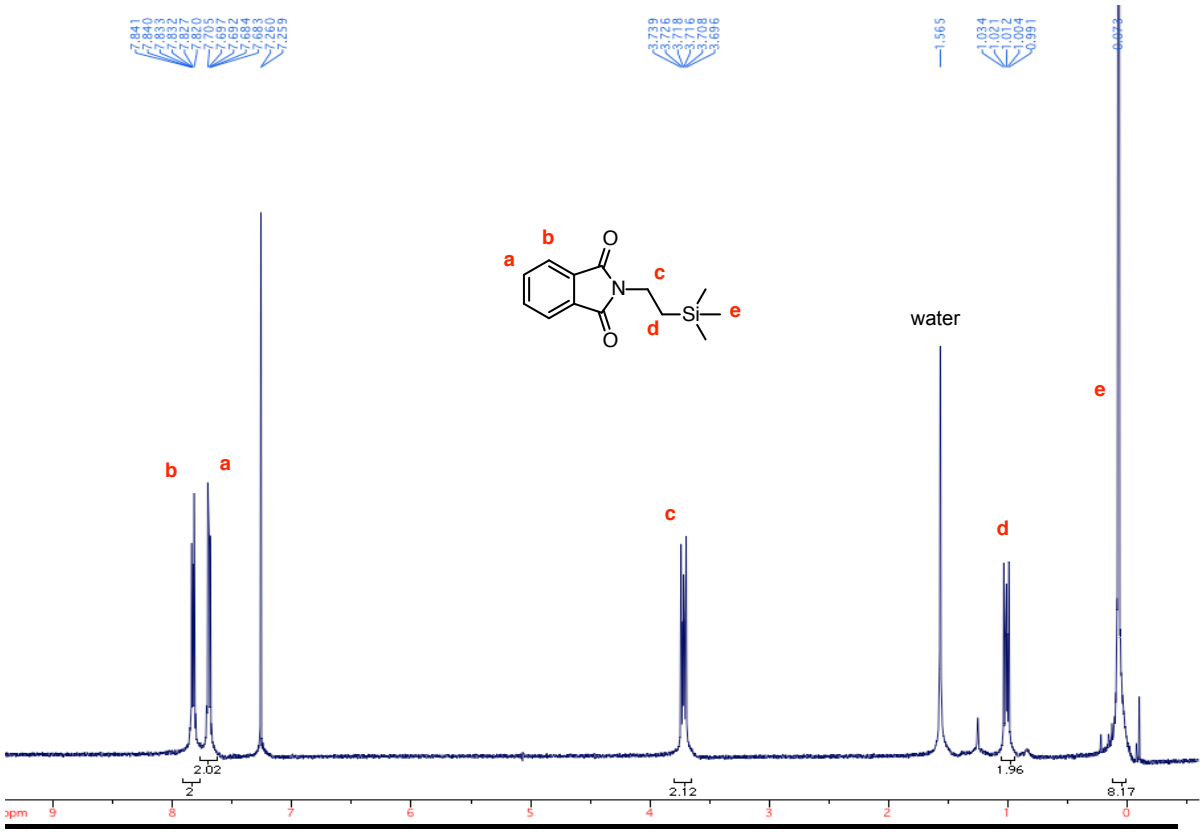
7.841
7.840
7.833
7.832
7.827
7.820
7.705
7.697
7.692
7.684
7.683
7.260
7.259
3.739
3.726
3.718
3.716
3.708
3.696
1.565
1.034
1.021
1.012
1.004
0.991
0.073
a
b
c
d
e
water
2.02
2.12
1.96
8.17
2
ppm 9
8
7
6
5
4
3
2
1
0

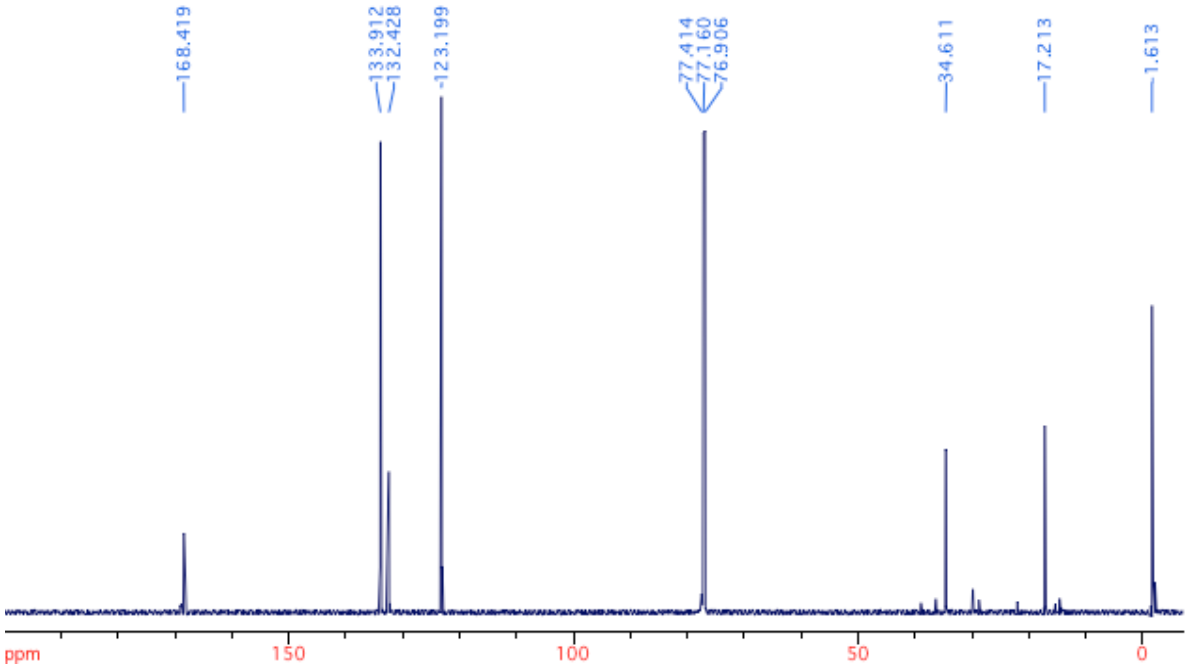
168.419
133.912
132.428
123.199
77.414
77.160
76.906
34.611
17.213
1.613
ppm
150
100
50
0

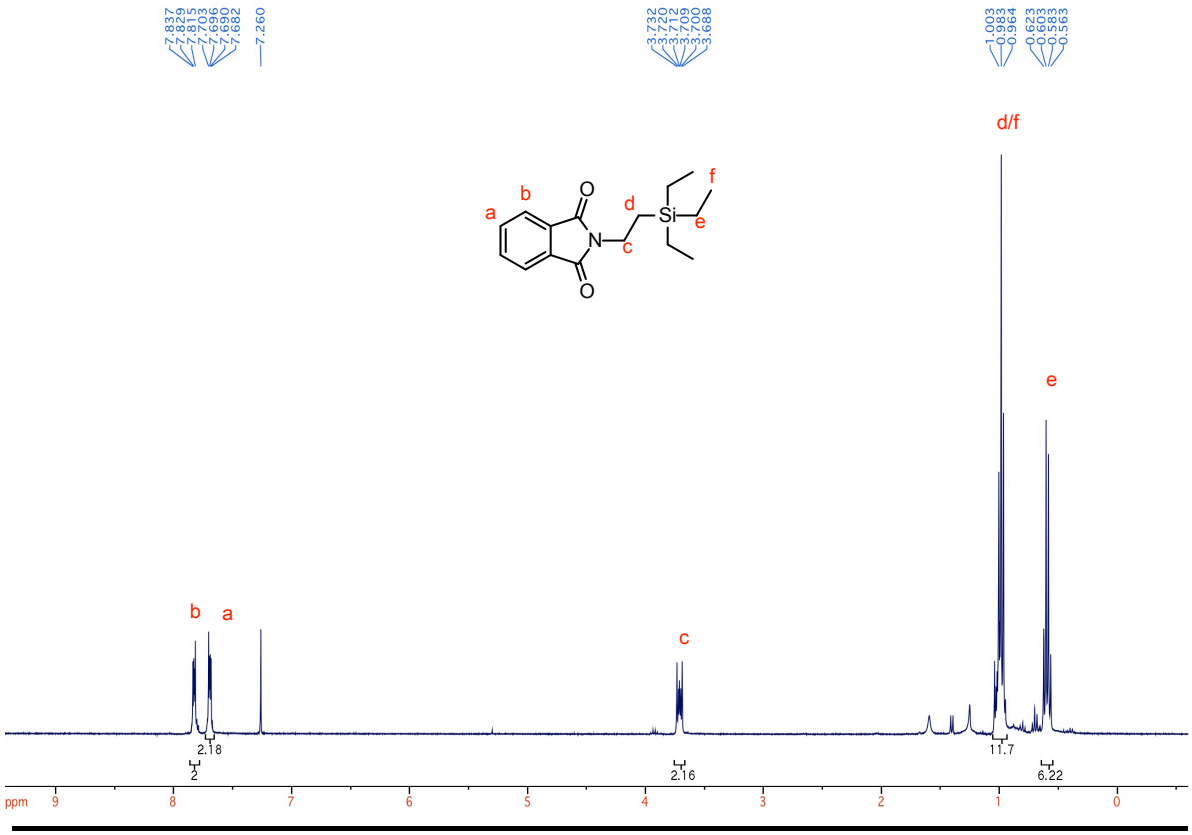
7.837
7.829
7.815
7.703
7.696
7.690
7.682
7.260
3.732
3.720
3.712
3.706
3.700
3.688
1.003
0.983
0.964
0.623
0.603
0.583
0.563
d/f
e
b
a
c
2.18
2.16
11.7
6.22
ppm

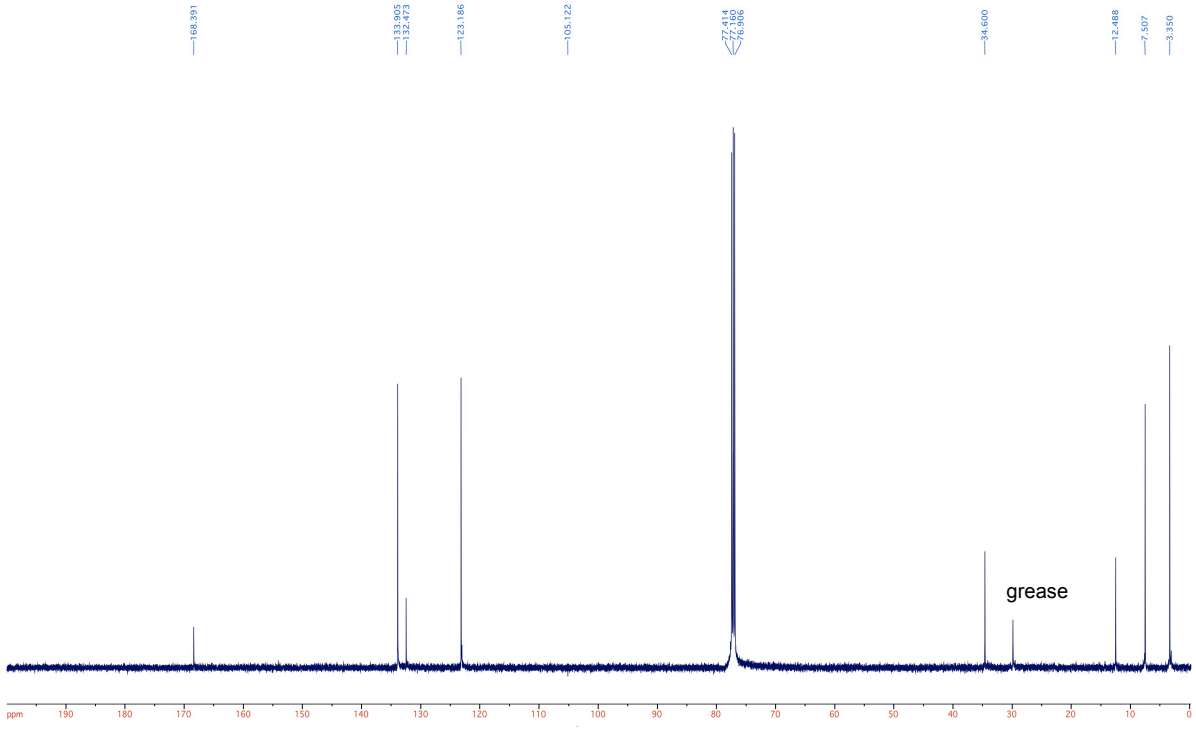
168.391
133.905
132.473
123.186
105.122
77.414
77.100
76.900
34.600
12.488
7.507
3.350
grease
ppm

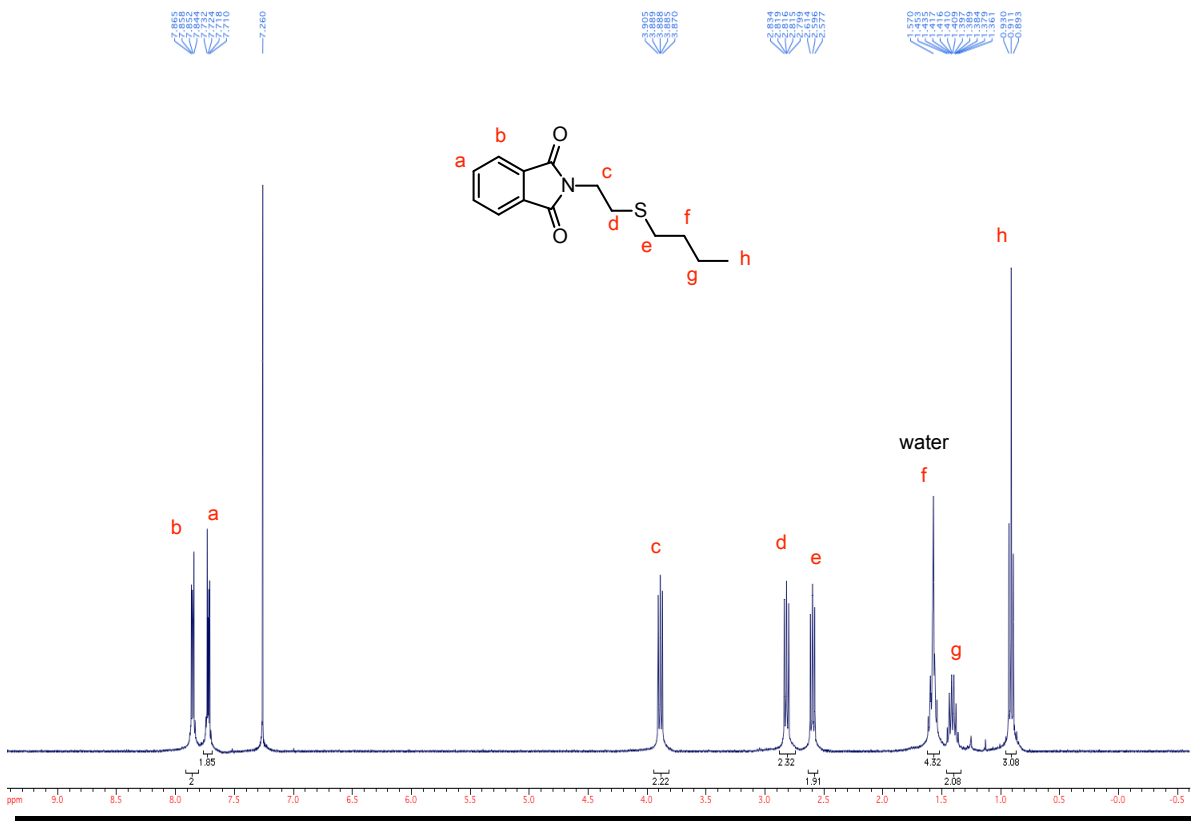
a
b
c
d
e
f
g
h
water
1.85
2.22
2.32
1.91
4.32
2.08
3.08
ppm

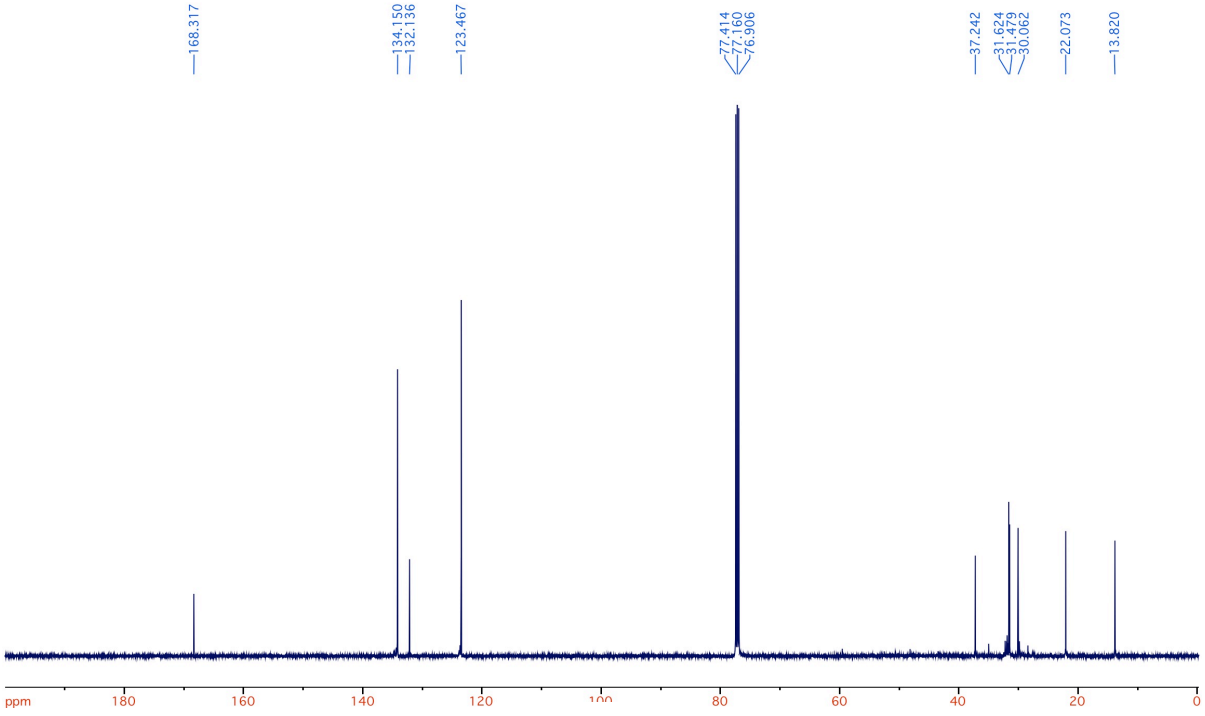
168.317
134.150
132.136
123.467
77.414
77.160
76.906
37.242
31.624
31.479
30.062
22.073
13.820
ppm

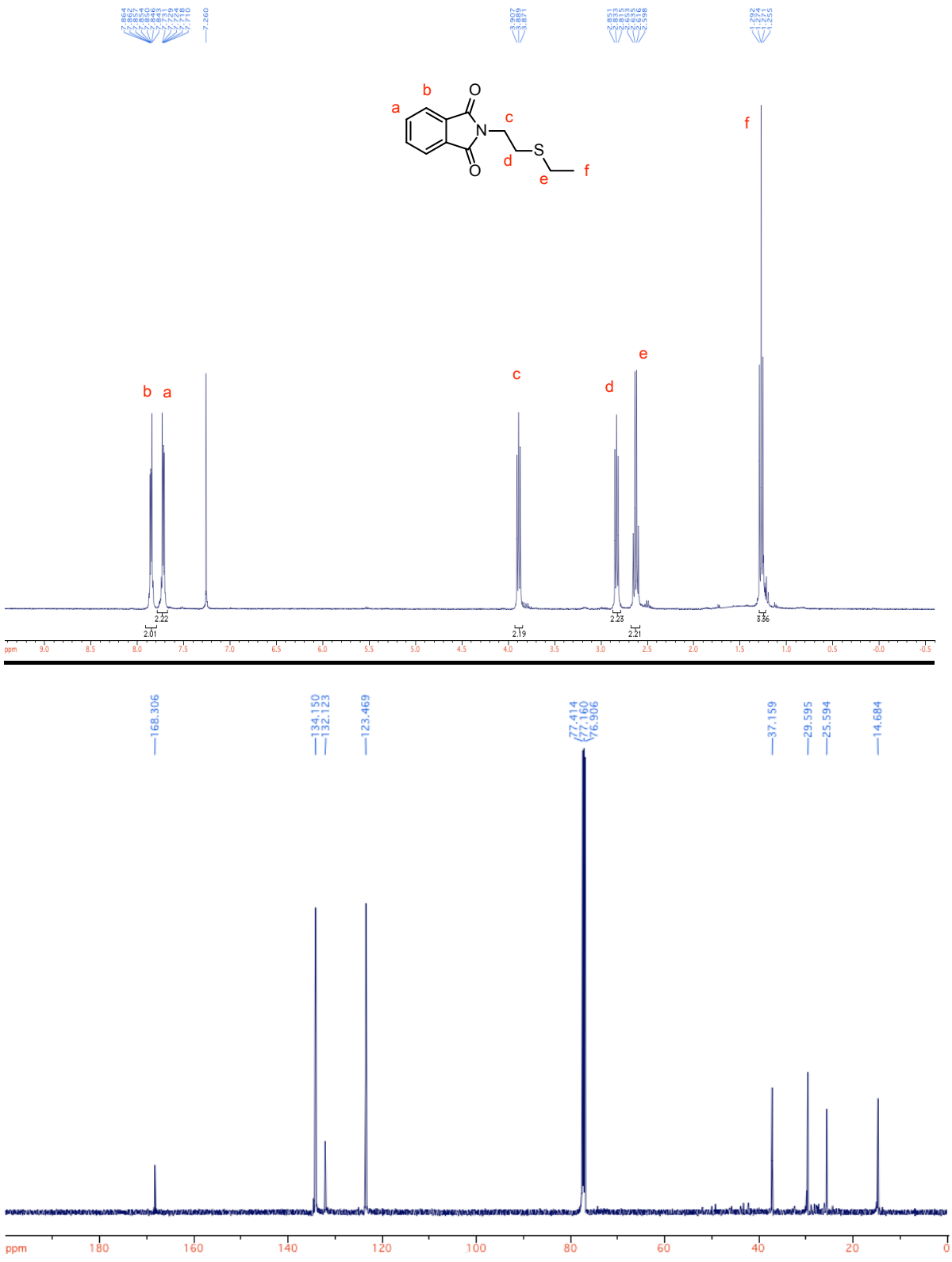
a
b
c
d
e
f
O
N
S
O
b a
c
d
e
f
2.01
2.22
2.19
2.23
2.21
3.36
ppm
9.0
8.5
8.0
7.5
7.0
6.5
6.0
5.5
5.0
4.5
4.0
3.5
3.0
2.5
2.0
1.5
1.0
0.5
-0.0
-0.5
168.306
134.150
132.123
123.469
77.414
77.160
76.906
37.159
29.595
25.594
14.684
ppm
180
160
140
120
100
80
60
40
20
0

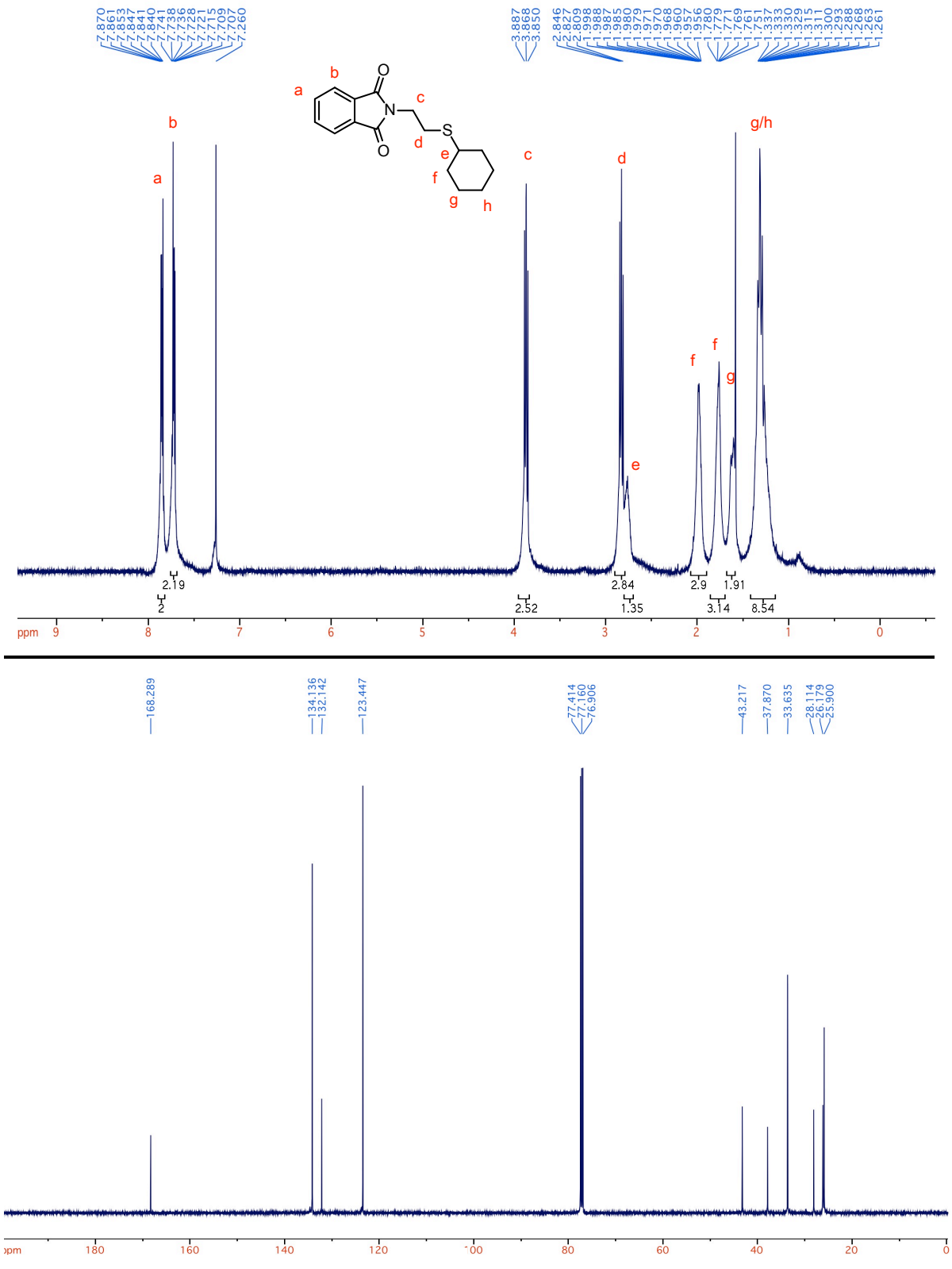
7.870
7.861
7.853
7.847
7.841
7.840
7.741
7.738
7.736
7.728
7.721
7.715
7.709
7.707
7.260
3.887
3.868
3.850
2.846
2.827
2.809
1.998
1.988
1.987
1.985
1.980
1.979
1.971
1.970
1.968
1.960
1.957
1.956
1.780
1.779
1.771
1.769
1.761
1.737
1.333
1.330
1.329
1.315
1.311
1.300
1.293
1.288
1.268
1.263
1.261
a
b
c
d
e
f
g
h
g/h
2.19
2
2.52
2.84
1.35
2.9
1.91
3.14
8.54
ppm
9
8
7
6
5
4
3
2
1
0
168.289
134.136
132.142
123.447
77.414
77.160
76.906
43.217
37.870
33.635
28.114
26.179
25.900
180
160
140
120
100
80
60
40
20
0

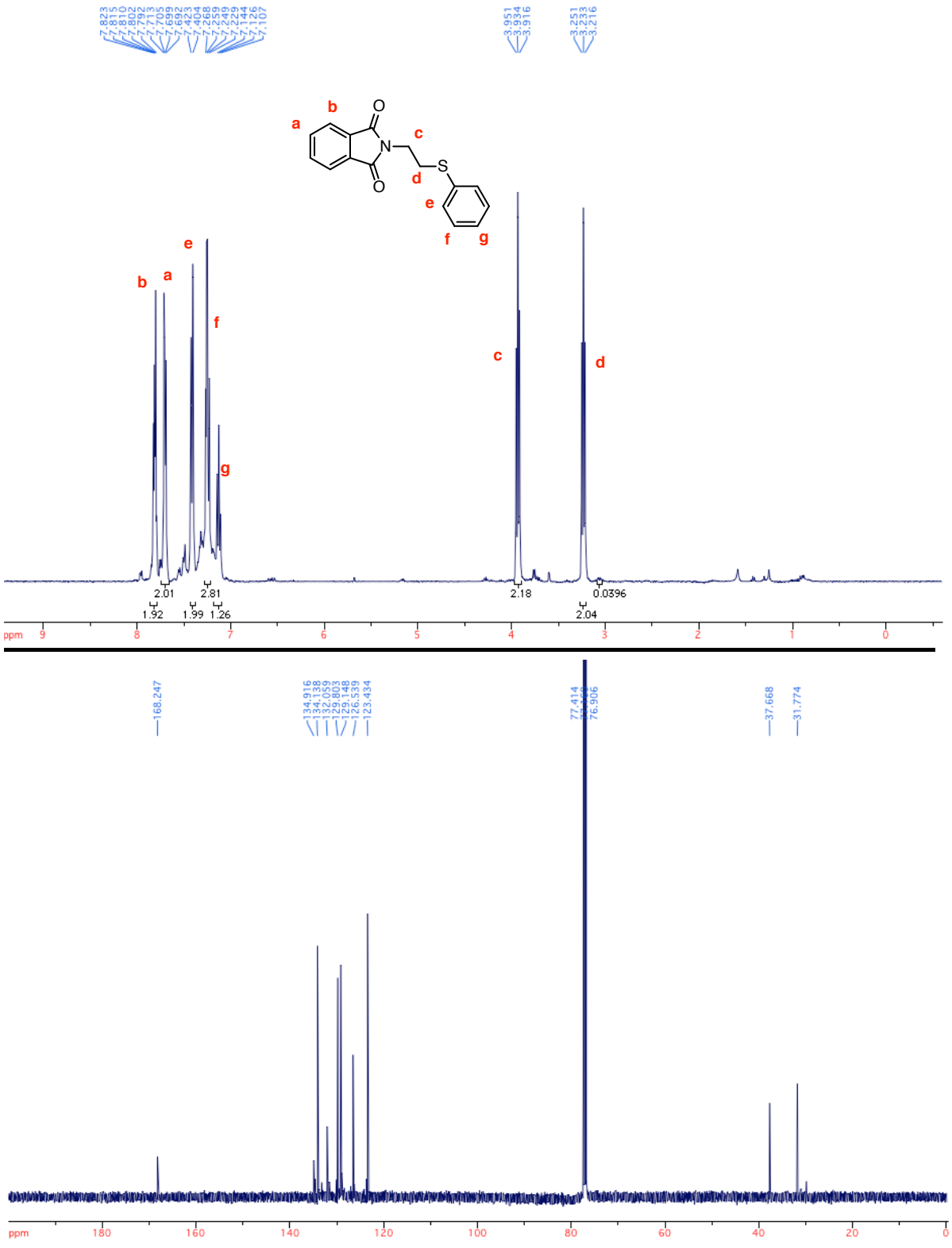
7.823
7.815
7.810
7.802
7.792
7.713
7.705
7.699
7.692
7.423
7.404
7.268
7.259
7.249
7.239
7.144
7.126
7.107
3.951
3.934
3.916
3.251
3.233
3.216
a
b
c
d
e
f
g
2.01
1.92
2.81
1.99
1.26
2.18
0.0396
2.04
ppm
9
8
7
6
5
4
3
2
1
0
168.247
134.916
134.138
132.059
129.803
129.148
126.539
123.434
77.414
77.088
76.906
37.668
31.774
ppm
180
160
140
120
100
80
60
40
20
0

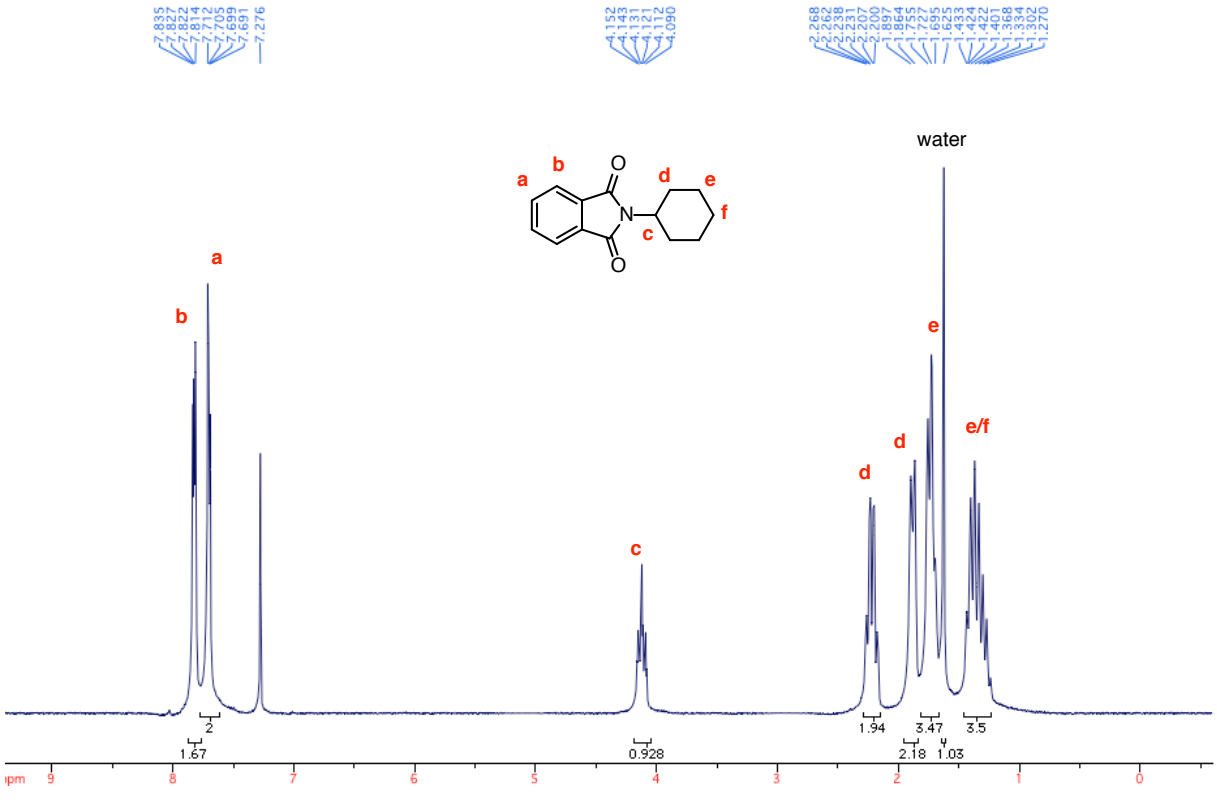
7.835
7.827
7.822
7.814
7.712
7.705
7.699
7.691
7.276
4.152
4.143
4.131
4.121
4.112
4.090
2.268
2.262
2.238
2.231
2.207
2.200
1.897
1.864
1.855
1.727
1.695
1.625
1.433
1.424
1.422
1.401
1.368
1.334
1.302
1.270
a
b
c
d
e
f
water
b
a
c
d
d
e
e/f
2
1.67
0.928
1.94
3.47
2.18
1.03
3.5
ppm
9
8
7
6
5
4
3
2
1
0

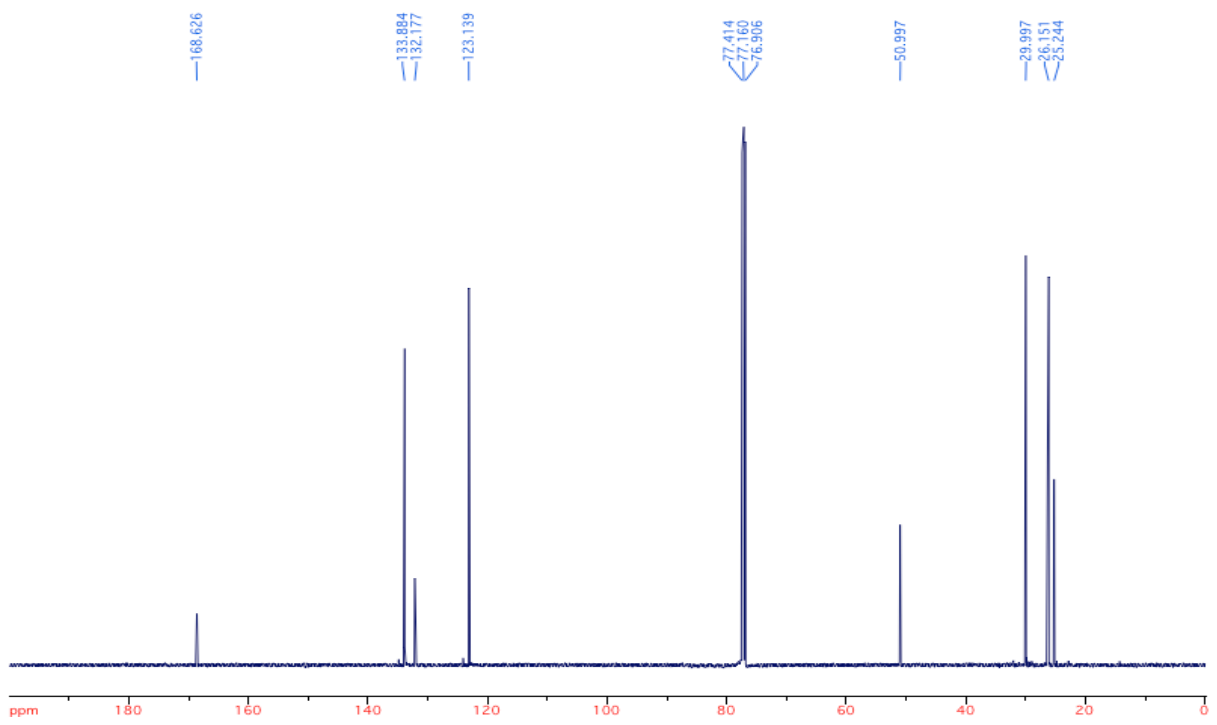
168.626
133.884
132.177
123.139
77.414
77.160
76.906
50.997
29.997
26.151
25.244
ppm
180
160
140
120
100
80
60
40
20
0

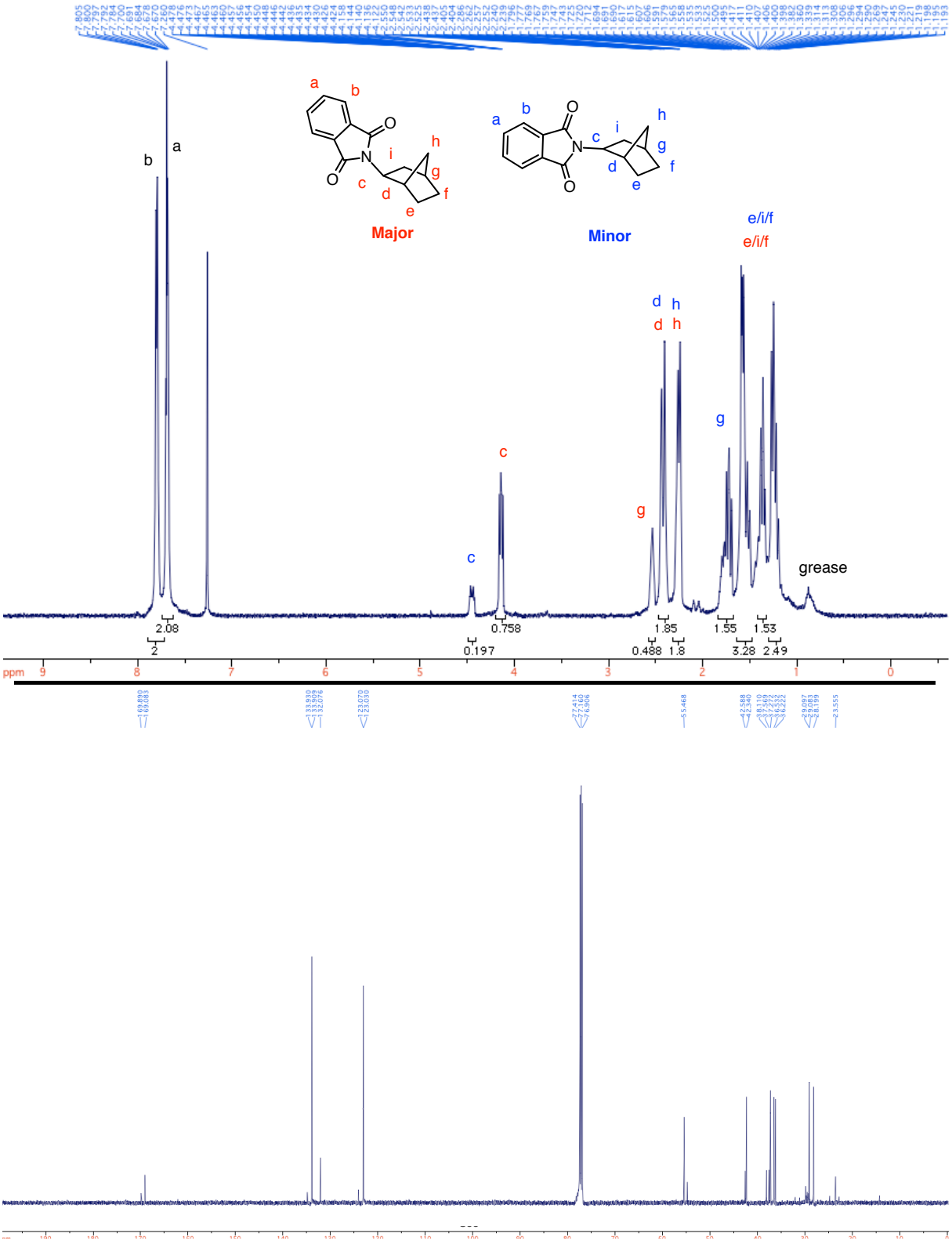
Major
Minor
grease
e/i/f
e/i/f
2.08
0.758
0.197
1.85
1.55
1.53
0.488
1.8
3.28
2.49
ppm

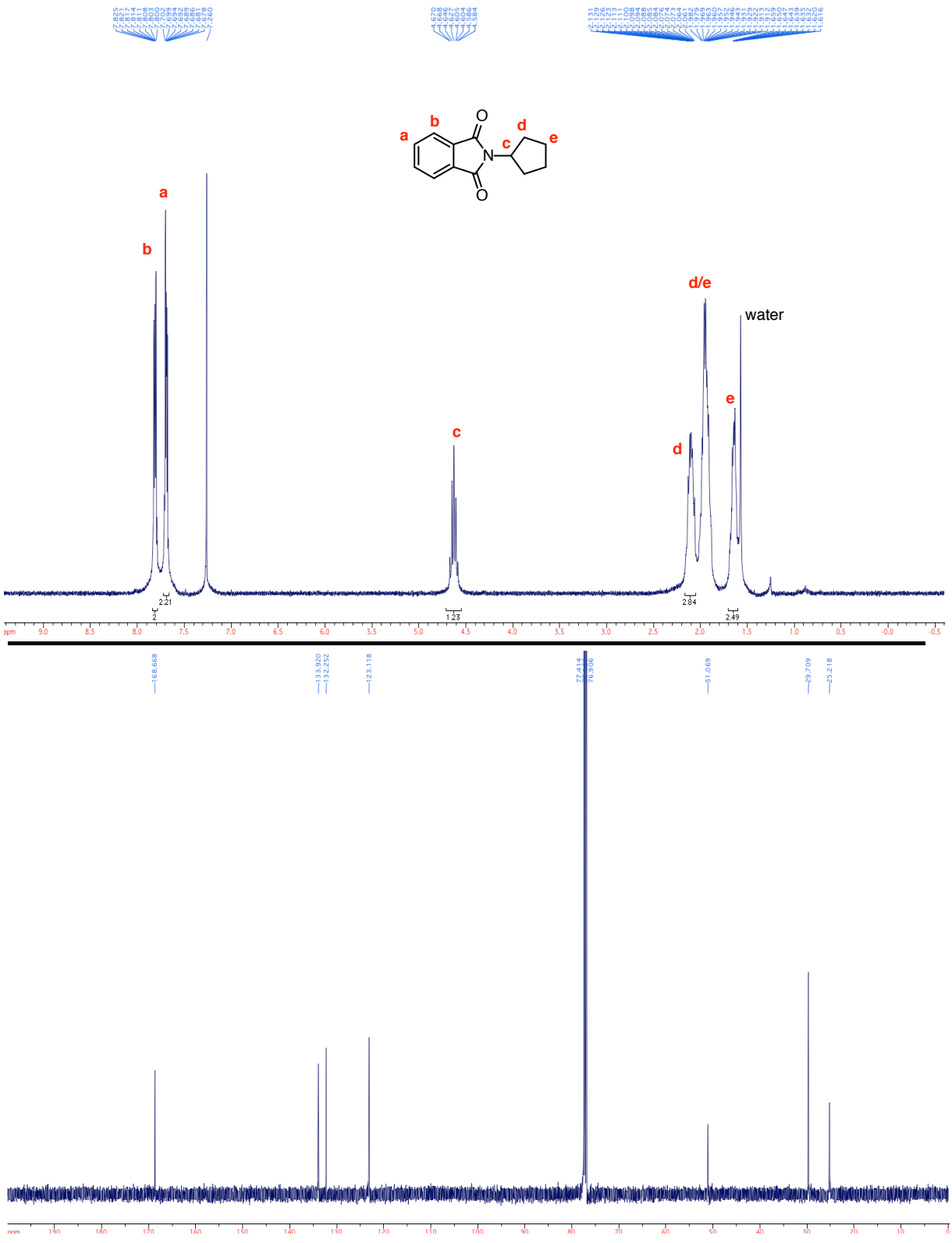
a
b
c
d
e
O
N
O
b
a
c
d/e
water
e
d
2.21
1.23
2.84
2.49
ppm

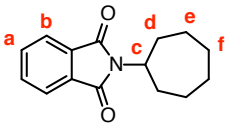
a
b
c
d
e
f
O
N
O

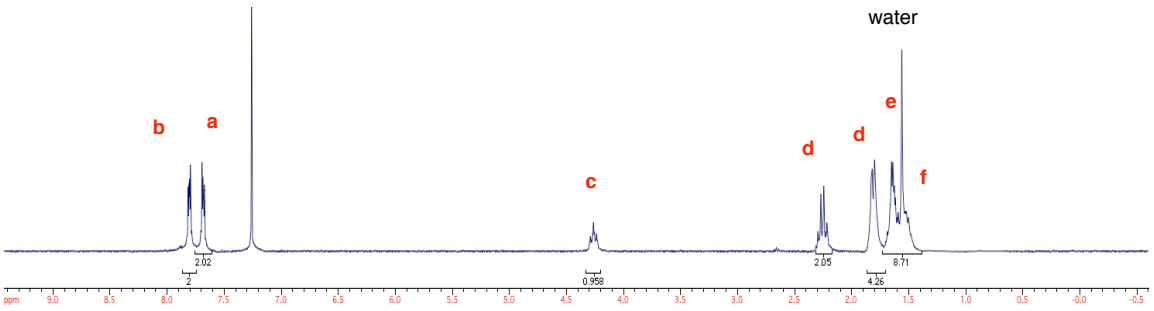
water
b
a
c
d
d
e
f
2.02
2
0.958
2.05
8.71
4.26
ppm

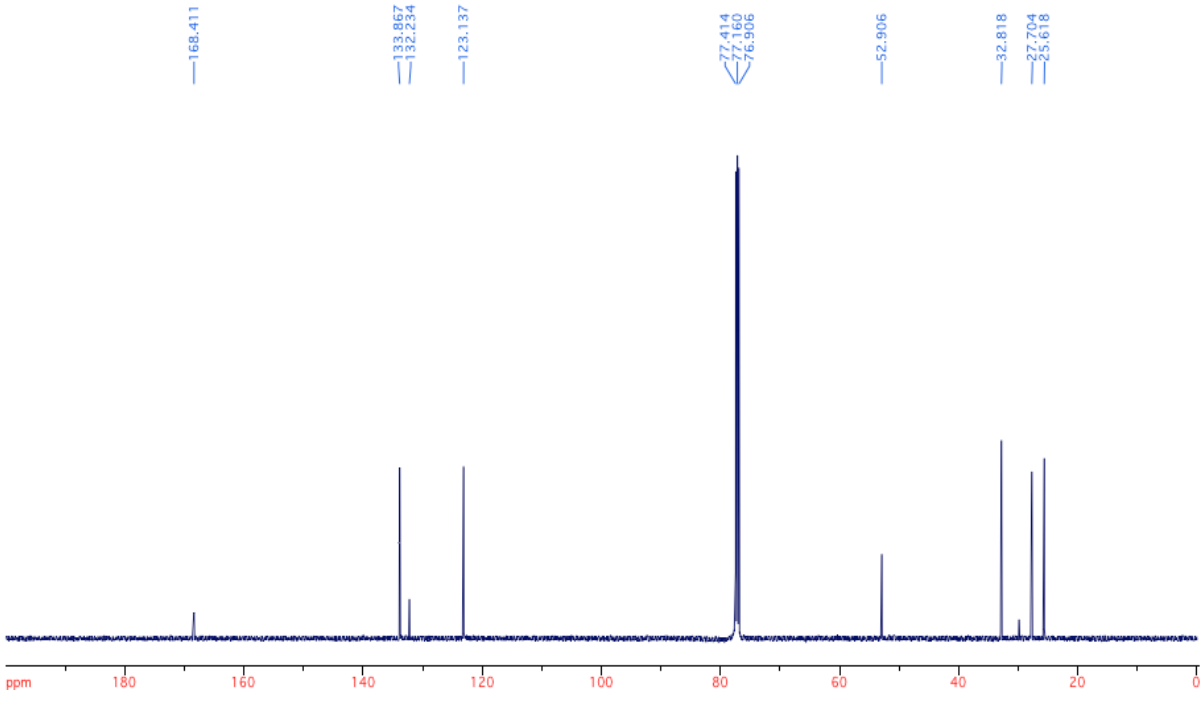
168.411
133.867
132.234
123.137
77.414
77.160
76.906
52.906
32.818
27.704
25.618
ppm

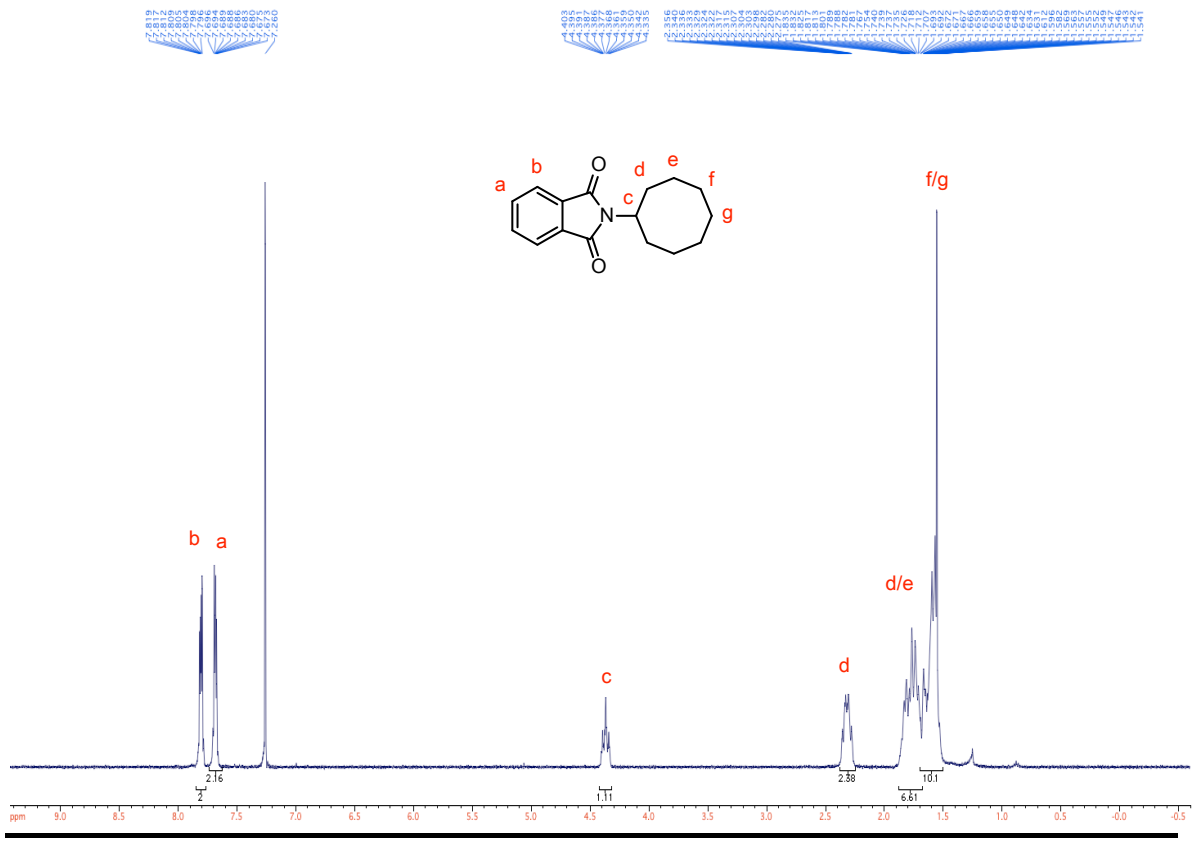
a
b
c
d
e
f
g
O
N
O
b
a
c
d
d/e
f/g
2.16
2
1.11
2.38
10.1
6.61
ppm

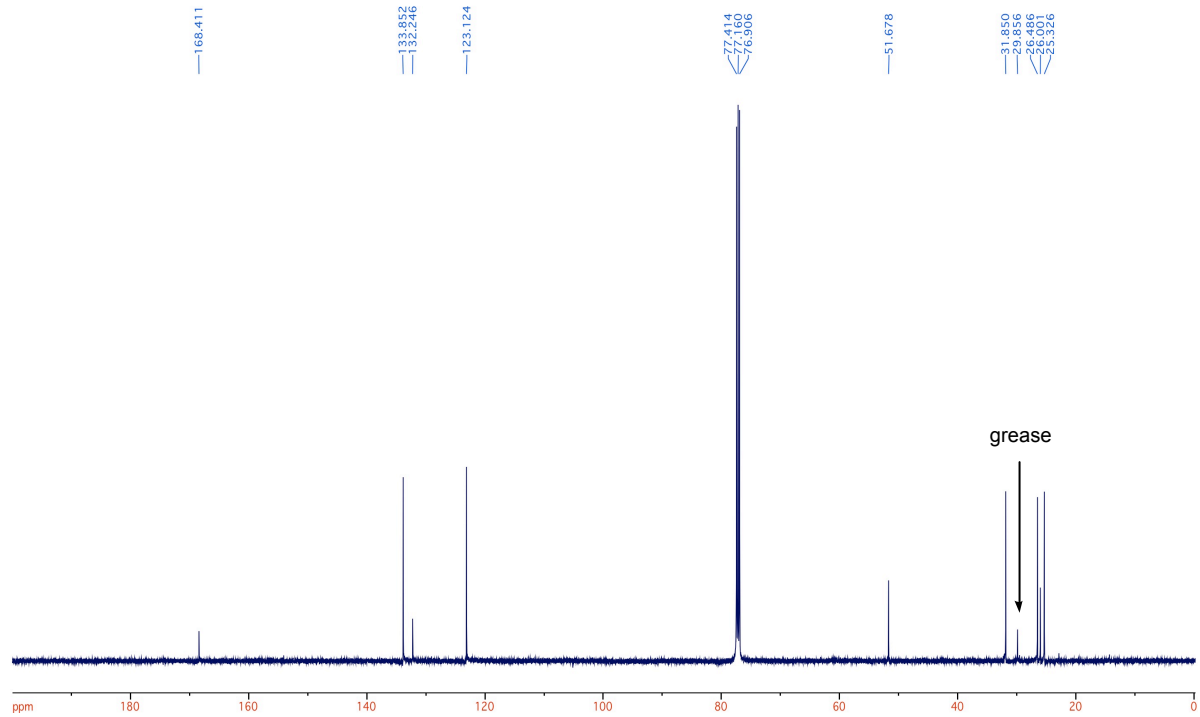
168.411
133.852
132.246
123.124
77.414
77.160
76.906
51.678
31.850
29.856
26.486
26.001
25.326
grease
ppm

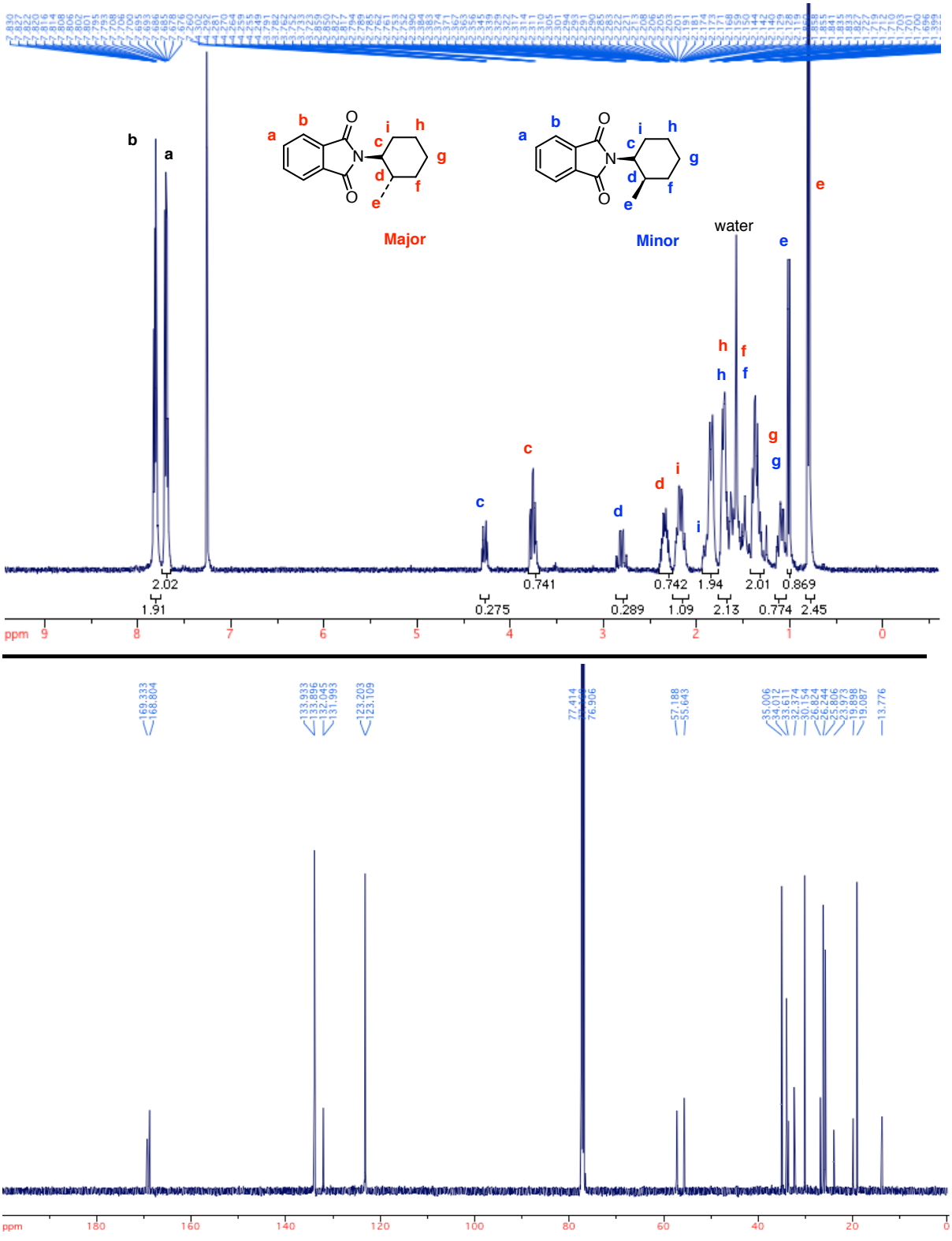
Major
Minor
water
2.02
1.91
0.275
0.741
0.289
0.742
1.09
1.94
2.13
2.01
0.774
0.869
2.45
ppm

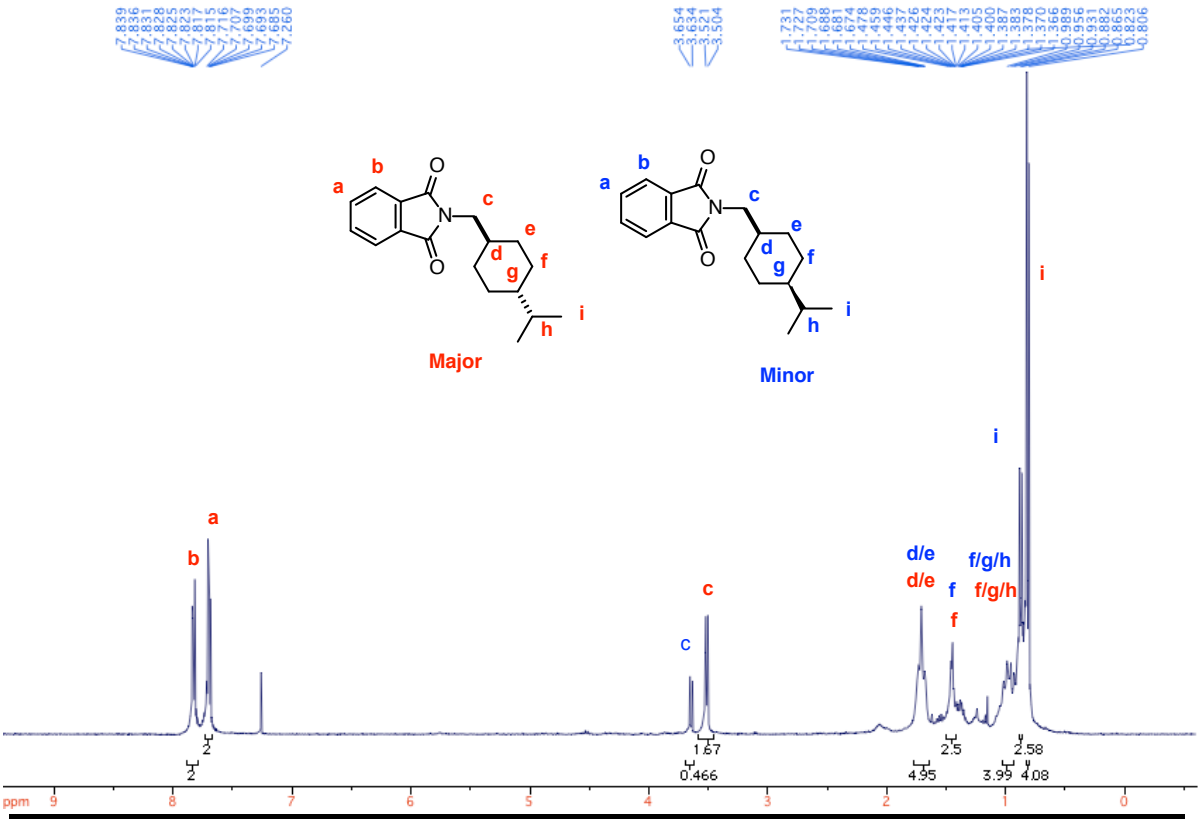
Major
Minor
a
b
c
d/e
f/g/h
i
2
1.67
0.466
2.5
4.95
2.58
3.99
4.08
ppm

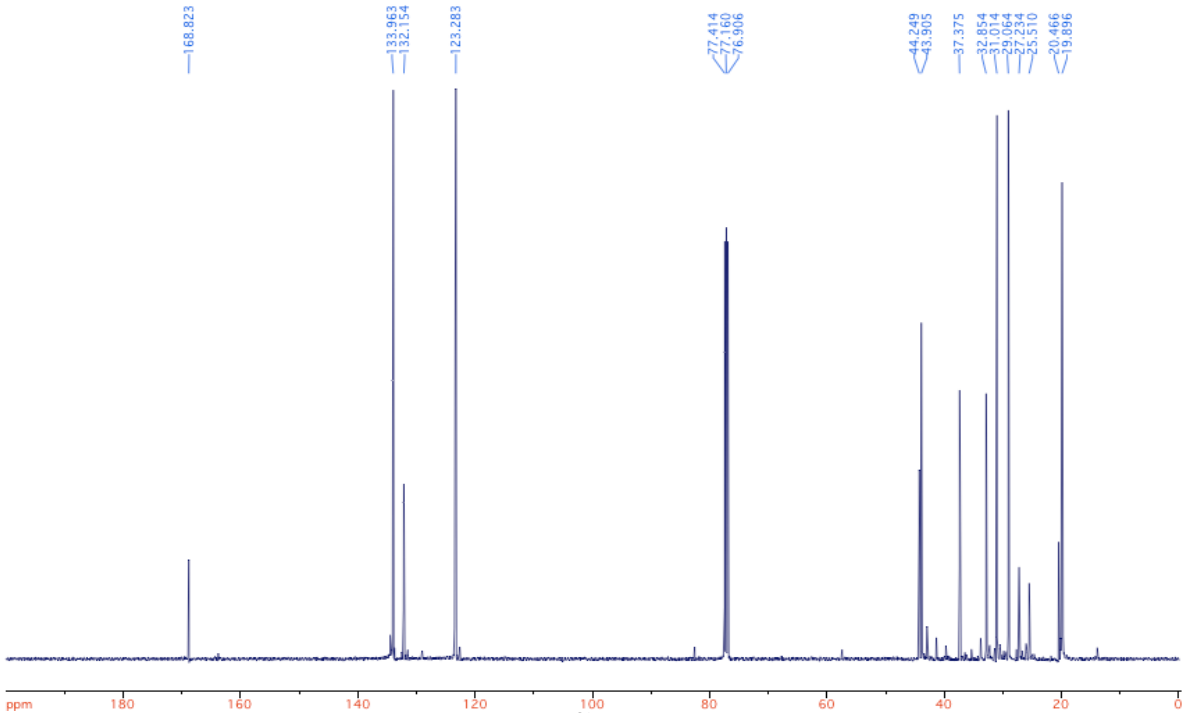
168.823
133.963
132.154
123.283
77.414
77.160
76.906
44.249
43.905
37.375
32.854
31.014
29.064
27.234
25.510
20.466
19.896
ppm

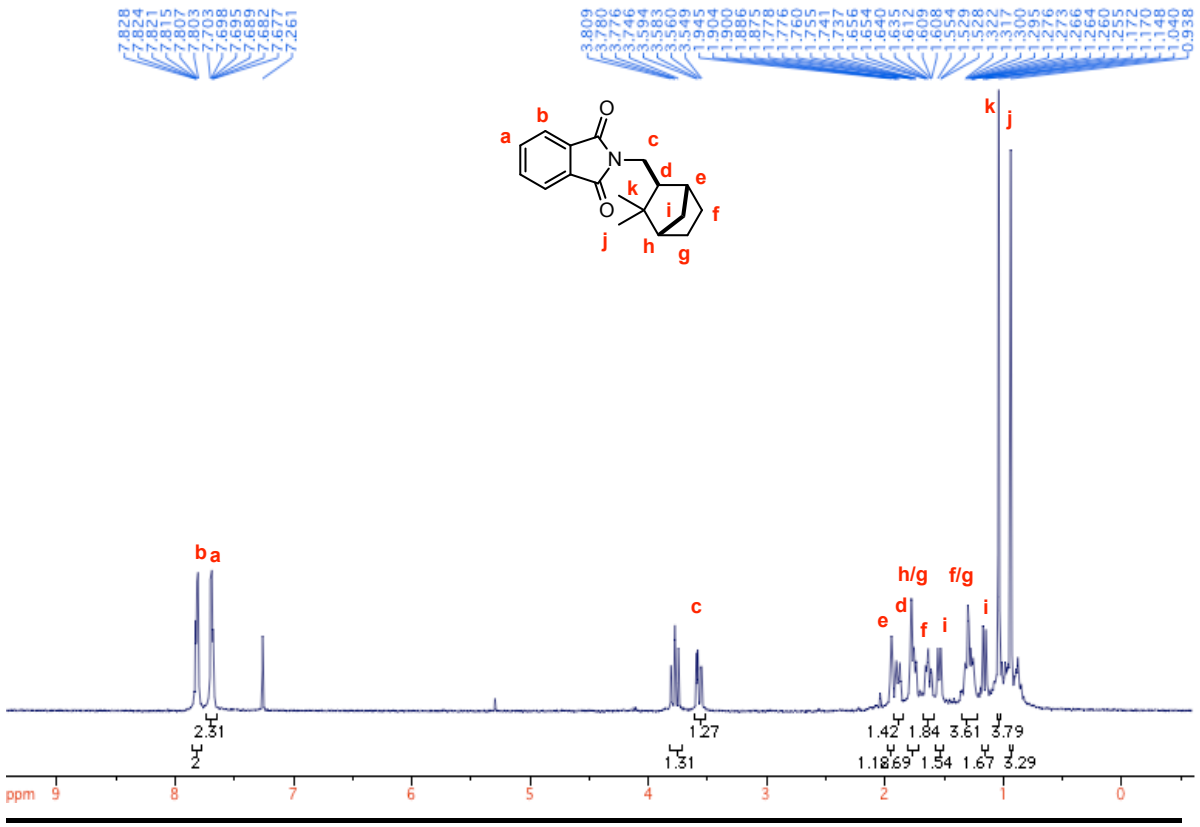
7.828
7.824
7.821
7.815
7.807
7.803
7.703
7.698
7.695
7.689
7.682
7.677
7.261
3.809
3.780
3.776
3.746
3.594
3.583
3.560
3.549
1.945
1.904
1.900
1.886
1.875
1.778
1.776
1.760
1.755
1.741
1.737
1.656
1.654
1.640
1.635
1.612
1.609
1.608
1.554
1.529
1.528
1.322
1.317
1.300
1.295
1.276
1.273
1.266
1.264
1.260
1.255
1.172
1.170
1.148
1.040
0.938
a
b
c
d
e
f
g
h
i
j
k
b a
c
e
d
h/g
f
i
f/g
i
k
j
2.31
2
1.27
1.31
1.42
1.18
1.84
69
1.54
3.61
1.67
3.79
3.29
ppm 9 8 7 6 5 4 3 2 1 0

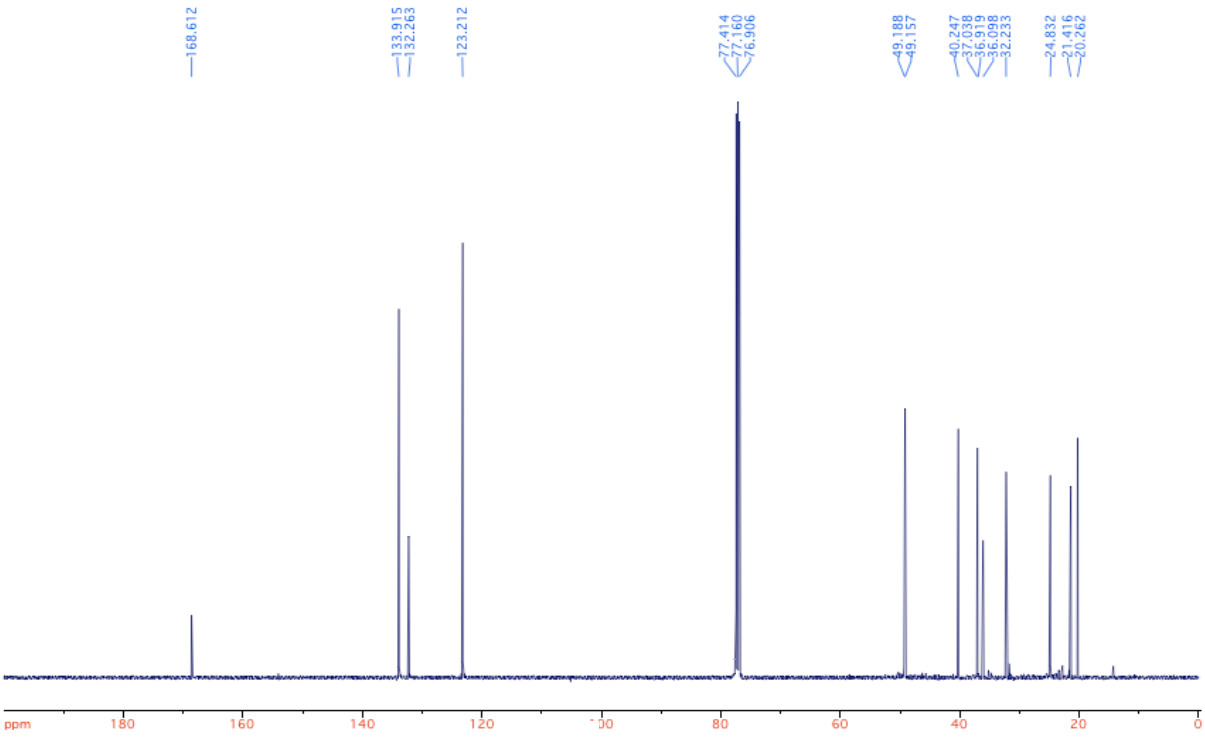
168.612
133.915
132.263
123.212
77.414
77.160
76.906
49.188
49.157
40.247
37.038
36.919
36.098
32.233
24.832
21.416
20.262
ppm 180 160 140 120 100 80 60 40 20 0

DEPT

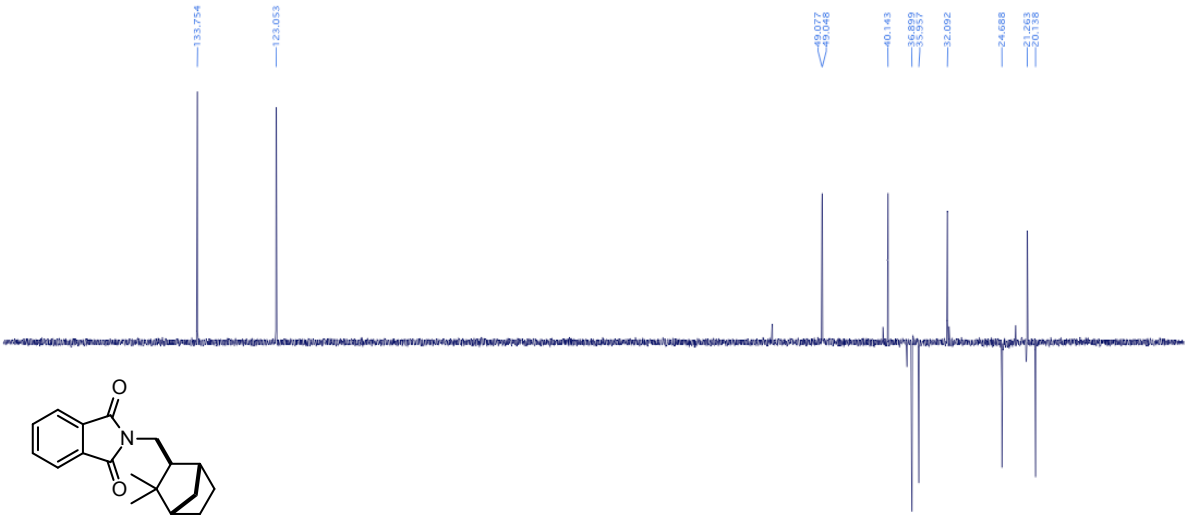
133.754
123.053
49.077
49.048
40.143
36.899
35.957
32.092
24.686
21.253
20.158
O
N
O

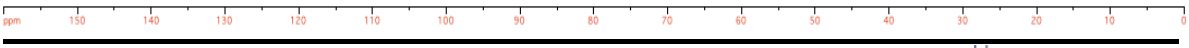
ppm
150
140
130
120
110
100
90
80
70
60
50
40
30
20
10
0

COSY

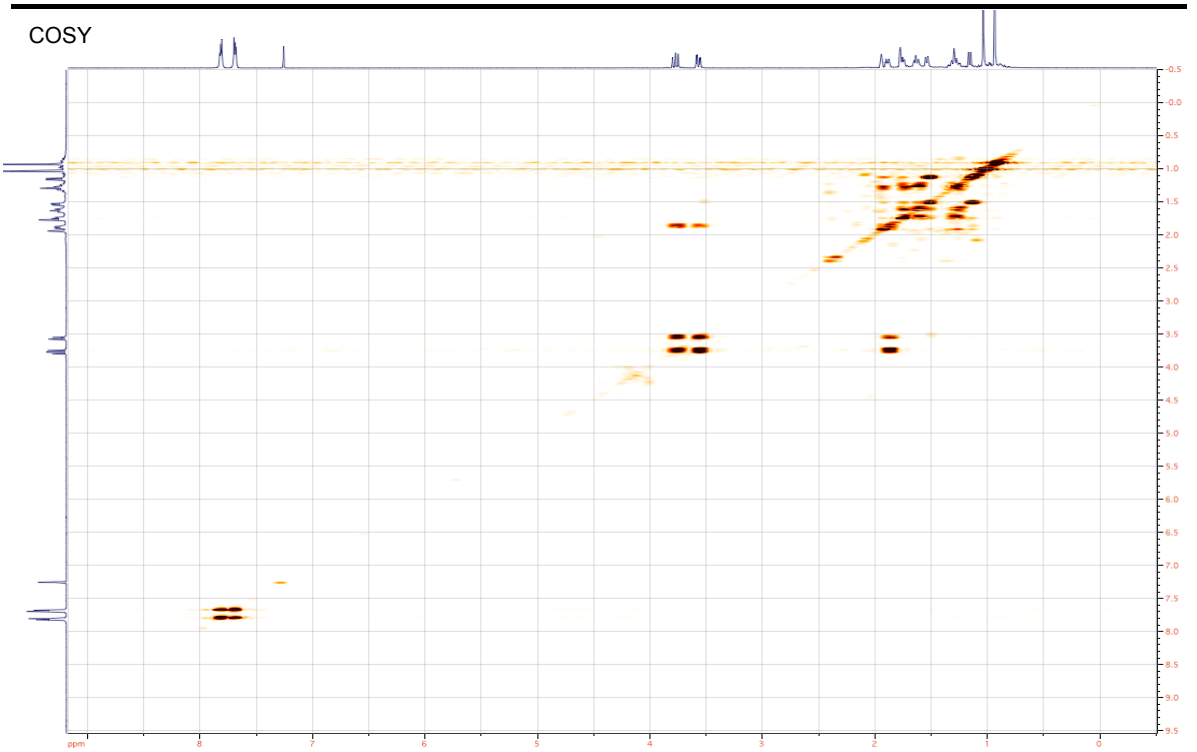
ppm
8
7
6
5
4
3
2
1
0

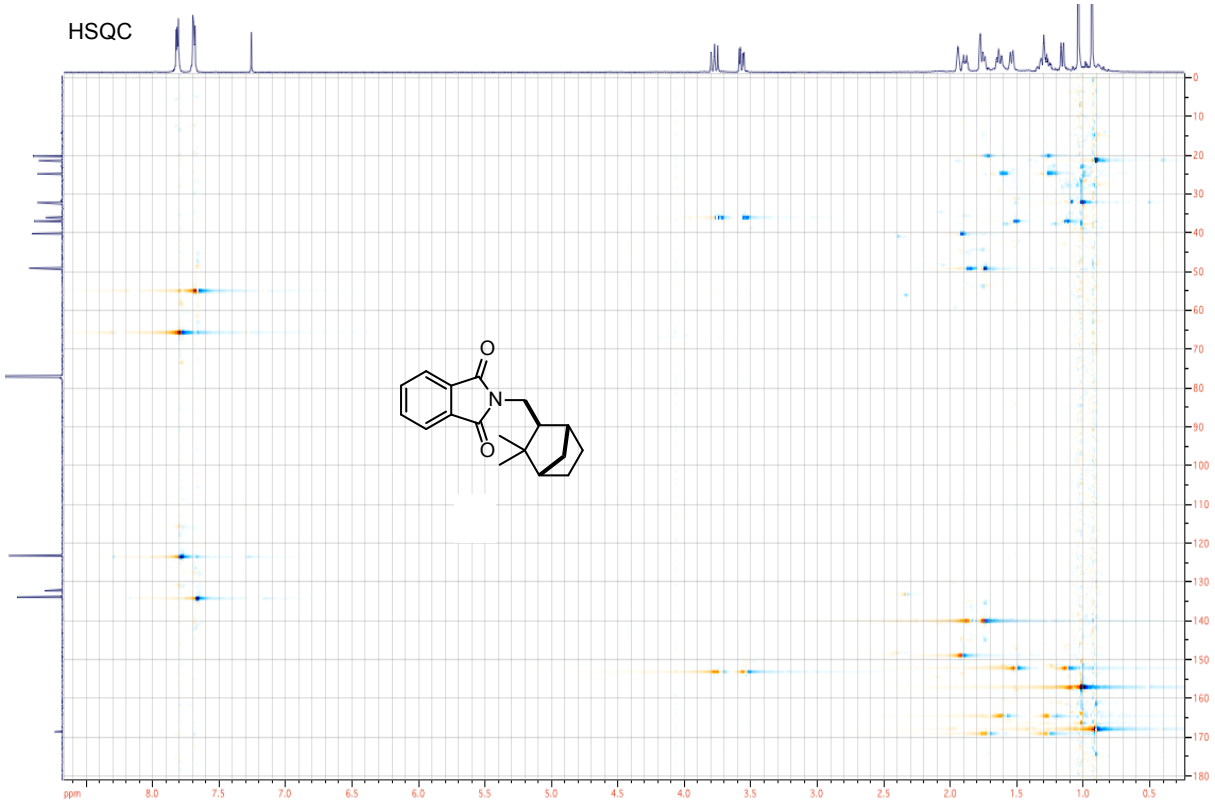
HSQC
O
N
O

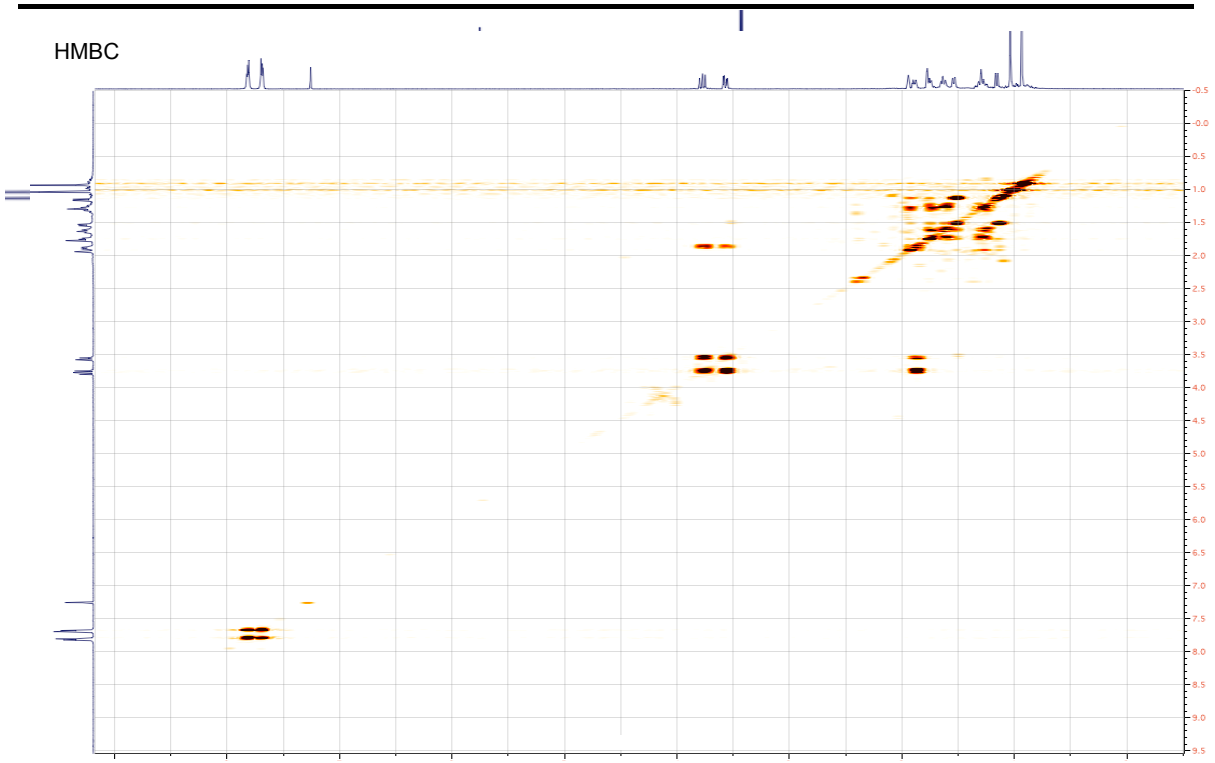
HMBC

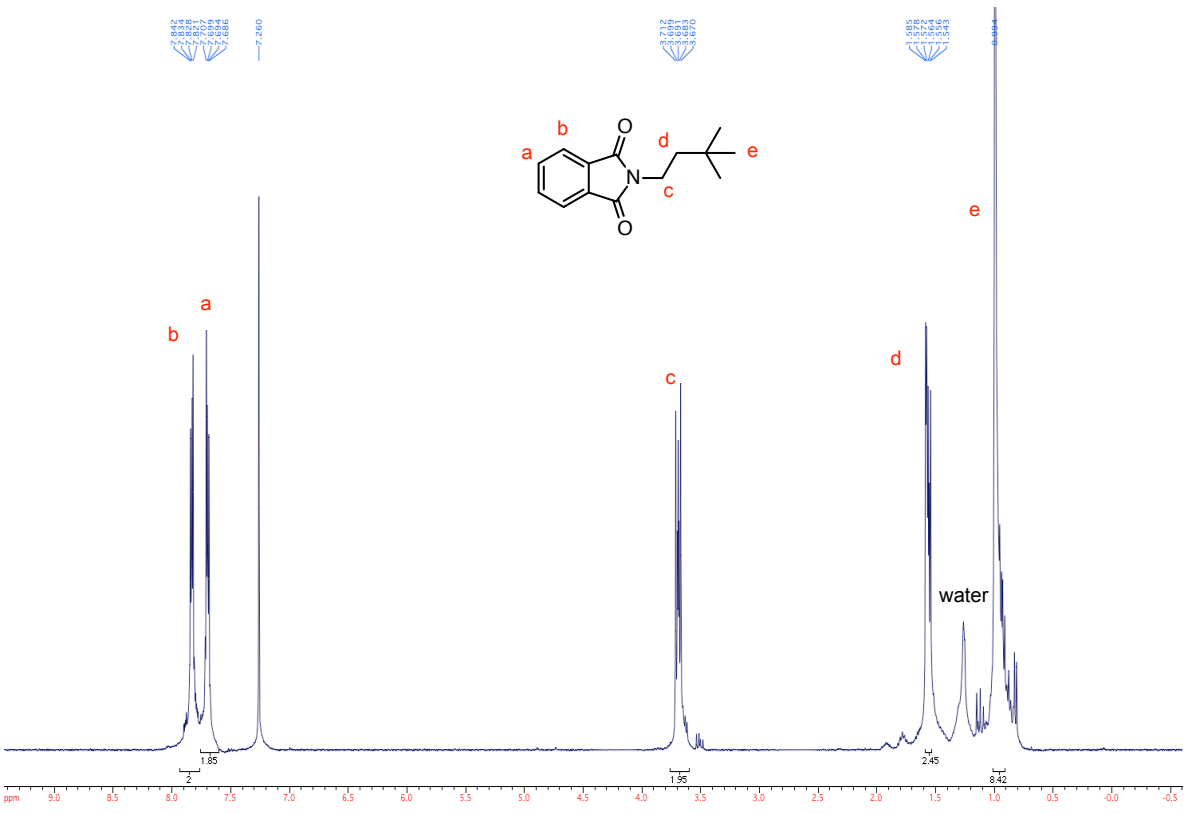
a
b
c
d
e
water
1.85
2
1.95
2.45
8.42
ppm

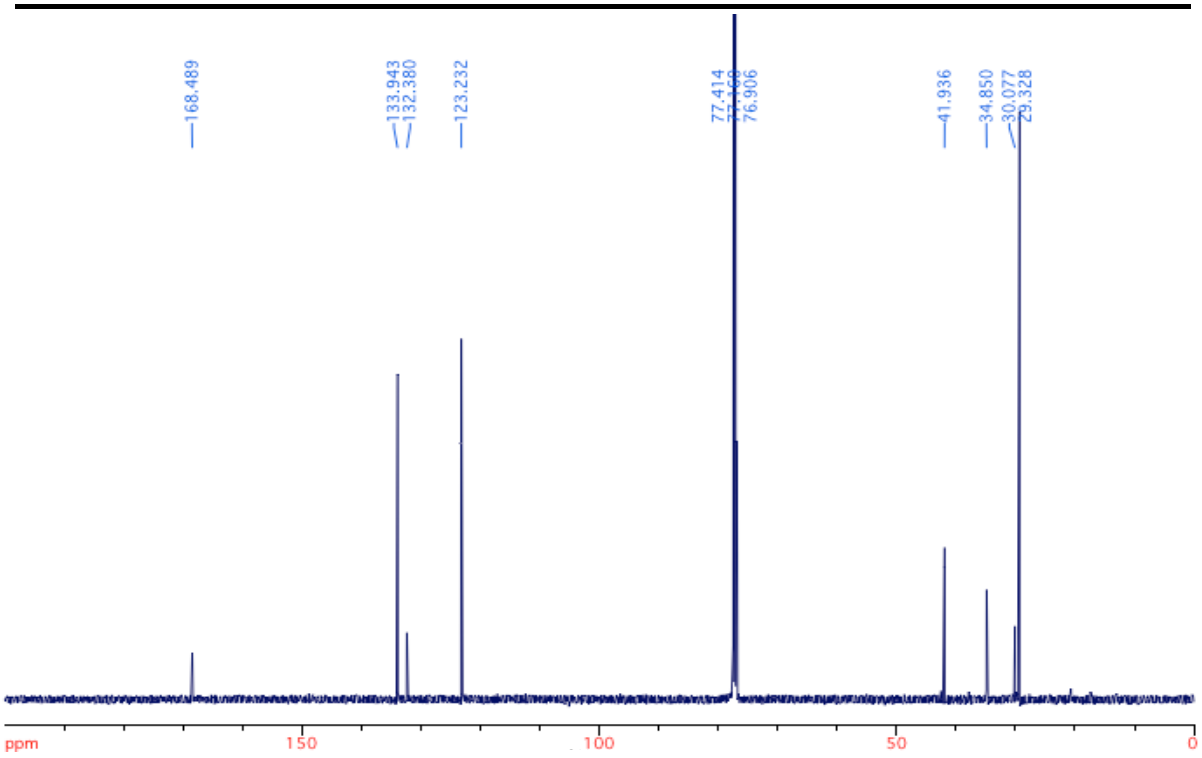
168.489
133.943
132.380
123.232
77.414
77.166
76.906
41.936
34.850
30.077
29.328
ppm
150
100
50
0

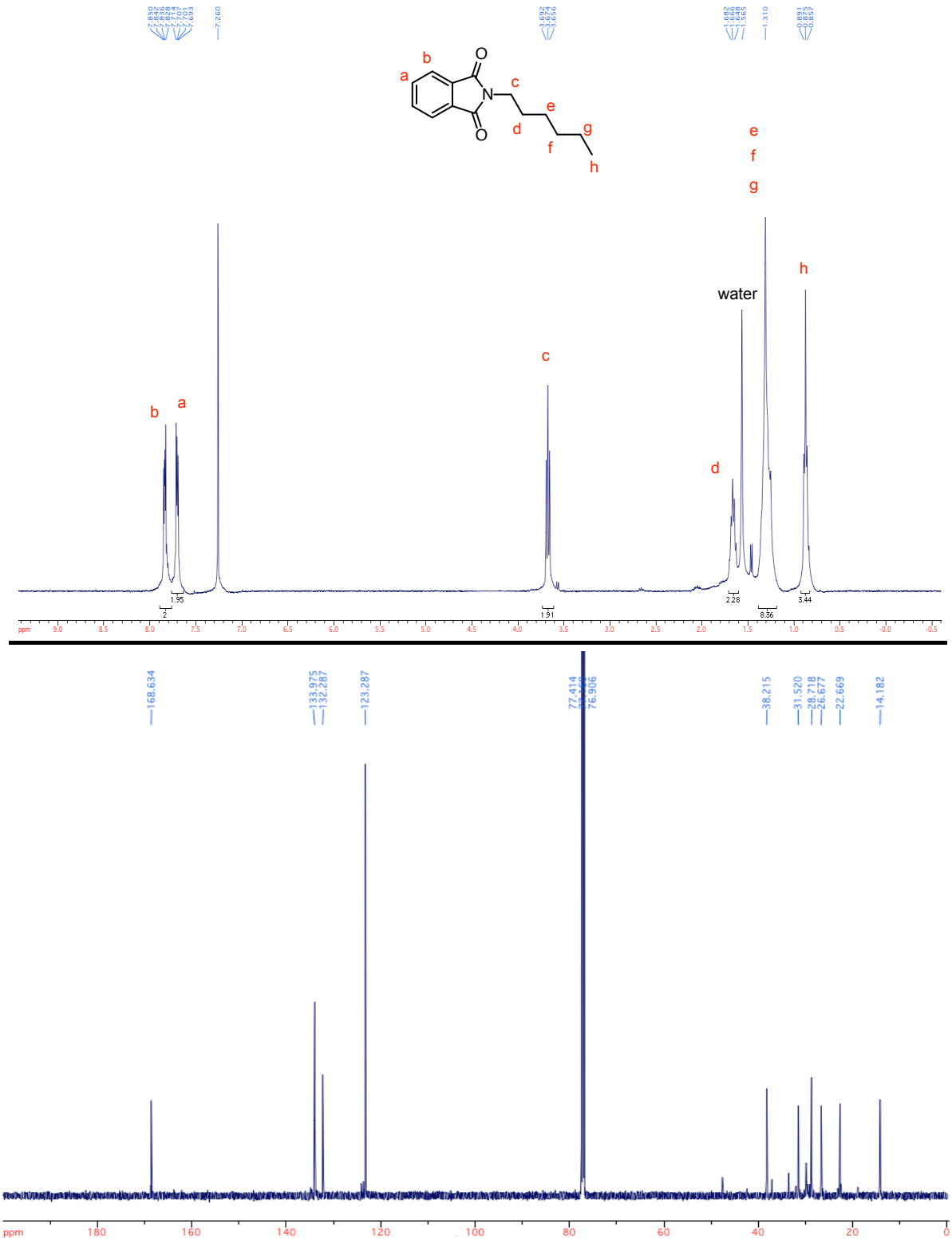
a
b
c
d
e
f
g
h
water
ppm

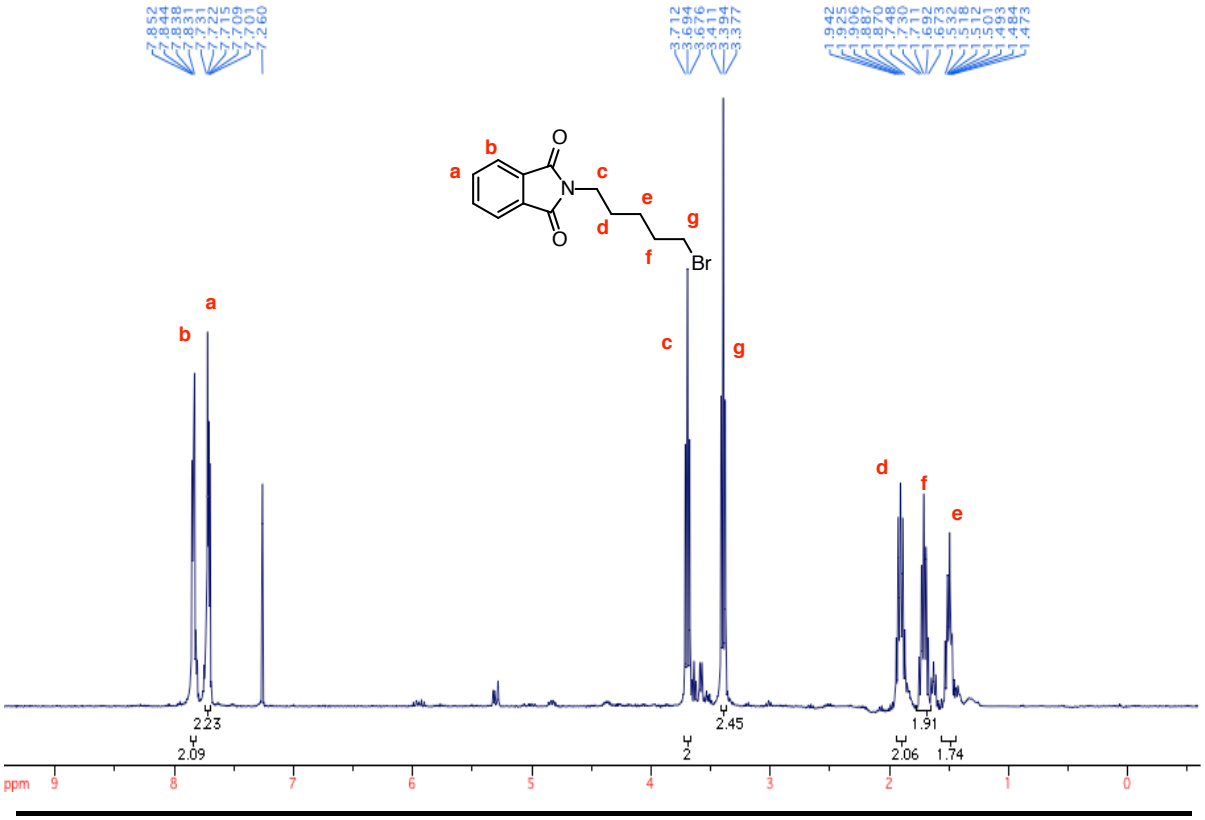
7.852
7.844
7.838
7.831
7.731
7.722
7.715
7.709
7.701
7.260
3.712
3.694
3.676
3.671
3.394
3.377
1.942
1.925
1.906
1.897
1.870
1.748
1.730
1.711
1.692
1.673
1.532
1.512
1.501
1.493
1.484
1.473
a
b
c
d
e
f
g
Br
2.23
2.09
2.45
2
1.91
2.06
1.74
ppm

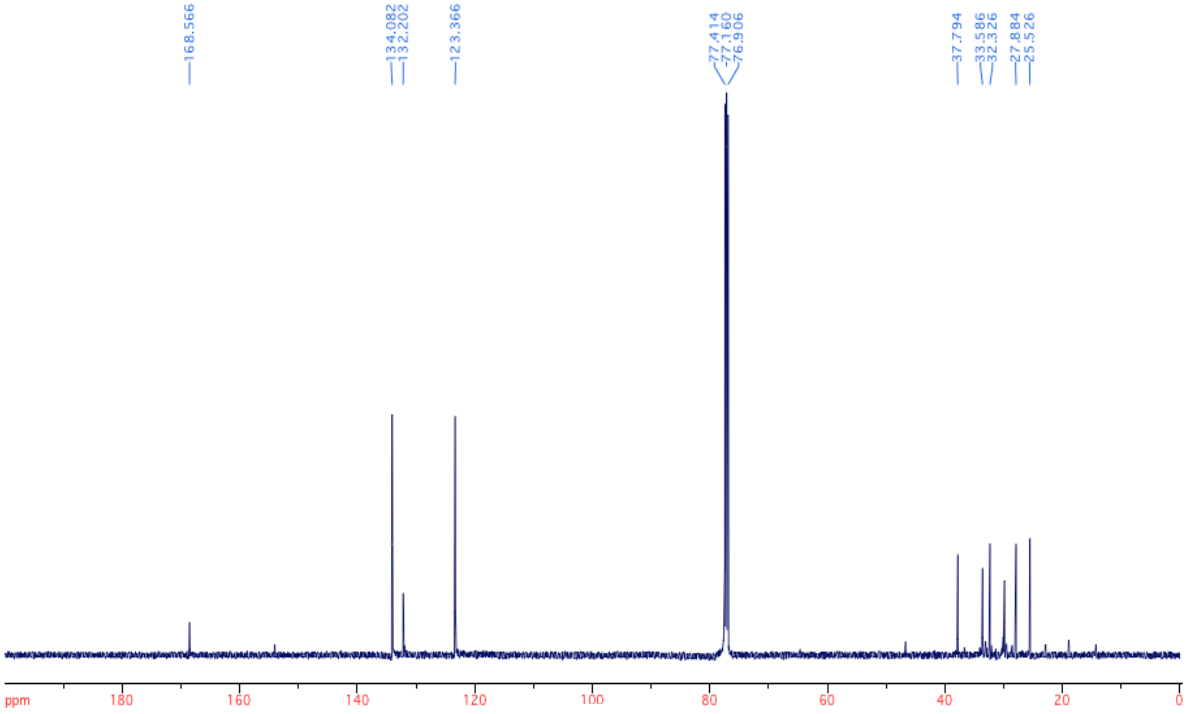
168.566
134.082
132.202
123.366
77.414
77.160
76.906
37.794
33.586
32.326
27.884
25.526
ppm

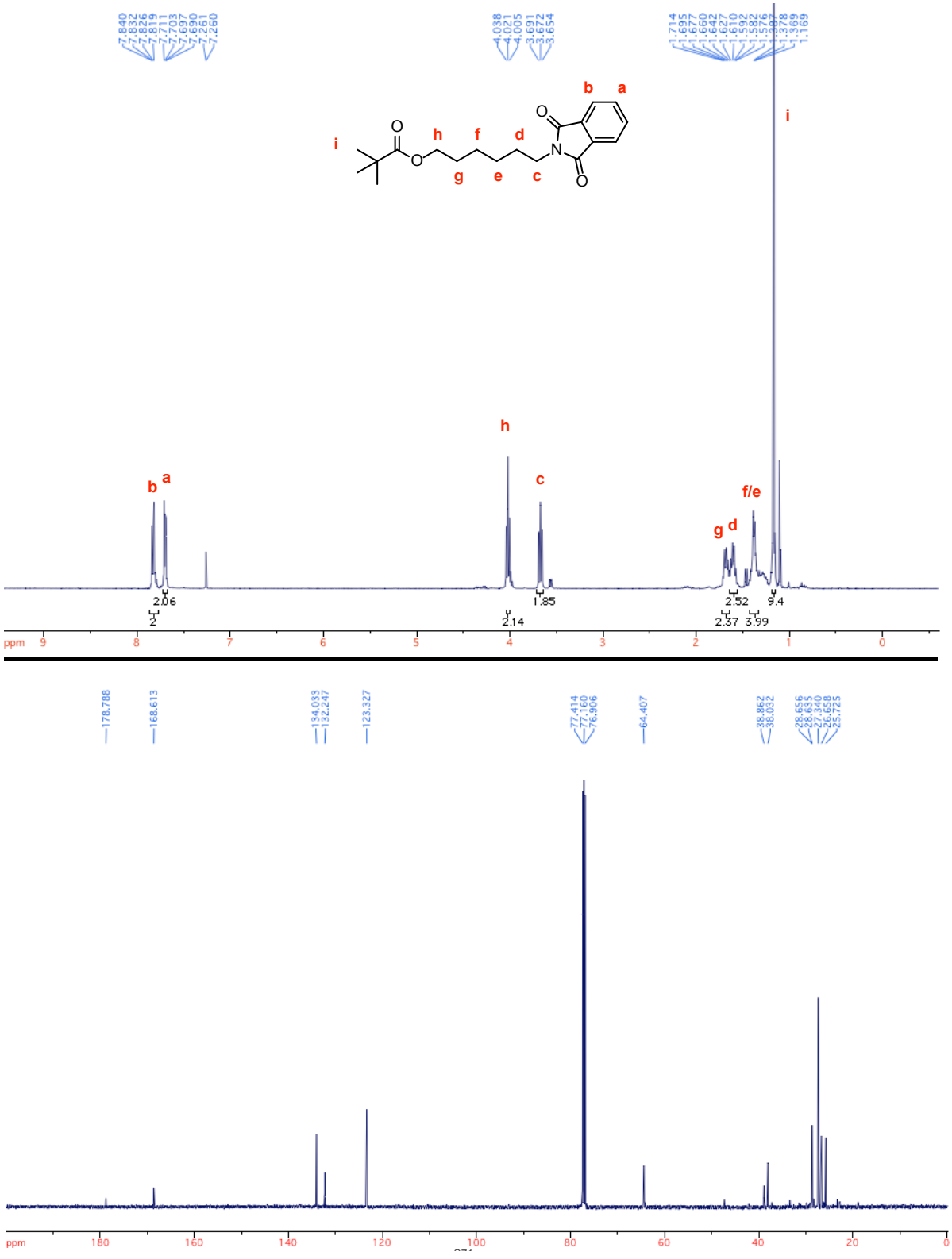
7.840
7.832
7.826
7.819
7.711
7.703
7.697
7.690
7.261
7.260
4.038
4.021
4.005
3.691
3.672
3.654
1.714
1.695
1.677
1.660
1.642
1.627
1.610
1.592
1.582
1.576
1.387
1.378
1.369
1.169
b a
i
h f d
g e c
O
O
O
O
N
b a
h
c
f/e
g d
i
2.06
2
2.14
1.85
2.52
2.37
9.4
3.99
ppm 9 8 7 6 5 4 3 2 1 0
178.788
168.613
134.033
132.247
123.327
77.414
77.160
76.906
64.407
38.862
38.032
28.656
28.635
27.340
26.658
25.725
ppm 180 160 140 120 100 80 60 40 20 0

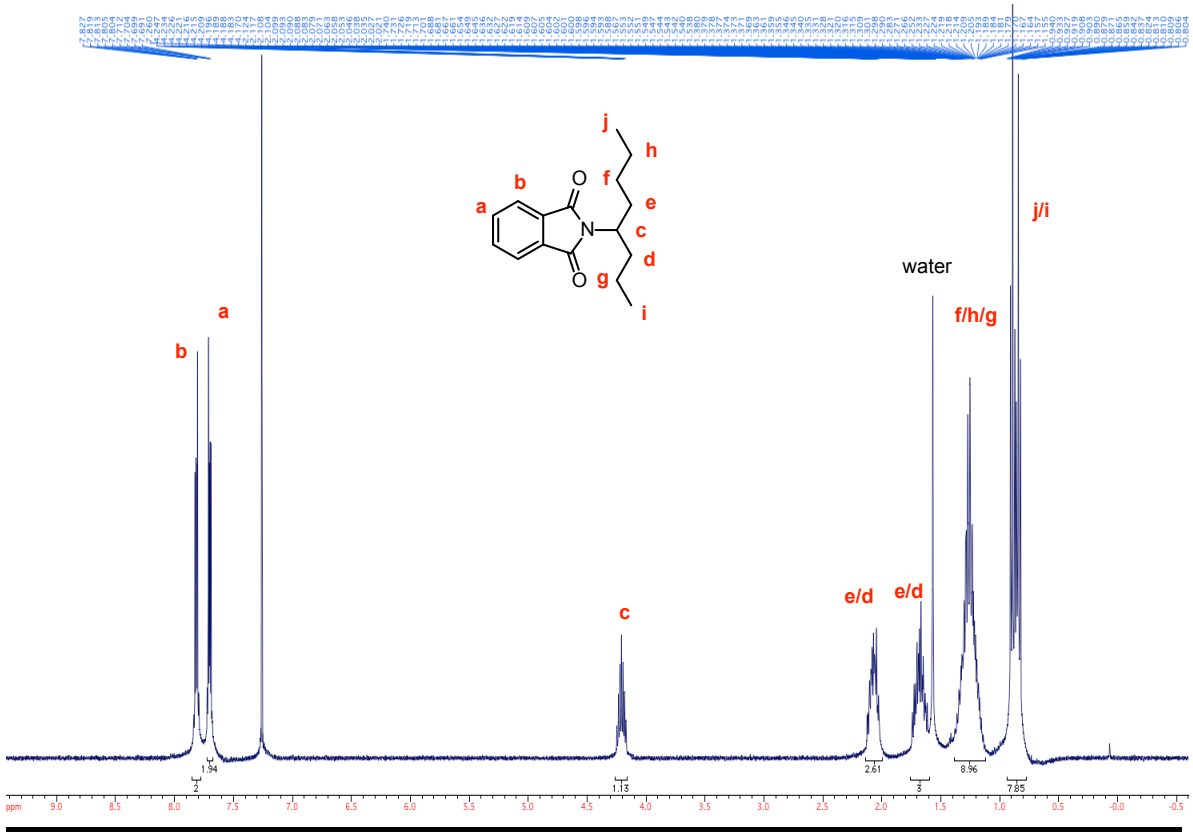
j
h
b
f
a
e
c
d
g
i
b
a
c
e/d
e/d
water
f/h/g
j/i
1.94
2
1.13
2.61
3
8.96
7.85
ppm

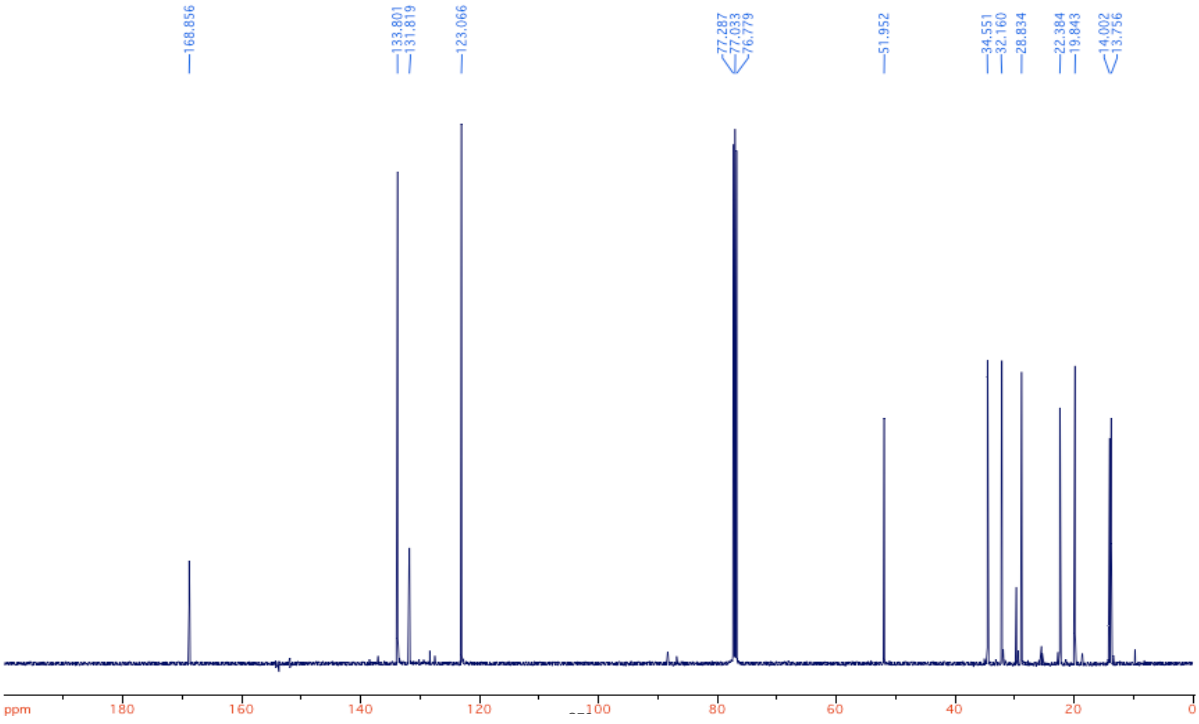
168.856
133.801
131.819
123.066
77.287
77.033
76.779
51.952
34.551
32.160
28.834
22.384
19.843
14.002
13.756
ppm

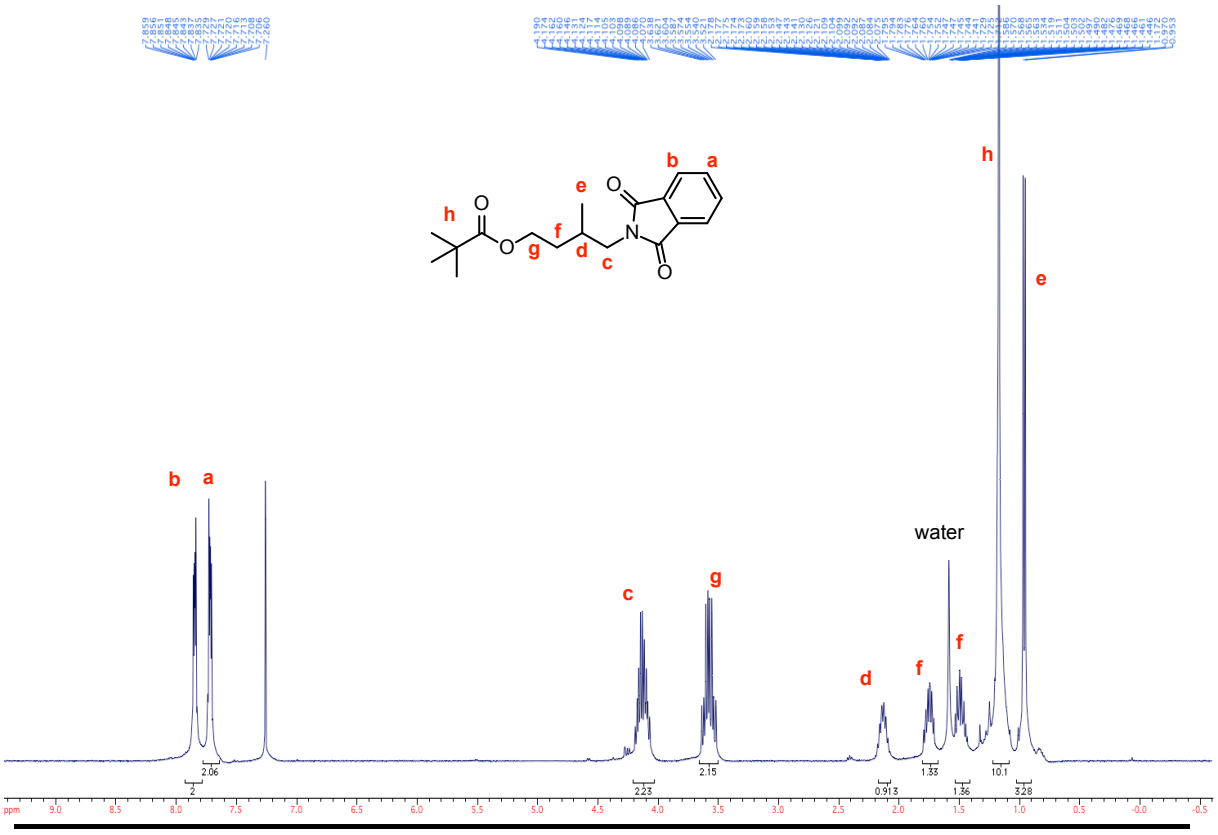
b
a
h
e
O
O
O
N
O
h
f
e
g
d
c
b
a
water
c
g
h
e
d
f
f
2.06
2.23
2.15
0.913
1.33
1.36
10.1
3.28
ppm
9.0
8.5
8.0
7.5
7.0
6.5
6.0
5.5
5.0
4.5
4.0
3.5
3.0
2.5
2.0
1.5
1.0
0.5
-0.0
-0.5

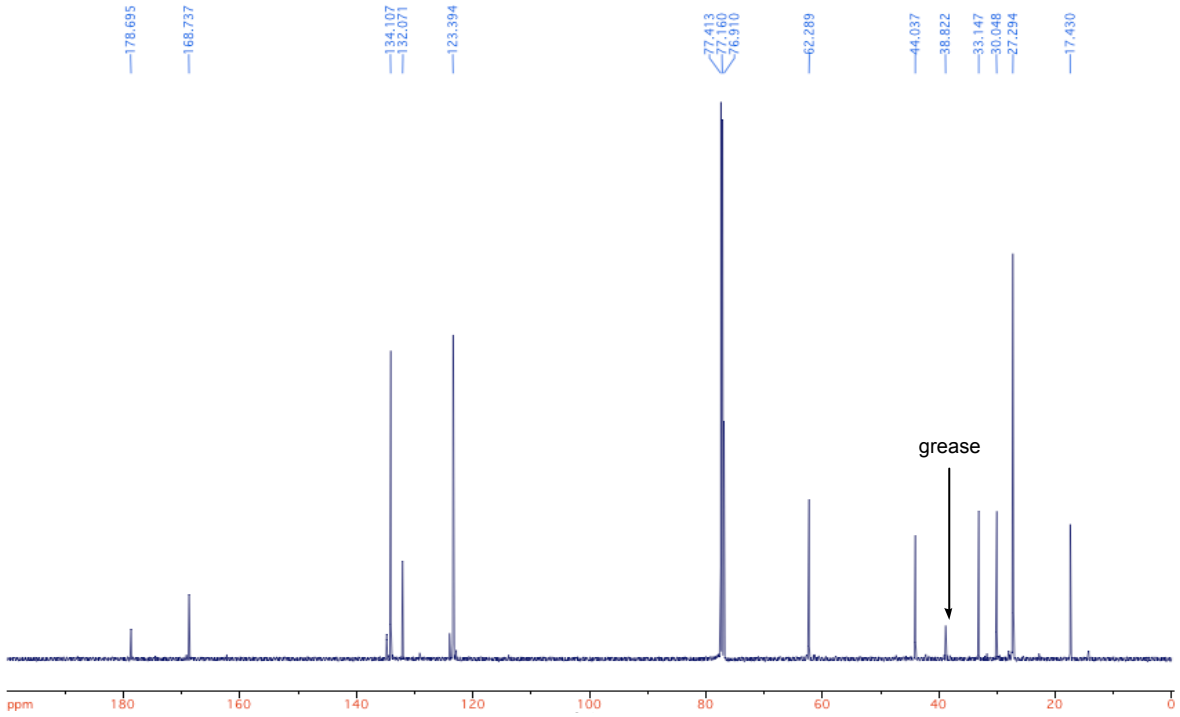
178.695
168.737
134.107
132.071
123.394
77.413
77.160
76.910
62.289
44.037
38.822
33.147
30.048
27.294
17.430
grease
ppm
180
160
140
120
100
80
60
40
20
0

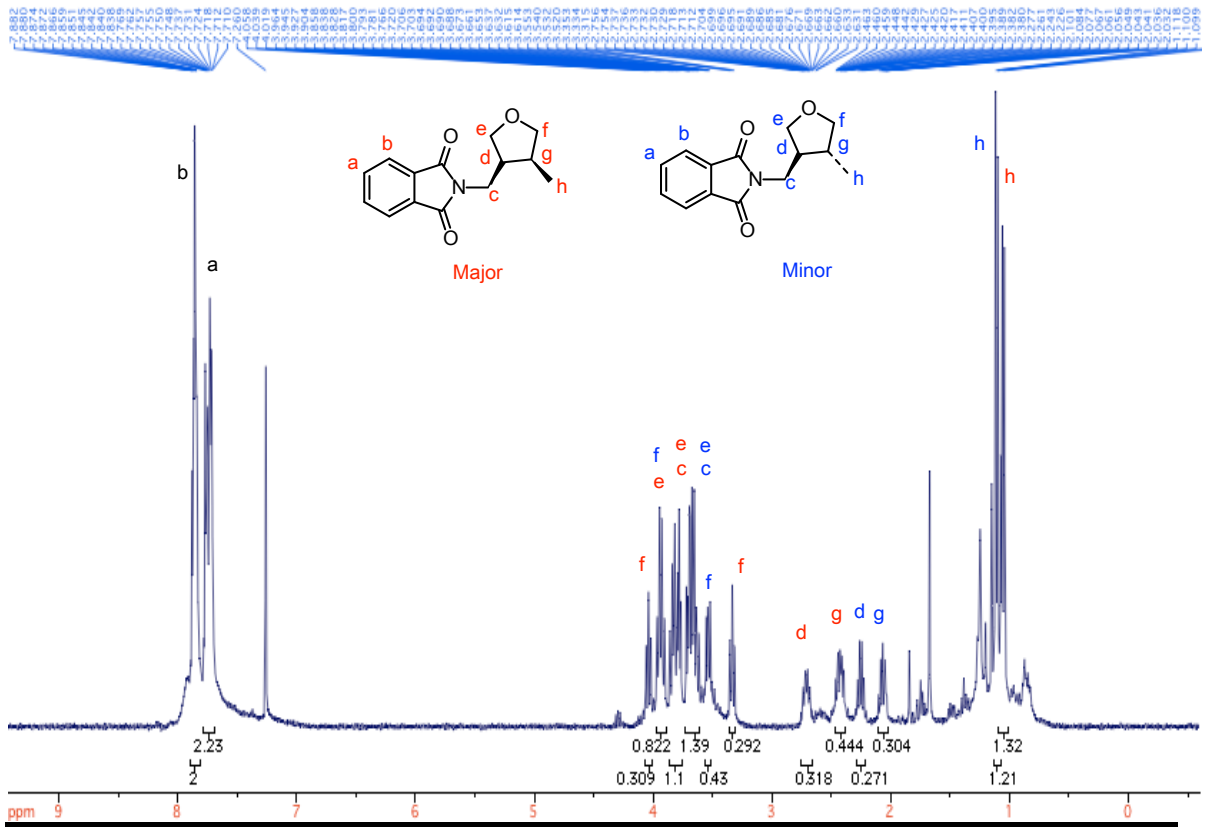
Major
Minor
2.23
2
0.822
0.309
1.39
1.1
0.292
0.43
0.444
0.318
0.304
0.271
1.32
1.21
ppm

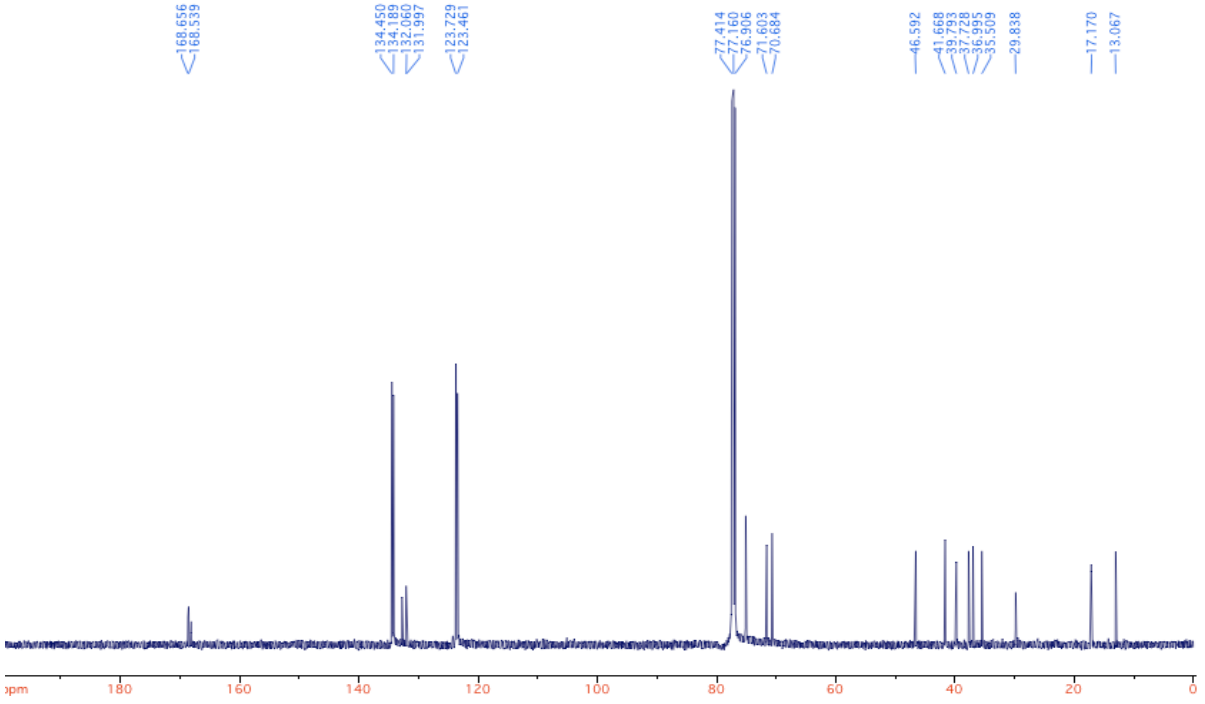
168.656
168.539
134.450
134.189
132.060
131.997
123.729
123.461
77.414
77.160
76.906
71.603
70.684
46.592
41.668
39.793
37.728
36.995
35.509
29.838
17.170
13.067
ppm

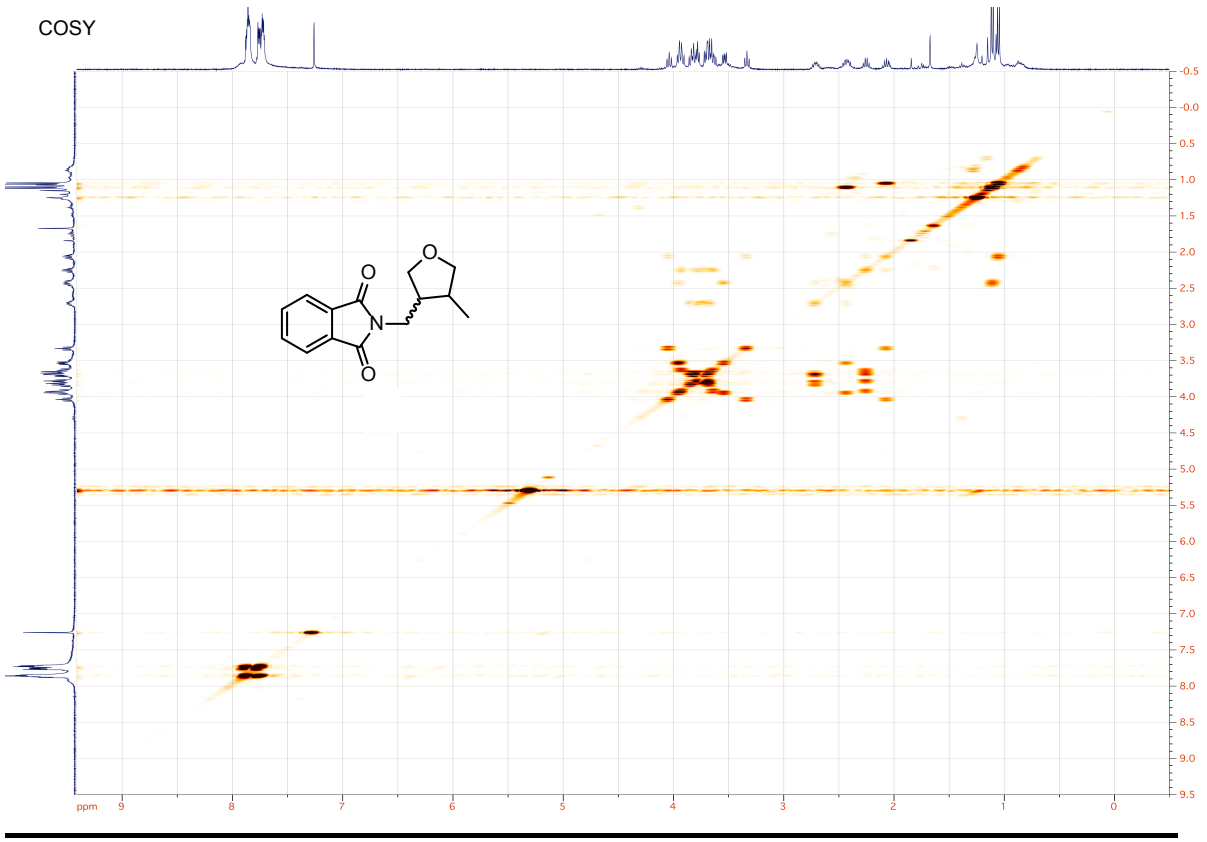
COSY
O
O
N
O
ppm
9
8
7
6
5
4
3
2
1
0
-0.5
-0.0
0.5
1.0
1.5
2.0
2.5
3.0
3.5
4.0
4.5
5.0
5.5
6.0
6.5
7.0
7.5
8.0
8.5
9.0
9.5

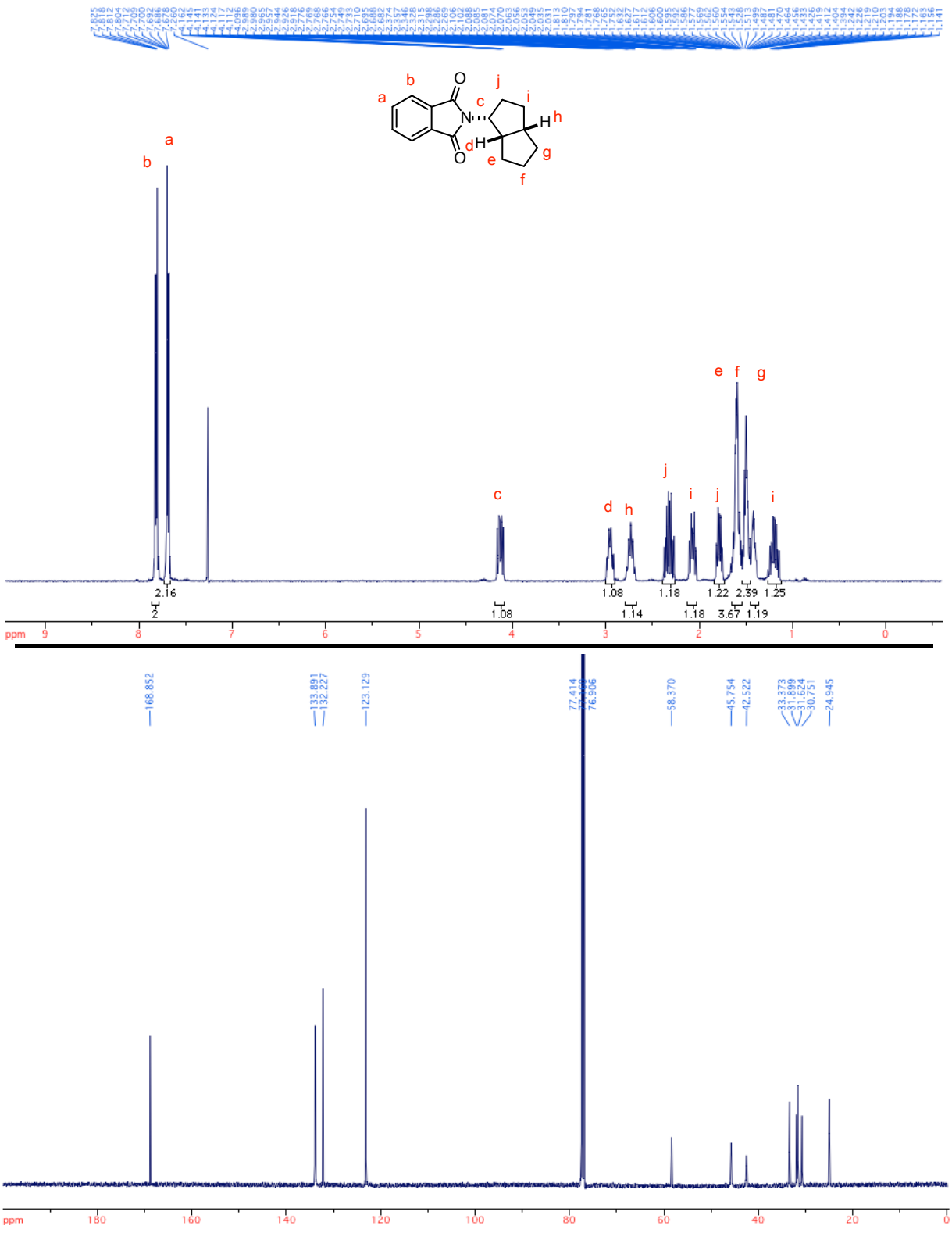
a
b
c
d
e
f
g
h
i
j
2.16
2
1.08
1.08
1.14
1.18
1.18
3.67
1.19
1.22
2.39
1.25
ppm
168.852
133.891
132.227
123.129
77.414
76.906
58.370
45.754
42.522
33.373
31.899
31.624
30.751
24.945

COSY

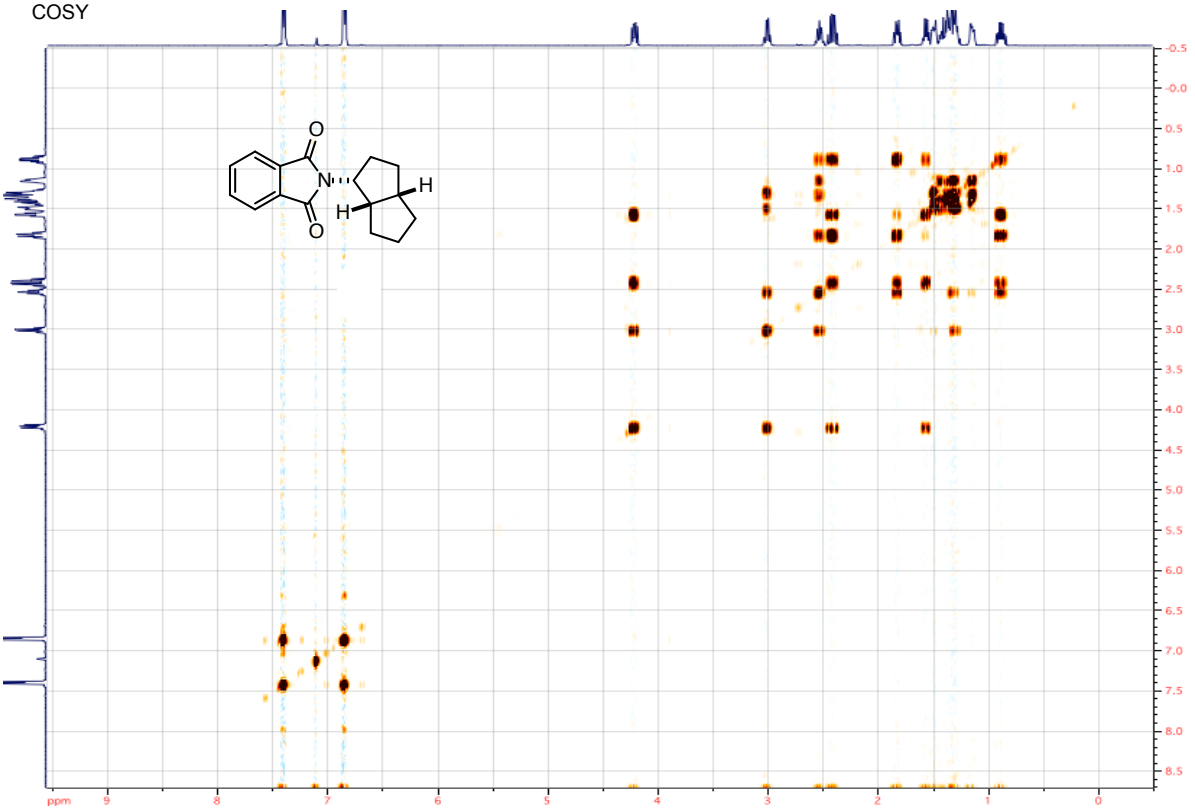
O
N
H
H
O
ppm
9
8
7
6
5
4
3
2
1
0

NOESY

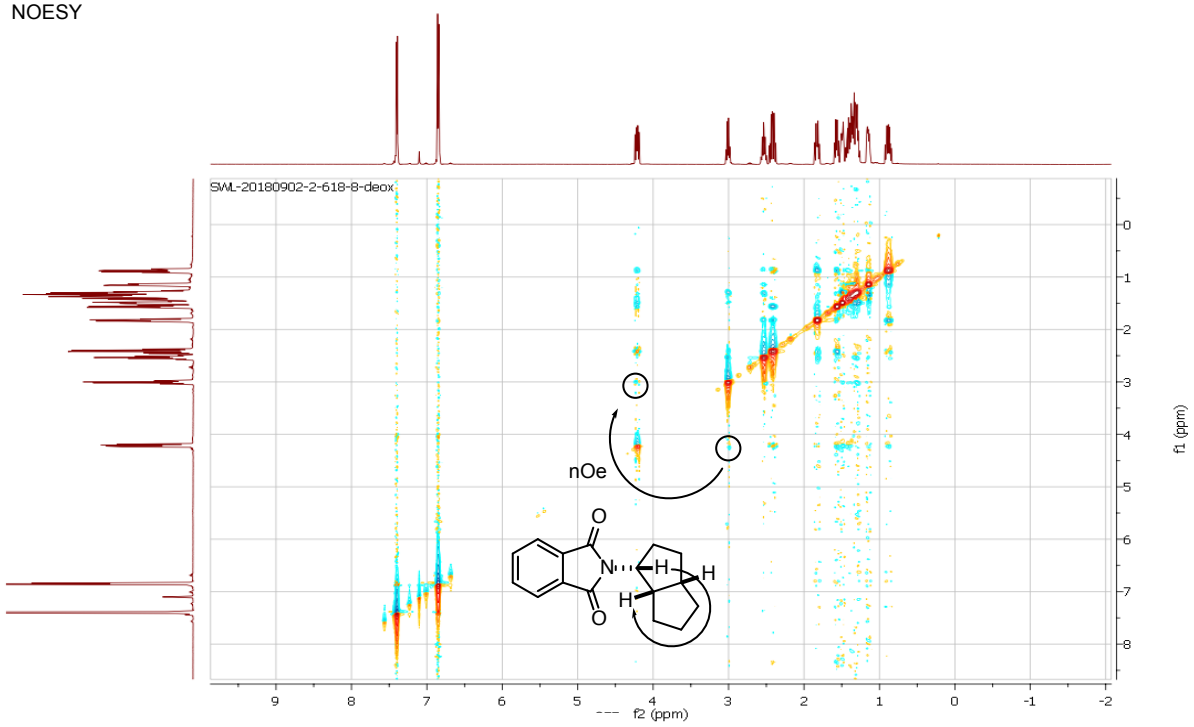
SML-20180902-2-618-8-deox
nOe
O
N
H
H
H
O
f2 (ppm)
f1 (ppm)

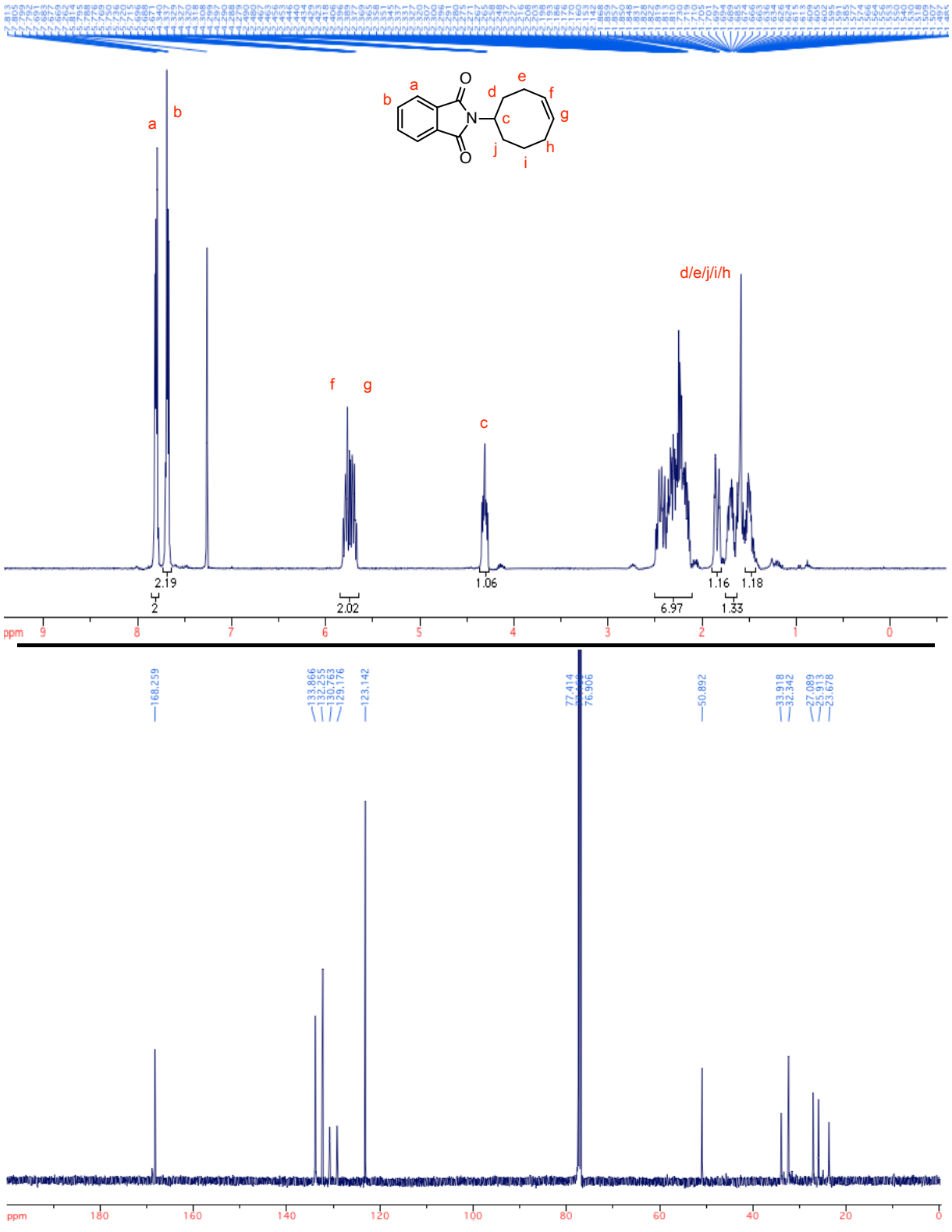
a
b
c
d
e
f
g
h
i
j
d/e/j/i/h
2.19
2
2.02
1.06
6.97
1.16
1.33
1.18
ppm
168.259
133.866
132.255
130.763
129.176
123.142
77.414
77.000
76.906
50.892
33.918
32.342
27.089
25.993
23.678

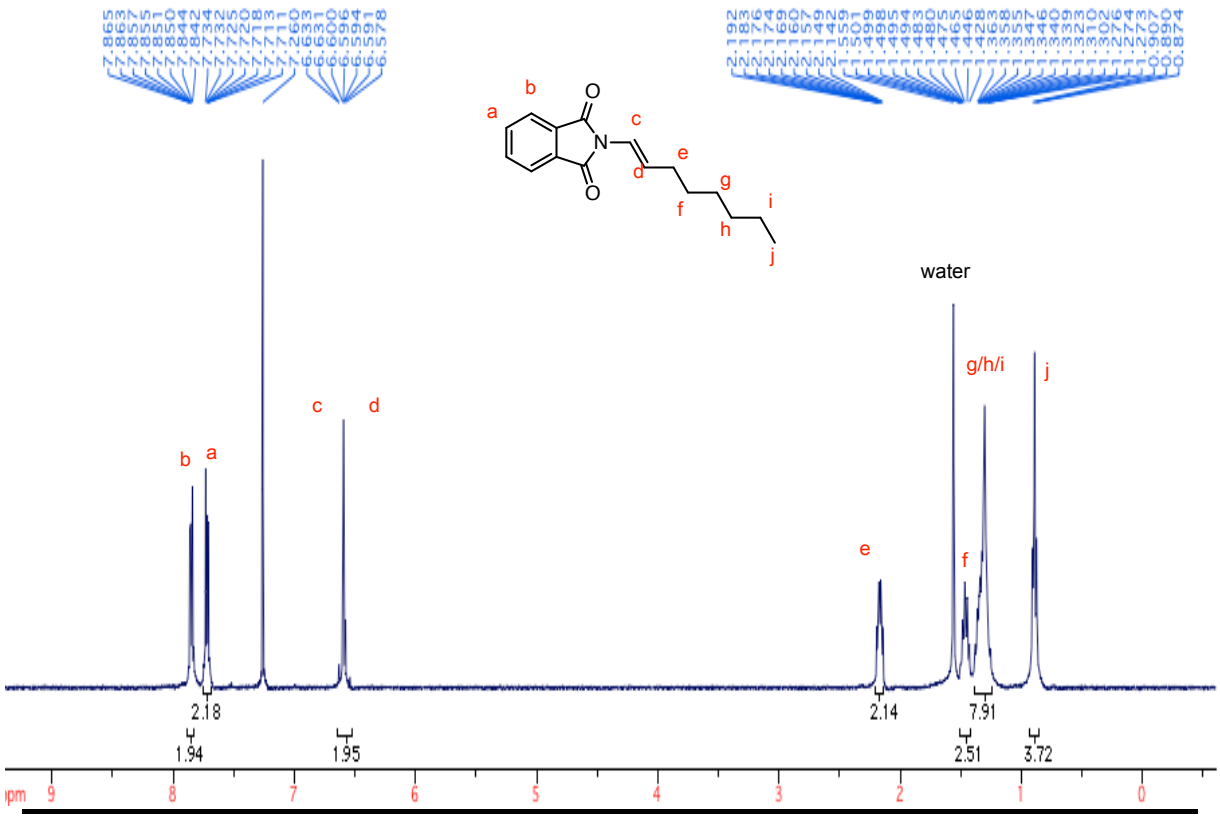
a
b
c
d
e
f
g
h
i
j
water
g/h/i
2.18
1.94
1.95
2.14
7.91
2.51
3.72
ppm

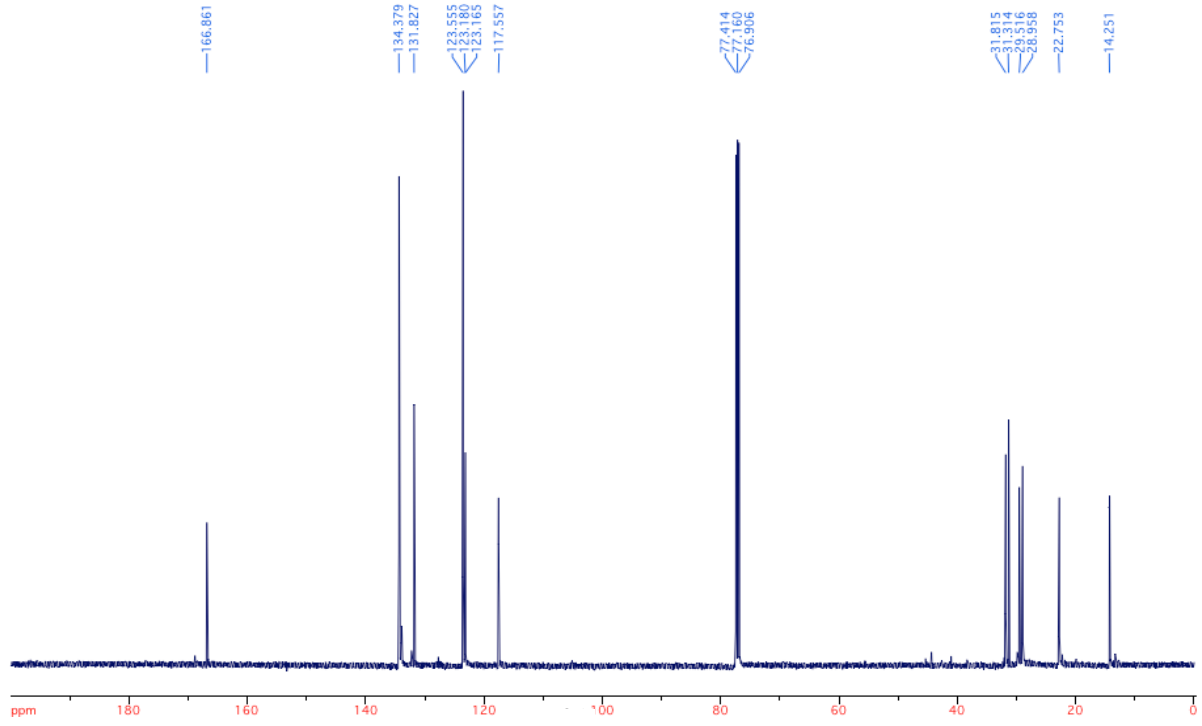
166.861
134.379
131.827
123.555
123.360
123.165
117.557
77.414
77.160
76.906
31.815
31.314
29.516
28.958
22.753
14.251
ppm

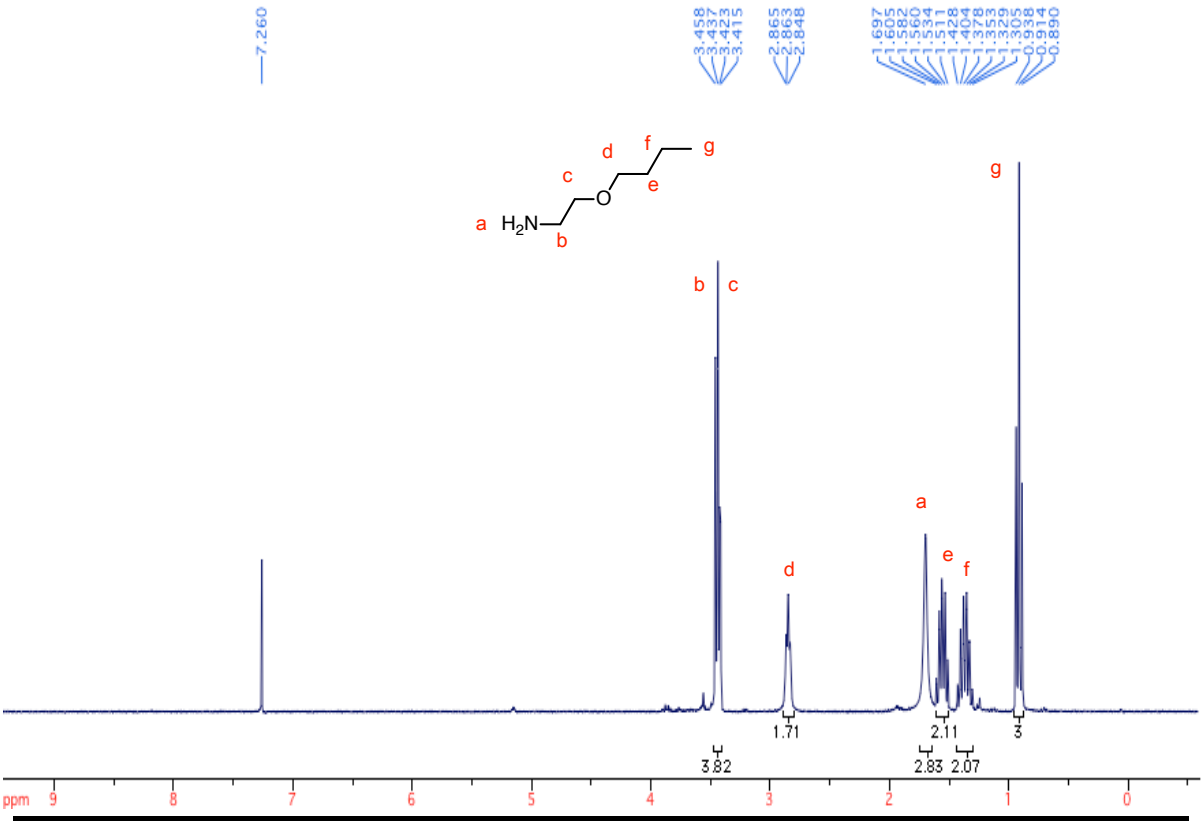
7.260
3.458
3.437
3.423
3.415
2.865
2.863
2.848
1.697
1.605
1.562
1.534
1.511
1.428
1.404
1.378
1.353
1.329
1.305
0.934
0.890
a
b
c
d
e
f
g
1.71
2.11
3
3.82
2.83
2.07
ppm

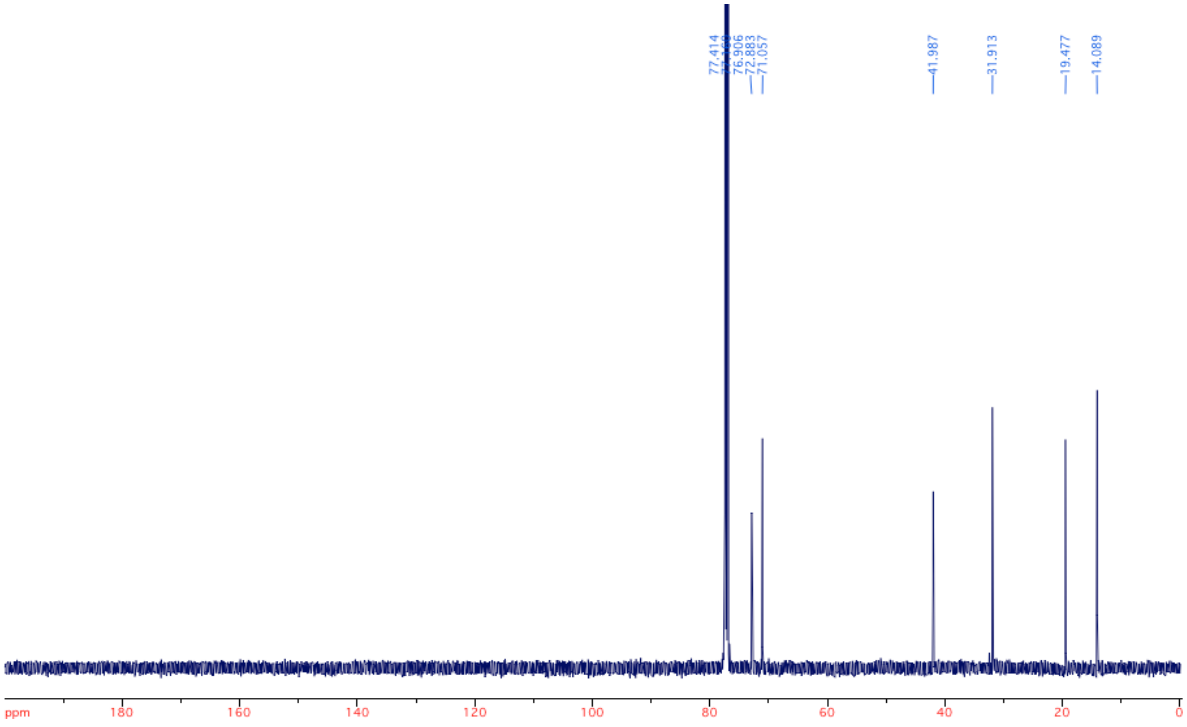
77.414
76.966
72.883
71.057
41.987
31.913
19.477
14.089
ppm

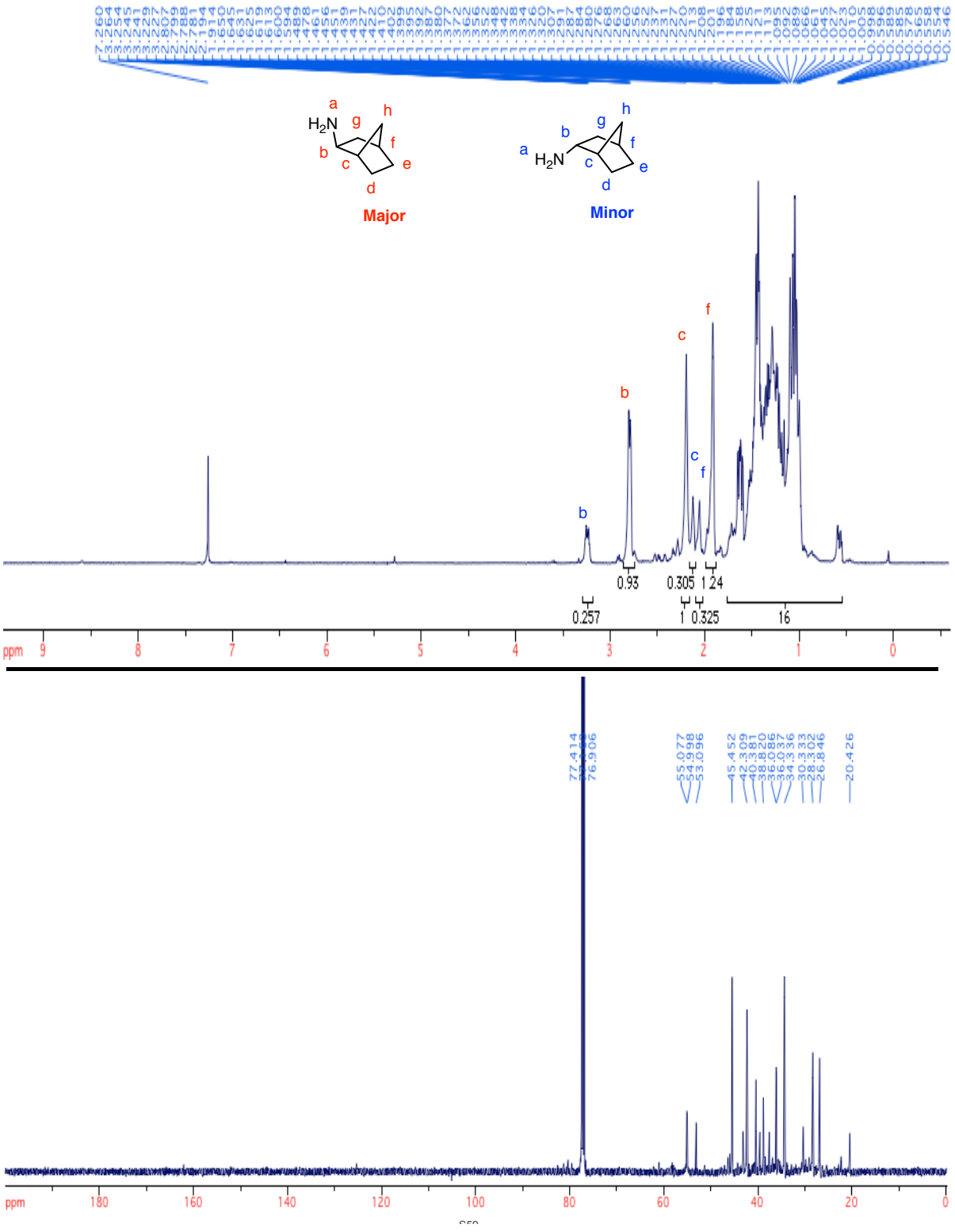
Major
Minor
0.93
0.305
1.24
0.257
1
0.325
16
ppm

## 1.7 References

[1] (a) Muller, T. E.; Beller, M. Metal-Initiated Amination of Alkenes and Alkynes. *Chem Rev.* **1998**, 675-704. (b) Hong, S.; Marks, T. J. Organolanthanide-Catalyzed Hydroamination. *Acc. Chem. Res.* **2004**, 673-686. (c) Muller, T. E.; Hultzsch, K. C.; Yus, M.; Foubelo, F.; Tada, M. Hydroamination: Direct Addition of Amines to Akenes and Alkynes. *Chem. Rev.* **2008**, 3795-3892. (d) Huang, L.; Arndt, M.; Gooßen, K.; Heydt, H.; Gooßen, L. Late Transition Metal-Catalyzed Hydroamination and Hydroamidation. *Chem. Rev.* **2015**, 2596-2697. (e) Coman, S. M.; Parvulescu, V. I. Nonprecious Metals Catalyzing Hydroamination and C-N Coupling reactions. *Org. Process Res. Dev.* **2015**, 1327-1355.

[2] (a) Ickes, A. R.; Ensign, S. C.; Gupta, A. K.; Hull, K. L. Regio- and Chemoselective Intermolecular Hydroamiantion of Allyl Imines for the Synthesis of 1,2-Diamines. *J. Am. Chem. Soc.* **2014**, 11256-11259. (b) Ensign, S. C.; Vanable, E. P.; Kortman, G. D.; Weir, L. J.; Hull, K. L. Anti-Markovnikov Hydroamination of Homoallylic Amines. *J. Am. Chem. Soc.* **2015**, 13748-13751.

[3] (a) Miller, D. C.; Ganley, J. M.; Musacchio, A. J.; Sherwood, T. C.; Ewing, W. R.; Knowles, R. R. Anti-Markovnikov Hydroamination of Unactivated Alkenes with Primary Alkyl Amines. *J. Am. Chem. Soc.* **2019**, 16590-16594. (b) Musacchio, A. J.; Nguyen, L. Q.; Beard, H.; Knowles, R. R. Catalytic Olefin Hydroamination with Aminium Radical Cations: A Photoredox Method for Direct C-N Bond Formation. *J. Am. Chem. Soc.* **2014**, 12217-12220.

[4] (a) Guin, J.; Mück-Lichtenfeld, C.; Frimme, S.; Studer, A. Radical Transfer Hydroamination with Aminated Cyclohexadienes Using Polarity Reversal Catalysis: Scope and Limitations. *J. Am. Chem. Soc.* **2007**, *129*, 4498-4503. (b) Kärkäs, M. D. Photochemical Generation of Nitrogen-Centered Amidyl, Hydrazonyl, and Imidyl Radicals: Methodology Developments and Catalytic Applications. *ACS Catal.* **2017**, *8*, 4999-5022.

[5] Chatilialoglu, C.; Studer, A. *Encyclopedia of Radicals in Chemistry, Biology and Materials Vol. 1-4*, Wiley: Chichester, UK, 2012.

[6] For a recent review of catalytic reactions using ammonia, see: Klinkenberg, J. L.; Hartwig, J. F. Catalytic Organometallic Reactions of Ammonia. *Angew. Chem. Int. Ed.* **2011**, *50*, 86-95.

[7] (a) Lünig, U.; Skell, P. S. Imidly Radicals. *Tetrahedron*, **1985**, *41*, 4289-4302. (b) Day, J. C.; Govindaraj, N.; McBain, . S.; Skell, P. S.; Tanko, J. M. The Chemistry of 1,8-Naphthalenedicarboximidyl and Phthalimidyl Raidcals. *J. Org. Chem.* **1986**, *51*, 4959-4963.

[8] Wuts, P. G. M.; Greene, T. W. *Greene's Protective Groups in Organic Synthesis*, 4th ed.; Wiley: Hoboken, 2007; pp 790−793.

[9] (a) Kim, H.; Kim, T.; Leed, D. G.; Roh, S. W.; Lee, C. Nitrogen-Centered Radical-Mediated C-H Imidation of Arenes and Heteroarenes Via Visible Light Induced Photocatalysis. *Chem. Commun.* **2014**, *50*, 9273-9276. (b) Allen, L. J.; Cabrera, P. J.; Lee, M.; Sandford, M. S. N-Acyloxyphthalimides as Nitrogen Radical Precursors in the Visible Light Photocatalyzed room

Temperature C-H Amination of Arenes and Heteroarenes. *J. Am. Chem. Soc.* **2014**, *136*, 5607-5610.

[10] (a) Day, J. C.; Katsaros, M. G.; Kocher, W. D.; Scott, A. E.; Skell, P. S.Addition Reactions of Imidyl Radicals with Olefins and Arenes. *J. Am. Chem. Soc.* **1978**, *100*, 1950-1951. (b) Kirsch, A.; Lünig, U.Imidly radicals 2. Radical Addition of N-Chlorophthalimide and N-Bromophthalimide to Alkenes. *J. Prakt. Chem./Chem.-Ztg.* **1998**, *340*, 129-134.

[11] Recupero, F.; Punta, C. Free Radical Functionalization of Organic Compounds Catalyzed by N-Hydroxyphthalimide. *Chem. Rev.* **2007**, *107*, 3800-3842.

[12] (a) Kharasch, M. S.; Mosher, R. A.; Bengelsdorf, I. S. Organophosphorus Chemistry. Addition Reaction of Diethyl Phosphate and the Oxidation of Triethyl Phosphite. *J. Org. Chem.* **1960**, *25*, 1000-1006. (b) Bentrude, W. G. Phosphoranyl Radicals – Their Structure, Formation, and Reactions. *Acc. Chem. Res.* **1982**, *15*, 117-125.

[13] Luo, Y.-R. *Handbook of Bond Dissociation Energies in Organic Compounds*; CRC Press: Boca Raton, 2003

[14] For a sample preparation, see: Patel, D. V.; Young, M. G.; Robinson, S. P.; Hunihan, L.; Dean, B. J.; Gordon, E. J. Hydroxamic Acid-Based Bisubstrate analog Inhibitors of Ras Farnesyl Protein Transferase. *J. Med. Chem.* **1996**, 4197-4210.

[15] Ames, D. E.; Grey, T. F. N-Hydroxy-imides. Part II. Derivatives of Homophthalic and Phthalic Acids. *J. Chem. Soc.* **1955**, 3518-3521.

[16] Newcomb, M. *Radicals in Organic Synthesis*; Wiley-VCH Verlag Gmbh: Weinheim, Germany, 2001; pp 327−329.

[17] Kharasch, M. S.; Jensen, E. V. Addition of Carbon Tetrachloride and Chloroform to Olefins. *Science* **1945**, 128.

[18] Rodygin, K. S.; Ananikov, V. P. An Efficient and Metal-Free Pathway to Vinyl Thioesters with Calcium Carbide as the Acetylene Source. *Green Chem.* **2016**, *18*, 482-486.

[19] Reid, W. B.; Spillane, J. J.; Krause, S. B.; Watson, D. A. Direct Synthesis of Alkenyl Boronic Esters from Unfunctionalized Alkenes: A Boryl-Heck Reaction. *J. Am. Chem. Soc.* **2016**, 5539-5542.

[20] Luo, W.; Lin, L.; Zhang, Y.; Liu, X.; Feng, X. Construction of Distant Stereocenters by Enantioselective Desymmetrizing Carbony-Ene Reaction. *Org. Lett.* **2017**, 3374-3377.

[21] Mendenhall, G. D. The Lewis Acid Catalyzed Reaction of Trans-Hyponitrite Ion with Alkyl Halides. *Tett. Lett.* **1983**, 451-452.

# Chapter 2: Intermolecular Aminoallylation of Alkenes using Allyl-Oxyphthalimides

## 2.1 Introduction

Methods that are capable of achieving the difunctionalization of an alkene are exceptionally powerful, as they can rapidly introduce complex molecular functionality in a single step.[1] Furthermore, the use of alkenes as starting materials is attractive because olefinic substrates are widely available and constitute a diverse class of molecules. As previously mentioned in Chapter 1, pioneering work from Kharasch demonstrated the difunctionalization of alkenes via ATRA using simple halogenated reagents such as carbon tetrachloride in the presence of light or a thermal radical initiator (Scheme 2.1). This work from Kharasch set the stage for the development of a wide array of ATRA mediated processes that allow for alkene difunctionalization.[2]

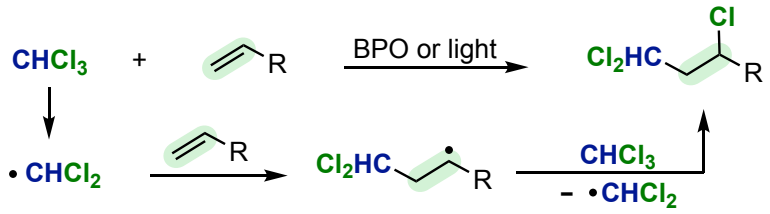


Scheme 2.1. ATRA difunctionalization of alkenes.

In the same vein as this, group transfer radical addition (GTRA) strategies are similar to ATRA, but allow for the transfer of more complex functionalities to an alkene, aside from just a single atom.[3] Particularly powerful in polymer synthesis, GTRA has found a wide range of applications in synthetic chemistry toward the synthesis of complex products from simple alkenes.

In light of the mechanistic evidence supporting an ATRA type mechanism for our hydroamination procedure as described in Chapter 1, we hypothesized that O-functionalized derivatives of NHPI could serve as alkene difunctionalization reagents by transferring a general group "G" to an alkene (Scheme 2.2). In pursuit of this theory, we sought to both provide further

evidence toward our mechanistic hypothesis for the hydroamination method, as well as develop a new method for the amino-difunctionalization of alkenes.

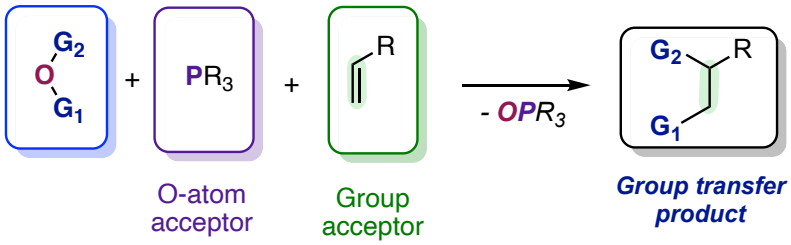


Scheme 2.2. General O-atom transfer, GTRA strategy.

In surveying the literature, we were inspired by the work of James Tanko[4] who had demonstrated the allyl-transfer capability of allyl-oxyphthalimides in the presence of benzylic substrates (Scheme 2.3). We hypothesized that in the presence of an effective O-atom transfer reagent such as a phosphite, these allyl-oxyphthalimides could be repurposed for the aminoallylation of alkenes.

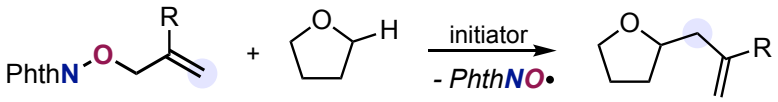


Scheme 2.3. Allyl-oxyphthalimides as ally-transfer reagents.

## 2.2 Reaction Optimization and Substrate Scope

We began this investigation by subjecting allyl-oxyphthalimide derivative **2.2a** to reaction conditions similar to those employed for our prior hydroamination procedure. We elected **2.2a** as the model substrate because we anticipated that the electron deficient character of this substrate would help facilitate productive reactivity with an electron rich, external alkene such as NBVE, which we also selected as a model substrate because of favorable polarity matching (10 equiv). In line with our previous experience, we also employed DLP (0.1 equiv) as radical initiator and triethyl phosphite (1.5 equiv) as O-atom transfer reagent in DCE at 90 °C (Table 2.1, entry 1).

Table 2.1. Aminoallylation reaction optimization. All reactions carried out with **2.2a** (1 equiv) and *n*-butyl vinyl ether (10 equiv) in the specified solvent (0.04 M) ubnless otherwise specified. [a]Determined by gas chromatography using mesitylene as an internal standard. [b]isolated yield of 26% following purification on silica gel.

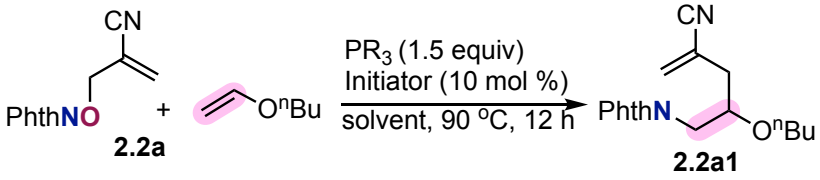


**2.2a** **2.2a1**

| Entry | $PR_3$ | Initiator | Solvent | Yield[a] |
|---|---|---|---|---|
| 1 | $P(OEt)_3$ | DLP | DCE | 34% |
| 2 | $P(OtBu)_3$ | DLP | DCE | <5% |
| 3 | $P(OiPr)_3$ | DLP | DCE | 20% |
| 4 | $P(OMe)_3$ | DLP | DCE | 45%[b] |
| 5 | $P(OMe)_3$ | AIBN | DCE | 21% |
| 6 | $P(OMe)_3$ | BPO | DCE | <5% |
| 7 | $P(OMe)_3$ | DLP | MeCN | 36% |
| 8[c] | $P(OMe)_3$ | DLP | Benzene | <5% |
| 9[d,e] | None | DLP | DCE | <5% |
| 10 | $P(OMe)_3$ | None | DCE | <5% |

As hypothesized, deoxygenative aminoallylation product **2.2a1** was produced and isolated, albeit in 34% yield. Interestingly, the main product from this reaction, isolated in 42% yield, was *N*-(*O*-ethyl) hydroxyphthalimide resulting from an Arbuzov-type, $S_N2$' substitution reaction (Scheme 2.4).

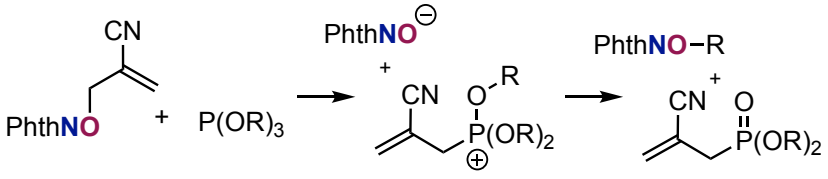


Scheme 2.4. Arbuzov-type side reactivity for aminoallylation.

In an effort to improve reaction efficiency and decrease the proclivity for the observed Arbuzov side reactivity, we explored the use of bulkier phosphites, as this would predictably diminish the ability of substitution to occur due to enhanced steric hinderance. Switching from triethyl phosphite to the bulkier tert-butyl variant indeed decreased the undesired Arbuzov reactivity, but also shunted the aminoallylation process, with only trace quantitites of **2.2a1** being formed (entry 2). Switching to triisopropyl phosphite similarly reduced the Arbuzov side reactivity, but unfortunately resulted in a mere 20% yield for the aminoallylation product (entry 3). Contrary to our initial hypothesis, the least bulky trimethyl phosphite resulted in the greatest yield of **2.2a1** (entry 4). Interestingly, O-atom transfer involving peroxy radicals and trimethyl phosphite has been demonstrated to be slower than with the isopropyl and ethyl variants,[5] but in this system, trimethyl phosphite allows for the desired radical reactivity to occur while keeping the undesired Arbuzov side reactivity to a minimum. We attribute this to the relatively low nucleophilicity of trimethyl phosphite as compared to the other phosphites screened.[6]

Further screening revealed that much like the our hydroamination procedure, this reaction was very sensitive to the nature of the radical initiator and solvent used. Common initiators such as AIBN and BPO resulted in decreased reaction efficiencies (entries 5 and 6), as did switching the solvent from DCE to benzene or acetonitrile, although acetonitrile was comparable to DCE (entries 7 and 8). Control experiments excluding the addition of phosphite and radical initiator indicated that both reagents were indeed necessary for productive reactivity (entries 9 and 10). It's important to note that even after exhaustive optimization studies, the optimized yield was unable to break past 45%. We attribute this to rapid decomposition of the allyl-oxyphthalimide substrates at the requisite reaction temperatures.

In line with our initial hypothesis, we found that electron deficient allyl-oxyphthalimides performed best in this transformation while electron neutral and electron rich substrates failed to deliver the desired aminoallylation product. In addition to compound **2.2a** bearing a vinyl cyano group, electron deficient allyl-oxyphthalimides **2.2b**, **2.2c**, and **2.2d** containing a vinyl ethyl ester, p-trifluoromethyl phenyl, and 3,5-bis-trifluoromethyl phenyl groups, respectively, resulted in production of the desired aminoallylation products with NBVE as the external alkene, albeit in modest yield. Less electron deficient substrates such as those bearing a vinyl amide or sulfoxide failed to deliver the desired products, as did electronically unbiased substrates including the parent allyl-oxyphthalimide, and those bearing a vinyl phenyl group or vinyl sulfide (Scheme 2.5).

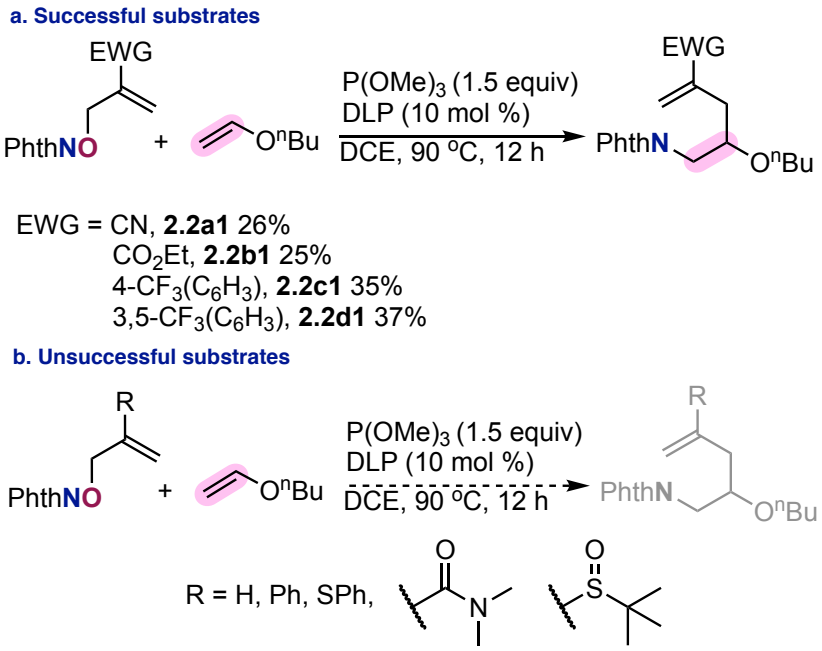


Scheme 2.5. Aminoallylation reaction scope on the part of the allyl-oxyphthalimide.

In addition to the necessity of an electron deficient allyl-oxyphthalimide for productive reactivity, we similarly observed stark electronic effects on the part of the external alkene. Electron rich vinyl ethers were found to take part in this aminoallylation transformation, while less electron rich olefins including vinyl silanes and sulfides resulted in only trace product formation. Other

alkenes such as styrene, vinyl acetate, and the strained norbornene failed to take part entirely (Scheme 2.6).

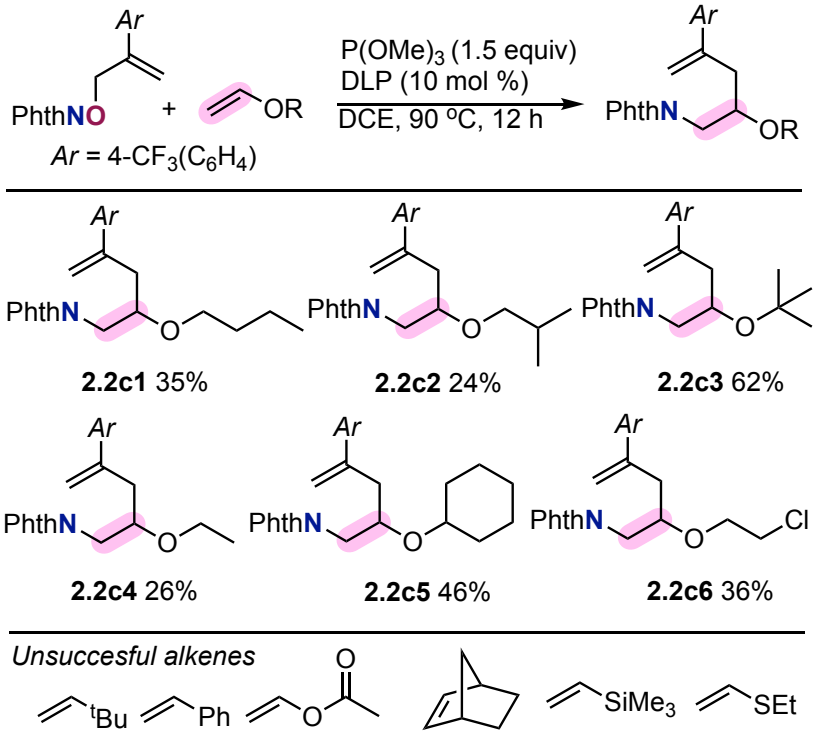


Scheme 2.6. Aminoallylation reaction scope on the part of the external alkene.

## 2.3 Mechanistic Discussion

Much like the previously disclosed hydroamination, we propose that this transformation occurs through a GTRA type radical chain mechanism based on our data (Scheme 2.7). Thermal radical initiation produces an imidoxyl radical through radical fragementation of the allyl-oxyphthalimide, and subsequent phosphite-mediated deoxygenation produces the requisite phthalimidyl radical which selectively adds to the external, electron rich vinyl ether, generating a carbon-centered radical intermediate. This nucleophilic species is now prone to add into the electron poor allyl-oxyphthalimide, producing the desired aminoallylation product and turning over the radical chain.

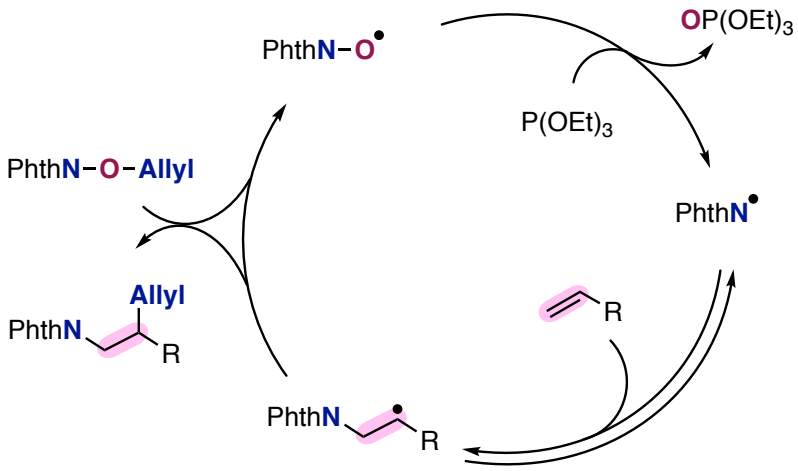


Scheme 2.7. Mechanistic hypothesis for aminoallylation.

In line with our initial hypothesis at the beginning of the development of this reaction, we found that this aminoallylation protocol was largely limited to electron deficient allyl-oxyphthalimides and electron rich external alkenes. This is ultimately a result of proper radical polarity matching. The intricacies of radical polarity matching are well documented with respect to hydrogen atom transfer processes[7] and for the addition of various radicalophiles into pi-systems.[8] For instance, it is well known that properly matched substrates react faster with one another than do mismatched reactants in radical processes (Scheme 2.8.a) as a result of minimizing the energy of the interaction with respect to molecular orbital theory (Scheme 2.8.b), and this work seen here compliments these trends.

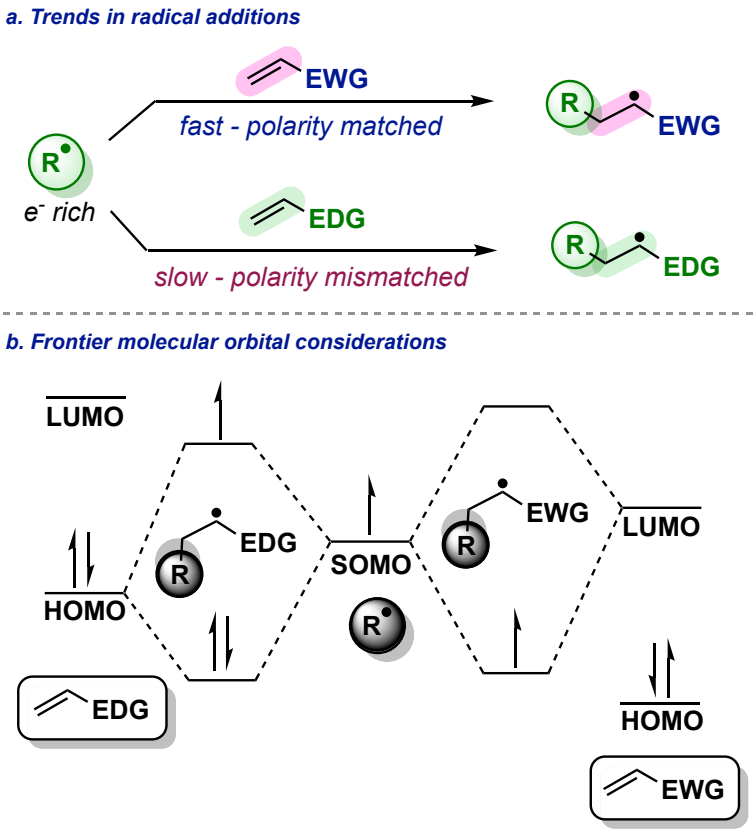


Scheme 2.8. Polarity matching effects in radical reactions.

As shown in Scheme 2.7, the electrophilic imidoxyl radical generated through thermal radical inititation interacts with the electron rich phosphite, generating yet another electrophilic species, the phthalimidyl radical. This electron deficient radical intermediate then preferentially engages with an electron rich alkene to generate a nucleophilic carbon centered radical, which finally preferentially adds into the allyl system of the electron-poor allyl-oxyphthalimde. While modest in yield, this systems serves as an excellent case study in radical polarity effects, of which the observed product is a direct result.

## 2.4 Conclusions

In an attempt to provide further evidence of an ATRA mechanistic pathway for our hydroamination procedure and to expand the method to the difunctionalization of alkenes, we sought to develop a method for the aminoallylation of alkenes using allyl-oxyphthalimide

derivatives of NHPI. While we were indeed able to observe productive, desired reactivity, the reactions was found to be fairly limited in scope and suffered from modest yields. Notwithstanding, our efforts did provide further evidence for an ATRA type pathway for our hydroamination reaction, and similarly stands alone as an excellent example in radical polarity effects.

Chapter 2 has been adapted from materials published in Lardy, S. W.; Schmidt, V. A. Regioselective Alkene Amination Strategies by Using Phosphite Mediated Deoxygenation, *Synlett*, **2019**, *30,* 2022, as well as Lardy, S. W.: Schmidt, V. A. Intermolecular Aminoallylation Using Allyl-oxyphthalimide Derivatives: A Case Study in Radical Polarity Effects, *Eur. J. Org. Chem.* **2019**, 6796. The dissertation author was the primary investigator of these publications.

## 2.5 Appendix

### 2.5.1 General Considerations

$^{1}H$, $^{13}C$, and $^{19}F$ NMR were recorded on Varian Mercury 400 MHz, Varian Unity/Inova 500 MHz, and Bruker 300 MHz spectrometers at 400, 126, and 282 MHz, respectively. All chemical shifts are reported relative to $SiMe_4$ using $^{1}H$ (residual) chemical shifts of the solvent as a secondary standard. $^{19}F$ chemical shifts are reported relative to a 2,2,2-trifluoroethanol ($CF_3CH_2OH$) internal standard at -77.16 ppm. GC analyses were performed using an Agilent Technologies 7890B gas chromatograph equipped with an Agilent 7693 autosampler and Agilent HP-5 capillary column (30 m x 0.320 mm x 250 μm). Standard method parameters: 1.2 mL/min flow rate with oven program 80 – 250 °C with a ramp rate of 25 °C/min and hold time of 8.7 minutes at 250 °C. High-resolution mass spectra were measured using an Agilent 6230 ESI-TOFMS. IR spectra were recorded on an FT/IR-4100typeA spectrometer with a TGS detector.

### 2.5.2 Preparation of Substrates

**General method 2A for the preparation of 2.2a and 2.2b**

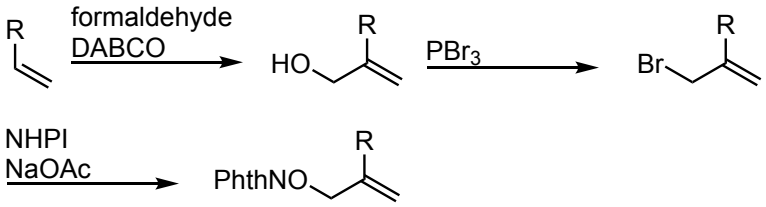


Scheme 2.9. Preparation of substrates **2.2a** and **2.2b**.

**Allylic alcohol:** Allylic alcohols derived from acrylates were prepared according to a procedure previously reported in the literature.[9]

**Allylic bromide:** Allylic bromides derived from acrylates were prepared according to a procedure previously reported in the literature.[9]

**Allyl-Oxyphthalimide:** Allyl-oxyphthalime derivatives derived from acrylates were prepared according to a procedure previously reported in the literature[9]

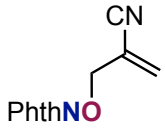


**2.2a** was synthesized as previously reported.[9] Analytical data for **2.2a**: **$^{1}$H-NMR** (400 MHz; $CDCl_3$): δ 7.86-7.82 (m, 2H), 7.80-7.76 (m, 2H), 6.24 (d, *J* = 10.6 Hz, 2H), 4.78 (s, 2H).**$^{13}$C-NMR** (126 MHz; $CDCl_3$): δ 163.3, 136.6, 135.0, 128.7, 123.9, 117.5, 116.6, 76.5. **HRMS** (ESI-TOF) Calc. for $[C_{12}H_8N_2O_3+H^+]^+$ = 229.0608, Found = 229.0609 **$R_f$** (25% EtOAc in hexanes): 0.13.

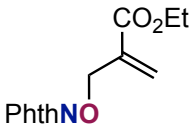


**2.2b** was synthesized as previously reported.[9] Analytical data for **2.2b: $^{1}$H-NMR** (400 MHz; $CDCl_3$): δ 7.86-7.82 (m, 2H), 7.80-7.76 (m, 2H), 6.24 (d, *J* = 10.6 Hz, 2H), 4.78 (s, 2H). **$^{13}$C-NMR** (126 MHz; $CDCl_3$): δ 163.3, 136.6, 135.0, 128.7, 123.9, 117.5, 116.6, 76.5. **HRMS** (ESI-TOF) Calc. for $[C_{12}H_8N_2O_3+H^+]^+$ = 229.0608, Found = 229.0609 **$R_f$** (25% EtOAc in hexanes): 0.13

**General method 2B for the preparation of 2.2c, 2.2d, and 2.2e**

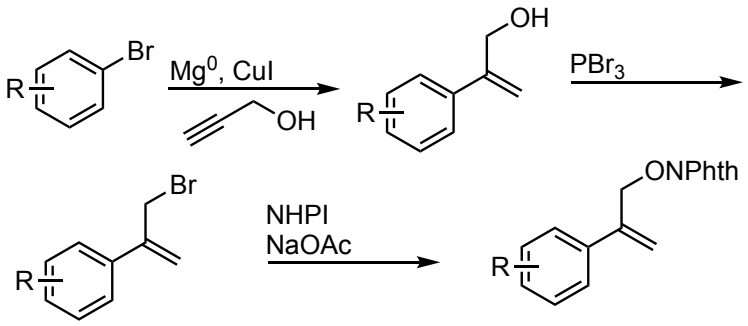


Scheme 2.10. Preparation of substrates **2.2c**, **2.2d**, and **2.2e**.

**Allylic alcohol:** Aryl allylic alcohols were prepared according to a modified procedure reported in the literature.[10] To a round bottom flask equipped with a reflux condenser and charged with a stir bar, magnesium turnings (2.0 equiv), and tetrahydrofuran (0.5 M) was added the corresponding aryl bromide (1.0 equiv). The reaction was allowed to stir for 2 h before CuI (0.06 equiv) was added. After an additional 0.5 h of stirring, propargyl alcohol (0.40 equiv) was added dropwise. The mixture was allowed to stir overnight, after which saturated ammonium chloride aqueous solution was added and the mixture was extracted with diethyl ether (3x). The organic extracts were then combined and dried over sodium sulfate. The solvent was removed in vacuo and the crude product was then purified by silica gel column chromatography to yield the corresponding allylic alcohol.

**Allylic bromide:** Aryl allylic bromides were prepared according to a procedure previously reported in the literature and used in the next step without further purification.[11]

**Allyl-Oxyphthalimide**: Allyl-oxyphthalimide derivatives were prepared from the corresponding bromides according to the general procedure in Method 2A.

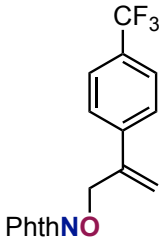


**2.2c** was synthesized according to method 2B in 13% yield over 3 steps as a fluffy white solid. Analytical data for **2.2c**: **Melting Point**: 115-117 °C. **IR (neat) ν cm$^{-1}$:** 1732, 1615, 1467, 1321, 1321, 1113, 699. **$^{1}$H-NMR** (400 MHz; $CDCl_3$): δ 7.84-7.75 (m, 6H), 7.65 (d, *J* = 8.7 Hz, 2H), 5.81 (s, 1H), 5.61 (s, 1H), 5.09 (s, 2H) **$^{13}$C-NMR** (126 MHz; $CDCl_3$): δ 163.3, 141.3, 140.26, 134.6, 130.1 (q, *J* = 32.5), 128.8, 126.6, 125.4 (q, J = 3.8 ), 124.1 (q, J = 271.9), 123.6, 121.9, 79.4. **$^{19}$F-NMR** (282 MHz; $CDCl_3$): δ -62.6. **HRMS** (ESI-TOF) Calc. for $[C_{18}H_{12}F_3NO_3+H^+]^+$ = 348.0842, Found = 348.0842. **$R_f$** (25% EtOAc in hexanes): 0.25.

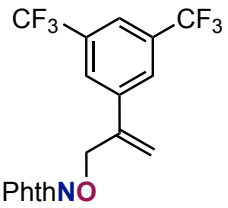


**2.2d** was synthesized according to method 2B in 10% yield over 3 steps as a crystalline white solid. Analytical data for **2.2d**: **Melting Point**: 132-134 °C. **IR (neat) ν cm$^{-1}$:** 1716, 1391, 1282, 113, 696. **$^{1}$H-NMR** (400 MHz; $CDCl_3$): δ 8.20 (s, 2H), 7.88-7.82 (m, 3H), 7.78-7.74 (m, 2H), 5.88 (s, 1H), 5.70 (s, 1H), 5.09 (s, 2H). **$^{13}$C-NMR** (126 MHz; $CDCl_3$): δ 163.5, 140.0, 139.3, 134.8, 132.0 (q, J = 33.3), 128.9, 126.83, 126.80, 123.5 (q, J = 272.8), 123.3, 122.0 (septet, J = 3.8), 79.4. **$^{19}$F-NMR** (282 MHz; CDCl3): δ -62.8. **HRMS** (ESI-TOF) Calc. for $[C_{19}H_{11}F_6NO_3+Na^+]^+$ = 438.0535, Found = 438.0536. **$R_f$** (25% EtOAc in hexanes): 0.28.

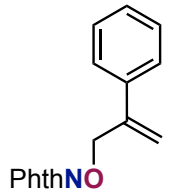


**2.2e** was synthesized according to method 2B. Analytical data for **2.2e**: **$^{1}$H-NMR** (400 MHz; $CDCl_3$): δ 7.83-7.81 (m, 2H), 7.76-7.73(m, 2H), 7.68-7.66 (m, 2H), 7.41-7.37 (m, 2H), 7.33-7.31 (m, 1H), 5.73 (s, 1H), 5.51 (s, 1H), 5.09 (s, 2H). **$^{13}$C-NMR** (126 MHz; $CDCl_3$): δ 163.6, 141.3, 137.9, 134.6, 129.0, 128.6, 128.3, 126.4, 123.6, 119.8, 79.8. **HRMS** (ESI-TOF) Calc. for $[C_{17}H_{13}NO_3+H^+]^+$ = 280.0968, Found = 280.0967. **$R_f$** (25% EtOAc in hexanes): 0.28.

**Method 2C for the preparation of 2.2f**

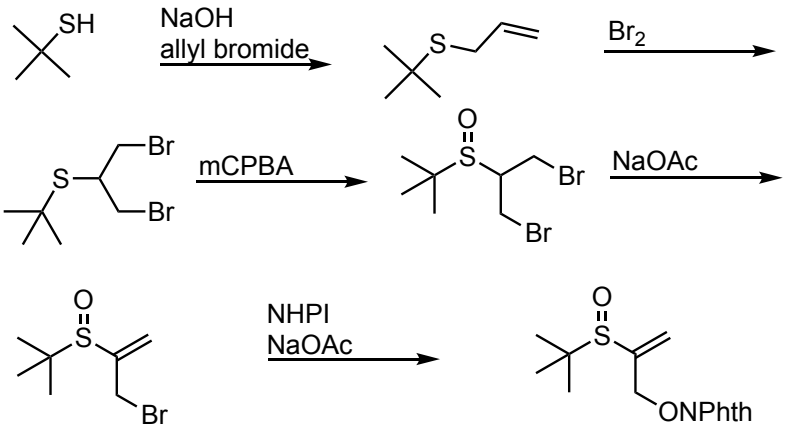


Scheme 2.11. Preparation of substrate **2.2f.**

**Allyl sulfide**: To a round bottom flask charged with a stir bar, $^{t}$bu-thiol (1 equiv), and water (0.5 M) was added sodium hydroxide (2 equiv). The reaction was allowed to stir at room temperature for 10 minutes before allyl bromide (1.1 equiv) was added dropwise. The reaction was left to stir overnight, after which it was extracted with ethyl acetate (3x). The combined organic layers were dried over sodium sulfate and the solvent was removed in vacuo to furnish the corresponding allyl sulfide quantitatively which was used in the next step without further purification.

**Dibromo sulfide**: The dibromo sulfide was prepared according to a procedure previously reported in the literature.[12]

**Dibromo sulfoxide**: The dibromo sulfoxide was prepared according to a procedure previously reported in the literature.[13]

**Bromo vinyl sulfoxide**: The bromo vinyl sulfoxide was prepared according to a procedure previously reported in the literature.[12]

**Allyl-Oxyphthalimide**: Allyl-oxyphthalimide derivatives were prepared from the corresponding bromides according to the general procedure in Method 2A.

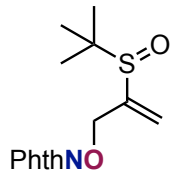


**2.2f** was synthesized according to method 2c in 26% yield over 5 steps as a fine brown powder. Analytical data for **2.2f**: **Melting Point:** 192-194 °C. **IR (neat) ν cm$^{-1}$:** 1709, 1394, 1288, 1113, 1098, 717. **$^{1}$H-NMR** (400 MHz; $CDCl_3$): δ 7.91-7.89 (m, *J* = 1.1 Hz, 2H), 7.79-7.77 (m, *J* = 1.1 Hz, 2H), 6.23 (s, 1H), 5.85 (s, 1H), 4.67 (s, 2H), 1.50 (s, 9H). **$^{13}$C-NMR** (126 MHz; $CDCl_3$): δ 167.5, 141.9, 134.6, 131.9, 129.1, 123.9, 61.2, 39.2, 23.7 **HRMS** (ESI-TOF) Calc. for $[C_{15}H_{17}NO_4S+H^+]^+$ = 308.0951, Found = 308.0949. **$R_f$** (50% EtOAc in hexanes): 0.08.

**Method 2D for the preparation of 2.2g**

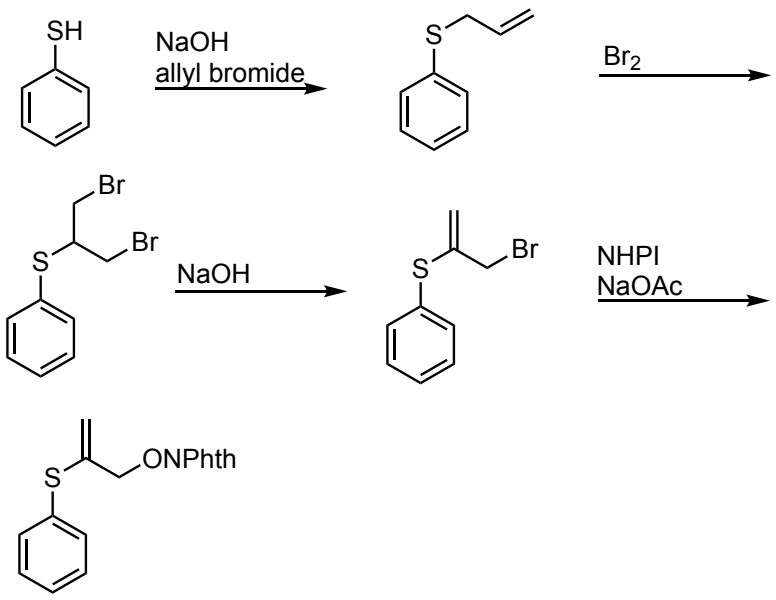


Scheme 2.12. Preparation of substrate **2.2g**.

**Allyl sulfide:** The allyl sulfide was prepared according to the procedure mentioned in Method C.

**Dibromo sulfoxide**: The dibromo sulfide was prepared according to a procedure previously reported in the literature.[13]

**Bromo vinyl sulfide**: The bromo vinyl sulfide was prepared according to a procedure previously reported in the literature.[12]

**Allyl-Oxyphthalimide**: Allyl-oxyphthalimide derivatives were prepared from the corresponding bromides according to the general procedure in Method 2A.

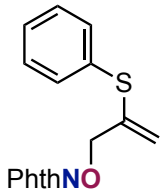


**2.2g** was synthesized according to method 2D in 69% yield over 4 steps as a fine off-white solid. Analytical data for **2.2g**: **Melting Point**: 57-59 °C. **IR (neat) ν cm$^{-1}$:** 1718, 979, 691. **$^{1}$H-NMR** (400 MHz; $CDCl_3$): δ 7.85-7.81 (m, 2H), 7.77-7.72 (m, 2H), 7.49-7.46 (m, 2H), 7.35-7.29 (m, 3H), 5.69 (s, 1H), 5.30 (s, 1H), 4.72 (s, 2H). **$^{13}$C-NMR** (126 MHz; $CDCl_3$): δ 163.4, 138.8, 134.6, 133.2, 132.0, 129.5, 129.0, 128.3, 123.7, 120.2, 78.7. **HRMS** (ESI-TOF) Calc. for $[C_{17}H_{13}NO_3+H^+]^+$ = 312.0689, Found = 312.0688. **$R_f$** (25% EtOAc in hexanes): 0.28.

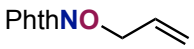


**2.2h** was synthesized as previously reported.[14] Analytical data for **2.2h**: **$^{1}$H-NMR** (400 MHz; $CDCl_3$): δ 7.85-7.80 (m, 2H), 7.77-7.72 (m, 2H), 6.17-6.07 (m, 1H), 5.40-5.33 (m, 2H), 4.74-4.68 (m, 2H). **$^{13}$C NMR** (126 MHz; $CDCl_3$): δ 163.9, 134.6, 131.4, 128.9, 123.7, 122.8, 79.0. **HRMS** (ESI-TOF) Calc. for $[C_{11}H_9NO_3+H^+]^+$ = 204.0655, Found = 204.0654. **$R_f$** (25% EtOAc in hexanes): 0.30.

**Method E for the preparation of 2.2i**

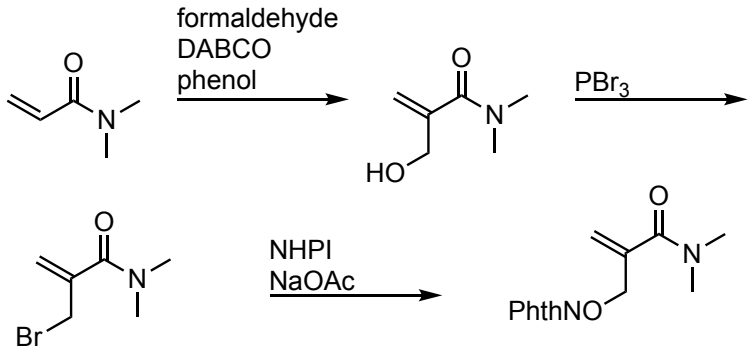


Scheme 2.13. Preparation of substrate **2.2i**.

**Allylic alcohol:** The allylic alcohol was prepared according to a procedure previously.[15]

**Allylic bromide:** The allylic bromide was prepared according to a procedure previously reported in the literature. reported in the literature.[15]

**Allyl-Oxyphthalimide**: Allyl-oxyphthalimide derivatives were prepared from the corresponding bromides according to the general procedure in Method 2A.

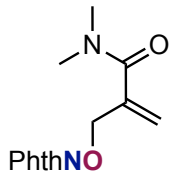


**2.2i** was synthesized according to method 2E in 7% yield over 3 steps as a fine white powder. Analytical data for **2.2i**: **Melting Point**: 133-134 °C. **IR (neat) ν cm$^{-1}$:** 1724, 1607, 1136, 876, 697. **$^{1}$H-NMR** (400 MHz; $CDCl_3$): δ 7.83-7.78 (m, 2H), 7.77-7.69 (m, 2H), 5.75 (s, 1H), 5.46 (s, 1H), 4.95 (s, 2H), 3.16 (s, 3H), 3.03 (s, 3H). **$^{13}$C-NMR** (126 MHz; $CDCl_3$): δ 169.4, 163.4, 138.3, 134.7, 134.3, 129.0, 123.7, 123.5, 122.1, 79.2. **HRMS** (ESI-TOF) Calc. for $[C_{14}H_{17}N_2O_4+H^+]^+$ = 275.1026, Found = 275.1028. **$R_f$** (50% EtOAc in hexanes): 0.08.

### 2.5.3 General Aminoallylation Procedure

****Caution: while no problems were encountered in this work, alkylhydroperoxides can undergo spontaneous and rapid exothermic decomposition and appropriate care should be taken in their handling****

To a 1-dram vial charged with a magnetic stir bar was added the respective allyl-PINO derivative (20 mg), dilauroyl peroxide (0.10 equiv), triethyl phosphite (1.5 equiv), olefin (10 equiv), and 1,2-dichloroethane (3 mL). The vial was capped and heated to 90 °C. Upon consumption of the *N-(O*-allyl)hydroxyphthalimide derivative as judged by TLC (25% EtOAc in hexanes), the reaction mixture was concentrated under reduced pressure and purified by flash column chromatography (10% EtOAc in hexanes).

### 2.5.4 Characterization of Products

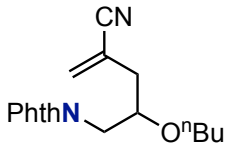


**2.2a1** was synthesized according to the general aminoallylation procedure in 26% yield (7 mg) as a clear oil. Analytica data for **2.2a1**: **IR (neat) ν cm$^{-1}$:** 2928, 2872, 1773, 1705, 1394, 1085, 713 **$^1$H-NMR** (400 MHz; $CDCl_3$): δ 7.87-7.85 (m, 2H), 7.77- 7.73 (m, 2H), 5.94 (s, 1H), 5.84 (s, 1H), 3.81 (s, 3H), 3.70- 3.65 (m, 1H), 3.50 (dt, *J* = 8.5, 6.9 Hz, 1H), 2.52-2.39 (m, 2H), 1.49 (dt, *J* = 14.4, 7.0 Hz, 2H), 1.34-1.25 (m, 2), 0.83 (t, *J* = 7.4 Hz, 3H). **$^{13}$C-NMR** (126 MHz; $CDCl_3$): δ 168.5, 134.3, 133.4, 132.1, 123.6, 119.7, 118.6, 75.4, 70.6, 40.3, 38.7, 32.0, 19.3, 13.9. **HRMS** (ESI-TOF) Calc. for $[C_{18}H_{20}N_2O_3+H^+]^+$ = 313.1547, Found = 313.1546. **$R_f$** (25% EtOAc in hexanes): 0.26.

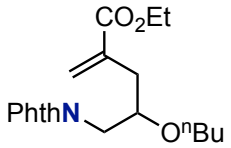


**2.2b1** was synthesized according to the general aminoallylation procedure in 26% yield (7 mg) as a clear oil. Analytical data for **2.2b1**: **IR (neat) ν cm$^{-1}$:** 2957, 2925, 2854, 1710, 1393, 1174, 1093, 1019, 714. **$^1$H-NMR** (400 MHz; $CDCl_3$): δ 7.87-7.83 (m, 2H), 7.74- 7.70 (m, 2H), 6.23 (s, 1H), 5.70 (s, 1H), 4.18 (q, *J* = 7.1 Hz, 2H), 3.84-3.70 (m, 3H), 3.46 (t, *J* = 6.4 Hz, 2H), 2.54-2.53 (m, 2H), 1.41-1.35 (m, 2H), 1.28-1.19 (m, 5H), 0.75 (t, *J* = 7.3 Hz, 3H). **$^{13}$C-NMR** (126 MHz; $CDCl_3$): δ 168.5, 167.0, 136.9, 134.1, 132.2, 127.8, 123.4, 75.7, 70.1, 60.9, 41.3, 36.2, 32.1, 19.2, 14.3, 13.9. **HRMS** (ESI-TOF) Calc. for $[C_{20}H_{25}NO_3+H^+]^+$ = 360.1805, Found = 360.1802 **$R_f$** (25% EtOAc in hexanes): 0.34

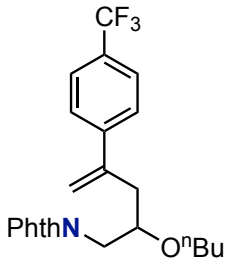


**2.2c1** was synthesized according to the general aminoallylation procedure in 35% yield (9 mg) as a clear oil. Analytical data for **2.2c1**: **IR (neat) ν cm$^{-1}$:** 2957, 2926, 2853, 1711, 1395, 1324, 1167, 1125, 1016, 723. **$^{1}$H-NMR** (400 MHz; $CDCl_3$): δ 7.85-7.82 (m, 2H), 7.74- 7.70 (m, 2H), 7.55 (d, *J* = 8.1 Hz, 2H), 7.48 (d, *J* = 8.2 Hz, 2H), 5.39 (s, 1H), 5.30 (s, 1H), 3.82-3.64 (m, 3H), 3.40- 3.30 (m, 2H), 2.82-2.70 (m, 2H), 1.35-1.12 (m, 2H), 0.90-0.82 (m, 2H), 0.72 (t, *J* = 7.3 Hz, 3H). **$^{13}$C-NMR** (126 MHz; $CDCl_3$): δ 168.5, 144.9, 144.2, 134.1, 132.1, 129.6 (q, J = 31.7), 126.7, 125.4 (q, J = 3.7), 124.1 (q, J = 117.7), 123.4, 117.3, 76.0, 70.0, 41.5, 39.4, 32.1, 19.2, 13.8. **$^{19}$F-NMR** (282 MHz; $CDCl_3$): δ -62.5. **HRMS** (ESI-TOF) Calc. for $[C_{24}H_{24}F_3NO_3+Na^+]^+$ = 454.1600, Found = 454.1594. **$R_f$** (25% EtOAc in hexanes): 0.45.

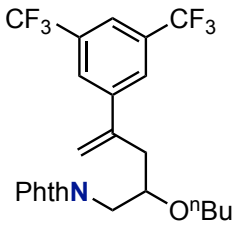


**2.2d1** was synthesized according to the general aminoallylation procedure in 37% yield (9 mg) as a clear oil. Analytical data for **2.2d1**: **IR (neat) ν cm$^{-1}$:** 2957, 2928, 2874, 2356, 2341, 1711, 1394, 1276, 1171, 1131, 723, 699. **$^{1}$H-NMR** (400 MHz; $CDCl_3$): δ 7.87-7.72 (m, 7H), 5.45 (s, 1H), 5.38 (s, 1H), 3.85-3.75 (m, 2H), 3.69-3.63 (m, 1H), 3.50-3.44 (m, 1H), 3.29 (dt, *J* = 9.0, 6.4 Hz, 1H), 2.76 (d, *J* = 6.3 Hz, 2H), 1.35-1.12 (m, 3H), 0.92-0.72 (m, 2H), 0.75 (t, *J* = 7.1 Hz, 3H). **$^{13}$C-NMR** (126 MHz; $CDCl_3$): δ 168.5, 143.6, 143.2, 134.2, 132.0, 131.7 (q, J = 33.2), 126.5, 123.5, 123.4 (q, J = 272.6), 121.2, 118.5, 76.3, 70.2, 41.1, 39.1, 32.0, 19.2, 13.8 **$^{19}$F-NMR** (282 MHz; $CDCl_3$): δ -62.9. **HRMS** (ESI-TOF) Calc. for $[C_{25}H_{23}F_6NO_3+H^+]^+$ = 500.1655, Found = 500.1649. **$R_f$** (25% EtOAc in hexanes): 0.47.

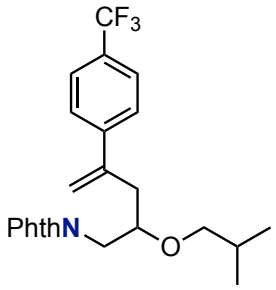


**2.2c2** was synthesized according to the general aminoallylation procedure in 24% yield (6 mg) as a clear oil. Analytical data for **2.2c2**: **IR (neat) ν cm$^{-1}$:** 2931, 1715, 1395, 1325, 1128, 718 **$^{1}$H-NMR** (400 MHz; $CDCl_3$): δ 7.85-7.82 (m, 2H), 7.74-7.71 (m, 2H), 7.55 (d, *J* = 8.0 Hz, 2H), 7.48 (d, *J* = 8.2 Hz, 2H), 5.40 (s, 1H), 5.30 (s, 1H), 3.84-3.65 (m, 3H), 3.13 (d, *J* = 6.5 Hz, 2H), 2.84-2.70 (m, 2H), 1.63-1.52 (m, 2H), 0.92-0.80 (m, 2H), 0.71 (d, *J* = 4.7 Hz, 6H). **$^{13}$C-NMR** (126 MHz; $CDCl_3$): δ 168.3, 144.7, 144.0, 134.0, 132.0, 129.6 (q, J = 32.0), 126.7, 125.4 (q, J = 3.8), 124.1 (q, J = 271.9), 123.2, 117.2, 75.9, 41.3, 39.2, 28.7, 19.19, 19.18. **$^{19}$F-NMR** (282 MHz; $CDCl_3$): δ -62.5. **HRMS** (ESI-TOF) Calc. for $[C_{24}H_{24}F_3NO_3+Na^+]^+$ = 454.1600, Found = 454.1597. **$R_f$** (25% EtOAc in hexanes): 0.47.

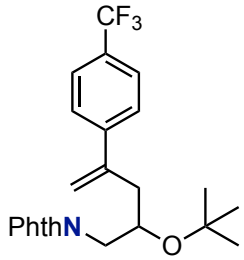


**2.2c3** was synthesized according to the general aminoallylation procedure in 64% yield (16 mg) as a clear oil. Analytical data for **2.2c3**: **IR (neat) ν cm$^{-1}$:** 2922, 2852, 1717, 1325, 1128, 720, 617. **$^{1}$H-NMR** (400 MHz; $CDCl_3$): δ 7.84 (m, 2H), 7.73 (m, 2H), 7.52 (d, *J* = 8.0 Hz, 2H), 7.44 (d, *J* = 8.0 Hz, 2H), 5.38 (s, 1H), 5.32 (s, 1H), 3.90 (quintet, *J* = 6.2 Hz, 1H), 3.71 (qd, *J* = 12.8, 6.2 Hz, 2H), 2.80-2.69 (m, 2H), 1.08-0.97 (m, 9H). **$^{13}$C-NMR** (126 MHz; $CDCl_3$): δ 168.5, 145.0, 144.2, 134.2, 132.2, 129.6 (q, J = 32.0) 126.7, 125.4 (q, J = 3.76), 124.1 (q, J = 271.9), 123.4, 117.5, 74.5, 68.0, 43.2, 41.6, 28.4. **$^{19}$F-NMR** (282 MHz; $CDCl_3$): δ -62.5. **HRMS** (ESI-TOF) Calc. for $[C_{24}H_{24}F_3NO_3+Na^+]^+$ = 454.1600, Found = 454.1594 **$R_f$** (25% EtOAc in hexanes): 0.42.

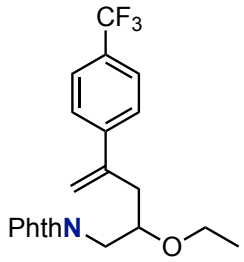


**2.2c4** was synthesized according to the general aminoallylation procedure in 26% yield (6 mg) as a clear oil. Analytical data for **2.2c4**: **IR (neat) ν cm$^{-1}$:** 2925, 2855, 1716, 1326, 1169, 1126, 1069, 725. **$^{1}$H-NMR** (400 MHz; $CDCl_3$): δ 7.86-7.81 (m, 2H), 7.75-7.70 (m, 2H), 7.54 (d, *J* = 8.2 Hz, 2H), 7.47 (d, *J* = 8.2 Hz, 2H), 5.40 (s, 1H), 5.31 (s, 1H), 3.80-3.71 (m, 3H), 3.15-3.13 (m, 1H), 2.75 (d, *J* = 5.8 Hz, 2H), 1.60-1.38 (m, 6H), 1.09-1.01 (m, 5H). **$^{13}$C-NMR** (126 MHz; $CDCl_3$): δ 168.5, 144.9, 144.2, 134.2, 132.1, 129.6 (q, J = 32.3), 126.7, 125.5 (q, J = 3.7), 124.1 (q, J = 271.9), 123.4, 117.2, 75.9, 65.6, 41.4, 39.5, 15.5. **$^{19}$F-NMR** (282 MHz; $CDCl_3$): δ -62.5. **HRMS** (ESI-TOF) Calc. for $[C_{22}H_{20}F_3NO_3+H^+]^+$ = 426.1287, Found = 426.1284. **$R_f$** (25% EtOAc in hexanes): 0.39.

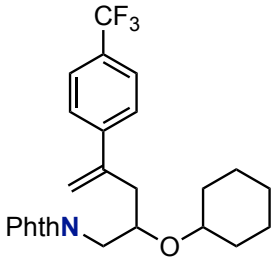


**2.2c5** was synthesized according to the general aminoallylation procedure in 46% yield (12 mg) as a clear oil. Analytical data for **2.2c5**: **IR (neat) ν cm$^{-1}$:** 2932, 2856, 1714, 1396, 1325, 1127, 1067, 723. **$^{1}$H-NMR** (400 MHz; $CDCl_3$): δ 7.86-7.82 (m, 2H), 7.75-7.70 (m, 2H), 7.55 (d, *J* = 8.2 Hz, 2H), 7.47 (d, *J* = 8.1 Hz, 2H), 5.39 (s, 1H), 5.30 (s, 1H), 3.79 (dd, *J* = 5.7, 3.3 Hz, 2H), 3.71-3.65 (m, 1H), 3.51-3.34 (m, 2H), 2.75 (ddd, *J* = 6.4, 3.7, 0.9 Hz, 2H), 0.98 (t, *J* = 7.0 Hz, 3H). **$^{13}$C-NMR** (126 MHz; $CDCl_3$): δ 168.5, 144.9, 144.2, 134.2, 132.1, 129.6 (q, J = 32.5), 126.7, 125.5 (q, J = 3.7), 124.1 (q, J = 271.9), 123.4, 117.2, 73.1, 42.3, 40.2, 32.7, 25.7, 24.2, 24.1. **$^{19}$F-NMR** (282 MHz; $CDCl_3$): δ -62.5. **HRMS** (ESI-TOF) Calc. for $[C_{26}H_{26}F_3NO_3+H^+]^+$ = 458.1938, Found = 458.1932 **$R_f$** (25% EtOAc in hexanes): 0.42

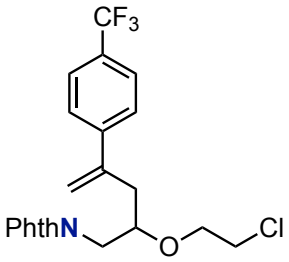


**2.2c6** was synthesized according to the general aminoallylation procedure in 36% yield (9 mg) as a clear oil. Analytical data for **2.2c6**: **IR (neat) ν cm$^{-1}$:** 2925, 2855, 1710, 1395, 1324, 1166, 1124, 1067, 724. **$^{1}$H-NMR** (400 MHz; $CDCl_3$): δ 7.85-7.82 (m, 2H), 7.76-7.71 (m, 2H), 7.57 (d, *J* = 8.2 Hz, 2H), 7.49 (d, *J* = 8.1 Hz, 2H), 5.43 (s, 1H), 5.33 (s, 1H), 3.87-3.74 (m, 3H), 3.64 (t, *J* = 5.4 Hz, 2H), 3.39 (t, *J* = 5.9 Hz, 2H), 2.81-2.79 (m, 2H). **$^{13}$C-NMR** (126 MHz; $CDCl_3$): δ 168.5, 144.6, 143.7, 134.7, 134.2, 132.1, 129.8 (q, J = 32.6), 126.7, 125.6 (q, J = 3.8), 124.5 (q, J = 204.5) 123.5, 117.8, 70.3, 43.1, 41.2, 39.4. **$^{19}$F-NMR** (282 MHz; $CDCl_3$): δ -62.5. **HRMS** (ESI-TOF) Calc. for $[C_{22}H_{19}ClF_3NO_3+H^+]^+$ = 438.1078, Found = 438.1076. **$R_f$** (25% EtOAc in hexanes): 0.34.

### 2.5.5 $^{1}$H, $^{13}$C, and 2-D NMR Spectra

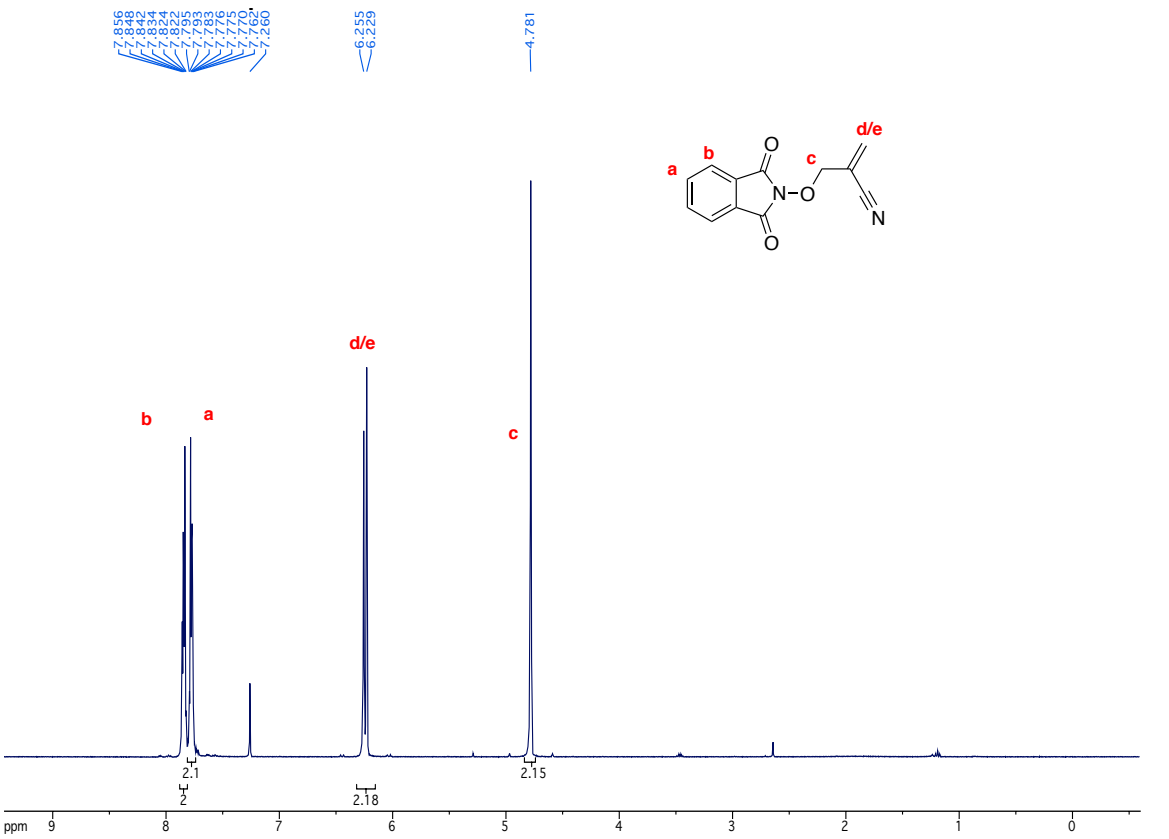
7.856
7.848
7.842
7.834
7.824
7.822
7.795
7.783
7.776
7.775
7.760
7.260
6.255
6.229
4.781
d/e
b
a
c
2.1
2
2.18
2.15
ppm
9
8
7
6
5
4
3
2
1
0

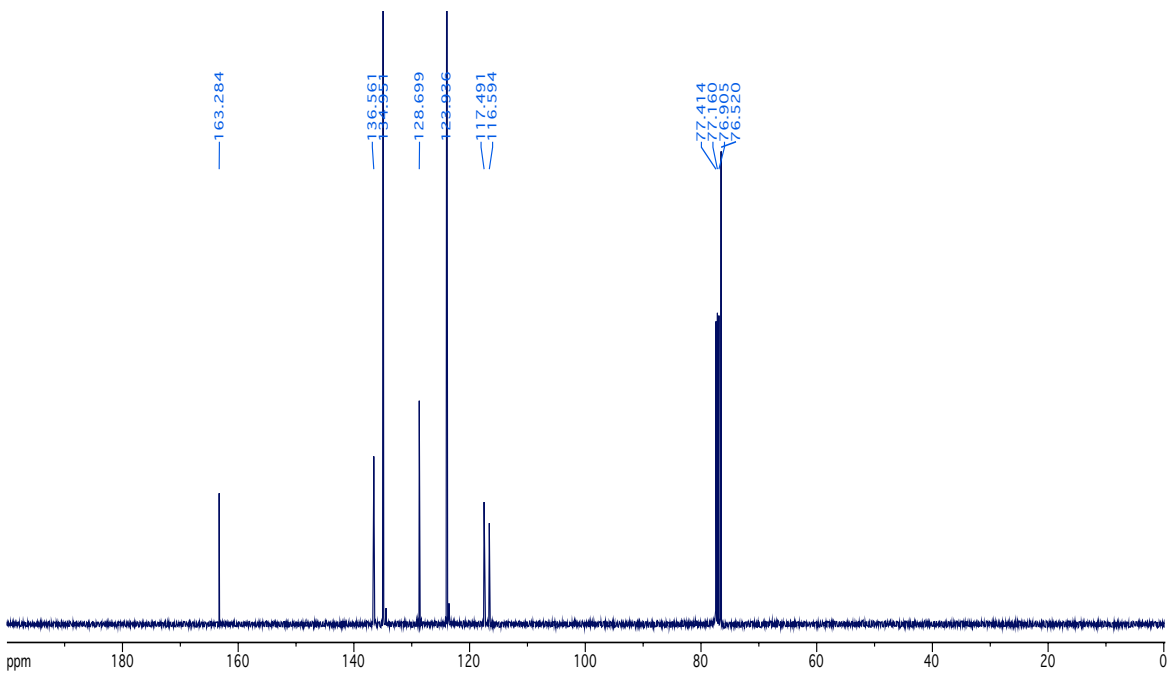
163.284
136.561
134.951
128.699
123.936
117.491
116.594
77.414
77.160
76.905
76.520
ppm
180
160
140
120
100
80
60
40
20
0

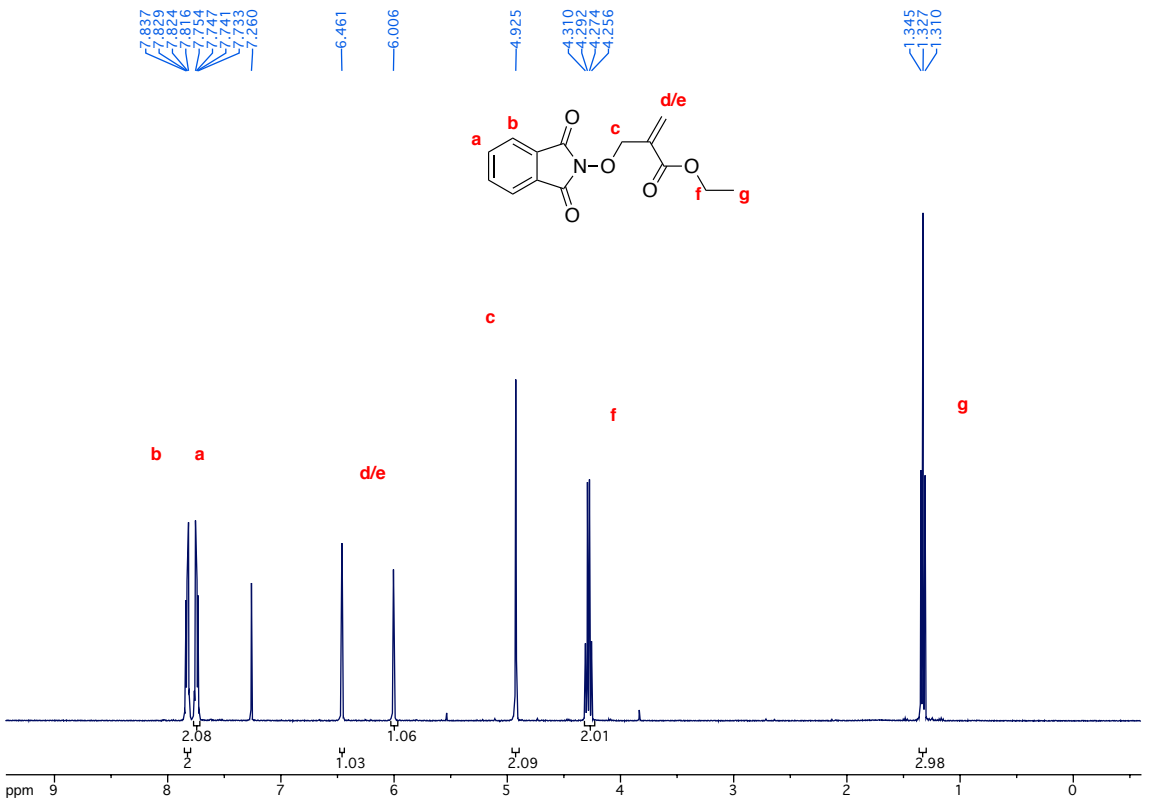
7.837
7.829
7.824
7.816
7.754
7.747
7.741
7.733
7.260
6.461
6.006
4.925
4.310
4.292
4.274
4.256
1.345
1.327
1.310
a
b
c
d/e
f
g
2.08
1.03
1.06
2.09
2.01
2.98
ppm

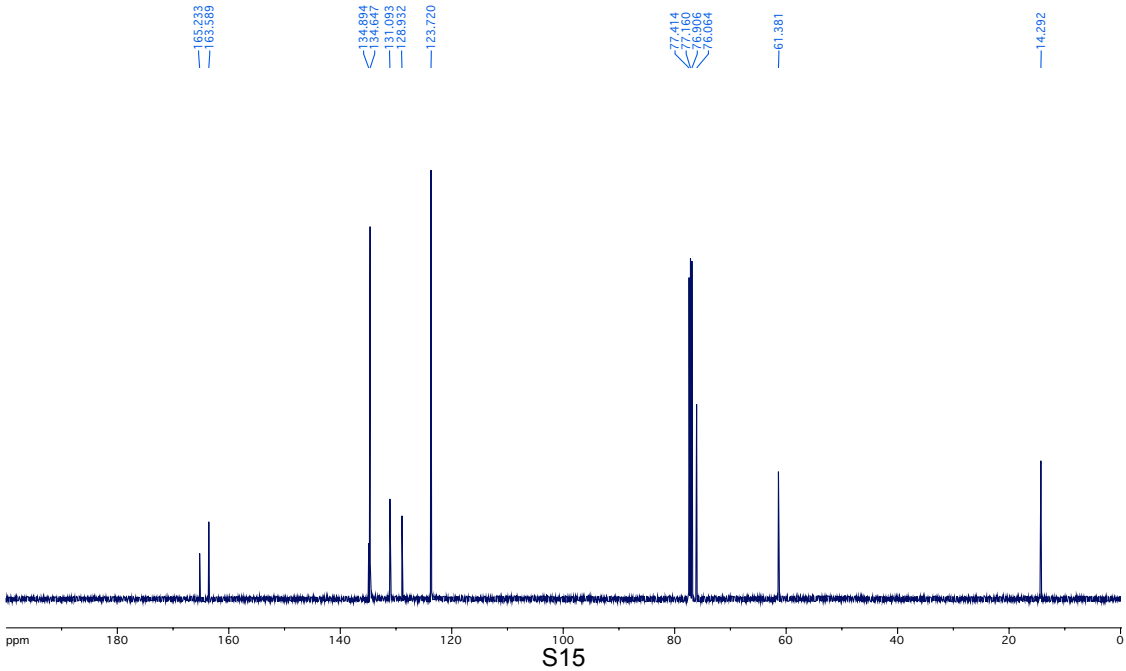
165.233
163.589
134.694
134.647
131.093
128.932
123.720
77.414
77.160
76.906
76.064
61.381
14.292
ppm

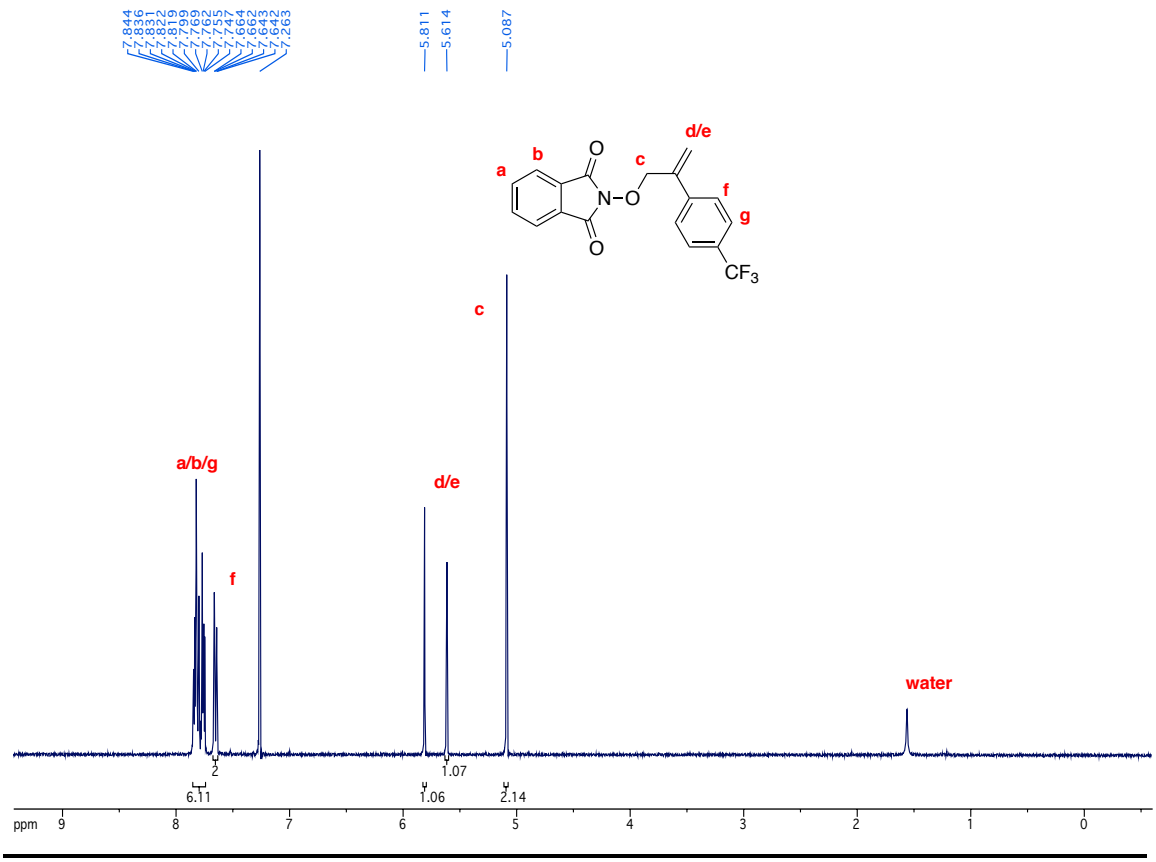
7.844
7.836
7.831
7.822
7.819
7.799
7.769
7.762
7.747
7.664
7.662
7.643
7.263
5.811
5.614
5.087
a
b
c
d/e
f
g
CF3
N–O
O
a/b/g
d/e
f
c
water
2
1.07
6.11
1.06
2.14
ppm
9
8
7
6
5
4
3
2
1
0

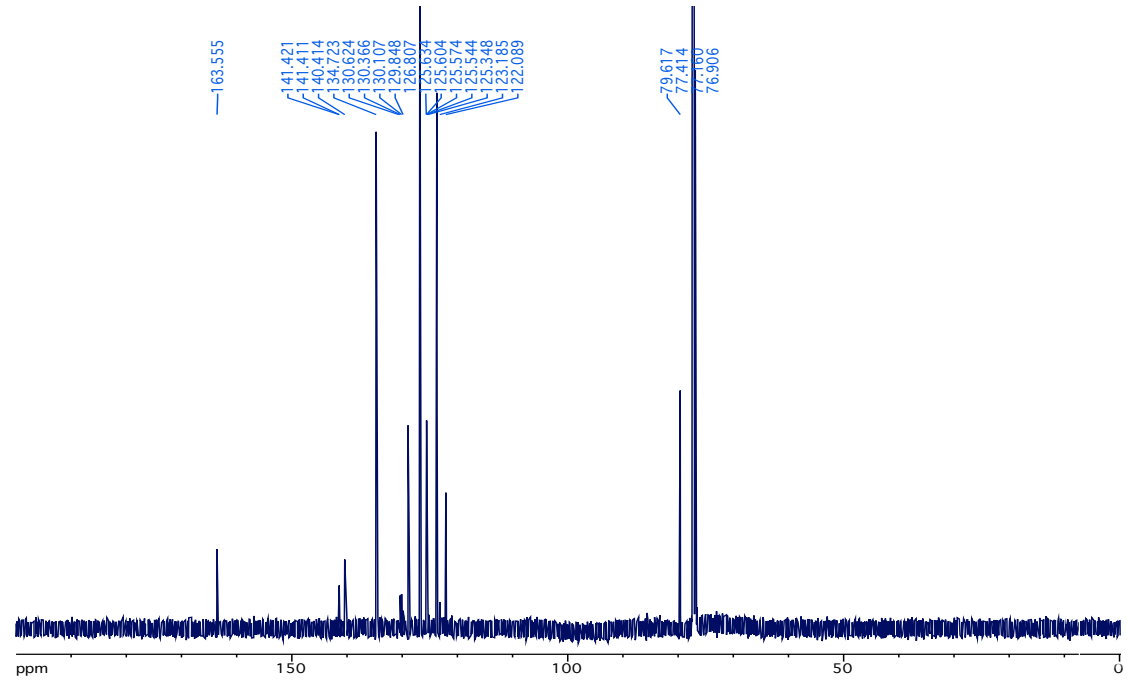
163.555
141.421
141.411
140.414
134.723
130.624
130.366
130.107
129.848
126.807
125.634
125.604
125.574
125.544
125.348
123.185
122.089
79.617
77.414
77.160
76.906
ppm
150
100
50
0

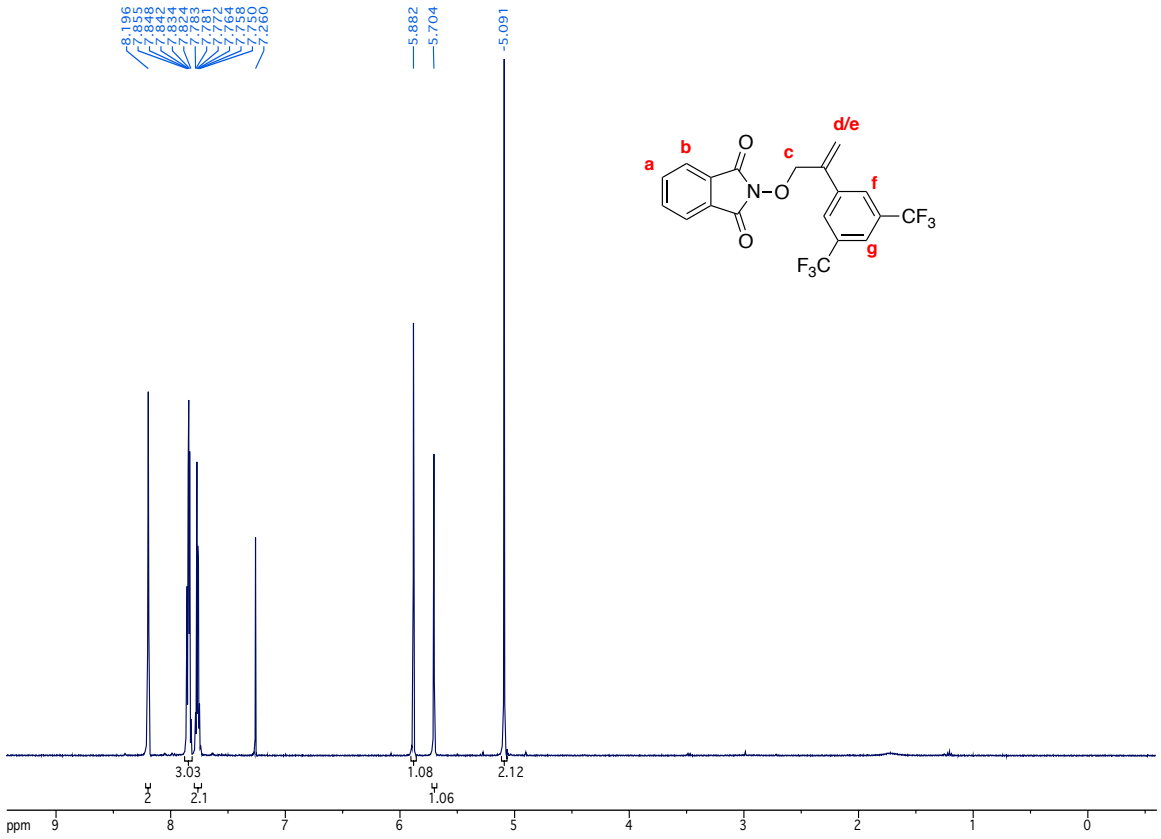
8.196
7.855
7.848
7.842
7.834
7.824
7.783
7.781
7.772
7.764
7.758
7.750
7.200
5.882
5.704
5.091
a
b
c
d/e
f
g
O
N–O
O
CF3
F3C
3.03
2.1
1.08
1.06
2.12
2
ppm
9
8
7
6
5
4
3
2
1
0

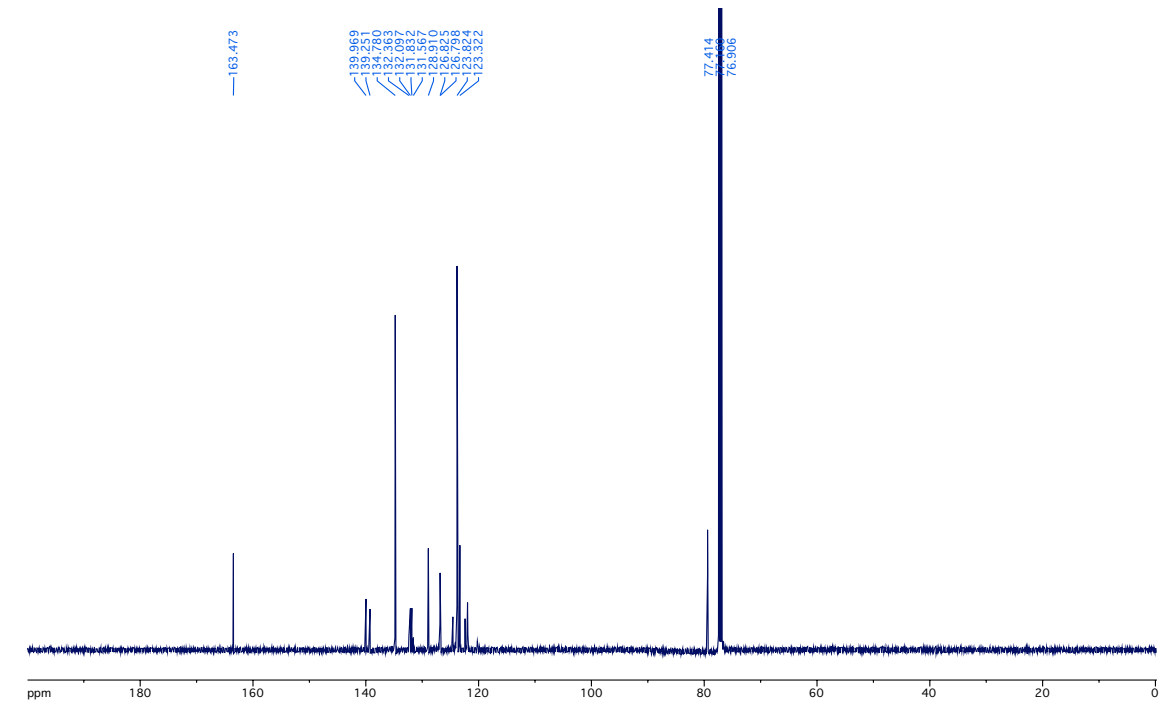
163.473
139.969
139.751
134.780
132.469
132.097
131.832
131.567
131.311
128.820
126.798
123.824
123.322
77.414
77.163
76.906
ppm
180
160
140
120
100
80
60
40
20
0

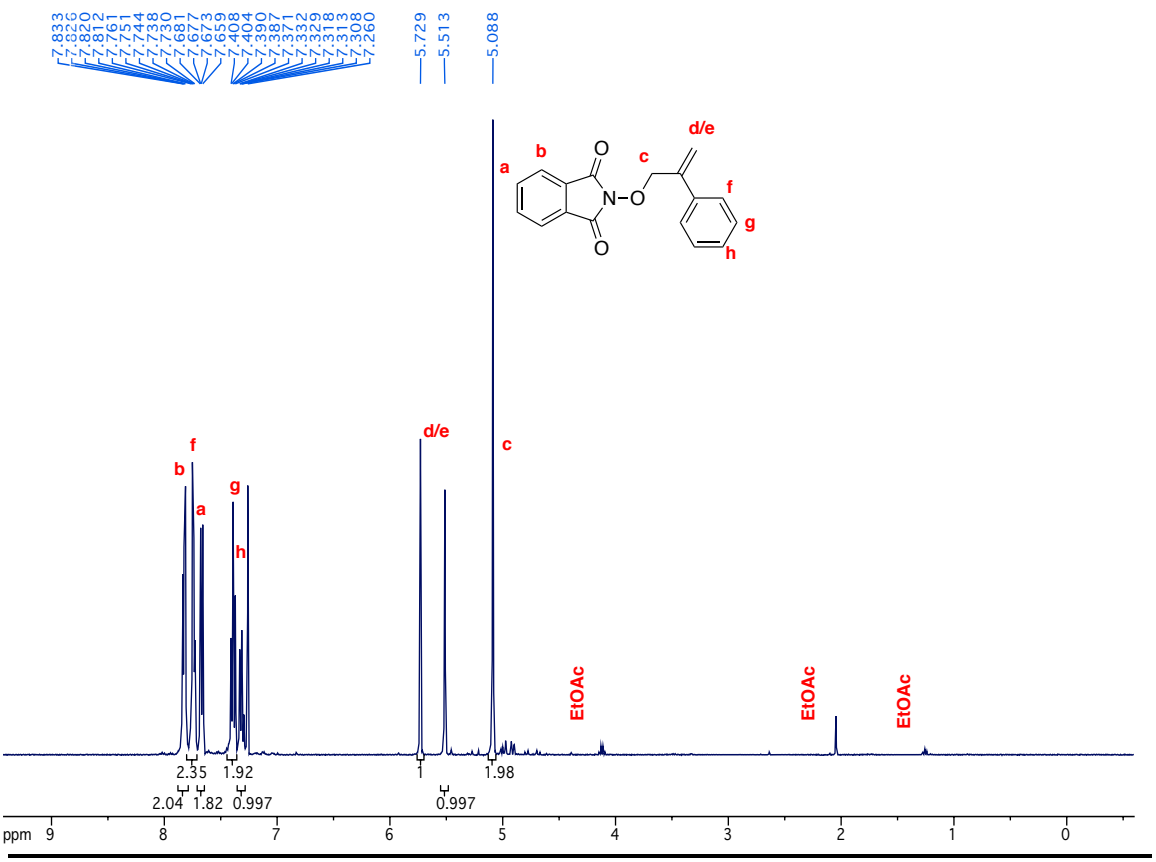
7.833
7.826
7.820
7.812
7.761
7.751
7.744
7.738
7.730
7.681
7.677
7.673
7.659
7.408
7.404
7.390
7.387
7.371
7.332
7.329
7.318
7.313
7.308
7.260
5.729
5.513
5.088
a
b
c
d/e
f
g
h
O
N–O
O
O
d/e
c
f
b
a
g
h
EtOAc
EtOAc
EtOAc
2.35
1.92
1
1.98
2.04
1.82
0.997
0.997
ppm
9
8
7
6
5
4
3
2
1
0

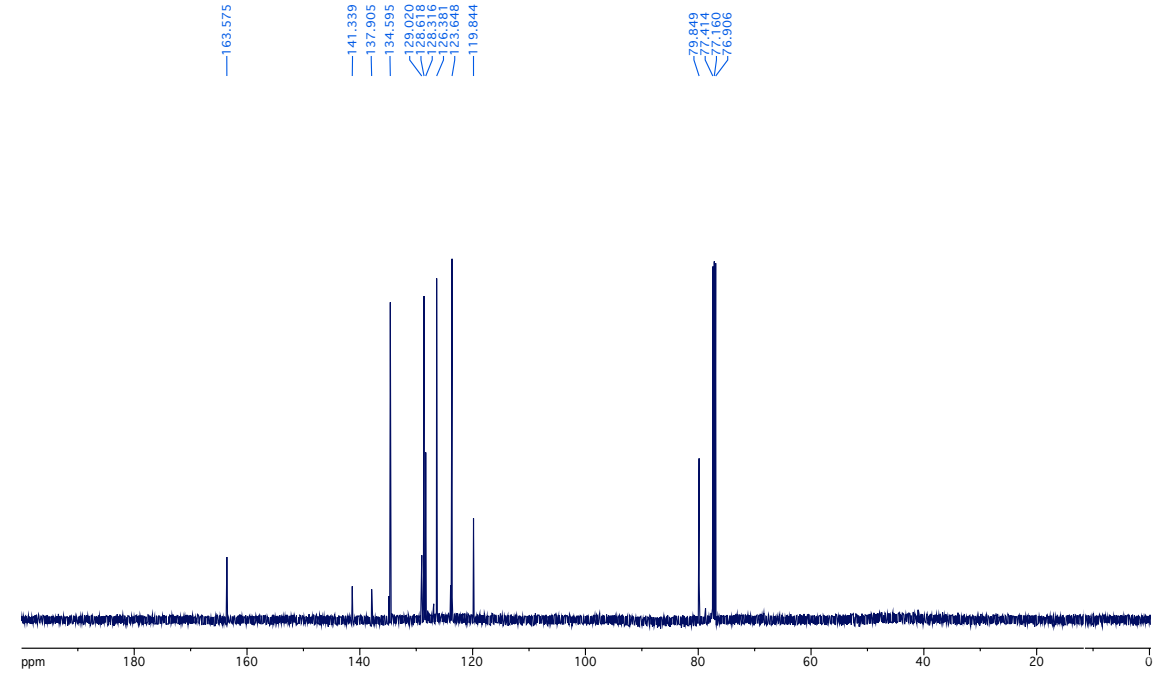
163.575
141.339
137.905
134.595
129.020
128.618
128.316
126.381
123.648
119.844
79.849
77.414
77.160
76.906
ppm
180
160
140
120
100
80
60
40
20
0

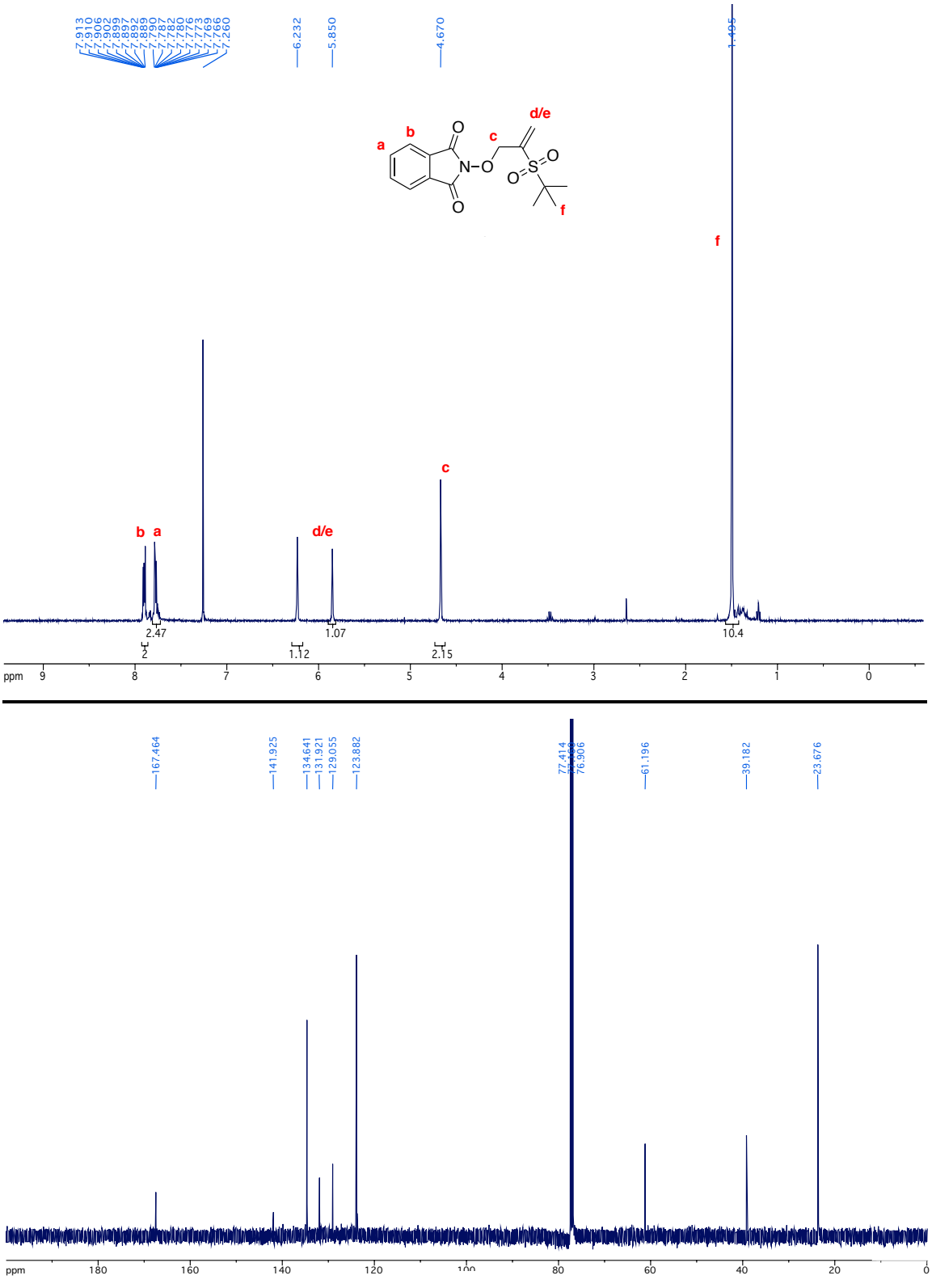
7.913
7.910
7.906
7.902
7.899
7.897
7.892
7.888
7.790
7.787
7.782
7.780
7.775
7.769
7.766
7.260
6.232
5.850
4.670
1.495
a
b
c
d/e
f
N
O
S
b a
d/e
c
f
2.47
1.07
10.4
2
1.12
2.15
ppm
9
8
7
6
5
4
3
2
1
0
167.464
141.925
134.641
131.921
129.055
123.882
77.414
77.000
76.906
61.196
39.182
23.676
ppm
180
160
140
120
100
80
60
40
20
0

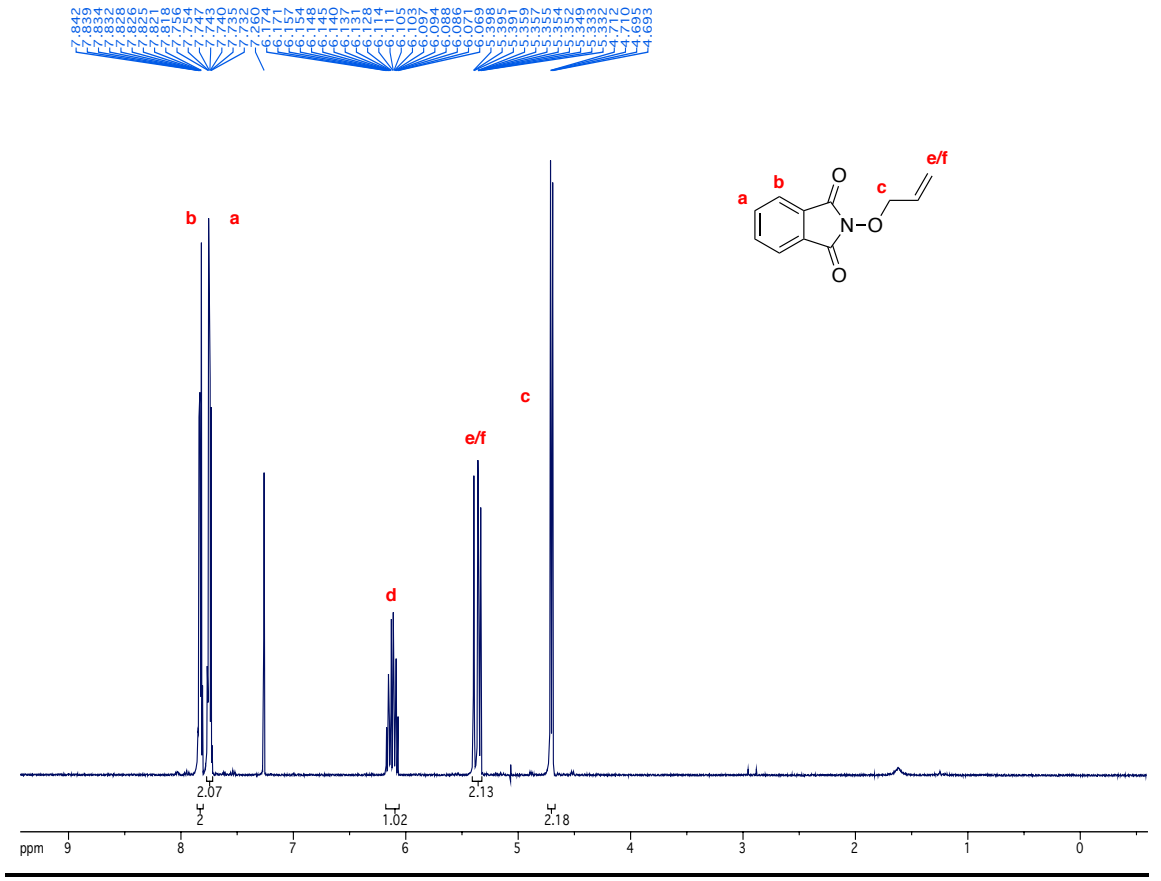
7.842
7.839
7.834
7.832
7.828
7.826
7.825
7.821
7.818
7.756
7.754
7.747
7.743
7.740
7.735
7.732
7.260
6.174
6.171
6.157
6.154
6.148
6.145
6.140
6.137
6.131
6.128
6.114
6.111
6.105
6.103
6.097
6.094
6.088
6.086
6.071
6.069
5.398
5.395
5.391
5.359
5.357
5.355
5.354
5.352
5.349
5.333
5.332
4.712
4.710
4.695
4.693
a
b
c
e/f
N–O
O
O
O
b
a
c
e/f
d
2.07
1.02
2.13
2.18
2
ppm
9
8
7
6
5
4
3
2
1
0

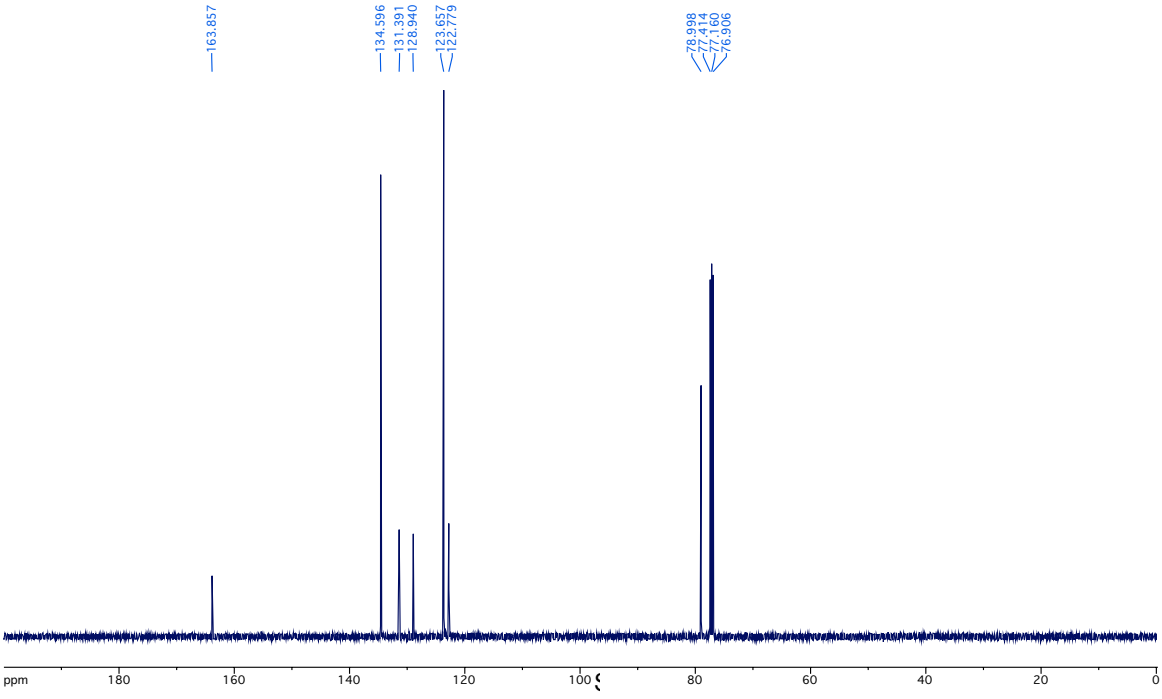
163.857
134.596
131.391
128.940
123.657
122.779
78.998
77.414
77.160
76.906
ppm
180
160
140
120
100
80
60
40
20
0

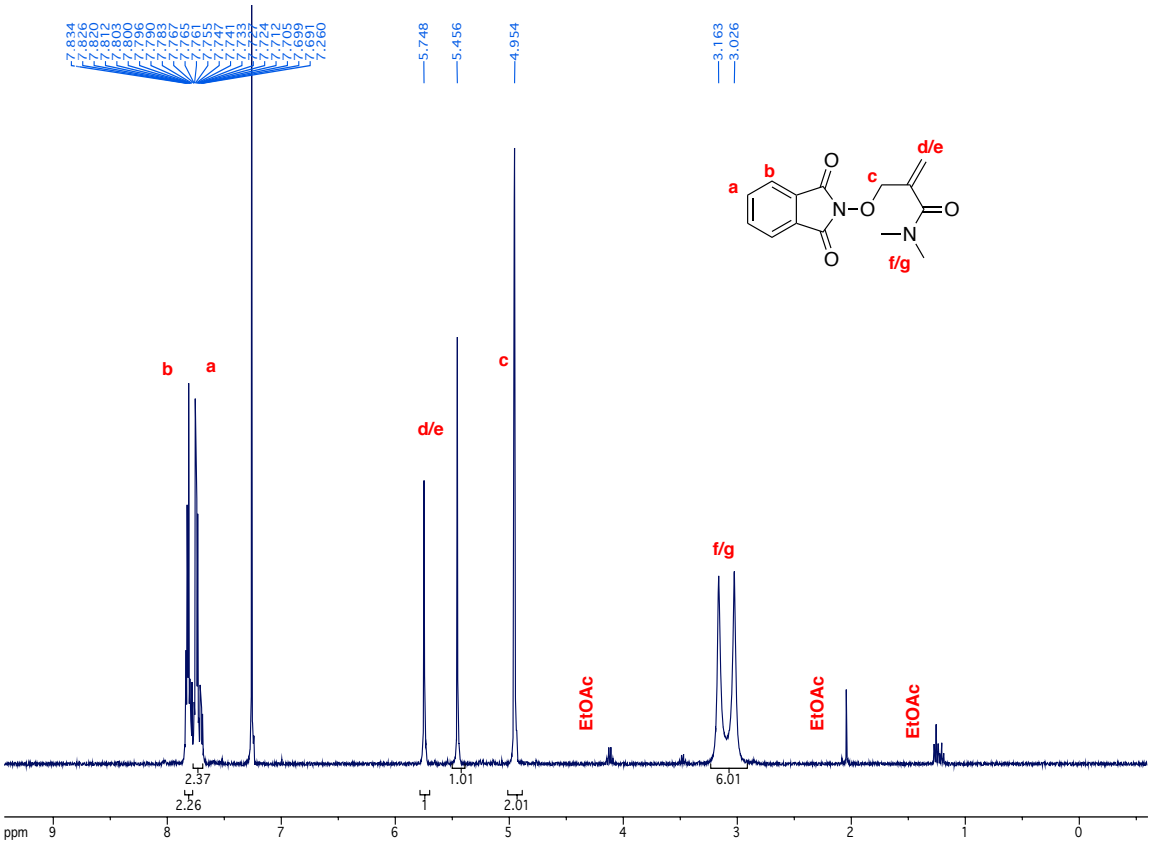
7.834
7.826
7.820
7.812
7.803
7.800
7.796
7.790
7.783
7.767
7.765
7.761
7.755
7.747
7.741
7.733
7.727
7.724
7.712
7.705
7.699
7.691
7.260
5.748
5.456
4.954
3.163
3.026
a
b
c
d/e
f/g
b
a
c
d/e
f/g
EtOAc
EtOAc
EtOAc
2.37
2.26
1
1.01
2.01
6.01
ppm

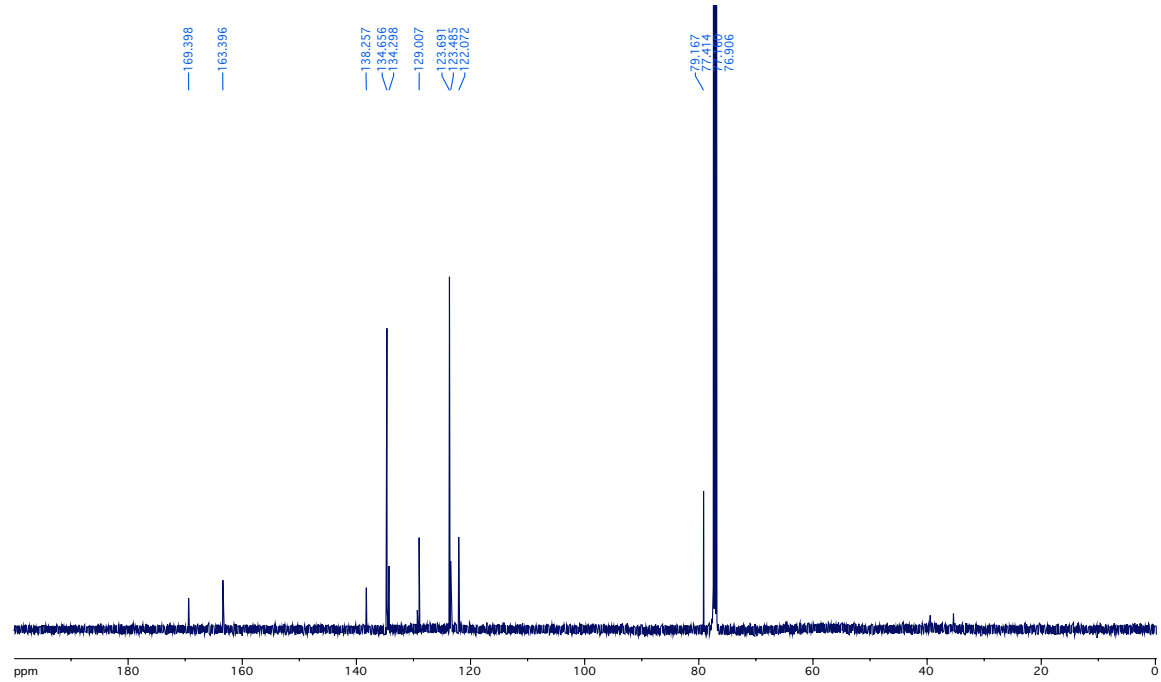
169.398
163.396
138.257
134.656
134.298
129.007
123.691
123.485
122.072
79.167
77.414
76.906
ppm

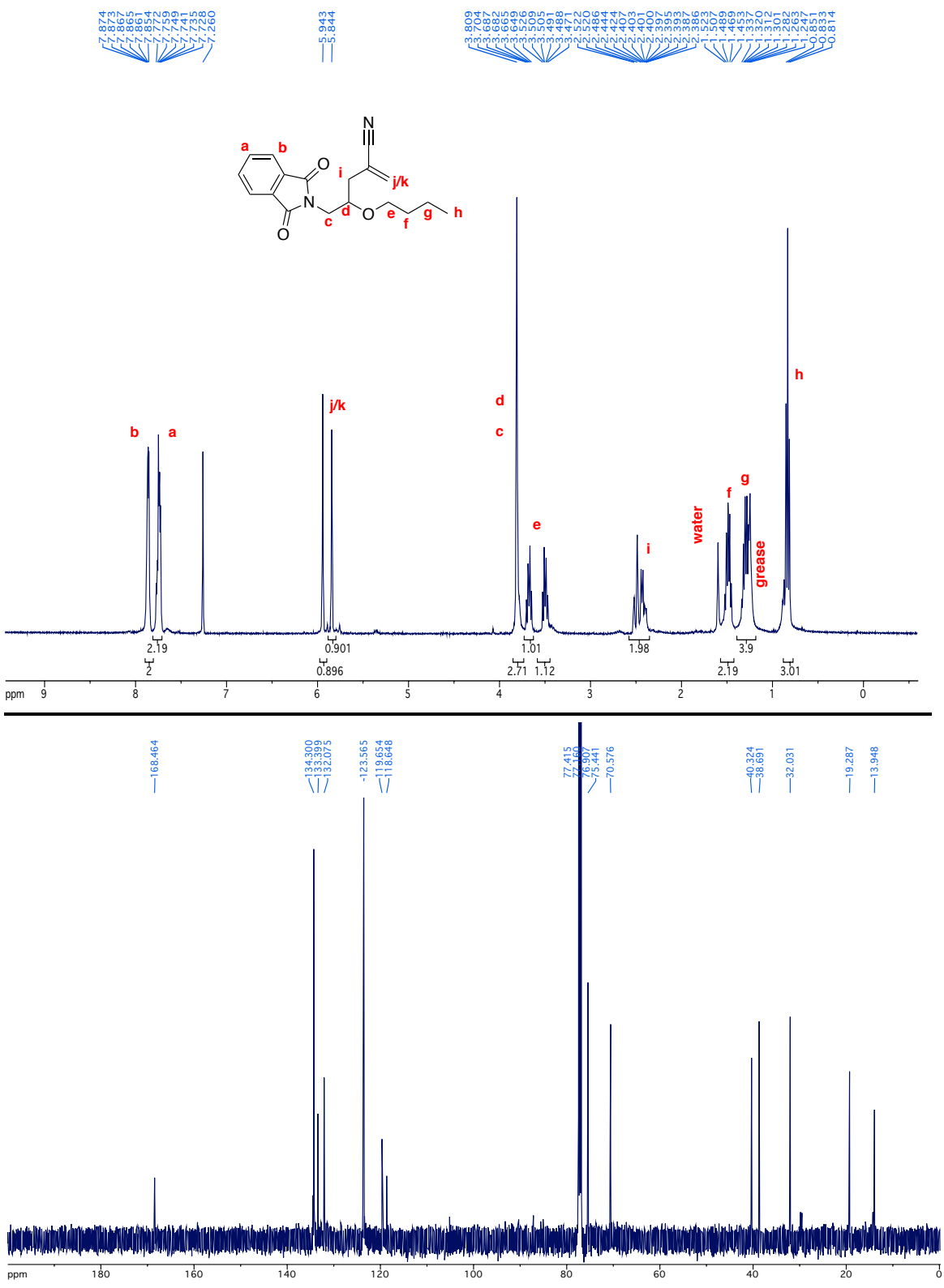
7.874
7.873
7.867
7.865
7.861
7.854
7.752
7.759
7.749
7.741
7.735
7.728
7.260
5.943
5.844
3.809
3.704
3.687
3.682
3.665
3.649
3.526
3.509
3.505
3.491
3.488
3.471
3.322
2.520
2.486
2.444
2.424
2.407
2.403
2.401
2.400
2.397
2.395
2.393
2.387
2.386
1.503
1.487
1.489
1.469
1.453
1.337
1.320
1.312
1.301
1.282
1.263
1.247
0.851
0.833
0.814
N
O
O
O
N
O
a
b
c
d
e
f
g
h
i
j/k
b
a
j/k
d
c
e
i
water
f
g
grease
h
2.19
0.901
1.01
1.98
3.9
3.01
2
0.896
2.71
1.12
2.19
ppm
9
8
7
6
5
4
3
2
1
0
168.464
134.300
133.999
132.075
123.565
119.654
118.648
77.415
77.160
76.907
75.441
70.576
40.324
38.691
32.031
19.287
13.948
ppm
180
160
140
120
100
80
60
40
20
0

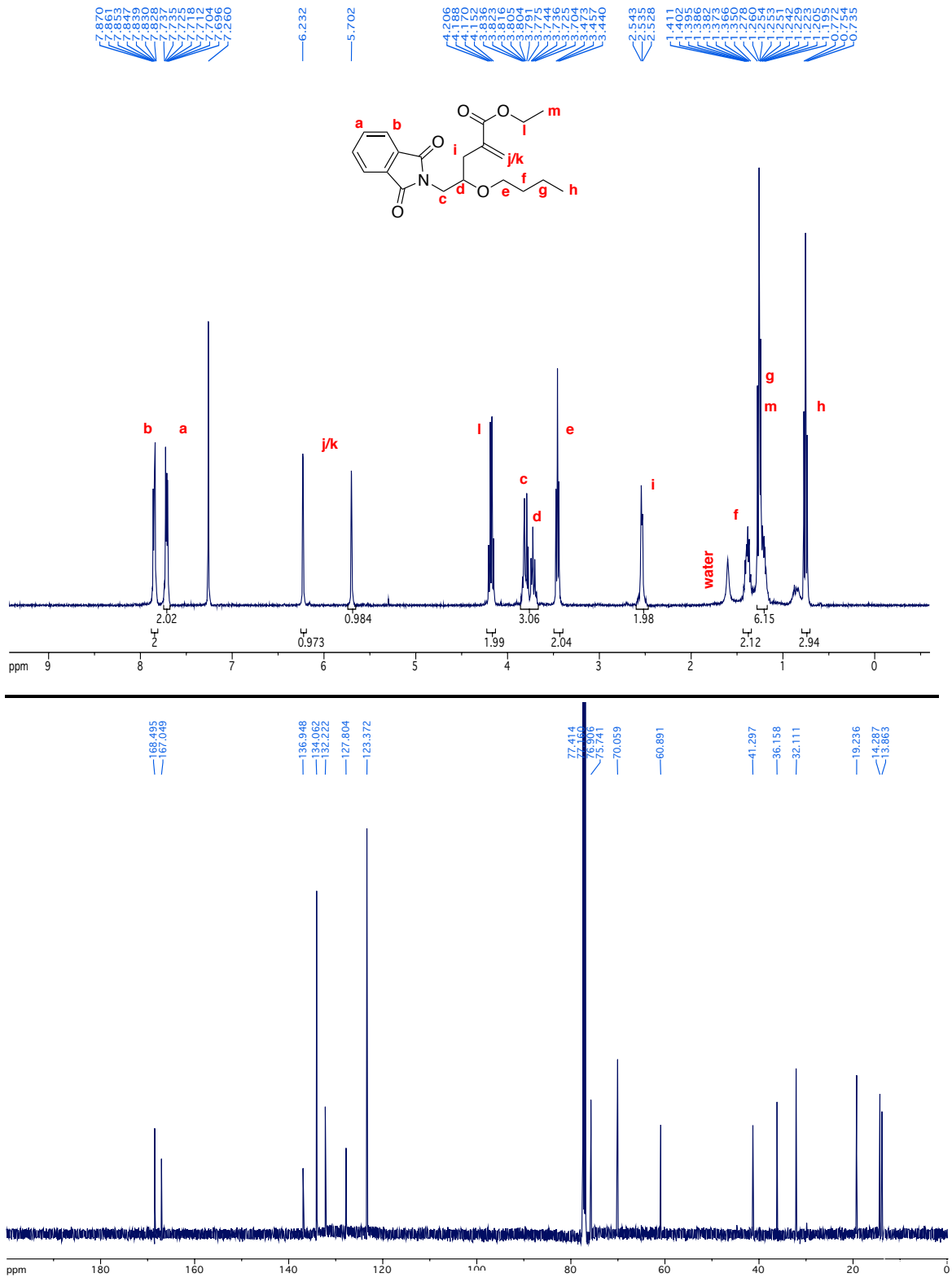
7.870
7.861
7.853
7.847
7.839
7.830
7.828
7.737
7.735
7.718
7.712
7.704
7.686
7.680
6.232
5.702
4.206
4.188
4.170
4.152
3.836
3.813
3.816
3.805
3.804
3.791
3.745
3.736
3.725
3.704
3.473
3.447
3.440
2.543
2.535
2.528
1.411
1.402
1.395
1.386
1.382
1.373
1.366
1.350
1.268
1.254
1.253
1.251
1.242
1.223
1.205
1.195
0.774
0.735
a
b
c
d
e
f
g
h
i
j/k
l
m
water
2.02
0.984
3.06
1.98
6.15
2
0.973
1.99
2.04
2.12
2.94
ppm
168.495
167.049
136.948
134.062
132.222
127.804
123.372
77.414
77.160
76.906
75.741
70.059
60.891
41.297
36.158
32.111
19.236
14.287
13.863

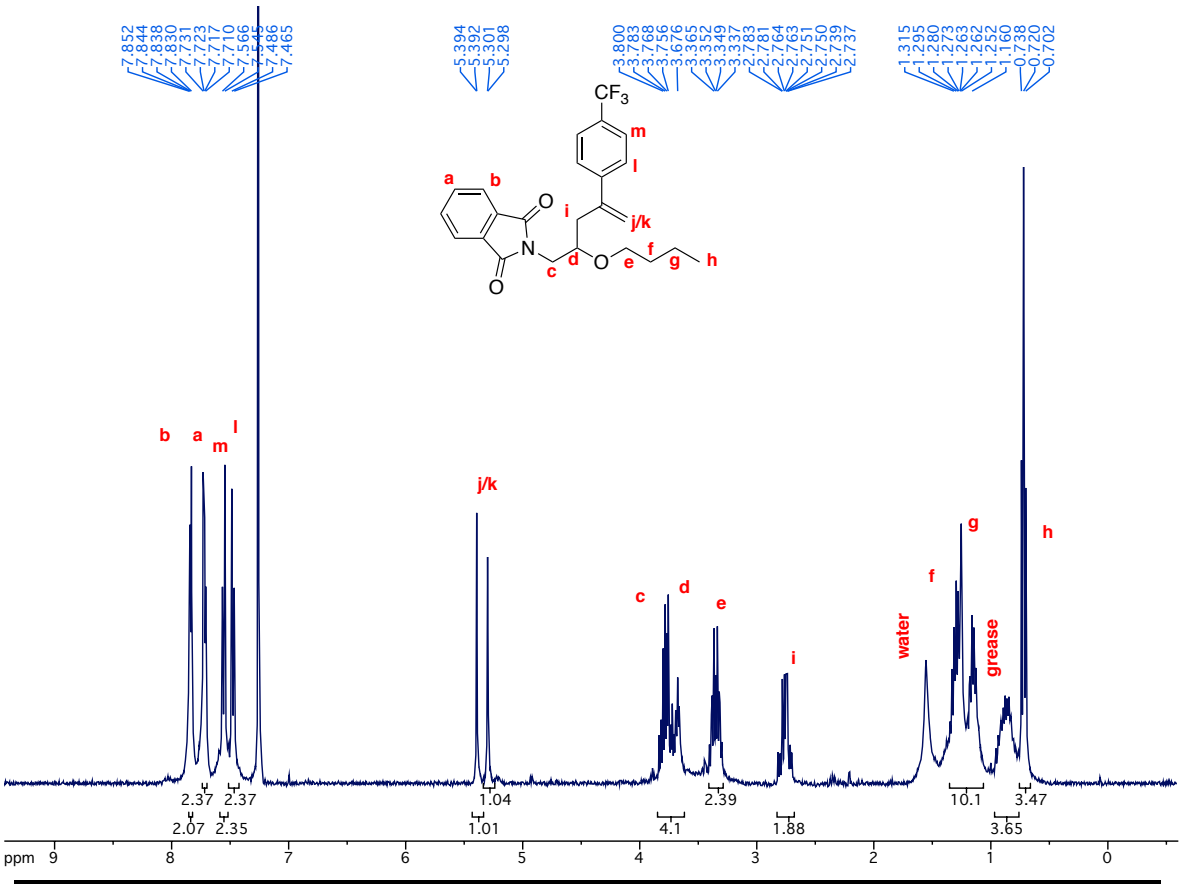
7.852
7.844
7.838
7.830
7.731
7.723
7.717
7.710
7.566
7.545
7.486
7.465
5.394
5.392
5.301
5.298
3.800
3.783
3.768
3.756
3.676
3.365
3.352
3.349
3.337
2.783
2.781
2.764
2.763
2.751
2.750
2.739
2.737
1.315
1.295
1.280
1.273
1.263
1.262
1.252
1.160
0.738
0.720
0.702
CF3
m
l
a
b
i
j/k
N
c
d
O
e
f
g
h
O
b
a
m
l
j/k
c
d
e
i
water
f
g
grease
h
2.37
2.37
1.04
2.39
10.1
3.47
2.07
2.35
1.01
4.1
1.88
3.65
ppm
9
8
7
6
5
4
3
2
1
0

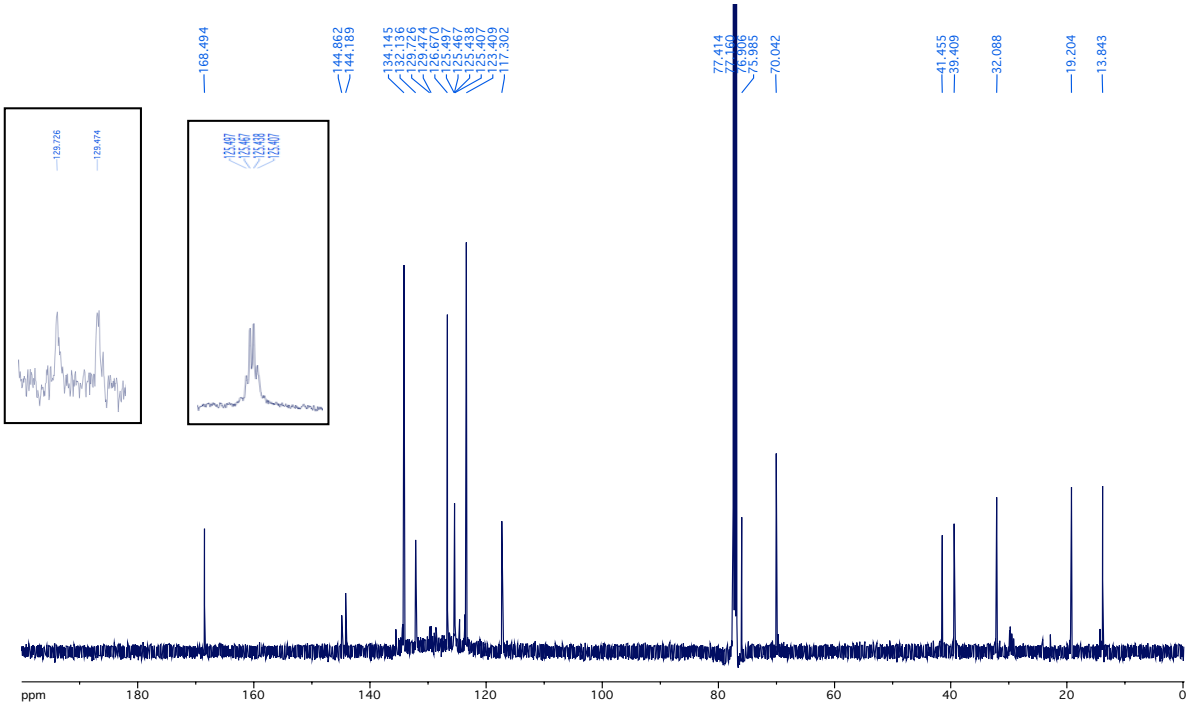
168.494
144.862
144.189
134.145
132.136
129.726
129.474
126.670
125.497
125.467
125.438
125.407
123.409
117.302
77.414
77.160
76.906
75.985
70.042
41.455
39.409
32.088
19.204
13.843
129.726
129.474
125.497
125.467
125.438
125.407
ppm
180
160
140
120
100
80
60
40
20
0

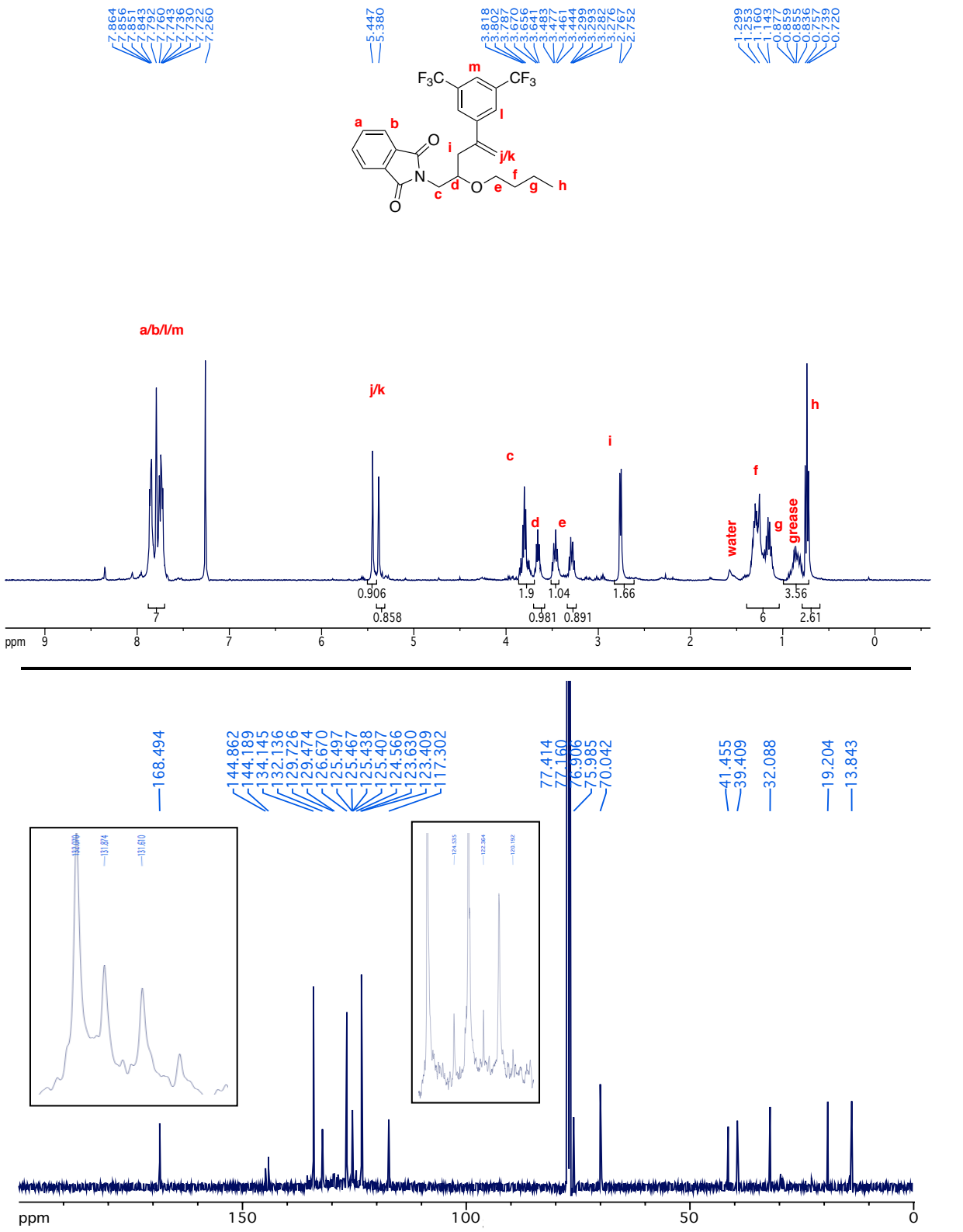
7.864
7.856
7.851
7.843
7.792
7.760
7.743
7.736
7.722
7.260
5.447
5.380
3.818
3.802
3.787
3.670
3.656
3.641
3.483
3.477
3.461
3.444
3.293
3.282
3.276
2.767
2.752
1.299
1.253
1.160
1.143
0.873
0.859
0.855
0.836
0.757
0.739
0.720
F3C
CF3
m
l
a
b
i
j/k
O
N
O
c
d
O
e
f
g
h
a/b/l/m
j/k
c
d
e
i
f
water
g
grease
h
0.906
1.9
1.04
1.66
3.56
7
0.858
0.981
0.891
6
2.61
ppm
9
8
7
6
5
4
3
2
1
0
168.494
144.862
144.189
134.145
132.136
129.726
129.474
126.670
125.497
125.467
125.438
125.407
124.566
123.630
123.409
117.302
77.414
77.160
76.906
75.985
70.042
41.455
39.409
32.088
19.204
13.843
131.874
131.610
124.535
122.364
120.192
ppm
150
100
50
0

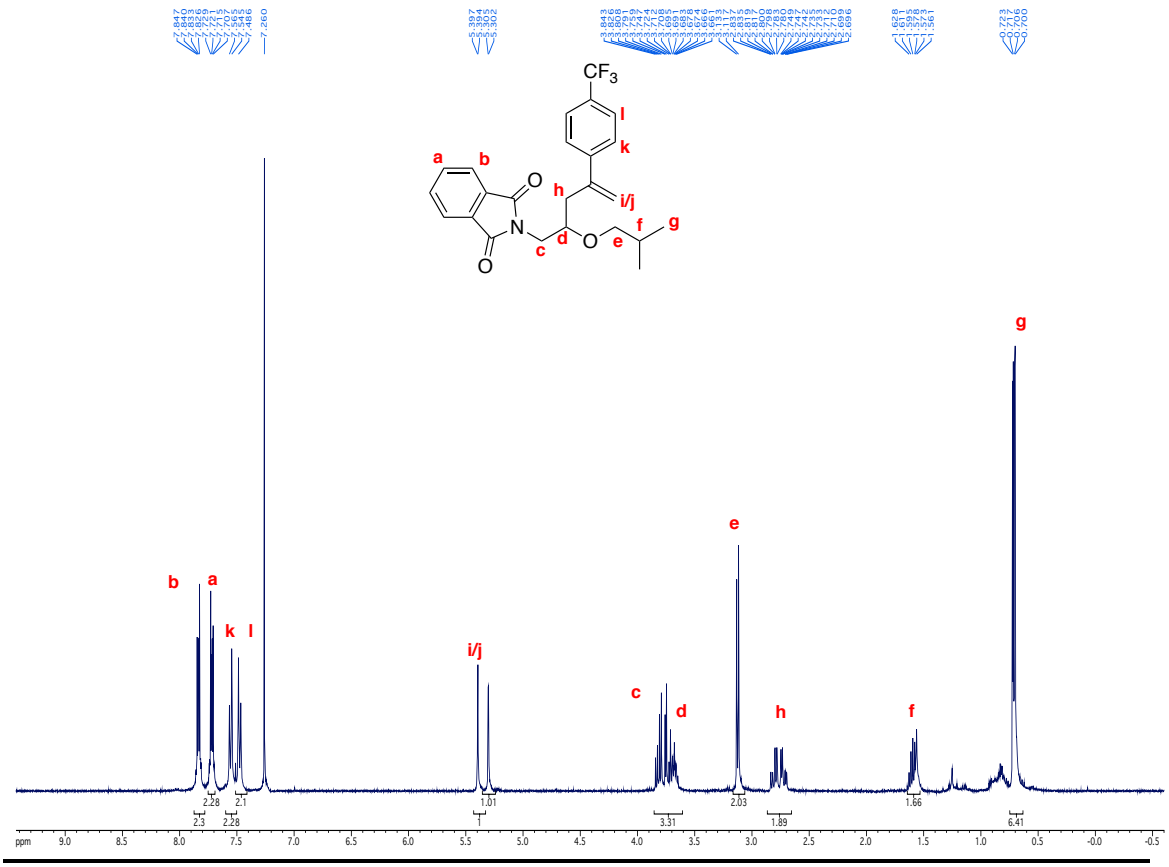
CF3
a
b
c
d
e
f
g
h
i/j
k
l
O
N
O
O
O
b
a
k
l
i/j
c
d
e
h
f
g
ppm

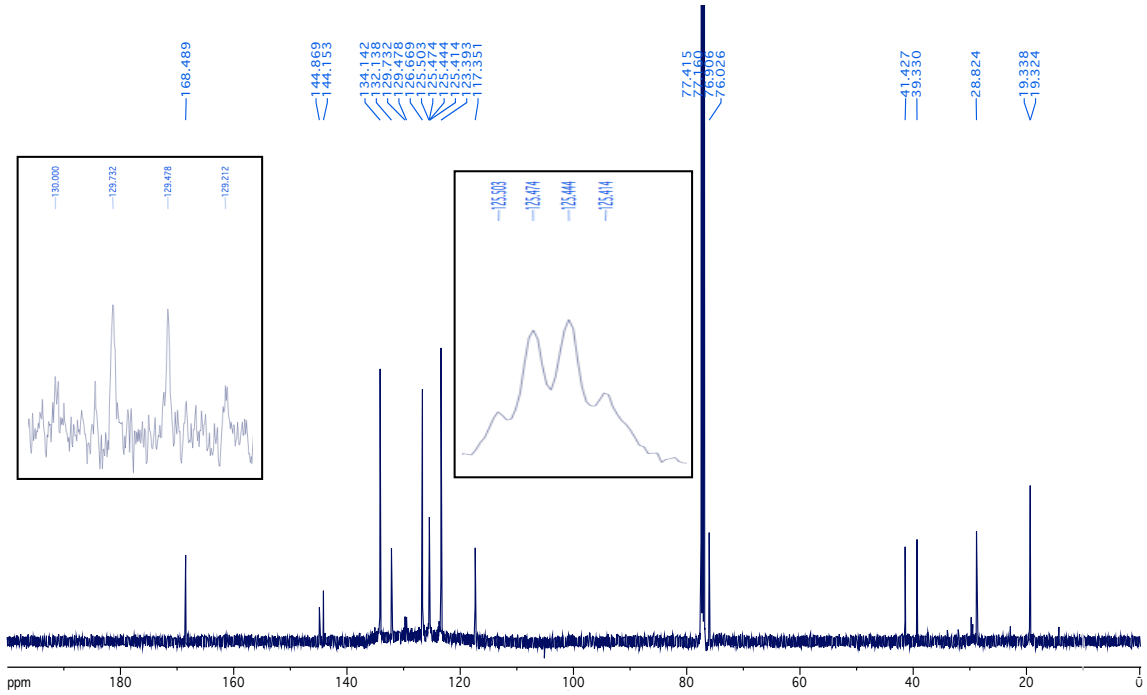
168.489
144.869
144.153
134.142
133.138
129.732
129.478
126.669
125.503
125.474
125.444
125.414
123.393
117.351
77.415
77.160
76.906
76.026
41.427
39.330
28.824
19.338
19.324
130.000
129.732
129.478
129.212
125.503
125.474
125.444
125.414
ppm

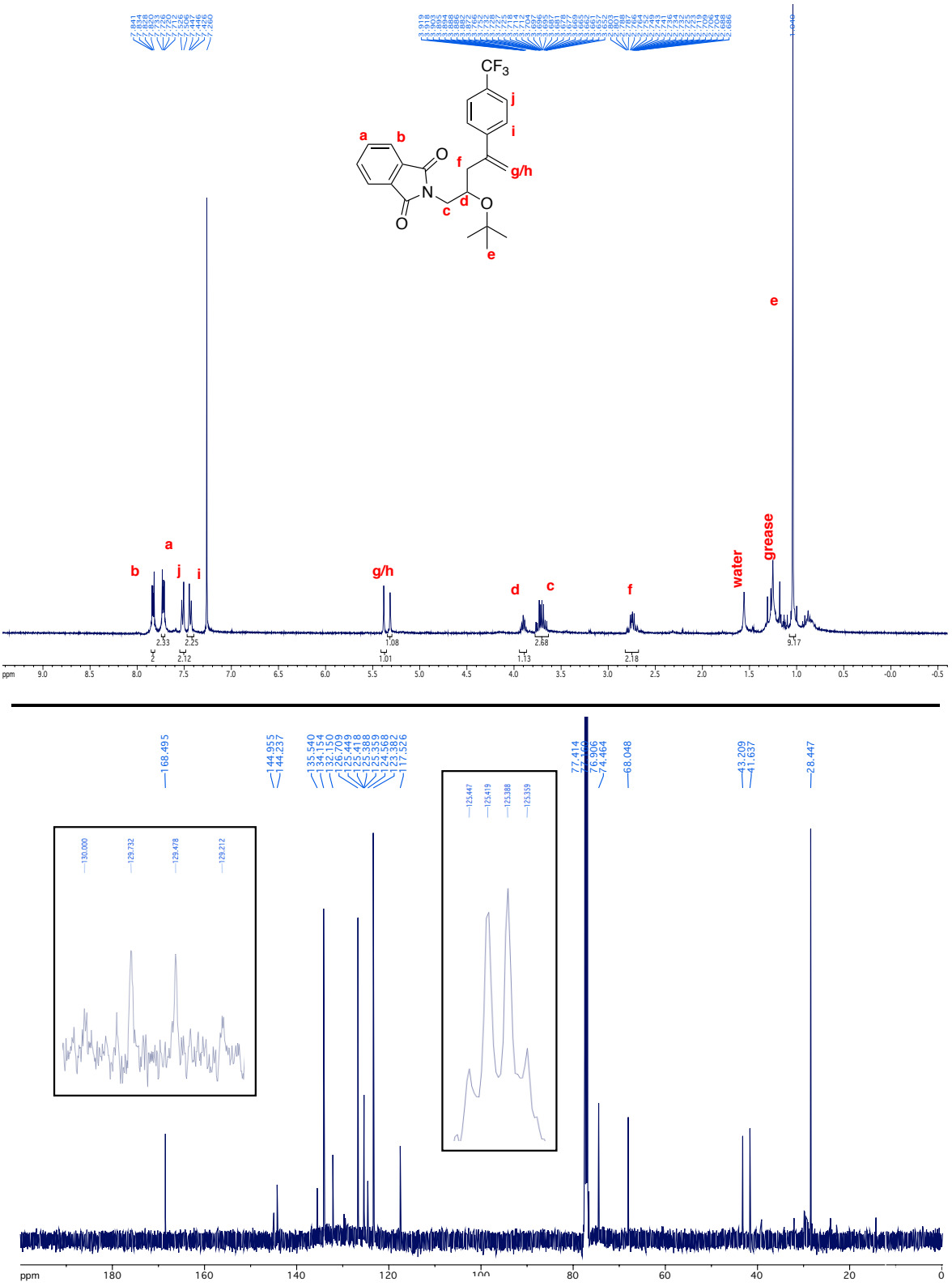
CF3
a
b
c
d
e
f
g/h
i
j
water
grease
ppm

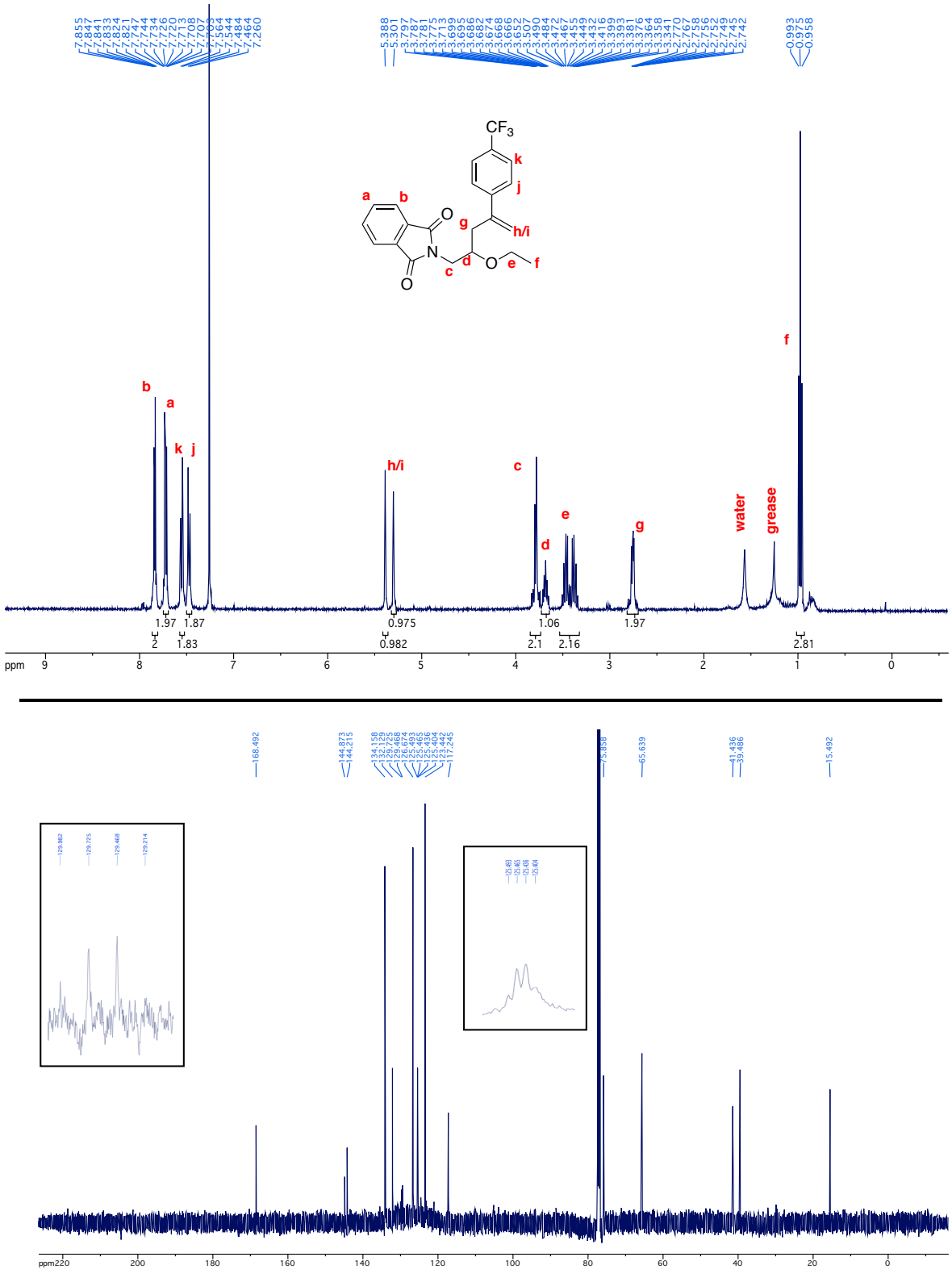
7.855
7.847
7.841
7.833
7.824
7.821
7.747
7.744
7.734
7.726
7.720
7.711
7.708
7.707
7.706
7.564
7.544
7.484
7.464
7.260
5.388
5.301
3.797
3.787
3.781
3.715
3.699
3.695
3.686
3.682
3.664
3.664
3.666
3.652
3.507
3.490
3.484
3.467
3.455
3.449
3.432
3.416
3.399
3.393
3.381
3.376
3.364
3.358
3.341
2.770
2.767
2.758
2.756
2.749
2.745
2.742
0.993
0.975
0.958
CF3
k
j
a
b
O
g
h/i
N
c
d
O
e
f
O
b
a
k
j
h/i
c
e
d
g
water
grease
f
1.97
1.87
0.975
1.06
1.97
2
1.83
0.982
2.1
2.16
2.81
ppm
9
8
7
6
5
4
3
2
1
0
168.492
144.873
144.215
134.158
132.129
129.725
128.468
126.674
125.493
125.485
125.436
125.424
125.422
117.245
75.858
65.639
41.436
39.486
15.492
129.382
129.725
129.468
129.214
125.493
125.485
125.436
125.424
ppm220
200
180
160
140
120
100
80
60
40
20
0

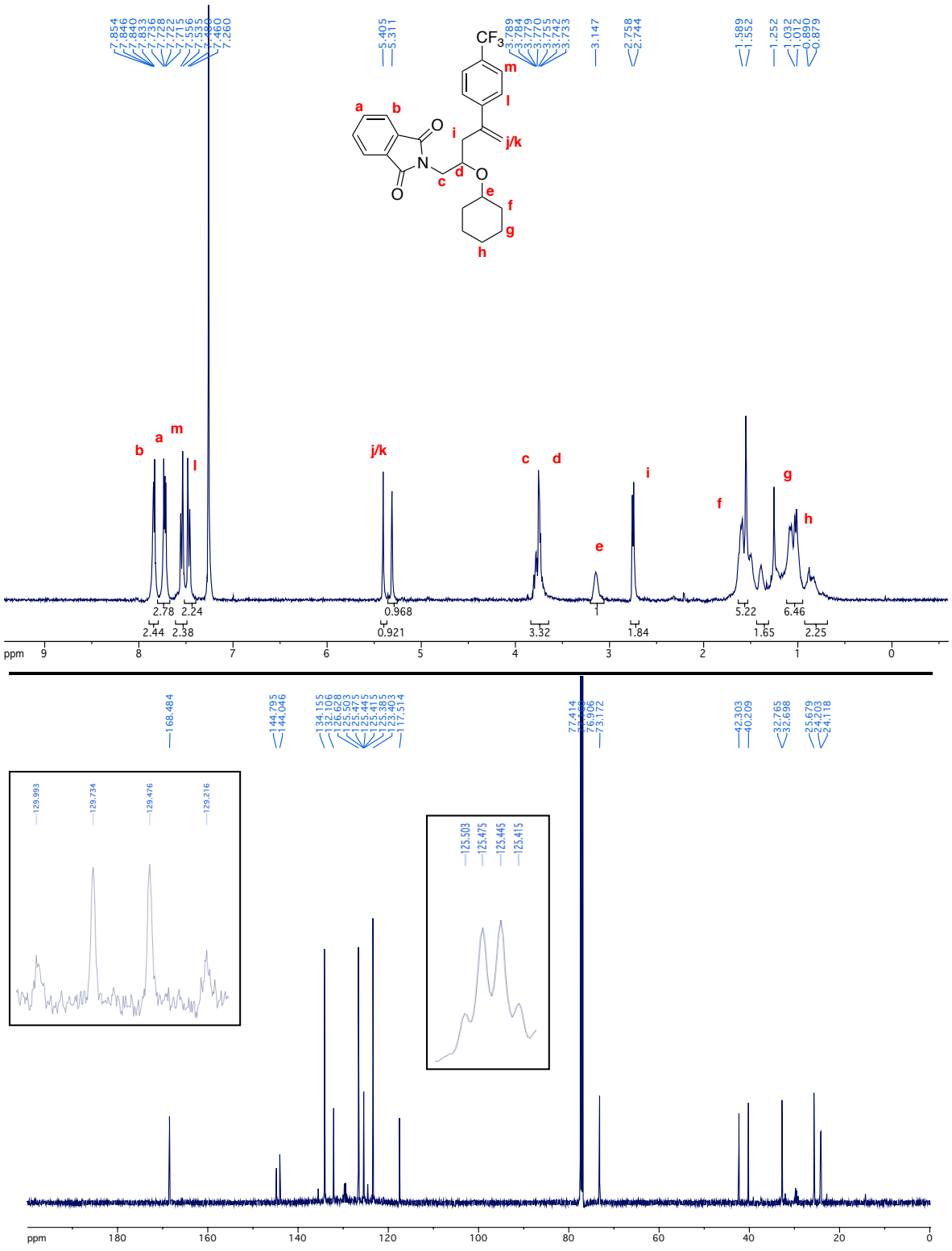
7.854
7.846
7.840
7.833
7.726
7.728
7.722
7.715
7.556
7.535
7.485
7.460
7.260
5.405
5.311
3.789
3.784
3.779
3.770
3.755
3.742
3.733
3.147
2.758
2.744
1.589
1.552
1.252
1.032
1.012
0.890
0.879
CF3
a
b
i
j/k
m
l
c
d
O
e
f
g
h
N
O
O
b
a
m
l
j/k
c
d
e
i
f
g
h
2.78
2.24
0.968
1
5.22
6.46
2.44
2.38
0.921
3.32
1.84
1.65
2.25
ppm
9
8
7
6
5
4
3
2
1
0
168.484
144.795
144.046
134.155
132.106
126.628
125.503
125.475
125.445
125.415
125.385
123.403
117.514
77.414
77.000
76.586
73.172
42.303
40.209
32.765
32.698
25.679
24.703
24.118
129.993
129.734
129.476
129.216
125.503
125.475
125.445
125.415
ppm
180
160
140
120
100
80
60
40
20
0

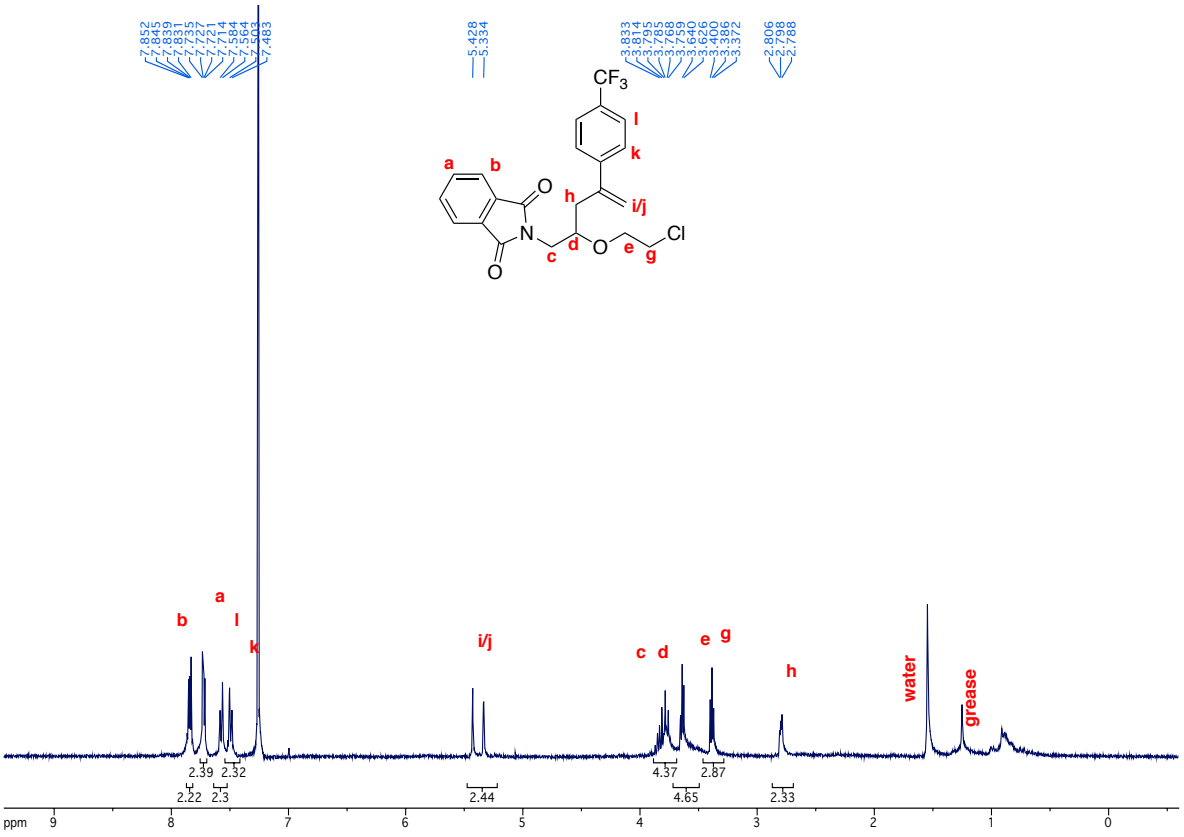
7.852
7.845
7.839
7.831
7.727
7.721
7.714
7.564
7.503
7.483
5.428
5.334
3.833
3.814
3.795
3.785
3.768
3.758
3.640
3.626
3.400
3.386
3.372
2.806
2.788
CF3
l
k
a
b
h
i/j
O
N
O
c
d
O
e
g
Cl
a
b
l
k
i/j
c d
e g
h
water
grease
2.39
2.32
2.22
2.3
2.44
4.37
2.87
4.65
2.33
ppm
9
8
7
6
5
4
3
2
1
0

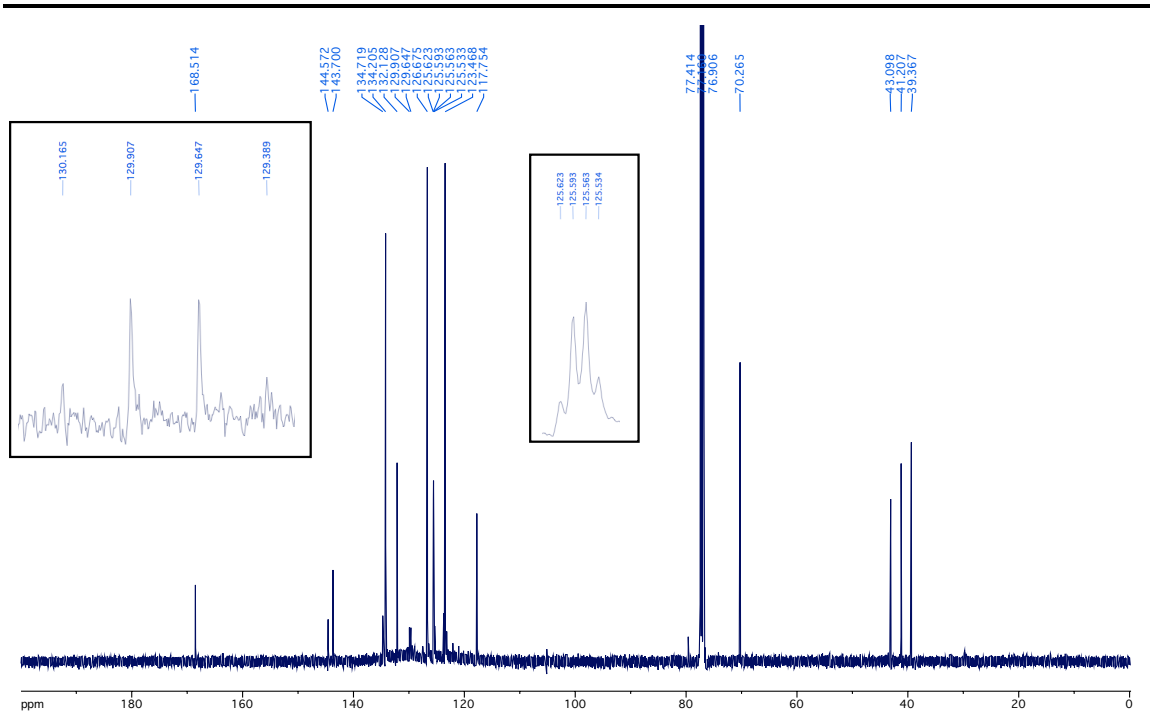
168.514
144.572
143.700
134.719
134.205
132.128
129.907
129.647
126.675
125.623
125.593
125.563
125.534
123.468
117.754
77.414
77.163
76.906
70.265
43.098
41.207
39.367
130.165
129.907
129.647
129.389
125.623
125.593
125.563
125.534
ppm
180
160
140
120
100
80
60
40
20
0

## 2.6 References


[1] (a) Patai, S. in *The Chemistry of alkenes*, Wiley Interscience **1964**, vol 1. (b) Lan, X.; Wang, N.; Xing, Y. Recent Advances in Radical Difunctionalization of Simple Alkenes. *Eur. J. Org. Chem.* **2017**, 5821-5851.

[2] (a) Renaud, P.; Sibi, P. in *Radical in Organic Synthesis Volume 1: Basic Principles*; Wiley-VCH. **2001**; pp. 72. (b) Clark, A. J. Atom Transfer Radical Cyclisation Reactions Mediated by Copper Complexes. *Chem. Soc. Rev.* **2002**, *31*, 1-11.

[3] (a) Gossage, R. A.; van de Kuil, L. A.; van Koten, G. Diaminarylnickel(II) "Pincer" Complexes: Mechanistic Considerations in the Kharasch Addition Reaction, Controlled Polymerization, and Dendrimeric Transition Metal Catalysts. *Acc. Chem. Res.* **1998**, *31*, 423-431. (b) Minisci, F. Free-Radical Additions to Olefins in the Presence of Redox Systems. *Acc. Chem. Res.* **1975**, 165-171. (c) Iqbal, J.; Bhatia, B.; Nayyar, N. K. Transition Metal-Promoted Free-Radical Reactions in Organic Synthesis: The Formation of Carbon-Carbon Bonds. *Chem. Rev.* **1994**, *94*, 519-564.

[4] (a) Patil, S.; Chen, L.; Tanko, J. M. C-H Bond Functionalization with the Formation of a C-C Bond: A Free Radical Condensation Reaction Based on Phthalimido-*N*-oxyl Radical. *Eur. J. Org. Chem.* **2014**, 502-505. (b) Patil, S.; Chen, L.; Tanko, J. M. Effect of Lewis Acids and Low Temperature Initiators on the Allyl Transfer Reaction Involving Phthalimido-*N*-Oxyl radical. *Tetrahedron Lett.* **2014**, 7029-7033.

[5] Furmisky, E.; Howard, J. A. Absolute Rate Constants for the Reaction of tert-butylperoxy Radicals with Trivalent Phosphorus Compounds. *J. Am. Chem. Soc.* **1973**, *95*, 369-374.

[6] Mayr, H.; Patz, M. Scales of Nucleophilicity and Electrophilicity: A System for Ordering Polar Organic and Organometallic Reactions. *Angew. Chem. Int. Ed.* **1994**, *33*, 938-957.

[7] (a) Minisci, F.; Vismara, E.; Fontana, F.; Morini, G.; Serravalle, M. Polar Effects in Free-Radical Reactions. Solvent and Isotope Effects of Base Catalysis on the Regio- and Chemoselectivity of Protonated Heteroaromatic Bases by Nucleophilic Carbon-Centered Radicals. *J. Org. Chem.* **1987**, *52*, 730-736. (b) Pan, X.; Lacpte, E.; Lalevee, J.; Curran, D. P. Polarity Reversal Catalysis in Radical Reductions of Halidesby N-Heterocylcic Carbene Boranes. *J. Am. Chem. Soc.* **2012**, *134*, 5669-5674. (c) Robers, B. P. Polaryity-Reversal Catalysis of Hydrogen-Atom Abstraction Reactions: Concepts and Applications in Organic Reactions. *Chem. Soc. Rev.* **1999**, *28*, 25-35.

[8] Giese, B.; He, J.; Mehl, W. Polarity Effects in Radical Addition Reactions: Borderline Cases. *Chem. Ber.* **1988**, *121*, 2063.

[9] (a) Hill, J. S.; Isaacs, N. S. Functionalisation of the Alpha Position of Acrylate Systems by the Addition of Carbonyl Compounds: Highly Pressure-Dependent Reactions. *Tetrahedron Lett.* **1986**, 5007-5010. (b) Patil, S.;Chen, L.; Tanko, J. M. C-H Bond Functionalization with the Formation of a C-C Bond: A Free Radical Condensation Reaction Based on the Phthalimido-*N*-oxyl Radical. *Eur. J. Org. Chem.* **2014**, 502-505.

[10] Grzan, A.; Jaganathan, A.; Marzijarani, N. S.; Yousefi, R.; Whitehead, D. C.; Jackson, J. E.; Borhan, B. Solvent-Dependent Enantiodivergences in the Chlorocyclization of Unsaturated Carbamates. **2013**, *19*, 9015-9021.

[11] Hirano, K.; Biju, A. T.; Piel, I.; Glorius, F. N-Heterocyclic Carbene-Catalyzed Hydroacylation of Unactivated Double Bonds. *J. Am. Chem. Soc.* **2009**, *131*, 14190-14191.

[12] Auvray, P.; Knochel, P.; Normant, J. F. 3-Bromo-2-t-butylsulfonyl-1-propene. A Versatile Multi-Coupling Reagent Part 1. *Tetrahedron*, **1988**, *44*, 4495-4508.

[13] Knochel, P.; Normant, J. F. Synthèse de diènes-1,4 fonctionnalisés par addition de zinziques allyliques fonctionnalisés sur des alcynes vrais et leur cyclisation en hétérocycles ou carbocycles, *J. Organomet. Chem.* **1986**, *309*, 1-23.

[14] Song, G.; Lu, Q.; Xu, J.; Sun, L.; Wang, J.; Xu, B.; Cui, J.; Zhou, X.; Zhu, J.; Zheng, Y.; Fu, X. Aza bicyclic Derivatives and their Preparation and Use (by Machine Translation). CN105294674.

[15] Davoust, M.; Cantagrel, F.; Metzner, P.; Brière, J.-F. A Stereodivergent Synthesis of beta-hydroxy-alpha-methylene Lactones via Vinyl Epoxides. *Org. Biomol. Chem.* **2008**, *6*, 1981-1993.

# Chapter 3: Formal Aniline Synthesis from Phenols Using a Radical Smiles Rearrangement

## 3.1 Introduction

In addition to aliphatic amines, aryl amines (also known as anilines) are similarly an important class of molecules that are found in a wide array of pharmaceuticals, natural products, agrochemicals, and much more.[1] Classically, anilines have been prepared via a two step nitration, hydrogenation sequence, and while this procedure can suffer from harsh conditions, high temperatures, and mixed regioselectivities, this method has proven to be a tried and true method for the synthesis of primary anilines (Scheme 3.1.a).[2] To compliment this reactivity, a myriad of transition metal catalyzed coupling strategies have been developed by Ullman,[3] Buchwald,[4] Hartwig,[5] Chan,[6] and Lam[7] that take advantage of aryl halides/boronic acids and amine nucleophiles to forge new C-N bonds (Scheme 3.1.b). While many of the recently developed variants of these cross coupling strategies operate with relatively mild conditions and tolerate a host of functionalities,[8] the transition metals and designer ligands required to perform these reactions can render them prohibitively expensive for some.[9]

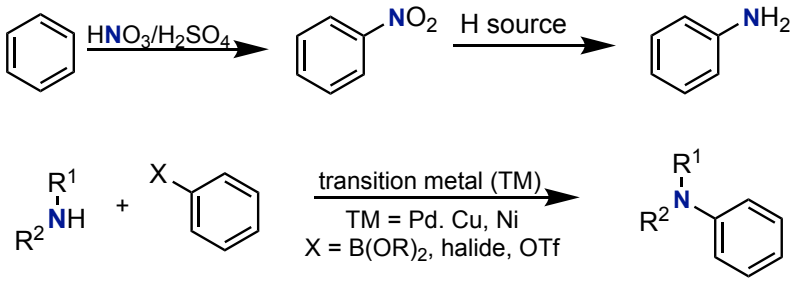


Scheme 3.1. Traditional methods for the preparation of aromatic amines.

While typical cross coupling strategies for the synthesis of anilines rely on the use of aryl halides or boronic acids, recent attention has shifted to the activation of aryl C-O bonds as a new route toward the synthesis of aromatic amines.[10] C-O activation is an attractive approach because it obviates the generation of stoichiometric halide waste, utilizes extremely abundant, lignin-biomass derived starting materials, and shifts focus from non-renewable, petroleum derived

chemicals to those that are renewable and found widely in nature (Scheme 3.2.a).[11] In particular, the Smiles rearrangement is a base mediated process that achieves intramolecular N-nucleophilic substitution at an aryl ether (Scheme 3.2.b).[12] Because the Smiles reaction is an $S_NAr$ process, electron deficient arenes are typically required to achieve good reaction efficiencies, though new evidence suggests that in some instances less activated arenes may be used.[13]

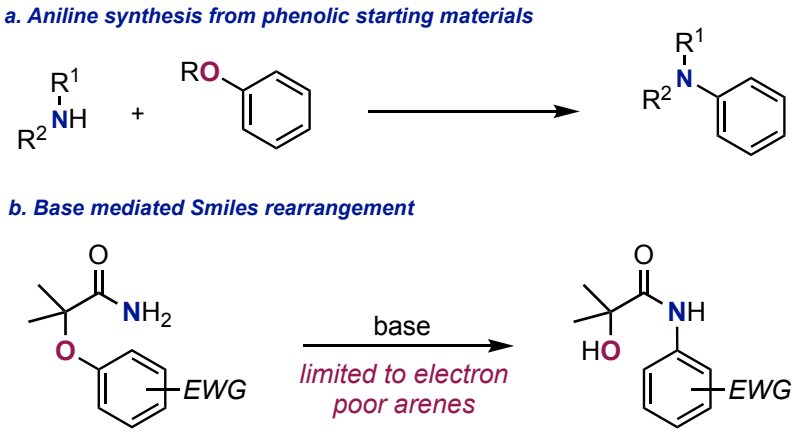


Scheme 3.2. Aniline synthesis via substitution at C-O bonds.

Recent efforts have lead to the development of radical mediated Smiles-type transformations that are largely unaffected by arene electronics,[14] though only a select few of these transformation employ a nitrogen-centered radicalophile for the synthesis of anilines.[15] Of note, Guo recently reported an electrochemical, radical-mediated Smiles reaction that utilized *O*-(2,4-dinitro)-phenyl hydroxamate esters as nitrogen-radical precursors for the formal synthesis of anilines from phenols.[16] Inspired by this work, we hypothesized that a similar transformation may be achieved using unfunctionalized hydroxamic acids without the need for an *O*-pendent electrophore.

## 3.2 Reaction Development and Substrate Scope

In light of the known propensity for amidyl radical to add into aromatic systems, we hypothesized that hydroxamic acids with the general structure presented below is Scheme 3.3

could be used for the formal synthesis of anilines from phenols. This structural scaffold was attractive to us because it can be easily synthesized from a wide range of different phenols in good to excellent yields (See appendix of this chapter for more information) and would allow for an intramolecular substitution at the aryl C-O bond of the phenol for the production of anilines.

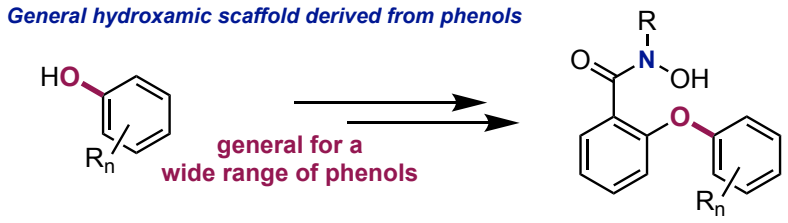


Scheme 3.3. General hydroxamic acid scaffold for the conversion of phenols to anilines.

We began our investigation by subjecting hydroxamic **3.2a1** to conditions similar to those used in our hydroamination and aminoallylation methods. In the presence of triethyl phosphite (1.5 equiv) and DLP (10 mol %) in DCE at 90 °C, we found that the desired amide **3.2b1** was produced in 83% isolated yield (Table 3.1, entry 1). Similar to our other methods, we found that this procedure was very sensitive to the nature of the thermal radical initiator used in the reaction. Common initiatros such as BPO and AIBN failed to produce any appreciable amounts of **3.2b1** (entries 2 and 3), though we found that di-tertbutyl peroxide (DTBP) improved reaction efficiency to 95% isolated yield (entry 4). Notably, we found that optimal yields were obtained when using a higher load of DTBP (50 mol% for entry 4), and ultimately we discovered that a super stoichiometric quantity of DTBP (5 equivalents) resulted in the highest reaction efficiency for a wide range of substrates. The 10-hour half life of DTBP has been document to be 125 °C in benzene,[17] making it one of the more stable thermal radical initiators that are commercially available. As a result of this, a higher load of the initiator is needed to produce the desired product in a 24 hour timeframe at the relatively low temperature of 90 °C. Control experiments where

radical initiator and phosphite were individually excluded did not result in the production of any of the desired product, thereby revealing their necessity in this process (entries 5 and 6).

Table 3.1. Radical Smiles rearrangement reaction optimization. [a]Reactions carried out with **3.2a1a** (1 equiv), $P(OEt)_3$ (1.5 equiv), and initiator (0.1 equiv) in 0.16M 1,2-dichloroethane at 90 °C for 24 h; AIBN = 2,2'-azobis(2-methylpropionitrile). [b]Yields determined by gas chromatography using mesitylene as an internal standard. [c]Carried out with 0.5 equiv initiator; isolated yield following silica gel chromatography.

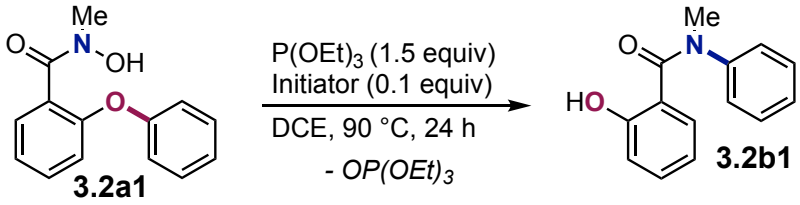


| Entry[a] | Initiator | Yield of 3.2b1[b] |
|---|---|---|
| 1 | $(undecylCO_2)_2$ | 83% |
| 2 | $(BzO)_2$ | < 5% |
| 3 | AIBN | < 5% |
| 4 | $(^tBuO)_2$ | 95%[c] |
| 5 | *none* | < 5% |
| 6 | $(^tBuO)_2$ and *no P(OEt)3* | < 5% |

With optimized conditions, we set out to explore the substrate scope of this reaction. We found that a wide range of phenol derivatives were amenable to this procedure including those bearing ortho-, meta-, and para-functionalities (Scheme 3.4, **3.2b2 – 3.2b16**). Within this class of substrates, electron rich methoxy groups were well tolerated, as was an electron deficient methyl ester and trifluofomethyl group. Halides and alkyl substituents were similarly tolerated. Of note, mono-substituted substrates resulted in generally high yields across the board, regardless of substitution pattern, electronics, or steric or steric bulk of the hydroxamic acid substrate.

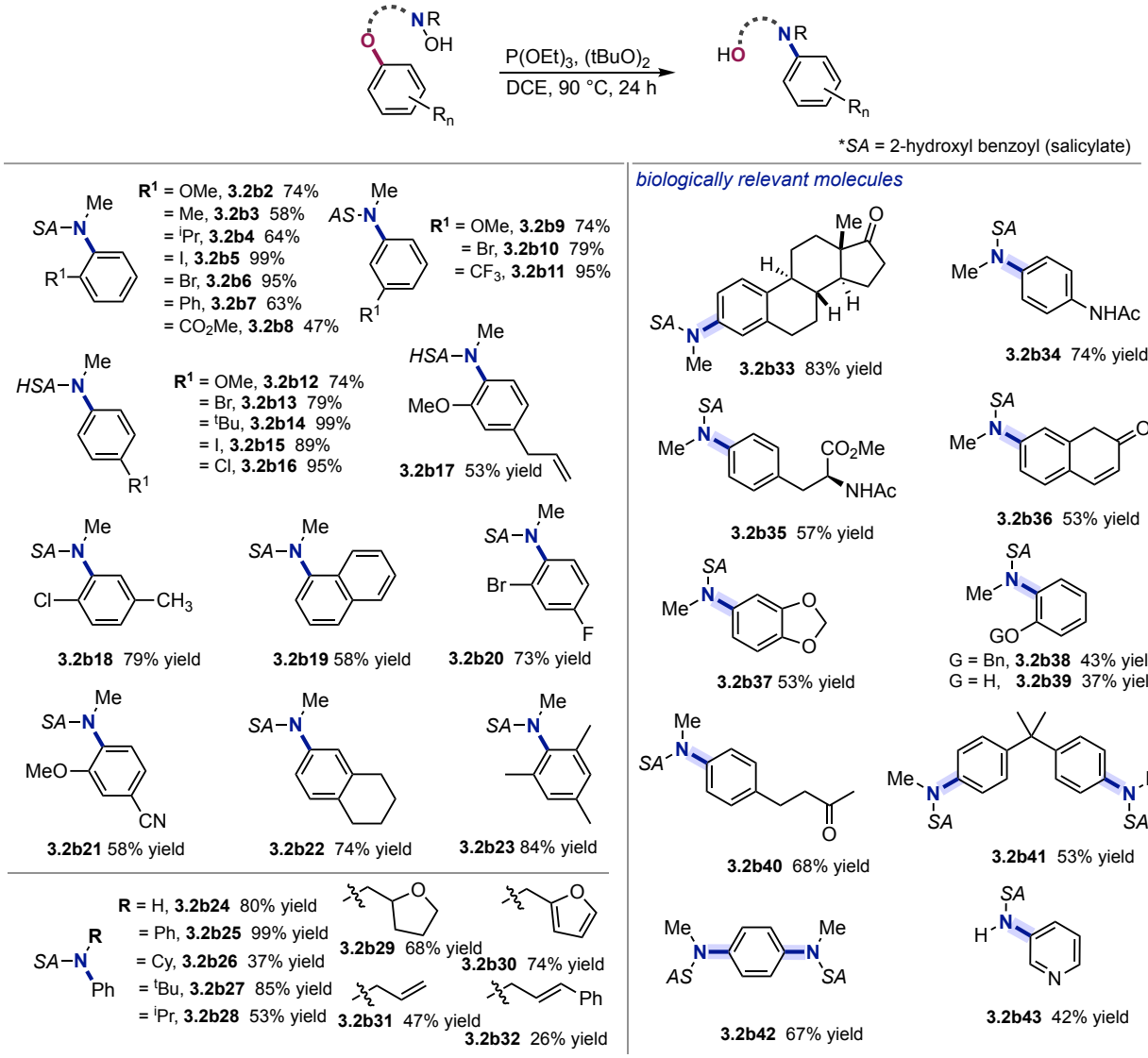


Scheme 3.4. Rearrangement substrate scope. All reactions carried out with the corresponding hydroxamic acid (1 equiv), $P(OEt)_3$ (1.5 equiv), and $(^tBuO)_2$ (5 equiv) in 0.16M 1,2-dichloroethane at 90 °C.

Poly-substituted substrates were similarly tolerated including that which was derived from eugenol, bearing a p-allyl group. The extended conjugation of 2-naphthol derived substrate participated in this reaction in modest yield, as did the dihalogenated substrate **3.2a20,** capable of undergoing further functionalization using traditional transition metal cross coupling. In addition to substitution at the phenol, we explored the tolerability of substitution at nitrogen beyond just a

simple methyl group, which previous reports were limited to. To our delight, we found that a variety of N-substituted hydroxamic acids were amenable to this protocol. For instance, alkyl groups such as a tert-butyl group, isopropyl group, and cyclohexyl group were all tolerated. Of note, we observed diminished yield when employing substrates **3.2a26** and **3.2a28,** and we hypothesize that this is a result of the presence of an abstractable, secondary hydrogen atom adjacent to the nitrogen atom. Abstraction at this cite by an amidyl radical or some other radical species could result in substrate decomposition and explain the decrease in yield. Furthermore, a phenyl group was tolerated, as were heterocyclic substrates **3.2a29** and **3.230** bearing a tetrhydrofunrayl and furanyl heterocycles. N-allyl and N-cinnamyl substrates similarly underwent this reaction, though in diminished yield. Again, we attribute this to the presence of the abstractable hydrogens alpha to the nitrogen atom. We found that N-unsubstituted substrate **3.2a24** produced the desired product in 80% yield, indicating that this procedure may be amenable to the synthesis of primary amines following hydrolysis.

In order to demonstrate the synthetic utility of this rearrangement protocol, we sought to perform this procedure on substrates derived from phenols with biological significance. Acetaminophen, a common over the counter analgesic successfully took part in this reaction, as did *N*-acetyl-L-tyrosine methyl ester. Sesamol, a suspected anti-microbial agent took part in this reaction to the desired amide product, along with umbilliferone, a member of the coumarin family. 2-benzyloxy phenol, a model of the alpha-O-4- linkage of lignin, took part in this reaction, as did the free phenol derivative. Raspbery ketone, the compound responsible for the pleasant smell of raspberries took part in this reaction, and produced the desired *N*-methyl amide in 68% yield. Polyphenolic substrates such as those derived from para-hydroquinone and bisphenol A (BPA)

similary took part in this reaction, as did the heterocyclic substrate derived from 3-hydroxypyridine.

Finally, we sought to explore the electronic effects of the aryl group not derived from the phenol of the hydroxamic acid. Interestingly, while no electronic effects were observed on the part of the phenol derived arene, the hydroxamyl arene bearing an electron decificent trifluormethyl group took part in this reaction in much higher yield than that with an electron donating methoxy group (Scheme x). We attribute this differentiation in reaction efficiency to the electronic effect these substituents have on the polarity of the amidyl radical produced following deoxygenation. This data suggests that more electron deficicent, electrophilic amidyl radicals take part in the desired rearrangement procedure more readily than do electronically rich amidyl radicals. This is most likely a result of proper polarity matching, where an electron poor amidly radical will react more favorably at the electron rich, ipso-phenol carbon.

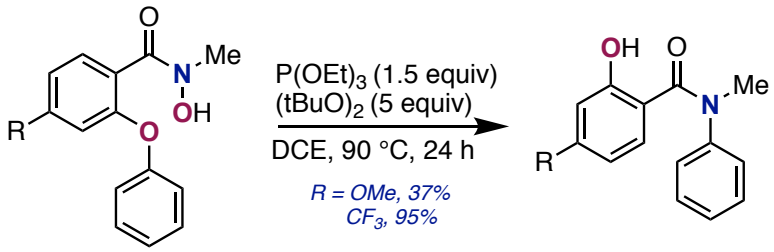


Scheme 3.5. Exploration of aromatic-tether electronics. All reactions carried out with the corresponding hydroxamic acid (1 equiv), $P(OEt)_3$ (1.5 equiv), and $(^tBuO)_2$ (5 equiv) in 0.16M 1,2-dichloroethane at 90 °C.

## 3.3 Synthetic Utility

We explored the utility of this reaction by performing the stepwise conversion of phenol to anilinium hydrochloride in 3 simple synthetic steps with a total yield of 70% and no chromatography needed (Scheme 3.6.a.). In addition to this, we were cable of converting the essential hormone estrone to the *N*-methyl analogue, again in just 3 steps with a total yield of 80% and without the need for purification by column chromatography (Scheme 3.6.b.).

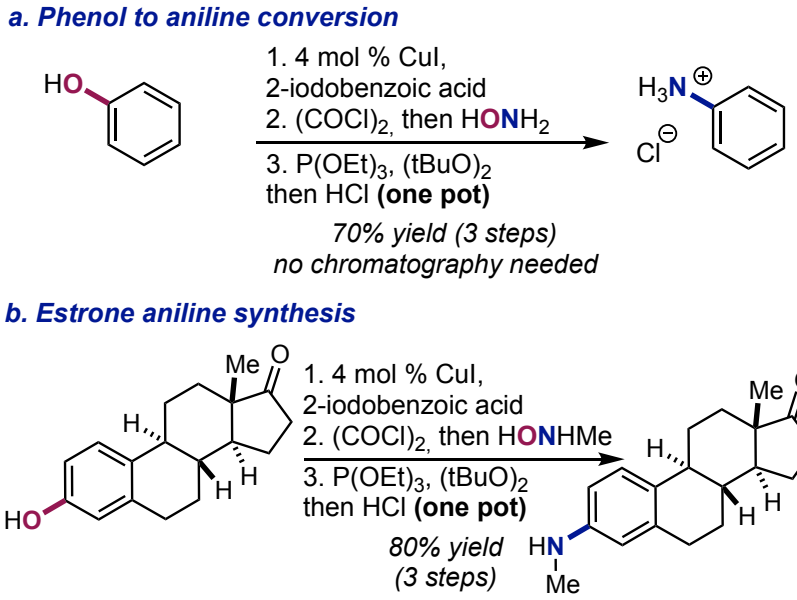


Scheme 3.6. Synthetic utility of direct phenol to aniline conversion. Detailed experimental procedures can be found in the Appendix.

Finally, we subjected amide **3.2a27** to base-mediated Smiles conditions employed by Turner[18] and Yamano[19] and found that in each case, no product was obtained and starting material was cleanly recovered (Scheme 3.7). This further emphasizes the utility of a radical-mediated approach.

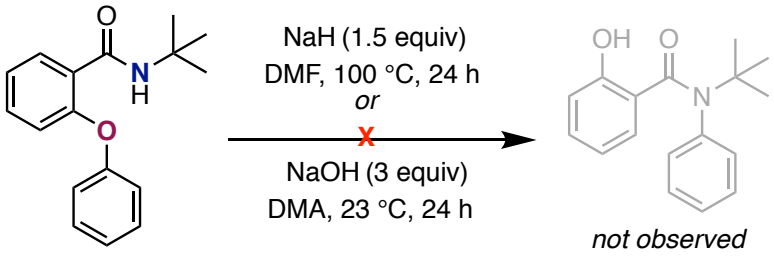


Scheme 3.7. Ineffective use of base-mediated conditions for substrate **3.2a27**.

## 3.4 Mechanistic Proposal

A mechanistic proposal in line with our data is presented in Scheme 3.8, radical initiation of the starting hydroaxamic acid generates an amidoxyl radical, which following deoxygenation, produces triethyl phosphate and the requisite amidyl radical. Addition, of the amidyl radical at the ipso-carbon of the phenol-derived arene produces a 6-membered intermediate and arene stabilized

radical. Homolytic elimination at oxygen results in rearomatization of the arene as well as the production of a stabilized, phenoxyl radical which upon hydrogen atom transfer, delivers the desired amide product and turns over the radical chain. This mechanism can be further understood by taking into account the bond dissociation energy of the bonds being formed and broken throughout the reaction. Deoxygenation of the hydroxamic acid breaks a very weak N-O bond and produces an appreciably strong P=O unit. Furthermore, the formation of a relatively strong aryl C-N linkage in exchange for the breaking of a relatively weak aryl C-O bond provides significant thermodynamic favorability for the reaction.

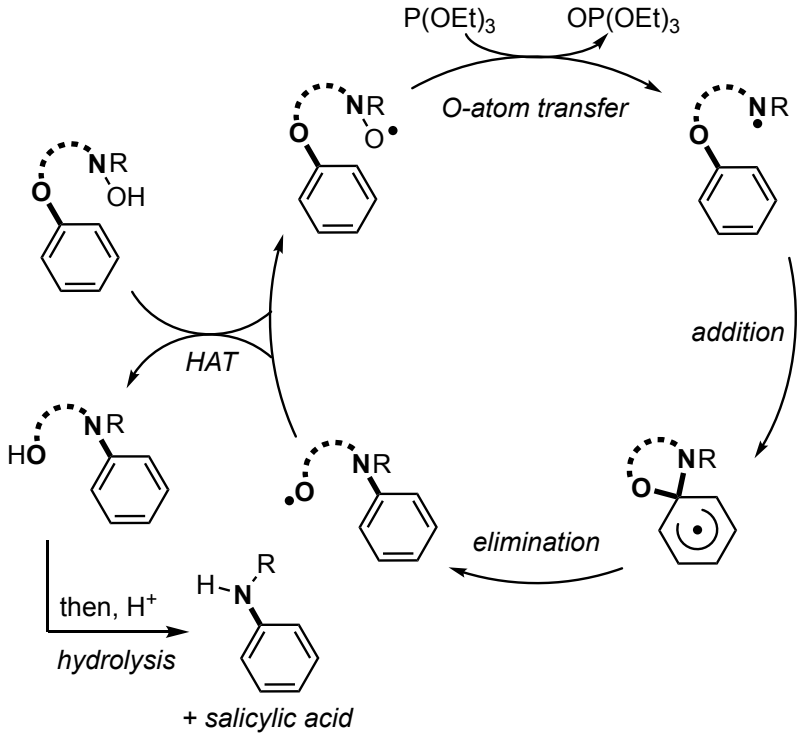


Scheme 3.8. Mechanistic proposal for radical-mediated Smiles rearrangement.

## 3.5 Conclusions

The synthesis of anilines has classically been achieved through a two-step nitration/hydrogenation sequence or a transition metal catalyzed cross coupling with an amine nucleophile. Because of growing concerns over our dependence on petroleum derived chemicals

and precious transition metal catalysts, attention has slowly but surely shifted toward the development of metal-free methods that take advantage of renewable, lignin derived, phenolic starting materials for the synthesis of anilines. Our work employs hydroxamic acid substrates that are easily prepared from a wide range of phenols for the formal conversion of phenols to anilines. Our strategy of a radical-mediated Smiles type rearrangement obviates the need for a precious transition metal catalyst or halogenated, aromatic electrophile. Furthermore, the radical approach allows us to perform this reaction successfully with both electron rich and electron poor substrates, whereas the classic, base-mediated Smiles reaction typically requires electron poor arenes to achieve acceptable yields.

Chapter 3 has been adapted from materials published in Lardy, S. W.; Luong, K. C.; Schmidt, V. A. Formal Aniline Synthesis from Phenols via Deoxygenative N-Centered Radical Substitution, *Chem. Eur. J.* **2019**, *25*, 15271. The dissertation author was the primary investigator of this publication.

## 3.6 Appendix

### 3.6.1 General Considerations

$^{1}H$, $^{13}C$, and $^{19}F$ NMR were recorded on Varian Mercury 400 MHz, Varian Unity/Inova 500 MHz, and Bruker 300 MHz spectrometers at 400, 126, and 282 MHz, respectively. All chemical shifts are reported relative to $SiMe_4$ using $^{1}H$ (residual) chemical shifts of the solvent as a secondary standard. $^{19}F$ chemical shifts are reported relative to a 2,2,2-trifluoroethanol ($CF_3CH_2OH$) internal standard at -77.16 ppm. GC analyses were performed using an Agilent Technologies 7890B gas chromatograph equipped with an Agilent 7693 autosampler and Agilent HP-5 capillary column (30 m x 0.320 mm x 250 μm). Standard method parameters: 1.2 mL/min flow rate with oven program 80 – 250 °C with a ramp rate of 25 °C/min and hold time of 8.7

minutes at 250 °C. Low-resolution mass spectra were measured using a DECA ESI-MS. High-resolution mass spectra were measured using an Agilent 6230 ESI-TOFMS.

### 3.6.2 Preparation of Substrates

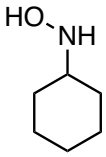

***N*-Cyclohexyl-hydroxylamine** was prepared from the corresponding ketone as previously reported.[20] Physical and spectral data was in accordance with the literature.

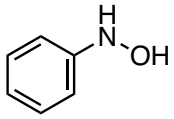

***N*-phenylhydroxylamine** was prepared from nitrobenzene as previously reported.[21] Physical and spectral data was in accordance with the literature.

**General Method A for the preparation of (*E*)-cinnamyl-hydroxylamine and *N*-(2-furanyl)-hydroxylamine**

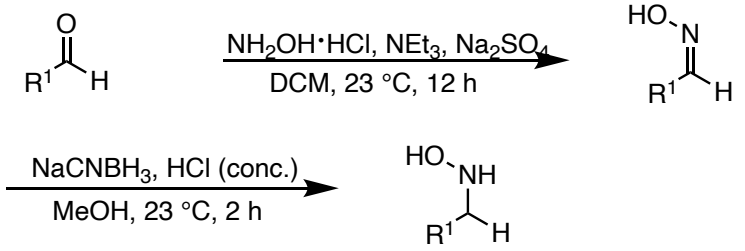


Scheme 3.9. Preparation of (*E*)-cinnamyl-hydroxylamine and *N*-(2-furanyl)-hydroxylamine.

**General Method A Procedure:** To a round bottom flask charged with a magnetic stir bar, hydroxylamine hydrochloride (3 equiv), triethylamine (5 equiv), sodium sulfate (10 equiv), and methylene chloride (0.2 M) was added the corresponding aldehyde (1 equiv). The reaction was allowed to stir at room temperature until complete consumption of the starting aldehyde was observed as judged by TLC (25% EtOAc in hexanes). Upon completion of the reaction, the organic solvent was decanted and washed with an aqueous, saturated solution of ammonium chloride and

then again with brine. The organic layer was then dried over sodium sulfate and the solvent was removed in vacuo to yield the crude oxime which was directly added to a roundbottom flask charged with a magnetic stir bar, a small amount of methyl orange indicator, and methanol (0.2 M). The flask was then cooled in an ice water bath and sodium cyanoborohydride (1.5 equiv) was added carefully. Concentrated hydrochloric acid was added dropwise with stirring to maintain a bright pink color. Once the reaction reached the point at which no more hydrochloric acid was necessary to maintain the bright pink color of the solution, the ice bath was removed and the reaction was allowed to stir for an additional two hours at room temperature. Upon completion of the reaction, a solution of saturated sodium bicarbonate was added to quench any excess hydrochloric acid and the aqueous layer was extracted three times with dichloromethane. The solvent was then removed in vacou to yield the crude hydroxylamine which was used without further purification for the synthesis of the corresponding hydroxamic acid.

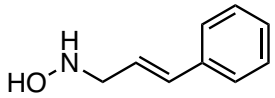


***N*-(*E*)-cinnamyl-hydroxylamine** was prepared from the corresponding aldehyde according to Method A and used directly for the synthesis of **3.2a32**.

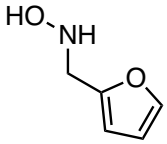


***N*-(2-furanyl)-hydroxylamine** was prepared from the corresponding aldehyde according to Method A and used directly for the synthesis of **3.2b30**.

**General Method B for the Preparation of Hydoxamic Acids**

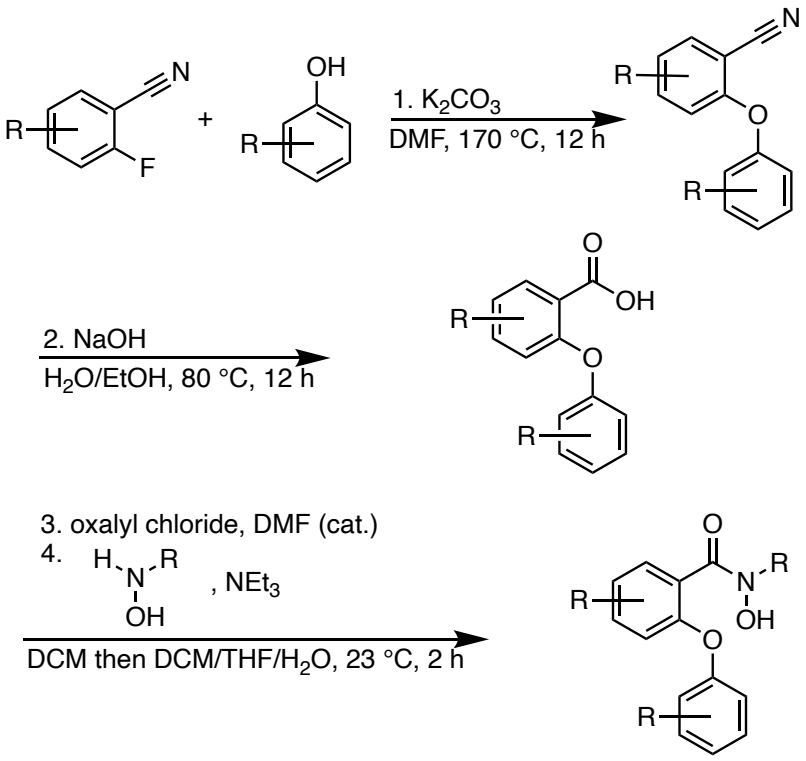


Scheme 3.10. General method B for the preparation of hydroxamic acids.

**Steps 1 and 2:** The carboxylic acid intermediate was prepared from the corresponding phenol and 2-fluorobenzonitrile according to a literature procedure.[22]

**Steps 3 and 4:** Hydroxamic acids were prepared according to an adapted procedure from the literature.[23] To a round bottom flask charged with the corresponding carboxylic acid (1 equiv), methylene chloride (0.5 M), and *N*,*N*-dimethylformamide (1.0 equiv) was added oxalyl chloride (4 equiv) dropwise. The reaction was allowed to stir for 1 h, after which the corresponding hydroxylamine or hydroxylamine hydrochloride (2 equiv) and triethylamine (4 equiv) dissolved in a 4:1 solution of tetrahydrofuran:distilled water (0.5 M) was added dropwise. The reaction was allowed to stir for an additional 10 minutes and was then quenched by the addition of 1 M HCl aqueous solution. The organic layer was separated and the aqueous layer was extracted twice with methylene chloride. The organic layers were then combined, dried over sodium sulfate and the solvent was removed in vacuo. Purification by flash column chromatography (25% EtOAc in

hexanes) afforded the corresponding hydroxamic acid. It's notable that many of the hydroxamic acids prepared were able to be purified by recrystallization and did not necessitate column chromatography. Additionally, we found that by increasing the equivalency of the hydroxylamine, we were able to greatly improve the overall yield. For the sake of cost-effectiveness, 2 equivalents were generally used in this work.

**General Method C for the Preparation of Hydroxamic Acids**

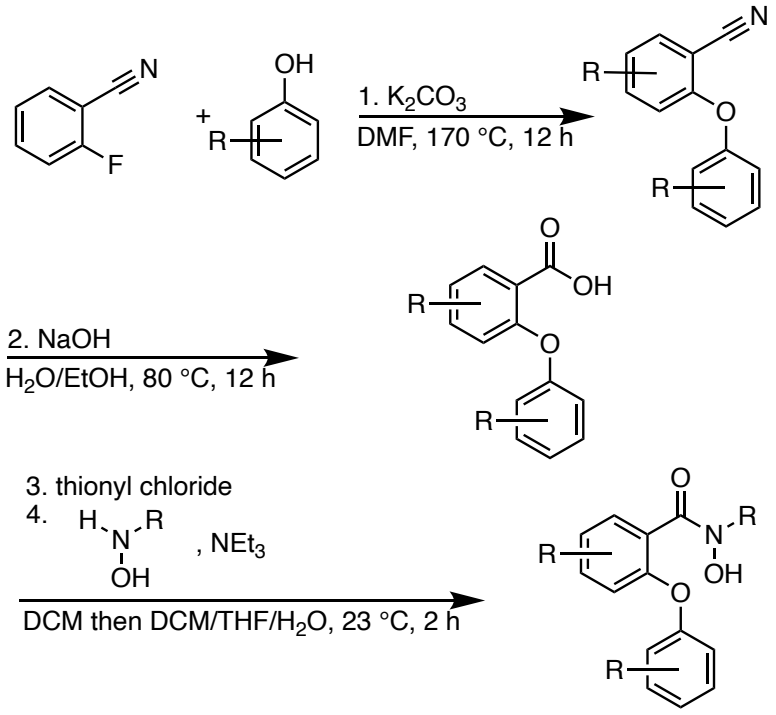


Scheme 3.11. General method C for the preparation of hydroxamic acids.

**Steps 1 and 2:** The carboxylic acid intermediate was prepared from the corresponding phenol and 2-fluorobenzonitrile according to a literature procedure.[22]

**Step 3:** A round bottom flask equipped with a reflux condenser and charged with a magnetic stir bar and thionyl chloride (10 equiv) was added the corresponding carboxylic acid. The reaction was heated to reflux for 1 h, allowed to cool to room temperature, and the excess thionyl chloride was removed in vacuo to furnish the corresponding acid chloride which was

immediately dissolved in methylene chloride (0.5 M) and added dropwise to a 4:1 tetrahydrofuran:distilled water solution containing the corresponding hydroxylamine or hydroxylamine hydrochloride (2 equiv) and triethylamine (4 equiv). The reaction was allowed to stir for an additional 10 minuntes and was then quenched by the addition of 1 M HCl aqueous solution. The organic layer was separated, and the aqueous layer was extracted twice with methylene chloride. The organic layers were then combined, dried over sodium sulfate and the solvent was removed in vacuo. Purification by recrystallization or flash column chromatography (25% EtOAc in hexanes) afforded the corresponding hydroxamic acid.

**General Method D for the Preparation of Substrates**

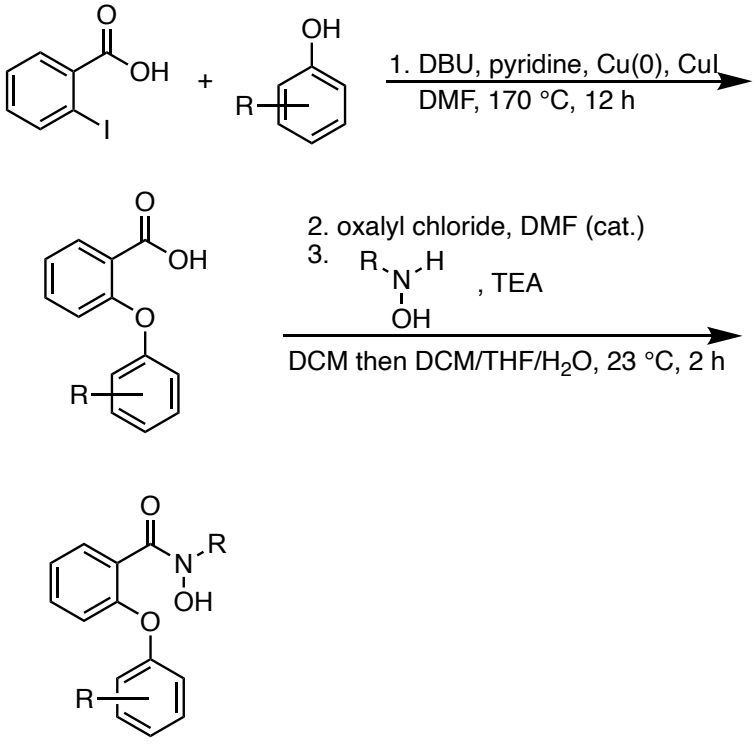


Scheme 3.12. General method D for the preparation of hydroxamic acids.

**General Method E for the Preparation of Substrates**

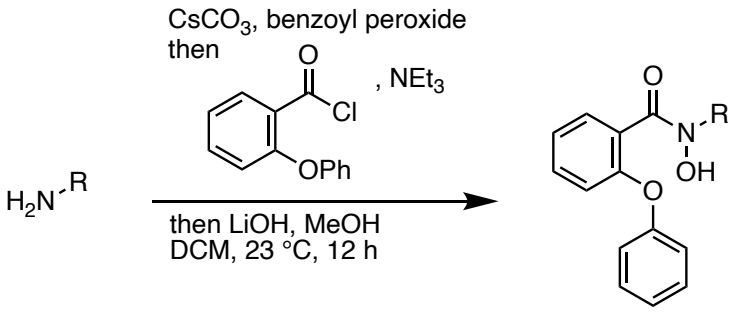


Scheme 3.13. General method E for the preparation of hydroxamic acids.

**One Pot Synthesis:** Hydroxamic acids were prepared from the corresponding primary amines according to a literature procedure.[24] Acid chlorides were prepared according to the procedure outlined in Method C.

**Step 1:** The carboxylic acid intermediate was prepared from the corresponding phenol and 2-iodobenzoic acid according to a literature procedure.[3]

**Steps 2 and 3:** The hydroxamic acids were prepared from the corresponding carboxylic acids in the same manner as in Method B.

**Method F for the preparation of 3.2a21**

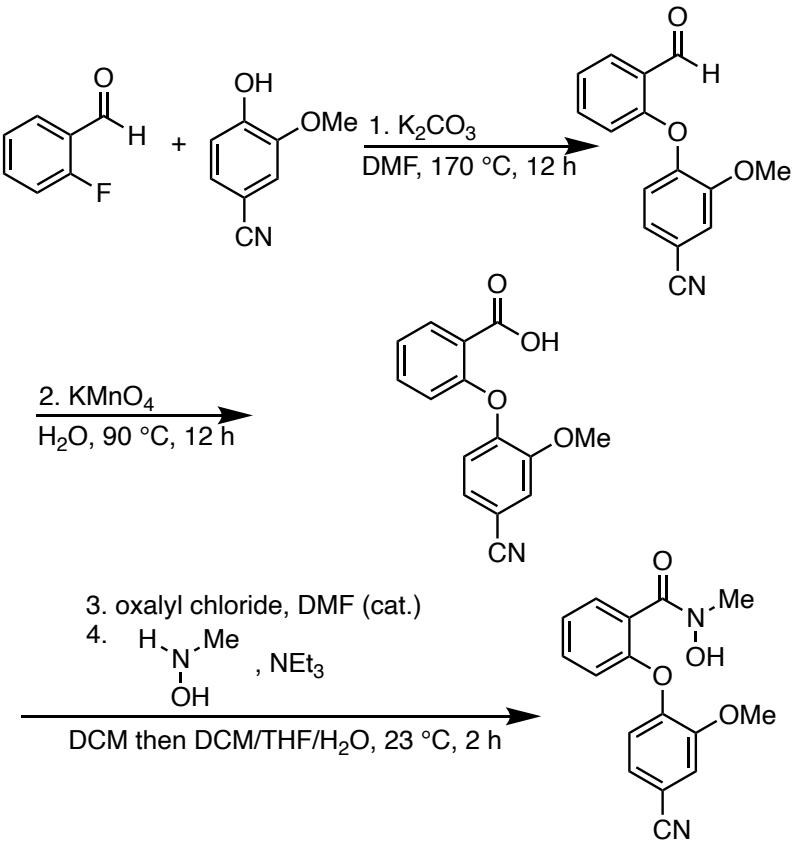


Scheme 3.14. Preparation of substrate **3.2a21**.

**Step 1**: The aldehyde intermediate was prepared according to a literature procedure.[25]

**Step 2:** To a round bottom flask equipped with a reflux condenser and charged with a magnetic stir bar, distilled water (0.2 M), and the corresponding aldehyde was added solid $KMnO_4$ (2 equiv). The reaction was heated to reflux and allowed to stir for 12 h. Upon completion of the reaction as judged by TLC (25% EtOAc in hexanes), an aqueous solution of 1 M HCl was added until pH 1 was obtained. The aqueous reaction mixture was then extracted three times with methylene chloride. The organic layers were combined, dried over sodium sulfate, and the solvent was removed in vacuo to provide the crude carboxylic acid which was used in the next step without further purification.

**Steps 3 and 4:** The hydroxamic acid was prepared from the corresponding carboxylic acid in the same manner as in Method B.

**General Method G for the preparation of Substrates**

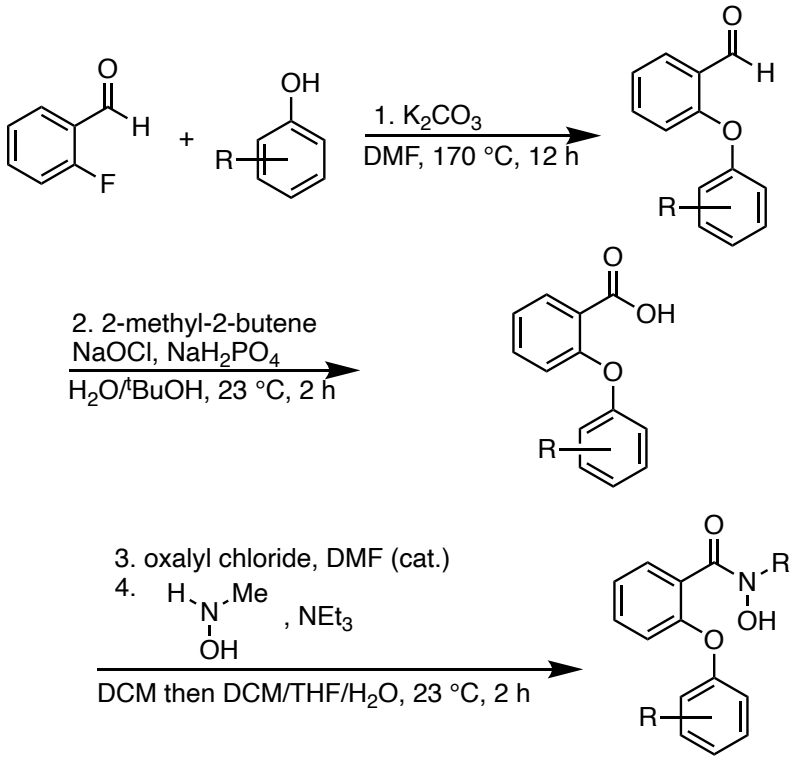


Scheme 3.15. General method G for the preparation of hydroxamic acids.

**Step 1**: The aldehyde intermediate was prepared according to a literature procedure.[6]

**Step 2:** The carboxylic acid intermediate was prepared from the corresponding aldehyde via Pinnick oxidation according to a procedure outlined in the literature.[26]

**Steps 3 and 4:** The hydroxamic acids were prepared from the corresponding carboxylic acids in the same manner as in Method B.

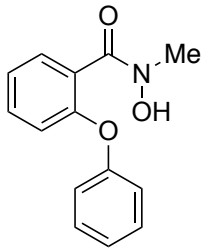


**3.2a1** was synthesized according to Method B in 35% yield as a fine white powder. **$^{1}$H-NMR** (400 MHz; $CDCl_3$): δ 7.47 (d, *J* = 7.8 Hz, 1H), 7.38-7.33 (m, 3H), 7.18-7.13 (m, 2H), 7.02-7.00 (m, 2H), 6.90 (d, *J* = 8.2 Hz, 1H), 3.34 (s, 3H). OH proton not observed. **$^{13}$C-NMR** (126 MHz; $CDCl_3$): δ 162.0, 156.2, 154.1, 131.9, 130.1, 129.8, 124.27, 124.19, 123.6, 119.4, 118.3, 36.7. **LRMS** (ESI-TOF) Calc. for $[C_{14}H_{13}NO_3+H^+]^+$ = 244.10, Found = 244.14. **$R_f$** (50% EtOAc in hexanes): 0.18.

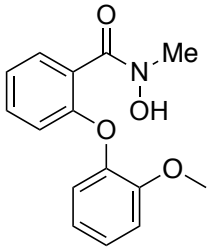


**3.2a2** was synthesized according to Method D in 64% yield as a fine white powder and as a mixture of rotational isomers. **$^{1}$H-NMR** (400 MHz; $CDCl_3$): δ 8.44 (s, 1H), 7.60 (d, *J* = 6.9 Hz, 1H), 7.46 (d, *J* = 6.9 Hz, 1H)*, 7.31-7.16 (m, 3H), 7.14-6.95 (m, 3H), 6.64 (t, *J* = 8.6 Hz, 1H), 3.86 (s, 3H), 3.77 (s, 3H)*, 3.43 (s, 3H), 3.41 (s, 3H)*. **$^{13}$C-NMR** (126 MHz; $CDCl_3$): δ 168.4, 162.3, 154.8, 154.0, 151.6, 150.9, 143.3, 142.1, 131.7, 131.3, 130.1, 129.6, 126.4, 126.0, 125.2, 122.96, 122.78, 122.48, 122.42, 122.36, 121.8, 121.4, 115.1, 113.01, 112.83, 112.5, 56.0, 55.8, 36.7, 36.3. **LRMS** (ESI-TOF) Calc. for $[C_{15}H_{15}NO_4+H^+]^+$ = 274.11, Found = 274.13. **$R_f$** (50% EtOAc in hexanes): 0.18. *indicates minor rotational isomer

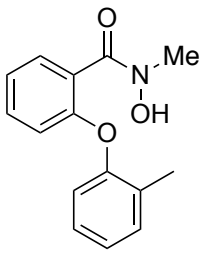

**3.2a3** was synthesized according to Method D in 13% yield as an off-white solid and as a mixture of rotational isomers. **$^{1}$H-NMR** (400 MHz; $CDCl_3$): δ 7.46 (d, *J* = 7.2 Hz, 1H), 7.32 (ddd, *J* = 8.5, 7.3, 1.5 Hz, 2H), 7.20-7.08 (m, 3H), 6.91 (d, *J* = 8.0 Hz, 1H), 6.68 (d, *J* = 8.3 Hz, 1H), 3.37 (s, 3H), 2.22 (s, 3H), 2.21 (s, 3H)*. OH proton not observed. **$^{13}$C-NMR** (126 MHz; $CDCl_3$): δ 162.3, 154.5, 153.6, 131.97, 131.86, 131.77, 130.2, 129.7, 127.5, 124.9, 122.8, 120.1, 116.3, 36.8, 16.4 . **LRMS** (ESI-TOF) Calc. for $[C_{15}H_{15}NO_3+H^+]^+$ = 258.11, Found = 258.16. **$R_f$** (50% EtOAc in hexanes): 0.22. *indicates minor rotational isomer

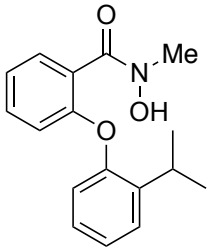

**3.2a4** was synthesized according to Method D in 81% yield as a white solid. **$^{1}$H-NMR** (400 MHz; $CDCl_3$): δ 7.43 (d, *J* = 7.4 Hz, 1H), 7.36-7.29 (m, 2H), 7.16 (dd, *J* = 5.4, 3.3 Hz, 2H), 7.09 (t, *J* = 7.4 Hz, 1H), 6.89 (d, *J* = 3.3 Hz, 1H), 6.72 (d, *J* = 8.3 Hz, 1H), 3.36 (s, 3H), 3.25-3.19 (m, 1H), 1.21 (d, *J* = 6.9 Hz, 6H). OH proton not observed. **$^{13}$C-NMR** (126 MHz; $CDCl_3$): δ 162.6, 154.8, 152.7, 140.4, 131.7, 129.5, 127.22, 127.18, 125.1, 123.6, 122.8, 120.0, 116.5, 37.0, 27.1, 23.1. **LRMS** (ESI-TOF) Calc. for $[C_{17}H_{19}NO_3+H^+]^+$ = 286.14, Found = 286.17. **$R_f$** (50% EtOAc in hexanes): 0.30.

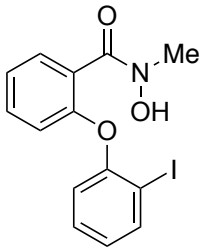


**3.2a5** was synthesized according to Method B in 57% yield as an off-white solid and as a mixture of rotational isomers. **$^{1}$H-NMR** (400 MHz; $CDCl_3$): δ 8.64 (s, 1H), 7.85 (d, *J* = 7.5 Hz, 1H), 7.67-7.49 (m, 1H), 7.40-7.36 (m, 1H), 7.32-7.27 (m, 1H), 7.20 (t, *J* = 7.3 Hz, 1H), 6.90 (t, *J* = 7.2 Hz, 2H), 6.81-6.76 (m, 1H), 3.44 (s, 3H). **$^{13}$C-NMR** (126 MHz; $CDCl_3$): δ 168.1, 161.8, 155.8, 155.6, 154.0, 153.2, 140.5, 140.0, 139.6, 132.0, 131.7, 130.6, 130.30, 130.11, 129.9, 127.6, 126.2, 125.9, 125.2, 124.2, 124.0, 120.0, 118.5, 117.9, 89.0, 87.8, 37.4, 36.7. **LRMS** (ESI-TOF) Calc. for $[C_{14}H_{12}INO_3+H^+]^+$ = 369.99, Found = 370.06. **HRMS** (ESI-TOF) Calc. for $[C_{14}H_{12}INO_3+H^+]^+$ = 369.9935, Found = 369.9932. **$R_f$** (50% EtOAc in hexanes): 0.20.

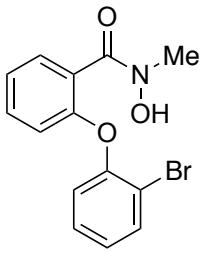


**3.2a6** was synthesized according to Method B in 56% yield as a fine white powder and as a mixture of rotational isomers. **$^{1}$H-NMR** (400 MHz; $CDCl_3$): δ 8.53 (s, 1H), 7.64 (d, *J* = 8.1 Hz, 1H), 7.53-7.49 (m, 1H), 7.38 (t, *J* = 8.5 Hz, 1H), 7.18 (t, *J* = 7.7 Hz, 1H), 7.06 (t, *J* = 7.5 Hz, 1H), 6.98 (d, *J* = 9.1 Hz, 1H), 6.90-6.87 (m, 1H), 6.74 (d, *J* = 8.8 Hz, 1H), 3.43 (s, 3H). **$^{13}$C-NMR** (126 MHz; $CDCl_3$): δ 168.0, 161.8, 153.3, 152.73, 152.68, 151.7, 134.0, 133.6, 132.0, 131.7, 130.7, 129.9, 129.33, 129.14, 127.3, 126.0, 125.6, 125.0, 123.89, 123.77, 121.3, 119.1, 117.9, 117.2, 115.2, 113.8, 37.1, 36.6. **LRMS** (ESI-TOF) Calc. for $[C_{14}H_{12}BrNO_3+H^+]^+$ = 322.01, Found = 322.12. **HRMS** (ESI-TOF) Calc. for $[C_{14}H_{12}BrNO_3+H^+]^+$ = 322.0073, Found = 322.0074. **$R_f$** (50% EtOAc in hexanes): 0.22.

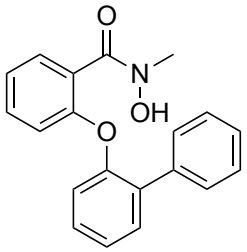

**3.2a7** was synthesized according to Method C in 91% yield as a white solid and as a mixture of rotational isomers. **$^{1}$H-NMR** (400 MHz; $CDCl_3$): δ 7.48-6.85 (m, 13H), 3.17 (s, 3H)*, 2.93 (s, 3H). OH proton not observed. **$^{13}$C-NMR** (126 MHz; $CDCl_3$): δ 168.2, 162.0, 154.1, 152.7, 137.72, 137.63, 137.0, 134.6, 134.1, 133.4, 133.1, 132.6, 131.8, 131.5, 131.3, 130.5, 129.7, 129.3, 129.07, 128.97, 128.93, 128.91, 128.5, 128.26, 128.17, 127.9, 127.5, 125.8, 124.8, 124.6, 124.2, 123.9, 123.1, 120.1, 118.5, 117.8, 117.4, 116.8, 36.42, 36.24. **LRMS** (ESI-TOF) Calc. for $[C_{20}H_{17}NO_3+H^+]^+$ = 320.13, Found = 320.20. **HRMS** (ESI-TOF) Calc. for $[C_{20}H_{17}NO_3+H^+]^+$ = 320.1281, Found = 320.1279. **$R_f$** (50% EtOAc in hexanes): 0.25. *indicates minor rotamer

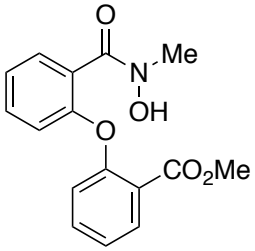

**3.2a8** was synthesized according to Method G in 59% yield as a thick clear oil. **$^{1}$H-NMR** (400 MHz; $CDCl_3$): 9.50 (s, 1H), 7.98 (d, $J$ = 7.8 Hz, 1H), 7.67 (d, $J$ = 7.6 Hz, 1H), 7.43 (q, $J$ = 7.3 Hz, 2H), 7.29-7.26 (m, 1H), 7.12 (t, $J$ = 7.6 Hz, 1H), 6.96 (d, $J$ = 8.1 Hz, 1H), 6.83 (d, $J$ = 8.4 Hz, 1H), 3.95 (s, 3H), 3.33 (s, 3H). **$^{13}$C-NMR** (126 MHz; $CDCl_3$): δ 167.8, 166.9, 157.2, 150.8, 134.9, 132.2, 131.5, 130.8, 128.4, 125.2, 122.9, 119.3, 119.1, 117.2, 52.9, 36.6. **HRMS** (ESI-TOF) Calc. for $[C_{16}H_{15}NO_5+H^+]^+$ = 302.1023, Found = 302.1020. **$R_f$** (50% EtOAc in hexanes): 0.22.

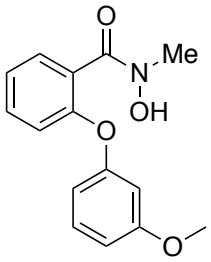


**3.2a9** was synthesized according to Method D in 63% yield as a fine brown powder. **$^1$H-NMR** (400 MHz; $CDCl_3$): δ 7.47 (d, *J* = 7.9 Hz, 1H), 7.41-7.36 (m, 1H), 7.23-7.21 (m, 1H), 7.17 (t, *J* = 7.5 Hz, 1H), 6.94 (d, *J* = 8.4 Hz, 1H), 6.69 (d, *J* = 6.4 Hz, 1H), 6.58 (dd, *J* = 4.4, 2.2 Hz, 2H), 3.78 (s, 3H), 3.33 (s, 3H). OH proton not observed. **$^{13}$C-NMR** (126 MHz; $CDCl_3$): δ 162.2, 161.1, 157.3, 153.9, 131.9, 130.4, 129.8, 124.4, 123.6, 118.5, 111.4, 109.9, 105.5, 55.6, 36.8. **LRMS** (ESI-TOF) Calc. for $[C_{15}H_{15}NO_4+H^+]^+$ = 274.11, Found = 274.11. **$R_f$** (50% EtOAc in hexanes): 0.18.

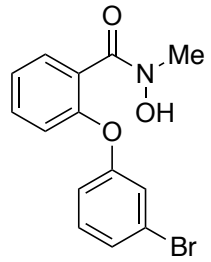


**3.2a10** was synthesized according to Method B in 55% yield as a fine white powder. **$^1$H-NMR** (400 MHz; $CDCl_3$): δ 8.6 (s, 1H), 7.50-7.41 (m, 2H), 7.25-7.16 (m, 4H), 6.94 (t, *J* = 7.9 Hz, 2H), 3.32 (s, 3H). **$^{13}$C-NMR** (126 MHz; $CDCl_3$): δ 161.8, 157.2, 153.2, 132.1, 131.1, 129.9, 127.2, 124.7, 124.4, 123.1, 122.2, 119.0, 117.6, 36.7. **LRMS** (ESI-TOF) Calc. for $[C_{14}H_{12}BrNO_3+H^+]^+$ = 322.01, Found = 322.09. **HRMS** (ESI-TOF) Calc. for $[C_{14}H_{12}BrNO_3+H^+]^+$ = 322.0073, Found = 322.0073. **$R_f$** (50% EtOAc in hexanes): 0.20.

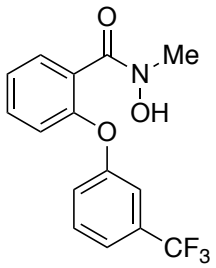

**3.2a11** was synthesized according to Method C in 95% yield as a fine white powder. **$^{1}$H-NMR** (400 MHz; $CDCl_3$): δ 7.51-7.38 (m, 4H), 7.27 (d, *J* = 0.5 Hz, 1H), 7.25-7.24 (m, 1H), 7.15 (d, *J* = 7.8 Hz, 1H), 6.96 (d, *J* = 8.4 Hz, 1H), 3.33 (s, 3H). OH proton not observed. **$^{13}$C-NMR** (126 MHz; $CDCl_3$): δ 161.6, 156.7, 152.9, 132.4 (q, *J* = 32.8 Hz), 132.1, 130.6, 129.8, 124.79, 124.61, 123.6 (q, *J* = 272.4 Hz), 121.9, 120.6 (q, *J* = 3.8 Hz), 119.0, 115.7 (q, *J* = 3.8 Hz), 36.6. **$^{19}$F NMR** (282 MHz; $CDCl_3$): δ -62.7. **LRMS** (ESI-TOF) Calc. for $[C_{15}H_{12}F_3NO_3+H^+]^+$ = 312.08, Found = 312.16. **HRMS** (ESI-TOF) Calc. for $[C_{15}H_{12}F_3NO_3+H^+]^+$ = 312.0842, Found = 312.0841. **$R_f$** (25% EtOAc in hexanes): 0.20.

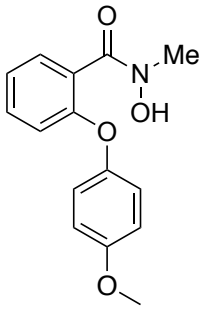

**3.2a12** was synthesized according to Method D in 64% yield as a tan woolen solid. **$^{1}$H-NMR** (400 MHz; $CDCl_3$): δ 7.44 (d, *J* = 6.7 Hz, 1H), 7.35-7.31 (m, 1H), 7.10 (t, *J* = 7.2 Hz, 1H), 6.97 (d, *J* = 9.0 Hz, 2H), 6.88 (d, *J* = 9.0 Hz, 2H), 6.79 (d, *J* = 8.4 Hz, 1H), 3.80 (s, 3H), 3.35 (s, 3H). OH proton not observed. **$^{13}$C-NMR** (126 MHz; $CDCl_3$): δ 162.4, 156.5, 155.2, 149.2, 131.8, 129.7, 123.5, 122.8, 121.1, 116.8, 115.1, 55.8, 36.8. **LRMS** (ESI-TOF) Calc. for $[C_{15}H_{15}NO_4+H^+]^+$ = 274.11, Found = 274.14. **$R_f$** (50% EtOAc in hexanes): 0.18.

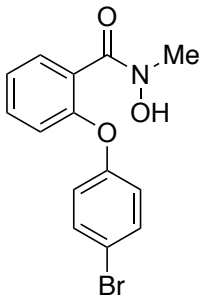


**3.2a13** was synthesized according to Method B in 36% yield as a tan solid. **$^1$H-NMR** (400 MHz; $CDCl_3$): δ 8.94 (s, 1H), 7.44-7.37 (m, 4H), 7.18 (t, *J* = 7.5 Hz, 1H), 6.91-6.87 (m, 3H), 3.30 (s, 3H). **$^{13}$C-NMR** (126 MHz; $CDCl_3$): δ 162.3, 155.6, 153.4, 133.0, 132.0, 129.7, 124.9, 124.1, 120.8, 118.7, 116.7, 37.2. **LRMS** (ESI-TOF) Calc. for $[C_{14}H_{12}BrNO_3+H^+]^+$ = 322.01, Found = 322.15. **HRMS** (ESI-TOF) Calc. for $[C_{14}H_{12}BrNO_3+H^+]^+$ = 322.0173, Found = 322.0072. **$R_f$** (50% EtOAc in hexanes): 0.20.

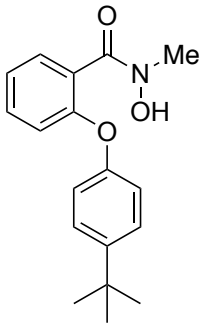


**3.2a14** was synthesized according to Method B in 45% yield as a fine white powder. **$^1$H-NMR** (400 MHz; $CDCl_3$): δ 7.48-7.45 (m, 1H), 7.36 (d, *J* = 8.4 Hz, 3H), 7.18-7.12 (m, 1H), 6.94 (d, *J* = 8.7 Hz, 2H), 6.90 (d, *J* = 8.4 Hz, 1H), 3.39 (s, 3H), 1.32 (s, 9H). OH proton not observed. **$^{13}$C-NMR** (126 MHz; $CDCl_3$): δ 162.1, 154.5, 153.6, 147.2, 131.9, 129.8, 126.9, 124.0, 123.2, 119.0, 117.8, 36.7, 34.5, 31.6. **LRMS** (ESI-TOF) Calc. for $[C_{18}H_{21}NO_3+H^+]^+$ = 300.16, Found = 300.16. **$R_f$** (50% EtOAc in hexanes): 0.25.

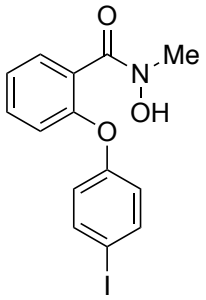

**3.2a15** was synthesized according to Method B in 46% yield as an off white powder. **$^{1}$H-NMR** (400 MHz; $CDCl_3$): δ 7.63 (d, *J* = 8.1 Hz, 2H), 7.47 (d, *J* = 6.8 Hz, 1H), 7.41 (t, *J* = 8.2 Hz, 1H), 7.21 (t, *J* = 7.5 Hz, 1H), 6.92 (d, *J* = 8.3 Hz, 1H), 6.77 (d, *J* = 8.1 Hz, 2H), 3.32 (s, 3H). OH proton not observed. **$^{13}$C-NMR** (126 MHz; $CDCl_3$): δ 162.0, 156.5, 153.3, 139.0, 132.1, 129.8, 124.8, 124.2, 121.1, 118.8, 87.2, 36.9. **LRMS** (ESI-TOF) Calc. for $[C_{14}H_{12}INO_3+H^+]^+$ = 369.99, Found = 370.08. **HRMS** (ESI-TOF) Calc. for $[C_{14}H_{12}INO_3+H^+]^+$ = 368.9935, Found = 369.9938. **$R_f$** (50% EtOAc in hexanes): 0.20.

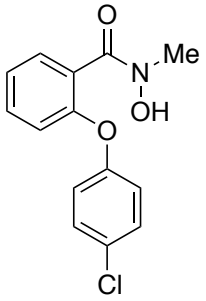

**3.2a16** was synthesized according to Method B in 63% yield as an off white powder. **$^{1}$H-NMR** (400 MHz; $CDCl_3$): δ 7.46 (d, *J* = 7.7 Hz, 1H), 7.42-7.38 (m, 1H), 7.32-7.28 (m, 2H), 7.19 (t, *J* = 7.4 Hz, 1H), 6.96-6.89 (m, 3H), 3.32 (s, 3H). OH proton not observed. **$^{13}$C-NMR** (126 MHz; $CDCl_3$): δ 162.1, 155.0, 153.6, 132.0, 130.0, 129.8, 129.3, 124.7, 124.1, 120.4, 118.6, 36.9. **LRMS** (ESI-TOF) Calc. for $[C_{14}H_{12}ClNO_3+H^+]^+$ = 278.06, Found = 278.17. **HRMS** (ESI-TOF) Calc. for $[C_{14}H_{12}ClNO_3+H^+]^+$ = 278.0578, Found = 278.0578. **$R_f$** (50% EtOAc in hexanes): 0.18.

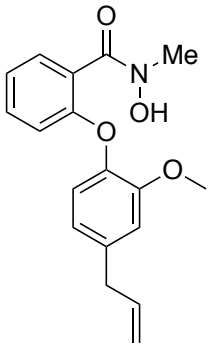


**3.2a17** was synthesized according to Method B in 36% yield as a yellow solid and as a mixture of rotational isomers. **$^{1}$H-NMR** (400 MHz; $CDCl_3$): δ 8.44 (s, 1H), 7.59 (d, *J* = 6.2 Hz, 1H), 7.45 (d, *J* = 6.5 Hz, 1H)*, 7.10-6.91 (m, 5H), 6.66 (q, *J* = 9.5 Hz, 1H), 6.40 (m, 2H), 6.26-6.21 (m, 1H), 5.86-5.78 (m, 1H)*, 3.85 (s, 3H), 3.76 (s, 3H)*, 3.42 (s, 3H), 3.40 (s, 3H)*, 1.93-1.90 (m, 2H). **$^{13}$C-NMR** (126 MHz; $CDCl_3$): δ 168.3, 162.1, 154.7, 154.0, 150.7, 150.3, 142.00, 142.00, 141.99, 140.7, 136.5, 136.0, 131.6, 131.2, 130.3, 129.5, 129.0, 127.5, 126.6, 126.0, 122.78, 122.62, 122.2, 119.1, 118.8, 114.9, 112.91, 112.82, 109.8, 109.5, 55.83, 55.64, 36.5, 36.2, 18.5, 14.7. **LRMS** (ESI-TOF) Calc. for $[C_{18}H_{19}NO_4+H^+]^+$ = 314.14, Found = 314.14. **$R_f$** (50% EtOAc in hexanes): 0.22. *indicates minor rotamer

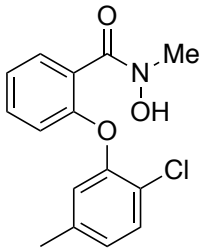


**3.2a18** was synthesized according to Method B in 56% yield as a white solid and as a mixture of rotational isomers. **$^1$H-NMR** (400 MHz; $CDCl_3$): δ 8.75 (s, 1H), 7.85 (s, 1H)*, 7.61 (d, *J* = 6.9 Hz, 1H)*, 7.46 (d, *J* = 7.4 Hz, 1H), 7.32 (dd, *J* = 14.9, 7.8 Hz, 2H), 7.20 (t, *J* = 6.5 Hz, 1H)*, 7.13 (t, *J* = 7.4 Hz, 1H), 6.93 (s, 1H), 6.82 (s, 1H), 6.75 (s, 1H)*, 6.67 (d, *J* = 8.1 Hz, 1H), 3.38 (s, 3H), 2.26 (s, 3H). **$^{13}$C-NMR** (126 MHz; $CDCl_3$): δ 167.9, 162.0, 153.9, 153.4, 152.2, 151.1, 150.8, 139.02, 138.86, 131.8, 131.5, 130.4, 130.1, 129.7, 127.0, 126.6, 126.1, 124.4, 123.7, 123.4, 123.0, 122.3, 121.7, 120.5, 117.4, 116.4, 37.2, 36.4, 21.15, 21.06. **LRMS** (ESI-TOF) Calc. for $[C_{15}H_{14}ClNO_3+H^+]^+$ = 292.07, Found = 292.15. **HRMS** (ESI-TOF) Calc. for $[C_{15}H_{14}ClNO_3+H^+]^+$ = 292.0735, Found = 292.0736. **$R_f$** (50% EtOAc in hexanes): 0.22. *indicates minor rotamer

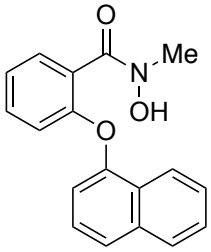


**3.2a19** was synthesized according to Method B in 54% yield as pale pink solid. **$^1$H-NMR** (400 MHz; $CDCl_3$): δ 8.56 (s, 1H), 8.12 (d, *J* = 7.8 Hz, 1H), 7.88 (d, *J* = 7.9 Hz, 1H), 7.67 (d, *J* = 8.2 Hz, 1H), 7.51 (dt, *J* = 15.6, 7.5 Hz, 3H), 7.40 (t, *J* = 8.0 Hz, 1H), 7.33 (t, *J* = 7.7 Hz, 1H), 7.17 (t, *J* = 7.6 Hz, 1H), 6.99 (d, *J* = 7.5 Hz, 1H), 6.81 (d, *J* = 8.1 Hz, 1H), 3.44 (s, 3H). **$^{13}$C-NMR** (126 MHz; $CDCl_3$): δ 162.1, 154.6, 152.0, 135.1, 132.0, 129.8, 128.0, 126.91, 126.77, 126.5, 125.8, 124.5, 124.0, 123.5, 121.8, 118.0, 114.4, 36.8. **LRMS** (ESI-TOF) Calc. for $[C_{18}H_{15}NO_3+H^+]^+$ = 294.11, Found = 294.14. **$R_f$** (50% EtOAc in hexanes): 0.10.

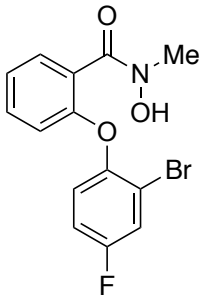


**3.2a20** was synthesized according to Method B in 82% yield as yellow plates and as a mixture of rotational isomers. **$^{1}$H-NMR** (400 MHz; $CDCl_3$): δ 8.68 (s, 1H), 7.64 (d, *J* = 6.4 Hz, 1H)*, 7.47 (d, *J* = 7.5 Hz, 1H), 7.39-7.35 (m, 2H), 7.17 (t, *J* = 7.4 Hz, 1H), 7.04-6.97 (m, 2H), 6.90 (dt, *J* = 1.1, 0.6 Hz, 1H)*, 6.79 (d, *J* = 7.7 Hz, 1H)*, 6.68 (d, *J* = 8.3 Hz, 1H), 3.41 (s, 3H). **$^{13}$C-NMR** (126 MHz; $CDCl_3$): δ 161.8, 159.0 (d, *J* = 248.2 Hz), 153.4, 148.8 (d, *J* = 3.4 Hz), 131.8, 131.1 (d, *J* = 136.5 Hz), 129.7, 124.7, 123.6, 122.4 (d, *J* = 8.8 Hz), 120.8 (d, *J* = 25.9 Hz), 116.3, 115.9 (d, *J* = 23.0 Hz), 37.2. **$^{19}$F NMR** (282 MHz; $CDCl_3$): δ -115.7 (q, *J* = 6.6 Hz). **LRMS** (ESI-TOF) Calc. for $[C_{14}H_{11}BrFN_2O_3+H^+]^+$ = 340.00, Found = 340.14. **HRMS** (ESI-TOF) Calc. for $[C_{14}H_{11}BrFN_2O_3+H^+]^+$ = 339.9979, Found = 339.9975. **$R_f$** (50% EtOAc in hexanes): 0.20. *indicates minor rotamer

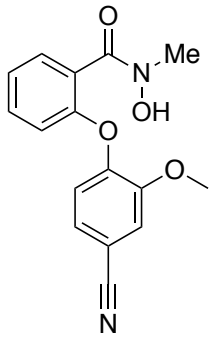


**3.2a21** was synthesized according to Method F in 66% yield as a white solid and as a mixture of rotational isomers. **$^{1}$H-NMR** (400 MHz; $CDCl_3$): δ 7.63 (d, *J* = 6.7 Hz, 1H)*, 7.48 (d, *J* = 7.2 Hz, 1H)*, 7.39 (t, *J* = 7.5 Hz, 2H), 7.26-7.21 (m, 3H), 7.00-6.95 (m, 2H), 6.81 (d, *J* = 8.0 Hz, 3H)*, 3.94 (s, 3H)*, 3.85 (s, 3H), 3.35 (s, 3H). OH proton not observed. **$^{13}$C-NMR** (126 MHz; $CDCl_3$): δ 167.8, 161.6, 152.7, 151.9, 151.1, 150.6, 148.9, 147.9, 132.1, 131.7, 130.8, 129.9, 126.65, 126.55, 126.1, 124.8, 124.4, 124.1, 120.55, 120.37, 118.7, 118.4, 117.8, 116.2, 115.7, 115.5, 108.6, 108.3, 56.6, 56.3, 36.9, 36.4. **LRMS** (ESI-TOF) Calc. for $[C_{16}H_{14}N_2O_4+H^+]^+$ = 299.10, Found = 299.15. **$R_f$** (50% EtOAc in hexanes): 0.10. *indicates minor rotamer

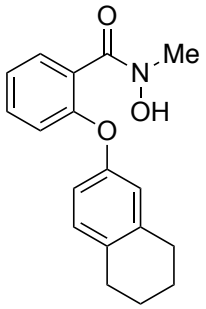

**3.2a22** was synthesized according to Method B in 24% yield as a greenish-brown solid. **$^{1}$H-NMR** (400 MHz; $CDCl_3$): δ 7.45 (d, *J* = 7.2 Hz, 1H), 7.37-7.32 (m, 1H), 7.11 (t, *J* = 7.4 Hz, 1H), 7.03 (d, *J* = 8.0 Hz, 1H), 6.87 (d, *J* = 8.2 Hz, 1H), 6.74 (d, *J* = 10.9 Hz, 2H), 3.35 (s, 3H), 2.73 (d, *J* = 6.1 Hz, 4H), 1.78 (dt, *J* = 4.5, 2.0 Hz, 4H). OH proton not observed. **$^{13}$C-NMR** (126 MHz; $CDCl_3$): δ 162.3, 154.6, 153.4, 139.1, 133.2, 131.8, 130.5, 129.7, 123.7, 123.0, 119.9, 117.5, 116.9, 36.8, 29.6, 28.9, 23.3, 23.0. **LRMS** (ESI-TOF) Calc. for $[C_{18}H_{19}NO_3+H^+]^+$ = 298.14, Found = 298.21. **HRMS** (ESI-TOF) Calc. for $[C_{18}H_{19}NO_3+H^+]^+$ = 298.1438, Found = 298.1437. **$R_f$** (50% EtOAc in hexanes): 0.30.

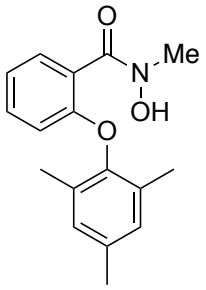

**3.2a23** was synthesized according to Method D in 15% yield as a yellow solid. **$^{1}$H-NMR** (400 MHz; $CDCl_3$): δ 7.41 (d, *J* = 7.4 Hz, 1H), 7.24 (dt, *J* = 7.3, 1.5 Hz, 2H), 7.04 (t, *J* = 7.1 Hz, 1H), 6.99 (s, 1H), 6.38 (d, *J* = 8.4 Hz, 1H), 3.40 (s, 3H), 2.36 (s, 3H), 2.17 (s, 3H), 2.05 (s, 3H). OH proton not observed. **$^{13}$C-NMR** (126 MHz; $CDCl_3$): δ 162.5, 154.0, 148.9, 133.6, 133.0, 131.8, 130.5, 129.8, 129.5, 129.2, 122.1, 121.9, 113.2, 36.9, 20.6, 16.3, 14.2. **HRMS** (ESI-TOF) Calc. for $[C_{17}H_{19}NO_3+H]^+$ = 285.1365, Found = 285.1365. **$R_f$** (50% EtOAc in hexanes): 0.10.

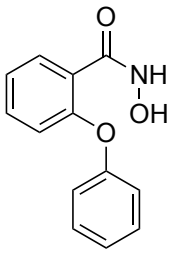


**3.2a24** was synthesized according to Method B in 67% yield as a fine white powder and as a mixture of rotational isomers. **$^{1}$H-NMR** (400 MHz; $CDCl_3$): δ 10.27 (s, 1H), 8.32-8.21 (m, 1H), 7.45-7.36 (m, 3H), 7.30-7.27 (m, 1H), 7.25-7.17 (m, 1H), 7.09 (dd, *J* = 8.7, 1.1 Hz, 2H), 7.02-7.00 (m, 1H), 6.88-6.76 (m, 1H). **$^{13}$C-NMR** (126 MHz; $CDCl_3$): δ 162.8, 156.1, 154.5, 134.9, 133.7, 133.4, 131.9, 130.51, 130.48, 130.1, 125.6, 124.3, 123.90, 123.87, 123.79, 123.5, 120.65, 120.55, 120.3, 118.6, 118.3, 117.1. **LRMS** (ESI-TOF) Calc. for $[C_{13}H_{11}NO_3+H^+]^+$ = 230.08, Found = 230.18. **HRMS** (ESI-TOF) Calc. for $[C_{13}H_{11}NO_3+H^+]^+$ = 230.0812, Found = 230.0813. **$R_f$** (25% EtOAc in hexanes): 0.22.

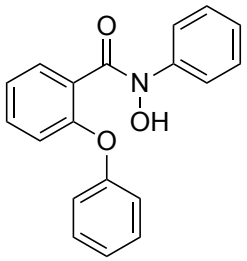


**3.2a25** was synthesized according to Method B in 84% yield as a fine tan powder. **$^{1}$H-NMR** (400 MHz; $CDCl_3$): δ 7.62-7.48 (m, 1H), 7.25 (d, *J* = 13.4 Hz, 9H), 7.12-7.08 (m, 2H), 6.67-6.47 (m, 2H). OH proton not observed. **$^{13}$C-NMR** (126 MHz; $CDCl_3$): δ 162.1, 155.3, 154.2, 138.3, 131.9, 130.1, 129.8, 128.8, 127.8, 124.9, 124.4, 124.1, 122.8, 119.9, 116.7. **LRMS** (ESI-TOF) Calc. for $[C_{19}H_{15}NO_3+H^+]^+$ = 306.11, Found = 306.12. **$R_f$** (50% EtOAc in hexanes): 0.25

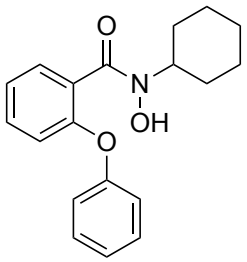

**3.2a26** was synthesized according to Method B in 92% yield as a fine white powder. **$^{1}$H-NMR** (400 MHz; $CDCl_3$): δ 7.42 (d, *J* = 7.5 Hz, 1H), 7.35 (q, *J* = 7.7 Hz, 3H), 7.14 (q, *J* = 7.4 Hz, 2H), 7.00 (d, *J* = 7.7 Hz, 2H), 6.89 (d, *J* = 8.3 Hz, 1H), 3.59 (t, *J* = 11.0 Hz, 1H), 1.86-1.76 (m, 6H), 1.58 (s, 1H), 1.13 (s, 3H). OH proton not observed. **$^{13}$C-NMR** (126 MHz; $CDCl_3$): δ 161.2, 156.1, 153.8, 131.4, 129.9, 129.4, 124.7, 124.1, 123.4, 119.2, 118.0, 59.1, 29.9, 25.3, 24.9. **LRMS** (ESI-TOF) Calc. for $[C_{19}H_{21}NO_3+H^+]^+$ = 312.16, Found = 312.24. **HRMS** (ESI-TOF) Calc. for $[C_{19}H_{21}NO_3+H^+]^+$ = 312.1594, Found = 312.1594. **$R_f$** (50% EtOAc in hexanes): 0.25.

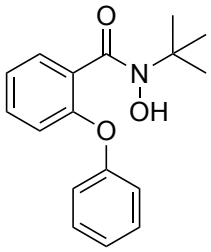

**3.2a27** was synthesized according to Method B in 88% yield as a white solid. **$^{1}$H-NMR** (400 MHz; $CDCl_3$): δ 7.47 (s, 1H), 7.36-7.32 (m, 3H), 7.19-7.11 (m, 2H), 7.01 (d, *J* = 7.6 Hz, 2H), 6.89 (d, *J* = 8.4 Hz, 1H), 1.37 (s, 9H). OH proton not observed. **$^{13}$C-NMR** (126 MHz; $CDCl_3$): δ 156.6, 154.1, 131.29, 131.28, 131.21, 130.1, 124.09, 124.05, 124.04, 124.02, 123.98, 61.5, 27.9. **LRMS** (ESI-TOF) Calc. for $[C_{17}H_{19}NO_3+H^+]^+$ = 286.14, Found = 286.01. **HRMS** (ESI-TOF) Calc. for $[C_{17}H_{19}NO_3+H^+]^+$ = 286.1438, Found = 286.1438. **$R_f$** (50% EtOAc in hexanes): 0.25.

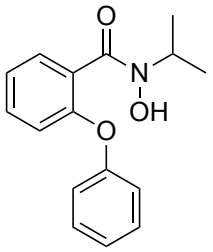

**3.2a28** was synthesized according to Method B in 87% yield as a pale orange solid. **$^{1}$H-NMR** (400 MHz; $CDCl_3$): δ 8.43 (s, 1H), 7.41 (d, *J* = 7.3 Hz, 1H), 7.36-7.32 (m, 3H), 7.14 (t, *J* = 7.4 Hz, 2H), 7.01 (d, *J* = 8.1 Hz, 2H), 6.88 (d, *J* = 8.3 Hz, 1H), 4.06 (dt, *J* = 12.9, 6.5 Hz, 1H), 1.30 (d, *J* = 6.5 Hz, 6H). **$^{13}$C-NMR** (126 MHz; $CDCl_3$): δ 161.3, 156.2, 154.0, 131.5, 130.1, 129.3, 124.9, 124.2, 123.5, 119.5, 118.1, 51.8, 20.0. **LRMS** (ESI-TOF) Calc. for $[C_{16}H_{17}NO_3+H^+]^+$ = 272.13, Found = 272.19. **HRMS** (ESI-TOF) Calc. for $[C_{16}H_{17}NO_3+H^+]^+$ = 272.1281, Found = 272.1281. **$R_f$** (25% EtOAc in hexanes): 0.22.

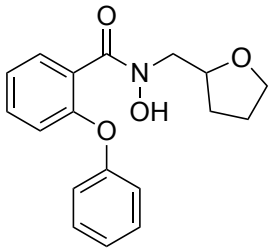

**3.2a29** was synthesized according to Method E in 25% yield as a yellow oil and as a mixture of rotational isomers. **$^{1}$H-NMR** (400 MHz; $CDCl_3$): δ 7.79-7.77 (m, 1H), 7.48 (d, *J* = 7.2 Hz, 2H), 7.43 (d, *J* = 7.7 Hz, 1H), 7.33-7.32 (m, 1H), 7.12 (t, *J* = 8.2 Hz, 1H), 7.02-7.00 (m, 1H), 6.88 (d, *J* = 8.3 Hz, 1H), 6.55-6.53 (m, 1H), 4.25 (d, *J* = 0.6 Hz, 1H)*, 4.10-4.06 (m, 1H), 3.90-3.65 (m, 3H), 3.59-3.51 (m, 1H)*, 3.35 (ddd, *J* = 13.7, 7.5, 4.9 Hz, 1H), 2.01 (td, *J* = 14.5, 11.2 Hz, 1H), 1.92 (s, 1H), 1.86-1.72 (m, 1H), 1.64-1.59 (m, 1H). OH proton not observed. **$^{13}$C-NMR** (126 MHz; $CDCl_3$): δ 167.7, 167.2, 162.9, 156.9, 156.3, 154.0, 153.3, 134.6, 131.73, 131.58, 131.1, 130.17, 129.99, 129.4, 128.7, 127.1, 124.2, 123.8, 123.4, 119.4, 118.8, 118.47, 118.31, 77.9, 68.3, 68.1, 53.4, 50.3, 43.7, 28.8, 26.1, 25.5. **LRMS** (ESI-TOF) Calc. for $[C_{18}H_{19}NO_4+H^+]^+$ = 314.14, Found = 314.10. **$R_f$** (50% EtOAc in hexanes): 0.15. *indicates minor rotamer

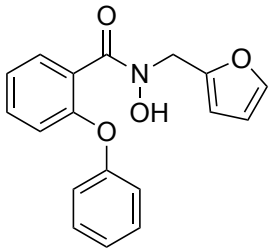

**3.2a30** was synthesized according to Method B in 66% yield as a tan solid and as a mixture of rotational isomers. **$^{1}$H-NMR** (400 MHz; $CDCl_3$): δ 7.65-7.51 (m, 1H), 7.65-7.51 (m, 1H)*, 7.45-7.29 (m, 3H), 7.19-7.12 (m, 2H), 7.03-6.91 (m, 4H), 6.31-6.28 (m, 2H), 4.94 (s, 2H)*, 4.76 (s, 2H). OH proton not observed. **$^{13}$C-NMR** (126 MHz; $CDCl_3$): δ 163.2, 157.3, 156.3, 154.3, 149.2, 148.2, 142.8, 135.0, 133.7, 132.07, 131.93, 130.5, 130.0, 127.3, 125.9, 124.5, 124.3, 123.95, 123.84, 123.5, 120.5, 119.5, 118.8, 118.56, 118.38, 117.5, 110.68, 110.55, 109.4, 109.0, 46.7, 45.1. **LRMS** (ESI-TOF) Calc. for $[C_{18}H_{15}NO_4+H^+]^+$ = 310.11, Found = 310.14. **$R_f$** (50% EtOAc in hexanes): 0.10. *indicates minor rotamer

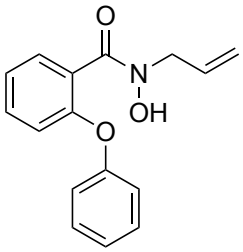

**3.2a31** was synthesized according to Method E in 21% yield as a tan solid and as a mixture of rotational isomers. **$^{1}$H-NMR** (400 MHz; $CDCl_3$): δ 7.44-7.42 (m, 1H), 7.37-7.33 (m, 3H), 7.15 (t, *J* = 7.4 Hz, 2H), 7.01 (d, *J* = 7.9 Hz, 2H), 6.88 (d, *J* = 8.3 Hz, 1H), 5.91-5.81 (m, 1H), 5.30-5.22 (m, 2H), 4.38 (s, 2H)*, 4.20 (s, 2H). OH proton not observed. **$^{13}$C-NMR** (126 MHz; $CDCl_3$): δ 162.7, 156.2, 154.2, 131.9, 131.5, 130.1, 129.6, 127.0, 124.3, 123.4, 119.6, 118.9, 118.2, 52.4. **LRMS** (ESI-TOF) Calc. for $[C_{16}H_{15}NO_3+H^+]^+$ = 270.11, Found = 270.18. **HRMS** (ESI-TOF) Calc. for $[C_{16}H_{15}NO_3+H^+]^+$ = 270.1125, Found = 270.1123. **$R_f$** (50% EtOAc in hexanes): 0.22. *indicates minor rotamer*

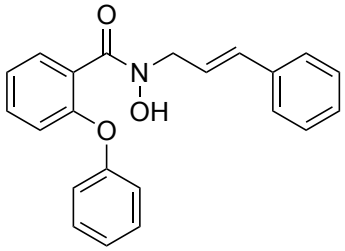

**3.2a32** was synthesized according to Method B in 43% yield as an orange solid and as a mixture of rotational isomers. **$^{1}$H-NMR** (400 MHz; $CDCl_3$): δ 7.47 (d, *J* = 6.8 Hz, 1H)*, 7.41-7.24 (m, 10H), 7.15 (q, *J* = 7.6 Hz, 2H), 6.96 (dd, *J* = 39.2, 7.8 Hz, 3H), 6.51 (d, *J* = 15.8 Hz, 1H), 6.23-6.19 (m, 1H), 4.54 (s, 2H)*, 4.36 (s, 2H). OH proton not observed. **$^{13}$C-NMR** (126 MHz; $CDCl_3$): δ 162.6, 156.1, 154.2, 136.2, 133.9, 132.0, 130.1, 129.7, 128.7, 128.1, 126.6, 124.3, 123.5, 122.6, 119.5, 118.5, 118.3, 52.1. **LRMS** (ESI-TOF) Calc. for $[C_{22}H_{19}NO_3+H^+]^+$ = 346.14, Found = 346.19. **$R_f$** (50% EtOAc in hexanes): 0.30. *indicates minor rotamer*

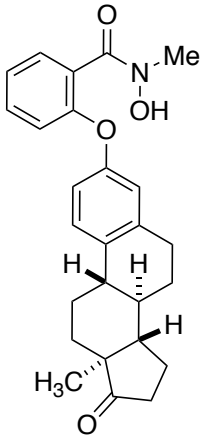


**3.2a33** was synthesized according to Method D in 99% yield as an off-white solid. **$^{1}$H-NMR** (400 MHz; $CDCl_3$): δ 7.47 (d, *J* = 6.9 Hz, 1H), 7.36 (t, *J* = 7.8 Hz, 1H), 7.23 (s, 1H), 7.15 (t, *J* = 7.1 Hz, 1H), 6.90 (d, *J* = 8.3 Hz, 1H), 6.79 (d, *J* = 7.8 Hz, 1H), 6.74 (s, 1H), 3.34 (s, 3H), 2.88-2.85 (m, 2H), 2.51 (dd, *J* = 19.0, 8.9 Hz, 1H), 2.41-2.39 (m, 1H), 2.27 (dt, *J* = 10.2, 5.2 Hz, 1H), 2.17-1.95 (m, 4H), 1.59-1.41 (m, 6H), 0.92 (s, 3H). OH proton not observed. **$^{13}$C-NMR** (126 MHz; $CDCl_3$): δ 162.1, 154.3, 154.0, 138.6, 135.8, 131.9, 129.8, 126.9, 124.0, 123.3, 119.5, 118.0, 116.7, 50.5, 48.1, 45.9, 44.2, 38.2, 36.7, 36.0, 31.6, 29.6 26.5, 25.9, 21.7, 14.0. **LRMS** (ESI-TOF) Calc. for $[C_{26}H_{29}NO_4+H^+]^+$ = 420.22, Found = 420.24. **$R_f$** (50% EtOAc in hexanes): 0.12.

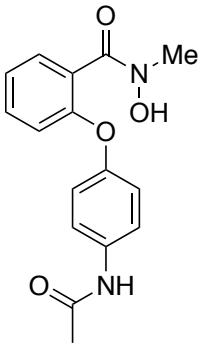


**3.2a34** was synthesized according to Method D in 95% yield as an off-white solid. **$^{1}$H-NMR** (400 MHz; DMSO-$d_6$): δ 9.92 (s, 1H), 9.84 (s, 1H), 7.55 (d, *J* = 5.7 Hz, 2H), 7.29 (d, *J* = 6.9 Hz, 2H), 7.10 (d, *J* = 5.7 Hz, 1H), 6.94 (d, *J* = 7.9 Hz, 2H), 6.76 (d, *J* = 7.8 Hz, 1H), 3.33 (s, 3H), 2.01 (s, 3H). **$^{13}$C-NMR** (126 MHz; DMSO-$d_6$): δ 173.2, 172.0, 158.8, 156.8, 140.3, 135.2, 133.5, 127.6, 125.5, 124.7, 122.5, 105.0, 41.0, 29.0. **LRMS** (ESI-TOF) Calc. for $[C_{16}H_{16}N_2O_4+H^+]^+$ = 301.12, Found = 301.10. **$R_f$** (50% EtOAc in hexanes): 0.02.

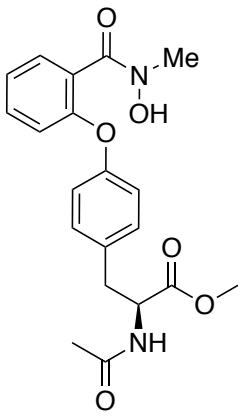

**3.2a35** was synthesized according to Method G in 14% yield as a yellow solid. **$^{1}$H-NMR** (400 MHz; $CDCl_3$): δ 7.47 (d, *J* = 7.5 Hz, 1H), 7.40 (t, *J* = 7.7 Hz, 1H), 7.19 (t, *J* = 7.4 Hz, 1H), 7.05 (d, *J* = 8.4 Hz, 2H), 6.95 (d, *J* = 8.2 Hz, 1H), 6.91 (d, *J* = 8.4 Hz, 2H), 6.01 (d, *J* = 7.7 Hz, 1H), 4.87 (q, *J* = 6.8 Hz, 1H), 3.75 (s, 3H), 3.30 (s, 3H), 3.14 (dd, *J* = 13.8, 5.5 Hz, 1H), 2.99 (dd, *J* = 13.7, 5.9 Hz, 1H), 2.01 (s, 3H). OH proton not observed. **$^{13}$C-NMR** (126 MHz; $CDCl_3$): δ 172.2, 170.1, 162.2, 155.7, 153.4, 132.0, 131.5, 130.8, 130.0, 124.8, 124.1, 119.2, 118.7, 53.3, 52.7, 37.7, 37.0, 23.3. **LRMS** (ESI-TOF) Calc. for $[C_{20}H_{22}N_2O_6+H^+]^+$ = 387.16, Found = 387.17. **$R_f$** (50% EtOAc in hexanes): 0.02.

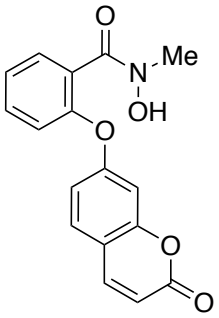

**3.2a36** was synthesized according to Method G in 45% yield as a pale brown solid. **$^1$H-NMR** (400 MHz; $CDCl_3$): δ 7.64 (d, *J* = 9.5 Hz, 1H), 7.50 (t, *J* = 8.6 Hz, 2H), 7.42 (dd, *J* = 8.9, 5.3 Hz, 1H), 7.31 (t, *J* = 7.5 Hz, 1H), 7.08 (d, *J* = 8.1 Hz, 1H), 6.88 (dd, *J* = 3.9, 2.0 Hz, 2H), 6.31 (d, *J* = 9.5 Hz, 1H), 3.31 (s, 3H). OH proton not observed. **$^{13}$C-NMR** (126 MHz; $CDCl_3$): δ 161.7, 160.9, 160.3, 155.6, 152.0, 143.2, 129.6, 129.3, 125.9, 125.5, 121.0, 120.6, 115.02, 114.86, 114.76, 106.0, 37.0. **LRMS** (ESI-TOF) Calc. for $[C_{17}H_{13}NO_5+H^+]^+$ = 312.09, Found = 312.14. **$R_f$** (50% EtOAc in hexanes): 0.02.

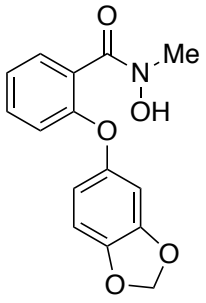

**3.2a37** was synthesized according to Method B in 98% yield as a white solid. **$^1$H-NMR** (400 MHz; $CDCl_3$): δ 7.43 (d, *J* = 7.0 Hz, 1H), 7.35 (t, *J* = 7.8 Hz, 1H), 7.12 (s, 1H), 6.84 (d, *J* = 8.3 Hz, 1H), 6.75 (d, *J* = 8.4 Hz, 1H), 6.56 (s, 1H), 6.48 (d, *J* = 8.3 Hz, 1H), 5.97 (s, 2H), 3.33 (s, 3H). OH proton not observed. **$^{13}$C-NMR** (126 MHz; $CDCl_3$): δ 162.3, 154.9, 150.4, 148.6, 144.5, 131.9, 129.7, 123.5, 123.1, 117.2, 112.4, 108.5, 102.4, 101.8, 36.9. **LRMS** (ESI-TOF) Calc. for $[C_{15}H_{13}NO_5+H^+]^+$ = 288.09, Found = 288.07. **$R_f$** (50% EtOAc in hexanes): 0.20

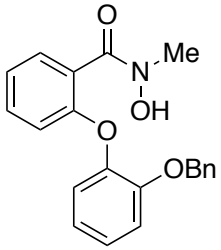


**3.2a38** was synthesized according to Method B in 67% yield as a pale yellow oil and as a mixture of rotational isomers. **$^{1}$H-NMR** (400 MHz; $CDCl_3$): δ 8.12 (s, 1H), 7.57 (d, *J* = 0.7 Hz, 1H)*, 7.41 (dd, *J* = 7.2, 0.7 Hz, 1H), 7.32-7.26 (m, 5H), 7.20-7.16 (m, 1H), 7.10 (s, 4H), 7.00-6.99 (m, 1H), 6.68 (dd, *J* = 16.7, 8.2 Hz, 1H), 5.12 (s, 2H)*, 4.99 (s, 2H), 3.29 (s, 3H)*, 3.06 (s, 3H). **$^{13}$C-NMR** (126 MHz; $CDCl_3$): δ 168.4, 162.3, 157.8, 154.9, 153.8, 150.7, 149.9, 143.2, 142.5, 136.2, 135.4, 134.6, 133.5, 131.5, 131.2, 130.1, 129.5, 128.8, 128.6, 128.0, 127.8, 127.4, 127.1, 126.1, 125.5, 123.3, 122.9, 122.5, 122.1, 121.93, 121.80, 114.6, 114.1, 113.3, 71.0, 70.6, 36.5, 36.3. **LRMS** (ESI-TOF) Calc. for $[C_{21}H_{19}NO_4+H^+]^+$ = 350.14, Found = 350.19. **$R_f$** (50% EtOAc in hexanes): 0.32.

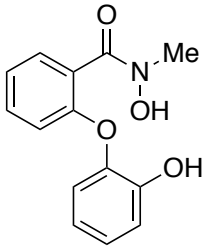


**3.2a39** was synthesized from the hydrogenolysis of compound **1al** following a general hydrogenolysis procedure outlined in the literature[27] in 99% yield as a clear oil and as a mixture of rotational isomers. **$^{1}$H-NMR** (400 MHz; $CDCl_3$): 7.76 (d, *J* = 7.7 Hz, 1H)*, 7.36-7.27 (m, 2H), 7.19-6.99 (m, 5H), 6.87 (t, *J* = 7.7 Hz, 1H), 3.45 (s, 3H), 2.99 (d, *J* = 4.8 Hz, 3H)*. OH protons not observed. **$^{13}$C-NMR** (126 MHz; $CDCl_3$): δ 168.1, 163.6, 156.17, 156.13, 149.9, 149.5, 143.0, 142.6, 132.6, 132.4, 129.9, 128.6, 126.90, 126.81, 124.5, 123.35, 123.18, 123.11, 122.6, 122.1, 120.2, 119.7, 118.4, 118.1, 117.7, 117.3, 37.7, 27.0. **HRMS** (ESI-TOF) Calc. for $[C_{14}H_{13}NO_4+H^+]^+$ = 260.0917, Found = 260.0915. **$R_f$** (50% EtOAc in hexanes): 0.32. *indicates minor rotamer

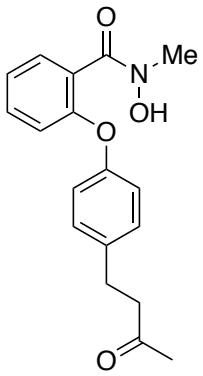

**3.2a40** was synthesized according to Method D in 72% yield as a dark oil. **$^{1}$H-NMR** (400 MHz; $CDCl_3$): δ 7.45 (d, *J* = 5.7 Hz, 1H), 7.36 (t, *J* = 7.7 Hz, 1H), 7.15 (d, *J* = 7.9 Hz, 3H), 6.92 (d, *J* = 8.2 Hz, 2H), 6.86 (d, *J* = 8.0 Hz, 1H), 3.33 (s, 3H), 2.87 (t, *J* = 7.3 Hz, 2H), 2.75 (t, *J* = 7.2 Hz, 2H), 2.15 (s, 2H). OH proton not observed. **$^{13}$C-NMR** (126 MHz; $CDCl_3$): δ 208.1, 162.2, 154.4, 137.0, 131.9, 131.0, 129.87, 129.75, 123.4, 119.49, 119.31, 118.0, 45.3, 36.8, 30.3, 29.0. **HRMS** (ESI-TOF) Calc. for $[C_{18}H_{19}NO_4+H^+]^+$ =314.1387, Found =314.1387. **$R_f$** (50% EtOAc in hexanes): 0.11.

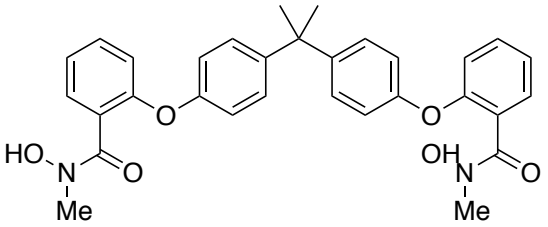

**3.2a41** was synthesized according to Method C in 84% yield as a white solid. **$^{1}$H-NMR** (400 MHz; $CDCl_3$): δ 7.46 (d, *J* = 7.3 Hz, 2H), 7.39-7.35 (m, 2H), 7.20-7.13 (m, 6H), 6.91 (d, *J* = 8.7 Hz, 6H), 3.32 (s, 6H), 1.66 (s, 6H). OH protons not observed. **$^{13}$C-NMR** (126 MHz; $CDCl_3$): δ 162.1, 154.19, 154.01, 146.5, 131.9, 129.8, 128.3, 124.1, 123.4, 118.8, 118.2, 42.4, 36.8, 31.1. **HRMS** (ESI-TOF) Calc. for $[C_{31}H_{30}N_2O_6+H^+]^+$ = 527.2177, Found = 527.2170. **$R_f$** (50% EtOAc in hexanes): 0.04.

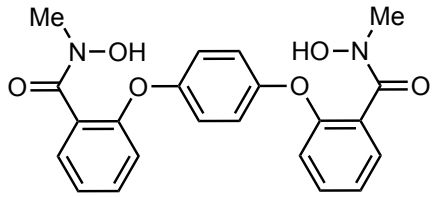


**3.2a42** was synthesized according to Method C in 73% yield as a white solid and as a mixture of rotational isomers. **$^1$H-NMR** (400 MHz; DMSO-$d_6$): δ 9.88 (s, 2H), 7.35 (s, 4H), 7.14 (s, 2H), 7.03 (s, 4H), 6.86 (s, 2H), 3.22 (s, 3H), 3.13 (s, 3H)*. **$^{13}$C-NMR** (126 MHz; DMSO-$d_6$): δ 167.0, 153.6, 131.1, 130.3, 128.6, 128.3, 123.5, 122.8, 120.7, 117.8, 36.0. **HRMS** (ESI-TOF) Calc. for $[C_{22}H_{20}N_2O_6+H^+]^+$ = 409.1394 Found = 409.1390. **$R_f$** (50% EtOAc in hexanes): 0.02. *indicates minor rotational isomer

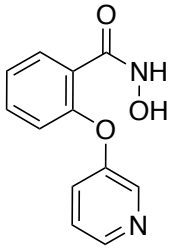


**3.2a43** was synthesized according to Method G in 54% yield as a pale brown solid. **$^1$H-NMR** (400 MHz; $CDCl_3$): δ 10.09 (s, 1H), 8.43 (s, 2H), 8.13 (d, *J* = 6.3 Hz, 1H), 7.41-7.31 (m, 3H), 7.22 (d, *J* = 7.6 Hz, 1H), 6.77 (d, *J* = 8.3 Hz, 1H). NH proton not observed. **$^{13}$C-NMR** (126 MHz; $CDCl_3$): δ 162.8, 154.5, 152.2, 145.7, 141.9, 133.1, 131.9, 127.3, 124.7, 124.4, 122.0, 117.8. **LRMS** (ESI-TOF) Calc. for $[C_{12}H_{10}N_2O_3+H^+]^+$ = 231.08, Found = 231.21 **HRMS** (ESI-TOF) Calc. for $[C_{12}H_{10}N_2O_3+H^+]^+$ = 231.0764, Found = 231.0765. **$R_f$** (50% EtOAc in hexanes): 0.02.

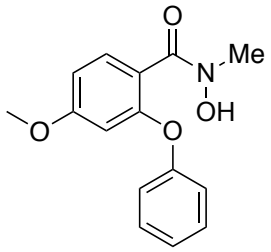

**3.2a44** was synthesized according to Method B in 45% yield as a yellow oil. **$^{1}$H-NMR** (400 MHz; $CDCl_3$): δ 7.42 (d, *J* = 6.9 Hz, 1H), 7.35 (t, *J* = 8.0 Hz, 2H), 7.14 (t, *J* = 7.4 Hz, 1H), 7.01 (d, *J* = 7.7 Hz, 2H), 6.70 (d, *J* = 8.5 Hz, 1H), 6.39 (d, *J* = 2.2 Hz, 1H), 3.74 (s, 3H), 3.35 (s, 3H). OH proton not observed. **$^{13}$C-NMR** (126 MHz; $CDCl_3$): δ 162.5, 162.3, 155.9, 155.4, 131.0, 130.1, 124.4, 119.4, 116.4, 109.0, 104.2, 55.7, 37.0. **LRMS** (ESI-TOF) Calc. for $[C_{15}H_{15}NO_4+H^+]^+$ = 274.11, Found = 274.17. **HRMS** (ESI-TOF) Calc. for $[C_{15}H_{15}NO_4+H^+]^+$ = 274.1074, Found = 274.1074. **$R_f$** (50% EtOAc in hexanes): 0.28.

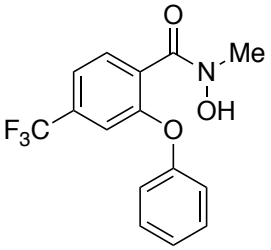

**3.2a45** was synthesized according to Method C in 45% yield as a tan solid. **$^{1}$H-NMR** (400 MHz; $CDCl_3$): δ 7.59 (d, *J* = 7.8 Hz, 1H), 7.43-7.39 (m, 3H), 7.23 (t, *J* = 7.4 Hz, 1H), 7.10 (s, 1H), 7.04 (d, *J* = 8.5 Hz, 2H), 3.35 (s, 3H). OH proton not observed. **$^{13}$C-NMR** (126 MHz; $CDCl_3$): δ 160.8, 155.1, 154.7, 134.0 (q, *J* = 33.1 Hz), 130.59, 130.47, 127.4, 125.3, 123.2 (q, *J* = 273.0 Hz), 120.0 (q, *J* = 3.6 Hz), 119.76, 114.5 (q, *J* = 3.7 Hz), 36.8. **$^{19}$F NMR** (282 MHz; $CDCl_3$): δ -63.1. **LRMS** (ESI-TOF) Calc. for $[C_{15}H_{12}F_3N_2O_3+H^+]^+$ = 312.08, Found = 312.18. **HRMS** (ESI-TOF) Calc. for $[C_{15}H_{12}F_3N_2O_3+H^+]^+$ = 312.0842, Found = 312.0843. **$R_f$** (50% EtOAc in hexanes): 0.22.

### 3.6.3 General Rearrangement Procedure

****Caution: while no problems were encountered in this work, alkylhydroperoxides can undergo spontaneous and rapid exothermic decomposition and appropriate care should be taken in their handling****

To a 1-dram vial charged with a magnetic stir bar was added the respective hydroxamic acid (20 mg), di-*tert*-butyl peroxide (5 equiv), triethyl phosphite (1.5 equiv), and 1,2-dichloroethane (0.5 mL). The vial was capped and heated to 90 °C. Upon consumption of the hydroxamic acid as judged by TLC (25% EtOAc in hexanes), the reaction mixture was concentrated under reduced pressure and purified by flash column chromatography (5-10% EtOAc in hexanes). It should be noted that in general, the starting hydroxamic acids stained orange with an $FeCl_3$ stain and the phenolic products stained purple.

### 3.6.4 Characterization of Products

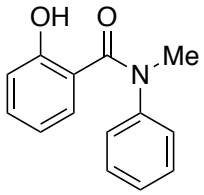


**3.2b1** was synthesized according to the general procedure in 99% (19 mg) yield as an oily residue. Physical and spectral data was in accordance with the literature.[22] $^1$H NMR and $R_f$ value provided for reference. **$^1$H-NMR** (400 MHz; $CDCl_3$): δ 10.90 (s, 1H), 7.34-7.30 (m, 2H), 7.26-7.23 (m, 1H), 7.18-7.10 (m, 3H), 6.93 (d, $J$ = 8.3 Hz, 1H), 6.66 (d, $J$ = 8.0 Hz, 1H), 6.38 (t, $J$ = 7.6 Hz, 1H), 3.49 (s, 3H). **$R_f$** (25% EtOAc in hexanes): 0.32.

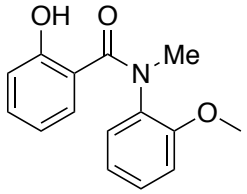


**3.2b2** was synthesized according to the general procedure in 74% yield (14 mg) as an oily residue. Physical and spectral data was in accordance with the literature.[22] $^1$H NMR and $R_f$ value provided for reference. **$^1$H-NMR** (400 MHz; $CDCl_3$): δ 10.58 (s, 1H), 7.26-7.21 (m, 1H), 7.13 (t, *J* = 7.26 Hz, 2H), 6.93-6.89 (m, 2H), 6.84 (d, *J* = 8.24 Hz, 1H), 6.75 (d, *J* = 7.72 Hz, 1H), 6.37 (t, *J* = 7.56 Hz, 1H), 3.66 (s, 3H), 3.36 (s, 3H). **$R_f$** (25% EtOAc in hexanes): 0.25.

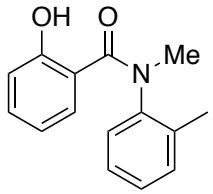


**3.2b3** was synthesized according to the general procedure in 58% yield (11 mg) as an oily residue. Physical and spectral data was in accordance with the literature.[22] $^1$H NMR and $R_f$ value provided for reference. **$^1$H-NMR** (400 MHz; $CDCl_3$): δ 11.28 (s, 1H), 7.21-7.11 (m, 5H), 6.91 (d, *J* = 8.3 Hz, 1H), 6.57 (d, *J* = 7.5 Hz, 1H), 6.34 (t, *J* = 7.4 Hz, 1H), 3.38 (s, 3H), 2.16 (s, 3H). **$R_f$** (25% EtOAc in hexanes): 0.35.

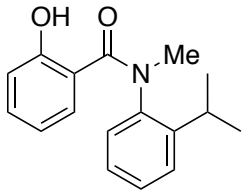


**3.2b4** was synthesized according to the general procedure in 64% yield (12 mg) as an oily residue. **$^1$H-NMR** (400 MHz; $CDCl_3$): δ 11.38 (s, 1H), 7.33-7.28 (m, 2H), 7.22-7.13 (m, 3H), 6.91 (d, *J* = 8.3 Hz, 1H), 6.59 (d, *J* = 7.9 Hz, 1H), 6.33 (t, *J* = 7.5 Hz, 1H), 3.41 (s, 3H), 2.88 (dt, *J* = 13.6, 6.8 Hz, 1H), 1.18 (d, *J* = 6.8 Hz, 3H), 0.83 (d, *J* = 6.8 Hz, 3H). **$^{13}$C-NMR** (126 MHz; $CDCl_3$): δ 171.5, 161.0, 145.2, 142.3, 132.9, 129.8, 128.8, 127.9, 127.4, 117.9, 117.5, 116.0, 39.9, 29.9, 27.9, 25.2, 22.5. **LRMS** (ESI-TOF) Calc. for $[C_{17}H_{19}NO_2+H^+]^+$ = 270.15, Found = 270.24. **HRMS** (ESI-TOF) Calc. for $[C_{17}H_{19}NO_2+H^+]^+$ = 270.1489, Found = 270.1487. **$R_f$** (25% EtOAc in hexanes): 0.40.

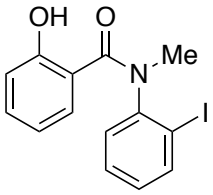


**3.2b5** was synthesized according to the general procedure in 99% yield (19 mg) as an oily residue. Physical and spectral data was in accordance with the literature.[28] $^1$H NMR and $R_f$ value provided for reference. **$^1$H-NMR** (400 MHz; $CDCl_3$): δ 10.89 (s, 1H), 7.87 (d, *J* = 7.92 Hz, 1H), 7.34 (t, *J* = 7.48 Hz, 1H), 7.22-7.16 (m, 2H), 7.01 (t, *J* = 7.40 Hz, 1H), 6.93 (d, *J* = 7.88 Hz, 1H), 6.62 (s, 1H), 6.40 (s, 1H), 3.38 (s, 3H). **$R_f$** (25% EtOAc in hexanes): 0.28.

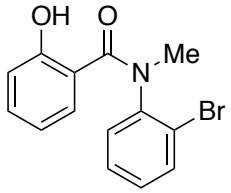


**3.2b6** was synthesized according to the general procedure in 95% yield (18 mg) as an oily residue. Physical and spectral data was in accordance with the literature.[22] $^1$H NMR and $R_f$ value provided for reference. **$^1$H-NMR** (400 MHz; $CDCl_3$): δ 10.72 (s, 1H), 7.62 (d, *J* = 8.0 Hz, 1H), 7.29 (t, *J* = 7.5 Hz, 1H), 7.18 (q, *J* = 7.2 Hz, 3H), 6.92 (d, *J* = 8.3 Hz, 1H), 6.66 (s, 1H), 6.41 (s, 1H), 3.39 (s, 3H). **$R_f$** (25% EtOAc in hexanes): 0.28.

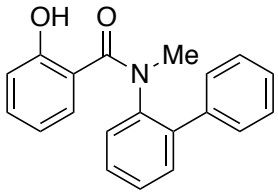


**3.2b7** was synthesized according to the general procedure in 63% yield (12 mg) as an oily residue. **$^1$H-NMR** (400 MHz; $CDCl_3$): δ 10.62 (s, 1H), 7.40-7.26 (m, 7H), 7.12 (t, *J* = 7.6 Hz, 1H), 6.98 (d, *J* = 6.2 Hz, 2H), 6.75 (d, *J* = 8.2 Hz, 1H), 6.66 (d, *J* = 7.7 Hz, 1H), 6.35 (t, *J* = 7.4 Hz, 1H), 3.35 (s, 3H). **$^{13}$C-NMR** (126 MHz; $CDCl_3$): δ 171.2, 161.0, 142.6, 139.1, 138.3, 132.7, 131.8, 129.4, 129.0, 128.7, 128.23, 128.13, 127.94, 127.91, 117.7, 117.3, 116.1, 39.7. **LRMS** (ESI-TOF) Calc. for $[C_{20}H_{17}NO_2+H^+]^+$ = 304.13, Found = 304.27. **HRMS** (ESI-TOF) Calc. for $[C_{20}H_{17}NO_2+H]^+$ = 304.1332, Found = 304.1328. **$R_f$** (25% EtOAc in hexanes): 0.32.

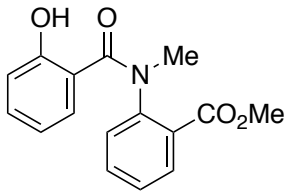


**3.2b8** was synthesized according to the general procedure in 47% (9 mg) yield as an oily residue. **$^1$H-NMR** (400 MHz; $CDCl_3$): δ 7.79 (d, *J* = 7.0 Hz, 1H), 7.58 (t, *J* = 7.5 Hz, 1H), 7.37 (d, *J* = 8.1 Hz, 2H), 7.13 (s, 1H), 6.89 (d, *J* = 7.5 Hz, 1H), 6.55 (s, 1H), 6.35 (s, 1H), 3.79 (s, 3H), 3.47 (s, 3H). OH proton not observed. **$^{13}$C-NMR** (126 MHz; $CDCl_3$): δ 171.5, 165.9, 160.1, 144.9, 133.6, 132.8, 131.9, 129.6, 129.0, 128.3, 127.8, 117.85, 117.70, 116.2, 52.8, 39.3. **HRMS** (ESI-TOF) Calc. for $[C_{16}H_{15}NO_4+H^+]^+$ = 286.1074, Found = 286.1070. **$R_f$** (25% EtOAc in hexanes): 0.05.

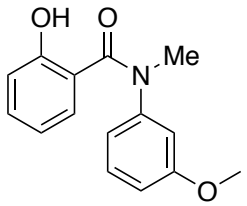


**3.2b9** was synthesized according to the general procedure in 74% yield (14 mg) as an oily residue. Physical and spectral data was in accordance with the literature.[29] $^1$H NMR and $R_f$ value provided for reference. **$^1$H-NMR** (400 MHz; $CDCl_3$): δ 10.94 (s, 1H), 7.23-7.15 (m, 2H), 6.92 (d, *J* = 8.3 Hz, 1H), 6.80-6.78 (m, 1H), 6.76-6.73 (m, 1H), 6.70-6.68 (m, 1H), 6.66-6.64 (m, 1H), 6.42 (t, *J* = 7.6 Hz, 1H), 3.73 (s, 3H), 3.48 (s, 3H). **$R_f$** (25% EtOAc in hexanes): 0.20.

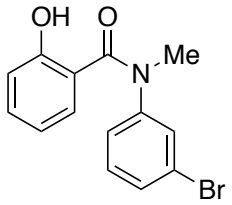


**3.2b10** was synthesized according to the general procedure in 79% yield (15 mg) as an oily residue. Physical and spectral data was in accordance with the literature.[22] $^1$H NMR and $R_f$ value provided for reference. **$^1$H-NMR** (400 MHz; $CDCl_3$): δ 10.69 (s, 1H), 7.38 (ddd, *J* = 8.0, 1.9, 1.0 Hz, 1H), 7.34 (t, *J* = 1.9 Hz, 1H), 7.22-7.14 (m, 2H), 7.00 (d, *J* = 8.0 Hz, 1H), 6.95 (d, *J* = 8.4 Hz, 1H), 6.69 (d, *J* = 6.4 Hz, 1H), 6.46 (t, *J* = 7.6 Hz, 1H), 3.47 (s, 3H). **$R_f$** (25% EtOAc in hexanes): 0.28.

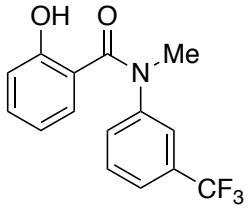


**3.2b11** was synthesized according to the general procedure in 95% yield (18 mg) as a white solid. Physical and spectral data was in accordance with the literature.[22] $^1$H NMR and $R_f$ value provided for reference. **$^1$H-NMR** (400 MHz; $CDCl_3$): δ 10.56 (s, 1H), 7.50 (d, *J* = 7.9 Hz, 1H), 7.44-7.41 (m, 2H), 7.24 (s, 1H), 7.20 (t, *J* = 7.8 Hz, 1H), 6.96 (d, *J* = 8.3 Hz, 1H), 6.61 (d, *J* = 6.5 Hz, 1H), 6.43 (t, *J* = 7.6 Hz, 1H), 3.52 (s, 3H). **$R_f$** (25% EtOAc in hexanes): 0.24.

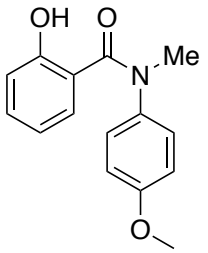


**3.2b12** was synthesized according to the general procedure in 74% yield (14 mg) as an oily residue. Physical and spectral data was in accordance with the literature.[22] $^1$H NMR and $R_f$ value provided for reference. **$^1$H-NMR** (400 MHz; $CDCl_3$): δ 11.02 (s, 1H), 7.16 (t, *J* = 7.8 Hz, 1H), 7.03 (d, *J* = 7.9 Hz, 2H), 6.92 (d, *J* = 8.3 Hz, 1H), 6.83 (d, *J* = 7.9 Hz, 2H), 6.69 (d, *J* = 8.1 Hz, 1H), 6.41 (t, *J* = 7.6 Hz, 1H), 3.79 (s, 3H), 3.45 (s, 3H). **$R_f$** (25% EtOAc in hexanes): 0.18.

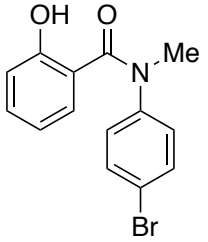


**3.2b13** was synthesized according to the general procedure in 79% yield (11 mg) as an oily residue. Physical and spectral data was in accordance with the literature.[22] $^1$H NMR and $R_f$ value provided for reference. **$^1$H-NMR** (400 MHz; $CDCl_3$): δ 10.69 (s, 1H), 7.44 (d, *J* = 8.6 Hz, 2H), 7.19 (t, *J* = 7.1 Hz, 1H), 6.98 (t, *J* = 10.3 Hz, 2H), 6.94 (d, *J* = 7.3 Hz, 1H), 6.68 (d, *J* = 6.5 Hz, 1H), 6.46 (t, *J* = 7.6 Hz, 1H), 3.46 (s, 3H). **$R_f$** (25% EtOAc in hexanes): 0.26.

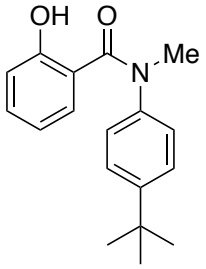


**3.2b14** was synthesized according to the general procedure in 99% yield (19 mg) as an oily residue. Physical and spectral data was in accordance with the literature.[22] $^{1}$H NMR and $R_f$ value provided for reference. **$^{1}$H-NMR** (400 MHz; $CDCl_3$): δ 11.03 (s, 1H), 7.32 (d, *J* = 8.5 Hz, 2H), 7.15 (t, *J* = 7.0 Hz, 1H), 7.03 (d, *J* = 8.5 Hz, 2H), 6.92 (d, *J* = 8.3 Hz, 1H), 6.66 (d, *J* = 6.6 Hz, 1H), 6.37 (t, *J* = 7.6 Hz, 1H), 3.47 (s, 3H), 1.30 (s, 9H). **$R_f$** (25% EtOAc in hexanes): 0.40.

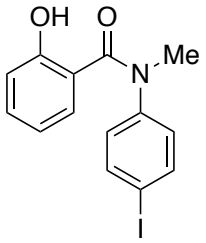


**3.2b15** was synthesized according to the general procedure in 89% yield (17 mg) as an oily residue. **$^{1}$H-NMR** (400 MHz; $CDCl_3$): δ 10.69 (s, 1H), 7.63 (d, *J* = 8.6 Hz, 2H), 7.20 (ddd, *J* = 8.4, 7.2, 1.4 Hz, 1H), 6.94 (dd, *J* = 8.3, 1.0 Hz, 1H), 6.86 (d, *J* = 8.6 Hz, 2H), 6.69 (dd, *J* = 8.0, 1.5 Hz, 1H), 6.48-6.44 (m, 1H), 3.46 (s, 3H). **$^{13}$C-NMR** (126 MHz; $CDCl_3$): δ 171.6, 160.7, 145.1, 138.93, 138.91, 133.2, 130.4, 128.6, 118.1, 115.7, 92.0, 39.3. **LRMS** (ESI-TOF) Calc. for $[C_{14}H_{12}INO_2+H^+]^+$ = 354.00, Found = 354.16. **HRMS** (ESI-TOF) Calc. for $[C_{14}H_{12}INO_2+H^+]^+$ = 353.9985, Found = 353.9982. **$R_f$** (25% EtOAc in hexanes): 0.28.

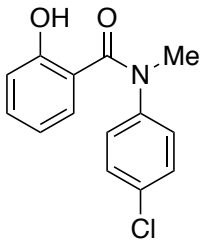


**3.2b16** was synthesized according to the general procedure in 95% yield (18 mg) as an oily residue. Physical and spectral data was in accordance with the literature.[16] $^1$H NMR and $R_f$ value provided for reference. **$^1$H-NMR** (400 MHz; $CDCl_3$): δ 10.70 (s, 1H), 7.29 (d, *J* = 8.5 Hz, 2H), 7.19 (t, *J* = 8.4 Hz, 1H), 7.05 (d, *J* = 8.5 Hz, 2H), 6.94 (d, *J* = 8.3 Hz, 1H), 6.68 (d, *J* = 8.0 Hz, 1H), 6.45 (t, *J* = 7.6 Hz, 1H), 3.46 (s, 3H). **$R_f$** (25% EtOAc in hexanes): 0.26.

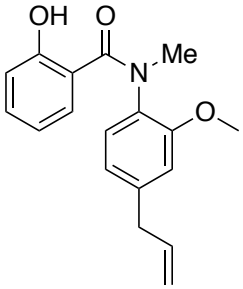


**3.2b17** was synthesized according to the general procedure in 53% yield (10 mg) as an oily residue and as a mixture of rotational isomers. **$^1$H-NMR** (400 MHz; $CDCl_3$): δ 10.61 (s, 1H), 7.13-7.02 (m, 3H), 6.92-6.73 (m, 4H), 6.39-6.23 (m, 3H), 5.82 (dd, *J* = 11.6, 7.2 Hz, 1H)*, 3.66 (s, 3H), 3.65 (s, 3H)*, 3.36 (s, 3H)*, 3.34 (s, 3H), 1.88 (ddd, *J* = 6.8, 3.3, 1.6 Hz, 2H). **$^{13}$C-NMR** (126 MHz; $CDCl_3$): δ 172.6, 159.9, 154.0, 138.8, 138.5, 132.5, 129.1, 128.20, 128.03, 121.9, 118.9, 117.39, 117.19, 112.8, 109.5, 55.6, 38.1, 18.7. **LRMS** (ESI-TOF) Calc. for $[C_{18}H_{19}NO_3+H^+]^+$ = 298.15, Found = 298.20. **$R_f$** (25% EtOAc in hexanes): 0.46. *indicates minor rotamer

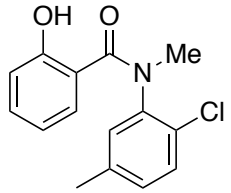


**3.2b18** was synthesized according to the general procedure in 79% yield (15 mg) as an oily residue. **$^1$H-NMR** (400 MHz; $CDCl_3$): δ 10.77 (s, 1H), 7.29 (d, *J* = 8.2 Hz, 1H), 7.18 (t, *J* = 7.4 Hz, 1H), 7.05 (d, *J* = 8.2 Hz, 1H), 6.99 (s, 1H), 6.92 (d, *J* = 8.3 Hz, 1H), 6.69 (s, 1H), 6.42 (s, 1H), 3.37 (s, 3H), 2.27 (s, 3H). **$^{13}$C-NMR** (126 MHz; $CDCl_3$): δ 172.0, 160.4, 138.7, 133.1, 130.6, 130.11, 130.04, 129.98, 129.1, 128.8, 117.88, 117.83, 116.4, 38.2, 20.9. **LRMS** (ESI-TOF) Calc. for $[C_{15}H_{14}ClNO_2+H^+]^+$ = 276.08, Found = 276.20. **HRMS** (ESI-TOF) Calc. for $[C_{15}H_{14}ClNO_2+H^+]^+$ = 276.0786, Found = 276.0786. **$R_f$** (25% EtOAc in hexanes): 0.36.

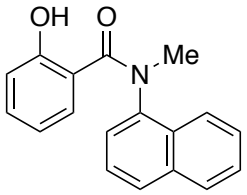


**3.2b19** was synthesized according to the general procedure in 58% yield (11 mg) as an oily residue. Physical and spectral data was in accordance with the literature.[29] $^1$H NMR and $R_f$ value provided for reference. **$^1$H-NMR** (400 MHz; $CDCl_3$): δ 11.22 (s, 1H), 7.98 (d, *J* = 8.2 Hz, 1H), 7.93 (d, *J* = 8.1 Hz, 1H), 7.82 (d, *J* = 8.1 Hz, 1H), 7.65-7.55 (m, 2H), 7.35 (t, *J* = 7.7 Hz, 1H), 7.15 (d, *J* = 7.1 Hz, 1H), 7.07 (t, *J* = 7.4 Hz, 1H), 6.89 (d, *J* = 8.3 Hz, 1H), 6.47 (d, *J* = 7.1 Hz, 1H), 6.15-6.14 (m, 1H), 3.52 (s, 3H). **$R_f$** (25% EtOAc in hexanes): 0.32.

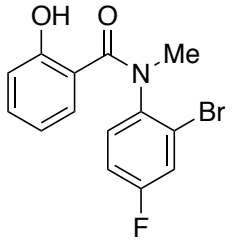


**3.2b20** was synthesized according to the general procedure in 73% yield (14 mg) as an oily residue. **$^{1}$H-NMR** (400 MHz; $CDCl_3$): δ 10.58 (s, 1H), 7.36 (dd, *J* = 7.8, 2.8 Hz, 1H), 7.20-7.17 (m, 2H), 7.04-6.92 (m, 2H), 6.67 (s, 1H), 6.46 (s, 1H), 3.37 (s, 3H). **$^{13}$C-NMR** (126 MHz; $CDCl_3$): δ 171.9, 162.2, 160.2 (d, *J* = 10.6), 133.1 (d, *J* = 13.7), 130.7, 128.9, 123.0 (d, *J* = 10.2), 121.25 (d, *J* = 41.0), 121.24 (d, *J* = 9.6), 118.10, 117.95, 117.89, 116.1, 38.3. **$^{19}$F NMR** (282 MHz; $CDCl_3$): δ -115.7 (q, *J* = 5.9 Hz). **LRMS** (ESI-TOF) Calc. for $[C_{14}H_{11}BrFNO_2+H^+]^+$ = 324.00, Found = 324.25. **HRMS** (ESI-TOF) Calc. for $[C_{14}H_{11}BrFNO_2+H^+]^+$ = 324.0030, Found = 324.0025. **$R_f$** (25% EtOAc in hexanes): 0.26.

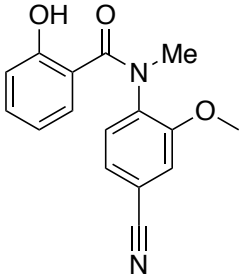


**3.2b21** was synthesized according to the general procedure in 58% yield (11 mg) as an oily residue. **$^{1}$H-NMR** (400 MHz; $CDCl_3$): δ 7.26 (s, 2H), 7.18 (t, *J* = 7.7 Hz, 1H), 7.05 (s, 1H), 6.93 (d, *J* = 8.1 Hz, 1H), 6.68 (d, *J* = 7.9 Hz, 1H), 6.42 (t, *J* = 7.6 Hz, 1H), 3.68 (s, 3H), 3.36 (s, 3H). OH proton not observed. **$^{13}$C-NMR** (126 MHz; $CDCl_3$): δ 172.7, 159.6, 154.3, 152.6, 138.7, 133.1, 129.0, 128.6, 125.7, 118.2, 116.8, 115.77, 115.68, 112.2, 56.2, 37.9. **LRMS** (ESI-TOFnegative ion) Calc. for $[C_{16}H_{14}N_2O_3-H^+]^-$ = 281.09, Found = 281.22. **HRMS** (ESI-TOF) Calc. for $[C_{16}H_{14}N_2O_3+H^+]^+$ = 283.1077, Found = 283.1076. **$R_f$** (25% EtOAc in hexanes): 0.12.

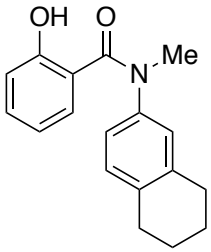


**3.2b22** was synthesized according to the general procedure in 74% yield (14 mg) as an oily residue. **$^1$H-NMR** (400 MHz; $CDCl_3$): δ 11.08 (s, 1H), 7.16 (t, *J* = 7.7 Hz, 1H), 6.98 (d, *J* = 7.9 Hz, 1H), 6.92 (d, *J* = 8.0 Hz, 1H), 6.77 (dd, *J* = 22.3, 9.1 Hz, 3H), 6.42 (t, *J* = 7.4 Hz, 1H), 3.45 (s, 3H), 2.73 (s, 2H), 2.67 (s, 2H), 1.77 (t, *J* = 3.1 Hz, 4H). **$^{13}$C-NMR** (126 MHz; $CDCl_3$): δ 171.5, 160.8, 142.5, 138.8, 136.4, 132.8, 130.6, 130.4, 126.8, 123.8, 117.87, 117.75, 116.2, 39.7, 29.4, 29.1, 23.08, 22.93. **LRMS** (ESI-TOF) Calc. for $[C_{18}H_{19}NO_2+H^+]^+$ = 282.15, Found = 282.26. **HRMS** (ESI-TOF) Calc. for $[C_{18}H_{19}NO_2+H^+]^+$ = 282.1489, Found = 282.1486. **$R_f$** (25% EtOAc in hexanes): 0.38.

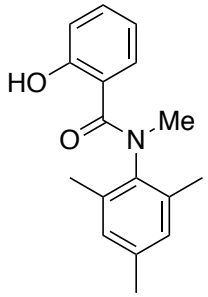


**3.2b23** was synthesized according to the general procedure in 84% yield (16 mg) as an oily residue. Physical and spectral data was in accordance with the literature.[22] $^1$H NMR and $R_f$ value provided for reference. **$^1$H-NMR** (400 MHz; $CDCl_3$): δ 11.42 (s, 1H), 7.18 (t, *J* = 7.0 Hz, 1H), 6.95 (s, 1H), 6.92 (d, *J* = 8.3 Hz, 2H), 6.52 (d, *J* = 8.0 Hz, 1H), 6.39 (t, *J* = 7.6 Hz, 1H), 3.27 (s, 3H), 2.35 (s, 3H), 2.27 (s, 3H), 2.06 (s, 3H). **$R_f$** (25% EtOAc in hexanes): 0.42.

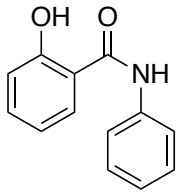


**3.2b24** was synthesized according to the general procedure in 80% yield (15 mg) as an oily residue. Physical and spectral data was in accordance with the literature.[30] $^1$H NMR and $R_f$ value provided for reference. **$^1$H-NMR** (400 MHz; $CDCl_3$): δ 11.98 (s, 1H), 7.92 (s, 1H), 7.58 (d, *J* = 8.6 Hz, 2H), 7.53 (d, *J* = 8.0 Hz, 1H), 7.48-7.39 (m, 3H), 7.21 (t, *J* = 6.9 Hz, 1H), 7.04 (d, *J* = 8.4 Hz, 1H), 6.93 (t, *J* = 7.6 Hz, 1H). **$R_f$** (25% EtOAc in hexanes): 0.29.

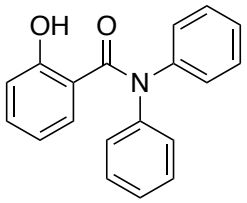


**3.2b25** was synthesized according to the general procedure in 99% yield (19 mg) as an oily residue. **$^1$H-NMR** (400 MHz; $CDCl_3$): δ 9.6 (s, 1H), 8.35 (dd, *J* = 7.9, 1.8 Hz, 1H), 7.63-7.61 (m, 2H), 7.45-7.41 (m, 3H), 7.33 (dd, *J* = 8.4, 7.5 Hz, 2H), 7.27-7.23 (m, 2H), 7.14-7.11 (m, 3H), 6.90 (dd, *J* = 8.2, 1.0 Hz, 1H). **$^{13}$C-NMR** (126 MHz; $CDCl_3$): δ 162.8, 155.4, 138.2, 133.3, 132.6, 130.52, 130.41, 129.2, 125.1, 124.4, 124.12, 124.05, 120.6, 119.7, 118.5. **LRMS** (ESI-TOF) Calc. for $[C_{19}H_{15}NO_2+H^+]^+$ = 290.12, Found = 290.20. **HRMS** (ESI-TOF) Calc. for $[C_{19}H_{15}NO_2+H^+]^+$ = 290.1176, Found = 290.1171. **$R_f$** (25% EtOAc in hexanes): 0.36.

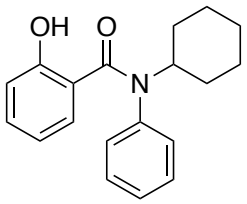


**3.2b26** was synthesized according to the general procedure in 37% yield (7 mg) as a white solid. Physical and spectral data was in accordance with the literature.[22] $^1$H NMR and $R_f$ value provided for reference. **$^1$H-NMR** (400 MHz; $CDCl_3$): δ 10.76 (s, 1H), 7.30 (dd, *J* = 5.2, 1.8 Hz, 3H), 7.07 (ddd, *J* = 5.6, 4.2, 1.8 Hz, 3H), 6.88 (d, *J* = 8.3 Hz, 1H), 6.63 (d, *J* = 8.0 Hz, 1H), 6.34 (t, *J* = 7.6 Hz, 1H), 4.70 (tt, *J* = 12.0, 3.5 Hz, 1H), 1.94 (d, *J* = 10.9 Hz, 2H), 1.80 (d, *J* = 13.5 Hz, 2H), 1.62 (d, *J* = 11.6 Hz, 2H), 1.50-1.39 (m, 2H), 1.32-1.22 (m, 2H). **$R_f$** (25% EtOAc in hexanes): 0.36.

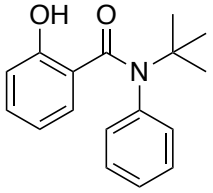


**3.2b27** was synthesized according to the general procedure in 85% yield (16 mg) as an oily residue. **$^1$H-NMR** (400 MHz; $CDCl_3$): δ 8.18 (dd, *J* = 7.8, 1.8 Hz, 1H), 7.48 (s, 1H), 7.36 (td, *J* = 7.5, 1.0 Hz, 3H), 7.26-7.23 (m, 1H), 7.17-7.13 (m, 1H), 6.98 (d, *J* = 8.7 Hz, 2H), 6.89 (d, *J* = 8.2 Hz, 1H), 1.35 (s, 9H). **$^{13}$C-NMR** (126 MHz; $CDCl_3$): δ 163.7, 156.1, 154.1, 132.4, 131.9, 130.1, 126.1, 124.27, 124.08, 119.5, 118.3, 51.2, 28.8. **LRMS** (ESI-TOF) Calc. for $[C_{17}H_{19}NO_2+H^+]^+$ = 270.15, Found = 270.19. **$R_f$** (25% EtOAc in hexanes): 0.36.

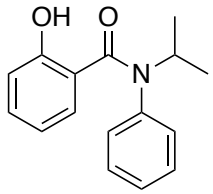


**3.2b28** was synthesized according to the general procedure in 53% yield (10 mg) as an oily residue. Physical and spectral data was in accordance with the literature.[22] $^{1}$H NMR and $R_f$ value provided for reference. **$^{1}$H-NMR** (400 MHz; $CDCl_3$): δ 10.80 (s, 1H), 7.32-7.29 (m, 3H), 7.08 (ddt, *J* = 7.2, 3.2, 1.7 Hz, 3H), 6.88 (d, *J* = 8.3 Hz, 1H), 6.65 (d, *J* = 8.0 Hz, 1H), 6.34 (t, *J* = 7.6 Hz, 1H), 5.08 (dquintet, *J* = 13.6, 6.8 Hz, 1H), 1.22 (d, *J* = 6.8 Hz, 6H). **$R_f$** (25% EtOAc in hexanes): 0.34.

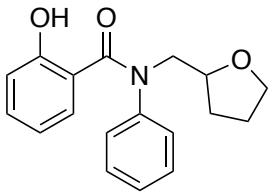


**3.2b29** was synthesized according to the general procedure in 68% yield (13 mg) as an oily residue. **$^{1}$H-NMR** (400 MHz; $CDCl_3$): δ 10.74 (s, 1H), 7.31-7.20 (m, 5H), 7.14 (t, *J* = 7.7 Hz, 1H), 6.91 (d, *J* = 8.3 Hz, 1H), 6.68 (d, *J* = 8.0 Hz, 1H), 6.38 (t, *J* = 7.6 Hz, 1H), 4.25 (dd, *J* = 7.0, 4.4 Hz, 1H), 4.15 (dd, *J* = 13.7, 4.1 Hz, 1H), 3.88 (q, *J* = 7.4 Hz, 1H), 3.78 (dt, *J* = 14.2, 7.3 Hz, 2H), 2.04-1.88 (m, 3H), 1.60 (dd, *J* = 11.9, 7.9 Hz, 1H). **$^{13}$C-NMR** (126 MHz; $CDCl_3$): δ 171.5, 160.5, 144.5, 132.8, 130.5, 129.6, 127.55, 127.42, 117.95, 117.80, 116.6, 76.4, 68.0, 55.4, 29.5, 25.7. **LRMS** (ESI-TOF) Calc. for $[C_{18}H_{19}NO_3+H^+]^+$ = 298.14, Found = 298.19. **$R_f$** (25% EtOAc in hexanes): 0.19.

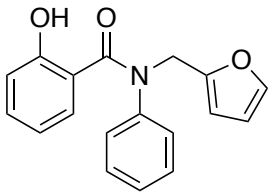


**3.2b30** was synthesized according to the general procedure in 74% yield (14 mg) as an oily residue. **$^1$H-NMR** (400 MHz; $CDCl_3$): δ 10.89 (s, 1H), 7.36 (s, 1H), 7.31-7.24 (m, 3H), 7.15 (t, *J* = 7.8 Hz, 1H), 7.08 (d, *J* = 7.3 Hz, 2H), 6.92 (d, *J* = 8.4 Hz, 1H), 6.69 (d, *J* = 8.1 Hz, 1H), 6.37 (t, *J* = 7.6 Hz, 1H), 6.28 (d, *J* = 13.8 Hz, 2H), 5.06 (s, 2H). **$^{13}$C-NMR** (126 MHz; $CDCl_3$): δ 171.4, 161.0, 154.1, 150.4, 143.9, 142.4, 133.1, 130.6, 129.7, 127.42, 127.42, 118.0, 116.0, 110.7, 109.5, 47.8 . **LRMS** (ESI-TOF) Calc. for $[C_{18}H_{15}NO_3+H^+]^+$ = 294.11, Found = 294.15. **$R_f$** (25% EtOAc in hexanes): 0.39.

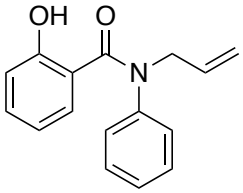


**3.2b31** was synthesized according to the general procedure in 47% yield (9 mg) as an oily residue. **$^1$H-NMR** (400 MHz; $CDCl_3$): δ 10.91 (s, 1H), 7.31 (t, *J* = 7.4 Hz, 3H), 7.16 (t, *J* = 7.7 Hz, 1H), 7.10 (d, *J* = 7.5 Hz, 2H), 6.93 (d, *J* = 8.3 Hz, 1H), 6.68 (d, *J* = 8.0 Hz, 1H), 6.38 (t, *J* = 7.6 Hz, 1H), 5.99 (ddt, *J* = 16.5, 11.0, 5.7 Hz, 1H), 5.22-5.18 (m, 2H), 4.51 (d, *J* = 5.8 Hz, 2H). **$^{13}$C-NMR** (126 MHz; $CDCl_3$): δ 171.2, 160.9, 144.0, 132.9, 132.6, 130.4, 129.72, 129.66, 127.29, 127.23, 118.15, 117.97, 116.1, 54.3. **LRMS** (ESI-TOF) Calc. for $[C_{16}H_{15}NO_2+H^+]^+$ = 254.13, Found = 254.23. **HRMS** (ESI-TOF) Calc. for $[C_{16}H_{15}NO_2+H^+]^+$ = 254.1176, Found = 254.1174. **$R_f$** (25% EtOAc in hexanes): 0.41.

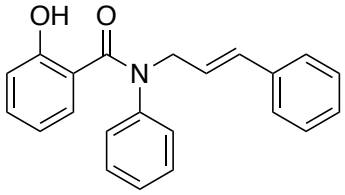


**3.2b32** was synthesized according to the general procedure in 26% yield (5 mg) as an oily residue. **$^1$H-NMR** (400 MHz; $CDCl_3$): δ 10.98 (s, 1H), 7.36-7.29 (m, 6H), 7.17-7.12 (m, 5H), 6.94 (d, *J* = 7.8 Hz, 1H), 6.70 (d, *J* = 6.6 Hz, 1H), 6.49 (d, *J* = 15.7 Hz, 1H), 6.41-6.34 (m, 2H), 4.66 (d, *J* = 6.3 Hz, 2H). **$^{13}$C-NMR** (126 MHz; $CDCl_3$): δ 171.1, 160.8, 151.1, 143.7, 136.4, 133.6, 130.3, 129.70, 129.60, 128.6, 127.39, 127.29, 126.55, 126.44, 123.6, 117.9, 115.9, 53.9. **LRMS** (ESI-TOF) Calc. for $[C_{22}H_{19}NO_2+H^+]^+$ = 330.15, Found = 330.18. **$R_f$** (25% EtOAc in hexanes): 0.39.

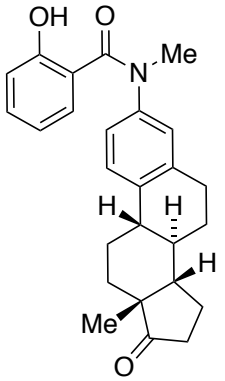


**3.2b33** was synthesized according to the general procedure in 83% yield (16 mg) as a white solid. Physical and spectral data was in accordance with the literature.[22] $^1$H NMR and $R_f$ value provided for reference. **$^1$H-NMR** (400 MHz; $CDCl_3$): δ 11.00 (s, 1H), 7.20 (m, 2H), 7.18-7.13 (m, 1H), 6.91 (dd, *J* = 8.3, 1.2 Hz, 1H), 6.88-6.83 (m, 1H), 6.74 (dd, *J* = 8.1, 1.6 Hz, 1H), 6.45-6.38 (m, 1H), 3.44 (s, 3H), 2.82 (dd, *J* = 8.8, 4.1 Hz, 2H), 2.50 (dd, *J* = 18.8, 8.5 Hz, 1H), 2.42-2.33 (m, 1H), 2.32-2.23 (m, 1H), 2.19-1.93 (m, 4H), 1.66-1.39 (m, 6H), 0.91 (s, 3H). **$R_f$** (25% EtOAc in hexanes): 0.15.

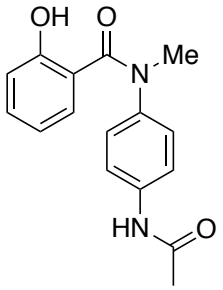


**3.2b34** was synthesized according to the general procedure in 74% yield (14 mg) as an oily residue. **$^1$H-NMR** (400 MHz; $CDCl_3$): δ 10.86 (s, 1H), 7.48 (d, *J* = 8.7 Hz, 3H), 7.15 (t, *J* = 7.8 Hz, 1H), 7.05 (d, *J* = 8.7 Hz, 2H), 6.91 (d, *J* = 8.3 Hz, 1H), 6.70 (d, *J* = 8.0 Hz, 1H), 6.40 (t, *J* = 7.6 Hz, 1H), 3.45 (s, 3H), 2.17 (s, 3H). **$^{13}$C-NMR** (126 MHz; $CDCl_3$): δ 171.4, 168.5, 160.5, 140.8, 136.9, 132.7, 130.4, 127.2, 120.6, 117.88, 117.82, 116.0, 39.4, 16.1 . **LRMS** (ESI-TOF) Calc. for $[C_{16}H_{16}N_2O_3+H^+]^+$ = 285.12, Found = 285.24. **HRMS** (ESI-TOF) Calc. for $[C_{16}H_{16}N_2O_3+H^+]^+$ = 285.1234, Found = 285.1233. **$R_f$** (25% EtOAc in hexanes): 0.02.

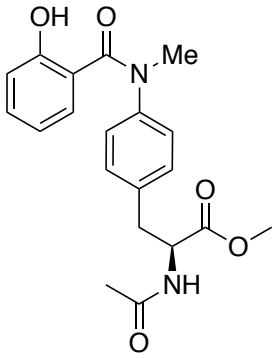


**3.2b35** was synthesized according to the general procedure in 57% yield (11 mg) as an oily residue. **$^1$H-NMR** (400 MHz; $CDCl_3$): δ 10.83 (s, 1H), 7.03 (s, 3H), 7.16 (td, *J* = 7.8, 1.4 Hz, 1H), 6.92 (d, *J* = 7.5 Hz, 1H), 6.59 (d, *J* = 8.0 Hz, 1H), 6.41 (t, *J* = 7.1 Hz, 1H), 5.91 (d, *J* = 7.8 Hz, 1H), 4.87 (dt, *J* = 7.6, 5.8 Hz, 1H), 3.70 (s, 3H), 3.47 (s, 3H), 3.17-3.02 (m, 2H), 1.98 (s, 3H). NH proton not observed. **$^{13}$C-NMR** (126 MHz; $CDCl_3$): δ 171.9, 171.5, 169.6, 160.7, 144.2, 135.2, 132.88, 132.77, 130.5, 126.8, 117.97, 117.78, 116.1, 53.1, 52.7, 39.3, 37.6, 23.4. **LRMS** (ESI-TOF) Calc. for $[C_{20}H_{22}N_2O_5+H^+]^+$ = 371.16, Found = 371.18. **$R_f$** (25% EtOAc in hexanes): 0.02.

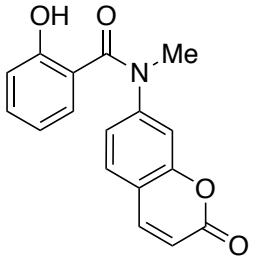


**3.2b36** was synthesized according to the general procedure in 53% yield (10 mg) as an oily residue. **$^1$H-NMR** (400 MHz; $CDCl_3$): δ 10.47 (s, 1H), 7.65 (d, *J* = 9.5 Hz, 1H), 7.38 (d, *J* = 8.3 Hz, 1H), 7.26-7.14 (m, 1H), 7.19-7.13 (m, 1H), 6.96 (ddd, *J* = 8.2, 5.5, 1.5 Hz, 2H), 6.73 (dd, *J* = 8.0, 1.5 Hz, 1H), 6.47-6.40 (m, 2H), 3.53 (s, 3H). **$^{13}$C-NMR** (126 MHz; $CDCl_3$): δ 172.0, 160.6, 160.2, 154.7, 148.4, 142.68, 133.6, 130.3, 128.8, 123.0, 118.33, 118.24, 117.3, 116.8, 115.7, 114.4, 39.2. **LRMS** (ESI-TOF) Calc. for $[C_{17}H_{13}NO_4+H^+]^+$ = 296.09, Found = 296.27. **HRMS** (ESI-TOF) Calc. for $[C_{17}H_{13}NO_4+H^+]^+$ = 296.0917, Found = 296.0913. **$R_f$** (25% EtOAc in hexanes): 0.02.

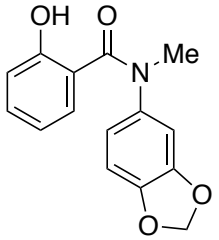


**3.2b37** was synthesized according to the general procedure in 53% yield (10 mg) as an oily residue. **$^1$H-NMR** (400 MHz; $CDCl_3$): δ 7.19 (t, *J* = 7.0 Hz, 1H), 6.93 (d, *J* = 8.3 Hz, 1H), 6.81 (d, *J* = 8.0 Hz, 1H), 6.71 (d, *J* = 8.2 Hz, 1H), 6.65 (d, *J* = 2.1 Hz, 1H), 6.55 (dd, *J* = 8.2, 2.2 Hz, 1H), 6.48 (t, *J* = 7.6 Hz, 1H), 6.00 (s, 2H), 3.43 (s, 3H). OH proton not observed. **$^{13}$C-NMR** (126 MHz; $CDCl_3$): δ 171.5, 160.8, 148.6, 146.8, 139.1, 132.9, 130.3, 120.4, 118.01, 117.97, 116.1, 108.8, 107.8, 102.0, 39.8. **HRMS** (ESI-TOF) Calc. for $[C_{15}H_{13}NO_4+H^+]^+$ = 272.0917, Found = 272.0915. **$R_f$** (25% EtOAc in hexanes): 0.27.

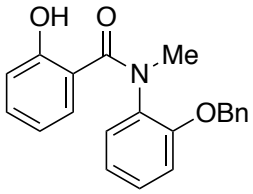


**3.2b38** was synthesized according to the general procedure in 53% yield (10 mg) as an oily residue. **$^{1}$H-NMR** (400 MHz; $CDCl_3$): δ 7.32 (q, *J* = 7.4 Hz, 3H), 7.19 (dt, *J* = 24.4, 7.4 Hz, 5H), 6.91 (dd, *J* = 11.6, 8.1 Hz, 3H), 6.79 (d, *J* = 7.6 Hz, 1H), 6.38 (q, *J* = 7.3 Hz, 1H), 5.00 (s, 2H), 3.40-3.36 (m, 3H). OH proton not observed. **$^{13}$C-NMR** (126 MHz; $CDCl_3$): δ 172.4, 160.4, 153.3, 136.4, 134.2, 132.4, 128.9, 128.6, 127.2, 126.8, 121.8, 121.5, 117.8, 117.6, 116.8, 113.8, 113.6, 70.3, 38.4. **HRMS** (ESI-TOF) Calc. for $[C_{21}H_{19}NO_3+H^+]^+$ = 334.1438, Found = 334.1434. **$R_f$** (25% EtOAc in hexanes): 0.40.

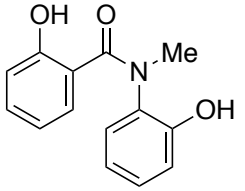


**3.2b39** was synthesized according to the general Smiles reaction procedure in 37% yield (7 mg) as an oily residue. **$^{1}$H-NMR** (400 MHz; $CDCl_3$): δ 7.21-7.15 (m, 2H), 7.01 (d, *J* = 7.2 Hz, 1H), 6.94-6.84 (m, 4H), 6.46 (t, *J* = 5.3 Hz, 1H), 3.37 (s, 3H). OH protons not observed. **$^{13}$C-NMR** (126 MHz; $CDCl_3$): δ 172.9, 160.0, 150.9, 133.1, 132.3, 129.6, 129.2, 128.4, 121.7, 118.3, 117.8, 117.3, 116.5, 38.4. **HRMS** (ESI-TOF) Calc. for $[C_{14}H_{13}NO_3+H^+]^+$ = 244.0968, Found = 244.0967. **$R_f$** (50% EtOAc in hexanes): 0.55.

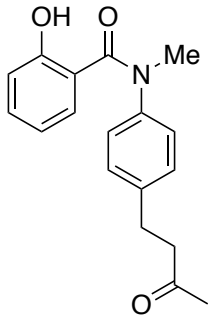

**3.2b40** was synthesized according to the general procedure in 68% yield (13 mg) as an oily residue. **$^1$H-NMR** (400 MHz; $CDCl_3$): δ 7.15 (dd, *J* = 15.1, 7.7 Hz, 3H), 7.02 (d, *J* = 8.0 Hz, 2H), 6.92 (d, *J* = 8.2 Hz, 1H), 6.66 (d, *J* = 7.8 Hz, 1H), 6.38 (t, *J* = 7.5 Hz, 1H), 3.46 (s, 3H), 2.88 (t, *J* = 7.3 Hz, 2H), 2.74 (t, *J* = 7.3 Hz, 2H), 2.13 (s, 3H). OH proton not observed. **$^{13}$C-NMR** (126 MHz; $CDCl_3$): δ 207.7, 171.6, 160.8, 143.3, 140.3, 132.8, 130.5, 129.7, 126.8, 117.94, 117.78, 116.1, 44.9, 39.5, 30.3, 29.2. **HRMS** (ESI-TOF) Calc. for $[C_{18}H_{19}NO_3+H^+]^+$ = 298.1438, Found = 298.1435. **$R_f$** (50% EtOAc in hexanes): 0.41.

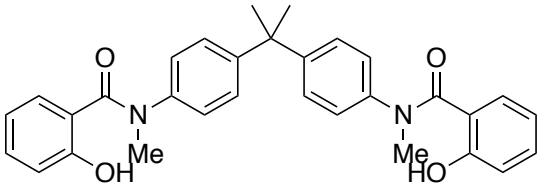

**3.2b41** was synthesized according to the general procedure using 3 equivalents of triethyl phosphite in 53% yield (10 mg) as a white solid. Purification by recrystallization. **$^1$H-NMR** (400 MHz; $CDCl_3$): δ 10.93 (s, 2H), 7.17-7.11 (m, 6H), 7.01 (d, *J* = 8.4 Hz, 4H), 6.92 (d, *J* = 8.3 Hz, 2H), 6.61 (dd, *J* = 8.0, 1.2 Hz, 2H), 6.34-6.30 (m, 2H), 3.48 (s, 6H), 1.64 (s, 7H). **$^{13}$C-NMR** (126 MHz; $CDCl_3$): δ 171.5, 160.8, 149.5, 142.9, 132.9, 130.5, 128.0, 126.4, 118.0, 117.5, 116.1, 42.8, 39.3, 30.7. **HRMS** (ESI-TOF) Calc. for $[C_{31}H_{30}N_2O_4+H^+]^+$ = 465.2278, Found = 485.2277. **$R_f$** (50% EtOAc in hexanes): 0.50.

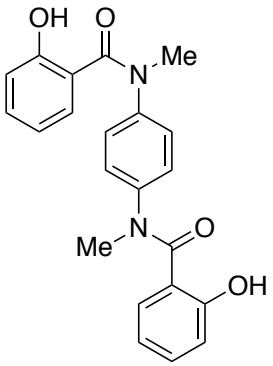


**3.2b42** was synthesized according to the general procedure using 3 equivalents of triethyl phosphite and acetonitrile as solvent in 67% yield (13 mg) as a white solid. **$^{1}$H-NMR** (400 MHz; DMSO-$d_6$): δ 9.71 (s, 2H), 7.09 (s, 6H), 6.91 (s, 2H), 6.65 (d, *J* = 25.5 Hz, 4H), 3.21 (s, 6H). **$^{13}$C-NMR** (126 MHz; DMSO-$d_6$): δ 168.5, 153.6, 141.6, 130.2, 128.1, 126.4, 124.2, 118.5, 115.7, 37.1. **HRMS** (ESI-TOF) Calc. for $[C_{22}H_{20}N_2O_4+H^+]^+$ = 377.1496, Found = 377.1496. **$R_f$** (50% EtOAc in hexanes): 0.09.

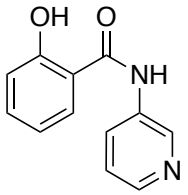


**3.2b43** was synthesized according to the general procedure in 42% yield (8 mg) as an oily residue. **$^{1}$H-NMR** (400 MHz; DMSO-$d_6$): δ 10.59 (s, 1H), 8.86 (d, *J* = 2.3 Hz, 1H), 8.34 (d, *J* = 4.7 Hz, 1H), 8.16 (d, *J* = 6.8 Hz, 1H), 7.94 (d, *J* = 7.8 Hz, 1H), 7.47-7.39 (m, 2H), 6.98 (t, *J* = 7.0 Hz, 2H). NH proton not observed. **$^{13}$C-NMR** (126 MHz; DMSO-$d_6$): δ 167.3, 158.7, 145.5, 142.85, 142.84, 135.4, 129.7, 128.3, 119.9, 119.2, 118.0, 117.3. **LRMS** (ESI-TOF) Calc. for $[C_{12}H_{10}N_2O_2\text{-}H^-]^+$ =213.07, Found = 213.29. **HRMS** (ESI-TOF) Calc. for $[C_{12}H_{10}N_2O_2+H^+]^+$ = 215.0815, Found = 215.0819. **$R_f$** (25% EtOAc in hexanes): 0.01.

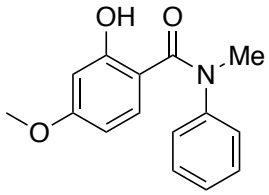


**3.2b44** was synthesized according to the general procedure in 37% yield (7 mg) as an oily residue. Physical and spectral data was in accordance with the literature.[16] $^1$H NMR and $R_f$ value provided for reference. **$^1$H-NMR** (400 MHz; $CDCl_3$): δ 11.75 (s, 1H), 7.36-7.32 (m, 3H), 7.13 (dd, *J* = 8.3, 1.2 Hz, 2H), 6.55 (d, *J* = 9.0 Hz, 1H), 6.42 (d, *J* = 2.6 Hz, 1H), 5.94 (dd, *J* = 9.0, 2.6 Hz, 1H), 3.72 (s, 3H), 3.46 (s, 3H). OH proton not observed. **$R_f$** (25% EtOAc in hexanes): 0.30.

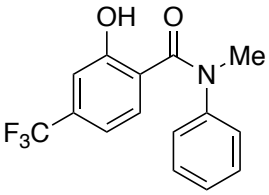


**3.2b45** was synthesized according to the general procedure in 95% yield (18 mg) as an oily residue. **$^1$H-NMR** (400 MHz; $CDCl_3$): δ 11.05 (s, 1H), 7.37-7.27 (m, 3H), 7.18 (s, 1H), 7.12-7.10 (m, 2H), 6.73 (d, *J* = 8.3 Hz, 1H), 6.62 (d, *J* = 8.4 Hz, 1H), 3.51 (s, 3H). OH proton not observed. **$^{13}$C-NMR** (126 MHz; $CDCl_3$): δ 170.3, 160.8, 144.6, 134.1 (q, *J* = 32.7 Hz) , 131.0, 130.1, 127.8, 126.7, 123.3 (q, *J* = 272.8 Hz), 119.0, 115.3 (dt, *J* = 7.5, 3.8 Hz), 114.2 (q, *J* = 3.7 Hz), 39.5. **LRMS** (ESI-TOF) Calc. for $[C_{15}H_{12}F_3NO_2+H^+]^+$ = 296.09, Found = 296.33. **HRMS** (ESI-TOF) Calc. for $[C_{15}H_{12}F_3NO_2+H^+]^+$ = 296.0893, Found = 296.0890. **$^{19}$F NMR** (282 MHz; $CDCl_3$): δ -63.6. **$R_f$** (25% EtOAc in hexanes): 0.25

### 3.6.5 General Amide Hydrolysis Procedure

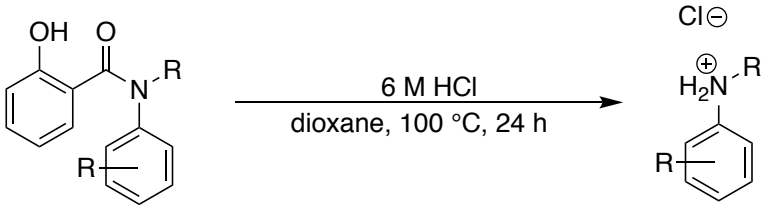


Scheme 3.16. General amide hydrolysis procedure.

To a 1-dram vial charged with a magnetic stir bar and amide (20 mg, 1 equiv) was added 0.5 mL 6 M aqueous HCl and 0.5 mL dioxane. The reaction was heated to 100 °C, and stirred for 24-72 h. The reaction was then allowed to cool to room temperature and extracted three times with ethyl acetate to remove the salicylic acid byproduct. Solvent was removed from the remaining aqueous fraction in vacuo to provide the aniline hydrochloride salt. Alternatively, the free amine can be isolated by suspending the hydrochloride salt in aqueous potassium carbonate solution, extracting with methylene chloride, combining the organic fractions and removing the solvent in vacuo.

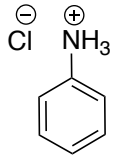


**Anilinium hydrochloride** was prepared using the general hydrolysis procedure using a 50:50 mixture dioxane:EtOH in lieu of pure dioxane in 70% yield (8 mg) over 3 steps starting from phenol as an oily residue. The rearrangement and hydrolysis reactions were carried out in one pot following a solvent switch. Spectral data was in accordance with the literature.[31]

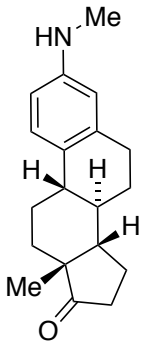


***N*-methyl aniline-estrone analog** was prepared according to the general hydrolysis procedure and isolated as the free amine in 80% yield (11 mg) over three steps starting from estrone as an oily residue. The rearrangement and hydrolysis reactions were carried out in one pot following a solvent switch. **$^{1}$H-NMR** (400 MHz; $CDCl_3$): δ 7.12 (d, *J* = 8.4 Hz, 1H), 6.47 (d, *J* = 8.4 Hz, 1H), 6.38 (s, 1H), 2.88-2.85 (m, 3H), 2.82 (s, 3H), 2.50 (dd, *J* = 18.8, 8.5 Hz, 2H), 2.38-2.36 (m, 1H), 2.23-2.06 (m, 3H), 2.00-1.92 (m, 2H), 1.62-1.47 (m, 5H), 0.90 (s, 3H). NH proton not observed. **$^{13}$C-NMR** (126 MHz; $CDCl_3$): δ 147.4, 137.4, 132.4, 129.0, 126.3, 112.7, 111.0, 50.5, 48.2, 44.1, 38.7, 36.1, 31.7, 31.2, 29.9, 26.8, 26.1, 21.7, 14.0. **LRMS** (ESI-TOF) Calc. for $[C_{19}H_{25}NO+H^+]^+$ = 284.20, Found = 284.24. **$R_f$** (25% EtOAc in hexanes): 0.12

### 3.6.6 Preparative Scale Procedure

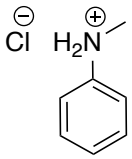


**N-methyl anilinium hydrochloride** was synthesized in 77% yield (447 mg) over three synthetic steps starting from phenol as an off-white solid. Spectral data was in accordance with the literature.[32]

**Step 1**: To a 100 mL roundbottom flask charged with a magnetic stir bar and DMF (50 mL) was added 2-iodobenzoic acid (1.0 g, 4.0 mmol, 1 equiv), 1,8-diazabicyclo[5.4.0]undec-7-ene (DBU, 1.8 mL, 3 equiv), phenol (0.76 g, 8.1 mmol, 2 equiv), pyridine (0.063 mL, 20 mol %), copper powder (11 mg, 4 mol %), and copper iodide (32 mg, 4 mol %). The reaction vessel was sealed with a rubber septum and sparged with $N_2$ for 10 mins. The mixture was then heated to 140 °C and allowed to stir for 12 h. Next, the reaction was allowed to cool to room temperature and was then poured into a 500 mL Erlenmeyer flask containing 200 mL of ice-cold 1M HCl aqueous solution. The mixture was then filtered to furnish the carboxylic acid intermediate (0.85 g, 3.97 mmol, 99% yield).

**Step 2**: The carboxylic acid (0.85 g, 3.97 mmol, 1 equiv) was added to a 100 mL round bottom flask charged with a magnetic stir bar and dissolved in dichloromethane (20 mL). *N*,*N*-dimethylformamide (0.31 mL, 1 equiv) was then added, followed by oxalyl chloride (1.8 mL, 5 equiv). The reaction was allowed to stir for 1 h at room temperature, after which a solution of N-methylhydroxylamine hydrochloride (2.0 g, 6 equiv) and triethylamine (4.5 mL, 8 equiv) dissolved in 20 mL of 9:1 tetrahydrofuran:water was added. The reaction was allowed to stir for an additional 1 h and was then transferred to a separatory funnel, washed once with 1M HCl aqueous solution, dried over sodium sulfate, and concentrated by rotary evaporation. The crude product was then recrystallized from hexanes to furnish **1a** (1.0 g, 4.1 mmol, ~quantitative yield).

**Step 3**: To a 100 mL round bottom flask equipped with a reflux condenser and charged with a magnetic stir bar was added **1a** (1.0 g, 4.1 mmol, 1 equiv), di-*tert*-butyl peroxide (3.7 mL, 5 equiv), triethyl phosphite (1.0 mL, 1.5 equiv), and 1,2-dichloroethane (25 mL). The flask was heated to 90 °C and allowed to stir for 24 hours. Upon consumption of the hydroxamic acid as judged by TLC (25% EtOAc in hexanes), the reaction mixture was concentrated under reduced

pressure and 7 mL 6 M aqueous HCl and 7 mL dioxane were added. The reaction was heated to 100 °C, and stirred for 48 h. The reaction was then allowed to cool to room temperature and extracted three times with ethyl acetate to remove the salicylic acid byproduct. Solvent was removed from the remaining aqueous fraction in vacuo to provide the N-methylaniline hydrochloride salt in 77% yield (447 mg, 3.1 mmol). Physical and spectral data was in accordance with the literature.

### 3.6.7 $^{1}$H and $^{13}$C NMR Spectra of Novel Compounds

**$^{1}$H-NMR** (400 MHz; $CDCl_3$)

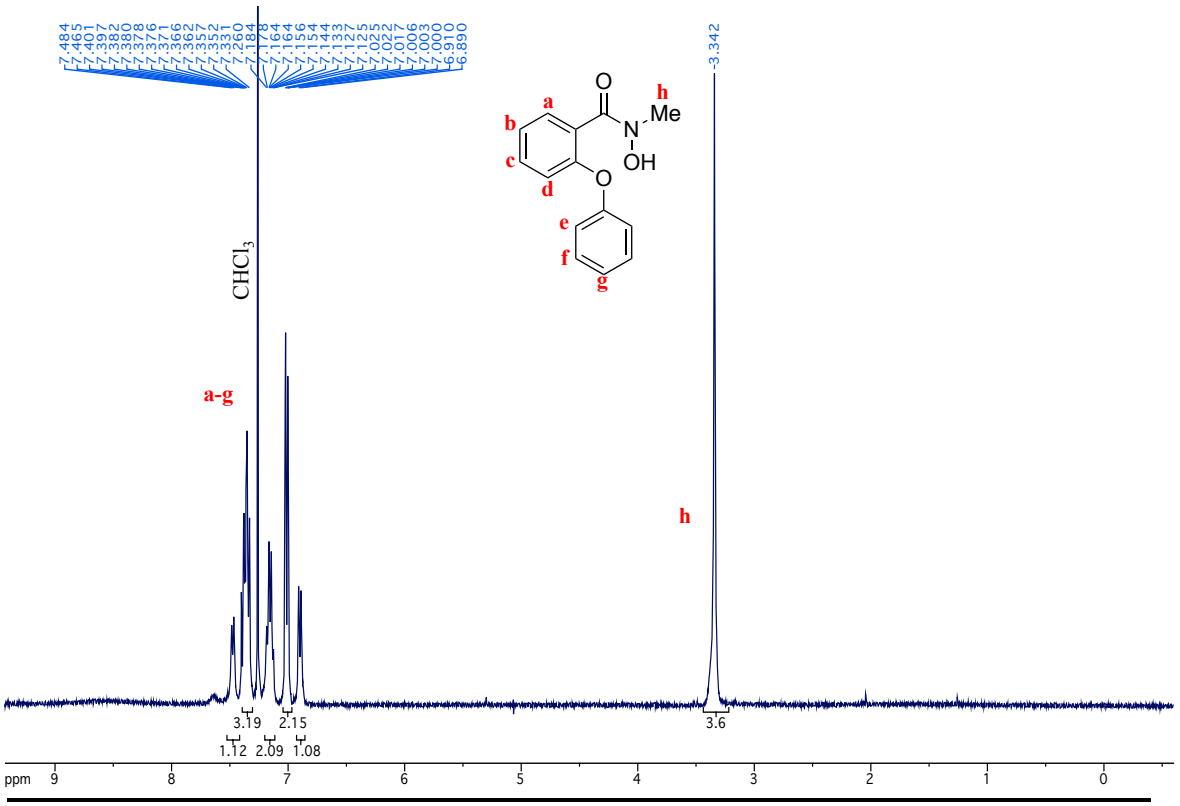


**$^{13}$C-NMR** (126 MHz; $CDCl_3$)

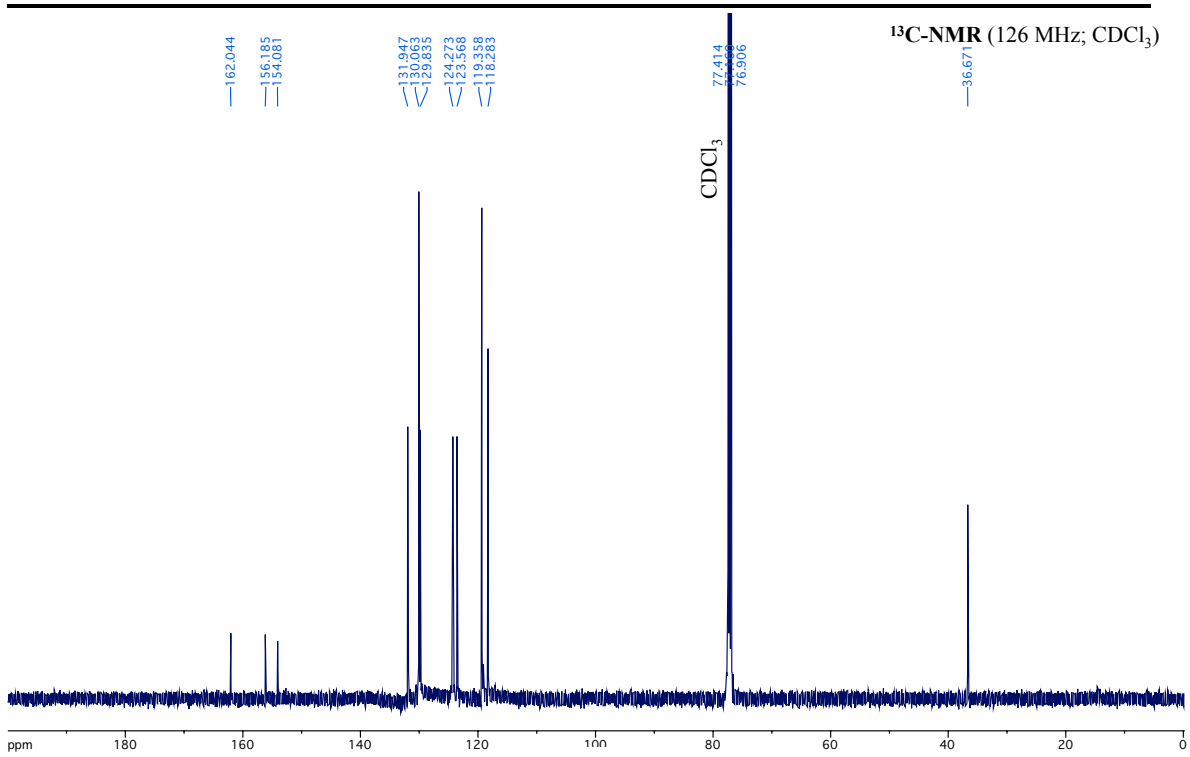

**$^{1}$H-NMR** (400 MHz; $CDCl_3$)

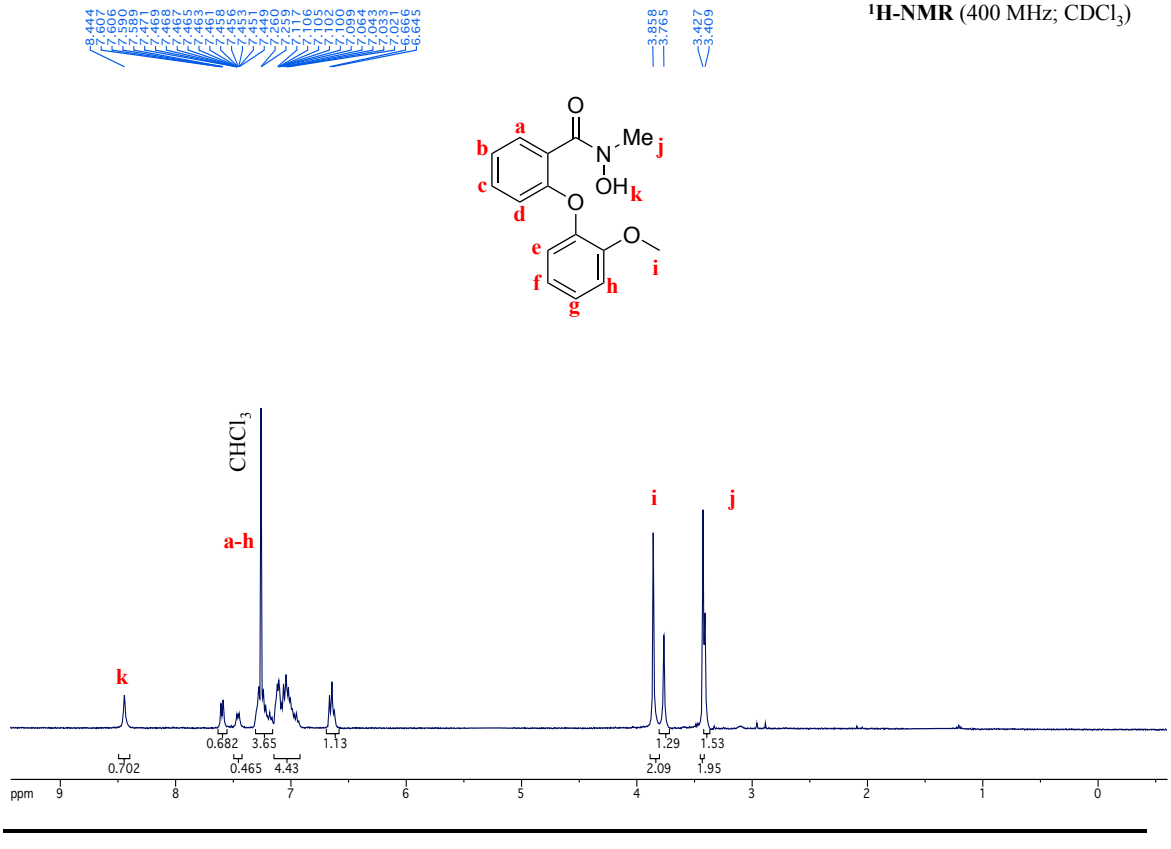


**$^{13}$C-NMR** (126 MHz; $CDCl_3$)

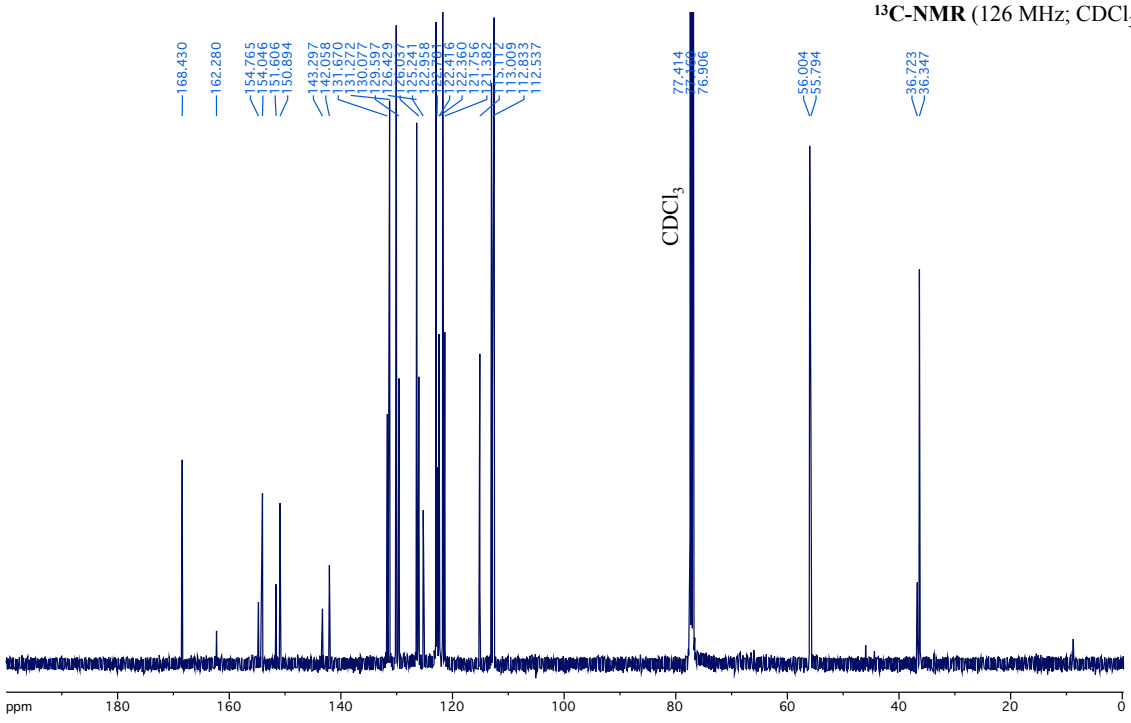

**$^{1}$H-NMR** (400 MHz; $CDCl_3$)

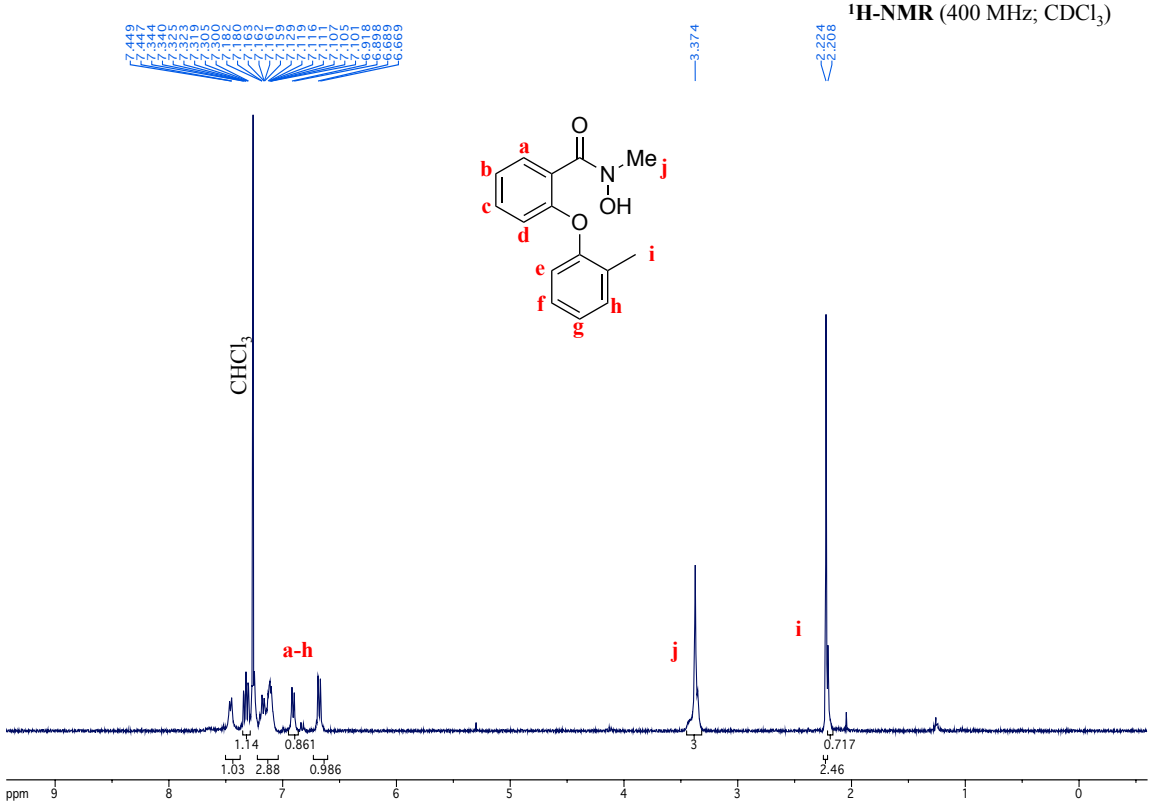


**$^{13}$C-NMR** (126 MHz; $CDCl_3$)

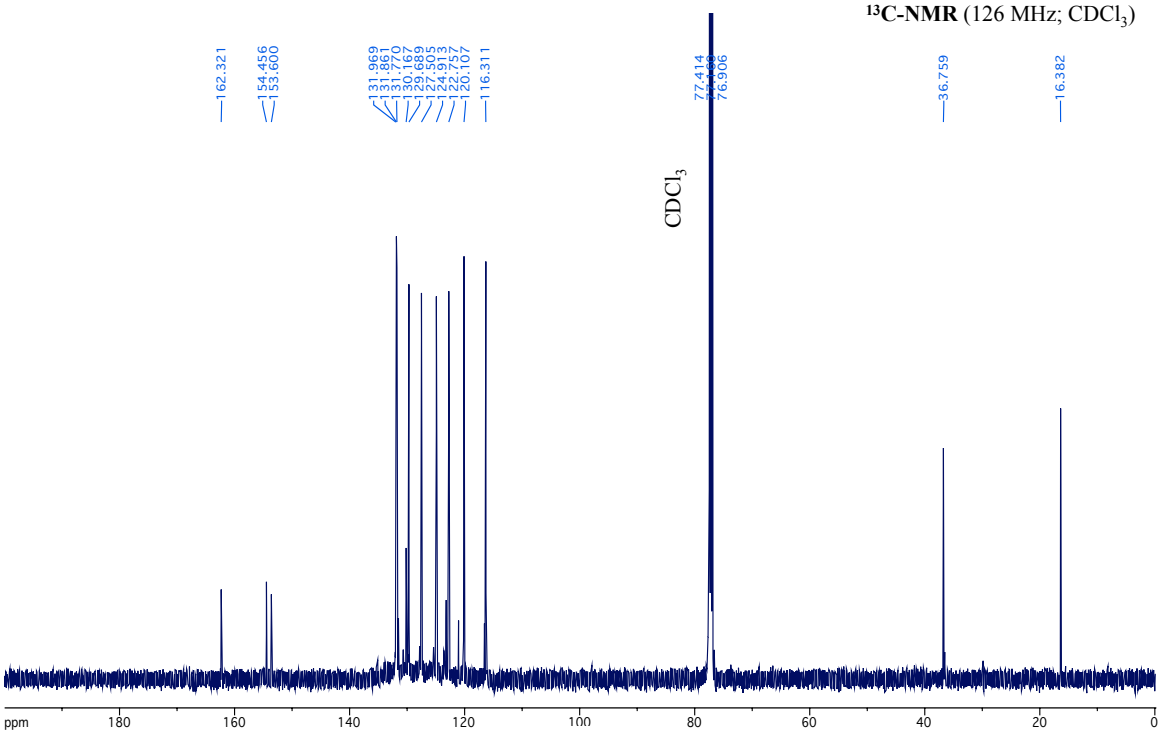

**$^{1}$H-NMR** (400 MHz; $CDCl_3$)

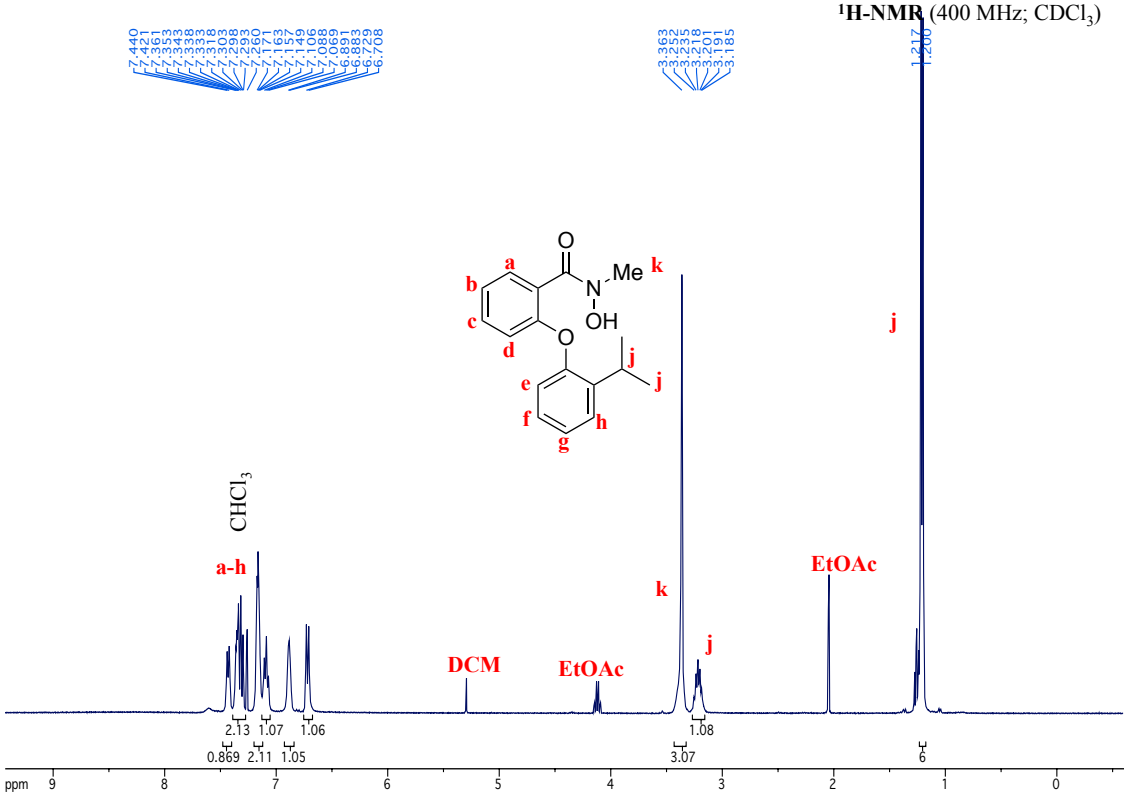


**$^{13}$C-NMR** (126 MHz; $CDCl_3$)

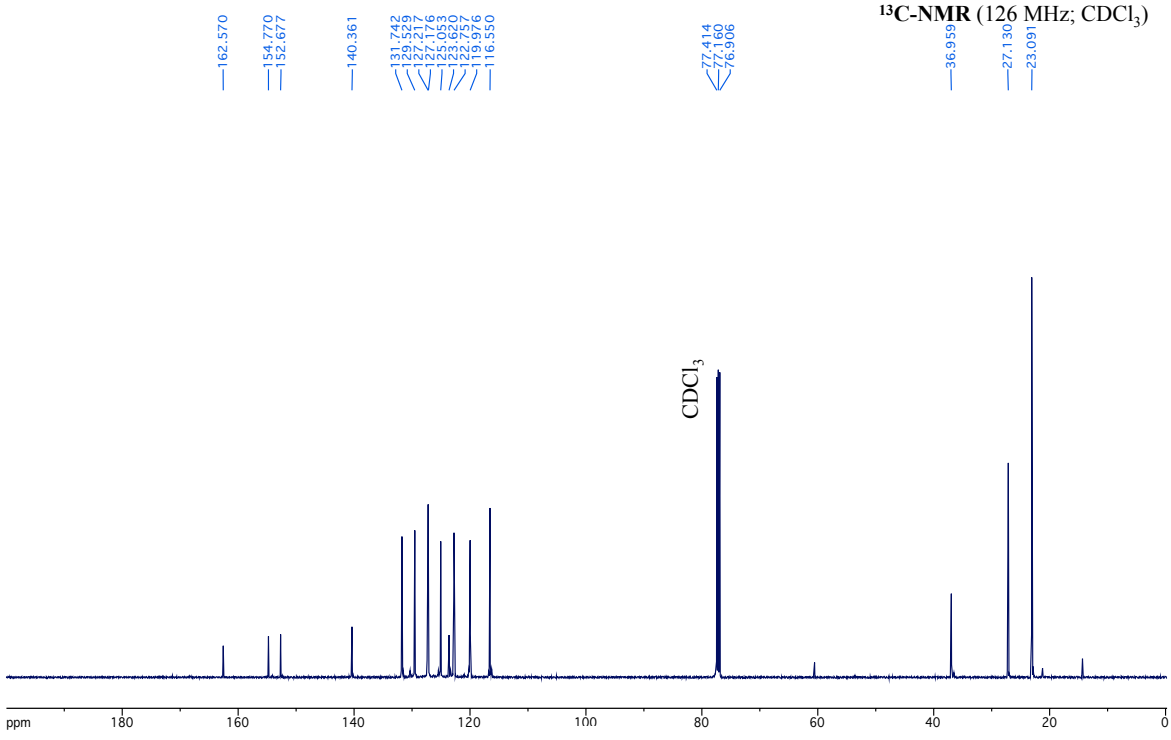

**$^{1}$H-NMR** (400 MHz; $CDCl_3$)

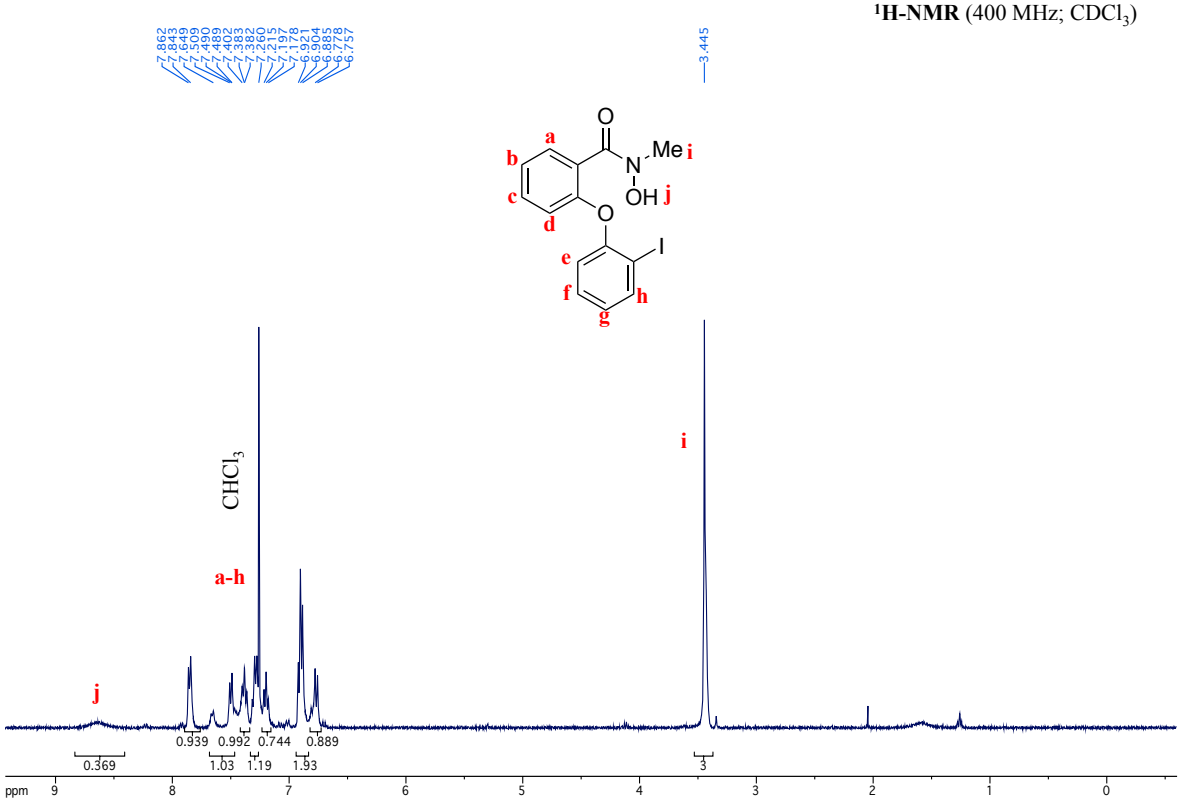


**$^{13}$C-NMR** (126 MHz; $CDCl_3$)

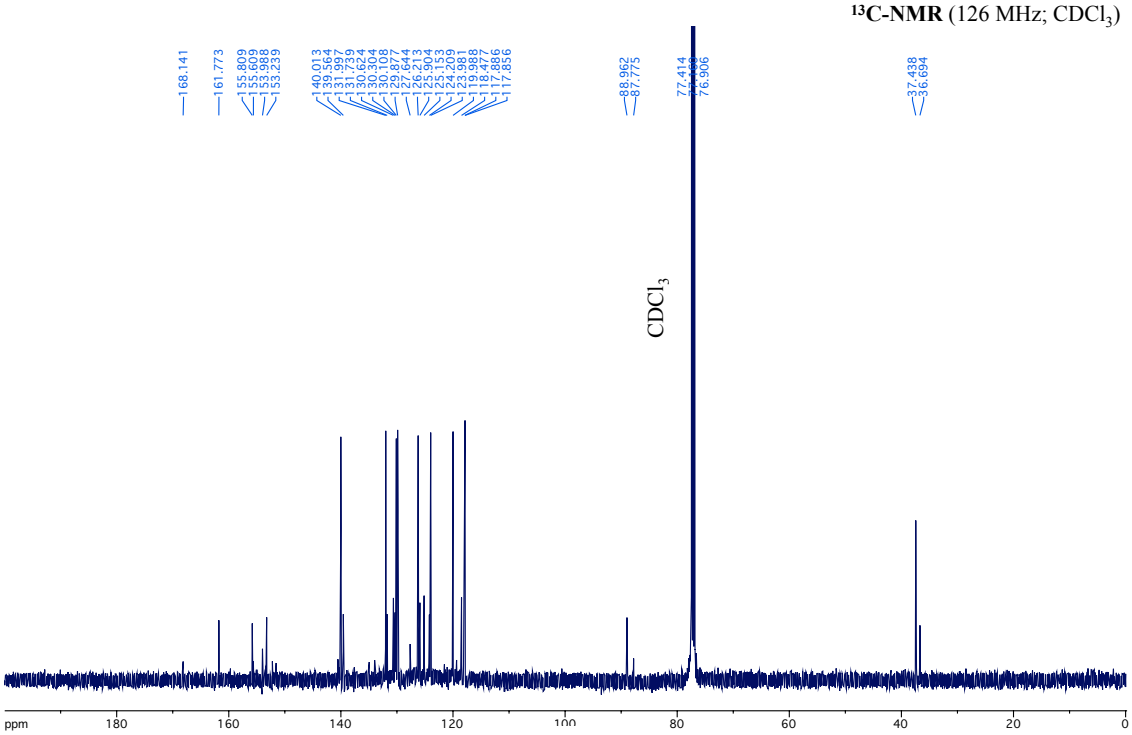

**$^{1}$H-NMR** (400 MHz; $CDCl_3$)

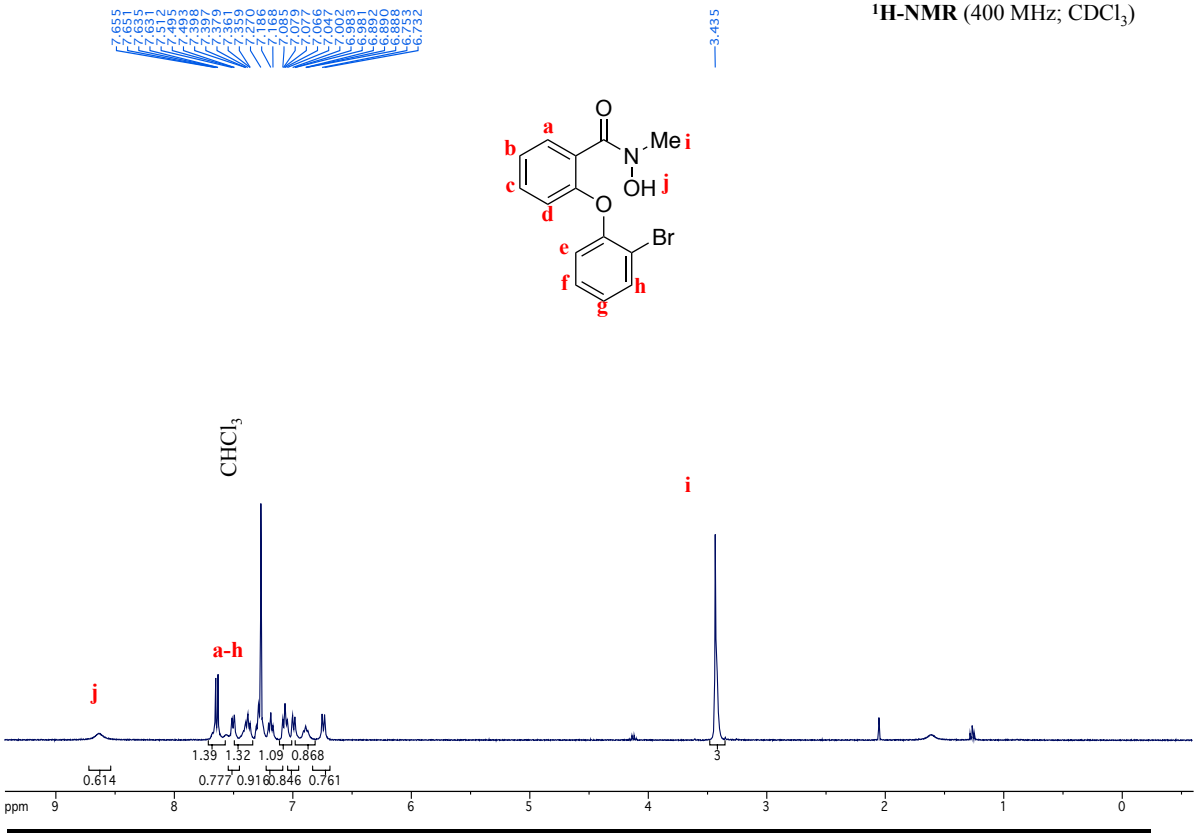


**$^{13}$C-NMR** (126 MHz; $CDCl_3$)

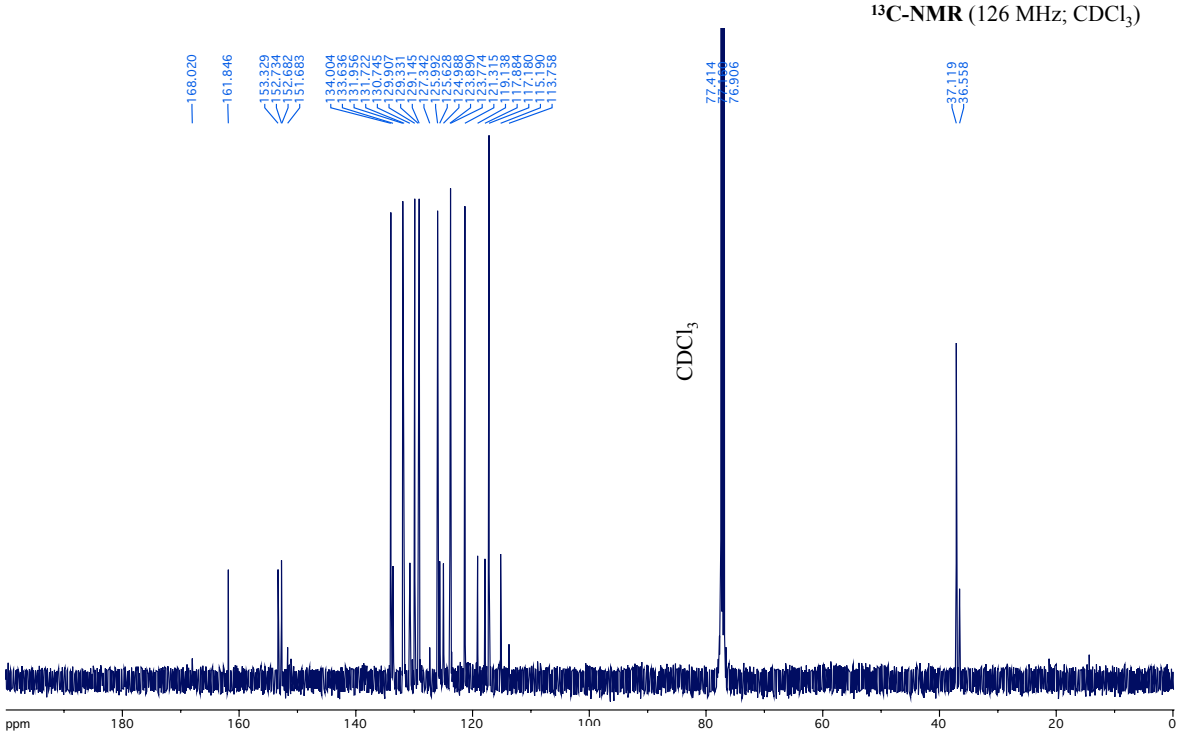

**$^{1}$H-NMR** (400 MHz; $CDCl_3$)

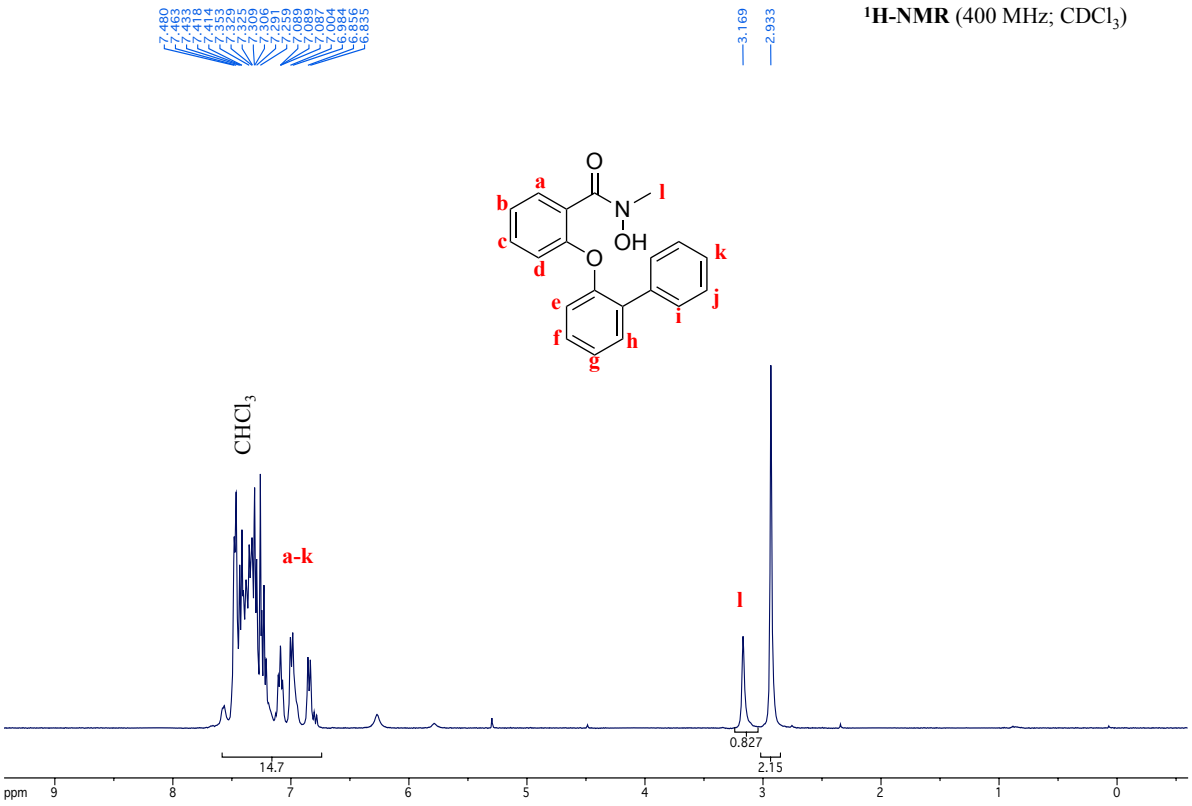


**$^{13}$C-NMR** (126 MHz; $CDCl_3$)

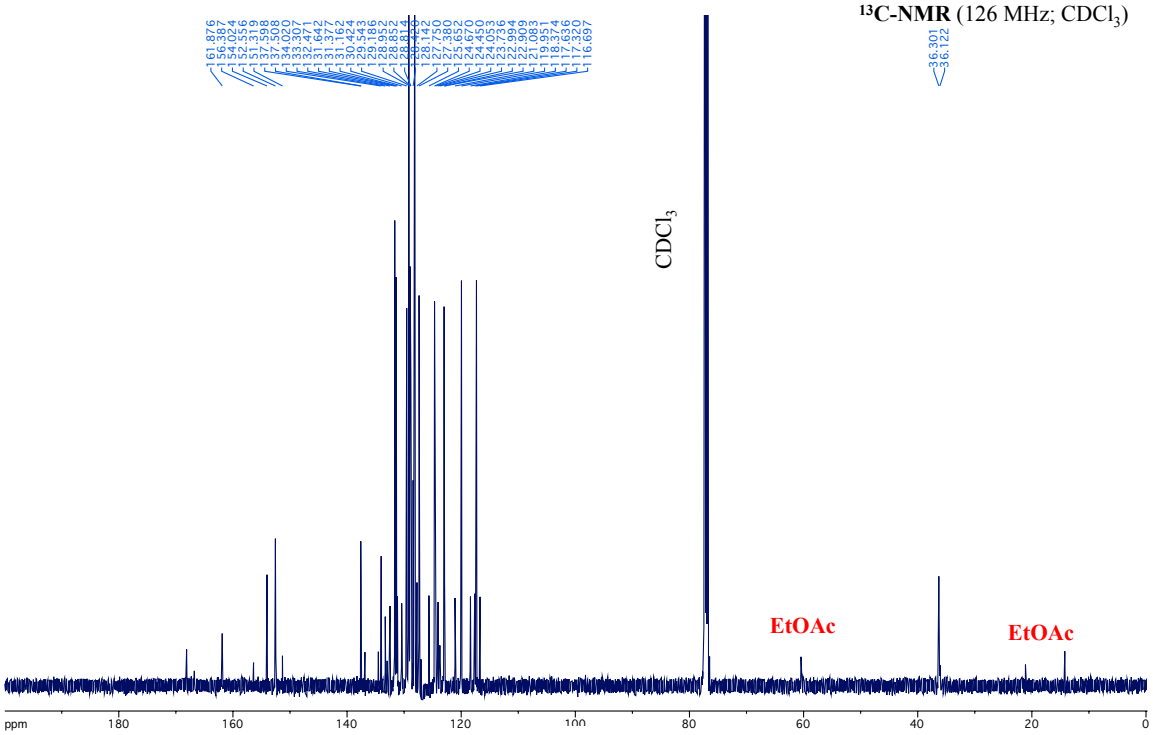

**$^1$H-NMR** (400 MHz; $CDCl_3$)

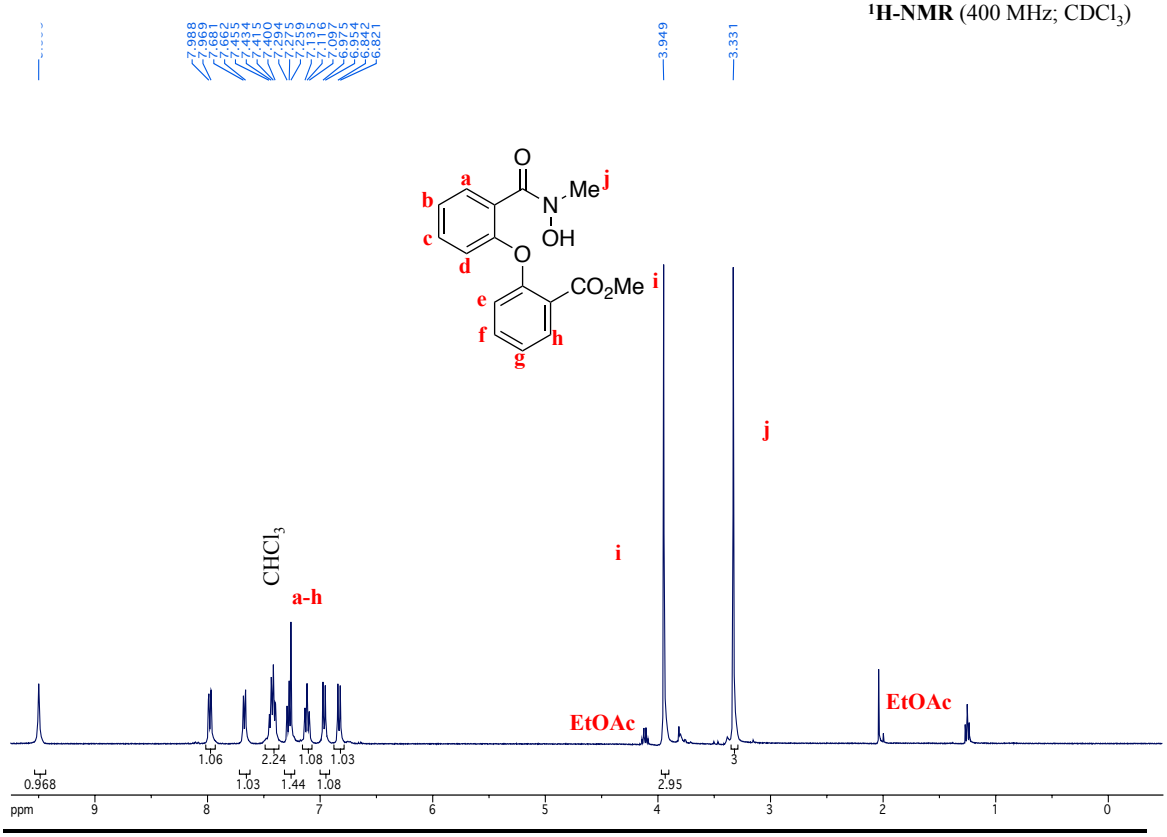


**$^{13}$C-NMR** (126 MHz; $CDCl_3$)

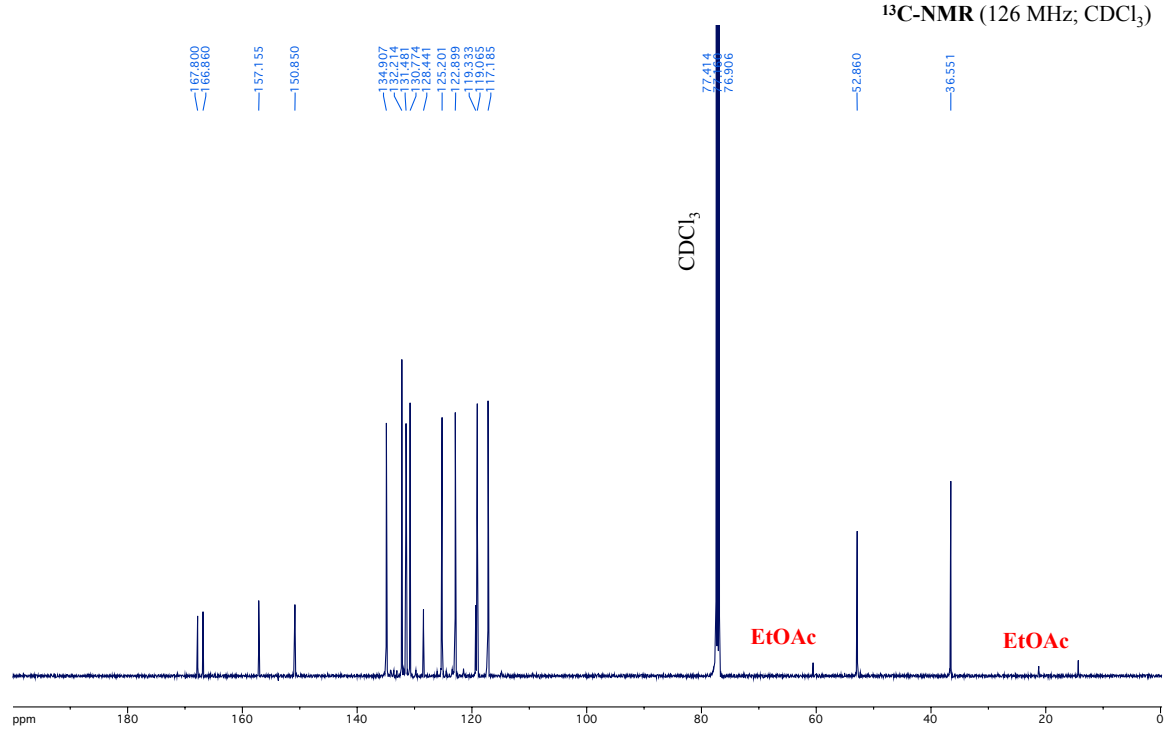

**$^{1}$H-NMR** (400 MHz; $CDCl_3$)

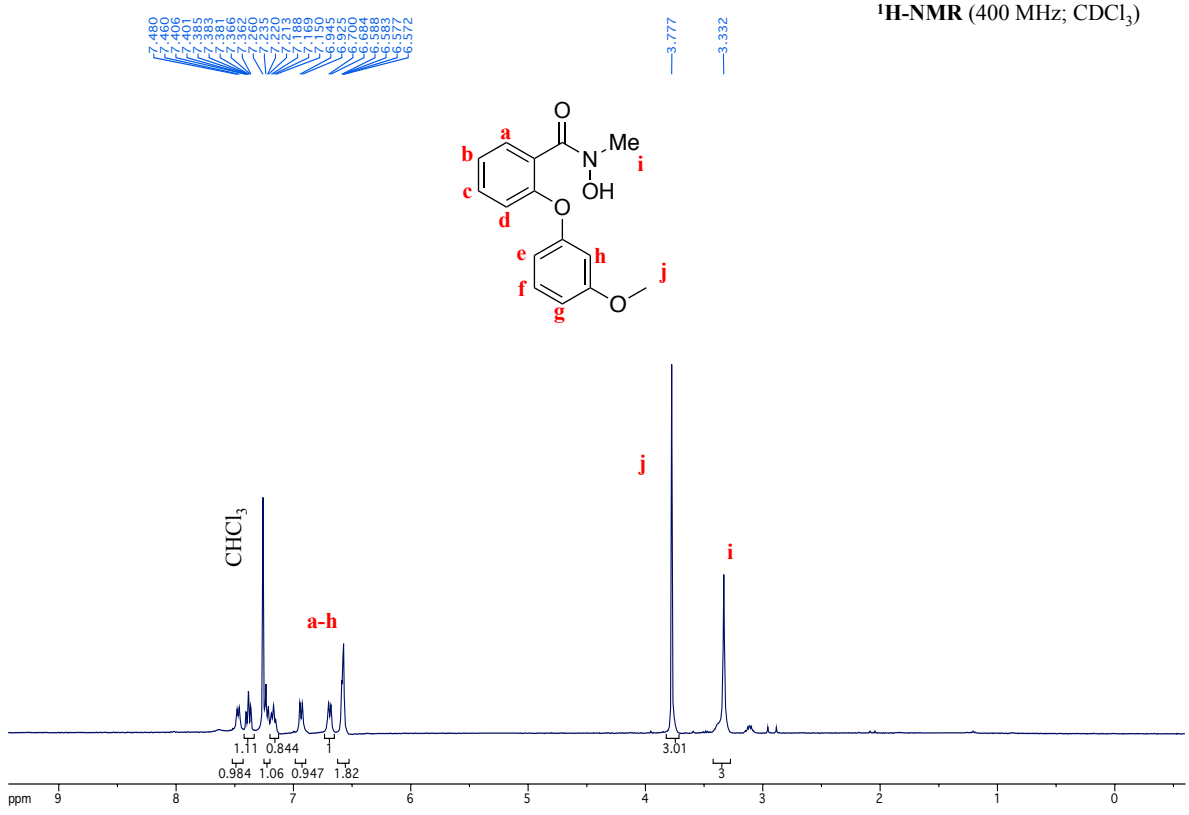


**$^{13}$C-NMR** (126 MHz; $CDCl_3$)

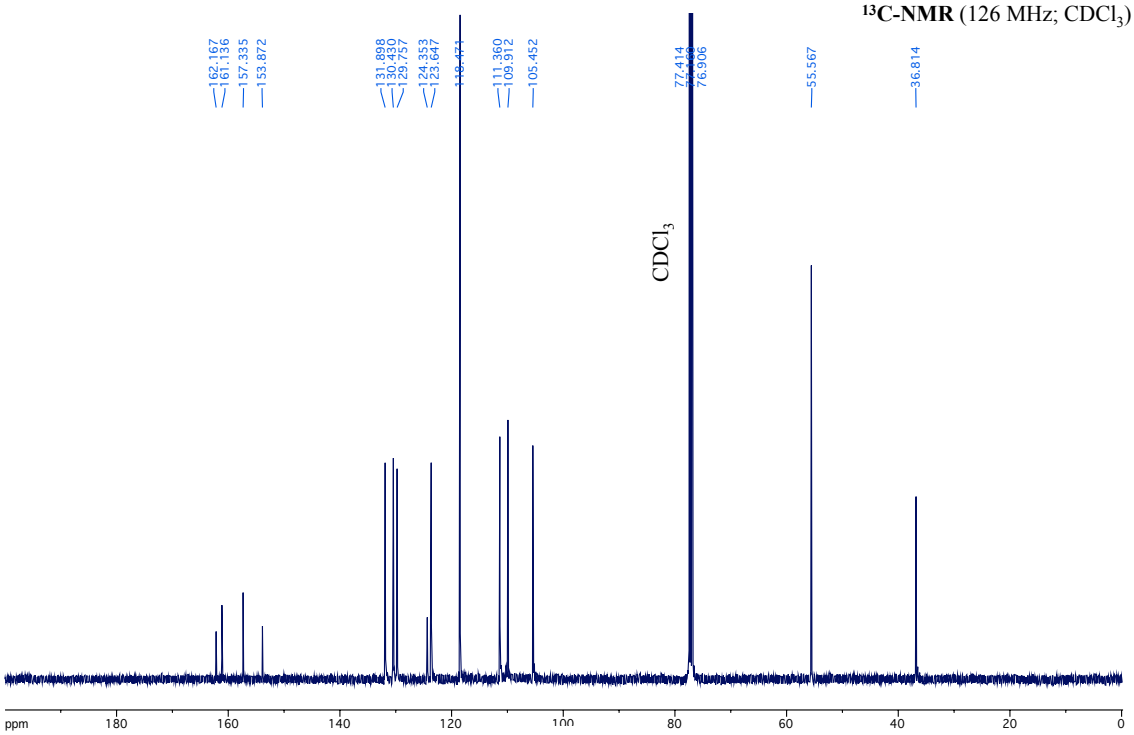

**$^{1}$H-NMR** (400 MHz; $CDCl_3$)

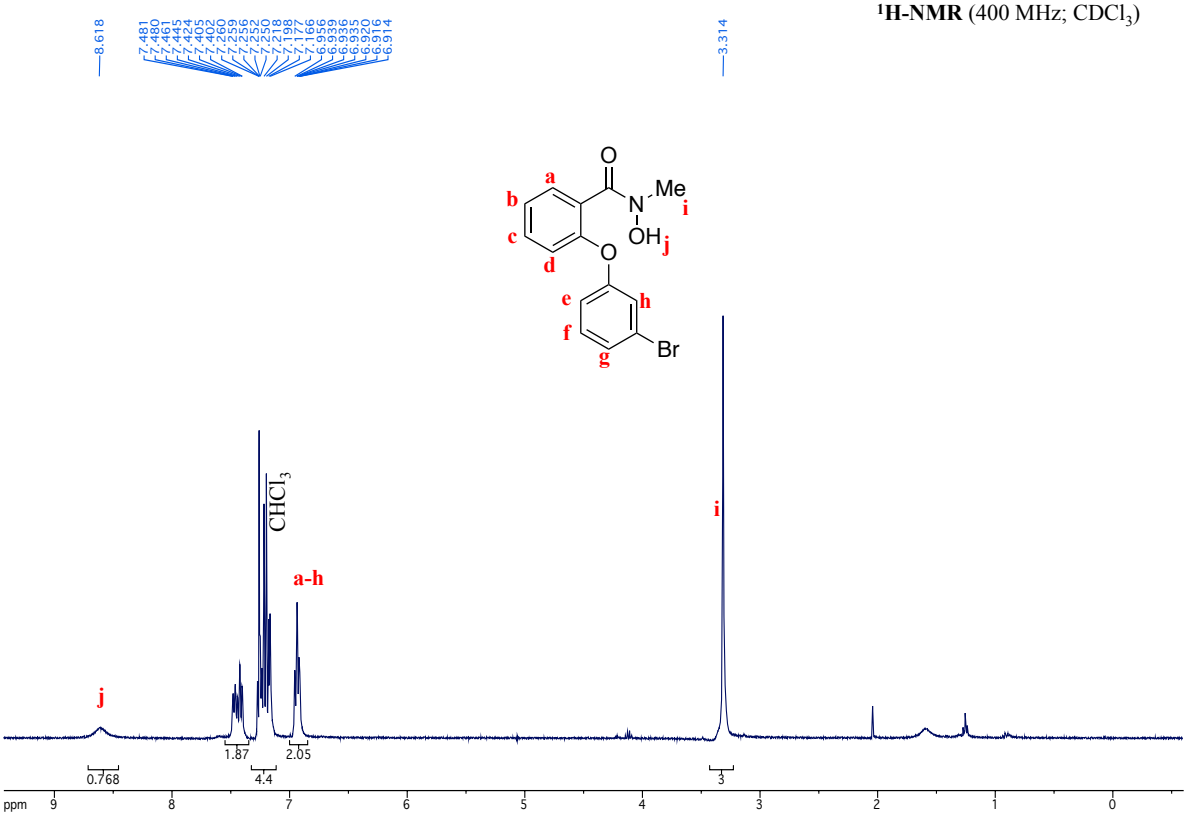


**$^{13}$C-NMR** (126 MHz; $CDCl_3$)

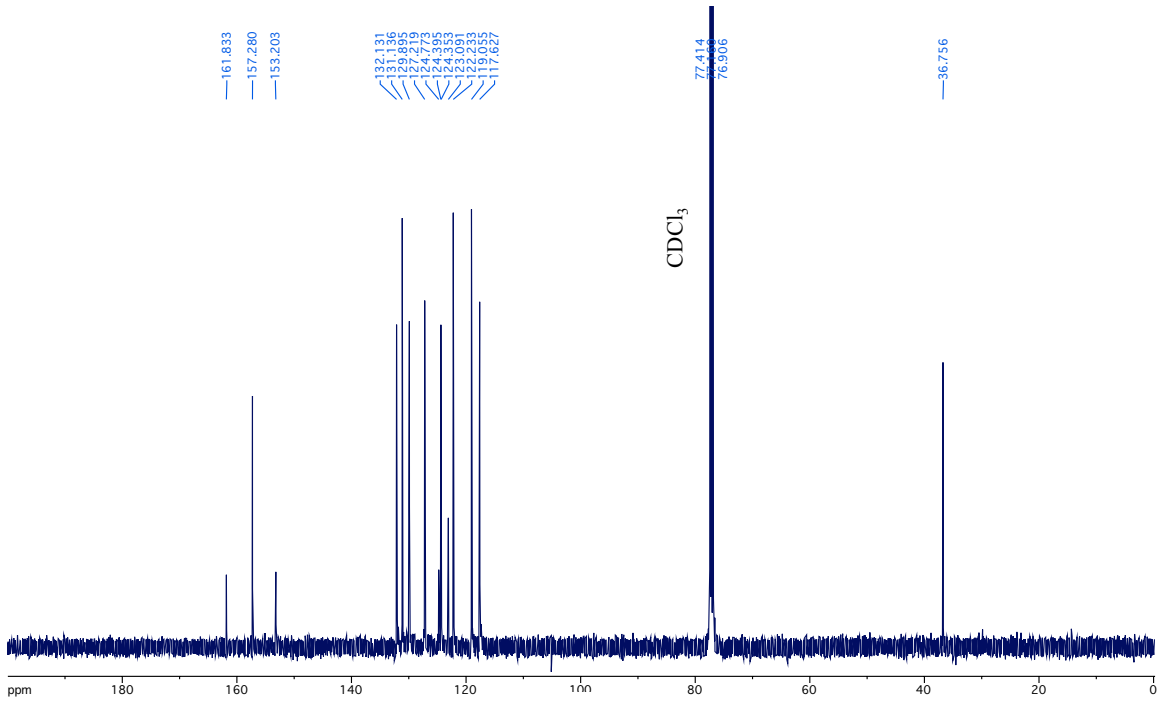

**$^{1}$H-NMR** (400 MHz; $CDCl_3$)

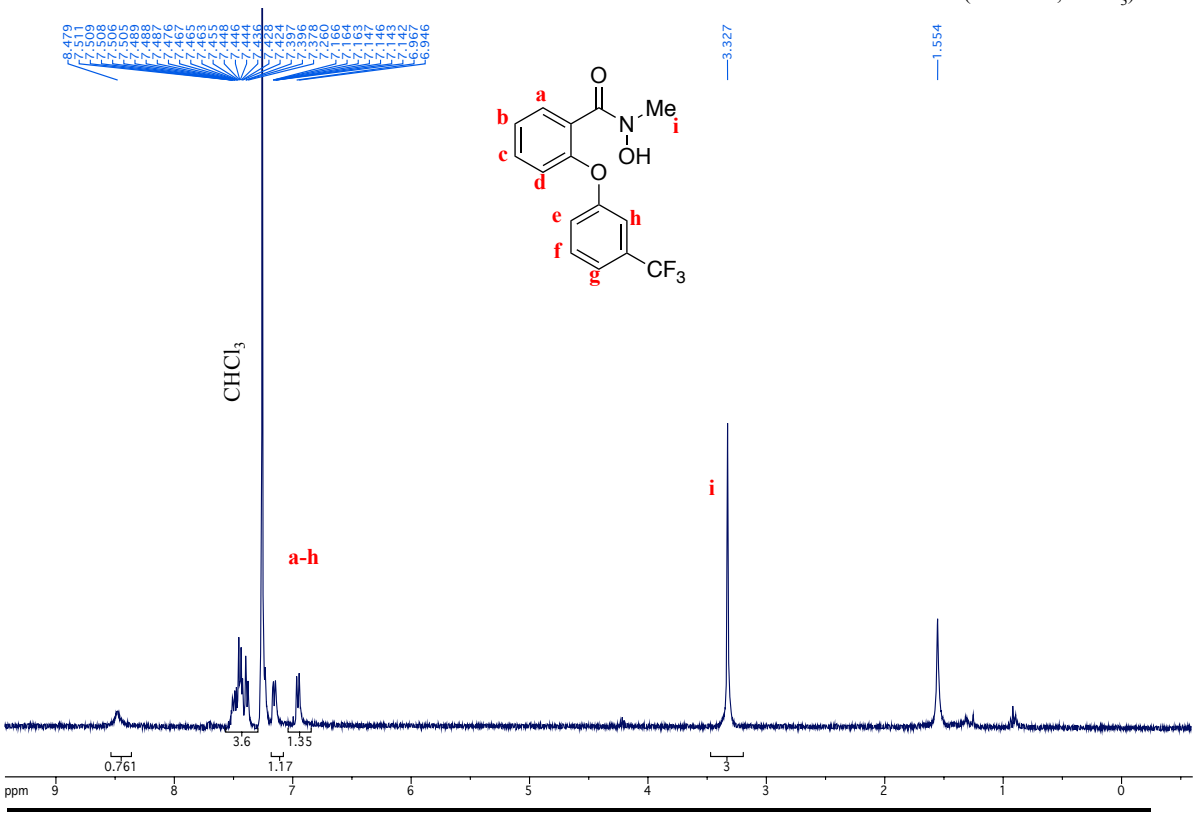


**$^{13}$C-NMR** (126 MHz; $CDCl_3$)

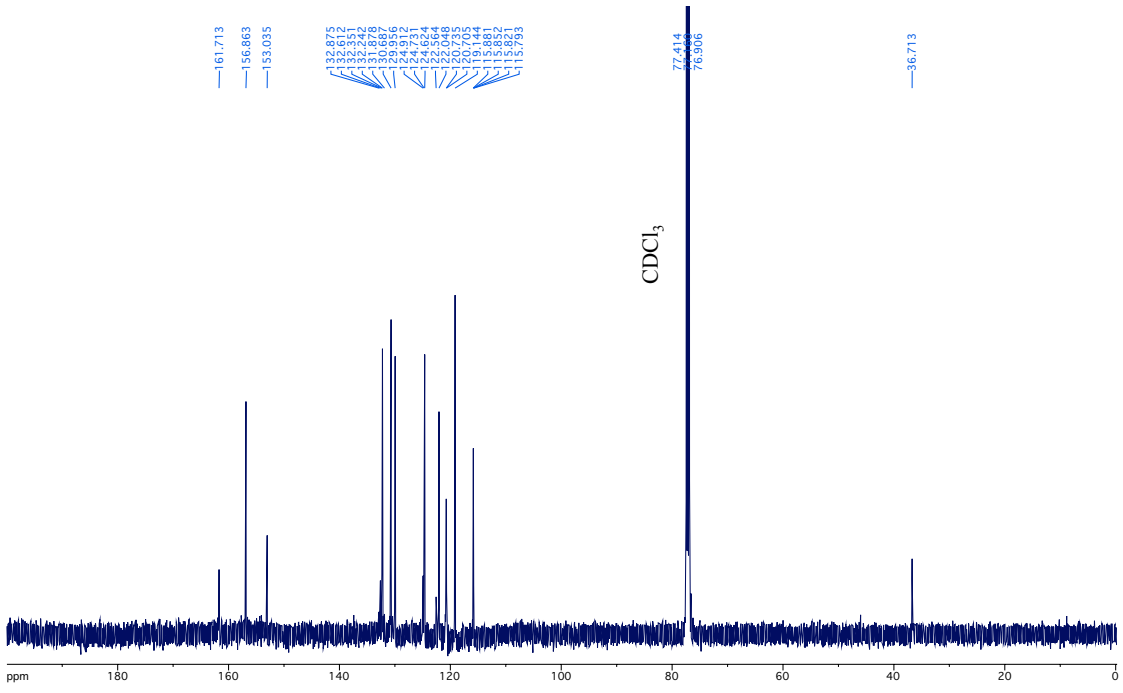

**$^{1}$H-NMR** (400 MHz; $CDCl_3$)

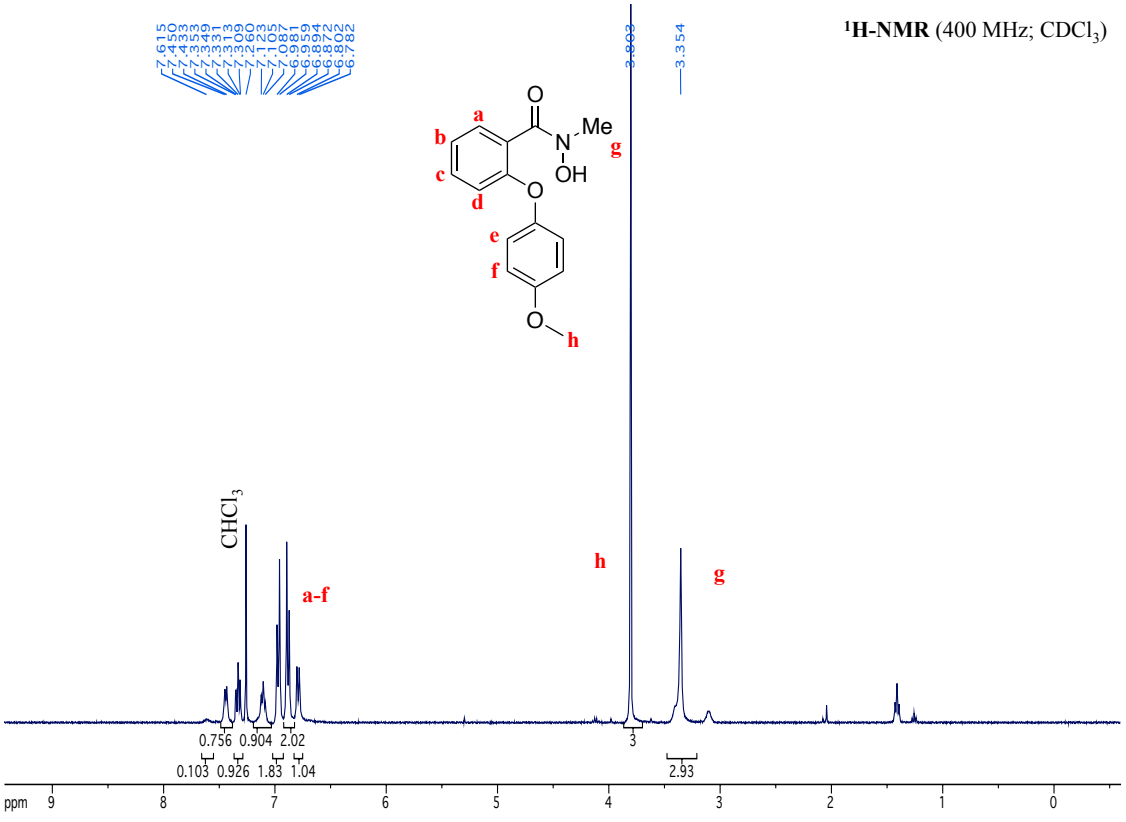


**$^{13}$C-NMR** (126 MHz; $CDCl_3$)

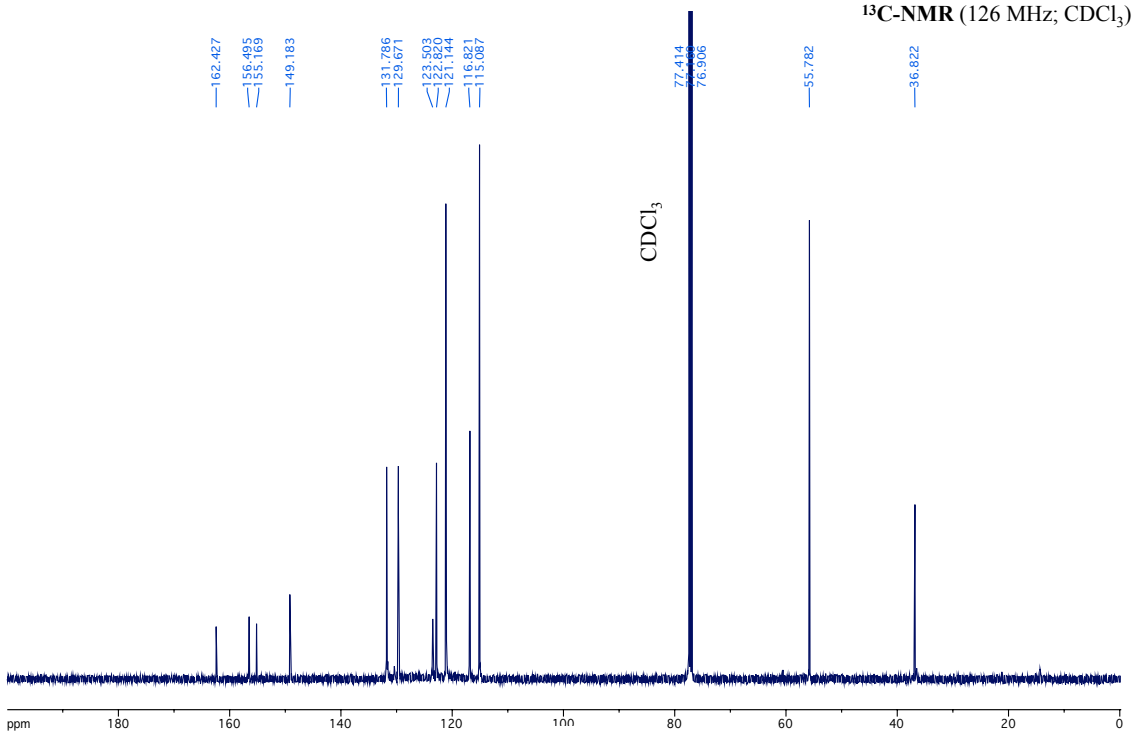

**$^{1}$H-NMR** (400 MHz; $CDCl_3$)

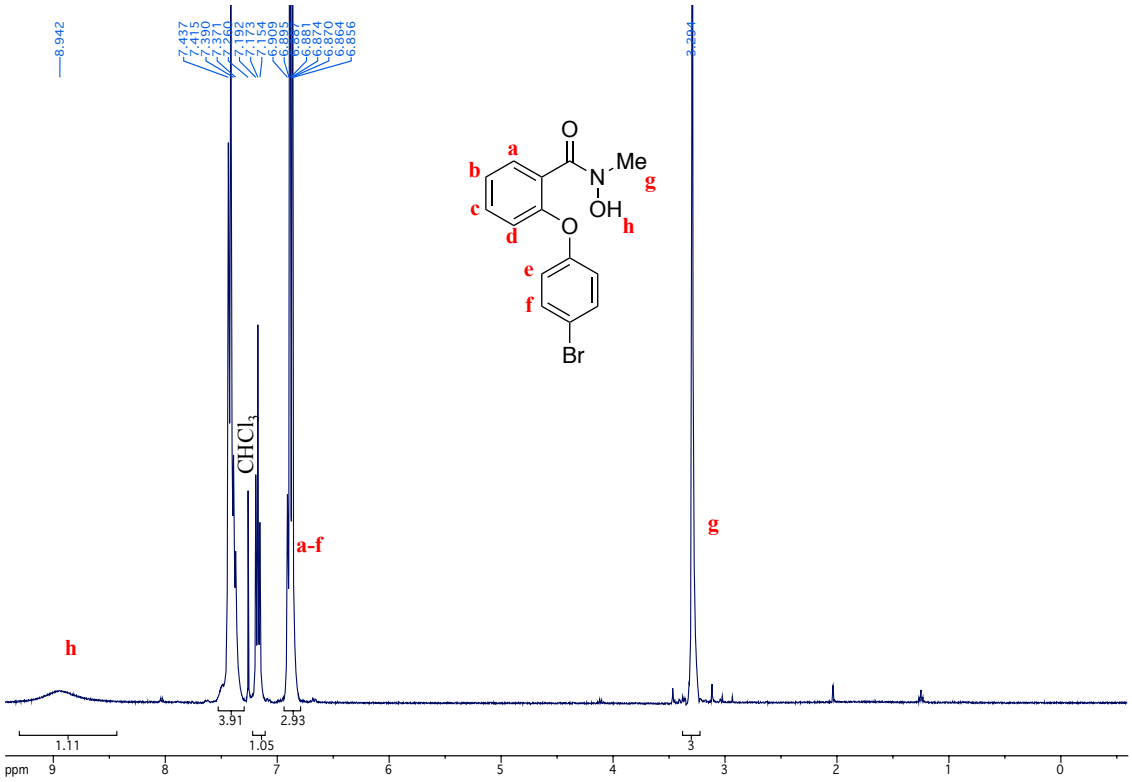


**$^{13}$C-NMR** (126 MHz; $CDCl_3$)

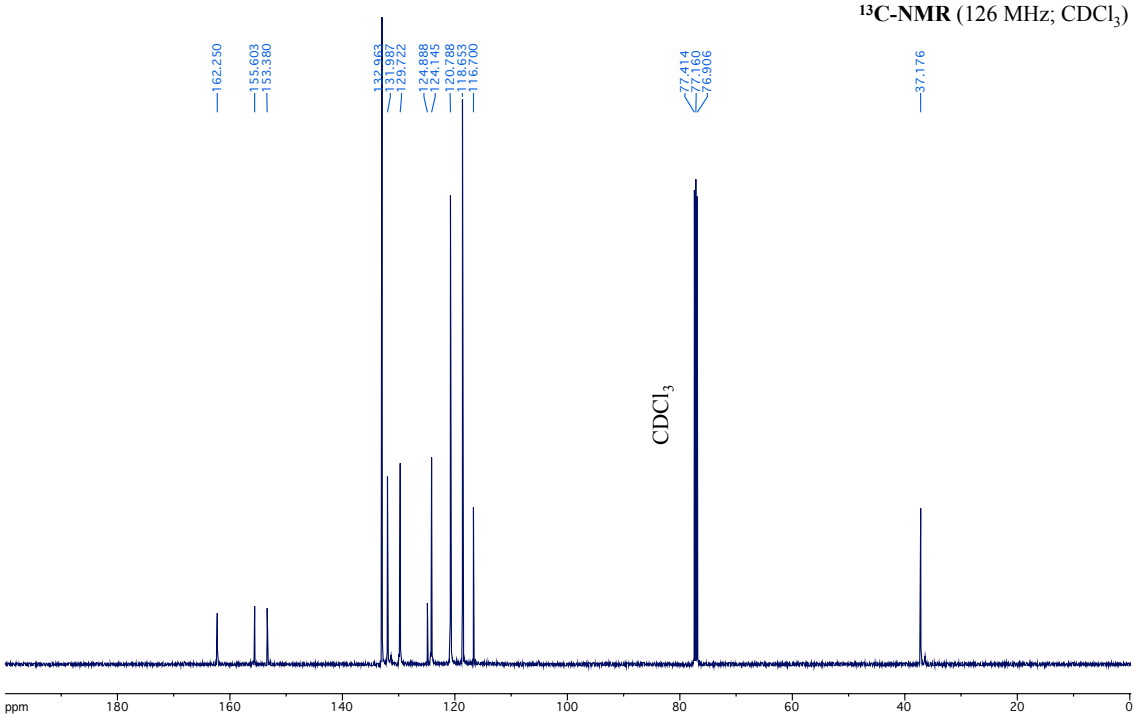

**$^{1}$H-NMR** (400 MHz; $CDCl_3$)

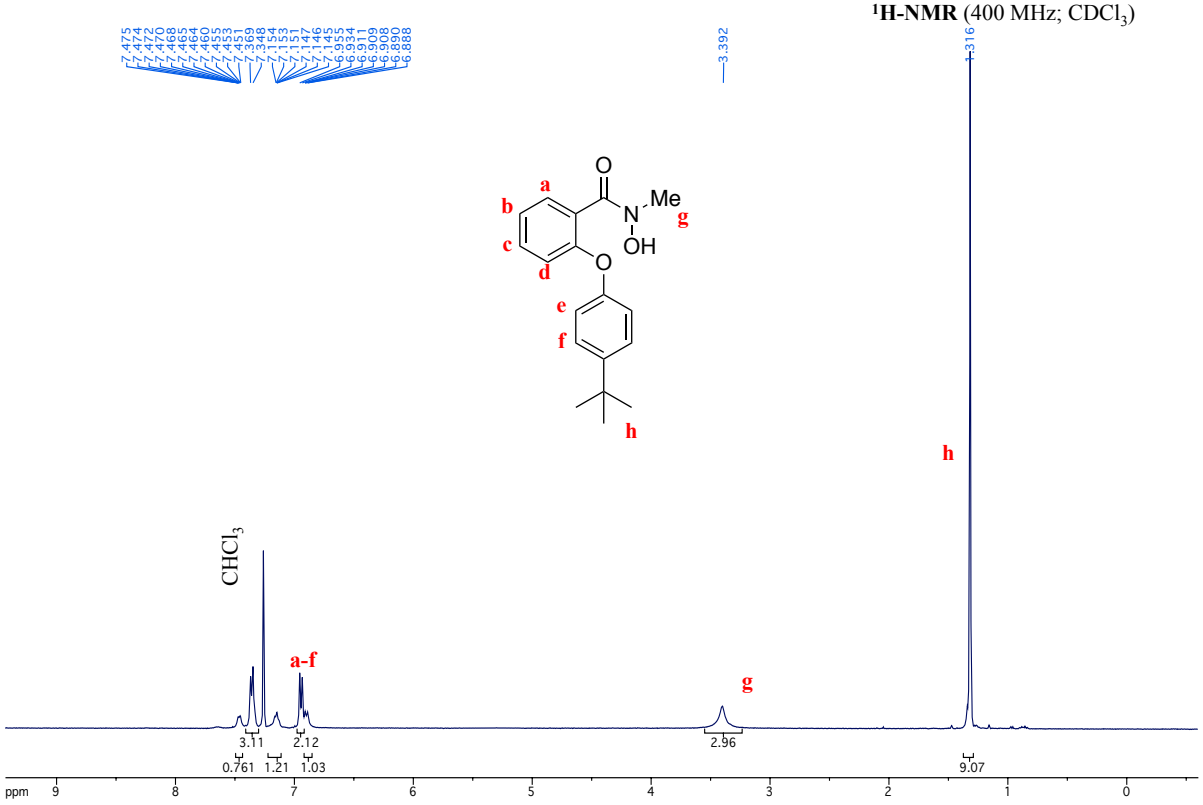


**$^{13}$C-NMR** (126 MHz; $CDCl_3$)

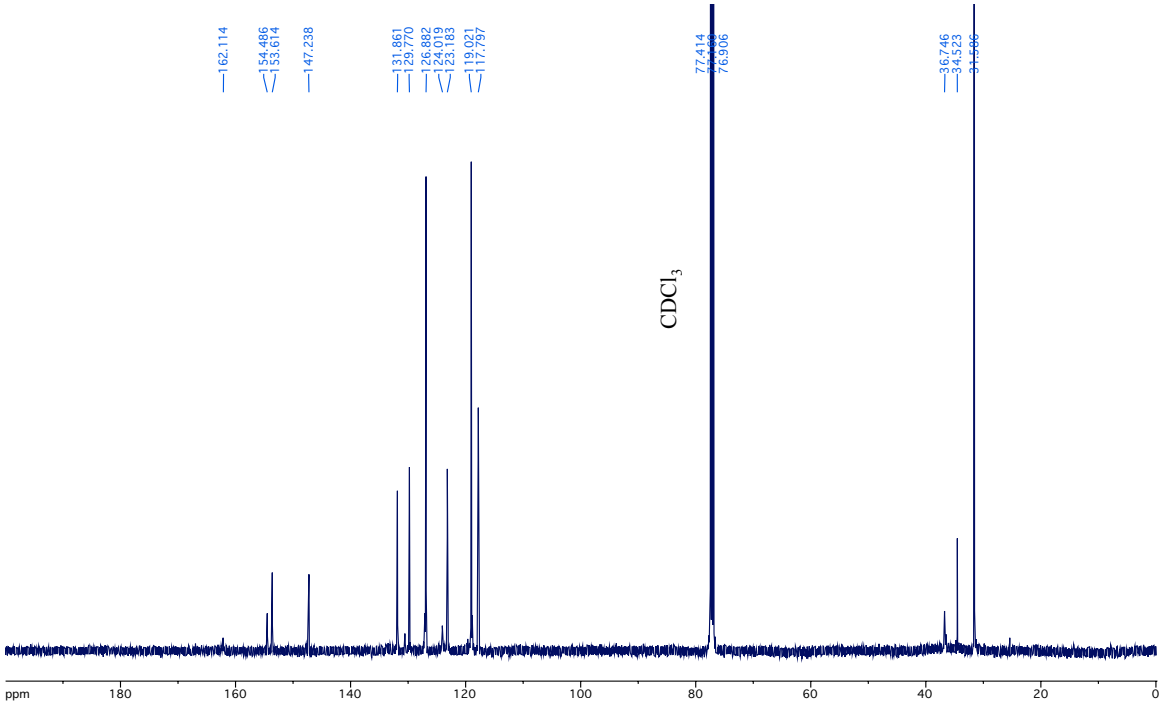

**$^{1}$H-NMR** (400 MHz; $CDCl_3$)

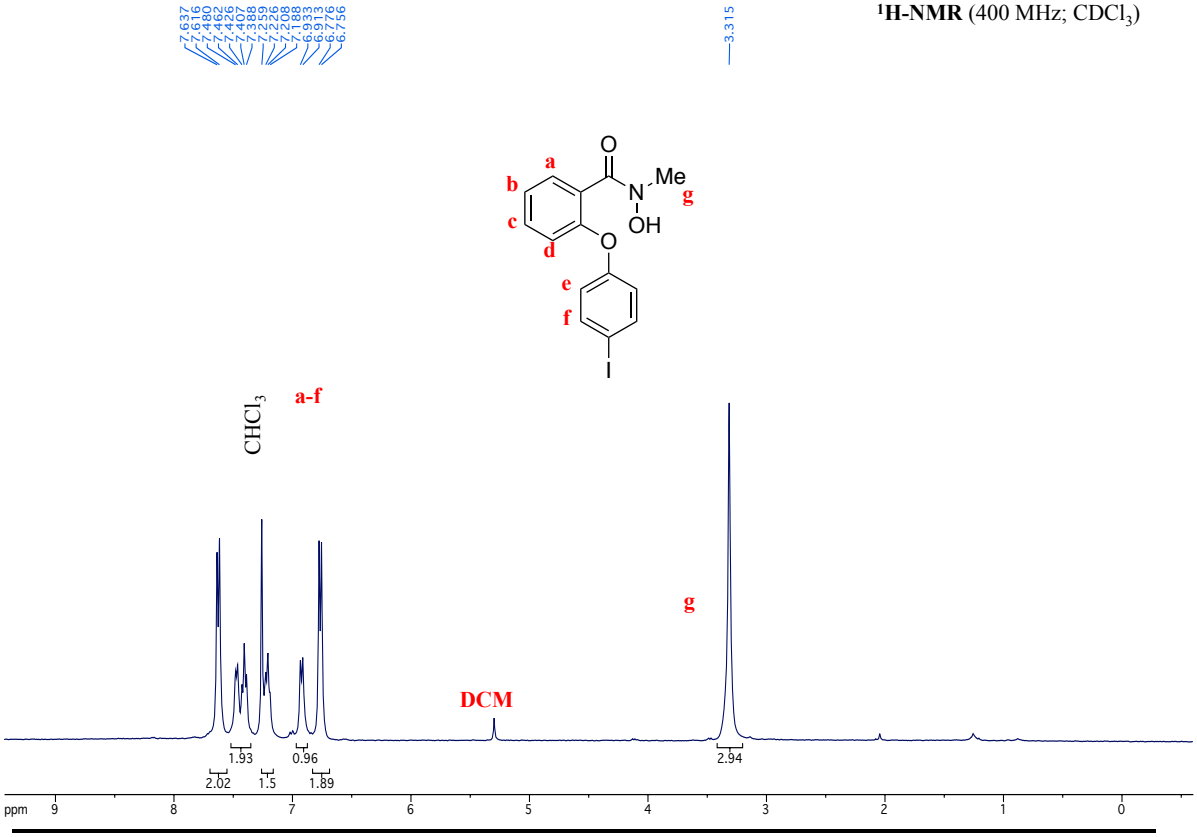


**$^{13}$C-NMR** (126 MHz; $CDCl_3$)

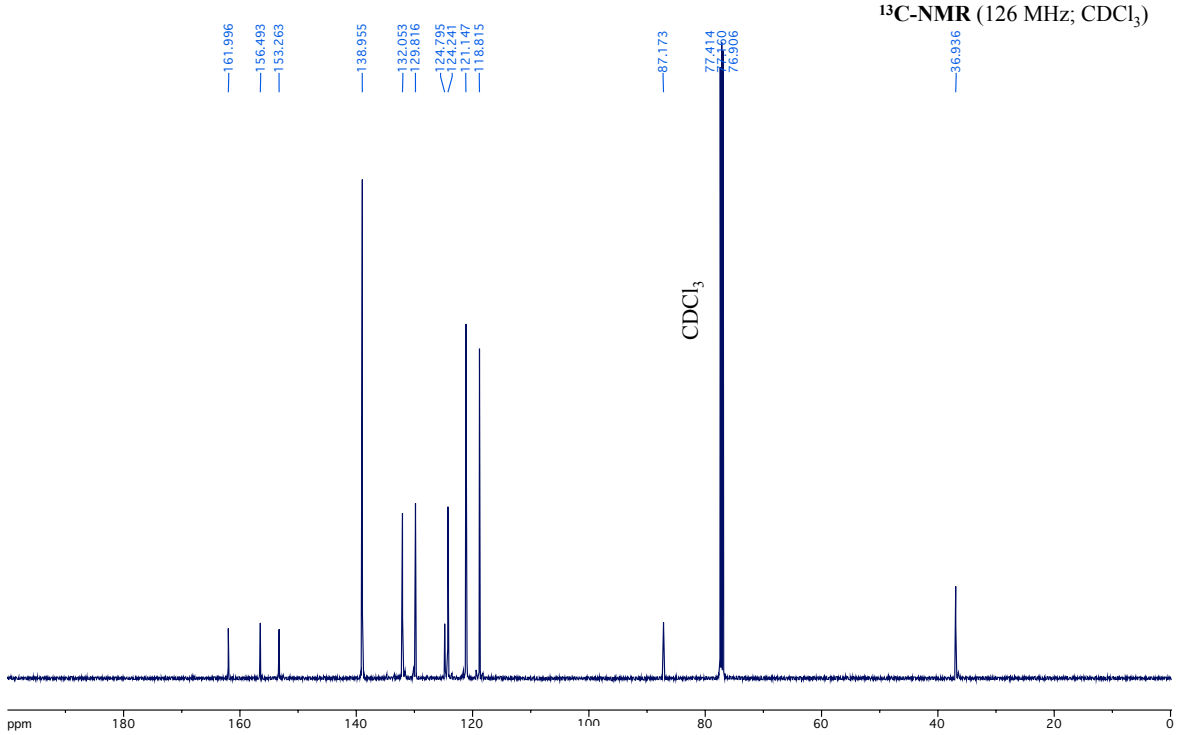

**$^{1}$H-NMR** (400 MHz; $CDCl_3$)

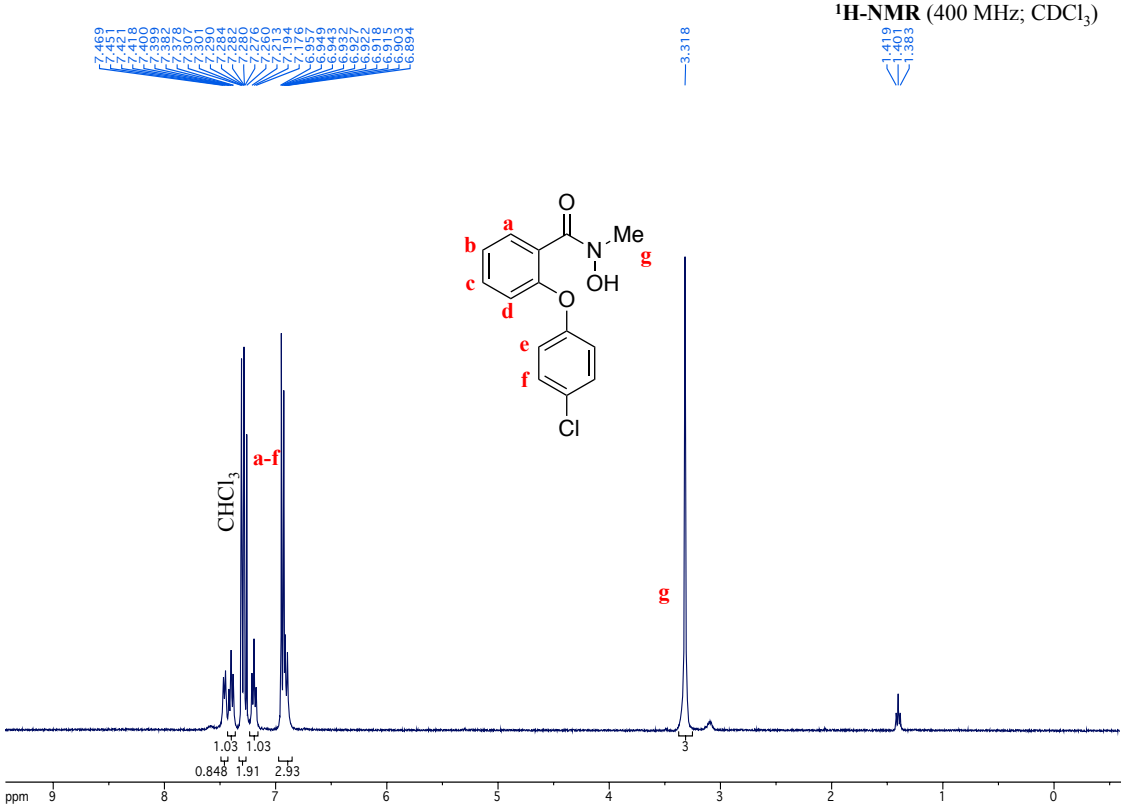


**$^{13}$C-NMR** (126 MHz; $CDCl_3$)

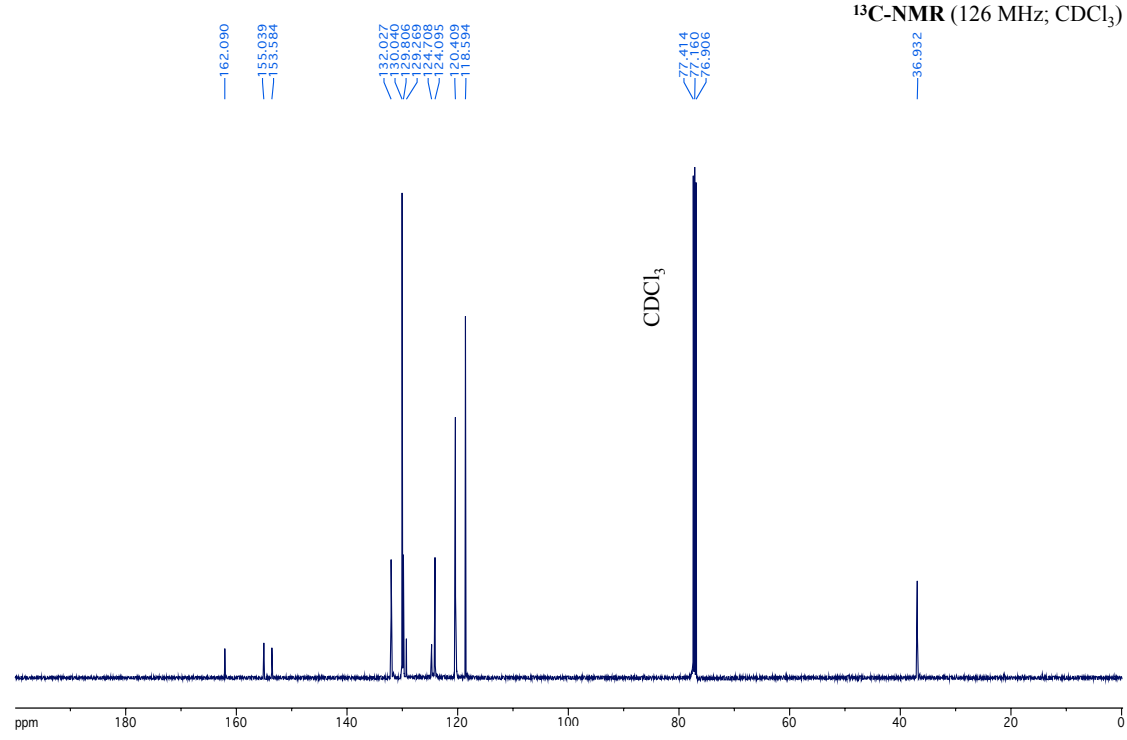

**$^{1}$H-NMR** (400 MHz; $CDCl_3$)

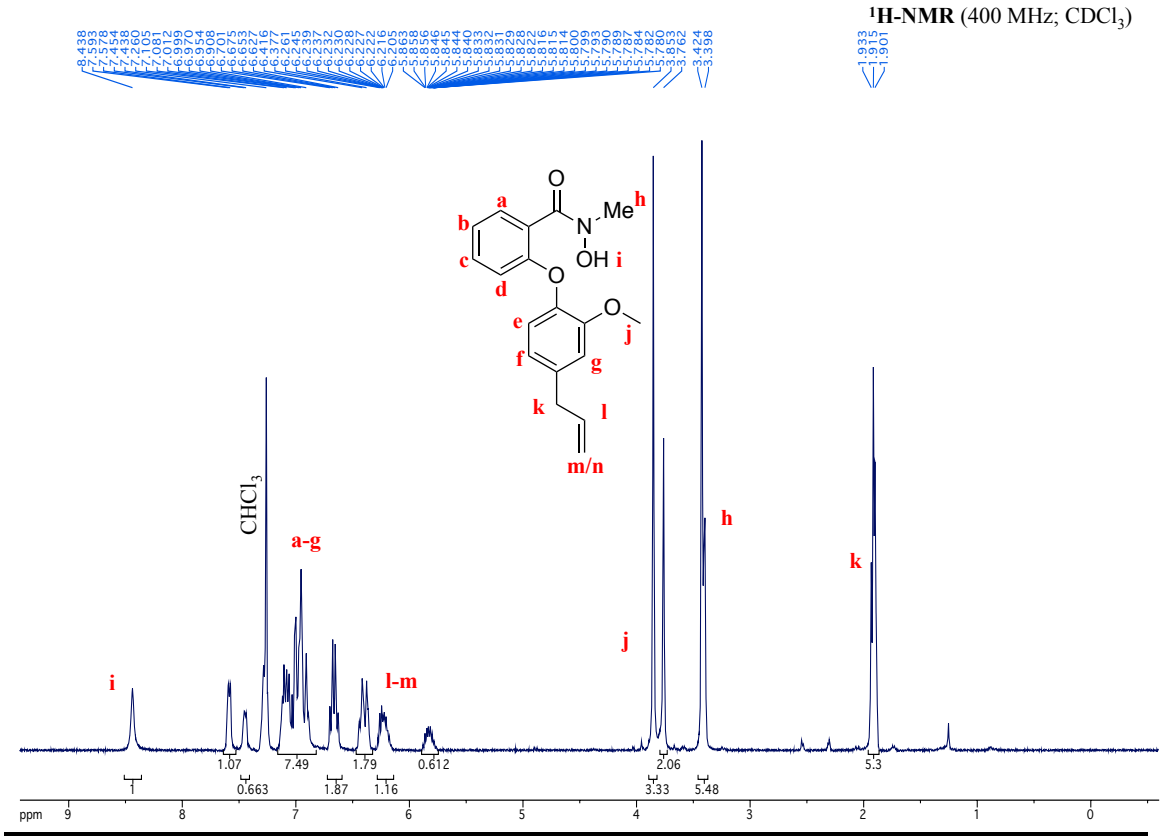


**$^{13}$C-NMR** (126 MHz; $CDCl_3$)

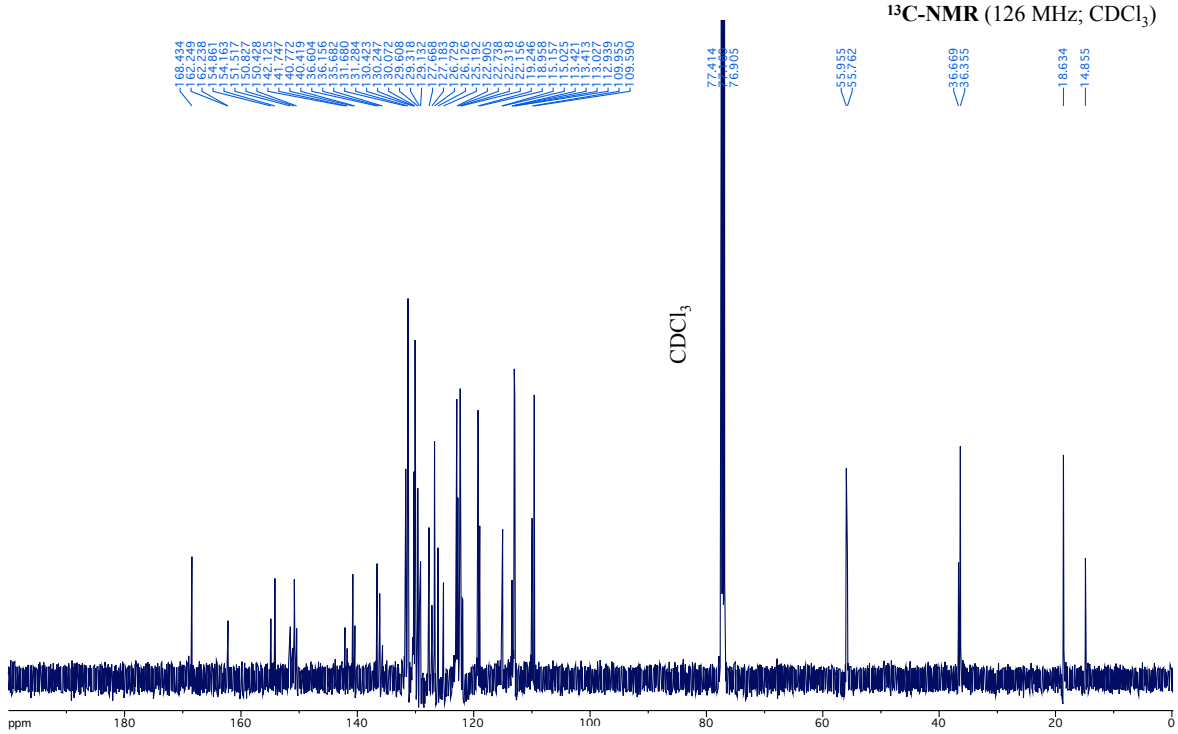

**$^{1}$H-NMR** (400 MHz; $CDCl_3$)

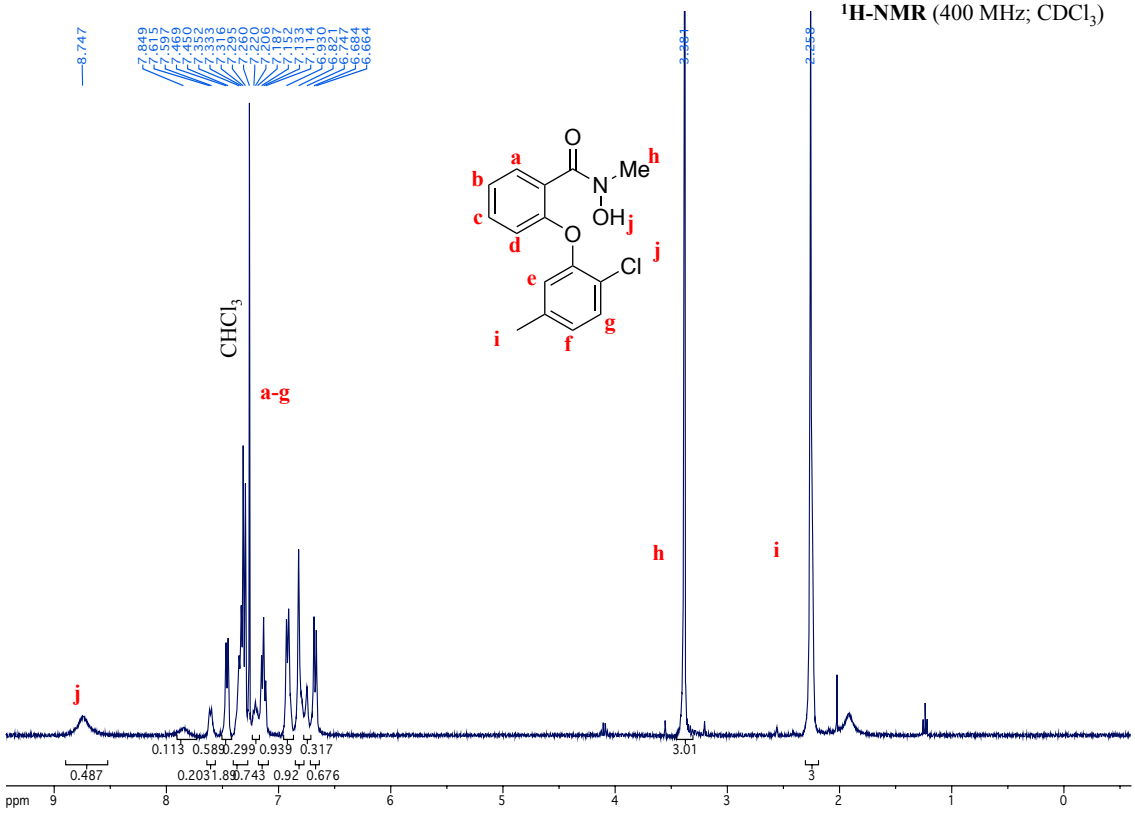


**$^{13}$C-NMR** (126 MHz; $CDCl_3$)

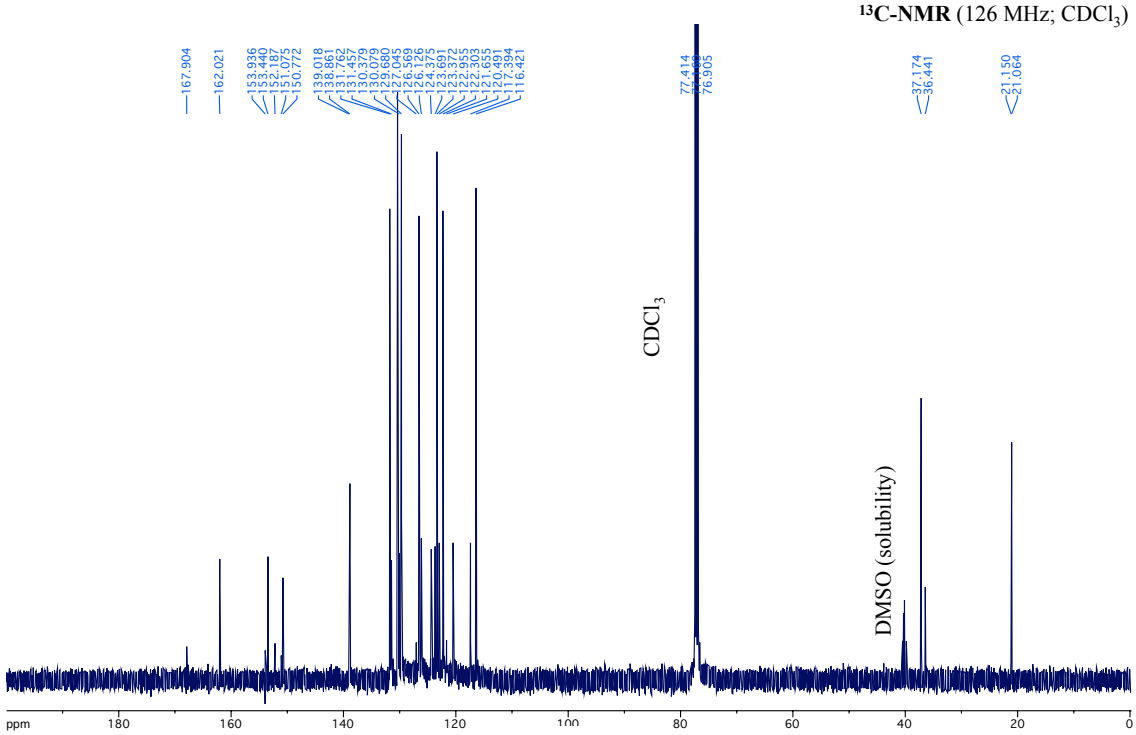

**$^{1}$H-NMR** (400 MHz; $CDCl_3$)

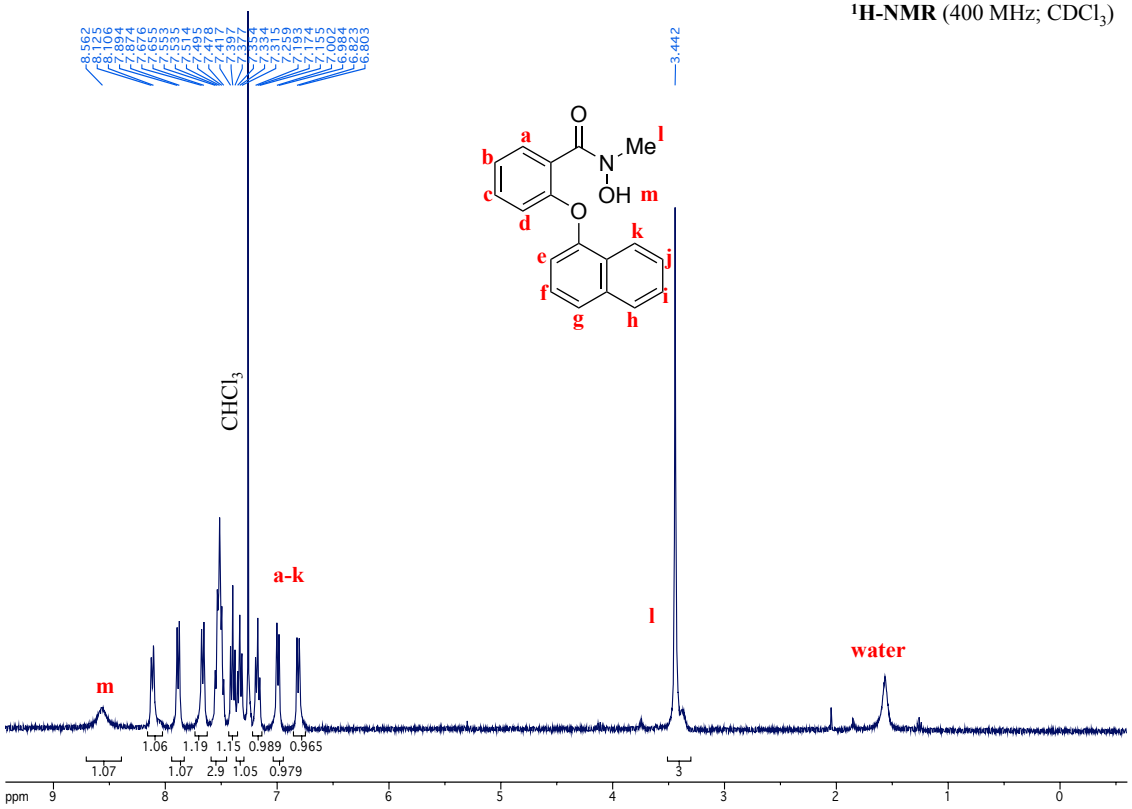





**$^{13}$C-NMR** (126 MHz; $CDCl_3$)

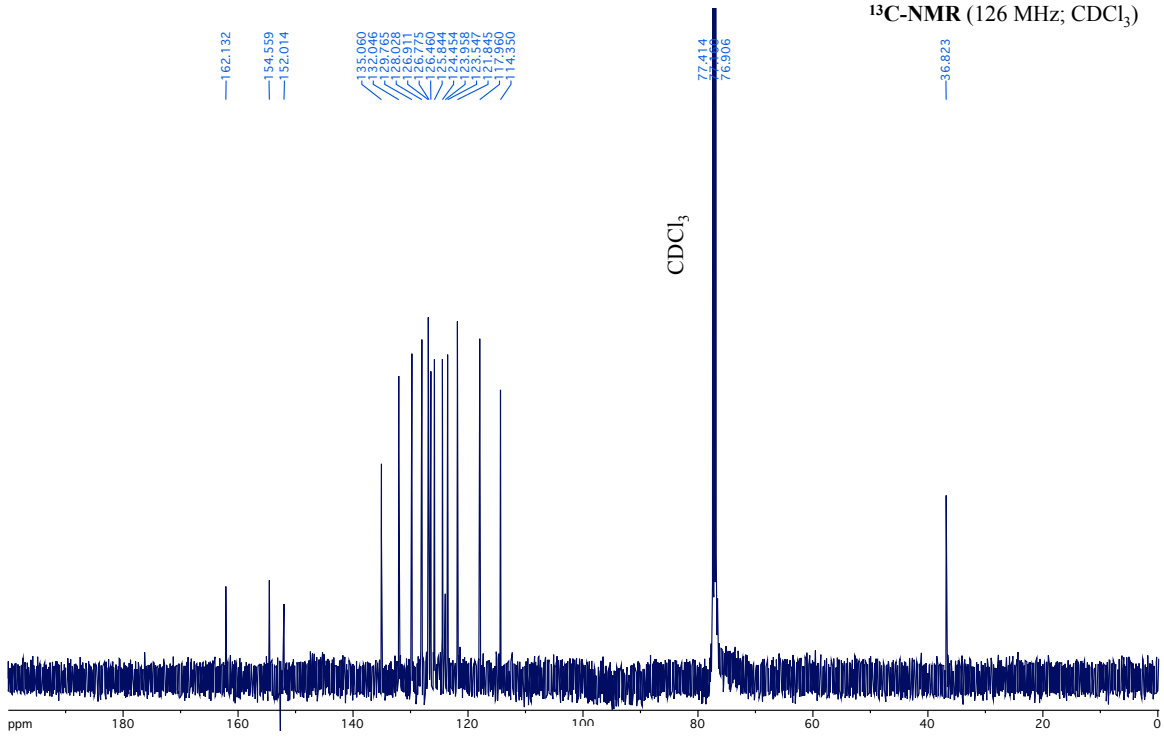

**$^{1}$H-NMR** (400 MHz; $CDCl_3$)

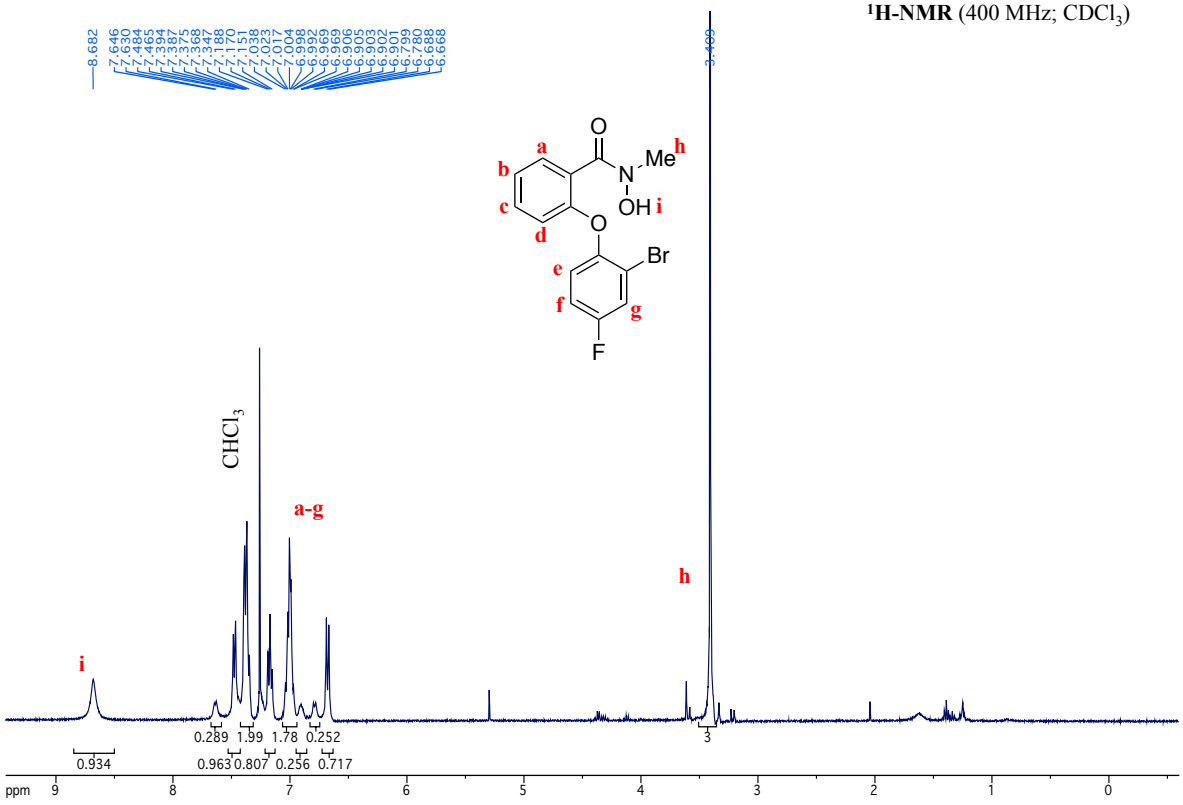


**$^{13}$C-NMR** (126 MHz; $CDCl_3$)

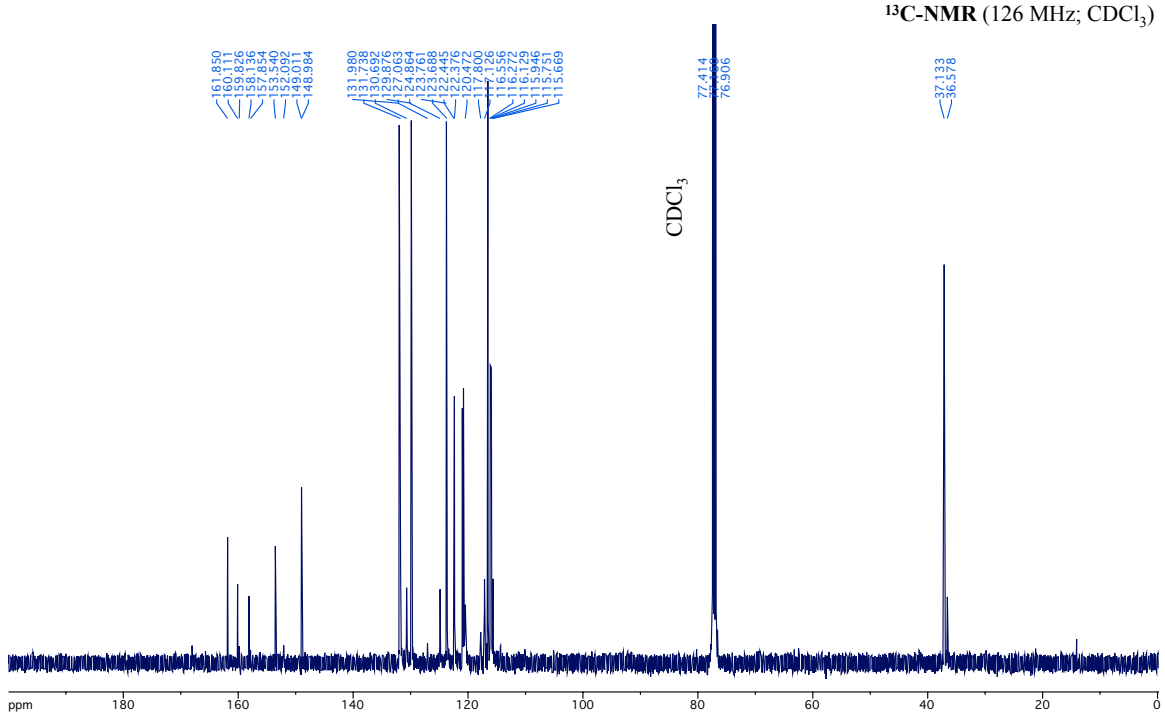

**$^{1}$H-NMR** (400 MHz; $CDCl_3$)

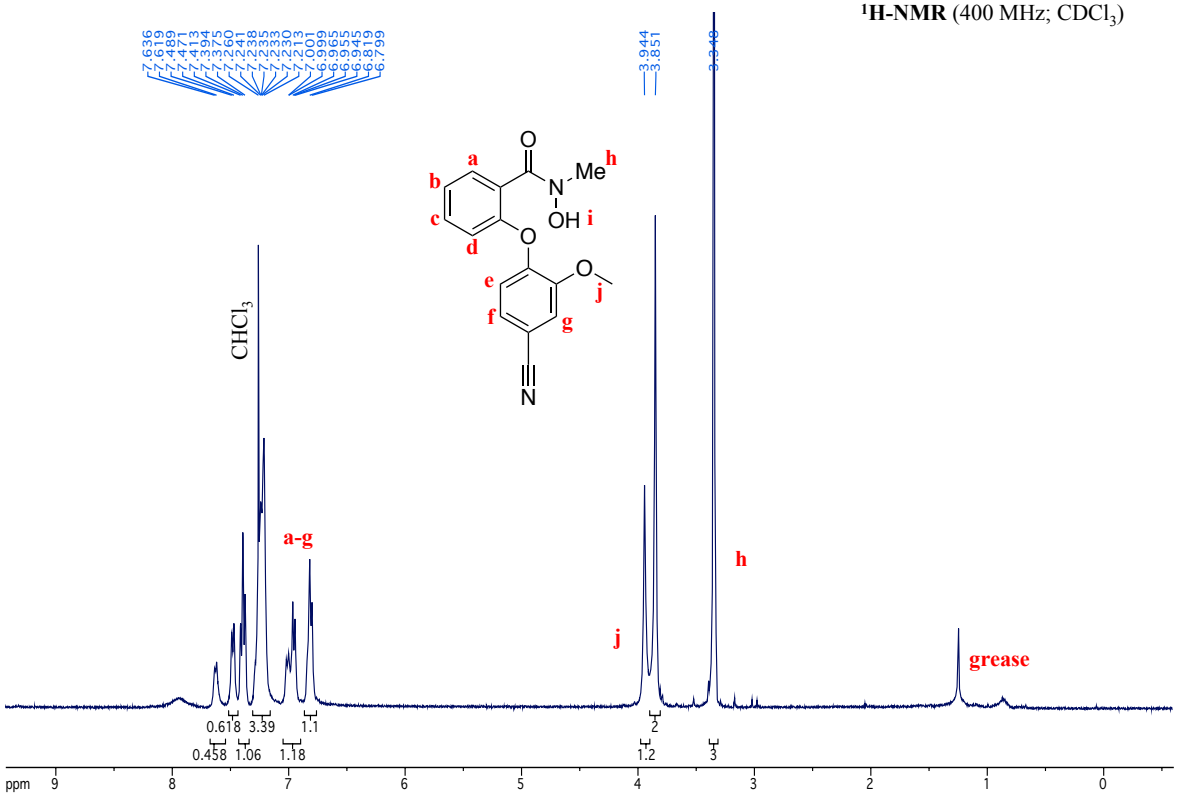


**$^{13}$C-NMR** (126 MHz; $CDCl_3$)

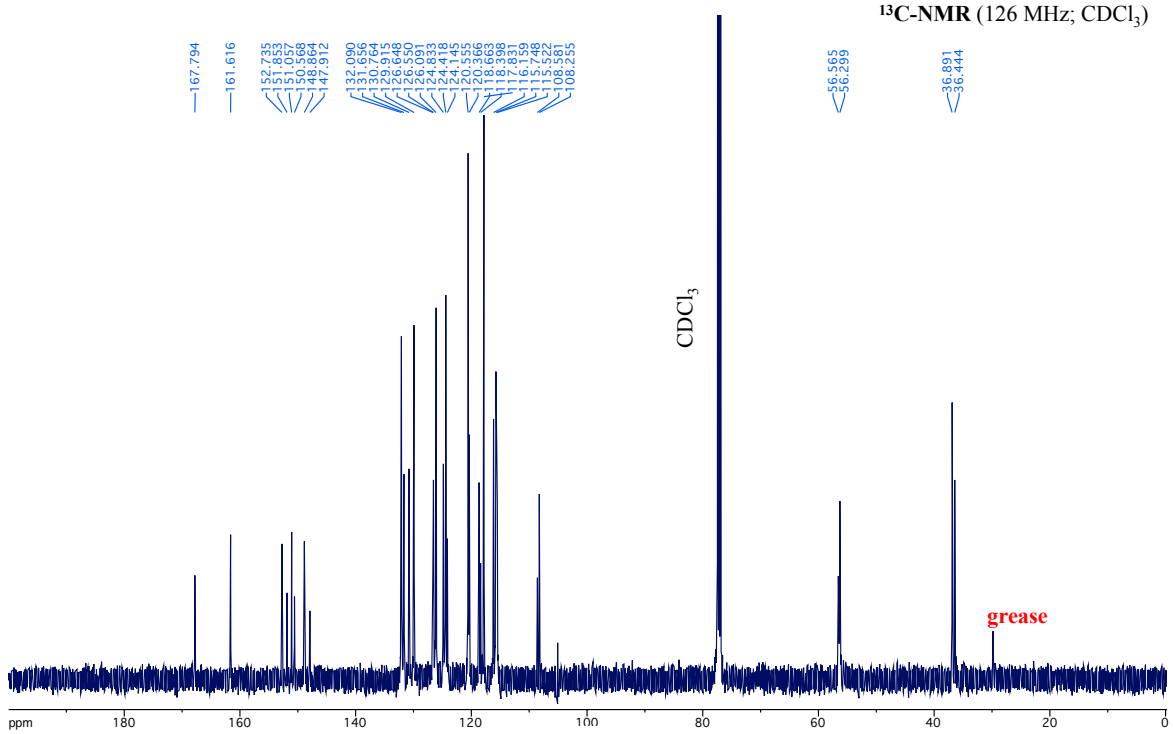

**$^{1}$H-NMR** (400 MHz; $CDCl_3$)

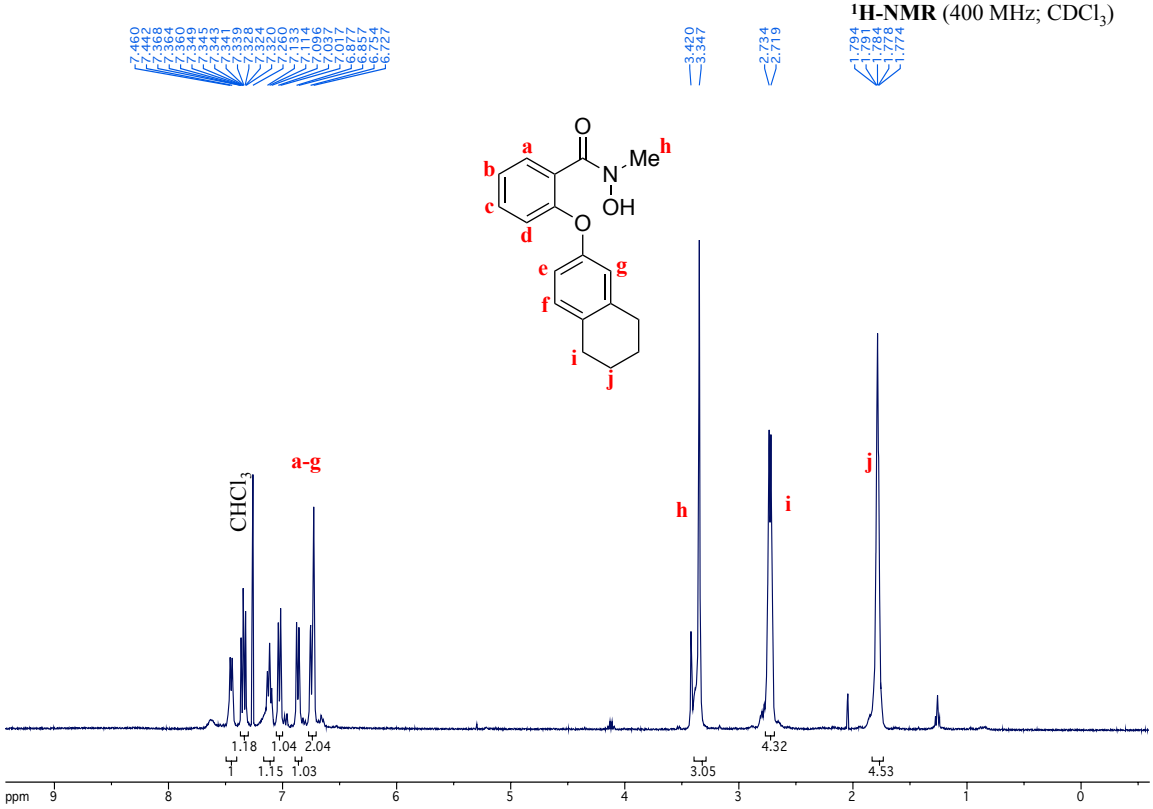


**$^{13}$C-NMR** (126 MHz; $CDCl_3$)

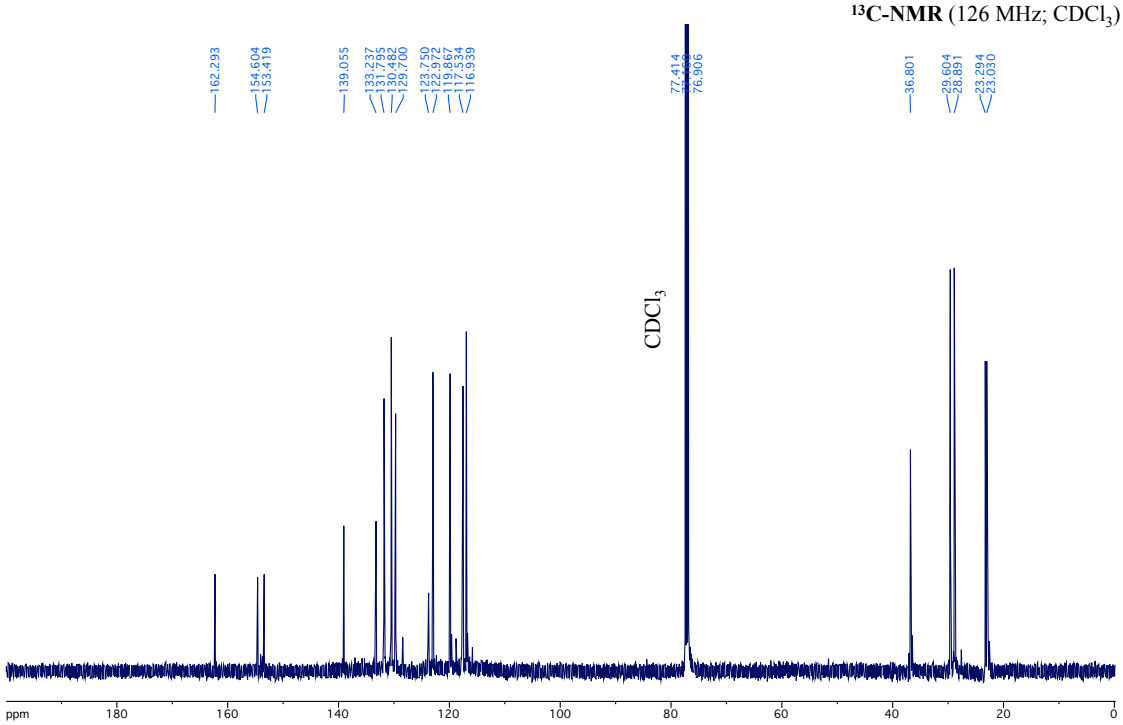

**$^{1}$H-NMR** (400 MHz; $CDCl_3$)

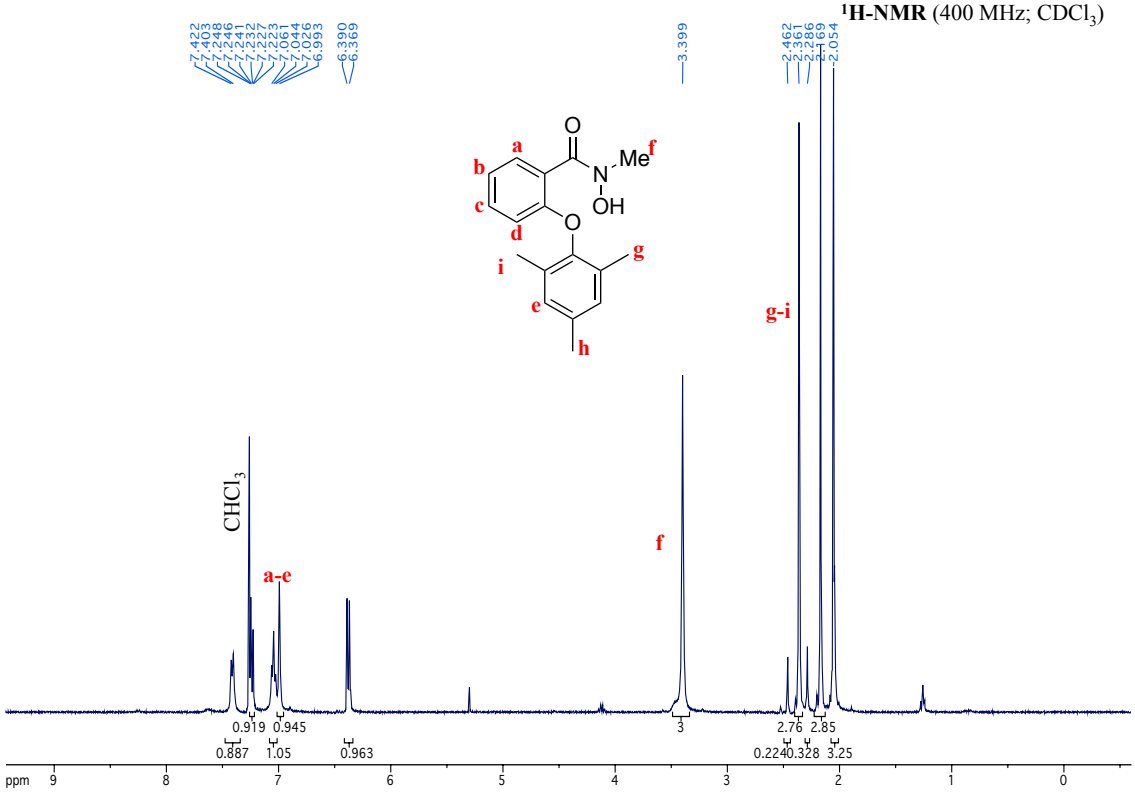


**$^{13}$C-NMR** (126 MHz; $CDCl_3$)

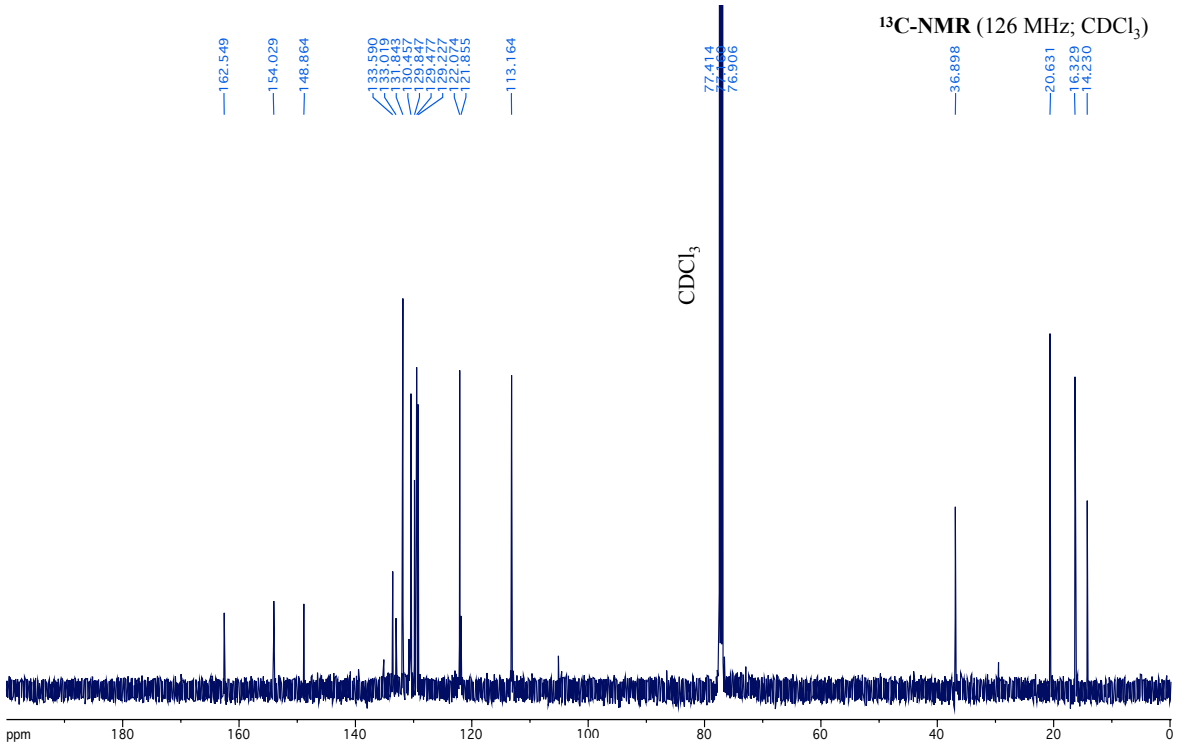

**$^{1}$H-NMR** (400 MHz; $CDCl_3$)

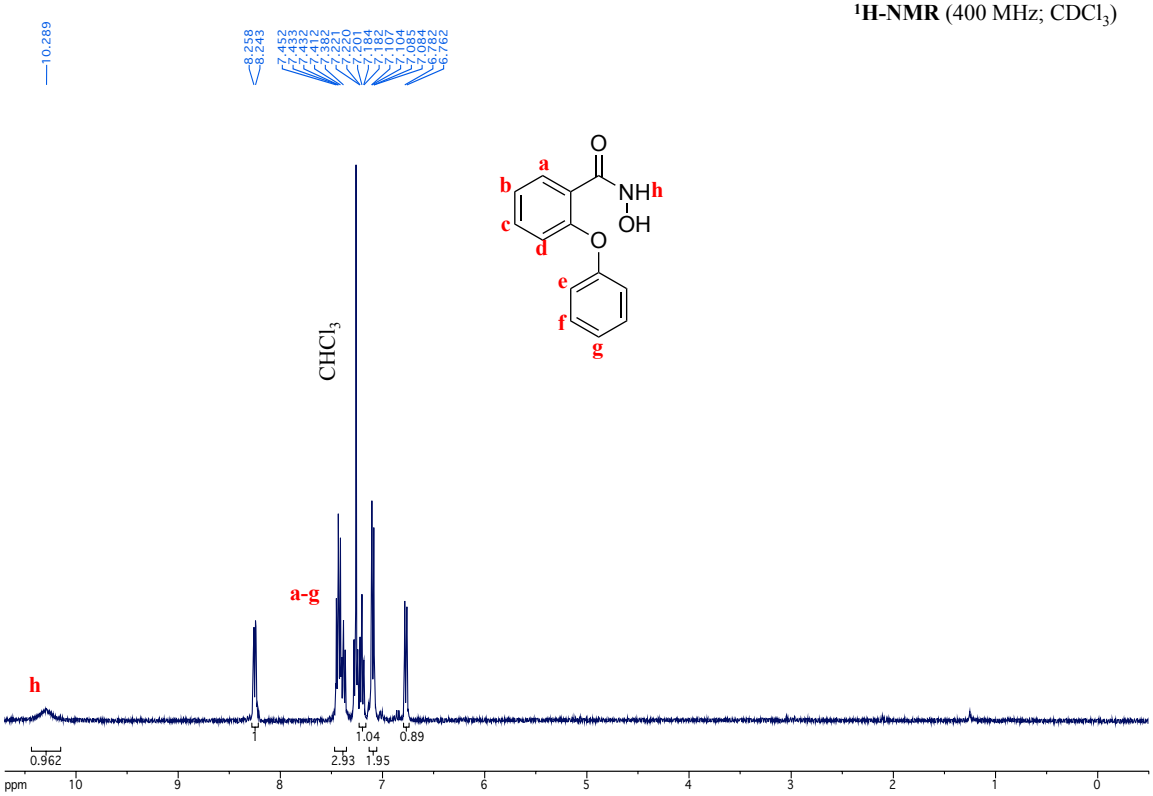


**$^{13}$C-NMR** (126 MHz; $CDCl_3$)

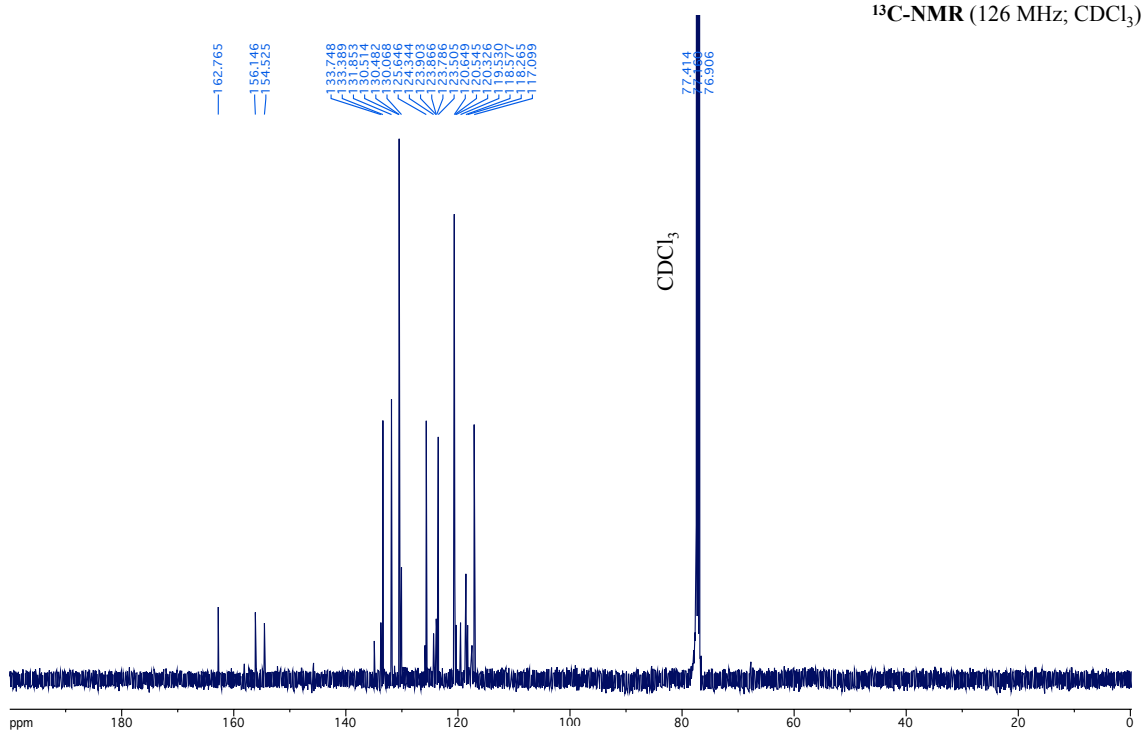

**$^{1}$H-NMR** (400 MHz; $CDCl_3$)

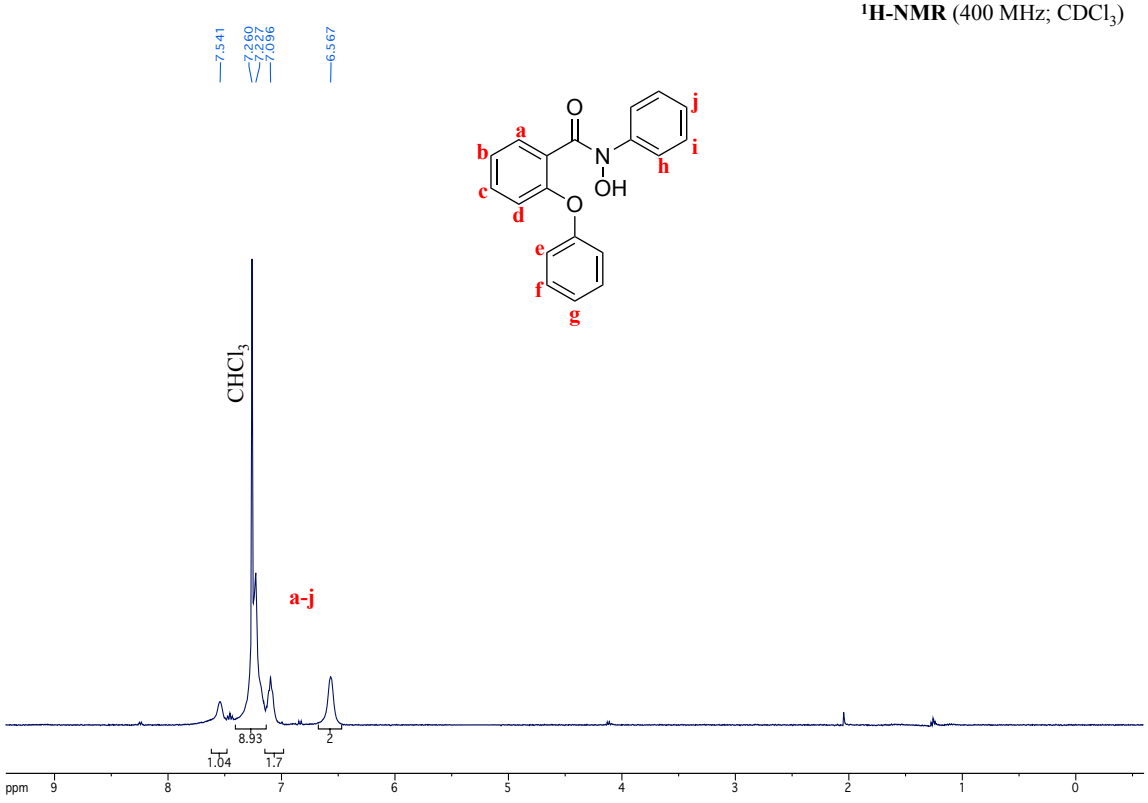


**$^{13}$C-NMR** (126 MHz; $CDCl_3$)

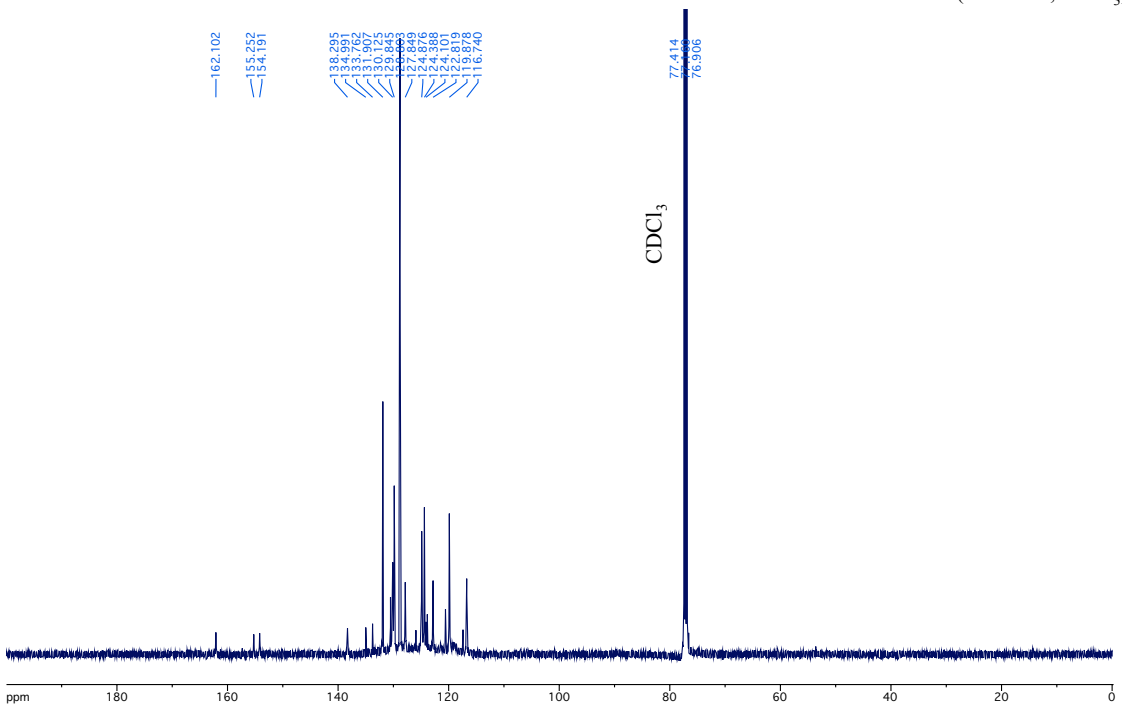

**$^{1}$H-NMR** (400 MHz; $CDCl_3$)

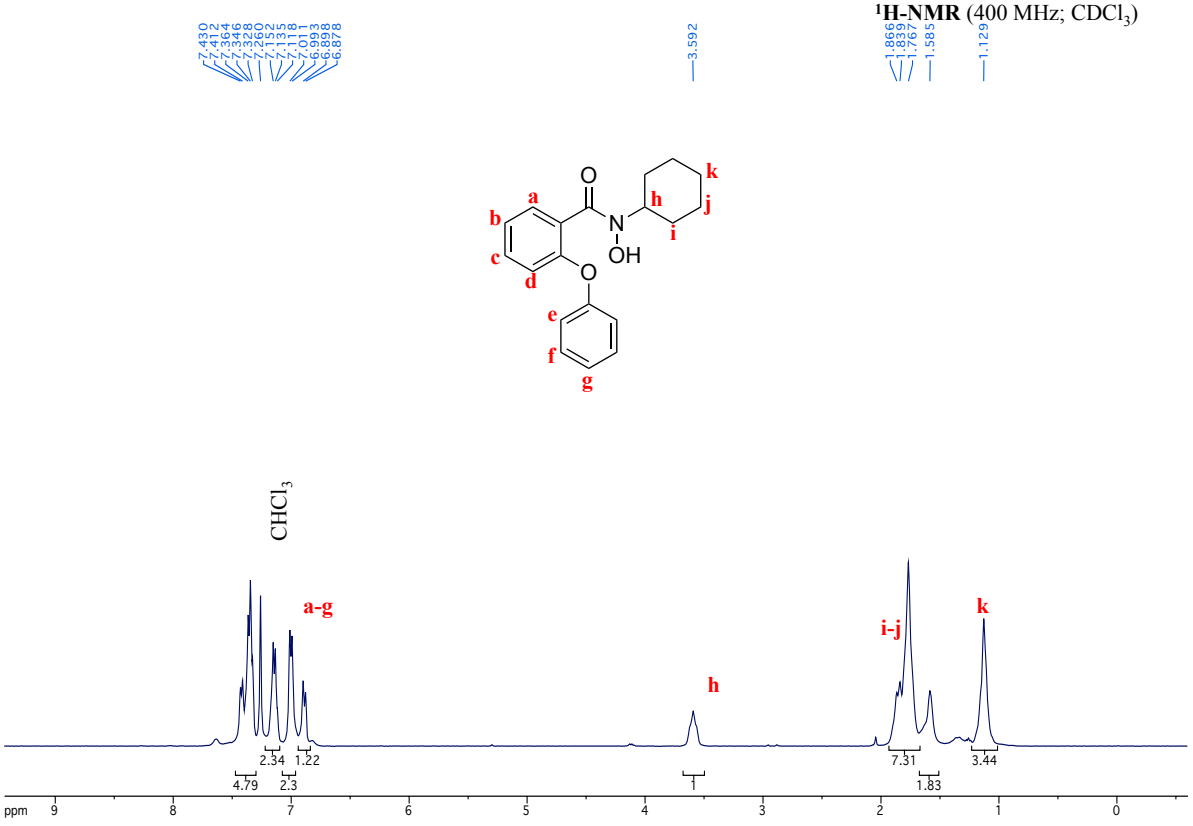


**$^{13}$C-NMR** (126 MHz; $CDCl_3$)

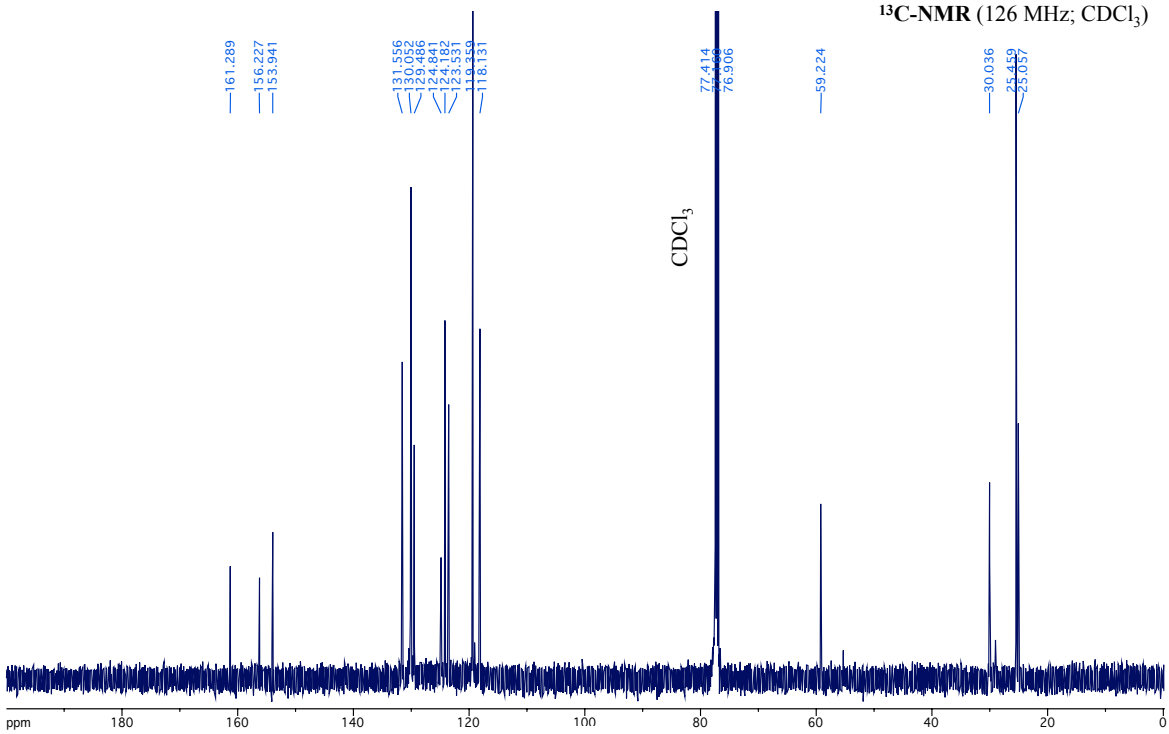

**$^{1}$H-NMR** (400 MHz; $CDCl_3$)

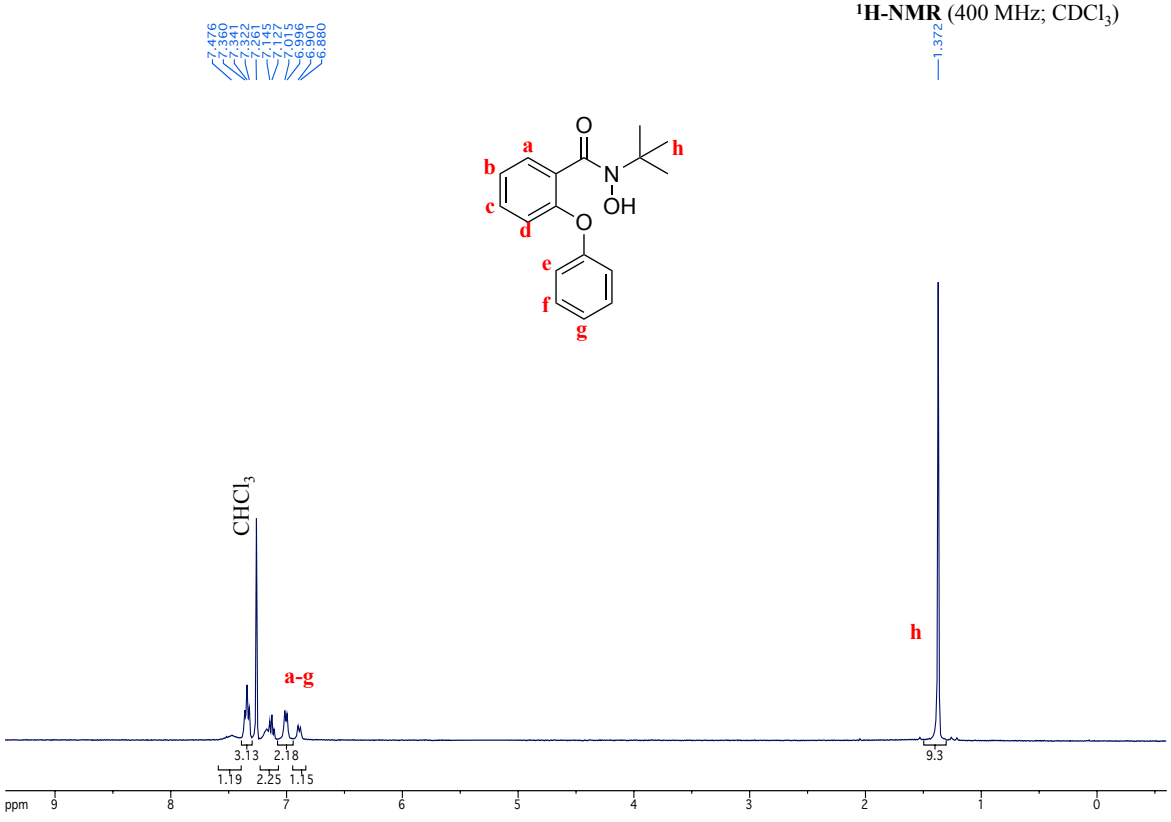


**$^{13}$C-NMR** (126 MHz; $CDCl_3$)

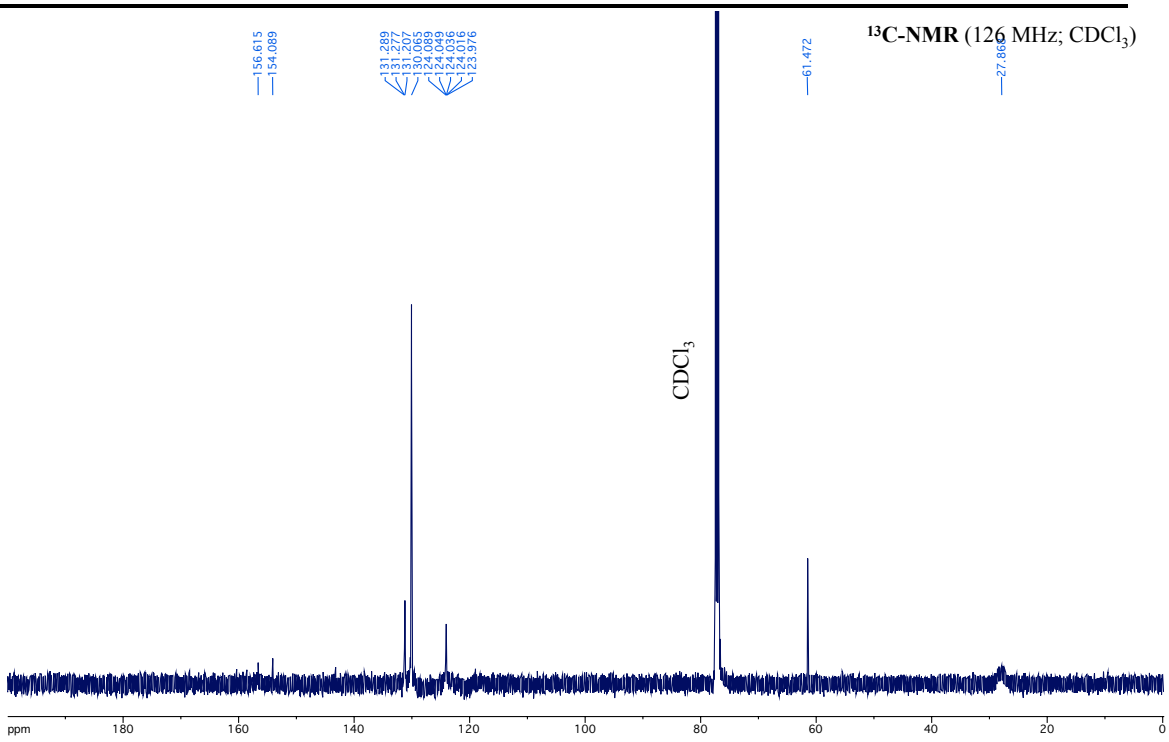

**$^{1}$H-NMR** (400 MHz; $CDCl_3$)

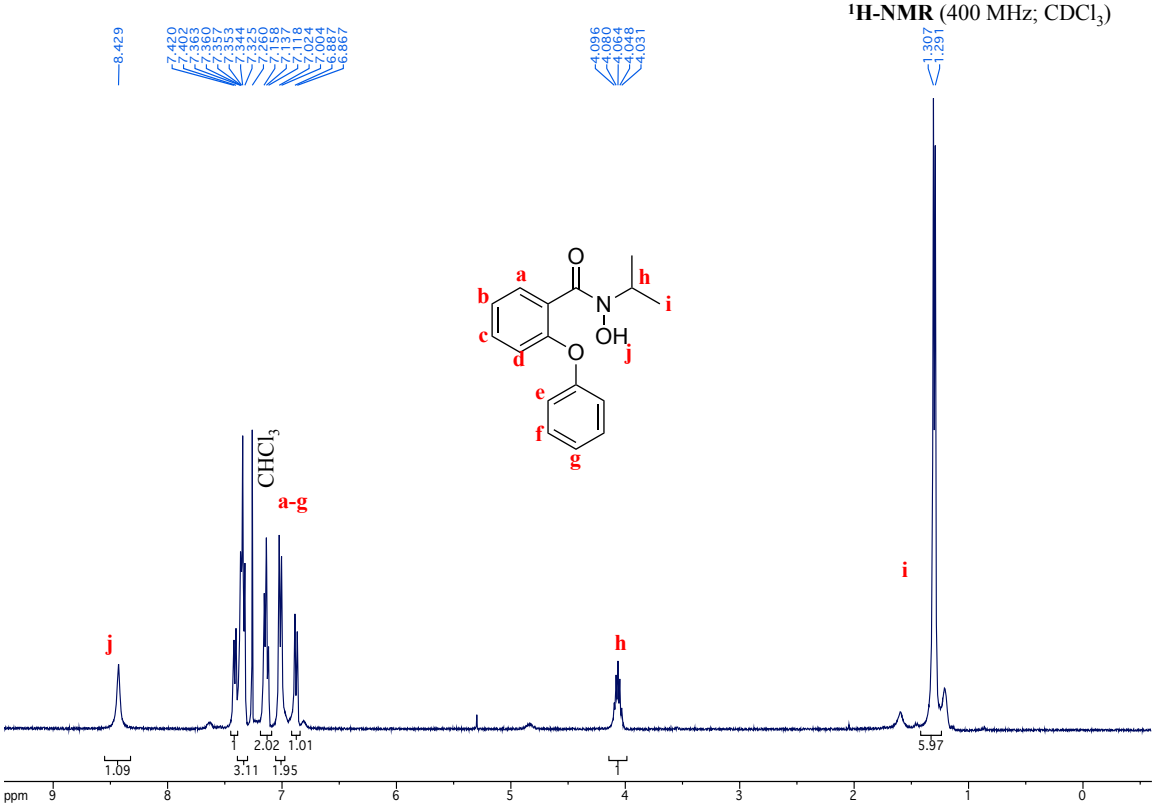


**$^{13}$C-NMR** (126 MHz; $CDCl_3$)

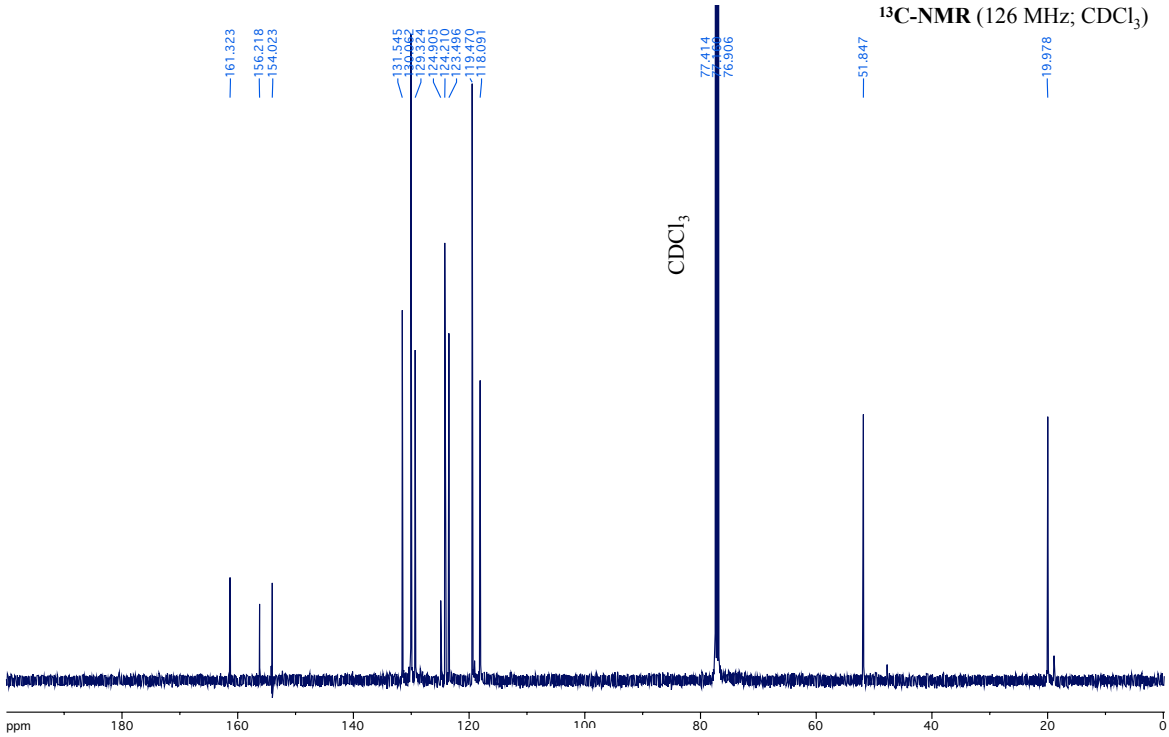

**$^{1}$H-NMR** (400 MHz; $CDCl_3$)

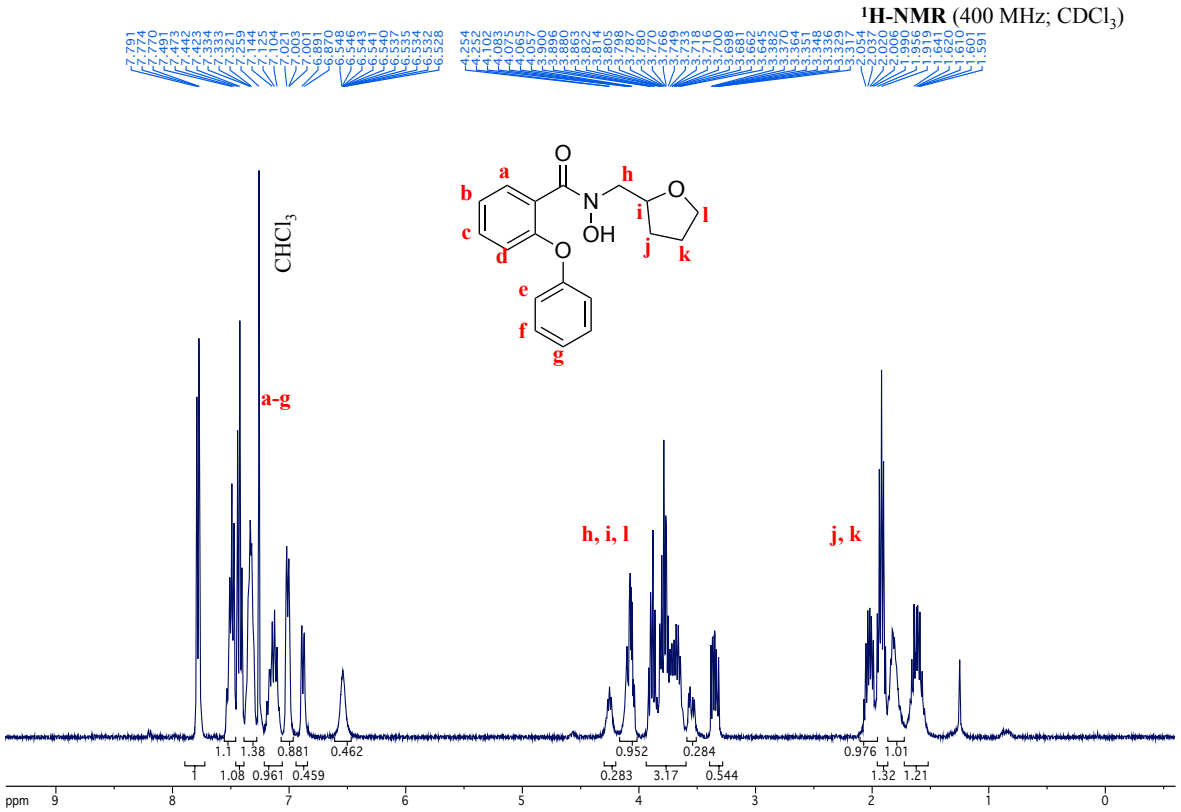


**$^{13}$C-NMR** (126 MHz; $CDCl_3$)

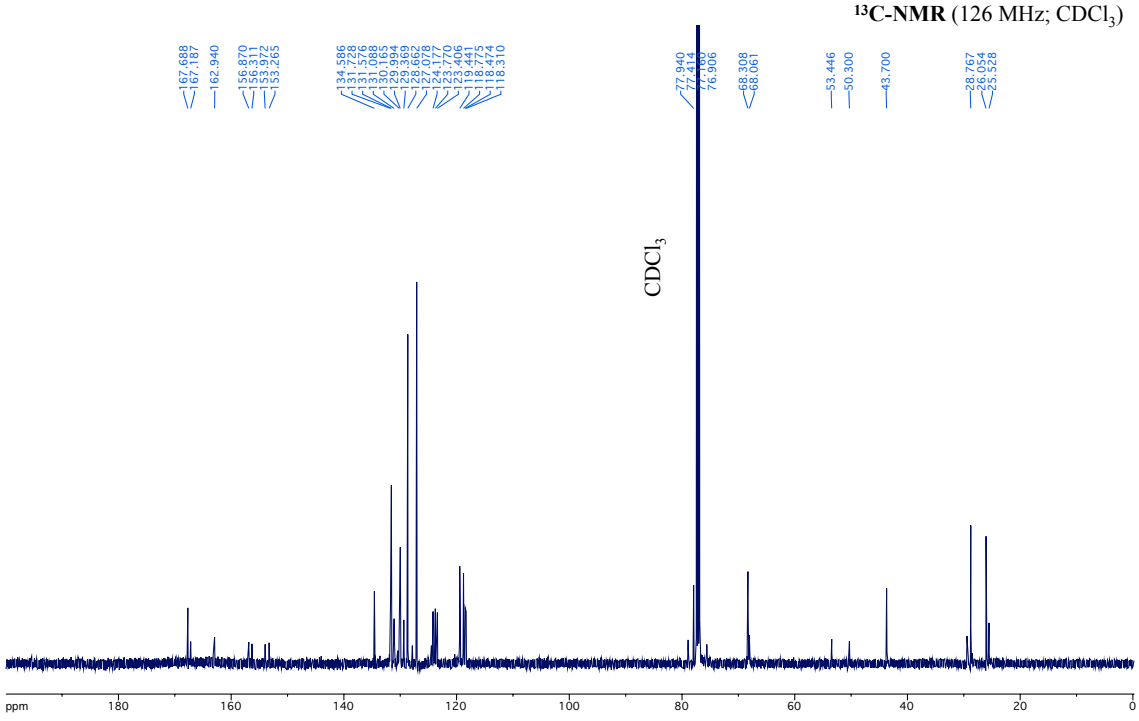

**$^{1}$H-NMR** (400 MHz; $CDCl_3$)

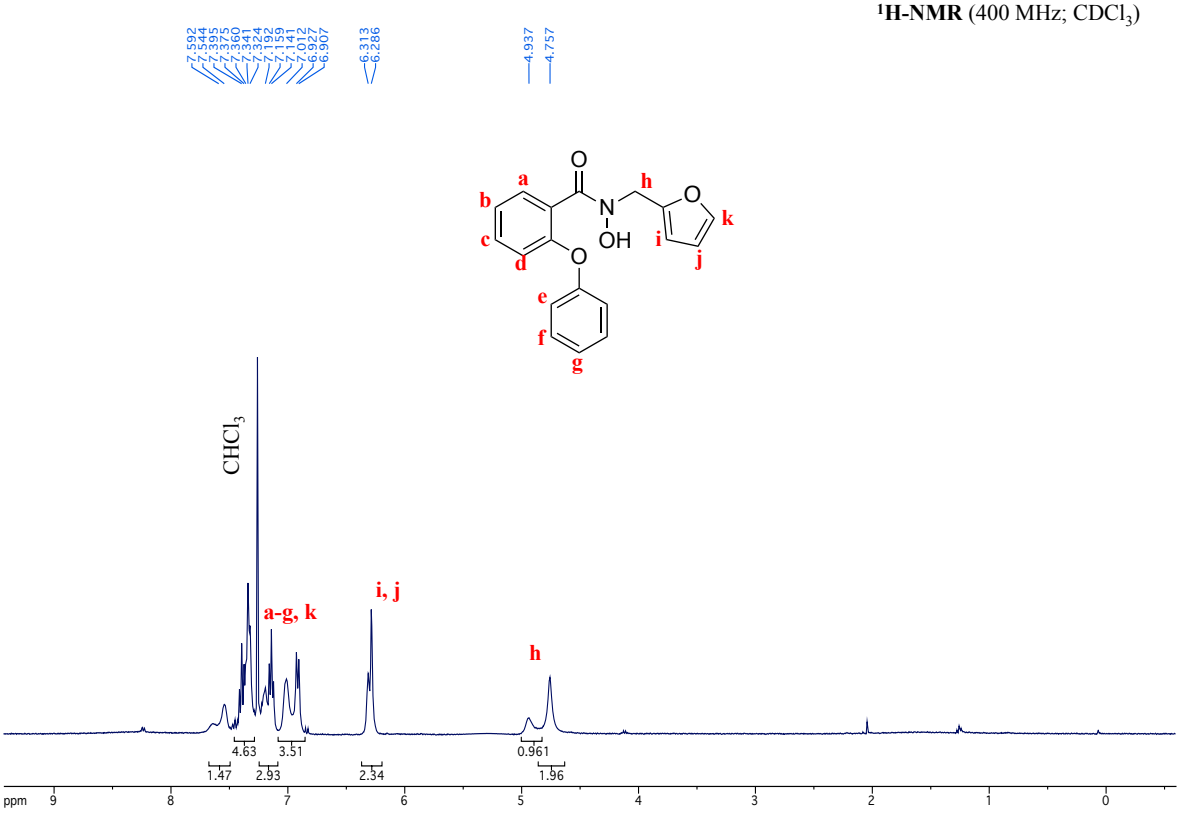


**$^{13}$C-NMR** (126 MHz; $CDCl_3$)

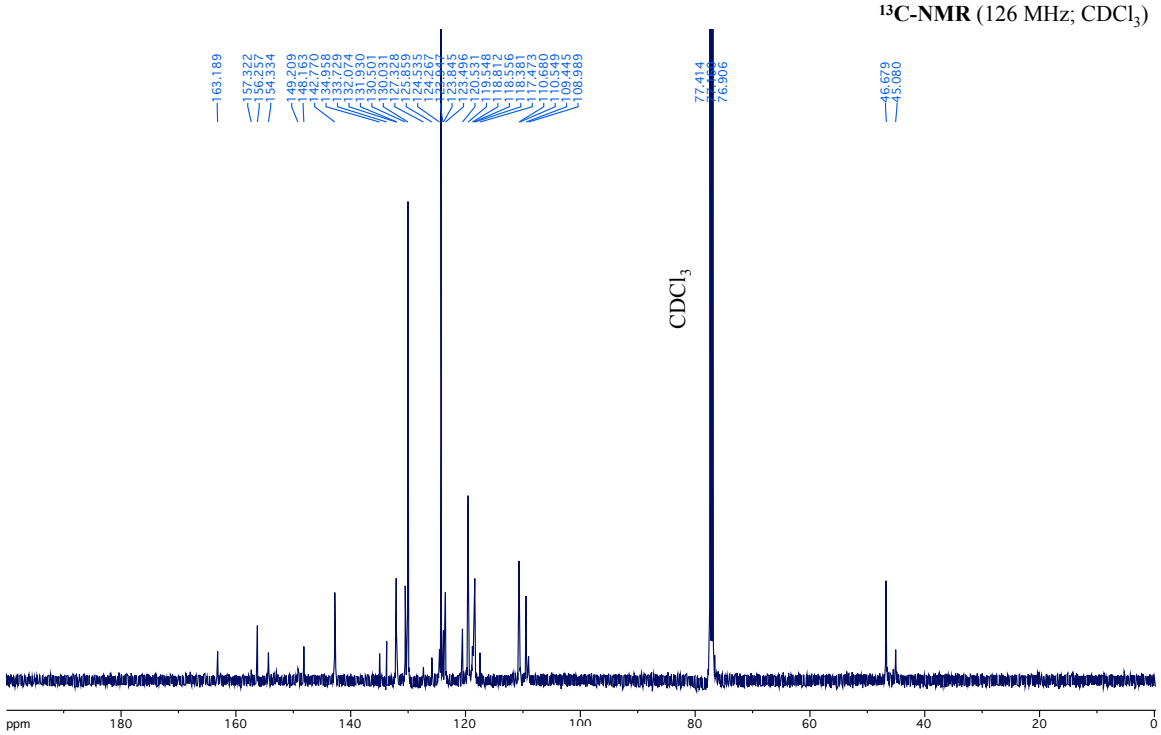

**$^{1}$H-NMR** (400 MHz; $CDCl_3$)

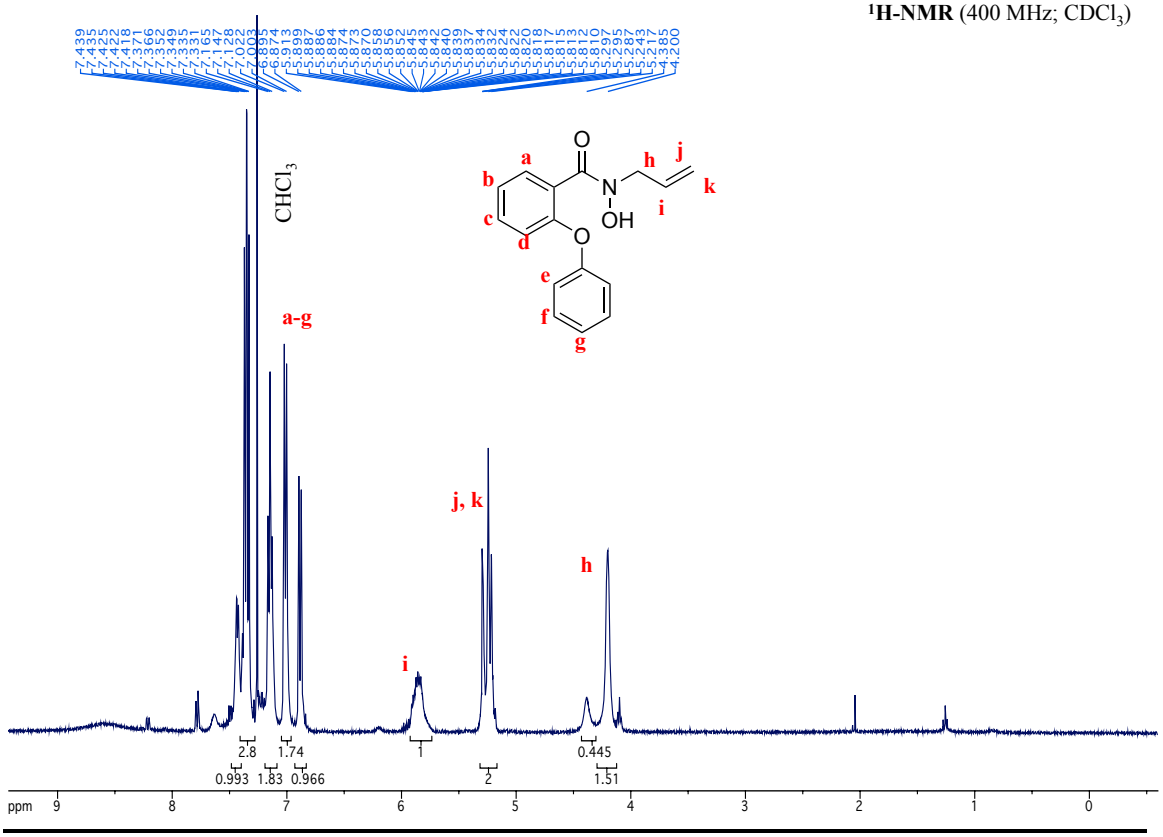


**$^{13}$C-NMR** (126 MHz; $CDCl_3$)

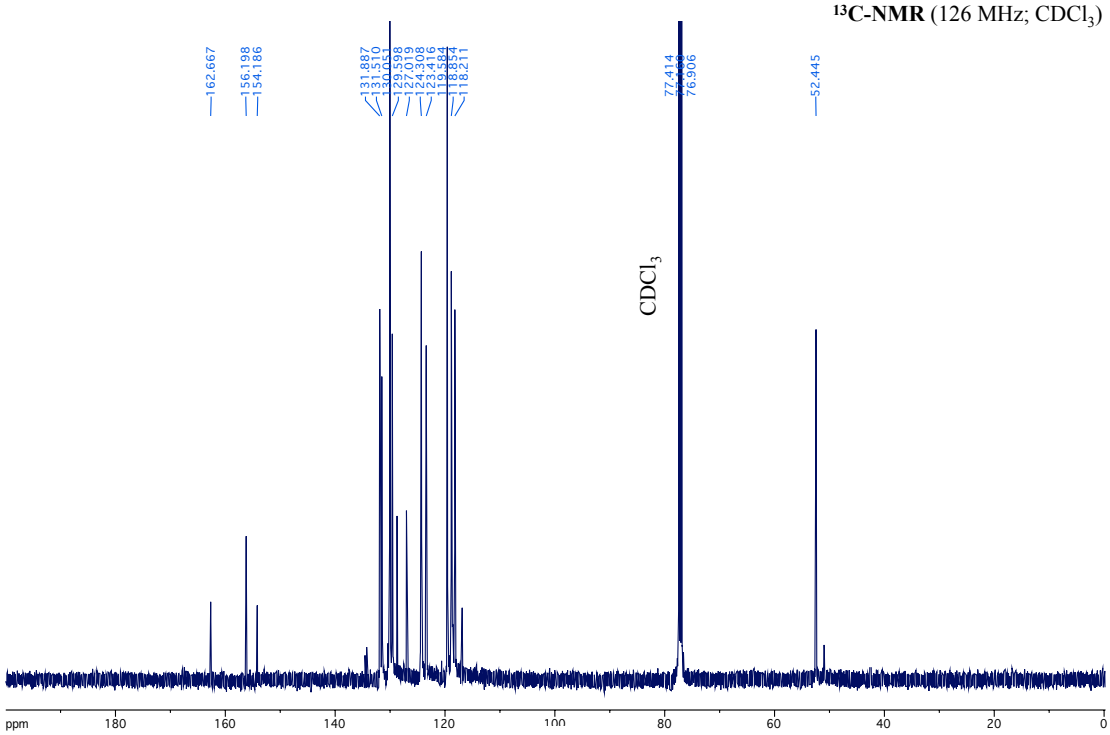

**$^{1}$H-NMR** (400 MHz; $CDCl_3$)

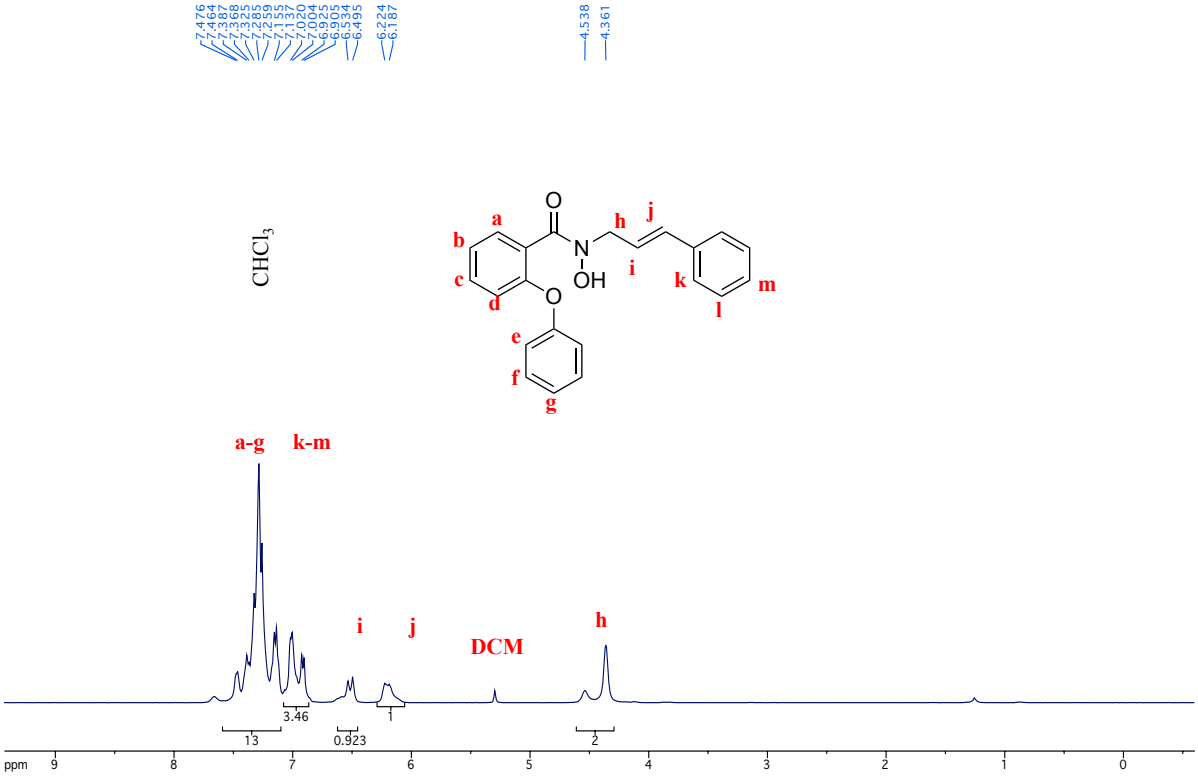


**$^{13}$C-NMR** (126 MHz; $CDCl_3$)

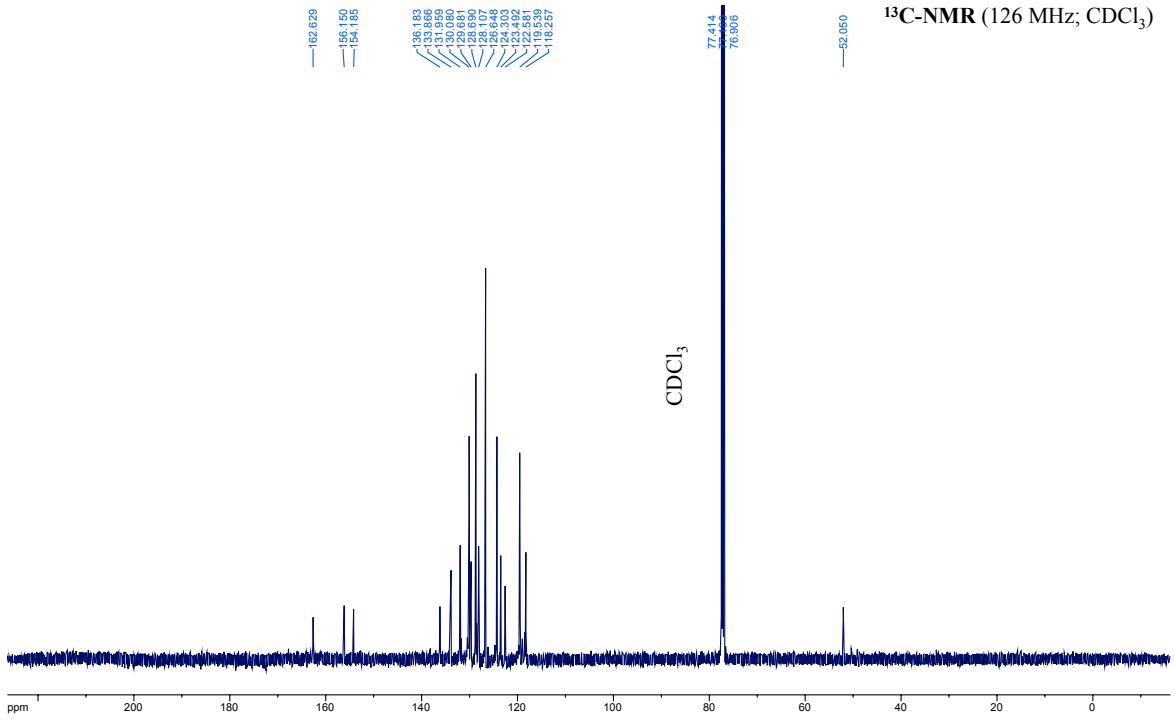

**$^{1}$H-NMR** (400 MHz; $CDCl_3$)

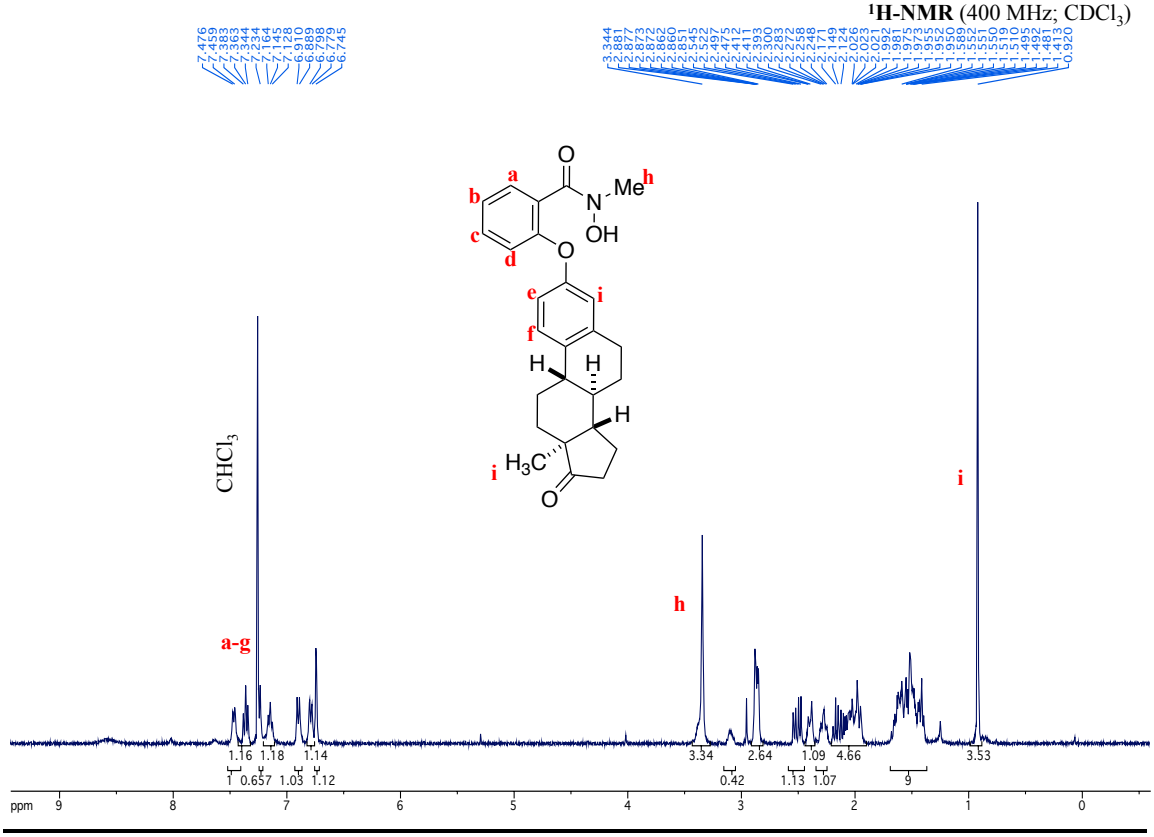


**$^{13}$C-NMR** (126 MHz; $CDCl_3$)

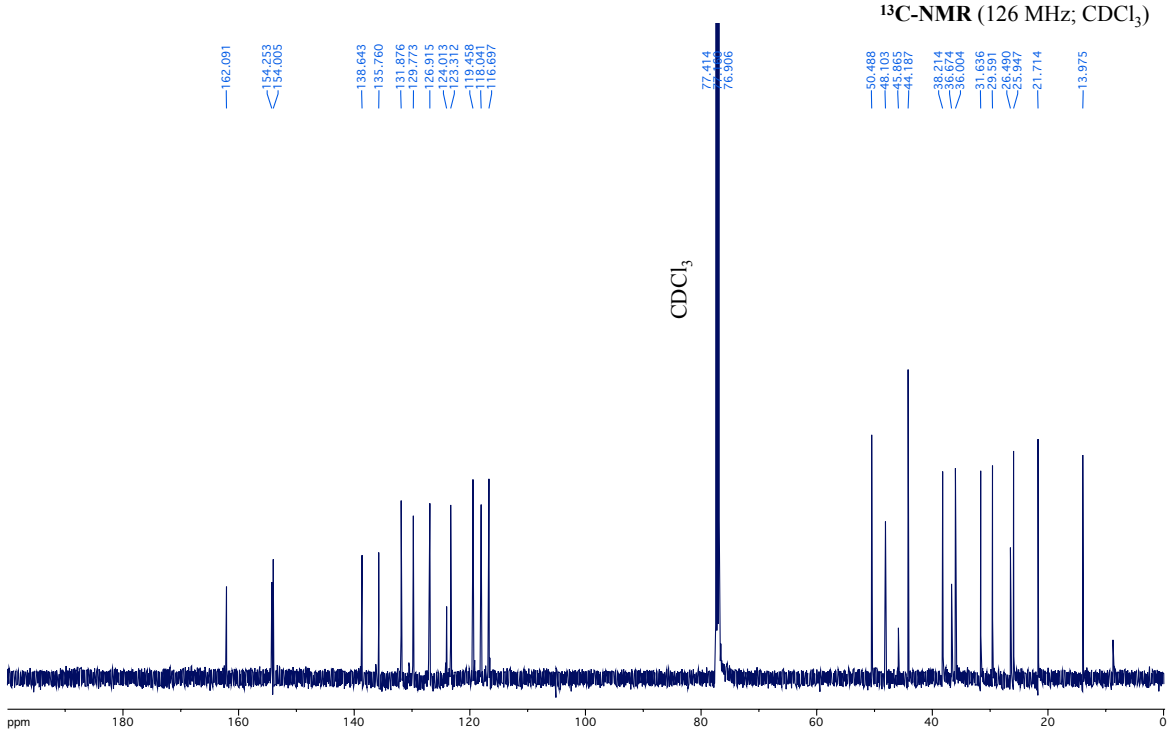

**$^{1}$H-NMR** (400 MHz; DMSO-d6)

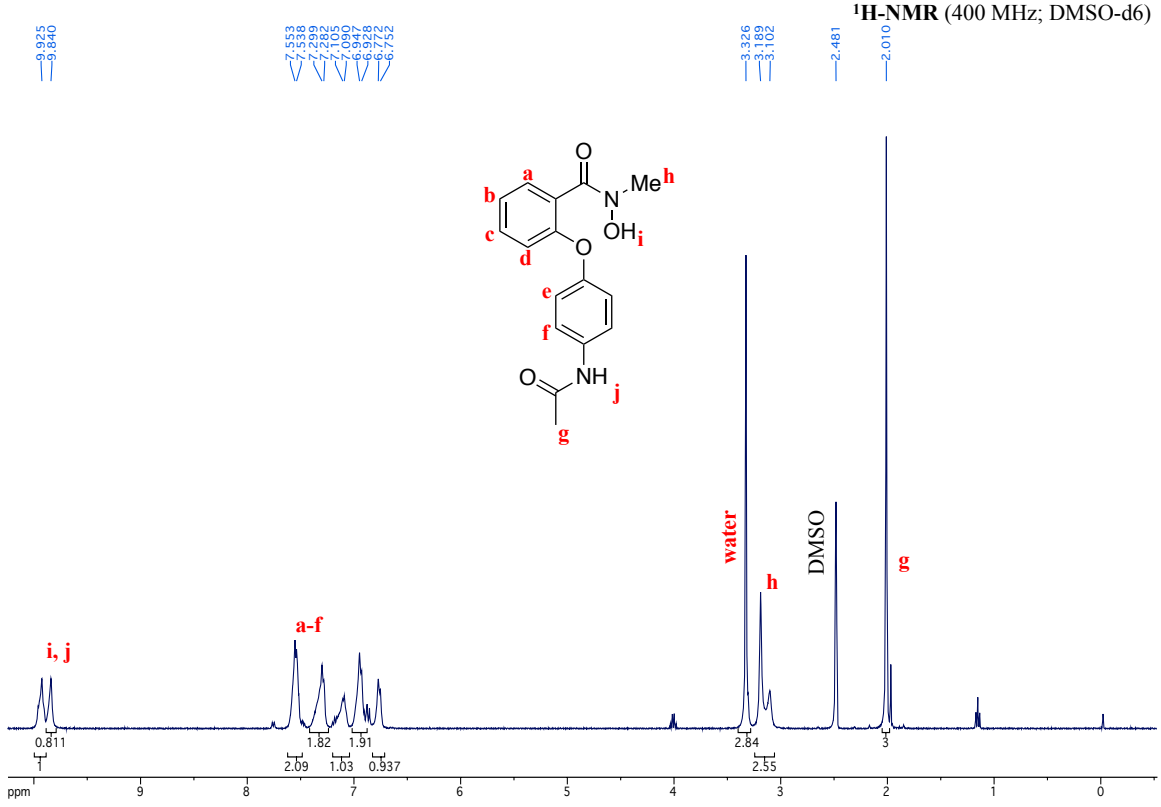


**$^{13}$C-NMR** (126 MHz; DMSO-d6)

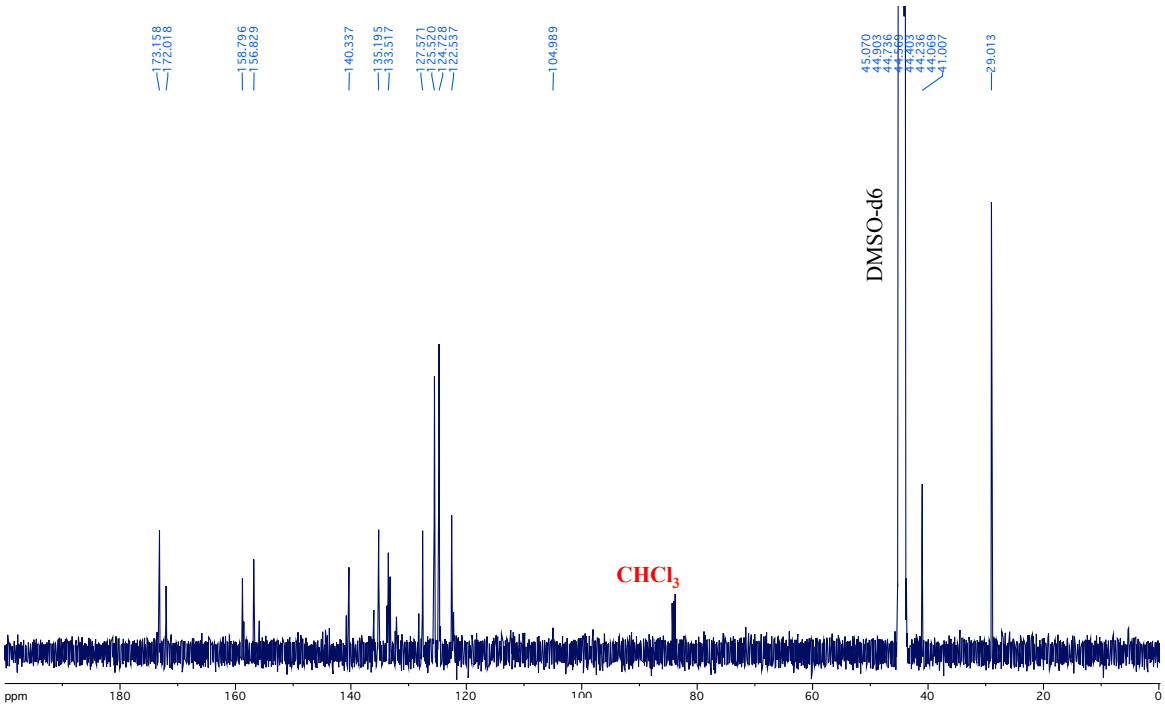

**$^{1}$H-NMR** (400 MHz; $CDCl_3$)

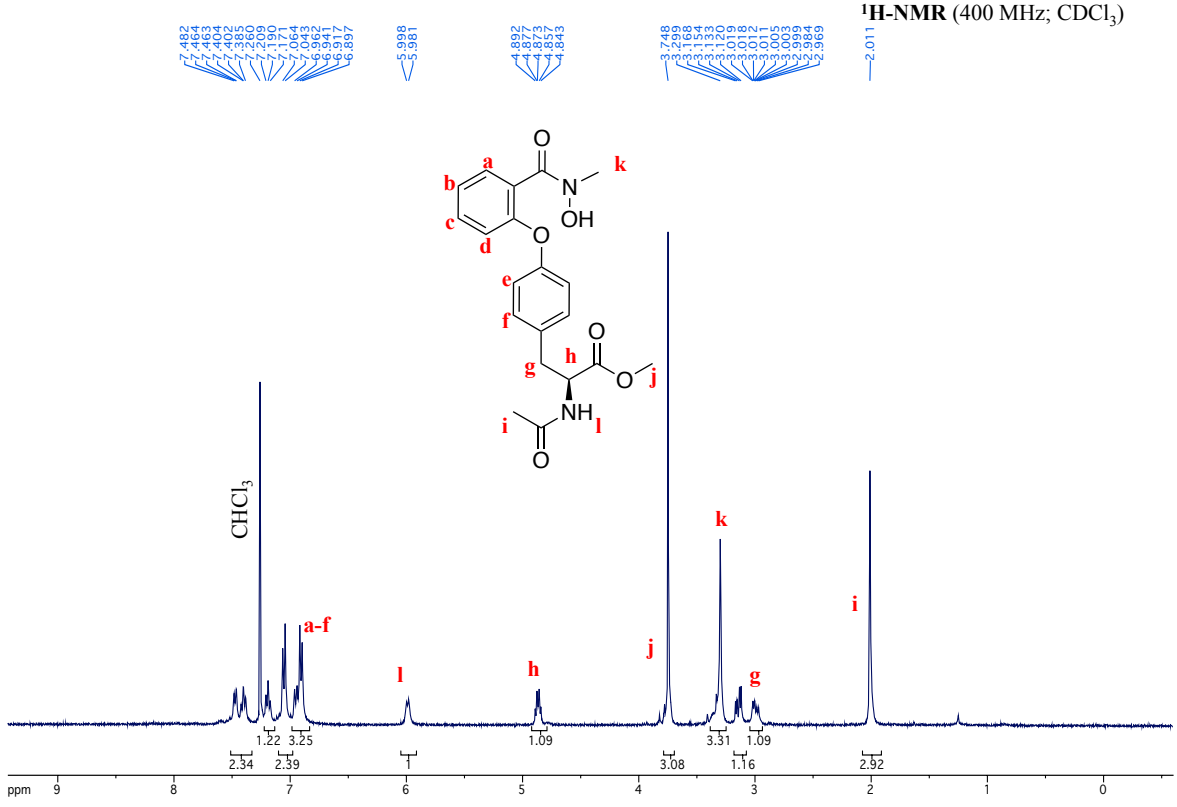


**$^{13}$C-NMR** (126 MHz; $CDCl_3$)

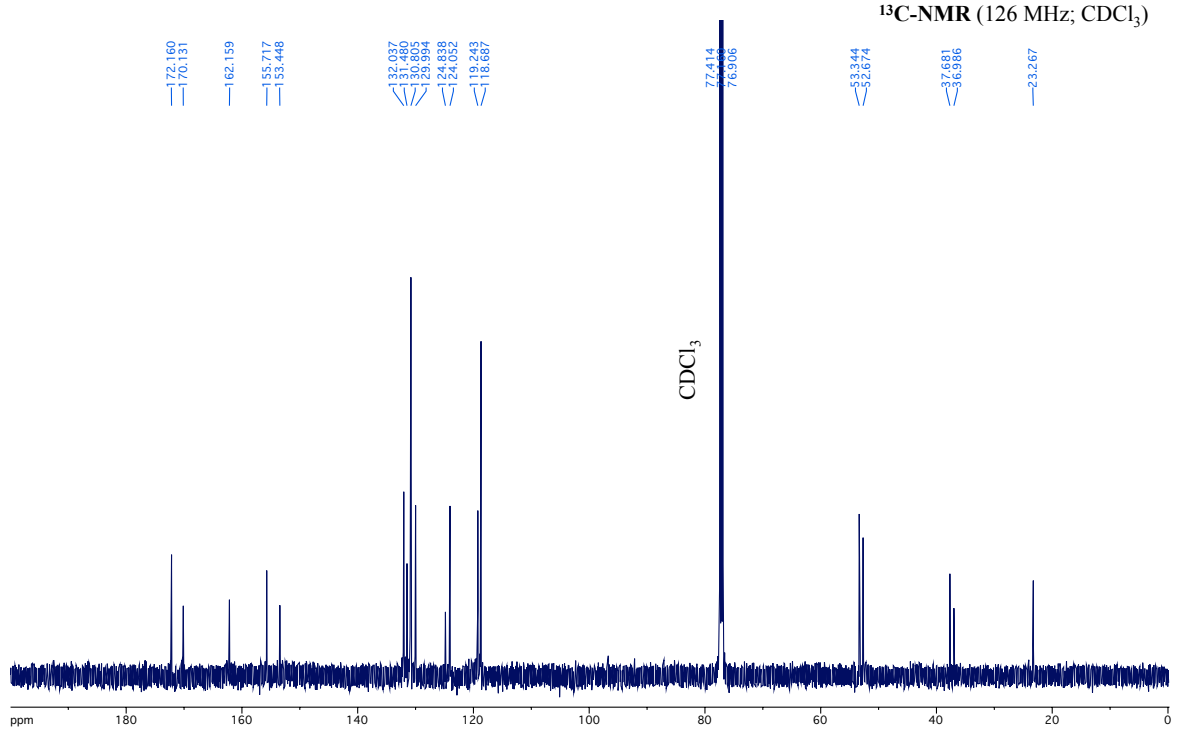

**$^{1}$H-NMR** (400 MHz; $CDCl_3$)

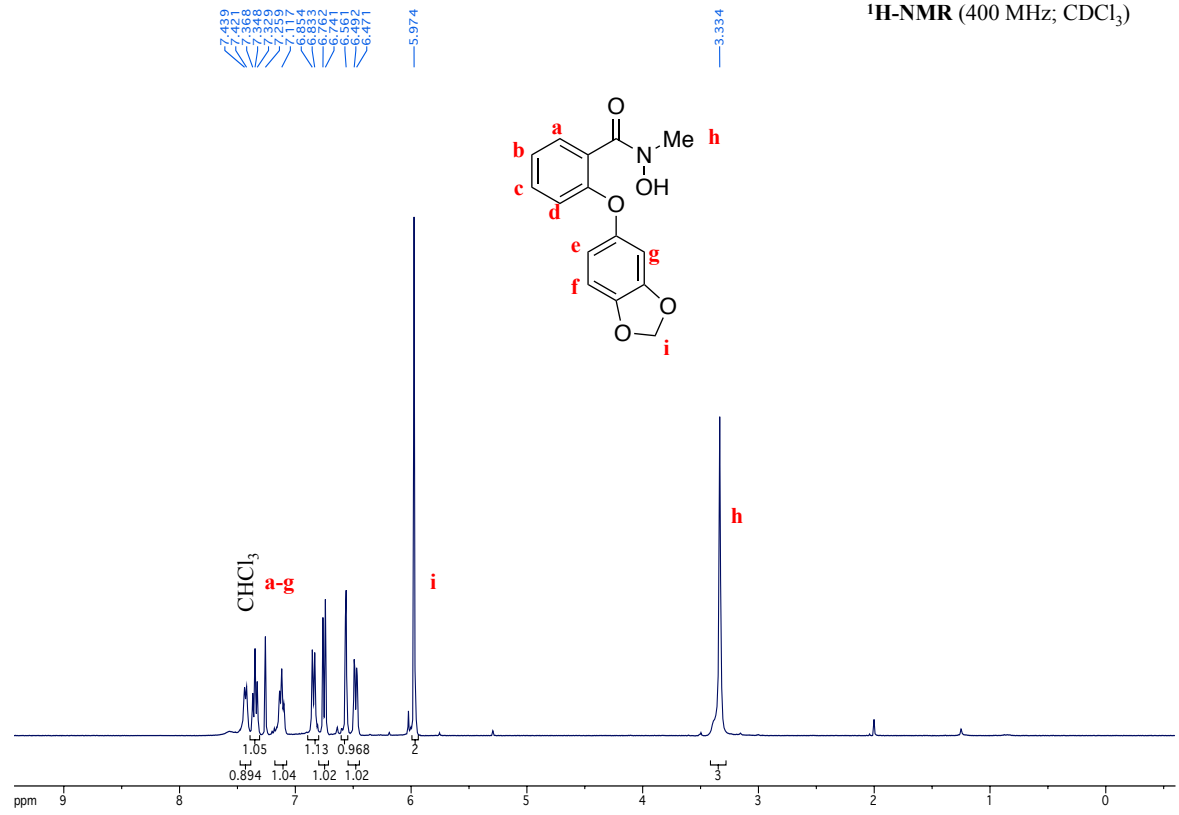


**$^{13}$C-NMR** (126 MHz; $CDCl_3$)

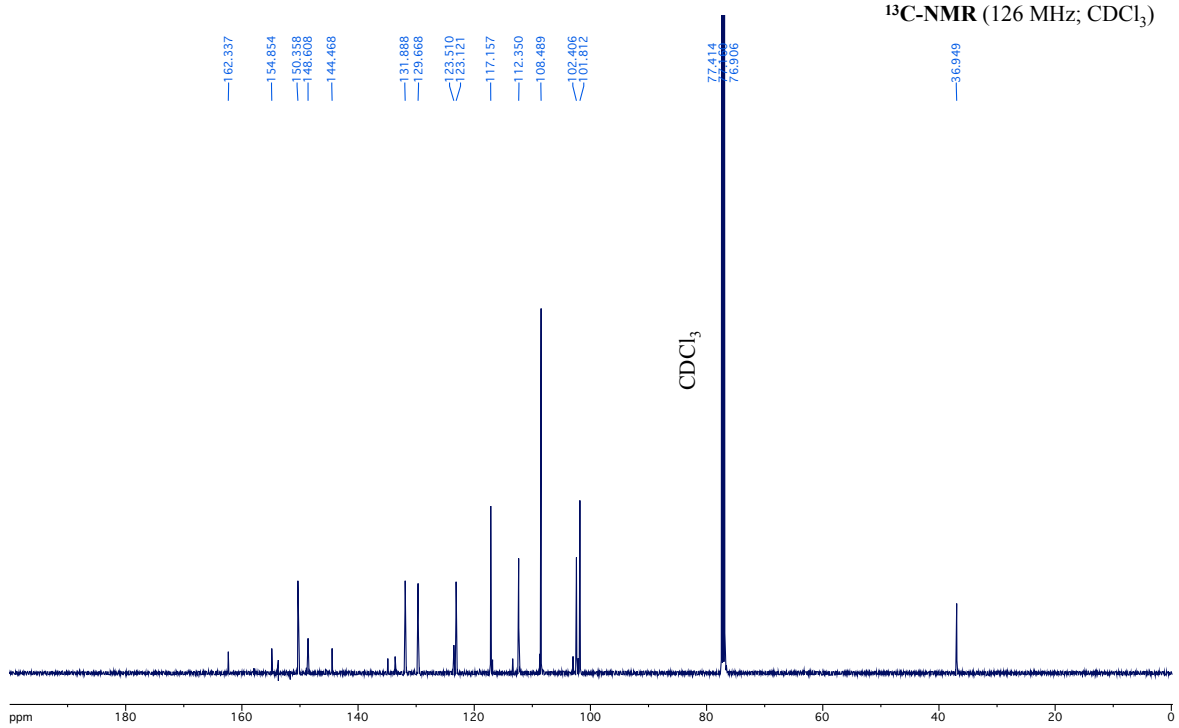

**$^{1}$H-NMR** (400 MHz; $CDCl_3$)

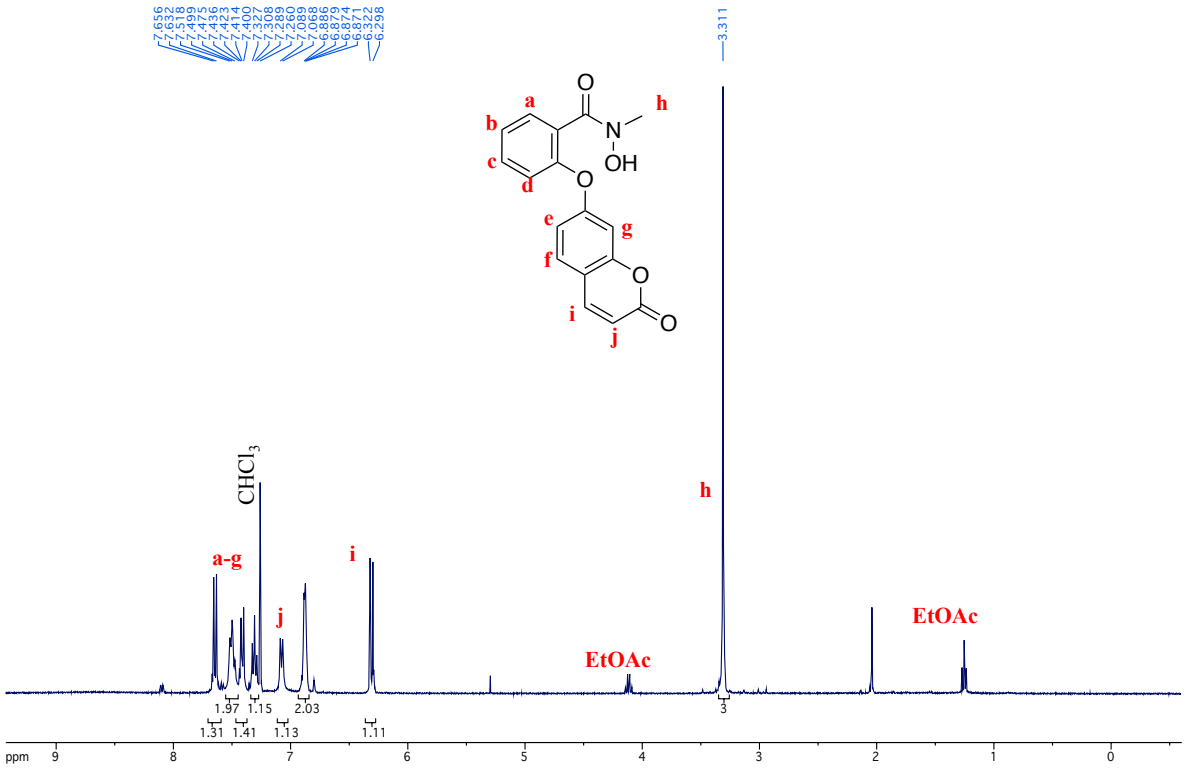


**$^{13}$C-NMR** (126 MHz; $CDCl_3$)

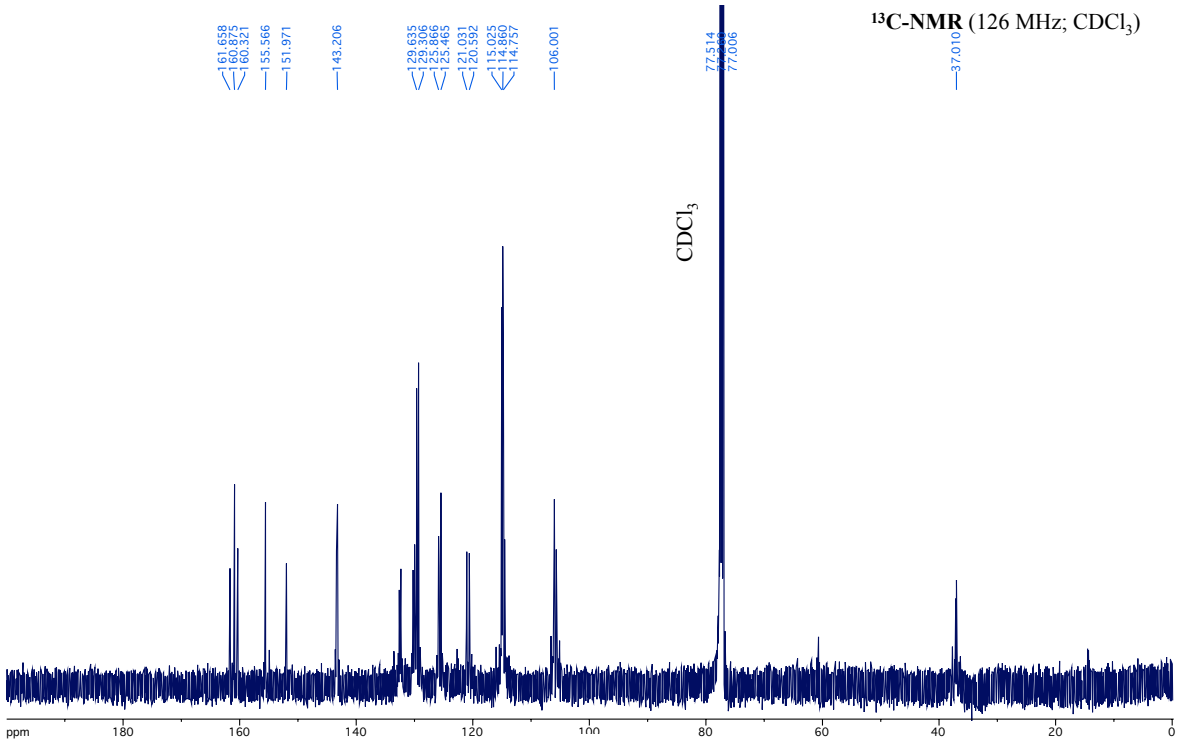

**$^{1}$H-NMR** (400 MHz; $CDCl_3$)

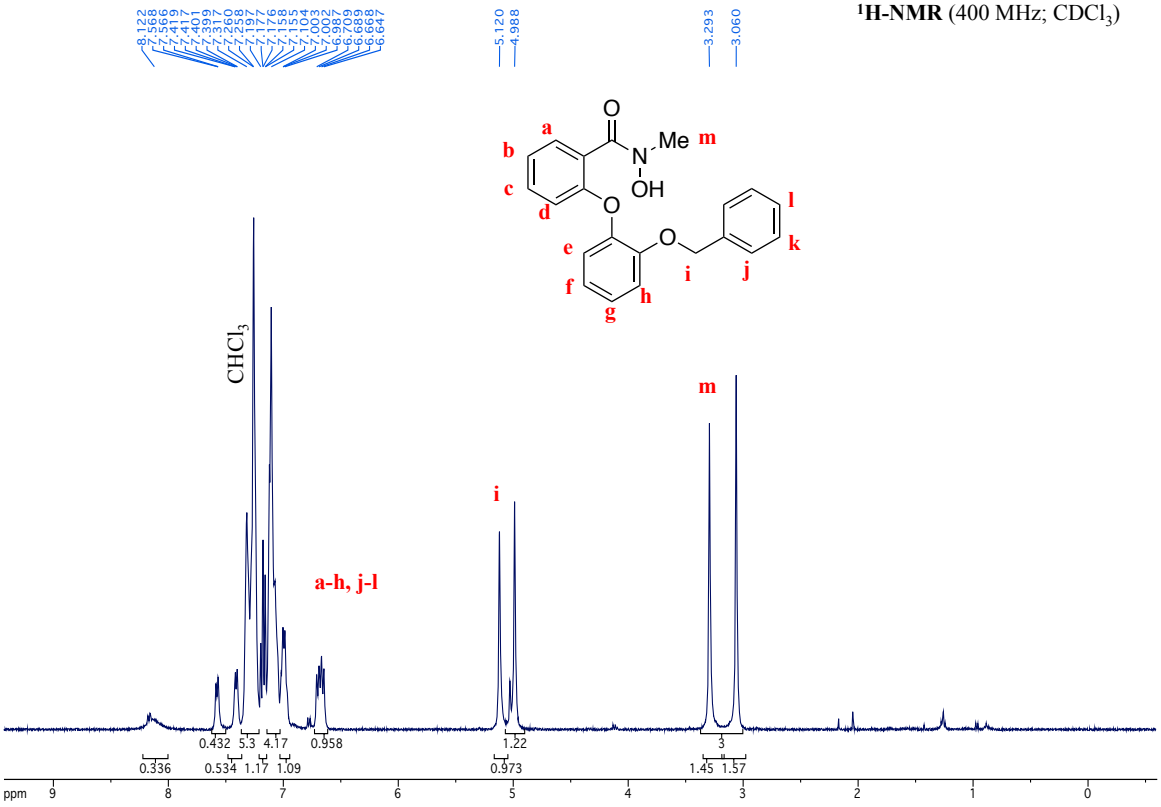


**$^{13}$C-NMR** (126 MHz; $CDCl_3$)

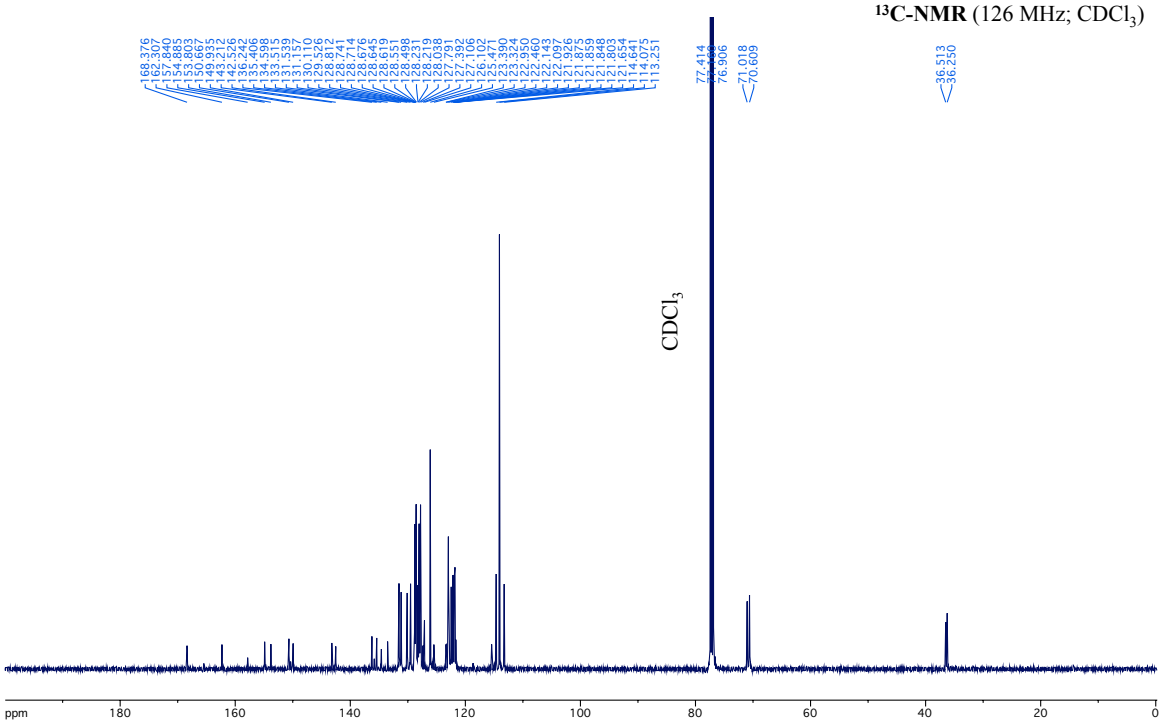

**$^1$H-NMR** (400 MHz; $CDCl_3$)

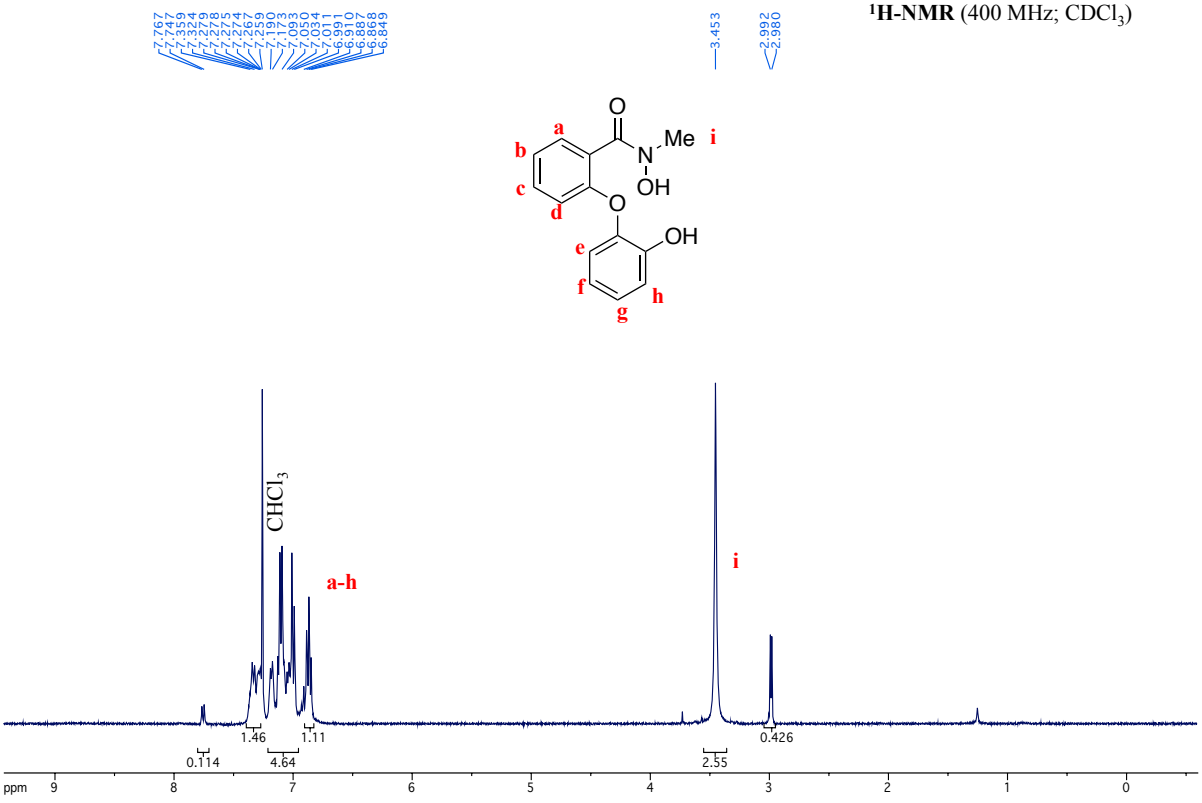


**$^{13}$C-NMR** (126 MHz; $CDCl_3$)

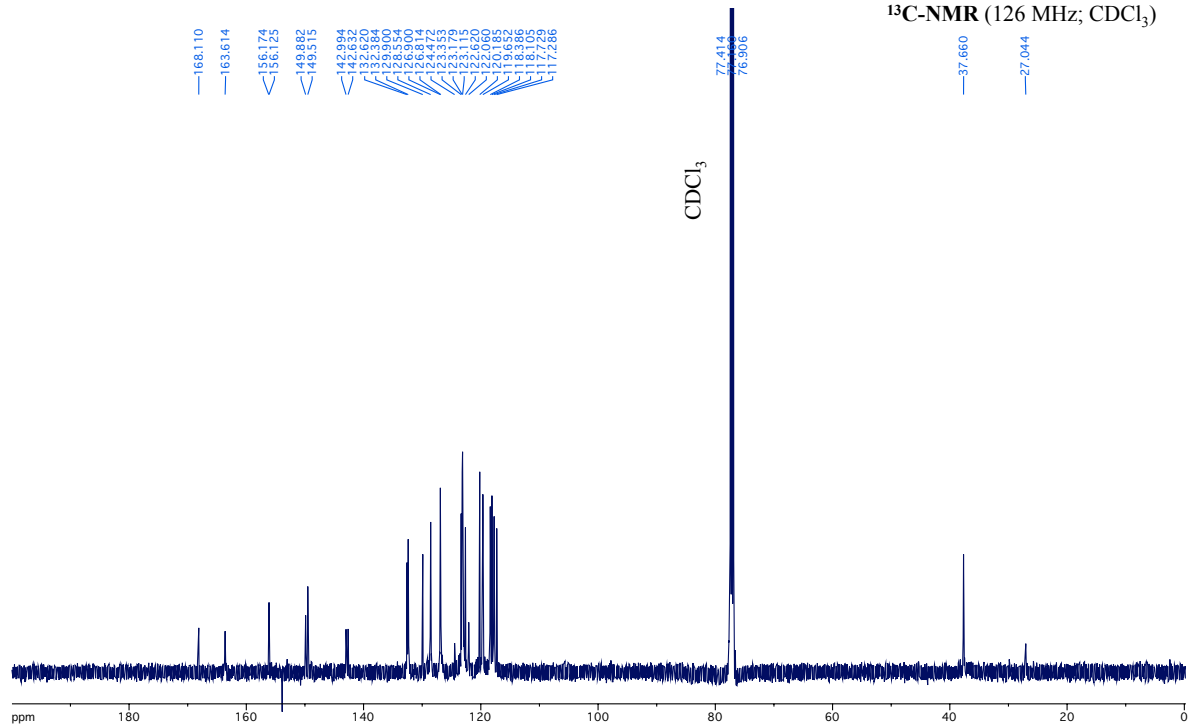

**$^{1}$H-NMR** (400 MHz; $CDCl_3$)

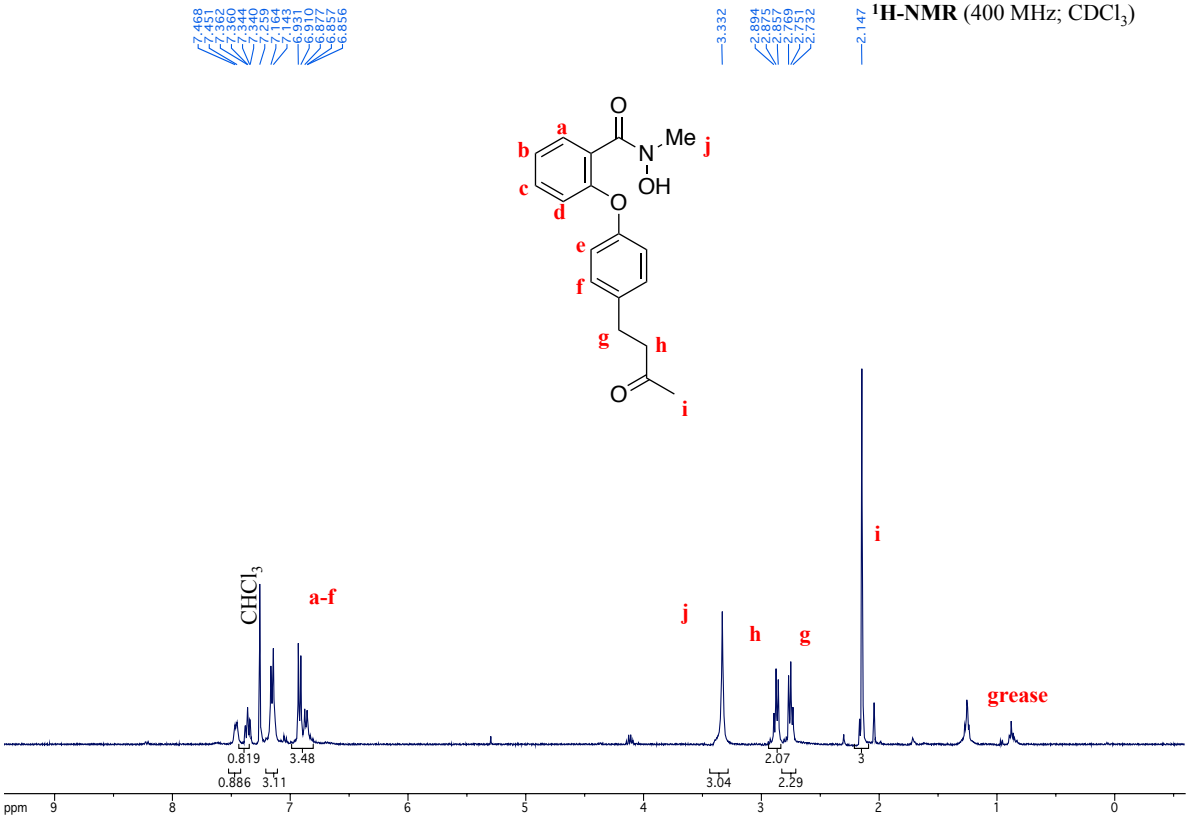


**$^{13}$C-NMR** (126 MHz; $CDCl_3$)

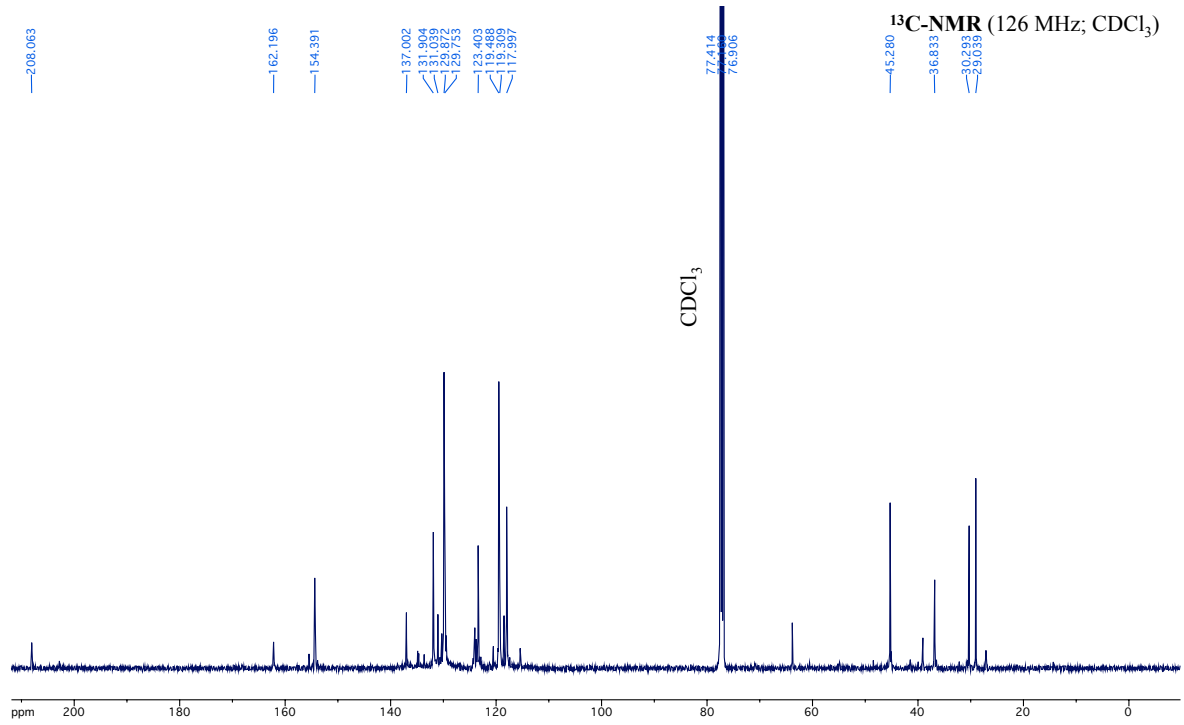

**$^{1}$H-NMR** (400 MHz; DMSO-$d_6$)

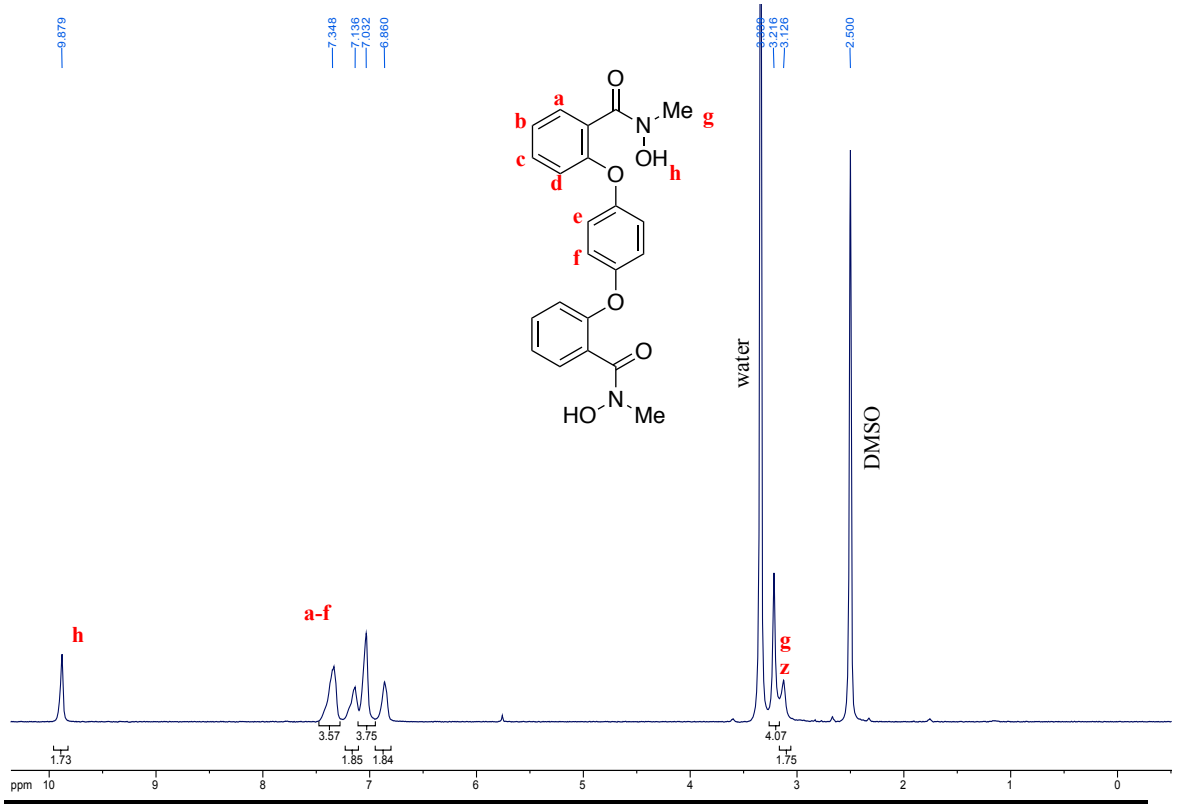


**$^{13}$C-NMR** (126 MHz; DMSO-$d_6$)

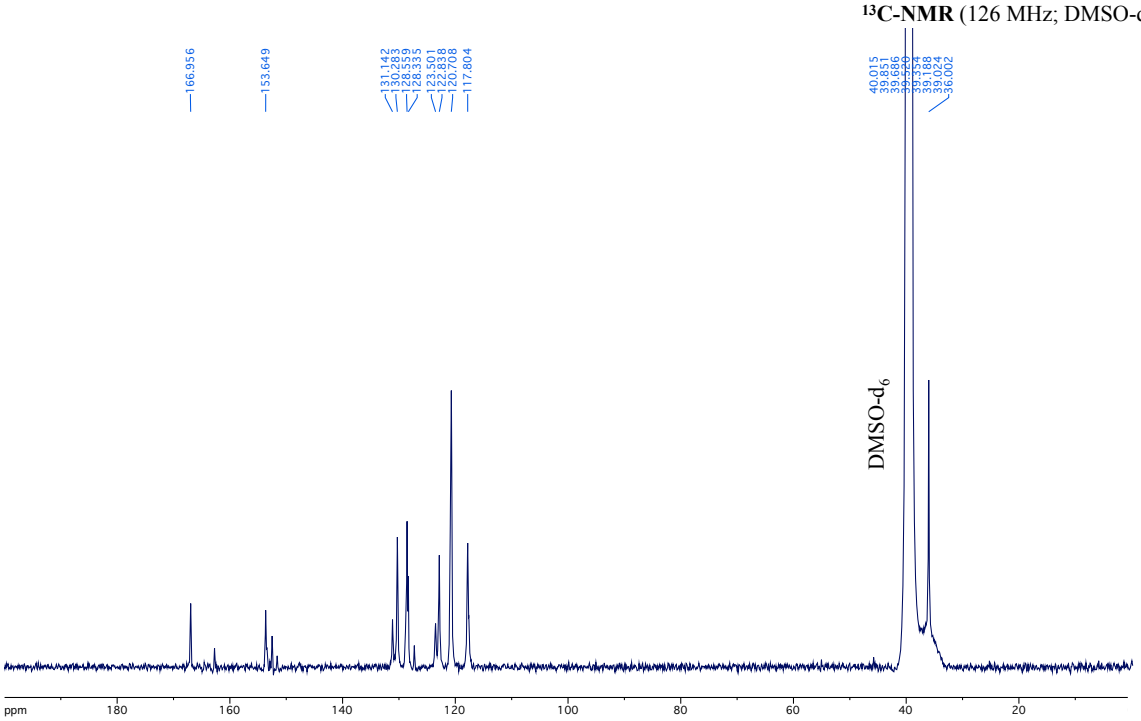

**$^{1}$H-NMR** (400 MHz; $CDCl_3$)

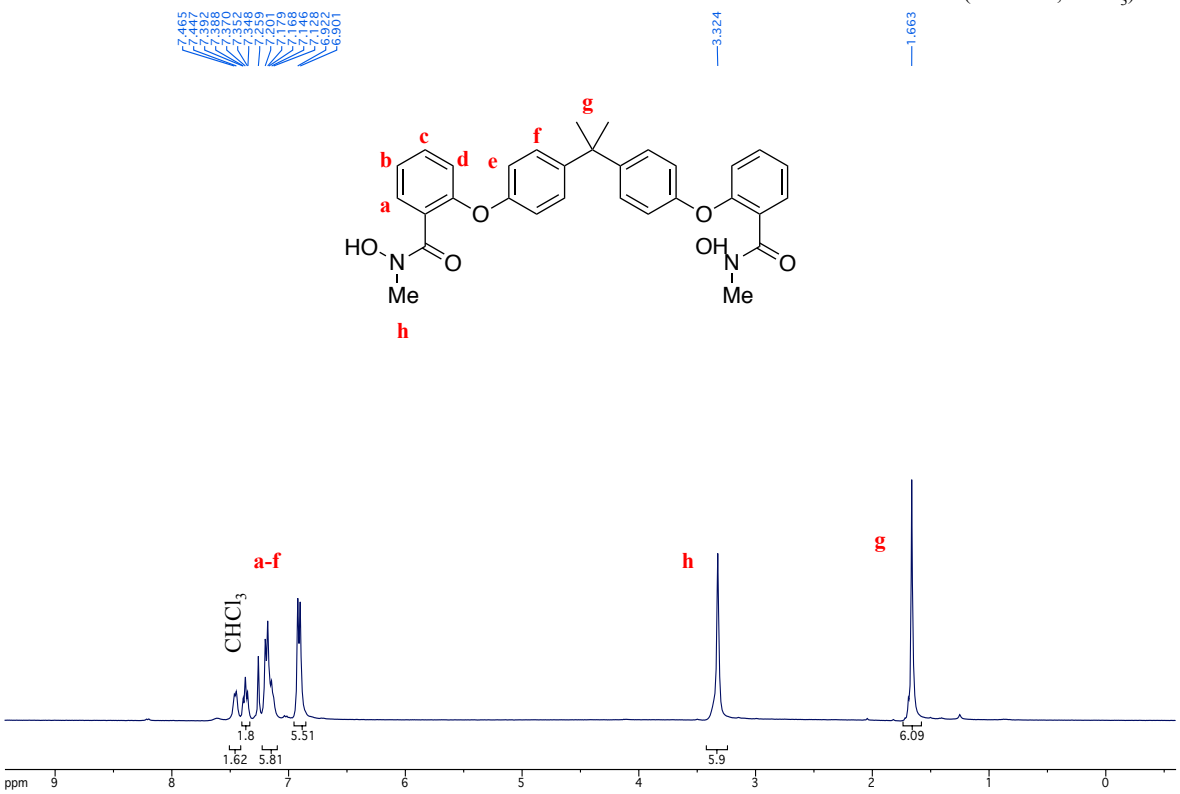


**$^{13}$C-NMR** (126 MHz; $CDCl_3$)

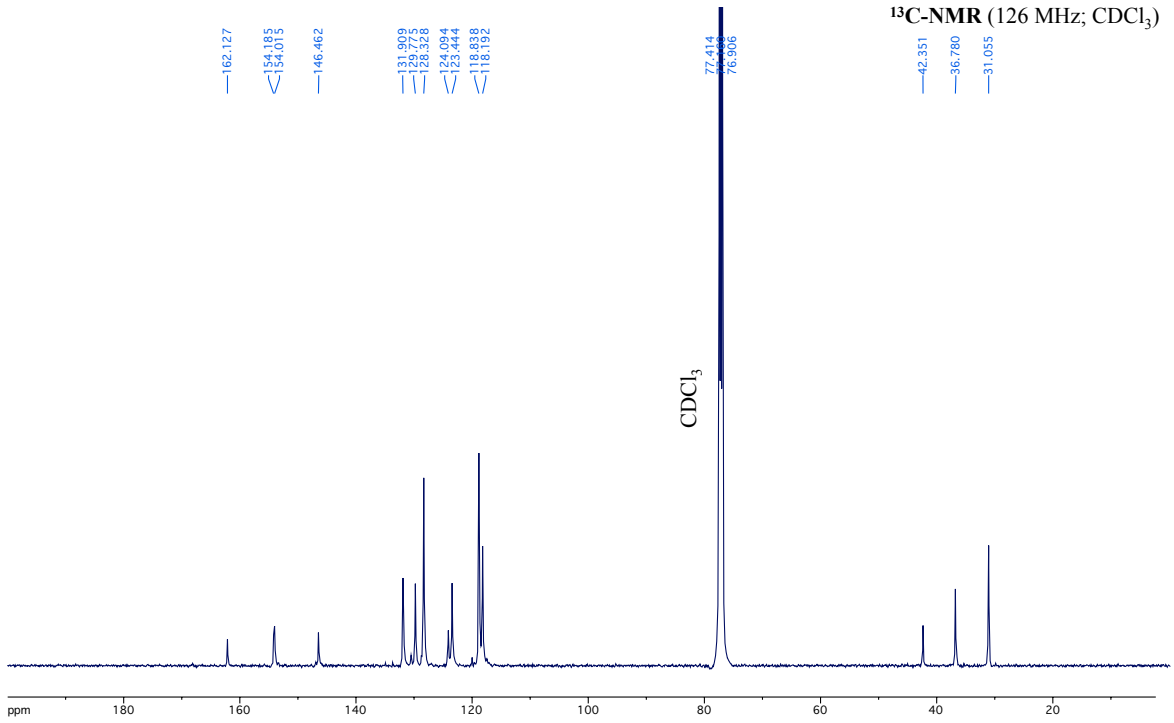

**$^{1}$H-NMR** (400 MHz; $CDCl_3$)

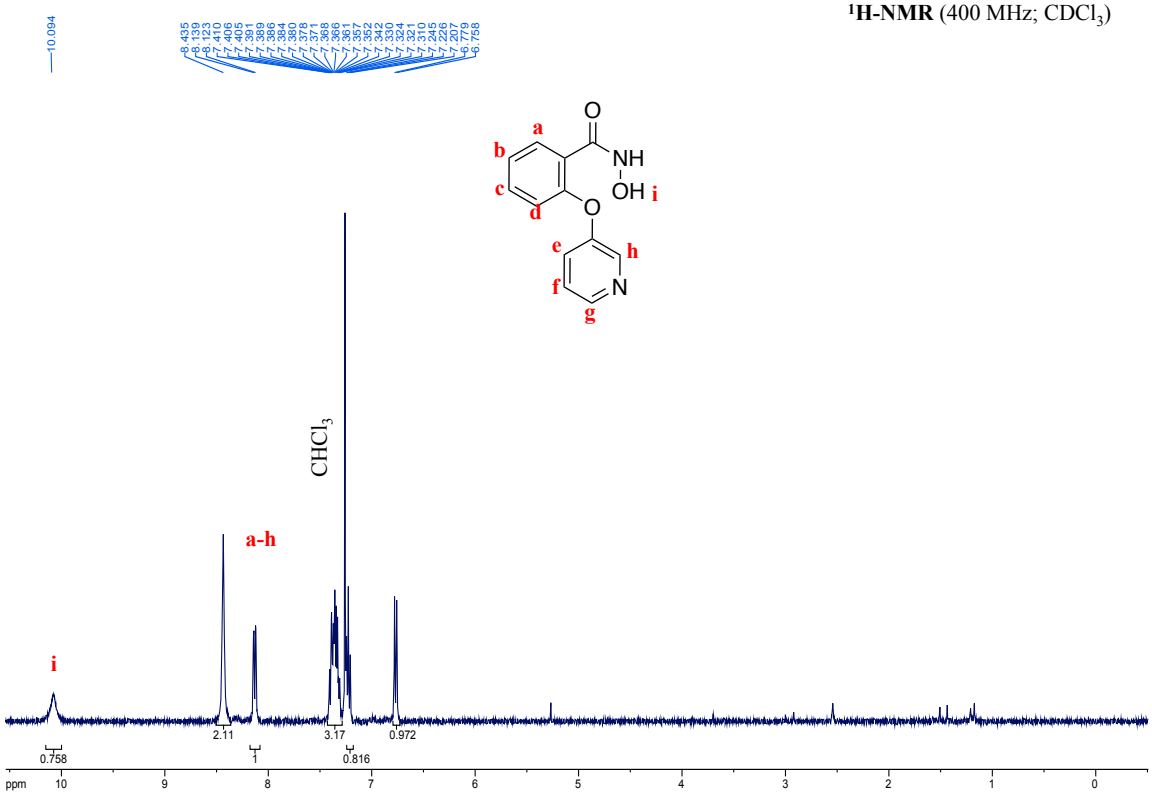


**$^{13}$C-NMR** (126 MHz; $CDCl_3$)

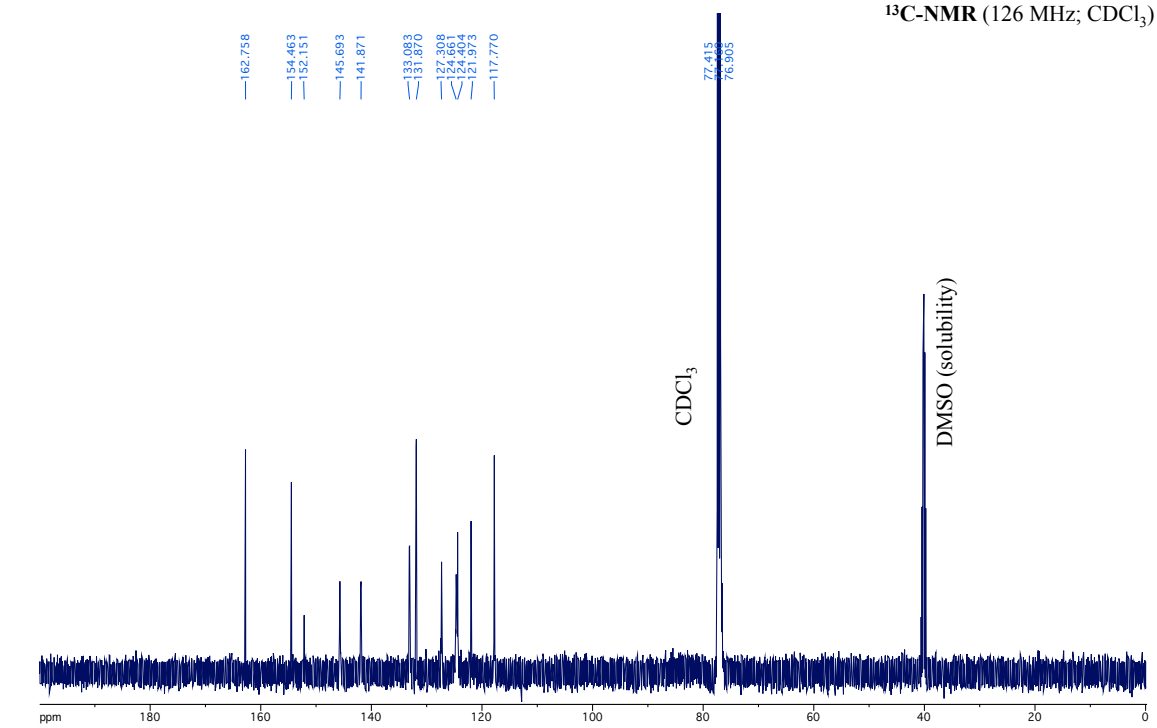

**$^{1}$H-NMR** (400 MHz; $CDCl_3$)

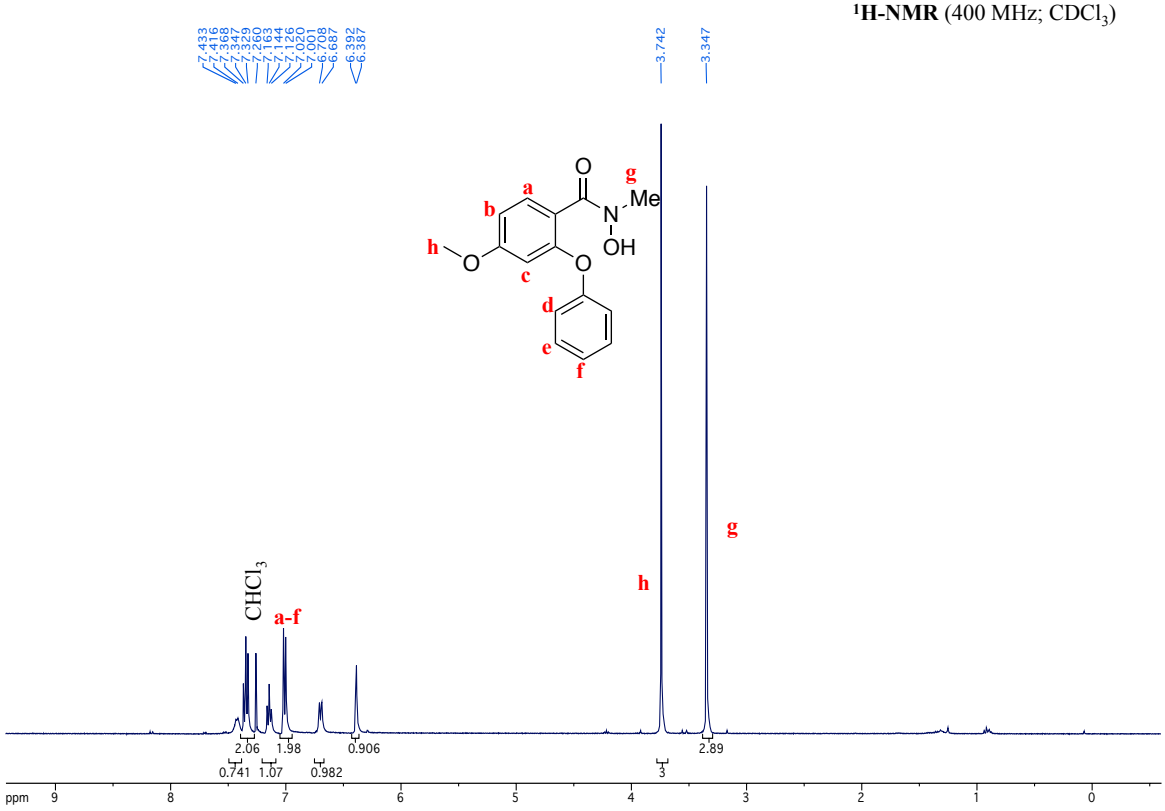


**$^{13}$C-NMR** (126 MHz; $CDCl_3$)

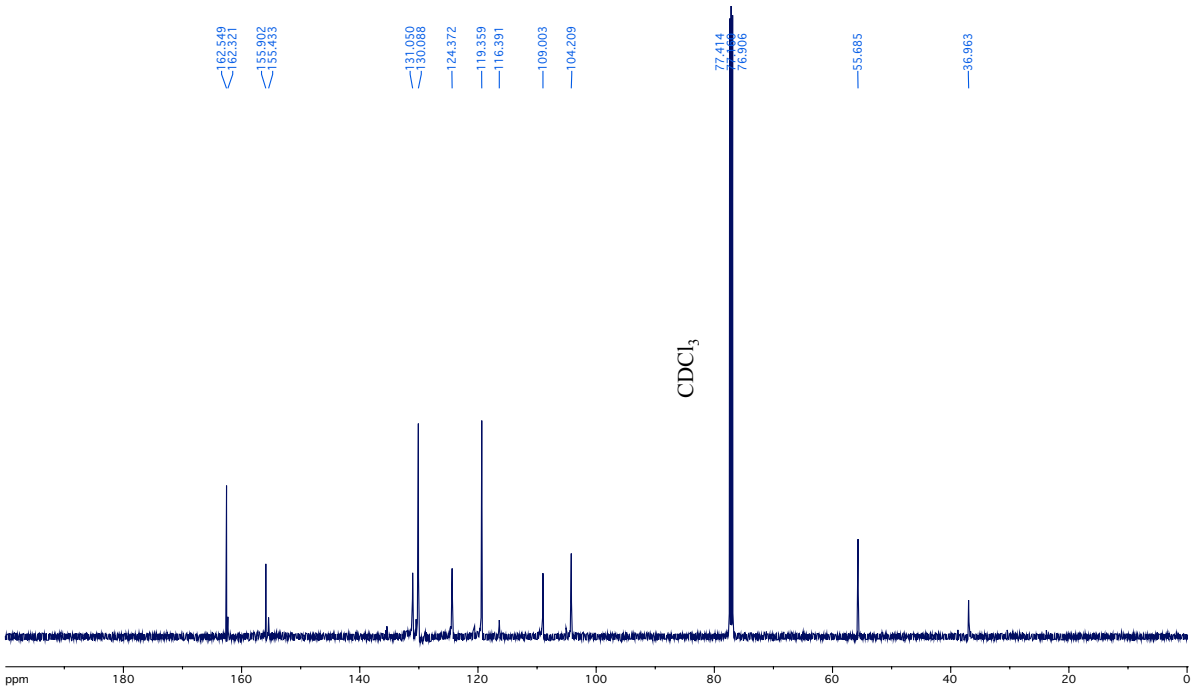

**$^{1}$H-NMR** (400 MHz; $CDCl_3$)

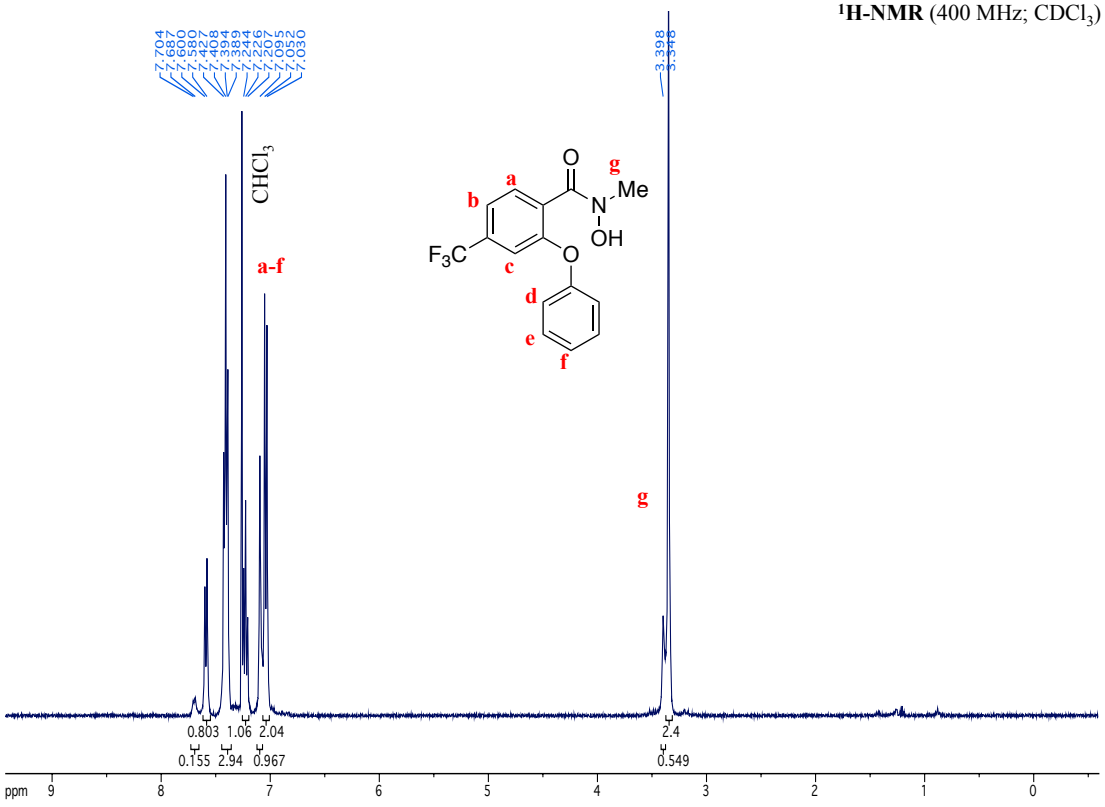


**$^{13}$C-NMR** (126 MHz; $CDCl_3$)

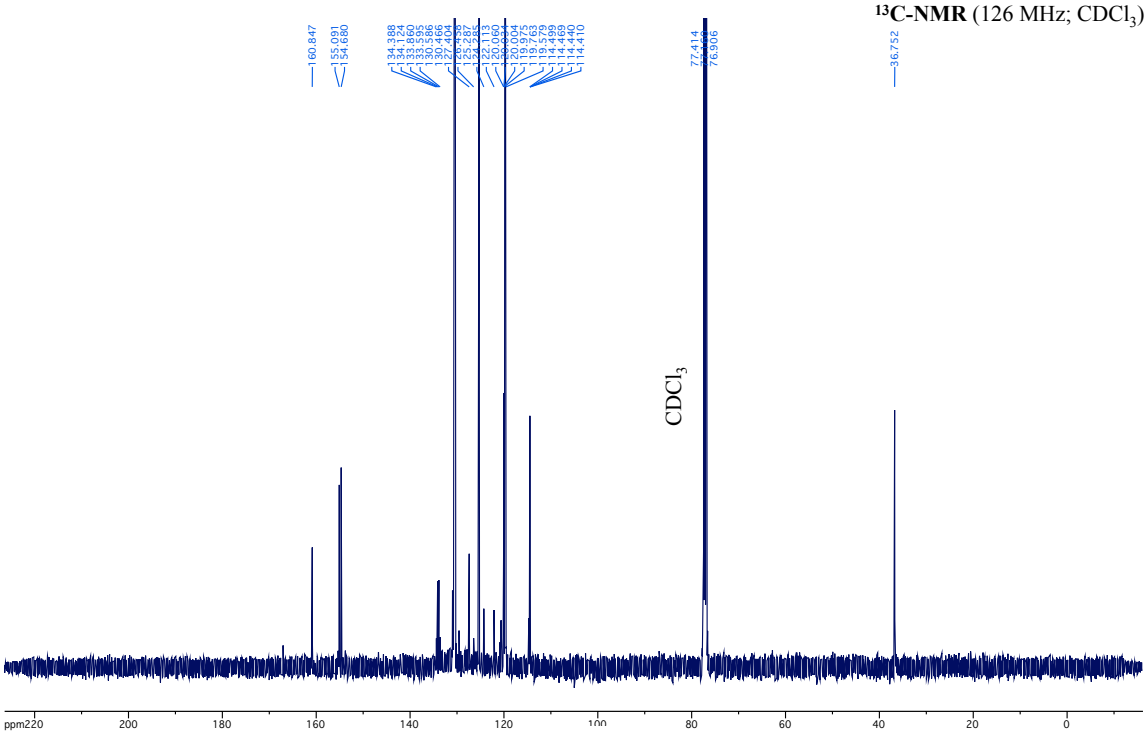

**$^{1}$H-NMR** (400 MHz; $CDCl_3$)

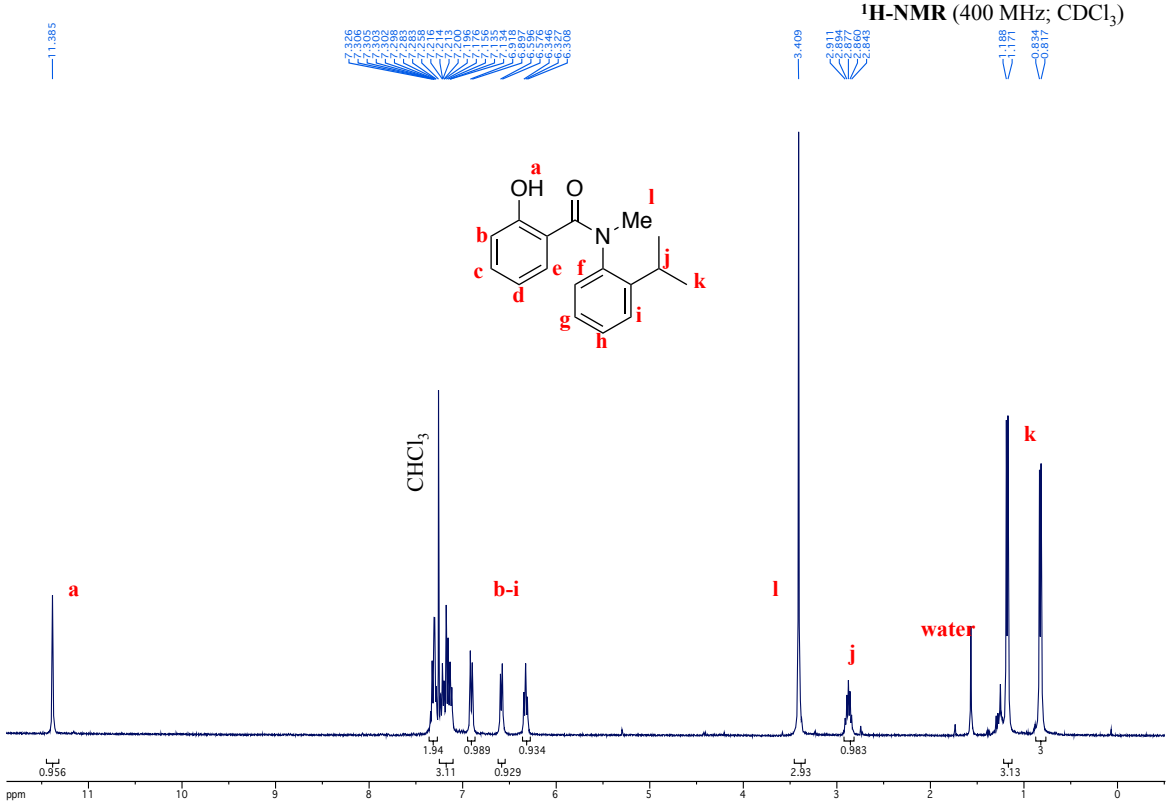


**$^{13}$C-NMR** (126 MHz; $CDCl_3$)

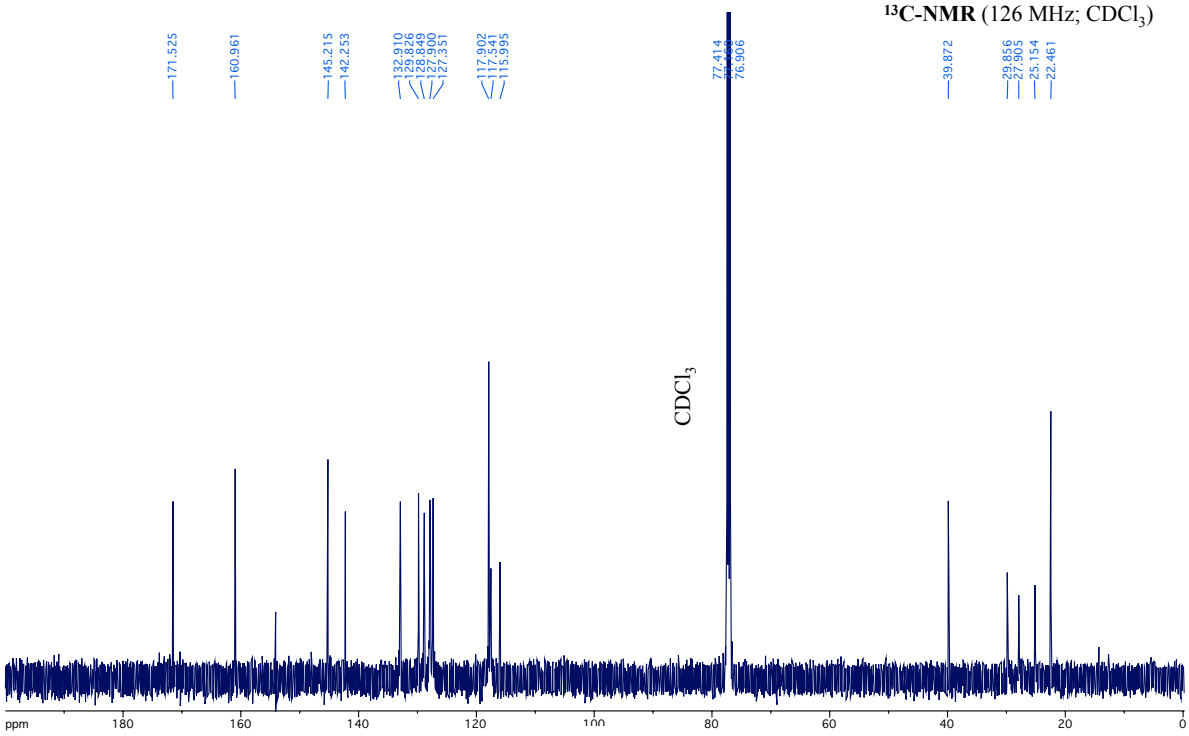

**$^{1}$H-NMR** (400 MHz; $CDCl_3$)

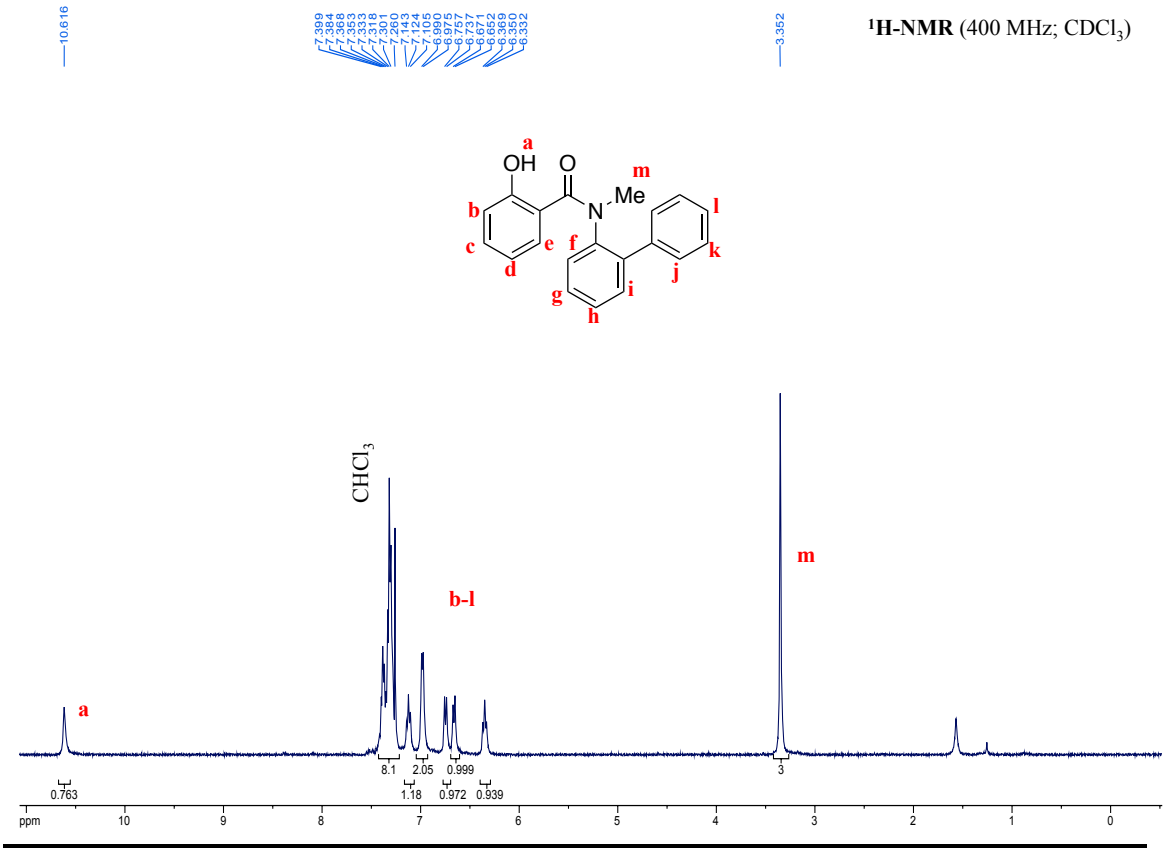


**$^{13}$C-NMR** (126 MHz; $CDCl_3$)

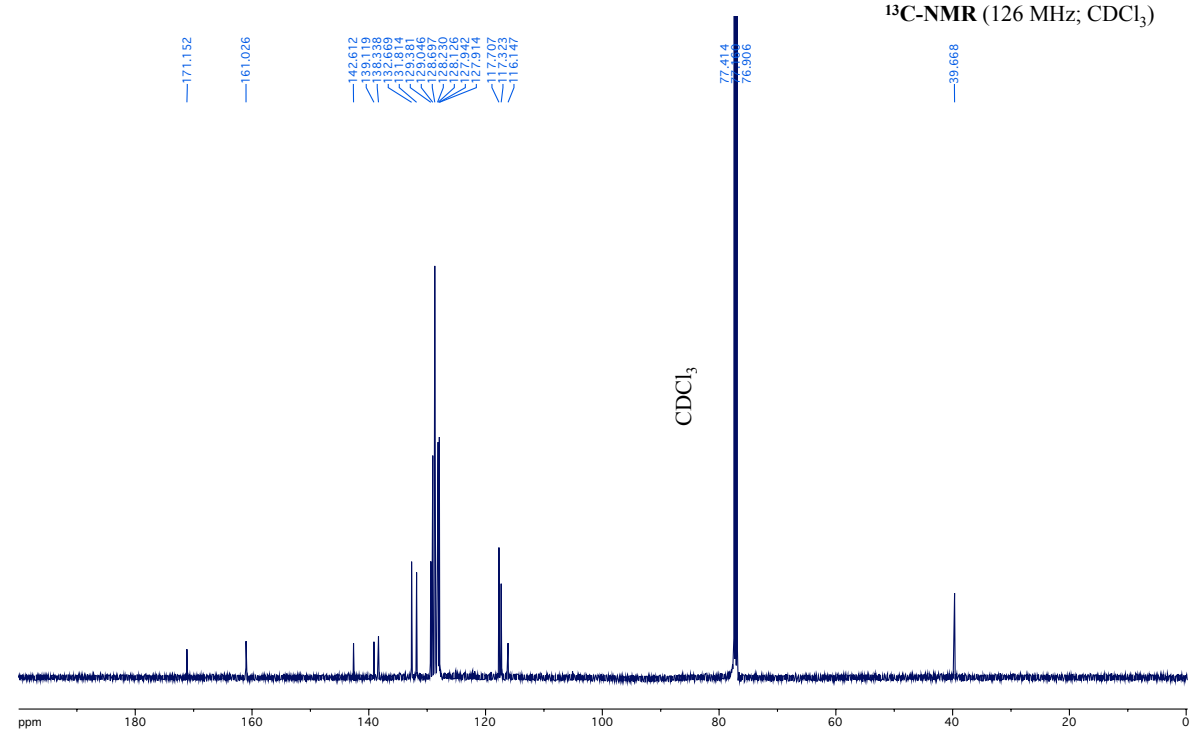

**$^{1}$H-NMR** (400 MHz; $CDCl_3$)

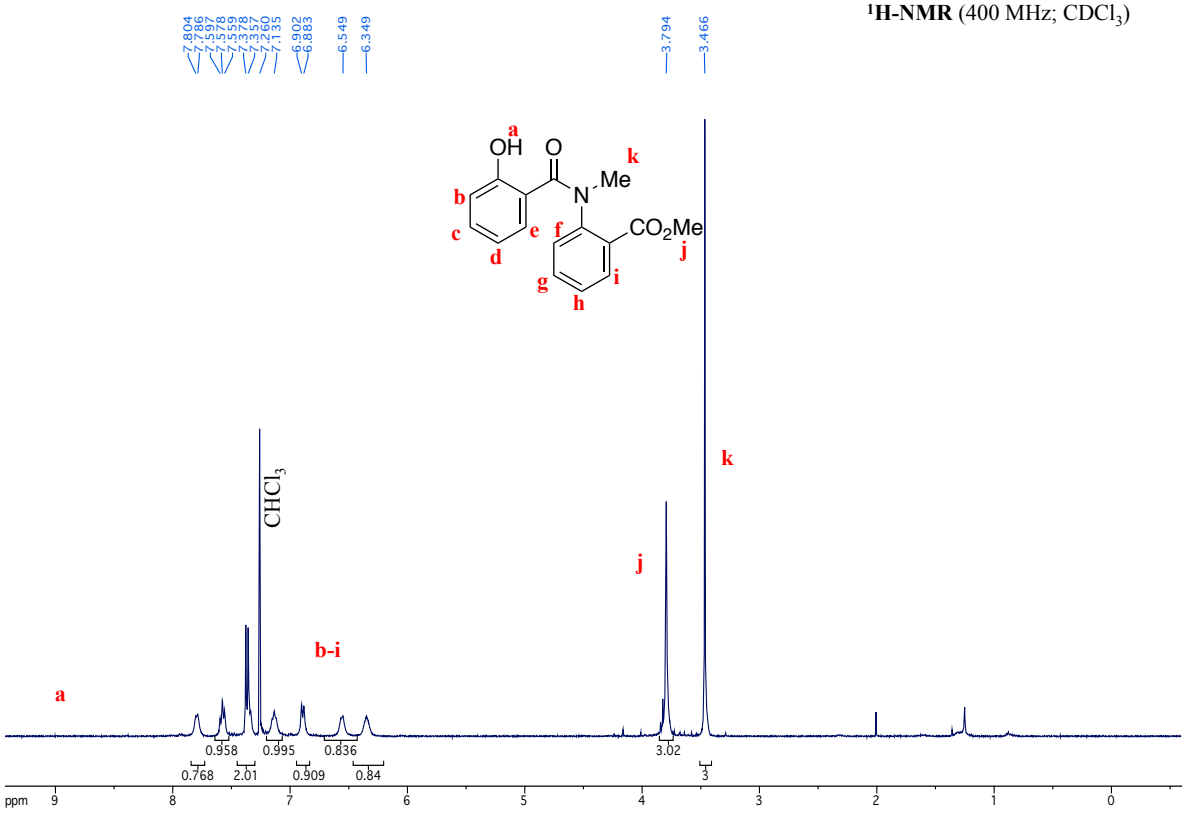


**$^{13}$C-NMR** (126 MHz; $CDCl_3$)

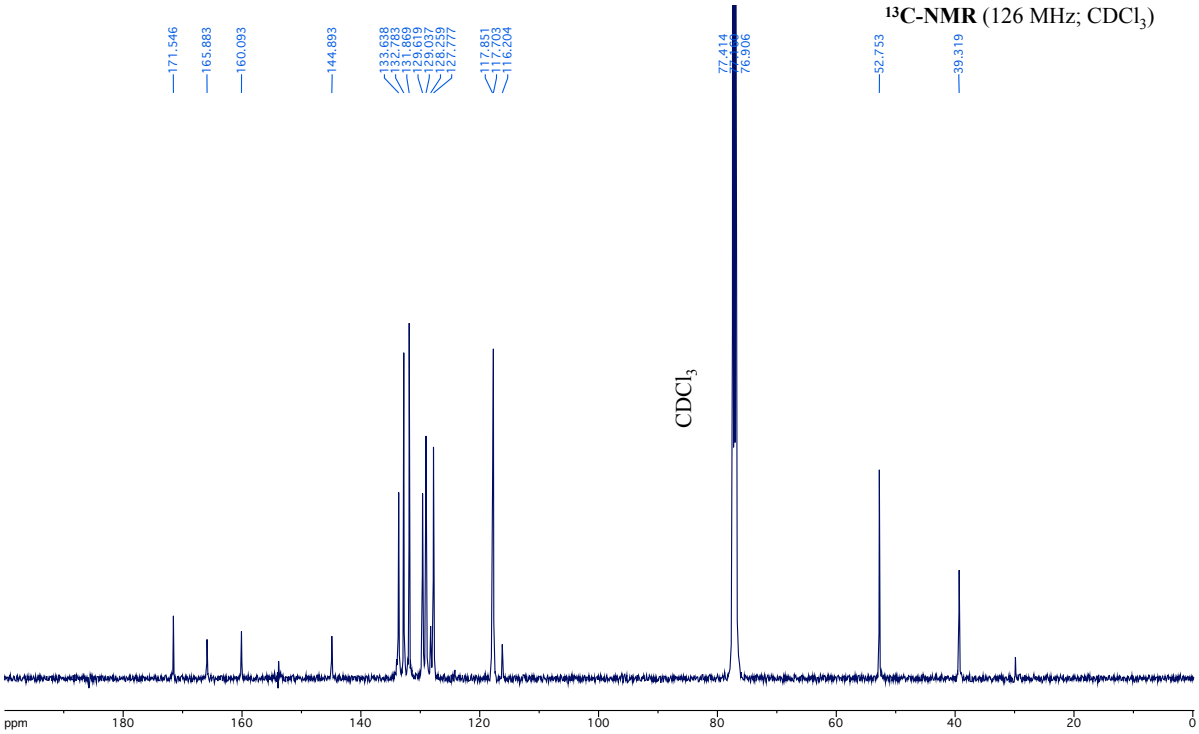

**$^{1}$H-NMR** (400 MHz; $CDCl_3$)

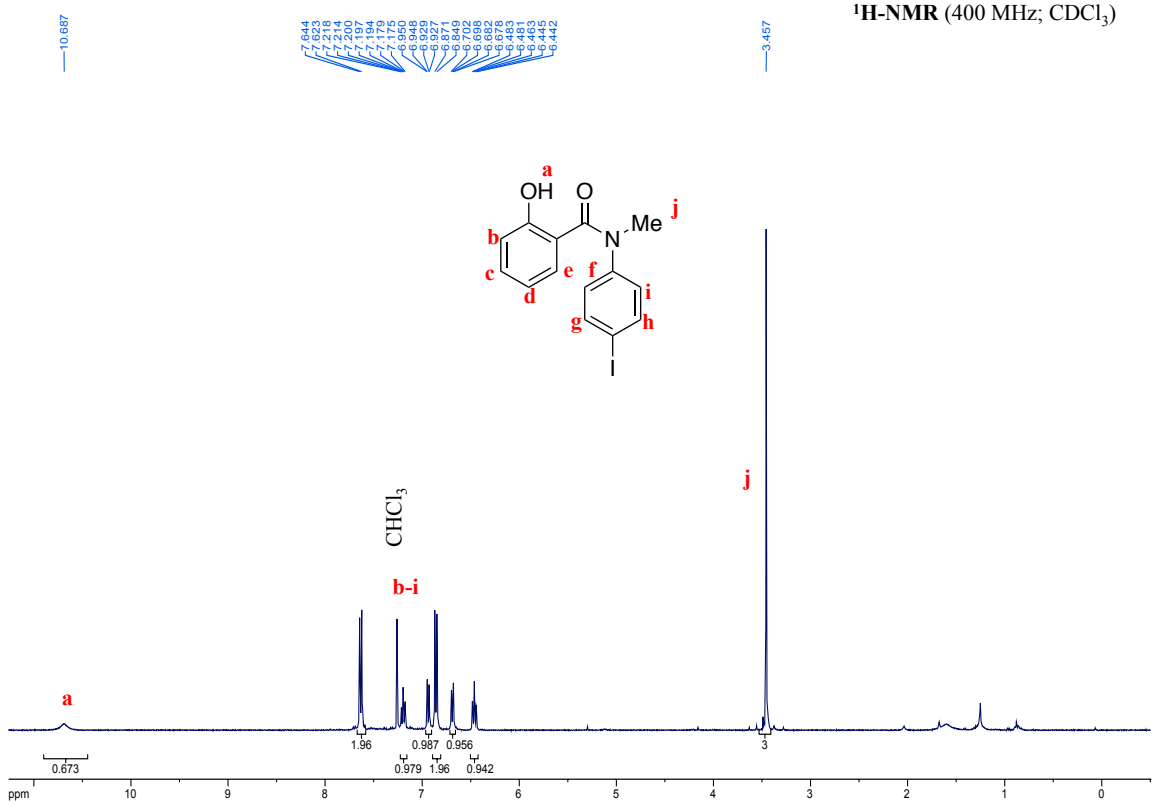


**$^{13}$C-NMR** (126 MHz; $CDCl_3$)

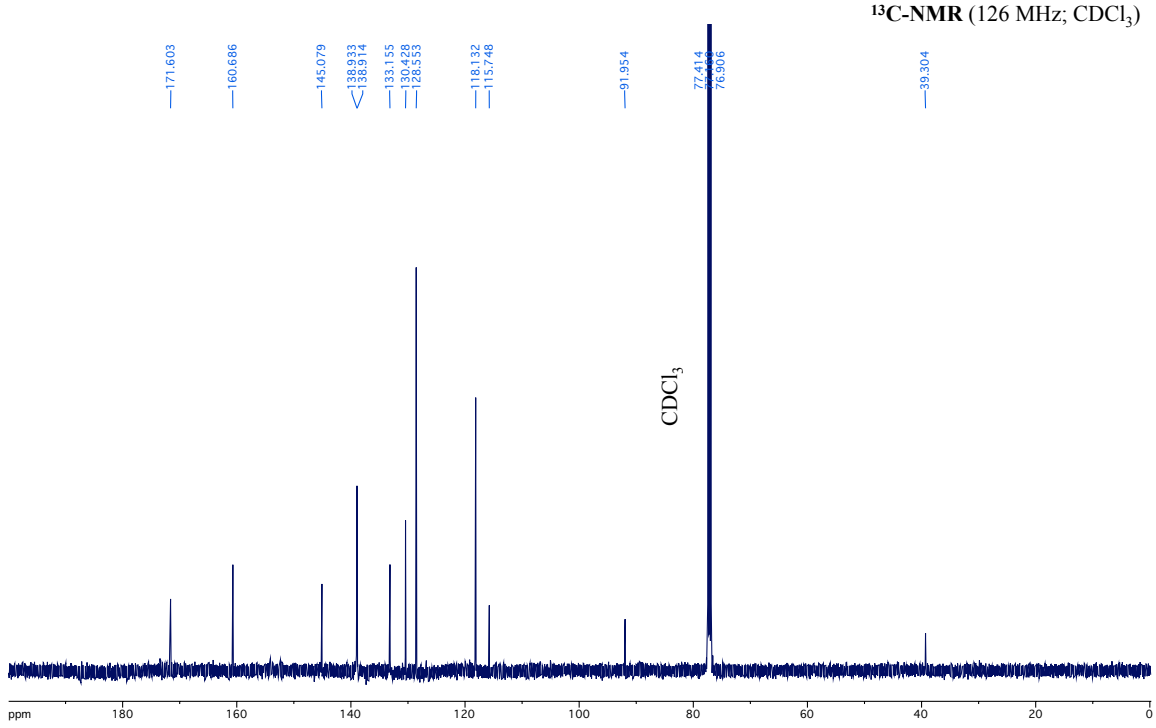

**$^1$H-NMR** (400 MHz; $CDCl_3$)

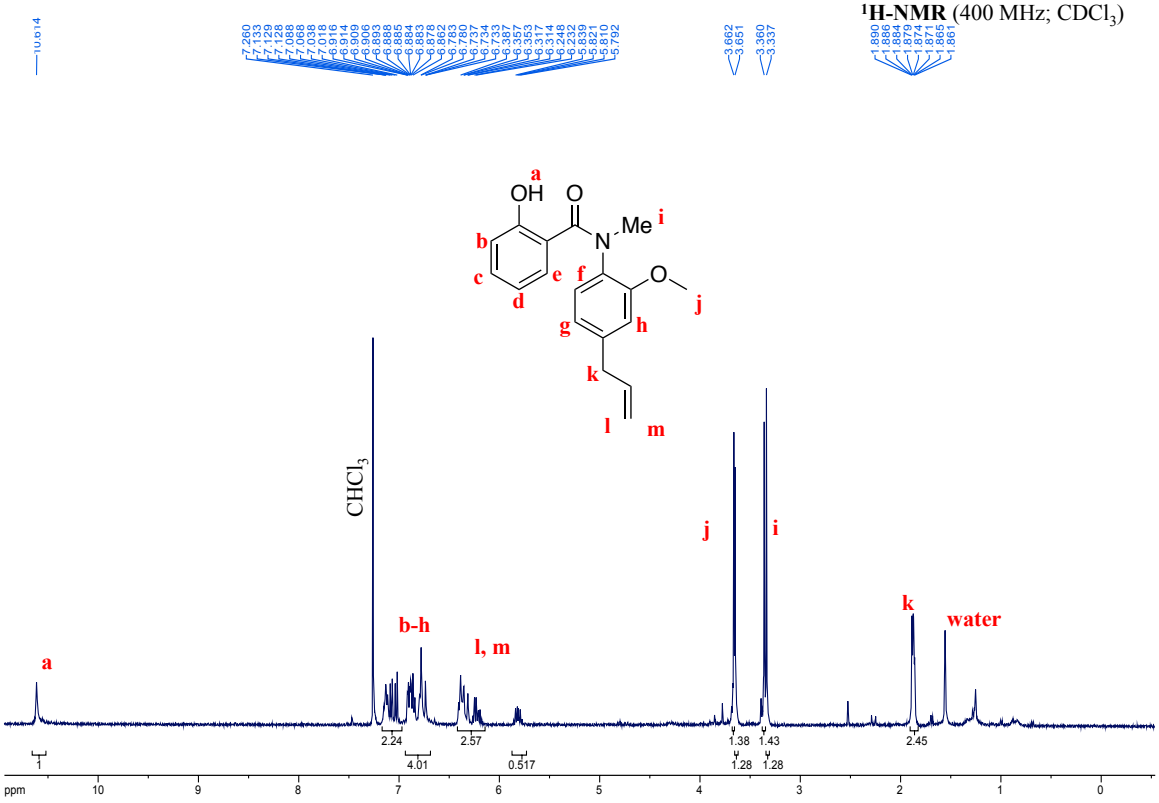


**$^{13}$C-NMR** (126 MHz; $CDCl_3$)

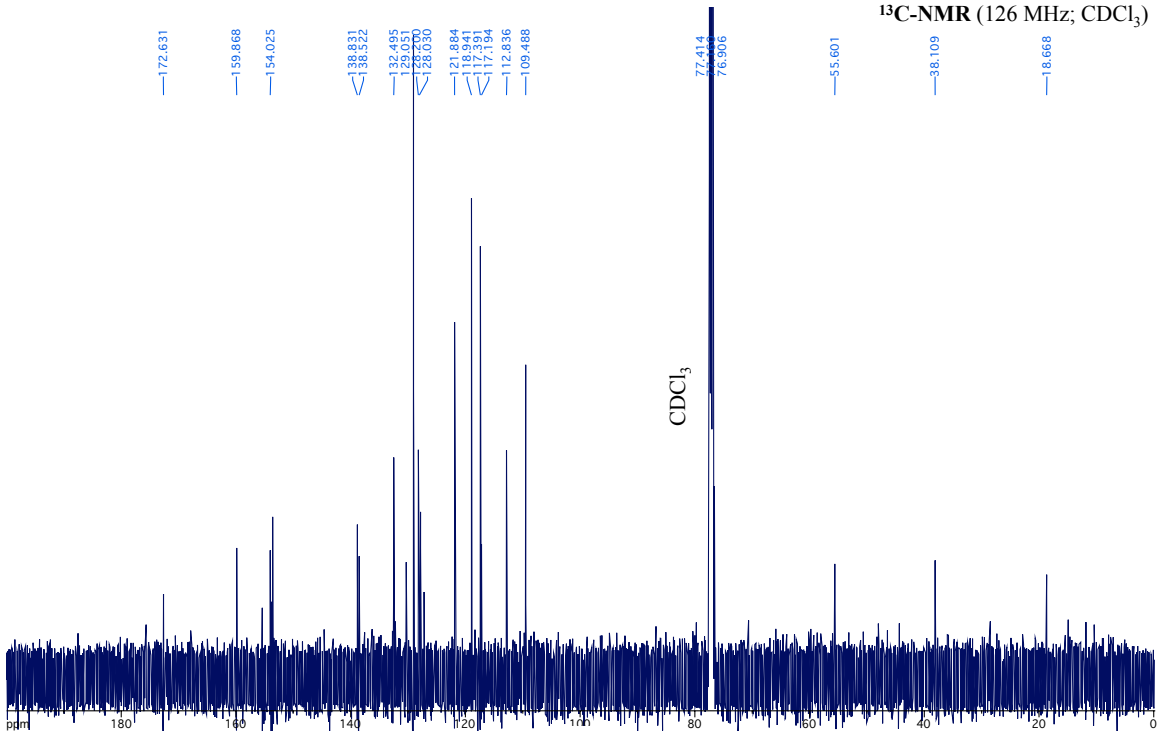

**$^{1}$H-NMR** (400 MHz; $CDCl_3$)

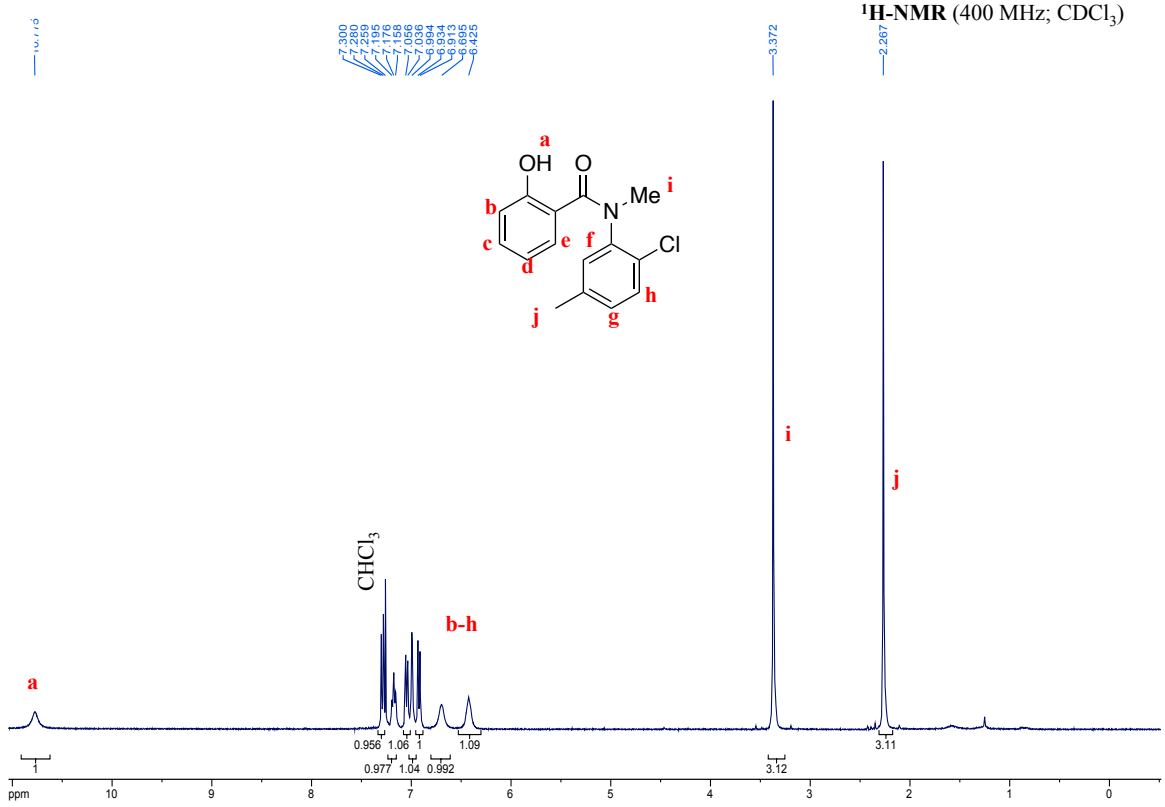


**$^{13}$C-NMR** (126 MHz; $CDCl_3$)

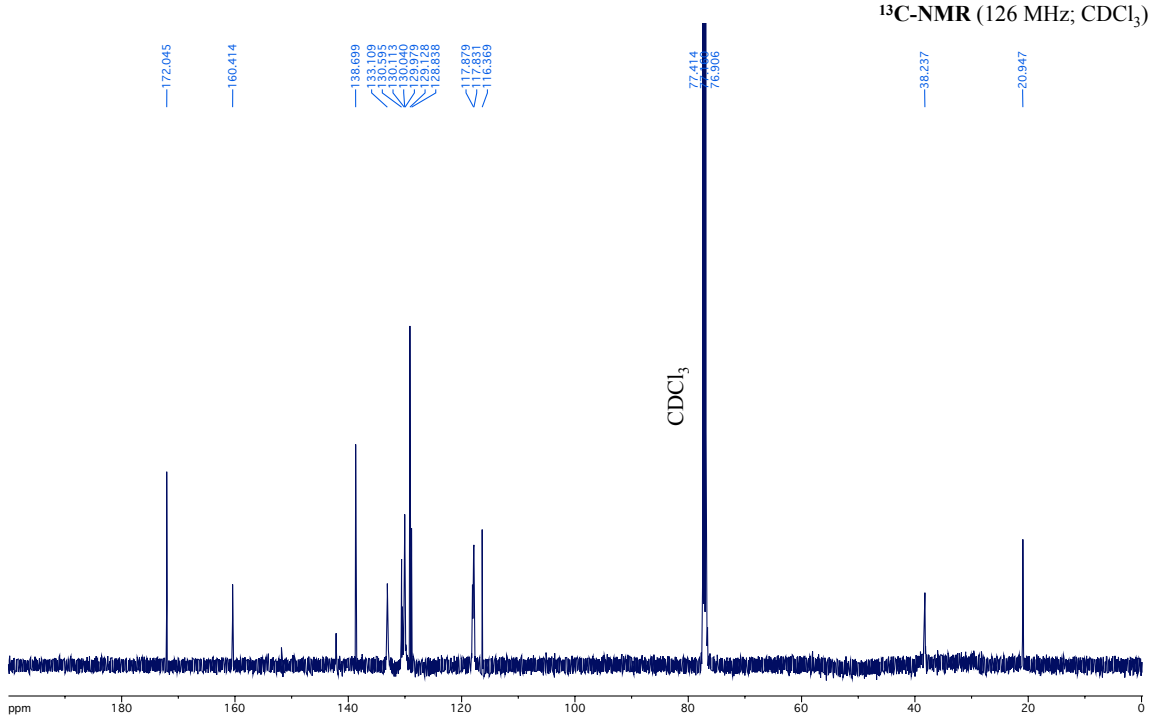

**$^{1}$H-NMR** (400 MHz; $CDCl_3$)

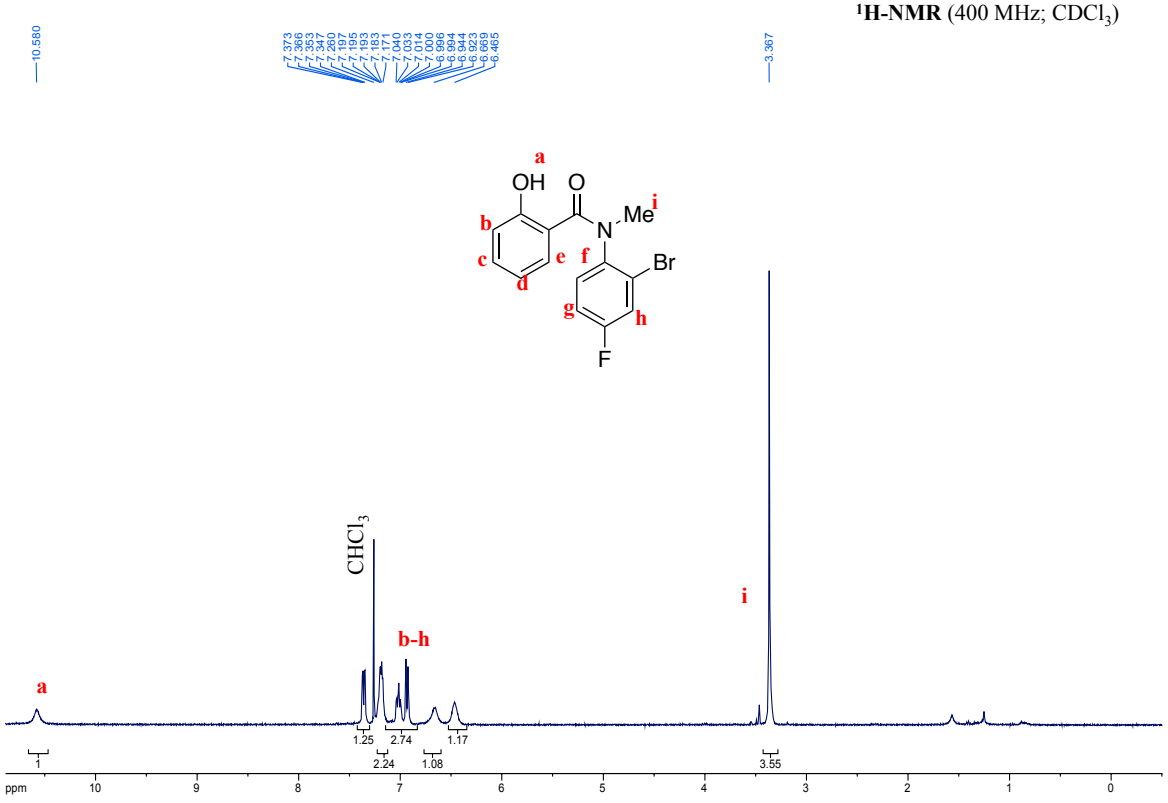


**$^{13}$C-NMR** (126 MHz; $CDCl_3$)

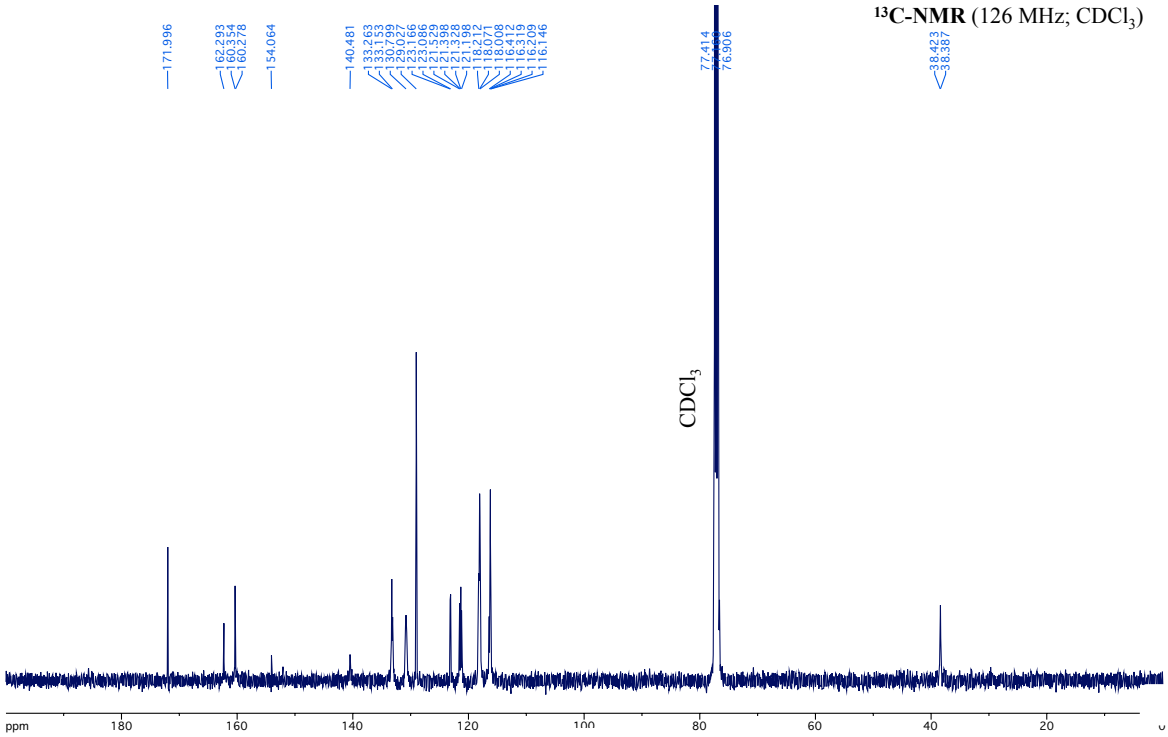

**$^{1}$H-NMR** (400 MHz; $CDCl_3$)

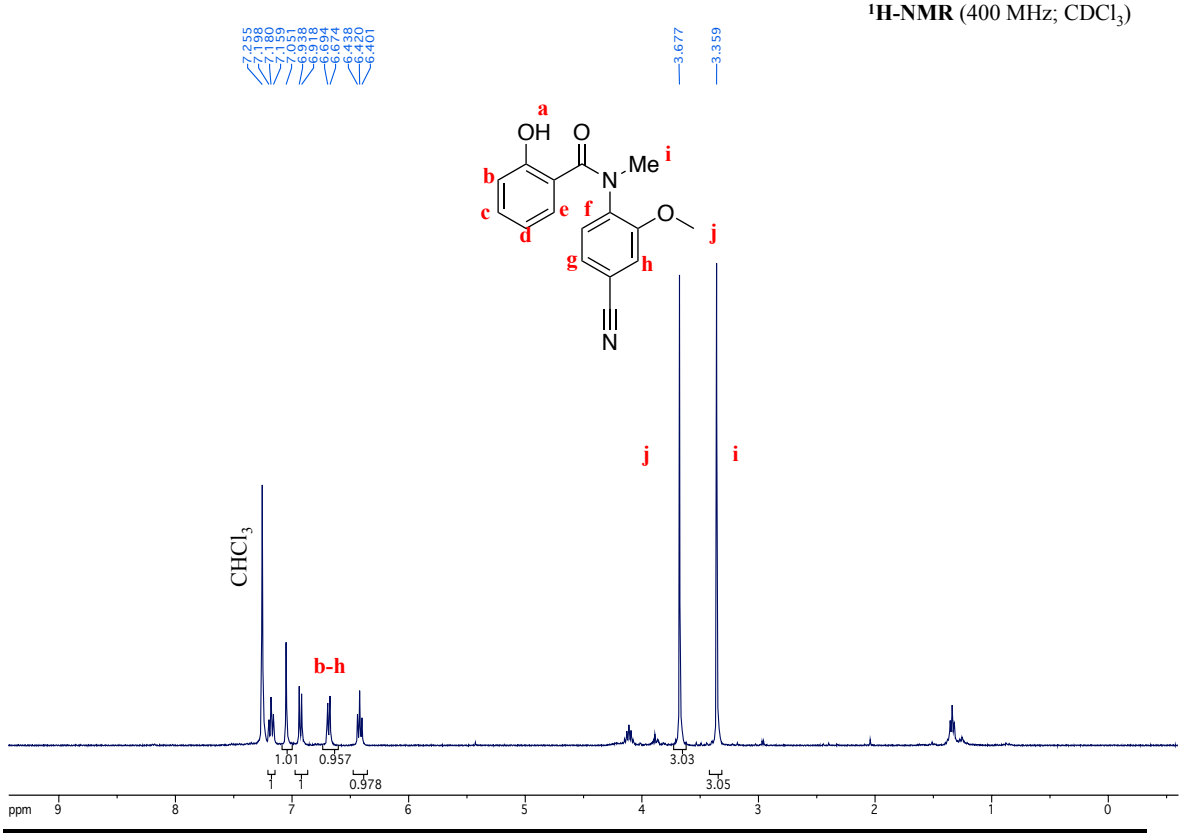


**$^{13}$C-NMR** (126 MHz; $CDCl_3$)

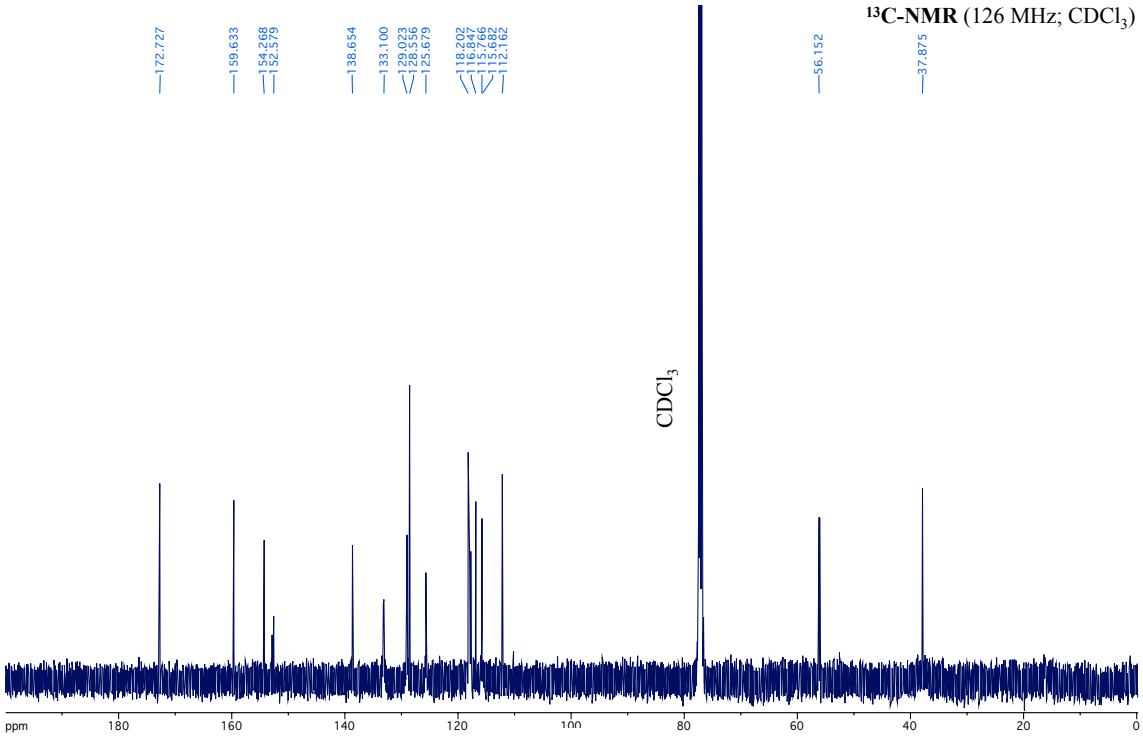

**$^{1}$H-NMR** (400 MHz; $CDCl_3$)

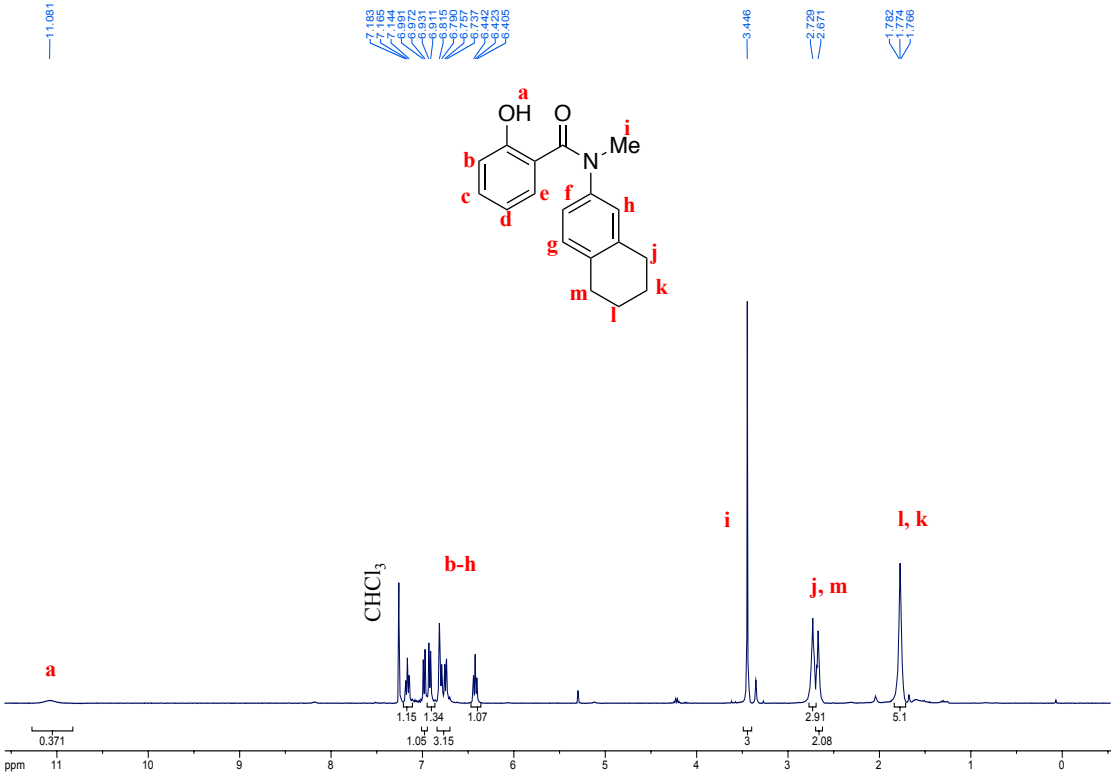


**$^{13}$C-NMR** (126 MHz; $CDCl_3$)

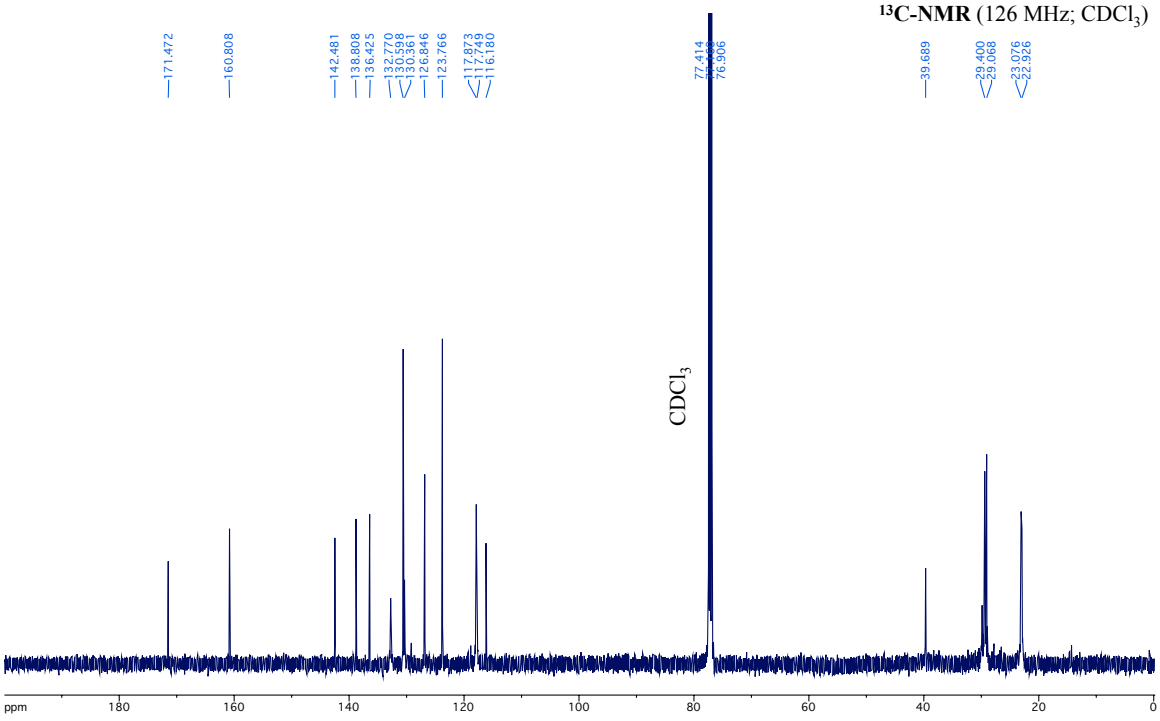

**$^{1}$H-NMR** (400 MHz; $CDCl_3$)

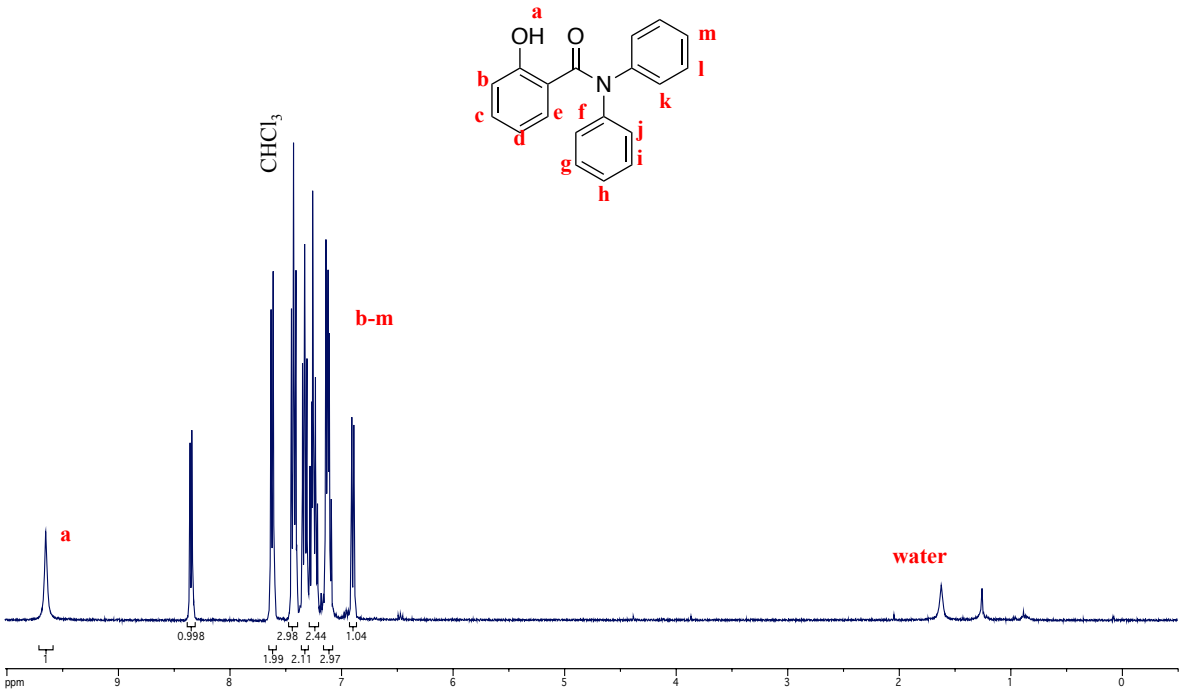


**$^{13}$C-NMR** (126 MHz; $CDCl_3$)

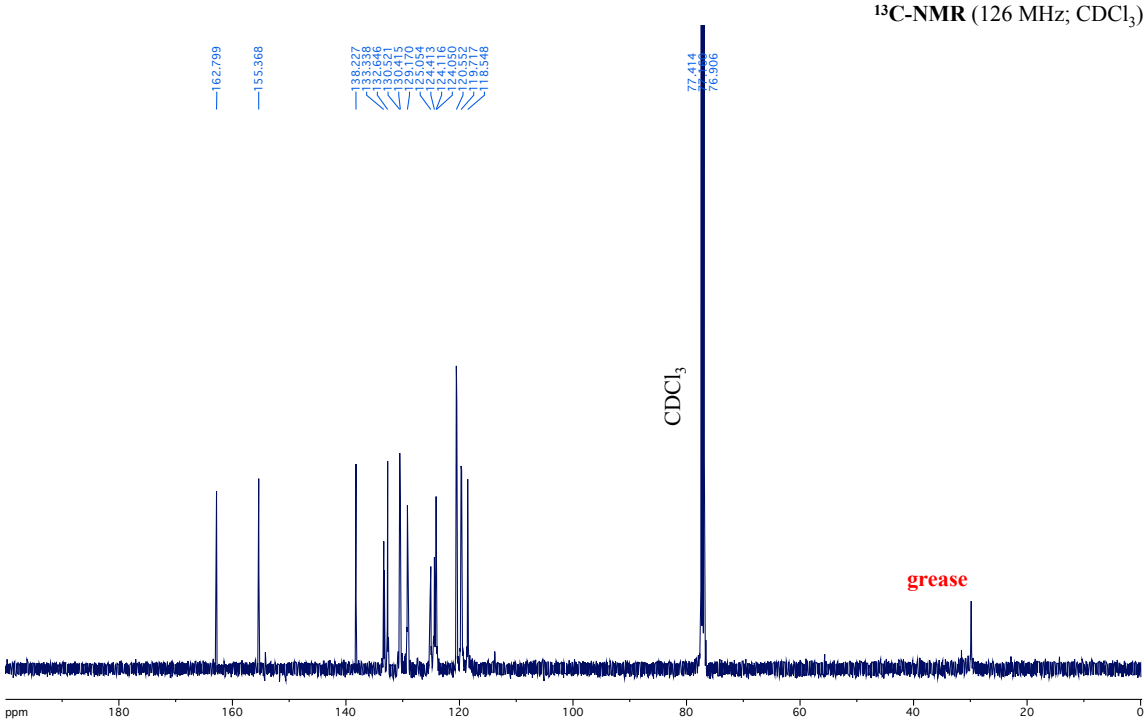

**$^{1}$H-NMR** (400 MHz; $CDCl_3$)

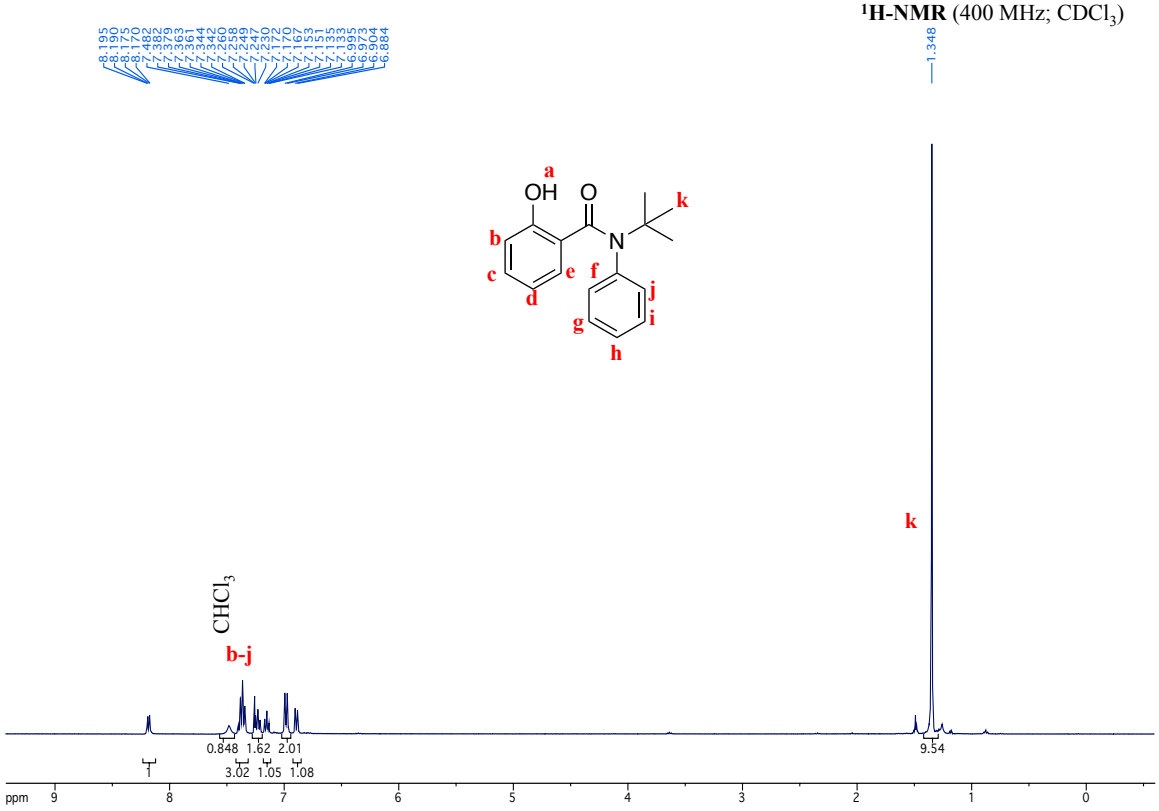


**$^{13}$C-NMR** (126 MHz; $CDCl_3$)

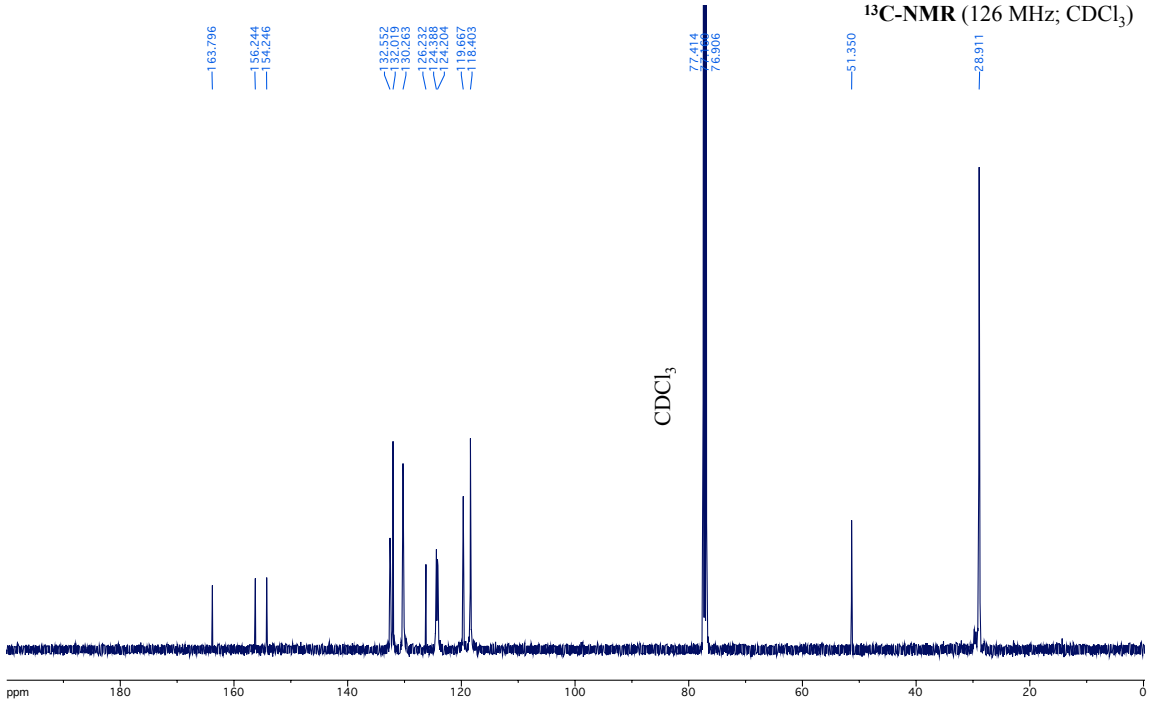

**$^{1}$H-NMR** (400 MHz; $CDCl_3$)

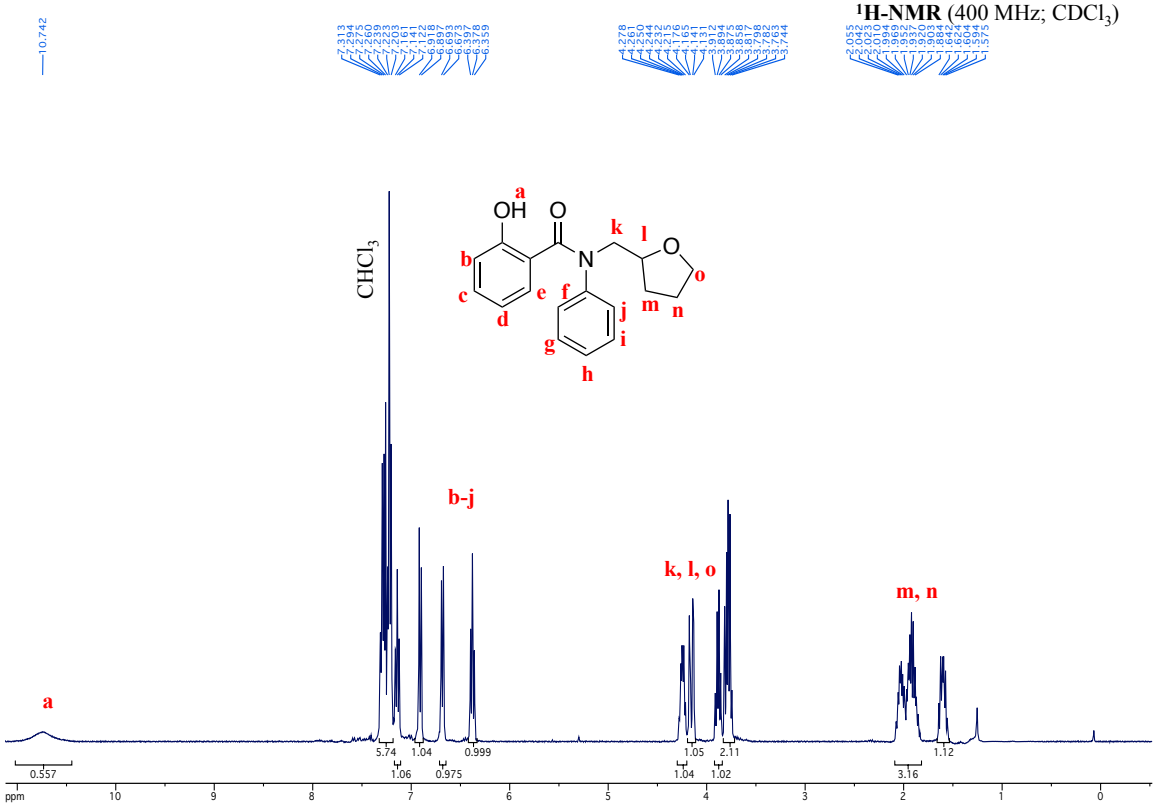


**$^{13}$C-NMR** (126 MHz; $CDCl_3$)

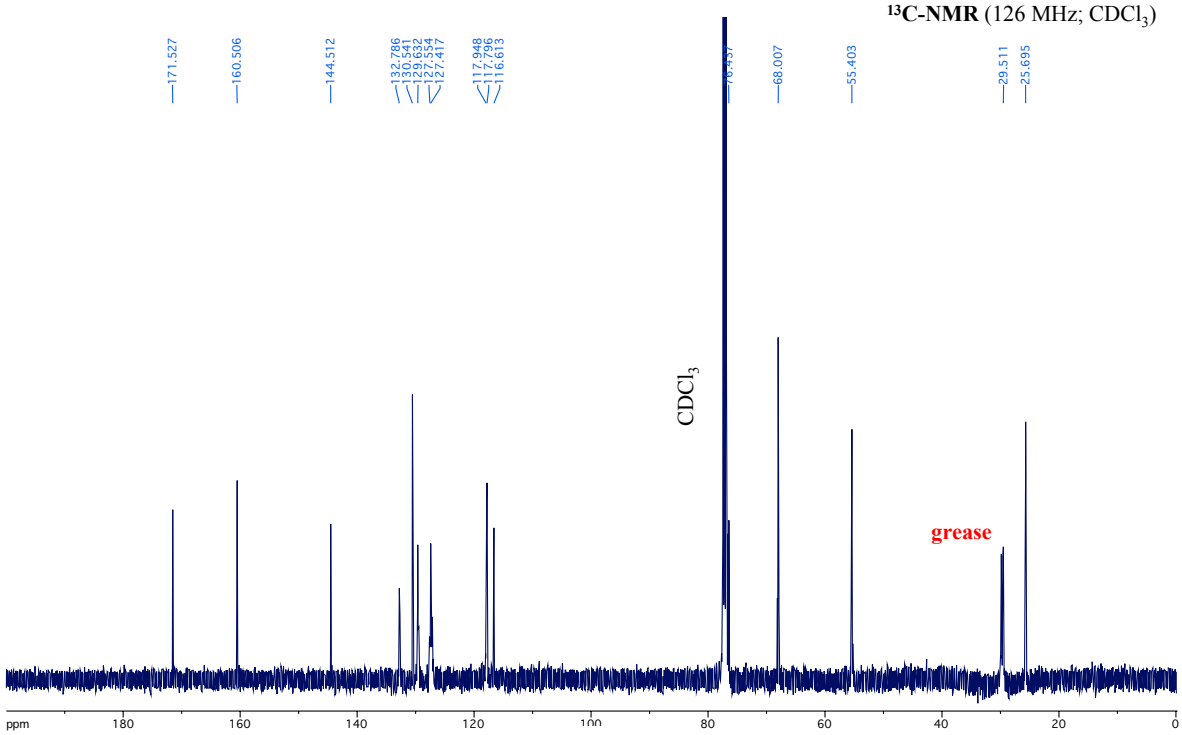

**$^{1}$H-NMR** (400 MHz; $CDCl_3$)

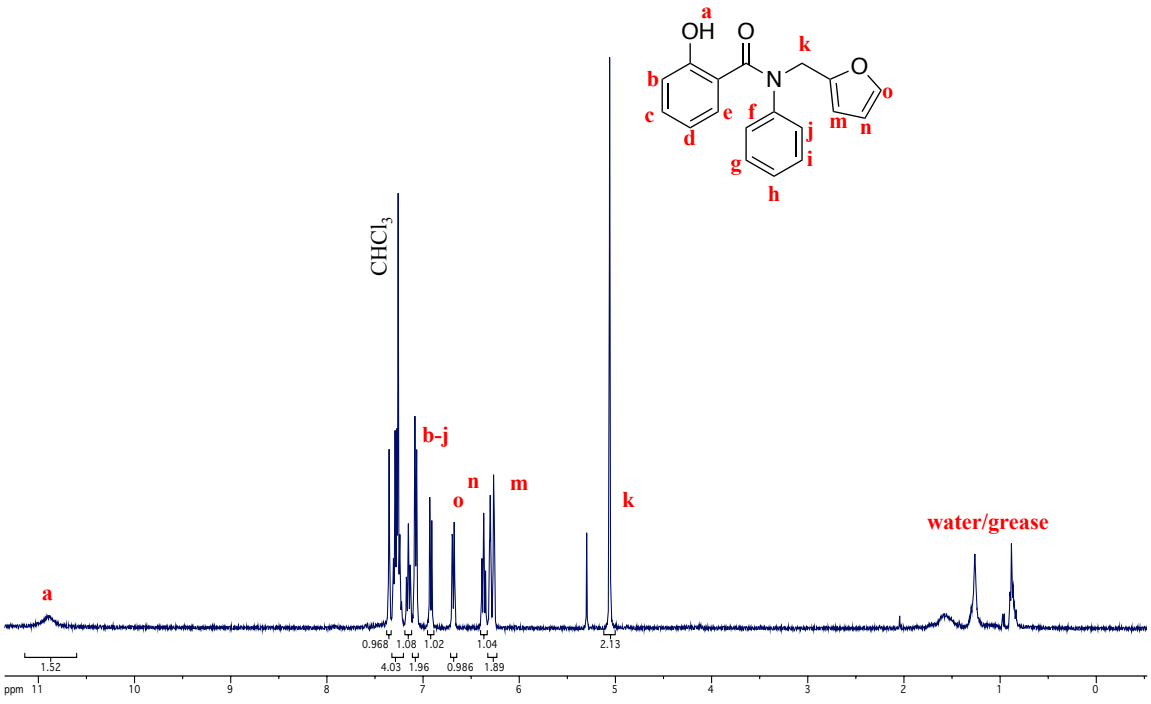


**$^{13}$C-NMR** (126 MHz; $CDCl_3$)

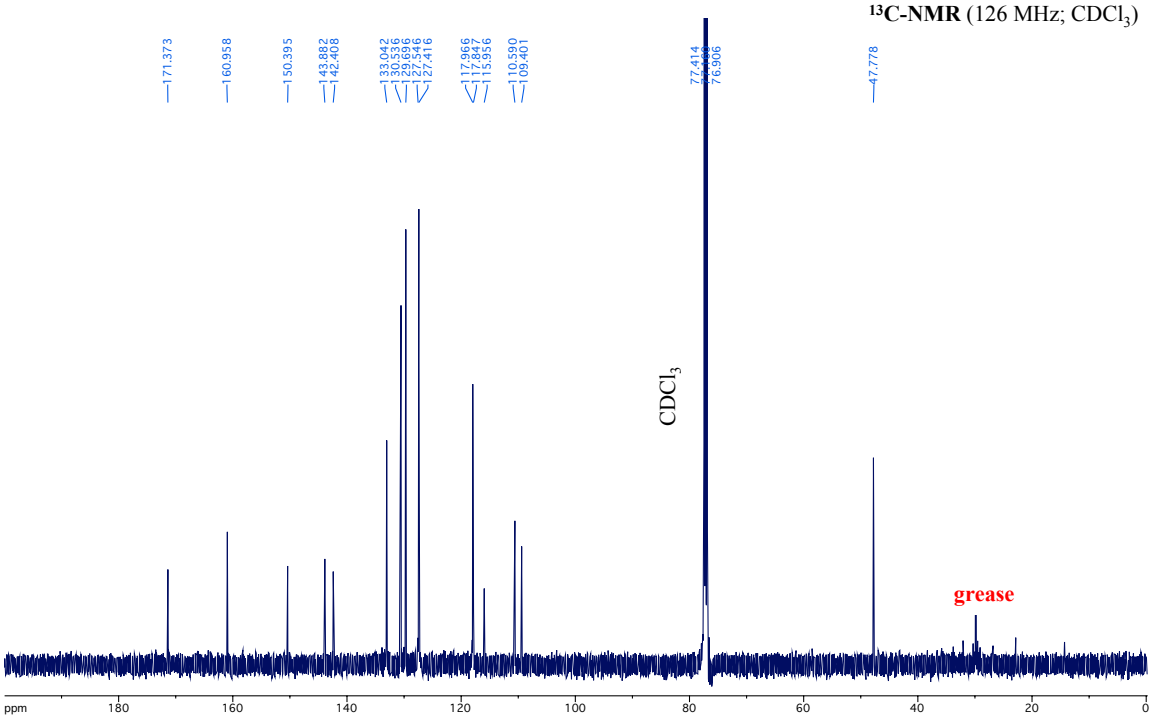

**$^1$H-NMR** (400 MHz; $CDCl_3$)

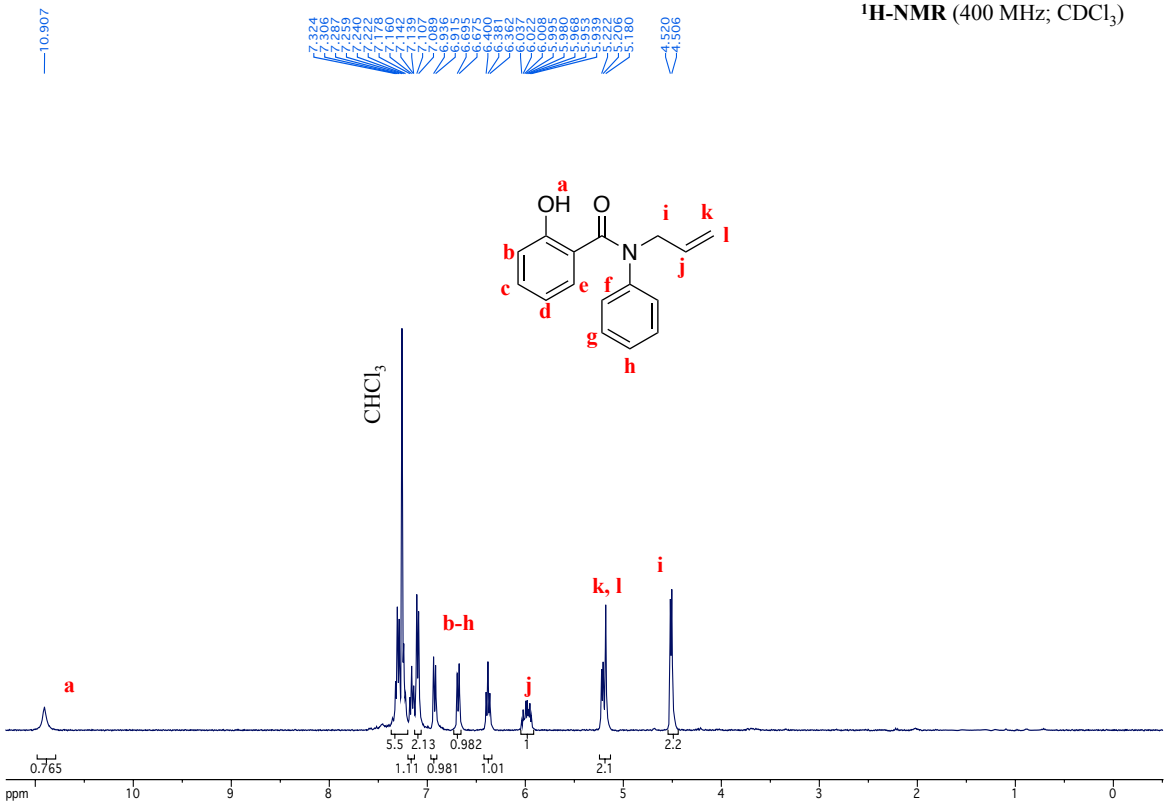


**$^{13}$C-NMR** (126 MHz; $CDCl_3$)

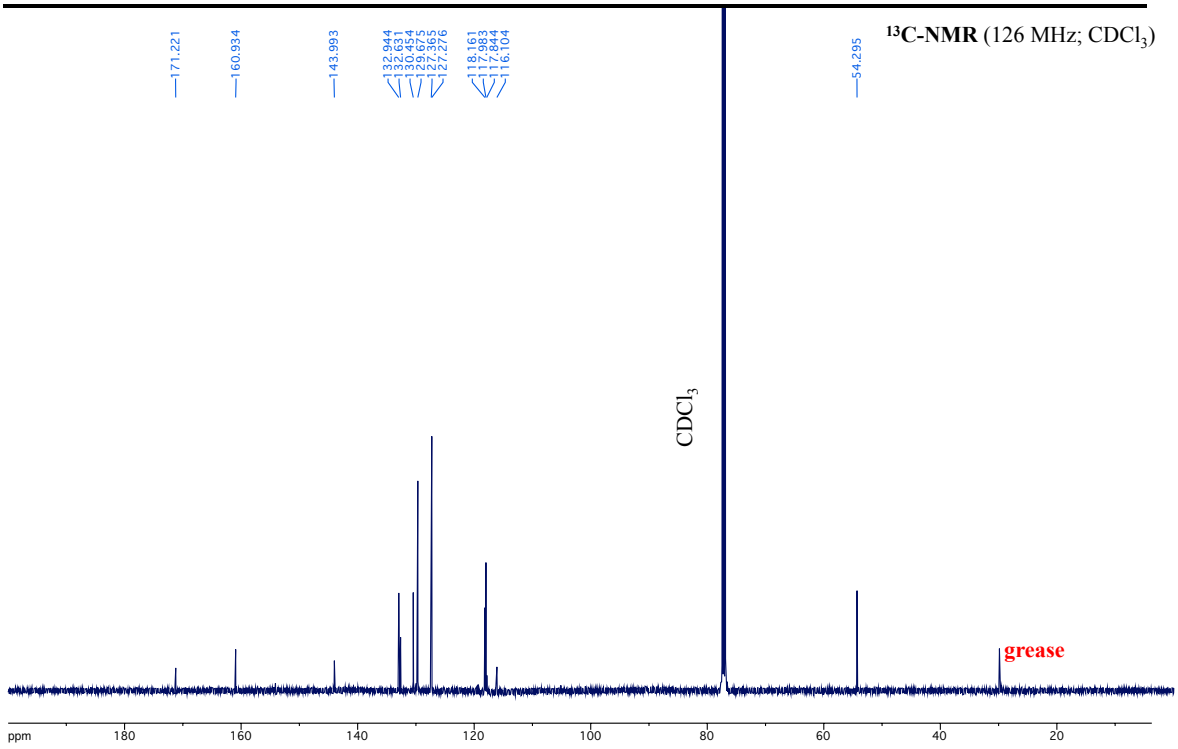

**$^{1}$H-NMR** (400 MHz; $CDCl_3$)

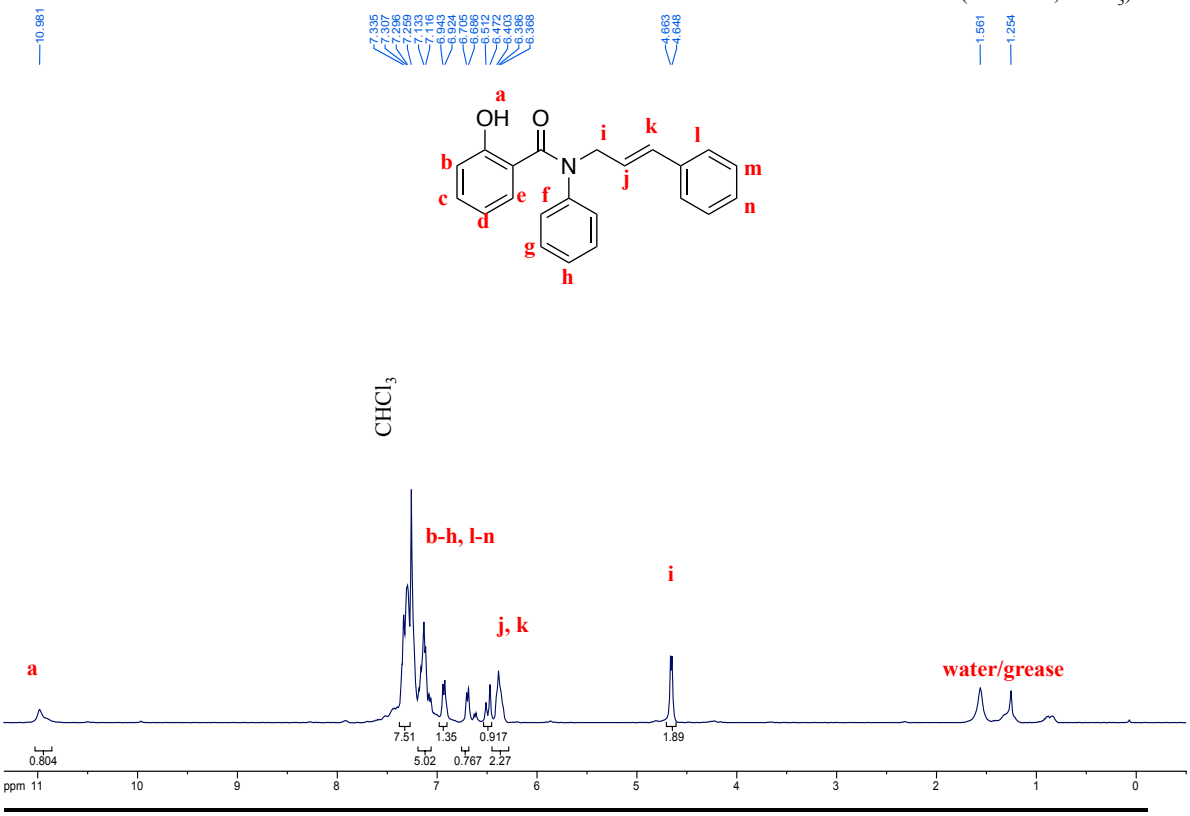


**$^{13}$C-NMR** (126 MHz; $CDCl_3$)

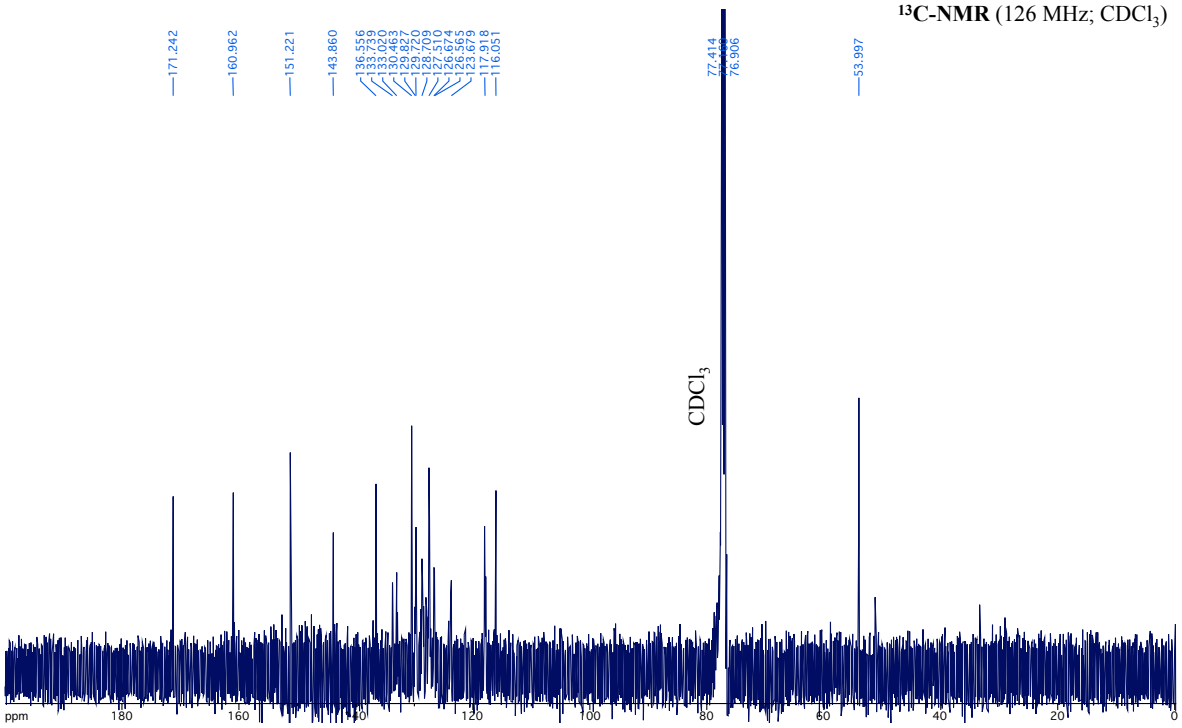

**$^{1}$H-NMR** (400 MHz; $CDCl_3$)

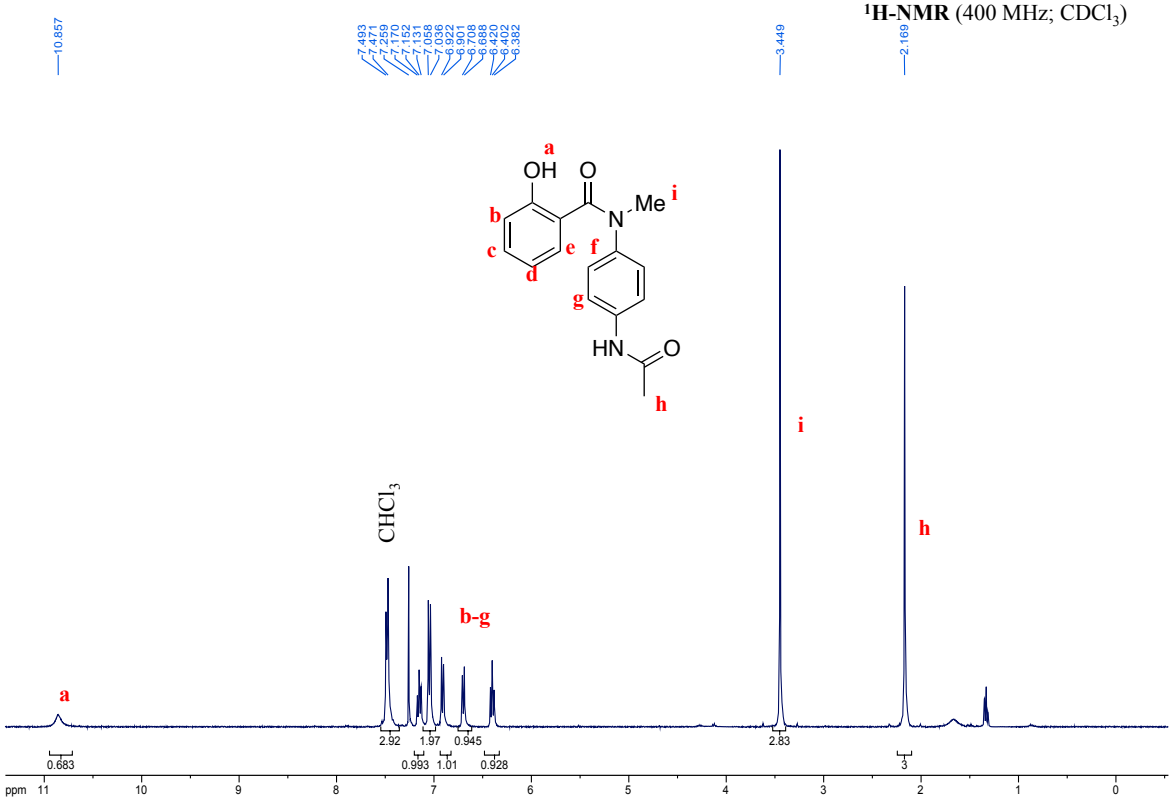


**$^{13}$C-NMR** (126 MHz; $CDCl_3$)

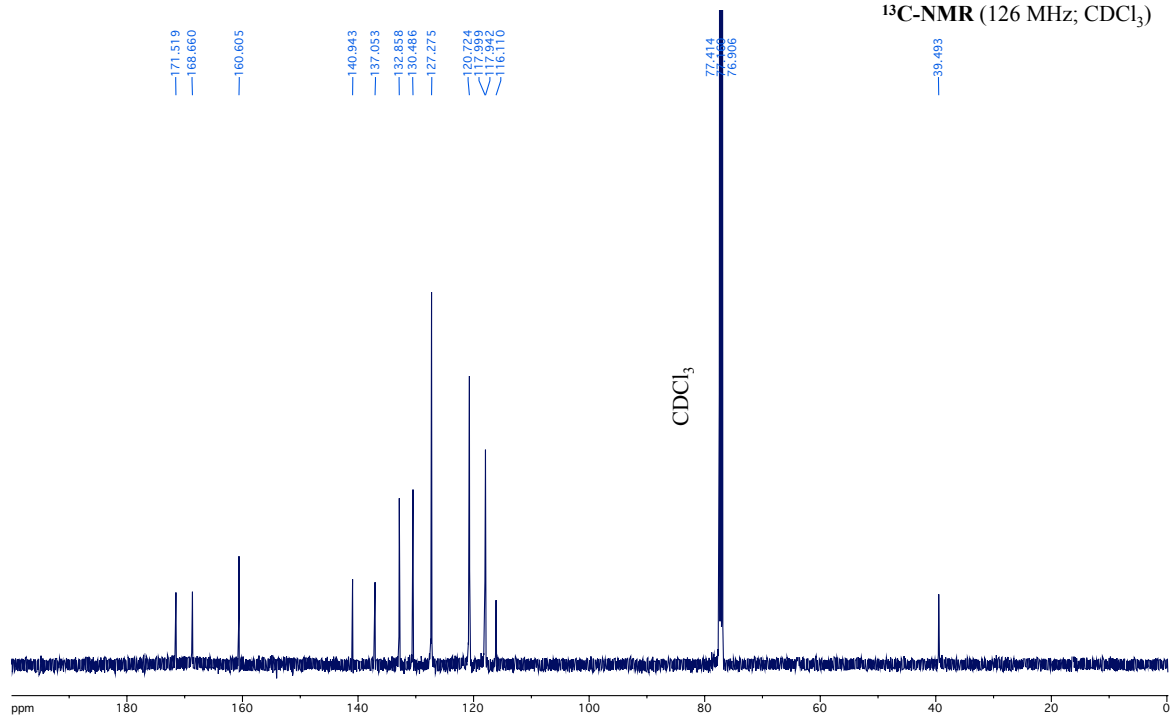

**$^{1}$H-NMR** (400 MHz; $CDCl_3$)

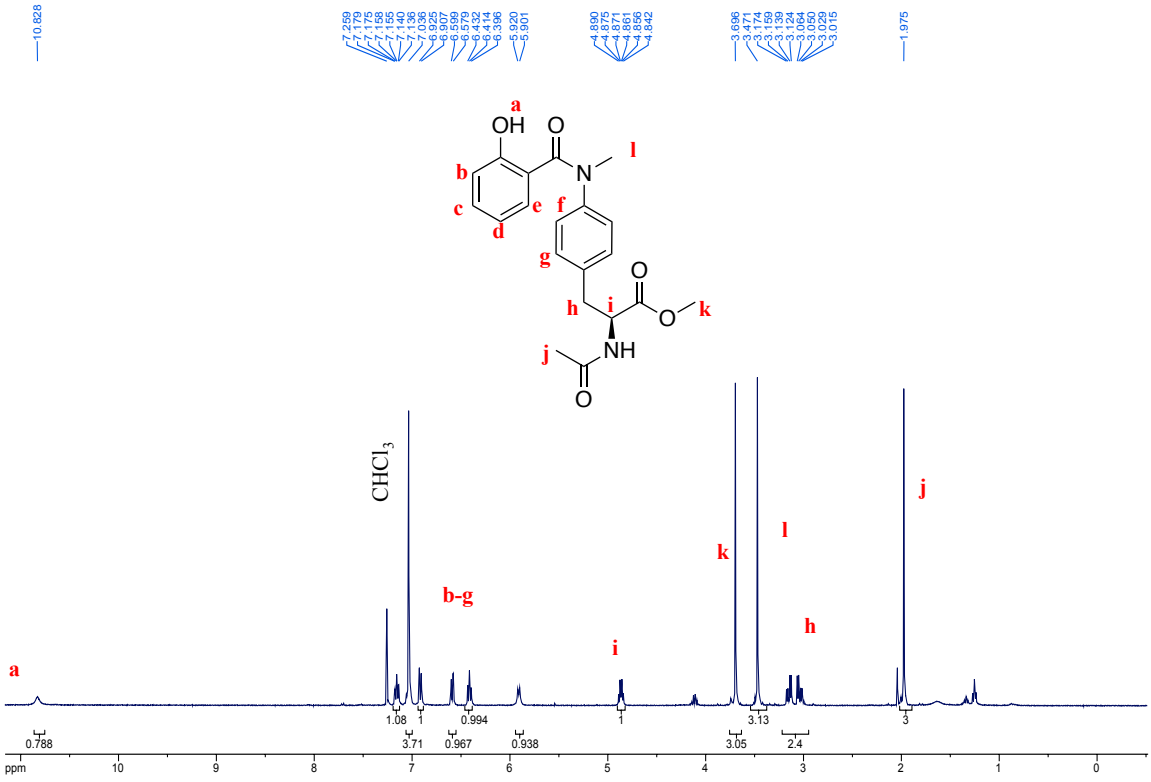


**$^{13}$C-NMR** (126 MHz; $CDCl_3$)

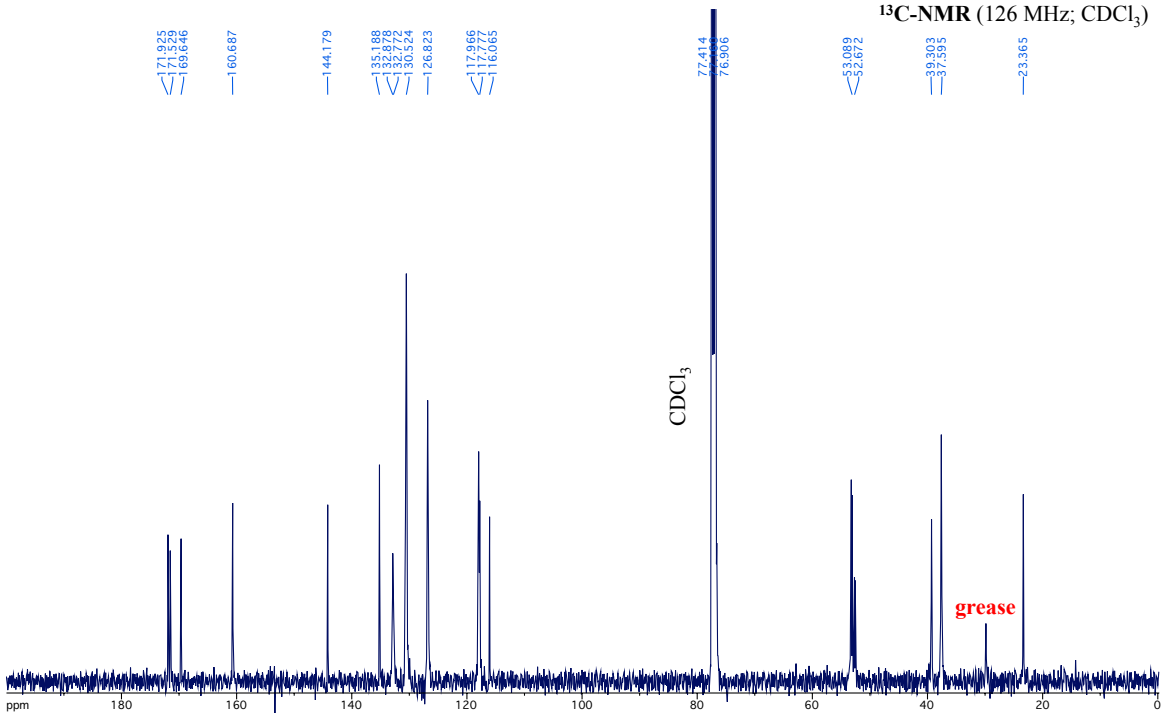

**$^{1}$H-NMR** (400 MHz; $CDCl_3$)

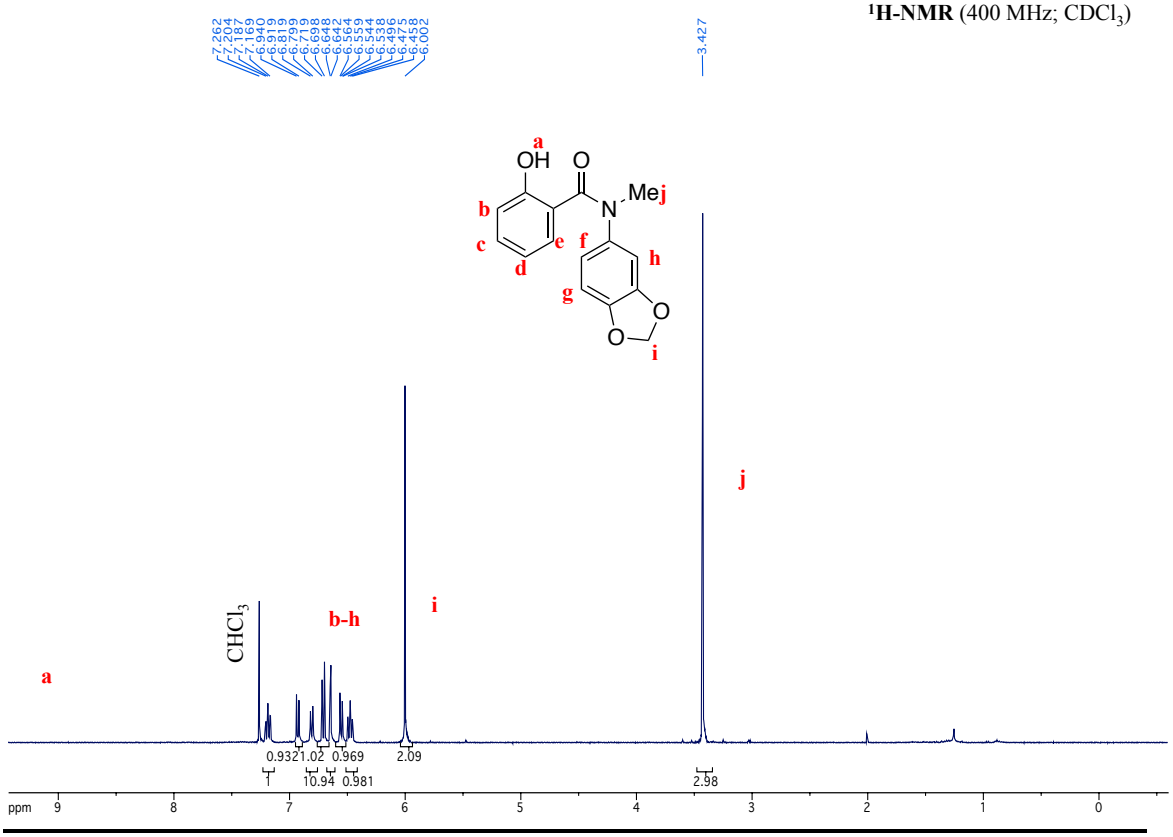


**$^{13}$C-NMR** (126 MHz; $CDCl_3$)

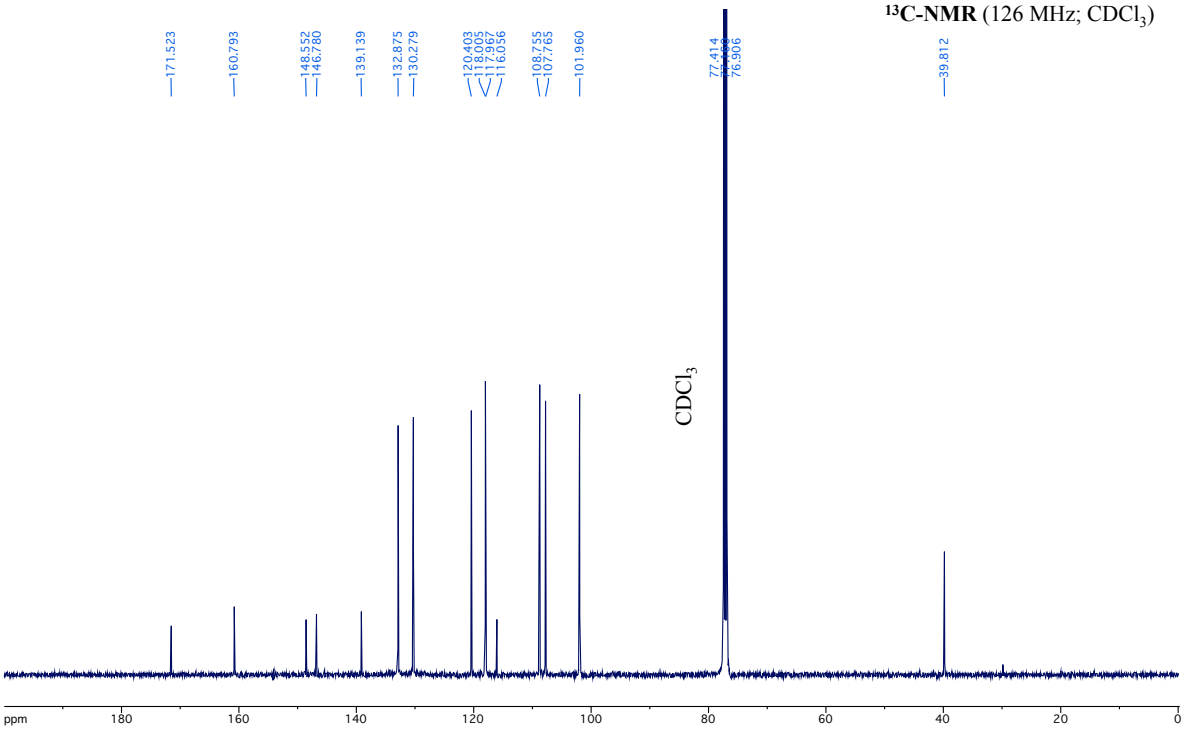

**$^{1}$H-NMR** (400 MHz; $CDCl_3$)

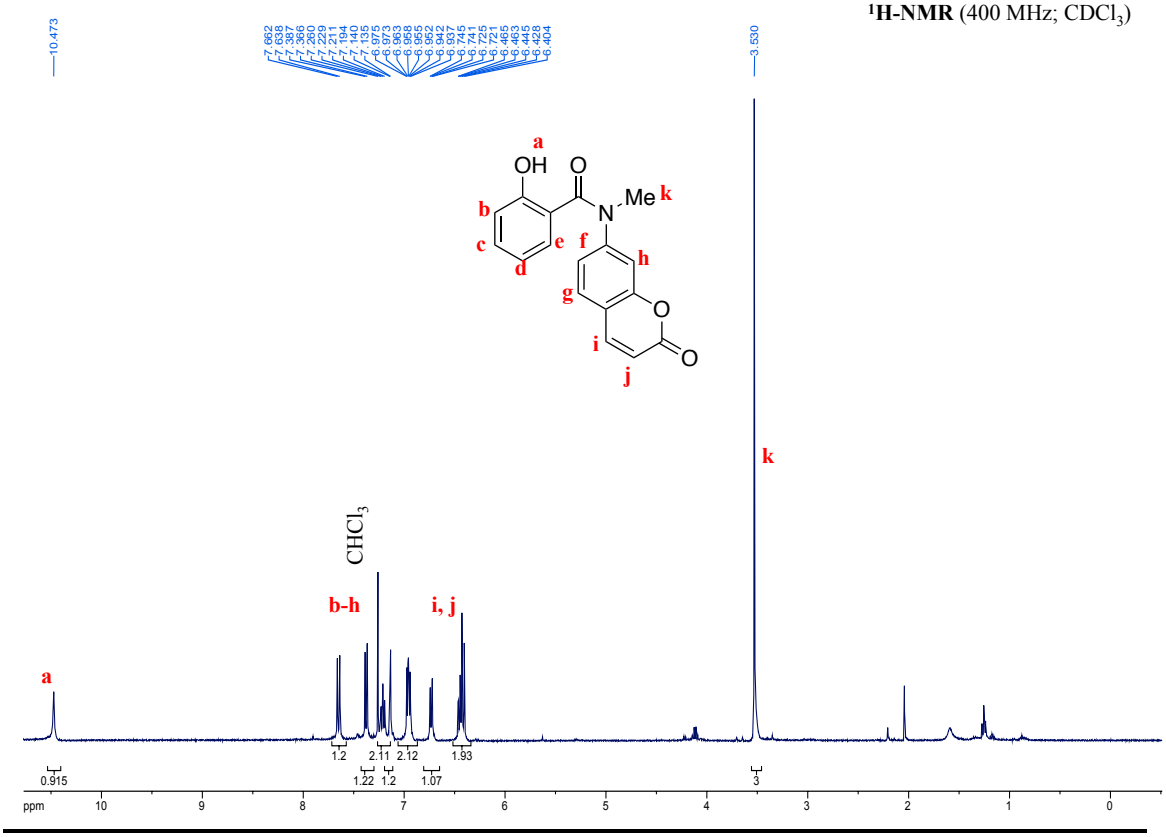


**$^{13}$C-NMR** (126 MHz; $CDCl_3$)

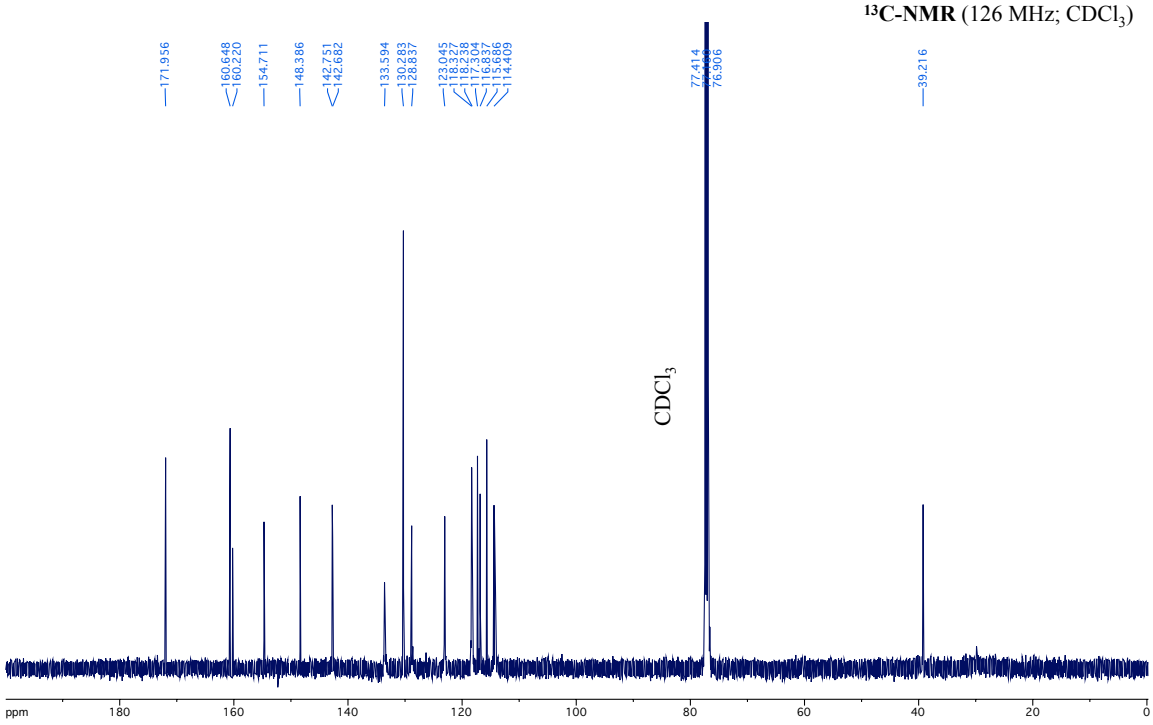

**$^{1}$H-NMR** (400 MHz; $CDCl_3$)

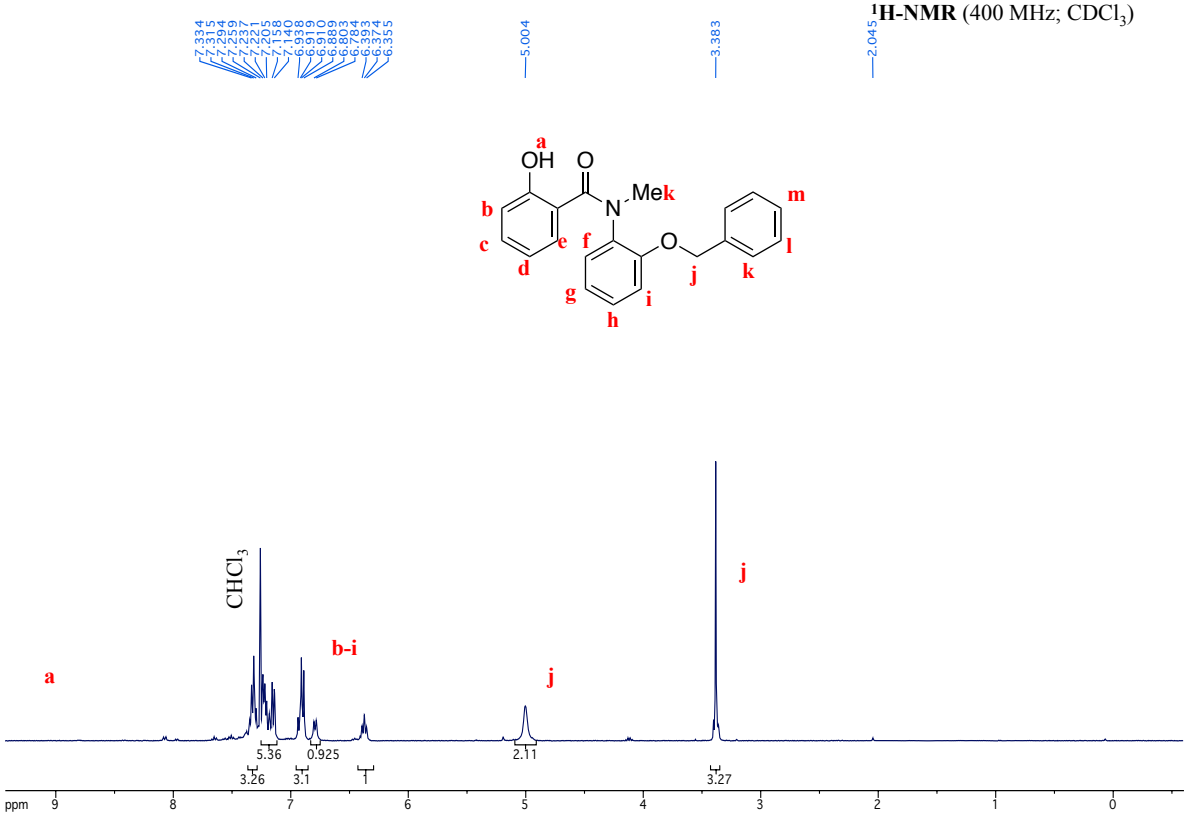


**$^{13}$C-NMR** (126 MHz; $CDCl_3$)

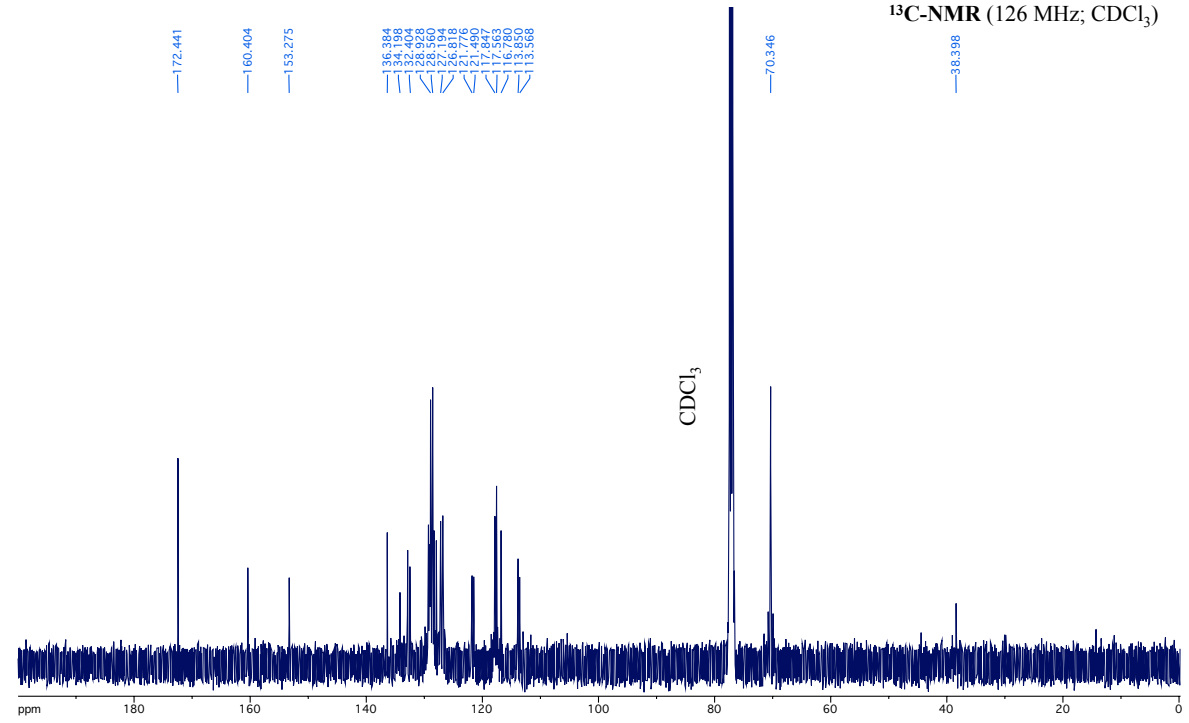

**$^{1}$H-NMR** (400 MHz; $CDCl_3$)

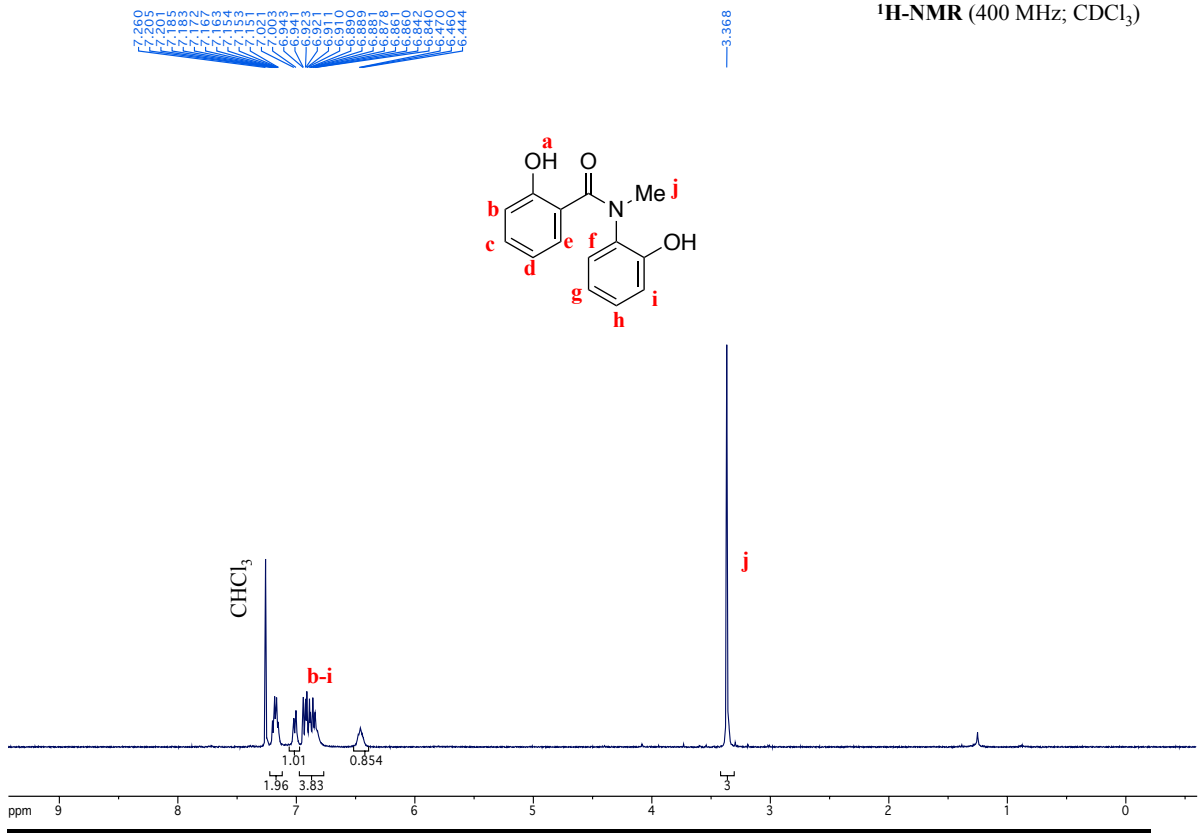


**$^{13}$C-NMR** (126 MHz; $CDCl_3$)

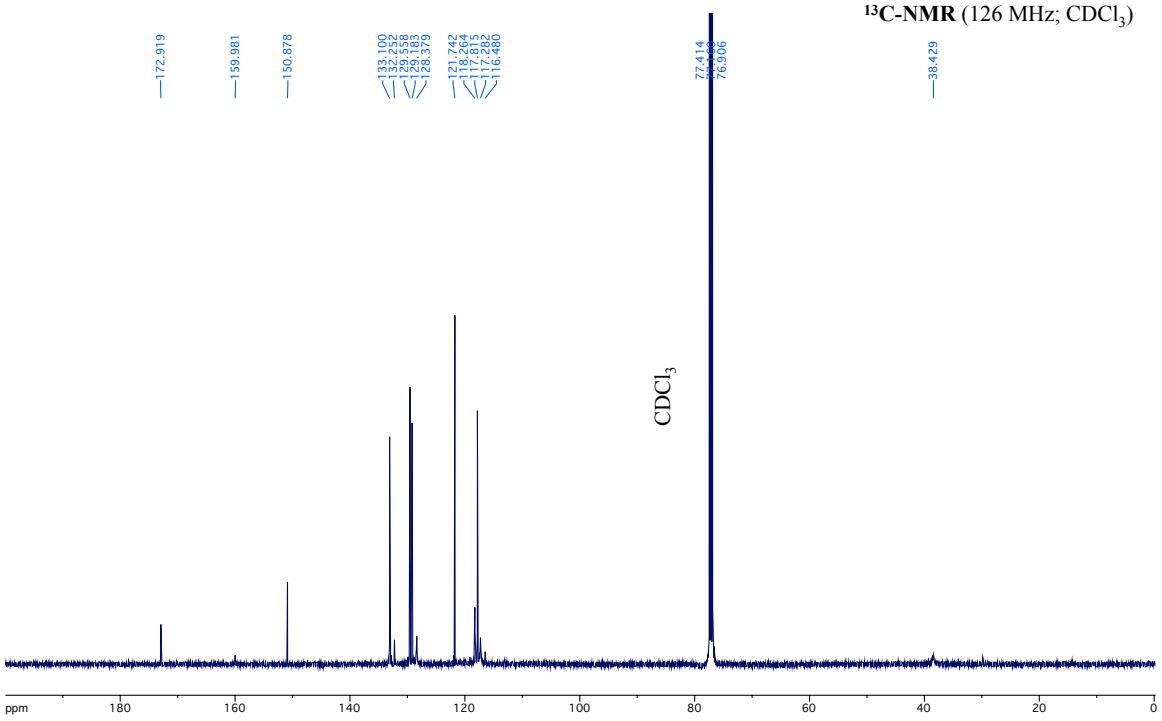

**$^{1}$H-NMR** (400 MHz; $CDCl_3$)

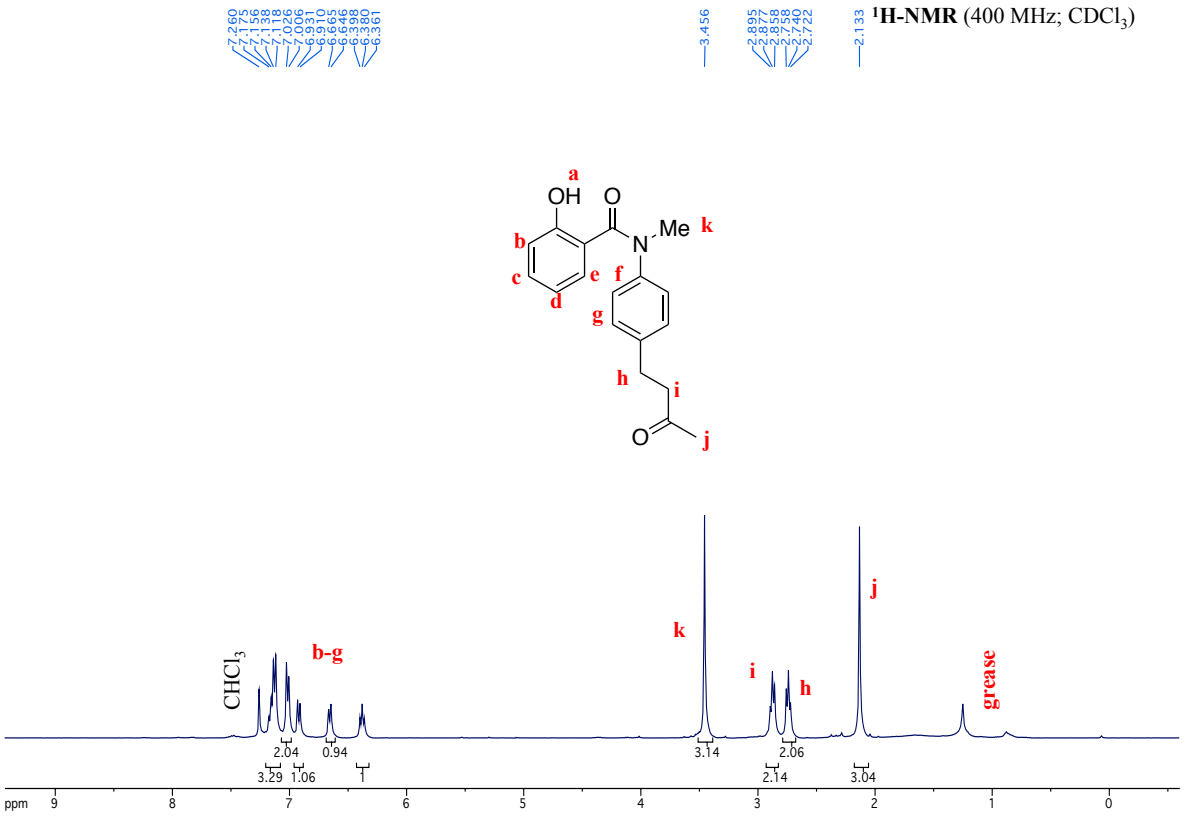


**$^{13}$C-NMR** (126 MHz; $CDCl_3$)

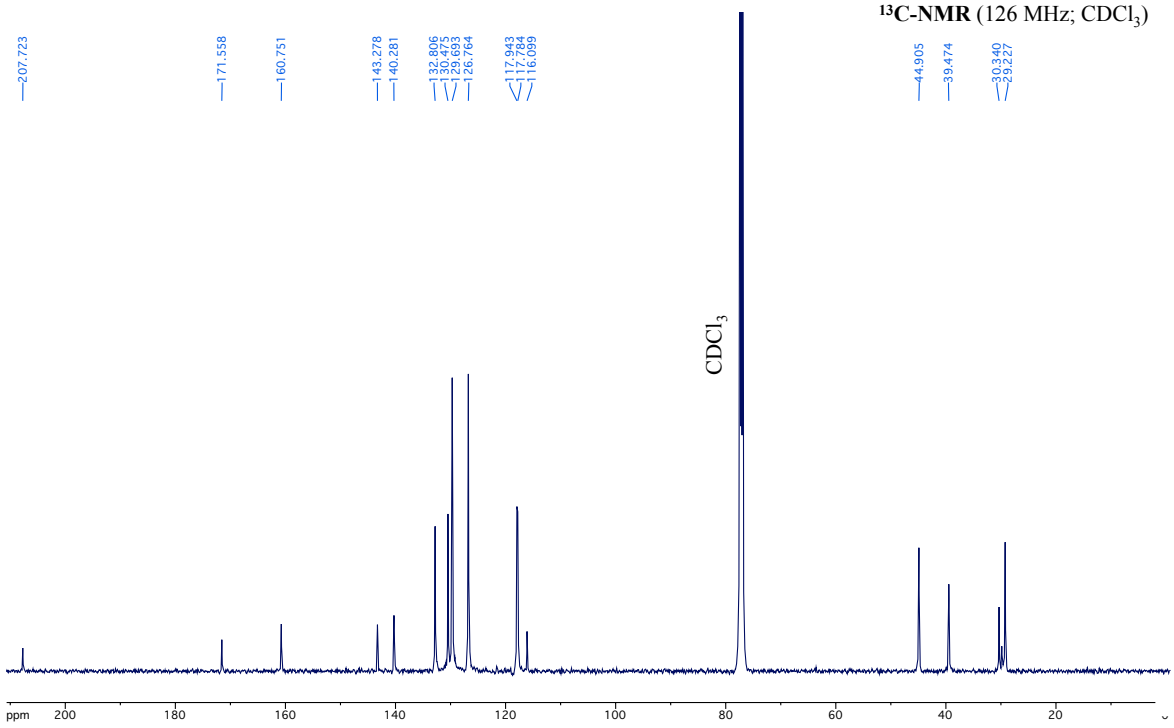

**$^{1}$H-NMR** (400 MHz; DMSO-d6)

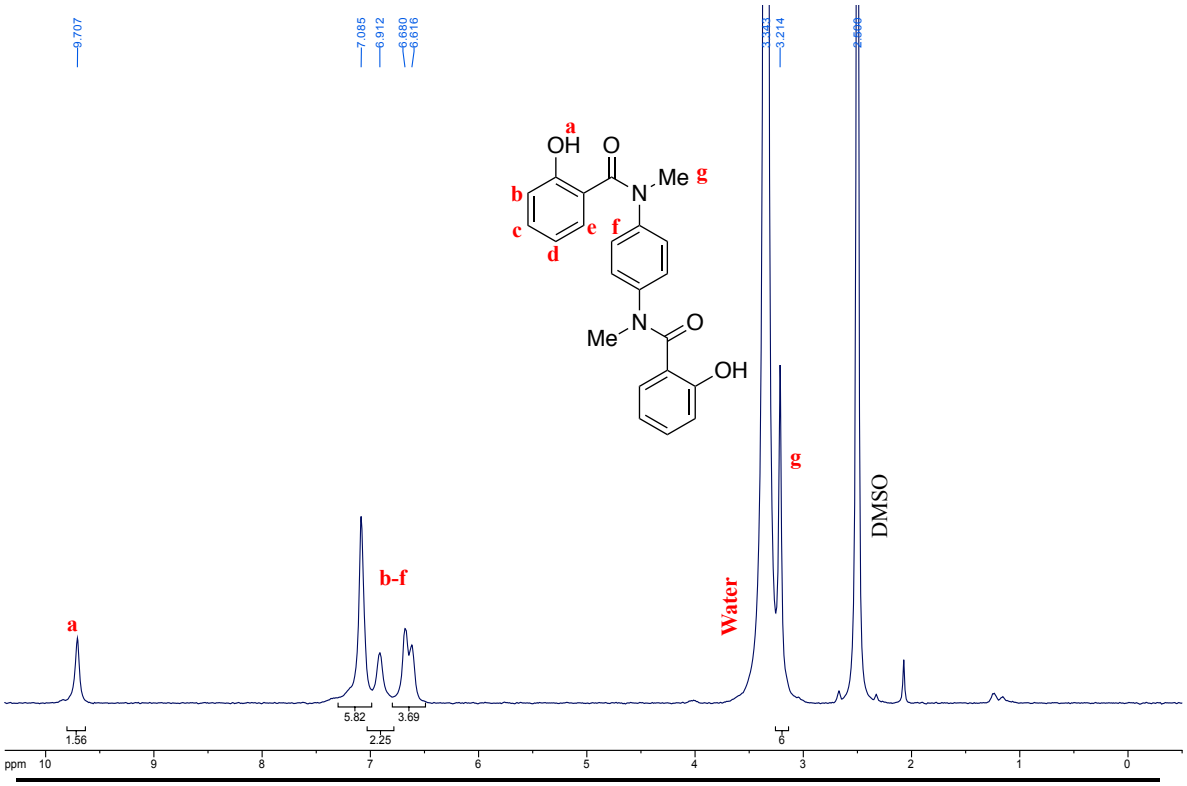


**$^{13}$C-NMR** (126 MHz; DMSO-d6)

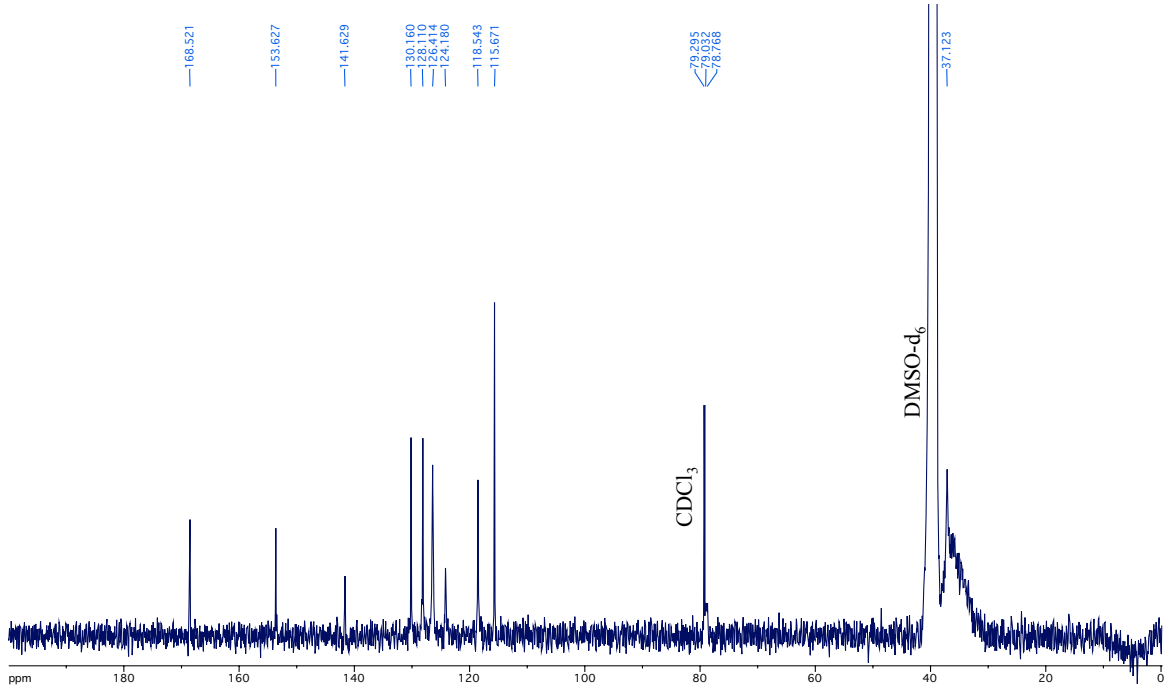

**$^1$H-NMR** (400 MHz; $CDCl_3$)

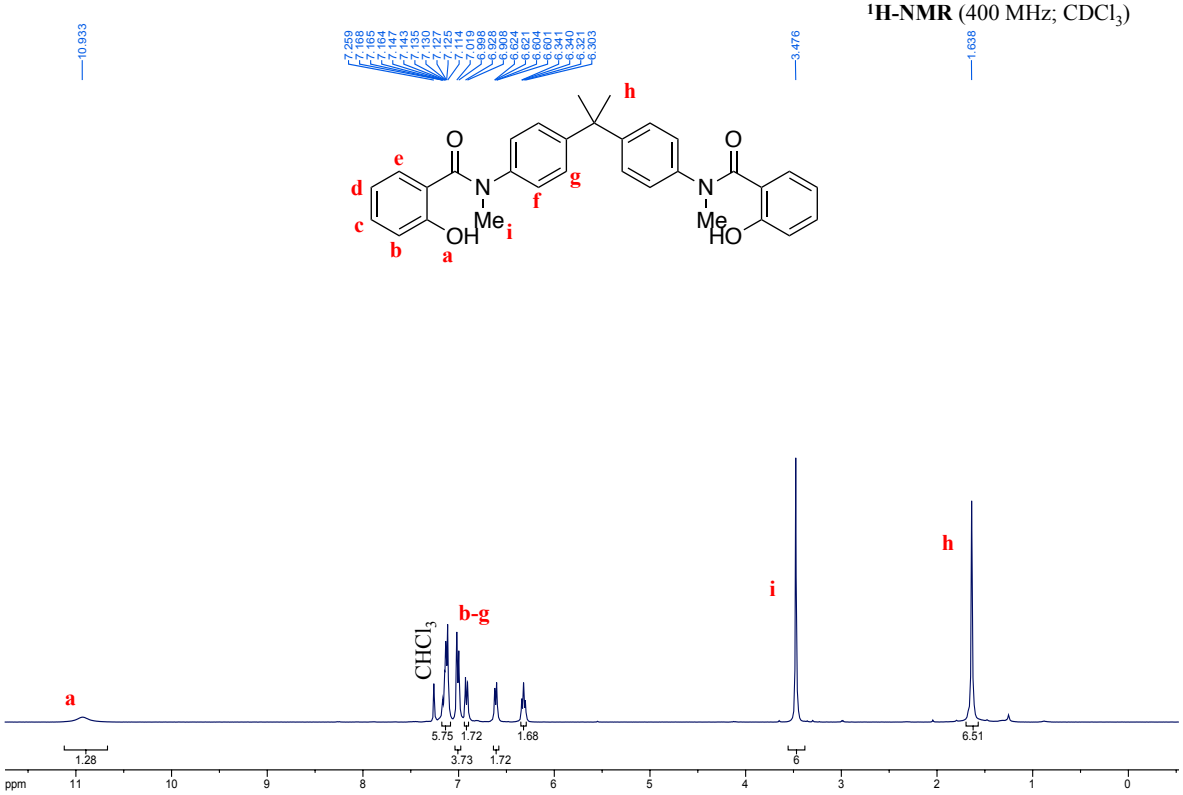


**$^{13}$C-NMR** (126 MHz; $CDCl_3$)

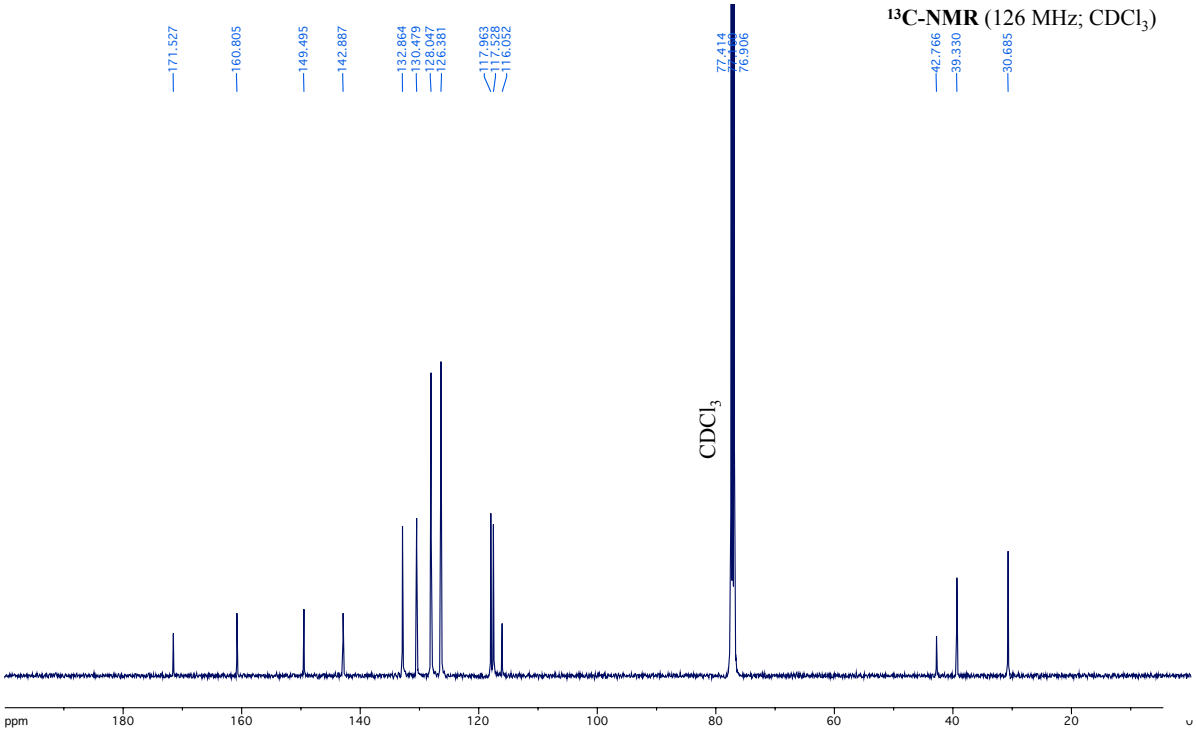

**$^{1}$H-NMR** (400 MHz; DMSO-d6)

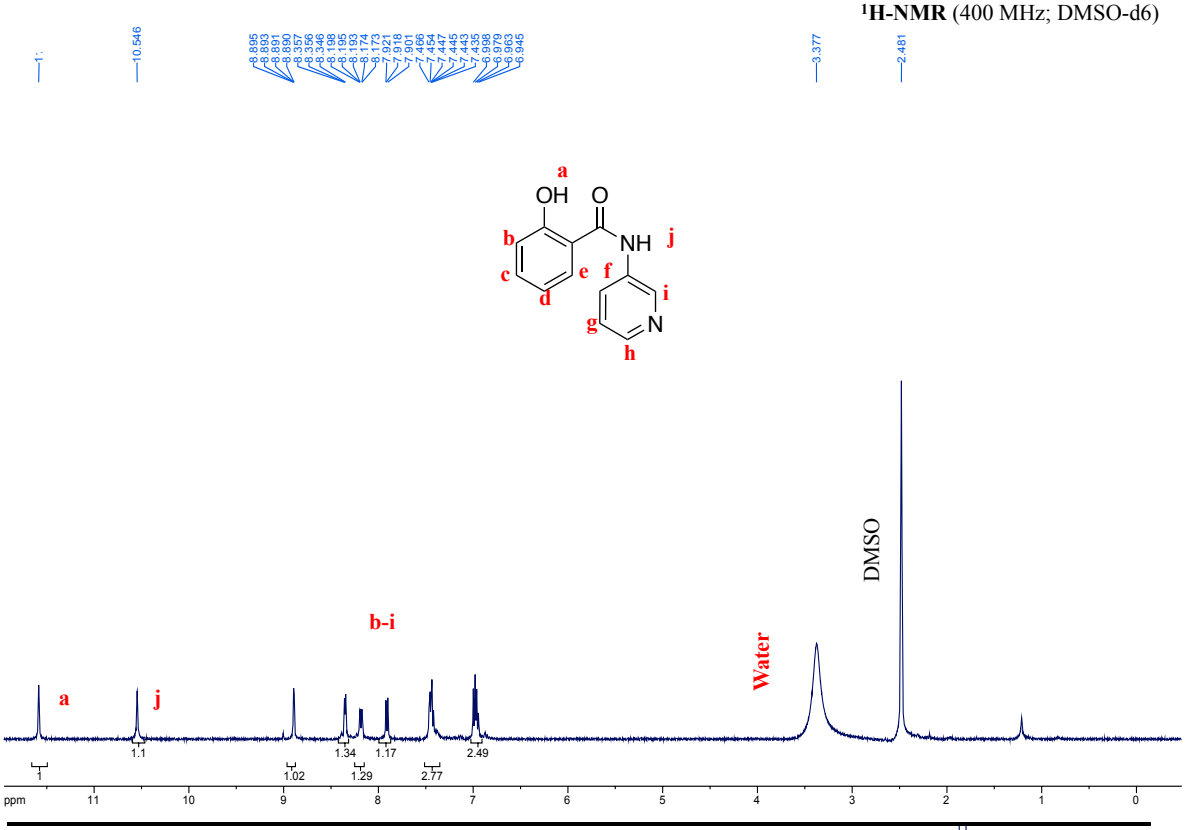


**$^{13}$C-NMR** (126 MHz; DMSO-d6)

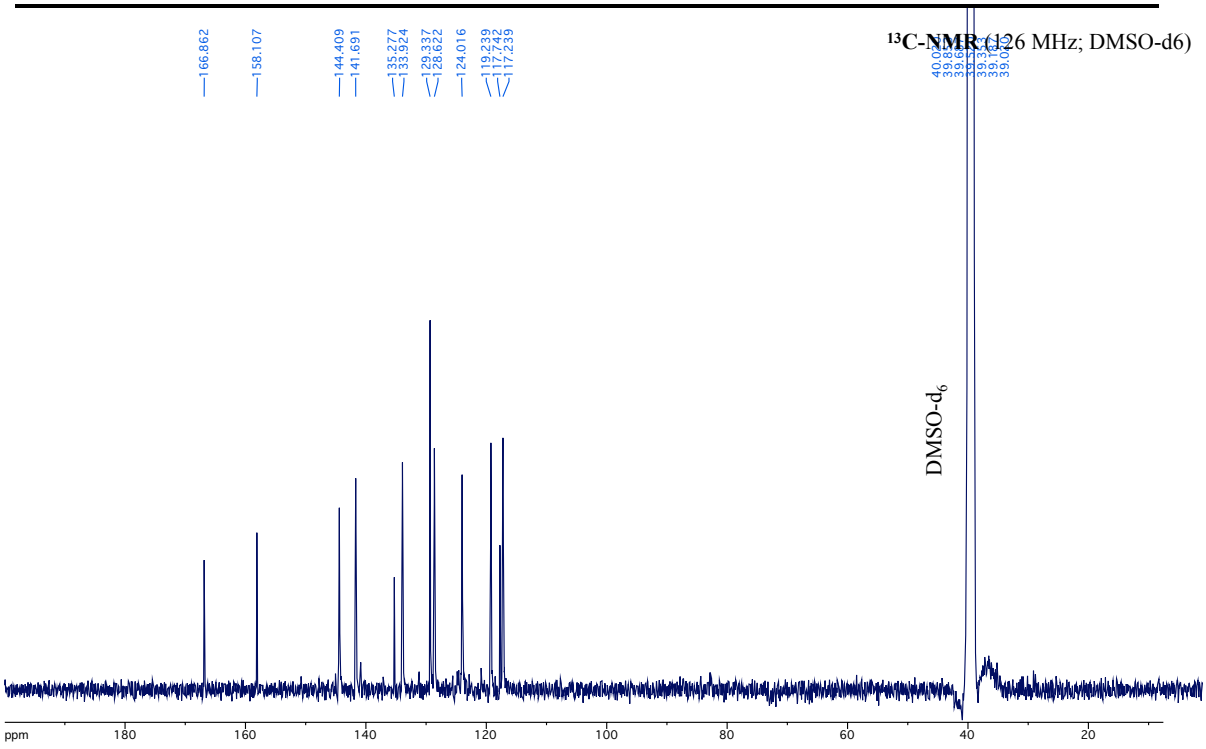

**$^{1}$H-NMR** (400 MHz; $CDCl_3$)

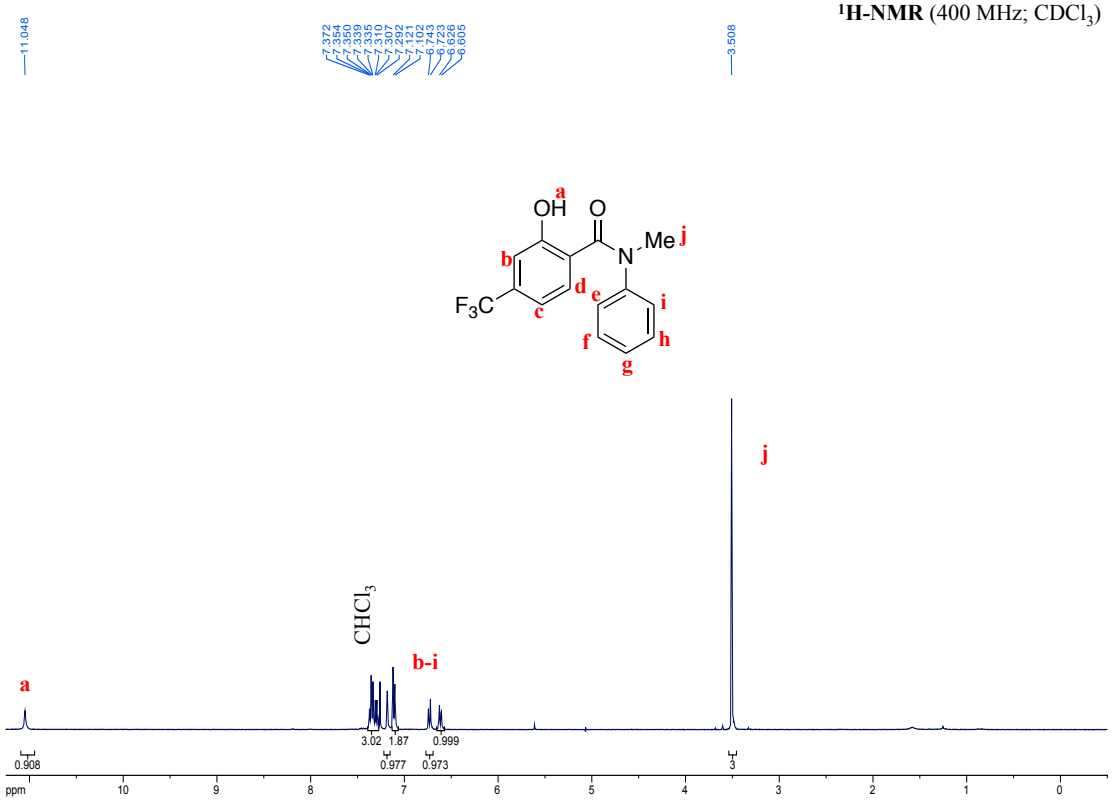


**$^{13}$C-NMR** (126 MHz; $CDCl_3$)

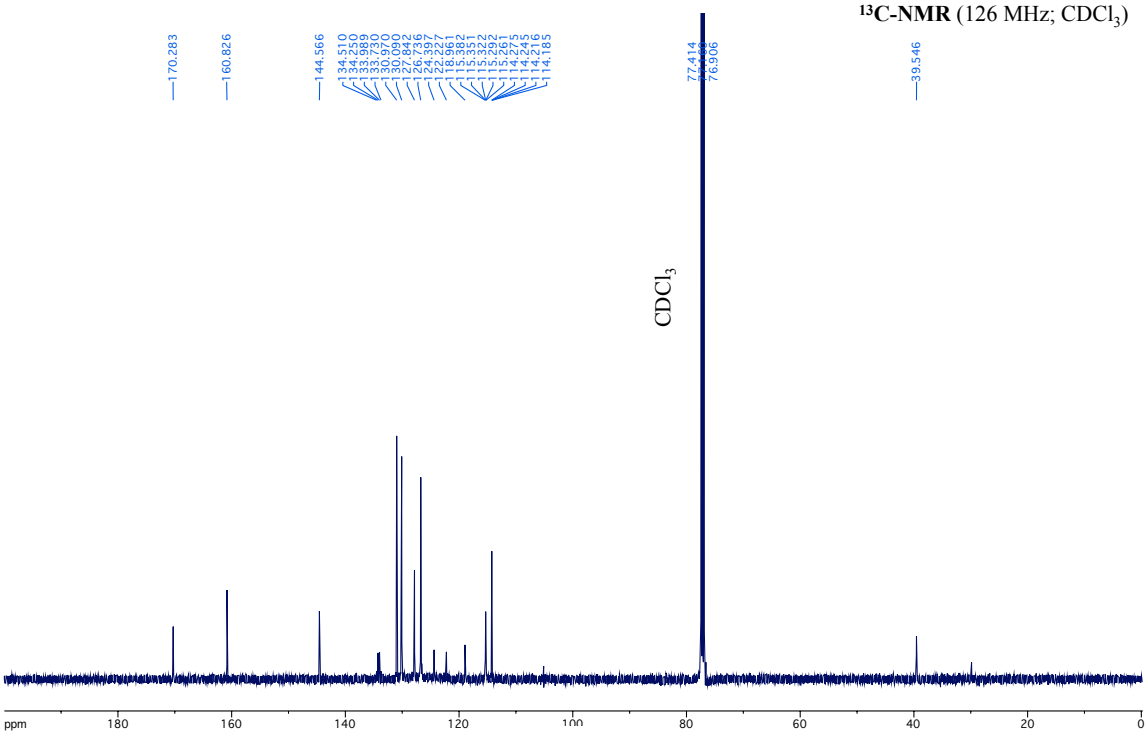

**$^1$H-NMR** (400 MHz; $CDCl_3$)

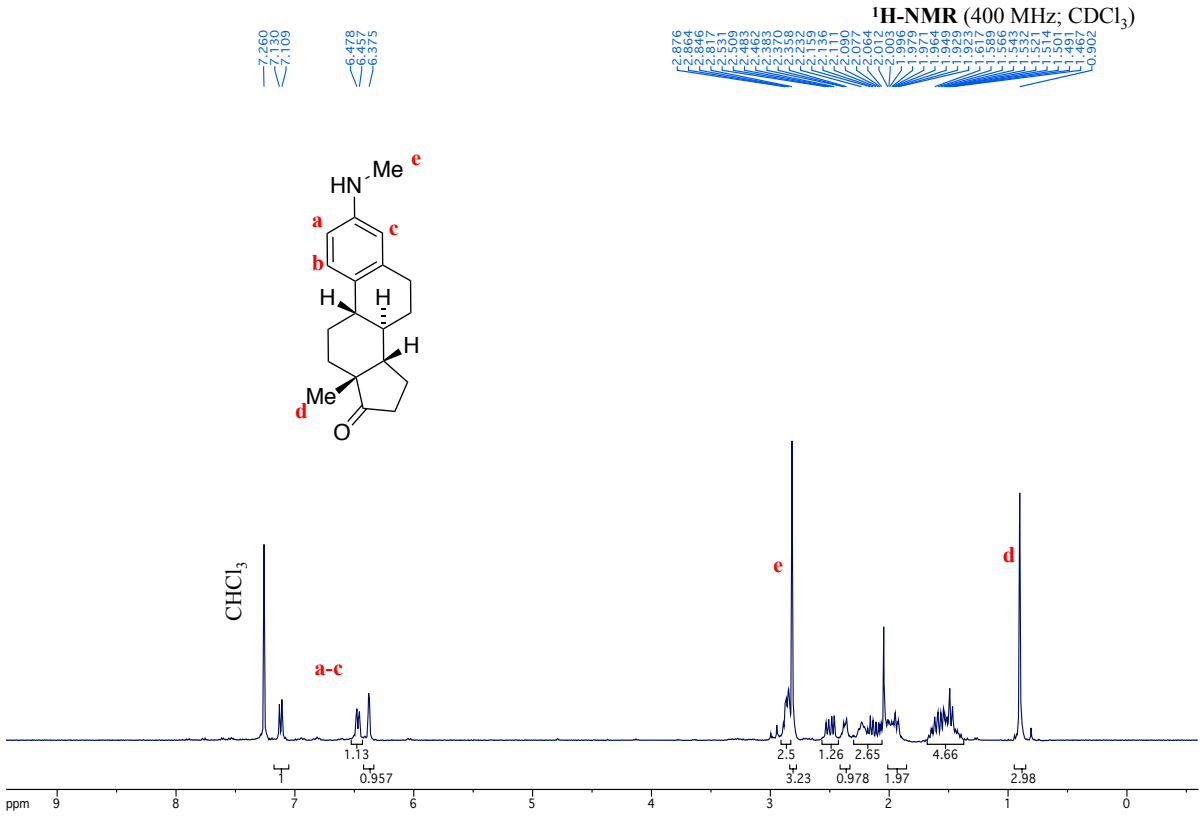


**$^{13}$C-NMR** (126 MHz; $CDCl_3$)

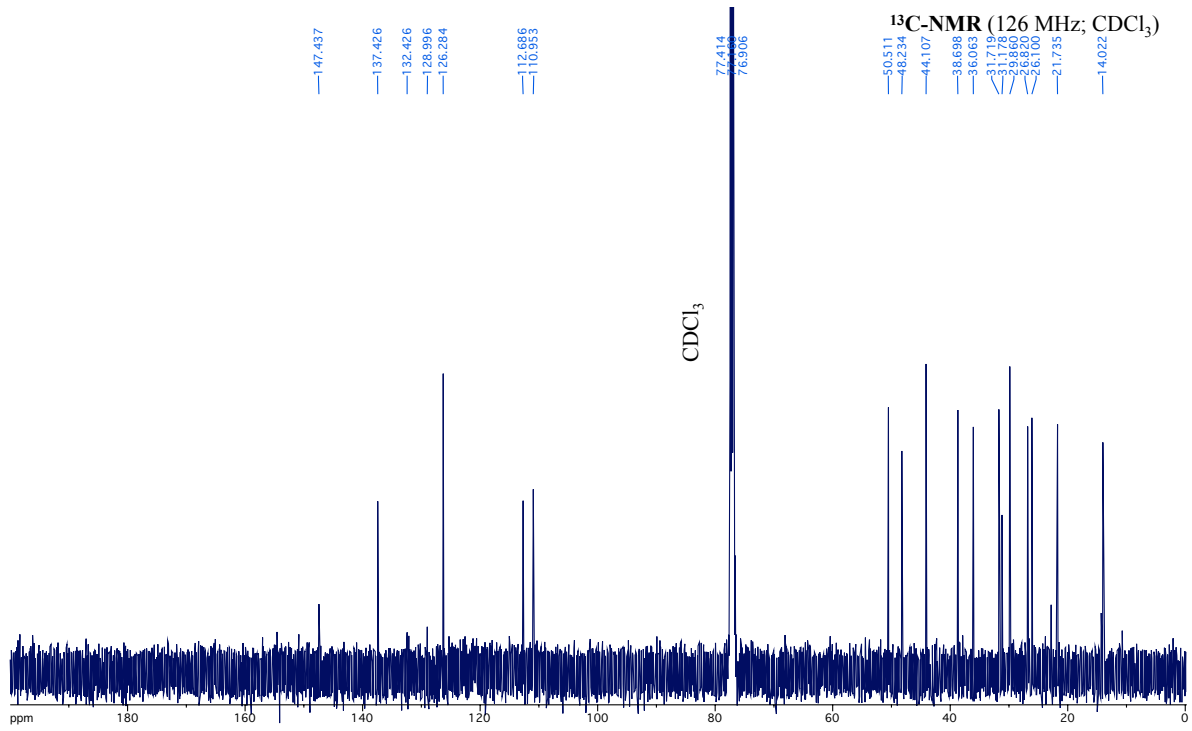

## 3.7 References


[1] Rappoport, R. in *The Chemistry of Anilines*, Wiley, 2007.

[2] Smith, M. B. in March's Advanced Organic Chemistry (7 ed), Wiley, 2015

[3] (a) Sambiagio, C.; Marsden, S. P.; Blacker, A. J.; McGowan, P. C. Copper catalysed Ullman type chemistry: from mechanistic aspects to modern development. *Chem. Soc. Rev.* **2014**, *43*, 3525 – 3550. DOI: 10.1039/C3CS60289C. (b) Creutz, S. E.; Lotito, K. J.; Fu, G. C.; Peters, J. C. Photoinduced Ullman C-N Coupling: Demonstrating the Viability of a Radical Pathway. *Science* **2012**, *338*, 647 – 651. DOI: 10.1126/science.1226458.

[4] Ryuiz-Castillo, P.; Buchwald, S. L. Applications of Palladium Catalyzed C-N Cross Coupling Reactions. *Chem. Rev.* **2016**, *116*, 12564 – 12564. DOI: 10.1021/acs.chemrev.6b00512

[5] (a) Shen, Q.; Shekhar, S.; Stambuli, J. P.; Hartwig, J. F. Highly Reactive, General, and Long-Lived Catalysts for Coupling Heteroaryl and Aryl Chlorides with Primary Nitrogen Nucleophiles. *Angew. Chem. Int. Ed*. **2005**, *44*, 1371−1375. DOI: 10.1002/anie.200462629. (b) Shen, Q.; Ogata, T.; Hartwig, J. F. Highly Reactive, General and Long-Lived Catalysts for Palladium-Catalyzed Amination of Heteroaryl and Aryl Chlorides, Bromides, and Iodides: Scope and Structure-Activity Relationships. *J. Am. Chem. Soc*. **2008**, *130*, 6586−6596. DOI: 10.1021/ja077074w.

[6] Chan, D. M. T.; Monaco, K. L.; Wang, R.-P.; Winters, M. P. New N- and O-arylations with phenylboronic acids and cupric acetate. *Tetrahedron Lett.* **1998**, *39*, 2933 – 2936. DOI: 10.1016/S0040-4039(98)00503-6.

[7] Lam, P. Y. S.; Clark, C. G.; Saubern, S.; Adams, J.; Winters, M. P.; Chan, D. M. T.; Combs, A. New aryl/heteroaryl C-N bond cross-coupling reactions via arylboronic acid/cupric acetate arylation. *Tetrahedron Lett.* **1998**, *39*, 2941-2944. DOI: 10.1016/S0040-4039(98)00504-8.

[8] (a) Hartwig, J. F., Shekhar, S., Shen, Q., Barrios-Landeros, F. in *PATAI'S Chemistry of Functional Groups*, Wiley, 2009 (b) Beletskaya, I. P.; Cheprakov, A. V. Copper in cross-coupling reactions: The post-Ullmann chemistry. *Coor. Chem. Rev.* **2004**, *248*, 2337-2364 DOI: 10.1016/j.ccr.2004.09.014 (c) Bariwal, J.; Van der Eycken, E. C-N bond forming cross-coupling reactions: an overview. *Chem. Soc. Rev.* **2013**, *42*, 9283-9303. DOI: 10.1039/c3cs60228a (d) Beletskaya, I, P.; Cheprakov, A, V. The Complementary Competitors: Palladium and Copper in C-N Cross-Coupling Reactions. *Organometallics* **2012**, *31*, 7753-7808. DOI: 10.1021/om300683c (e) Joseph, J. A.; Pritadarshini, S. Copper-Mediated C-X functionalization of Aryl Halides. *Org. Process Res. Dev.* **2017,** *21*, 1889-1924. DOI: 10.1021/acs.oprd.7b00285

[9] (a) Voth, S.; Hollett, J. W.; McCubbin, J. A. Transition-Metal-Free Access to Primary Anilines from Boronic Acids and a Common $+NH_2$ Equivalent. *J. Org. Chem.* **2015**, *80*, 2545-2553 DOI: 10.1021/jo5025078 (b) Chatterjee, N.; Goswami, A. Metal and base free synthesis of primary amines *via ipso* amination of organoboronic acids mediated by [bis(trifluoroacetoxy)iodo]benzene (PIFA). *Org. Biomol. Chem.* **2015**, *13*, 7940-7945. DOI: 10.1039/C5OB01070E (c) Llangovan,

A.; Sakthivel, P.; Sakthivel, P. Green and practical transition metal-free one-pot conversion of substituted benzoic acids to anilines using tosyl azide. *Org. Chem. Front.* **2016**, *3*, 1680-1685. DOI: 10.1039/C6QO00343E (d) Prakash, G. K. S.; Gurung, L.; Marinez, E. R.; Mathew, T.; Olah, G. A. Electrophilic amination of aromatics with sodium azide in BF3-H2O *Tetrahedron Lett.* **2016**, *57*, 288-291. DOI: 10.1016/j.tetlet.2015.11.104 (e) Sun, H.-B.; Gong, L.; Tian, Y.-B.; Wu, J.-G.; Zhang, X.; Liu, J.; Fu, Z.; Niu, D. Metal- and Base-Free Room-Temperature Amination of Organoboronic Acids with N-Alkyl Hydroxylamines. *Angew. Chem. Int. Ed.* **2018**, *57*, 9456-9460. DOI: 10.1002/anie.201802782

[10] For a gas phase, industrial example of direct phenol to aniline conversion, see: Becker, M.; Khoobiar, S. Process for the production of organic amines. US 3860650 A. January 14, 1975.
For more examples please see: (a) Rosen, B. M.; Quasdorf, K. W.; Wilson, D. A.; Zhang, N.; Resmerita, A.-M.; Garg, N. K.; Percec, V. Nickel-Catalyzed Cross-Couplings Involving Carbon-Oxygen Bonds. *Chem. Rev.* **2011**, *111*, 1346−1416. DOI: 10.1021/cr100259t. (b) Li, B.-J.; Yu, D.-G.; Sun, C.-L.; Shi, Z.-J. Activation of "Inert" Alkenyl/Aryl C-O Bond and Its Application in Cross-Coupling Reactions. *Chem. Eur. J.* **2011**, *17*, 1728−1759. DOI: 10.1002/chem.201002273. (c) Yamaguchi, J.; Muto, K.; Itami, K. Recent Progress in Nickel-Catalyzed Biaryl Coupling. *Eur. J. Org. Chem*. **2013**, 19−30. DOI: 10.1002/ejoc.201200914. (d) Cornella, J.; Zarate, C.; Martin, R. Metal-catalyzed activation of ethers *via* C-O bond cleavage: a new strategy for molecular diversity. *Chem. Soc. Rev.* **2014**, *43*, 8081−8097. DOI: 10.1039/C4CS00206G. (e) Tobisu, M.; Chatani, N. Cross-Couplings Using Aryl Ethers via C-O Bond Activation Enabled by Nickel Catalysts. *Acc. Chem. Res*. **2015**, *48*, 1717−1726. DOI: 10.1021/acs.accounts.5b00051. (f) Zeng, H.; Qiu, Z.; Domínguez-Huerta, A.; Hearne, Z.; Chen, Z.; Li, C.-J. An Adventure in Sustainable Cross-Coupling of Phenols and Derivatives via Carbon-Oxygen Bond Cleavage. *ACS Catal*. **2017**, *7*, 510−519. DOI: 10.1021/acscatal.6b02964. (g) Surry, D. S.; Buchwald, S. L. Dialkylbiaryl phosphines in Pd-catalyzed amination: a user's guide. *Chem. Sci*. **2011**, *2*, 27−50. DOI: 10.1039/C0SC00331J. (h) Ramgren, S. D.; Silberstein, A. L.; Yang, Y.; Garg, N. K. Nickel-Catalyzed Amination of Aryl Sulfamates. *Angew. Chem. Int. Ed*. **2011**, *50*, 2171−2173. DOI: 10.1002/anie.201007325. (i) Shimasaki, T.; Tobisu, M.; Chatani, N. Nickel Catalyzed Amination of Aryl Pivalates by the Cleavage of Aryl C-O Bonds. *Angew. Chem., Int. Ed*. **2010**, *49*, 2929−2932. DOI: 10.1002/anie.200907287. (j) Mesganaw, T.; Silberstein, A. L.; Ramgren, S. D.; Nathel, N. F. F.; Hong, X.; Liu, P.; Garg, N. K. Nickel-catalyzed amination of aryl carbamates and sequential site-selective cross-couplings. *Chem. Sci*. **2011**, *2*, 1766−1771. DOI: 10.1039/C1SC00230A. (k) Tobisu, M.; Shimasaki, T.; Chatani, N. $Ni^0$-catalyzed Direct Amination of Anisoles Involving the Cleavage of Carbon-Oxygen Bonds. *Chem. Lett*. **2009**, *38*, 710−711. DOI: 10.1246/cl.2009.710. (l) Tobisu, M.; Yasutome, A.; Yamakawa, K.; Shimasaki, T.; Chatani, N. Ni(0)/NHC-catalyzed amination of N-heteroaryl methyl ethers through cleavage of carbon-oxygen bonds. *Tetrahedron* **2012**, *68*, 5157−5161. DOI: 10.1016/j.tet.2012.04.005. (m) Chen, Z.; Chen, X.; So, C. M. Palladium-Catalyzed C($sp^2$)-N Bond Cross-Coupling with Triaryl Phosphates. *J. Org. Chem.* **2019**, *84*, 6366 – 6376. DOI: 10.1021/acs.joc.9b00703. (n) Dennis, J. M.; White, N. A.; Liu, R. Y.; Buchwald, S. L. Pd-Catalyzed C-N Coupling Reactions Facilitated by Organic Bases: Mechanistic Investigation Leads to Enhanced Reactivity in the Arylation of Weakly Binding Amines. *ACS Catal.* **2019**, *9*, 3822 – 3830. DOI: 10.1021/acscatal.9b00981. (o) Yue, H.; Guo, L.; Liu, X.; Rueping, M. Nickel-Catalyzed Synthesis of Primary Aryl and Heteroaryl Amines via C-O Bond Cleavage. *Org. Lett.* **2017**, *19*, 1788 – 1791. DOI: 10.1021/acs.orglett.7b00556. (p) Li, J.; Wang, Z.-X. Nickel-Catalyzed Amination of Aryl 2-Pyridyl Ethers via Cleavage of the

Carbon-Oxygen Bond. *Org. Lett.* **2017**, *19*, 3723 – 3726. DOI: 10.1021/acs.orglett.7b01549. (q) Liu, W.; Li, J.; Querard, P.; Li, C.-J. Transition-Metal-Free C-C, C-O, and C-N Cross-Couplings Enabled by Light. *J. Am. Chem. Soc.* **2019**, *141*, 6755 – 6764. DOI: 10.1021/jacs.9b02684. (r) Tay, N. E. S.; Nicewicz, D. A. Cation Radical Accelerated Nucleophilic Aromatic Substitution via Organic Photoredox Catalysis. *J. Am. Chem. Soc.* **2017**, *139*, 16100 – 16104. DOI: 10.1021/jacs.7b10076. (s) Nishizawa, A.; Takahira, T.; Yasui, K.; Fujimoto, H.; Iwai, T.; Sawamura, M; Chatani, N.; Tobisu, M. Nickel-Catalyzed Decarbxylation of Aryl Carbamates for Converting Phenols into Aromatic Amines. *J. Am. Chem. Soc.* **2019**, *141*, 7261 – 7265. DOI: 10.1021/jacs.9b02751.

[11] (a) Upton, B. M.; Kasko, A. M. Strategies for the Conversion of Lignin to High-Value Polymeric Materials: Review and Perspective. *Chem. Rev*. **2016**, *116*, 2275-2306. DOI: 10.1021/acs.chemrev.5b00345. (b) Li, C.; Zhao, X.; Wang, A.; Huber, G. W.; Zhang, T. Catalytic Transformation of Lignin for the Production of Chemicals and Fuels. *Chem. Rev*. **2015**, *115*, 11559-11624. DOI: 10.1021/acs.chemrev.5b00155.

[12] For recent advances on the Smiles rearrangement please see (a) Holden, C. M.; Greaney, M. F. Modern Aspects of the Smiles Rearrangement. *Chem. Eur. J.* **2017**, *23*, 8992-9008. DOI: 10.1002/chem.201700353. (b) Costil, R.; Dale, H. J. A.; Fey, N.; Whitecombe, G.; Matlock, J. V.; Clayden, J. Heavily Substituted Atropisomeric Diarylamines by Unactivated Smiles Rearrangement of N-Aryl Anthranilamides. *Angew. Chem. Int. Ed.* **2017**, *56*, 12533-12537. DOI: 10.1002/anie.201706341. (c) Mizuno, M.; Yamano, M. A New Practical One-Pot Conversion of Phenols to Anilines. *Org. Lett.* **2005**, *7*, 3629-3631. DOI: 10.1021/ol051080k. (d) Bayles, R.; Johnson, M. C.; Maisey, R. F.; Turner, R. W. A Smiles Rearrangement Involving Non-Activated Aromatic Systems; the Facile Conversion of Phenols to Anilines. *Synthesis* **1977**, *1*, 33-34. DOI: 10.1055/s-1977-24263. (e) Weidner, J. J.; Peet, N. P. Direct conversion of hydroxy aromatic compounds to heteroarylamines via a one-pot smiles rearrangement procedure. *J. Heterocyclic Chem.* **1997**, *34*, 1857 – 1860. DOI: 10.1002/jhet.5570340636.

[13] (a) Lennox, A. J. J. Meisenheimer Complexes in $S_NAr$ Reactions: Intermediates or Transition Steates? *Angew. Chem. Int. Ed.* **2018**, *57*, 14686-14688. (b) Leonard, D. J.; Ward, J. W.; Clayden, J. Asymmetric α-Arylation of Amino Acids. *Nature*, **2018**, 105-109.

[14] a) Li, J.; Liu, Z.; Wu, S.; Chen, Y. Acyl Radical Smiles Rearrangement To Construct Hydroxybenzophenones by Photoredox Catalysis. *Org. Lett.* **2019**, *21*, 2077-2080. DOI: 10.1021/acs.orglett.9b00353. (b) Chen, Z.-M.; Zhang, X.-M.; Tu, Y.-Q. Radical Aryl migration reactions and synthetic applications. *Chem. Soc. Rev.* **2015**, *44*, 5220-5245. DOI: 10.1039/C4CS00467A. (c) Allart-Simon, I.; Gérard, S.; Sapi, J. Radical Smiles Rearrangement: An Update. *Molecules*, **2016**, *21*, 878. DOI: 10.3390/molecules21070878. (d) Li, W.; Xu, W.; Xie, J.; Yu, S.; Zhu, C. Distal radical migration strategy: an emerging synthetic means. *Chem. Soc. Rev.* **2018**, *47*, 654-667. DOI: 10.1039/C7CS00507E. (e) Wang, S.-F.; Cao, X.-P.; Li, Y. Efficient Aryl Migration from an Aryl Ether to a Carboxylic Acid Group To Form an Ester by Visible-Light Photoredox Catalysis. *Angew. Chem. Int. Ed.* **2017**, *56*, 13809-13813. DOI: 10.1002/anie.201706597.

[15] (a) Zhou, T.; Luo, F.-X.; Yang, M.-Y.; Shi, Z.-J. Silver-Catalyzed Long-Distance Aryl Migration from Carbon Center to Nitrogen Center. *J. Am. Chem. Soc.* **2015**, *137*, 14586-14589. DOI: 10.1021/jacs.5b10267. (b) Shu, W.; Genoux, A.; Li, Z.; Nevado, C. γ-Functionalizations of Amines through Visible-Light-Mediated Redox-Netural C-C Bond Cleavage. *Angew. Chem. Int. Ed.* **2017**, *56*, 10521-10524. DOI: 10.1002/anie.201704068.

[16] Chang, X.; Zhang, Q.; Guo, C. Electrochemical Reductive Smiles Rearrangement for C-N Bond Formation. *Org. Lett.* **2019**, *21*, 10-13. DOI: 10.1021/acs.orglett.8b03178.

[17] Sigma Aldrich Catalog

[18] Bayles, R.; Johnson, M. C.; Maisey, R. F.; Turner, R. W. A Smiles Rearrangement Involving Non-Activated Aromatic Systems; the Facile Conversion of Phenols to Anilines. *Synthesis* **1977**, *1*, 33-34. DOI: 10.1055/s-1977-24263.

[19] Mizuno, M.; Yamano, M. A New Practical One-Pot Conversion of Phenols to Anilines. *Org. Lett.* **2005**, *7*, 3629-3631. DOI: 10.1021/ol051080k.

[20] Ortiz, G. X.; Hemric, B. N.; Wang, Q. *Org. Lett*. **2017**, *19*, 1314-1317.

[21] Schmidt, V. A.; Alexanian, E. *Angew. Chem. Int. Ed.* **2010**, *49*, 4491-4494.

[22] Chang, X.; Zhang, Q.; Guo, C. *Org. Lett.* **2019**, *21*, 10-13.

[23] Boger, D. L. CYCLIC N-ACYL O-AMINONPHENOL CBI DERIVATIVE. WO/2014/160586

[24] Banerjee, A.; Yamamoto, H. *Chem. Sci.* **2019**, *10*, 2124-2129.

[25] Yonekawa, M.; Koyama, Y.; Kuwata, S.; Takata, T. *Org. Lett.* **2012**, *14*, 1164-1167.

[26] Kraus, G. A.; Roth, B. *J. Org. Chem.*, **1980**, *45*, 4825-4830.

[27] Jayasekara, P. S.; Jacobson, K. A. *Synthetic Communications*, **2014**, *44*, 2344-2347.

[28] Roussea, G.; Robert, F.; Landais, Y. *Chem. Eur. J.*, **2009**, *15*, 11160-11173

[29] Shang, S; Zhang-Negrerie, D.; Du, Y.; Zhao, K. *Angew. Chem. Int. Ed.* **2014**, *53*,

[30] Nimnual, P.; Tummatorn, J.; Thongsornkleeb, C.; Ruchirawat, S. *J. Org. Chem.* **2015**, *80*, 8657-8667.

[31] Guan, Q.; Jiang, M.; Wu, J.; Zhai, Y.; Wu, Y.; Bao, K.; Zhang, W. *Green Chem.* **2016**, *18*, 5794-5799.

[32] Wang, H.; Huang, Y.; Dai, X.; Shi, F. *Chem. Commun.*, **2017**, *53*, 5542-5545.

# Chapter 4: Thiol Catalyzed Aerobic Debenzylation of Amines and Alcohols

## 4.1 Introduction

Thiols are ubiquitous in radical, open-shell chemistry owing to their ability to serve as excellent H-atom donors.[1] Carbon-centered radicals abstract H-atoms from thiols at near diffusion-controlled rates for certain substrates, making them ideal terminal reductants. In spite of this well known reactivity, the H-atom transfer event between thiols and C-radicals in reality exists as an equilibrium, meaning that thiyl radicals can similarly act as H-atom abstractors. The inherent electrophilicity of thiyl radicals makes them poised to abstract from electron rich hydrogens such as those from silanes,[2] boranes,[3] aldehyedes,[4] and C-H bonds adjacent to heteroatoms.[5] Dilman recently showed that the tetrafluoropyridinyl-thiyl radical generated from purple light-mediated homolysis of the disulfide could be used to perform a C-H abstraction of unactivated alkanes toward C-H thiolation (Scheme 4.1).[6]

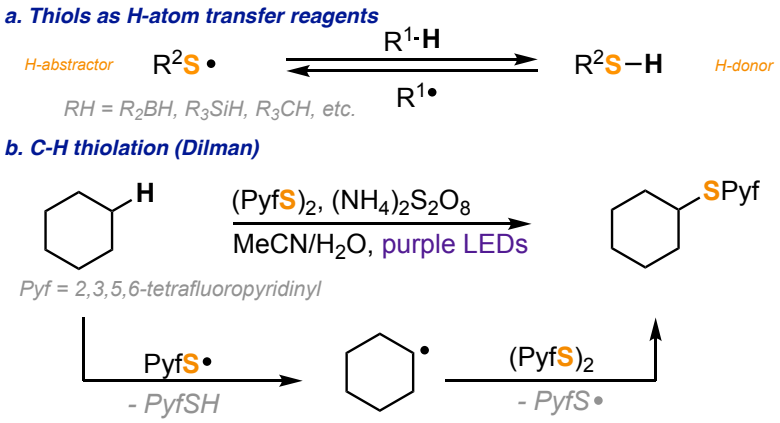


Scheme 4.1. Capability of thiols as H-atom abstraction reagents.

Benzyl (Bn) and p-methoxybenzyl (PMP) protecting groups have become common place in organic synthesis, and the efficient installation and removal of these groups is of the utmost importance.[7] Currently the most frequently employed strategies for the removal of Bn and PMB groups are hydrogenolysis with Pd/C and hydrogen gas,[8] and oxidative cleavage with dichloro-5,6-p-benzoquinone (DDQ),[9] respectively.

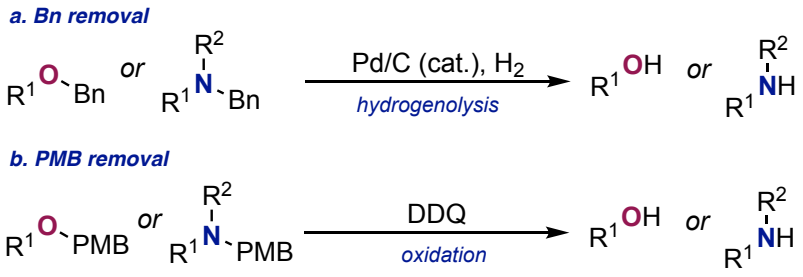


Scheme 4.2. Traditional benzyl deprotection strategies.

In spite of the tried and true methods for Bn and PMB deprotection, there is an ongoing drive to develop increasingly mild methods to perform the same overall transformation. A recently developed strategy for deprotection relies on the H-atom abstraction at the benzylic position of a Bn or PMB protected amine or alcohol. Parsons reported a debenzylation procedure for Bn-protected amides using stoichiometric *N*-bromosuccinimide (NBS)[10]. The in-situ generated imidyl radical performed a site-selective C-H abstraction at the benzylic position of the substrate to generate a carbon-centered radical. This intermediate then abstracted a bromine atom from a second equivalent of NBS to provide an alpha-bromo benzylic species which was hydrolyzed under the reaction conditions to provide the desired amide. Recently, Togo developed a method wherein a KBr and Oxone couple us used for the stoichiometric generation of bromine radical in situ that acts as the active H-atom abstraction species.[11] Subsequent oxidation of the benzylic radical intermediated provided the deprotected amine or ketone in the case of alcohol deprotection.

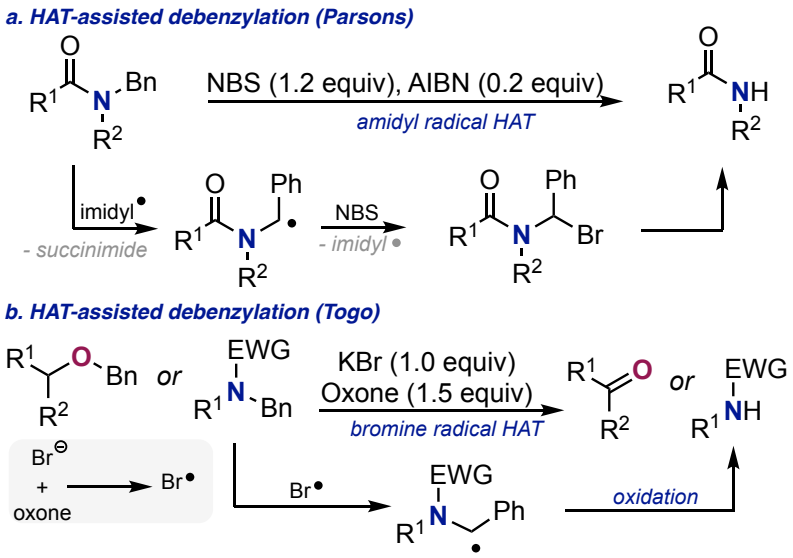


Scheme 4.3. HAT-mediated debenzylation strategies.

In our own efforts, we developed a HAT-mediated debenzylation protocol that uses catalytic thiol and atmospheric $O_2$ as the terminal oxidant, applicable to a variety of functionalized alcohols and amine substrates (Scheme 2e). This method operates with predictable chemoselectivity and is amenable to substrates that would be challenging for hydrogenolysis, DDQ, or acid based deprotection strategies such as those containing alkenes, carbamate protecting groups, acyl-amines, nitriles, ketones, and acetals. Our approach uses only a catalytic amount of thiol with ambient oxygen as the sole oxidant.[12] The key to this strategy lies in the ability of the abstracting thiyl radical to be easily regenerated in-situ via a radical chain process, thereby precluding the need for stoichiometric reagents other than air.

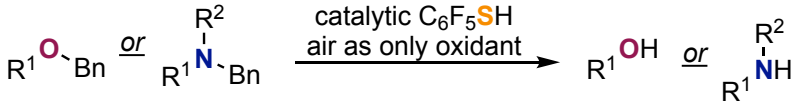


Scheme 4.4. Radical debenzylation using the thiyl radical.

## 4.2 Reaction Development and Substrate Scope

We discovered that a substantial amount of p-anisaldehyde and N-methyl aniline were produced when PMB-N-methyl aniline was reacted with a catalytic amount of radical initiator and

methyl thioglycolate in aqueous media. We explored this debenzylation reactivity using amine **1** and found that the major product formed was imine **2** rather than simply aniline (**3**) (Table 4.1). An initial reaction including PMB-aniline **1**, 5 mol% methyl thioglycolate, and 5 mol% 2-2'-azobis(2-methylpropionitrile) (AIBN) heated to 80 $^{o}$C in chlorobenzene for 1.5 hours resulted in only 29% conversion of **1** and an 11% combined yield of imine **2** and aniline **3** (Table 1, Entry 1). We hypothesized that imine formation was the result of either a) direct formation of imine under the reaction conditions, or b) the in-situ condensation of amine and p-anisaldehyde following debenzylation. While using thiophenol in place of methyl thioglycolate increased conversion and yield (Entry 2), the use of pentafluorothiophenol substantially improved reaction efficiency to 68% conversion and a 41% total yield of desired products (Entry 3). The reaction was further improved to 78% total yield by including a second addition of thiol and initiator after 1.5 hours, and extending the total reaction time to 3 hours (entry 4). Increasing the amount of thiol and initiator to 10 mol% resulted in 94% conversion and a total yield of 91% (entry 5). An acidic workup effectively funneled all material to the debenzylated amine as the sole product in 71% yield.

Table 4.1. Radical debenzylation reaction optimization. (a) All reactions performed on a 0.2 mmol scale of **4.3a1**. (b) Conversion and yields were determined by $^1$H NMR using dibromomethane as an internal standard from crude reaction mixtures. (c) 3 h total reaction time, with a second addition of thiol and initiator added after 1.5 h for a total of 10 mol% PFTP and 10 mol% AIBN added. (d) 10 mol% of PFTP and AIBN used, 3 h total reaction time, and a second addition of thiol and initiator added after 1.5 hours for a total of 20 mol% PFTP and 20 mol% AIBN used. (f) $^1$H NMR yield following acid workup (See Appendix for details).

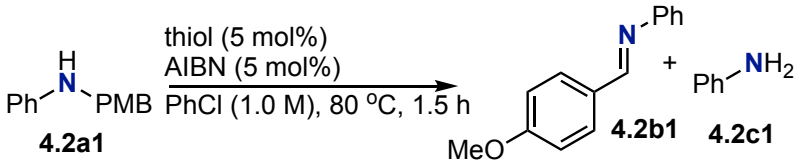


| Entry | Reaction Conditions[a] | Conversion[b] | Yield (**4.2b1** : **4.2c1**)[b] |
|---|---|---|---|
| 1 | methyl thioglycolate | 29% | 9% : 2% |
| 2 | thiophenol | 33% | 17% : 6% |
| 3 | $C_6F_5SH$ | 68% | 32% : 9% |
| 4 | $C_6F_5SH$[c] | 97% | 62% : 16% |
| 5 | $C_6F_5SH$[d] | 94% | 74% : 17% (0% : 71%)[f] |
| 6 | $C_6F_5SH$, no initiator | 7% | 2% : 0% |
| 7 | no thiol | 6% | 3% : 0% |
| 8 | $C_6F_5SH$, degassed[e] | 20% | 4% : 0% |

We observed that the individual exclusion of AIBN (or initiator) (entry 6), thiol (entry 7), or $O_2$ (entry 8), resulted in only trace amount of debenzylation. Combined, these results indicate that debenzylation occurs via a radical rather than acid-mediated pathway xiv and that thiol and oxygen are required.

With proper reaction conditions and a mechanistic understanding of this debenzylation process, we sought to explore the breadth of its applicability to the removal of PMB and Bn groups from amines (Scheme 4.5). Primary, PMB-protected anilines were easily deprotected and were generally found to be the most successful substrates. Several deprotected anilines were isolated in near quantitative yield including **4.2c1**, **4.2c7**, and **4.2c3** bearing a sensitive acetamide group that may be intolerant to classic PMB removal methods involving acid catalysis.[13] Other substrates possessing sensitive functionality such as ketone **4.2c2**, bis-aryl ether **4.2c5**, nitrile **4.2c6**, primary

TBS-protected alcohol **4.2c8**, and acetal **4.2c12** were all deprotected in good to great yield. Carbazole **x** underwent these conditions smoothly, as did the free hydroxyl bearing substrate **4.2c9**. Carbamates **4.2c10** and **4.2c11** similarly were successful substrates, indicating that this method is amenable for the chemoselective removal of PMB groups over Cbz groups, and tolerates the acid-sensitive Boc protecting group.

Increasing the substitution at nitrogen generally decreased reaction efficiency, as seen in substrates **4.2c13**, **4.2c14**, and **4.2c15**. Several biologically relevant, PMB-protected molecules were successfully debenzylated under our conditions providing sulfadiazine (**4.2c16**), sulfamethoxazole (**4.2c17**), and cholic acid derivative **4.2c19** in moderate to good yield. PMB-protected n-butyl amine was similarly deprotected providing **4.2c18**. We found that relatively electron-deficient substates such as PMB-protected amides, carbamates and sulfonamides were ineffectively deprotected using our protocol, resulting in the recovery of starting material in each case. This unique reactivity makes our method complimentary to those previously reported by Togo and Parsons, wherein the most successful substrates were amides and sulfonamides.

Bn- and PMP-ethers could similarly be deprotected using nearly identical conditions to reveal the corresponding alcohol. 2-Indanol and 1-octanol were both isolated from their Bn-protected congeners in modest yield. Olefinic substrates such as PMB-protected Citronellol and (1R)-(-) nopol that may not be amenable to typical hydrogenolysis conditions proved to be effectively deprotected in spite of the known propensity for thiyl radicals to engage with alkenes in thiol-ene chemistry.[14] (-)-Menthol was obtained from its PMB-derivative with no erosion of stereochemistry. Acid sensitive 2-trimethylsilyl 1-ethanol and 3-hydroxypropanenitrile were similarly obtained under our conditions. More complex substrates including 2-(5-methyl-2-phenyloxazol-4-yl)ethanol, serine derivate (**4.2c27**), diosgenin, and stigmasterol were all isolated

following from their PMP-protected derivatives in modest to great yields. Compound **4.2c29** was isolated from its O-PMB protected congener leaving the PMB-protected amide untouched, thus highlighting the unique chemoselectivity of this method. PMB-protected phenols and esters were ineffective substrates under our conditions, resulting in the recovery of starting material in both cases.

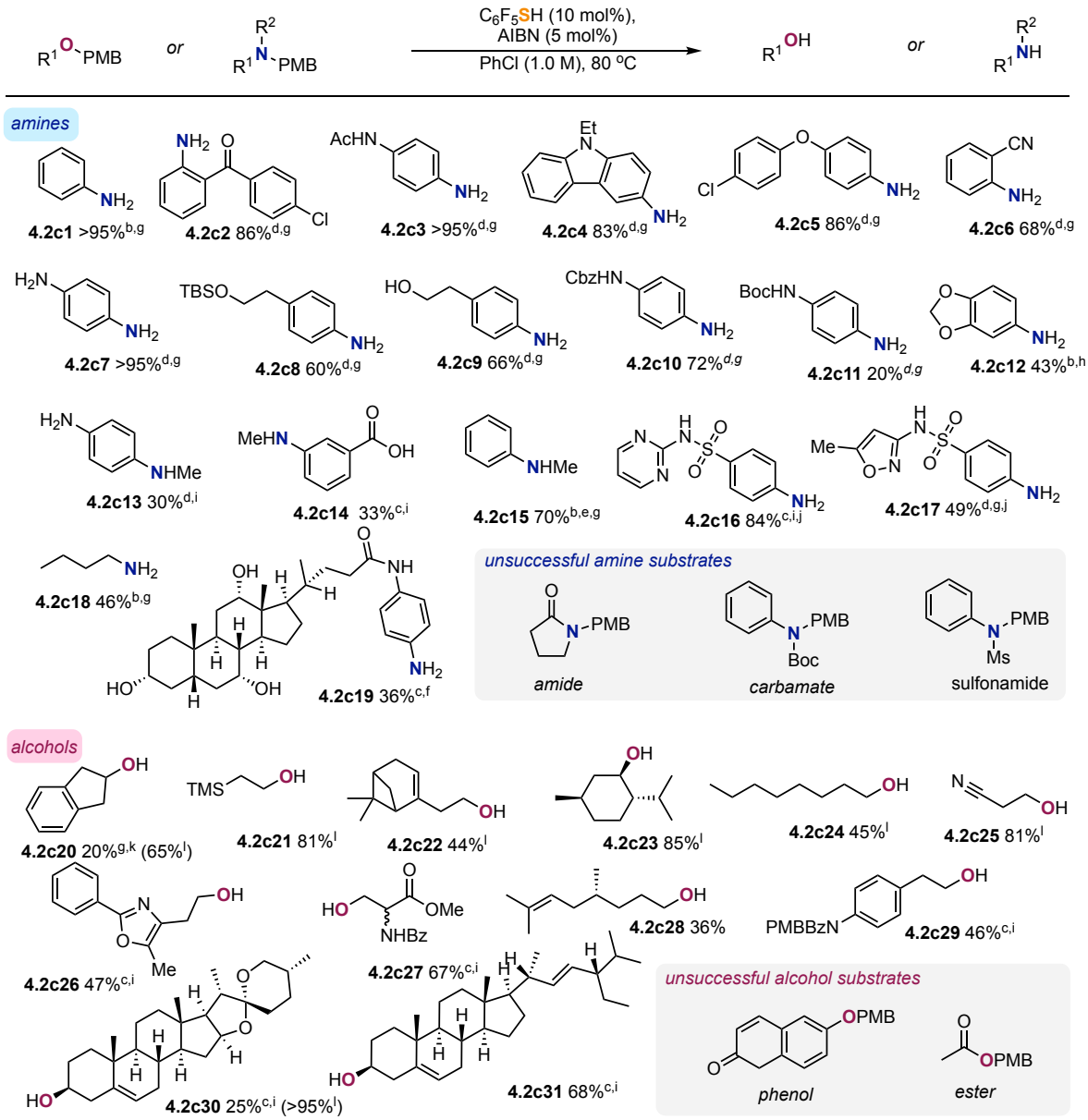


Scheme 4.5. Thiol catalyzed debenzylation substrate scope. (a) All yields are of isolated products, except where otherwise noted. (b) Isolated as the hydrochloride salt via aqueous workup of the crude reaction mixture. (c) Isolated by silica gel column chromatography. (d) Isolated via silica gel column chromatography following hydrolytic workup using either aqueous 5 M HCl, hydrazine monohydrate in methanol, or hydroxylamine hydrochloride in 1:1 water:THF (see SI for full experimental details). (e) Obtained from the reaction with the benzyl, not PMB-protected starting material. (f) Reaction was performed with 2 additions of thiol and initiator for a total reaction time of 2 hours. (g) Reaction was performed with 3 additions of thiol and initiator for a total reaction time of 3 hours. (h) Reaction was performed with 4 additions of thiol and initiator for a total reaction time of 4 hours. (i) Reaction was performed with 4 additions of thiol and initiator for a total reaction time of 4 hours. (j) MeCN used as solvent. (k) Isolated by silica gel column chromatography following removal of aldehyde byproduct via $NaHSO_3$ column. (l) $^1H$ NMR yield of crude reaction mixture using dibromomethane as internal standard. (m) TBHN used in place of AIBN, and reaction performed at 50 °C. 4 total additions of thiol and initiator added every 30 min. for a total reaction time of 2 hours.

Further investigation revealed that our debenzylation procedure was amenable to the selective oxidation of several substrates (Scheme 4.6). Compound **4.2a32** was smoothly converted to **4.2c32** under our conditions, a procedure that typically requires temperatures up to 140 °C,[15] or strong oxidants such as potassium permanganate.[16] Similarly, p-methoxy benzyl alcohol was quantitatively oxidized to p-anisaldehyde under our reaction conditions.

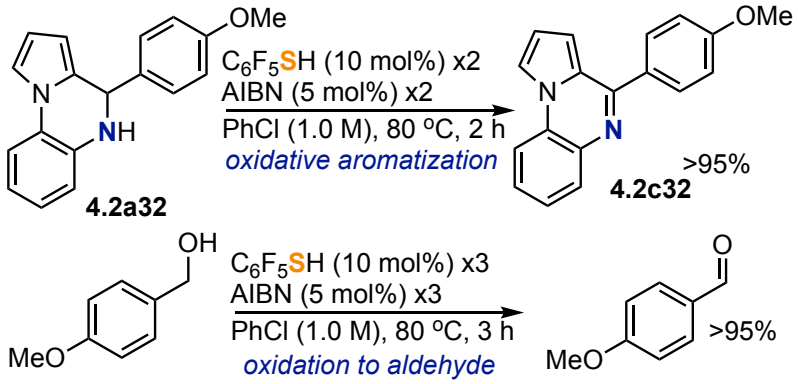


Scheme 4.6. Oxidative transformations using debenzylation conditions. (a) $^{1}$H NMR yields of crude reaction mixture using dibromomethane as internal standard.

## 4.3 Mechanistic Investigation

This data led to the proposed mechanism for debenzylation shown in Scheme 4.7. Radical initiation generates an electrophilic, thiyl radical from pentafluorothiophenol which then preferentially abstracts a relatively weak, electron-rich, benzylic H-atom from the substrate.[17] Molecular oxygen then may either perform a single electron oxidation[18] or radical trapping [19] of the benzylic radical intermediate to generate a benzylic carbocation or peroxy radical intermediate, respectively. Either pathway is possible and lead to a common benzylic peroxy radical intermediate.[20] H-Atom transfer between this intermediate and pentafluorothiophenol would generate a benzylic peroxide species as propagate the chain process by regenerating thiyl radical. Finally, elimination of hydrogen peroxide anion followed by hydrolysis furnishes the desired amine or alcohol product.

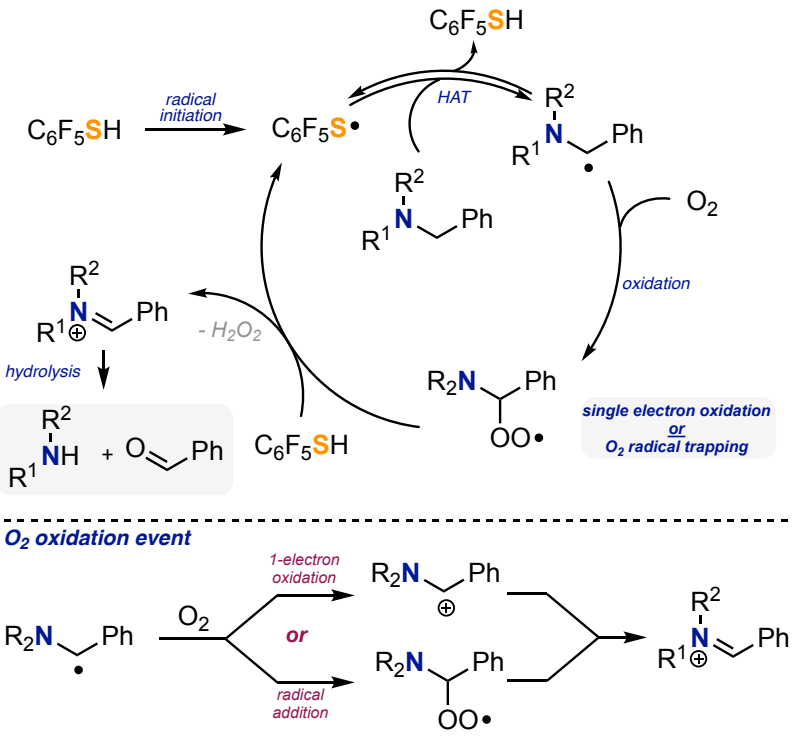


Scheme 4.7. Mechanistic proposal for thiol catalyzed debenzylation.

We turned to DFT to understand the importance of the thiol selection in this reaction as we observed that the use of pentafluorothiophenol achieved significantly higher reaction efficiencies than any other thiol surveyed. We considered the S-H bond dissociation energies[21] and the electron affinities[22] of their corresponding thiyl radicals of the three thiols that were investigated in Table 4.1 (Scheme 4.8). These calculations indicated that pentafluorothiophenol had both the lowest S-H BDE (79.4 kcal/mol) and the greatest, most exothermic electron affinity (EA) (68.5 kcal/mol). While the inclusion of electron withdrawing groups typically increases the BDEs in a molecule, the presence of fluorine at the ortho and para positions of an aromatic thiol has been shown to decrease the S-H BDE, which likely explains the ~4 kcal/mol difference between pentafluorothiophenol and thiophenol.[23] Similarly, the electron withdrawing-nature of the fluorine group is likely responsible for the electron affinity of the pentafluorothiyl radical being substantially higher than that of either methyl thioglycolate or thiophenol.[24] The weak S-H BDE

and high electron affinity of pentafluorothiophenol thiyl radical facilitates the chemoselective C-H abstraction of the weak benzylic alpha amino H-atoms of the substrate.

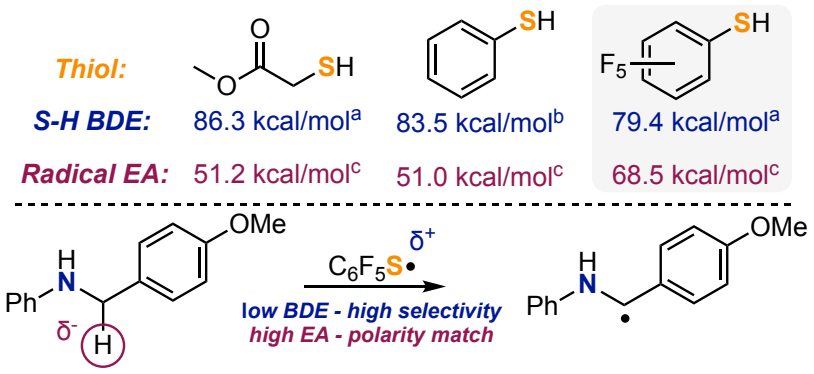


Scheme 4.8. Significance of thiol selection for chemoslective benzyl removal.

To further illustrate the importance of substrate electronics on our observed reactivity, we prepared the benzyl- and 4-trifluoromethylbenzyl- protected congeners of substrate **4.2a1** and observed significantly slower reactivity for these two substrates. The decreased reactivity of the more electronically-deficient analogues further illustrates substrate electronics on this thiol catalyzed aerobic debenzylation.

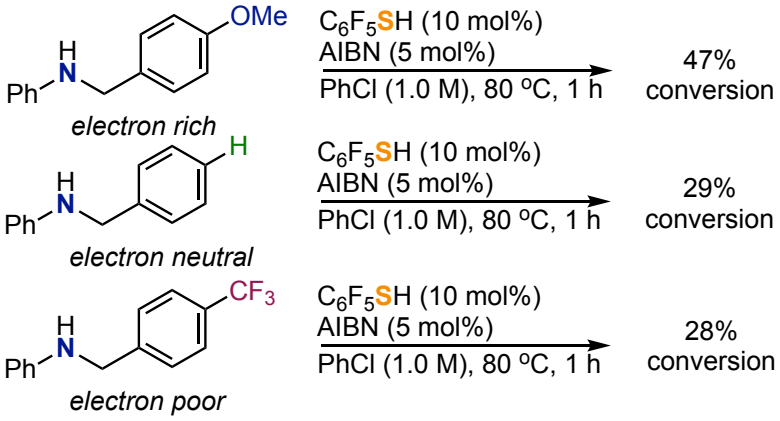


Scheme 4.9. Significance of substrate electronics on thiol catalyzed debenzylation.

## 4.4 Conclusions

The great utility of protecting groups in organic synthesis inherently creates a drive toward the develop of methods that improve the overall efficiency of the either the installation or removal

of these groups. In our efforts, we have made a small step in this direction by exploring a thiol catalyzed, aerobic debenzylation of amines and alcohols. In contrast to typical methods for the removal of Bn or PMB protecting groups that utilize precious transition metals (Pd), strong acids (TFA), or harsh oxidants (DDQ), our HAT approach uses but a substoichiometric amount of thiol and $O_2$ present in an ambient atmosphere as the only oxidant.

Chapter 4 has been adapted from materials prepared to be published in Lardy, S. W.; Schmidt, V. A. Thiol Catalyzed Aerobic Debenzylation of Alcohols and Amines. The dissertation author was the primary investigator of this publication.

## 4.5 Appendix

### 4.5.1 General Considerations

$^{1}H$, $^{13}C$, and $^{19}F$ NMR were recorded on a Brucker AVA 300 MHz or JEOL 400 MHz spectrometer. All chemical shifts are reported relative to $SiMe_4$ using $^{1}H$ (residual) chemical shifts of the solvent as a secondary standard. $^{19}F$ chemical shifts are reported relative to a 2,2,2-trifluoroethanol ($CF_3CH_2OH$) internal standard at -77.16 ppm. GC analyses were performed using an Agilent Technologies 7890B gas chromatograph equipped with an Agilent 7693 autosampler and Agilent HP-5 capillary column (30 m x 0.320 mm x 250 μm). Standard method parameters: 1.2 mL/min flow rate with oven program 80 – 250 °C with a ramp rate of 25 °C/min and hold time of 8.7 minutes at 250 °C. Low-resolution mass spectra were measured using a DECA ESI-MS. High-resolution mass spectra were measured using an Agilent 6230 ESI-TOFMS.

### 4.5.2 Preparation of Substrates

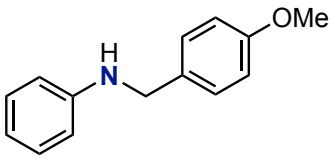


**4.2a1** was prepared in a manner similar to that which has been previously reported:[25] a mixture of aniline (1 equiv), p-anisaldehyde(1 equiv), and ethanol (0.2 M) was heated to reflux for 12 h. The reaction mixture was then cooled to room temperature and $NaBH_4$ (1.2 equiv) was added carefully in small portions. The reaction mixture was then allowed to stir at room temperature for 2 hours, at which point water was added and mixture was extracted with dichloromethane. The organic fractions were collected, dried over sodium sulfate, and the solvent was removed under reduced pressure. The crude product was then purified by column chromatography on silica gel using 2-10% ethyl acetate in hexanes as eluent to yield **4.2a1** in 85% yield (performed on up to 20 g scale). This same procedure (and in some case, with slight modification when noted) was used to prepare many of the other PMB- and Bn-protected amines below. Physical and spectral data was in accordance with the literature.[25]

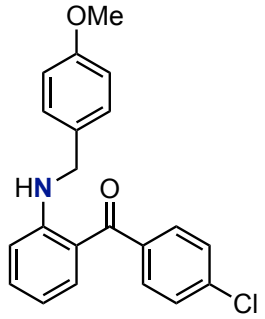


**4.2a2** was prepared analogously to **4.2a1** but by using $NaBH(OAc)_3$ (prepared immediately prior to use by slowly adding $NaBH_4$ to acetic acid (5 equiv relative to $NaBH_4$)) in lieu of $NaBH_4$ in 32% yield (1.4 g). **4.2a2** was purified by recrystallization from hexanes/ethyl acetate to give a bright yellow solid. **$^1$H-NMR** (300 MHz; $CDCl_3$): δ 7.61-7.57 (m, 2H), 7.61-7.57 (m, 2H), 7.50-7.44 (m, 3H), 7.50-7.44 (m, 3H), 7.40-7.32 (m, 3H), 7.40-7.32 (m, 3H), 6.93-6.90 (m, 2H), 6.93-6.90 (m, 2H), 6.80-6.77 (m, 1H), 6.80-6.77 (m, 1H), 6.61-6.55 (m, *J* = 1.0 Hz, 1H), 6.61-6.55 (m, *J* = 1.0 Hz, 1H), 4.46 (s, 2H), 4.46 (s, 2H), 3.83 (s, 3H), 3.83 (s, 3H). **$^{13}$C-NMR** (75 MHz; $CDCl_3$): δ 197.9, 158.9, 151.6, 138.8, 137.1, 135.20, 135.13, 130.53, 130.38, 128.43, 128.35, 117.2, 114.19, 114.17, 112.2, 55.3, 46.5. **HRMS** (ESI-TOF) Calc. for $[C_{21}H_{19}ClNO_2]^+$ = 352.1099, Found = 352.1097

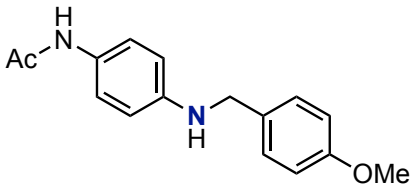


**4.2a3** was prepared analogously to compound **4.2a1** in 69% yield (2.3 g). **4.2a3** was purified by recrystallization from hexanes/ethyl acetate. **$^1$H-NMR** (300 MHz; $CDCl_3$): δ 7.56 (s, 1H), 7.30-7.26 (m, 4H), 6.89 (d, $J$ = 8.4 Hz, 2H), 6.58 (d, $J$ = 8.6 Hz, 2H), 4.23 (s, 2H), 3.82 (s, 3H), 2.11 (s, 3H). **$^{13}$C-NMR** (75 MHz; $CDCl_3$): δ 168.4, 158.8, 145.3, 131.3, 128.8, 128.4, 122.4, 114.0, 113.1, 55.3, 48.0, 24.2. **HRMS** (ESI-TOF) Calc. for $[C_{16}H_{18}N_2O_2Na]^+$= 293.1260, Found = 293.1263.

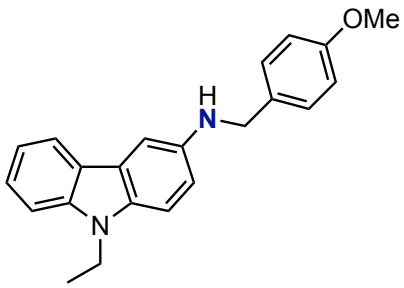


**4.2a4** was prepared analogously to compound **4.2a1** starting from in 49% yield (2.0 g). Physical and spectral data was in accordance with the literature.[26]

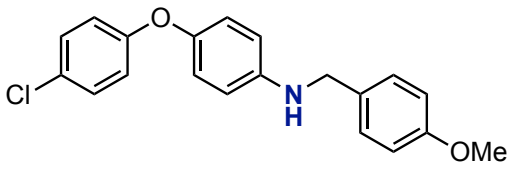


**4.2a5** was prepared analogously to **4.2a1** in 59% yield as a dark purple solid (2.0 g). **$^{1}$H-NMR** (300 MHz; $CDCl_3$): δ 7.33 (d, *J* = 8.6 Hz, 2H), 7.24 (d, *J* = 9.0 Hz, 2H), 6.93-6.86 (m, 6H), 6.66 (d, *J* = 8.8 Hz, 2H), 4.27 (s, 2H), 3.84 (s, 3H). **$^{13}$C-NMR** (75 MHz; $CDCl_3$): δ 159.0, 157.8, 147.4, 145.2, 131.2, 129.4, 128.9, 126.8, 121.2, 118.3, 114.1, 113.9, 55.3, 48.3. **HRMS** (ESI-TOF) Calc. for $[C_{20}H_{18}ClNO_2]^+$= 339.1021, Found = 339.1017.

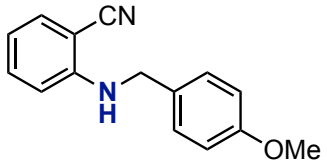


**4.2a6** was prepared by the reaction of 2-fluorobenzonitrile (1 equivalent), 4-methoxy-N-benzylamine (1 equiv), and potassium carbonate (2 equivalents) in DMF (0.5 M) at 130 °C for 36 hours. The reaction was then allowed to cool to room temperature, water was added, and the mixture was extracted with DCM, The organic fractions were then colleted, dried over sodium sulfate, and evaporated under reduced pressure. The crude material was then subjected to flash column chromatography (25% EtOAc in hexanes) to provide compound **4.2a6** in 18% yield (500 mg)**.** Physical and spectral data was in accordance with the literature.[27]

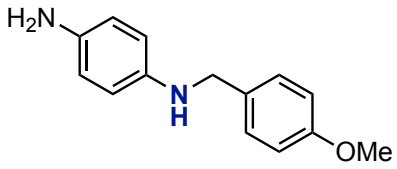


**4.2a7** was prepared by heating a mixture of compound **4.2a3** and KOH (5 equivlants) in a 1:9 ethanol:water (0.5 M) to reflux for 16 hours. The reaction was then allowed to cool to room temperature, water was added, and the precipitated solid was filtered and dried to yield compound **x** as an off white solid in 95% yield (1.0 g). **$^{1}$H-NMR** (300 MHz; $CDCl_3$): δ 7.32 (d, *J* = 8.7 Hz, 2H), 6.91 (d, *J* = 8.7 Hz, 2H), 6.64 (d, *J* = 8.8 Hz, 2H), 6.57 (d, *J* = 8.8 Hz, 2H), 4.22 (s, 2H), 3.83 (s, 3H), 3.36 (s, 3H). **$^{13}$C-NMR** (75 MHz; $CDCl_3$): δ 158.8, 141.4, 137.9, 131.9, 128.9, 116.9, 114.6, 114.0, 55.3, 48.9 **HRMS** (ESI-TOF) Calc. for $[C_{14}H_{16}N_2O]^+$= 228.1257, Found = 228.1262.

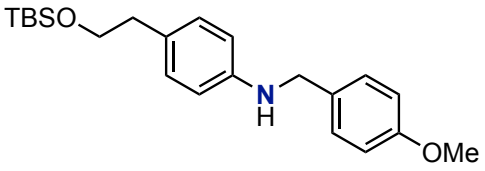


**4.2a8** was prepared by the reaction of TBSCl (1.1 equiv), imidazole (1.5 equiv), and compound **x** in DCM (0.5 M) at room temperature for 16 hours. The reaction was then washed once with water, the organic layer was dried over sodium sulfate, and evaporated under reduced pressure. The title compound was isolated by flash column chromatography (5% EtOAc in hexanes) in 78% yield as an orange oil (2.6 g). **$^{1}$H-NMR** (300 MHz; $CDCl_3$): 7.33 (d, *J* = 8.7 Hz, 2H), 7.06 (d, *J* = 8.5 Hz, 2H), 6.92 (d, *J* = 8.7 Hz, 2H), 6.62 (d, *J* = 8.5 Hz, 2H), 4.27 (s, 2H), 3.83 (d, *J* = 9.7 Hz, 4H), 3.78 (t, *J* = 7.4 Hz, 3H), 2.77 (s, 2H), 0.95-0.93 (m, 9H), 0.06 (s, 6H). **$^{13}$C-NMR** (75 MHz; $CDCl_3$): δ 158.8, 146.6, 131.5, 129.9, 128.8, 128.0, 114.0, 112.9, 65.1, 55.3, 48.1, 38.8, 26.0, 18.4, -5.3. **HRMS** (ESI-TOF) Calc. for $[C_{22}H_{34}NO_2Si]^+$= 372.2353, Found = 372.2355.

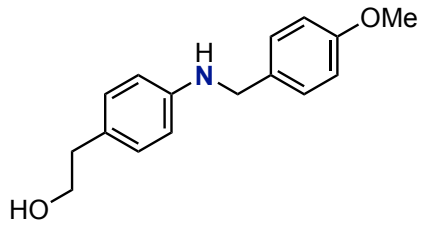


**4.2a9** was prepared analogously to compound **4.2a1** in 82% yield (2.6 g). Physical and spectral data was in accordance with the literature.[28]

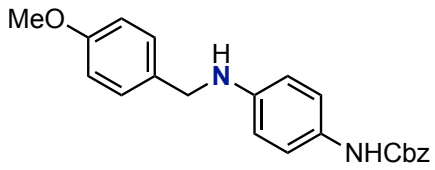


**4.2a10** was prepared by first installing a Cbz group at one end of 1,4-phenylenediamine following a reported procedure.[29] From this intermediate, **4.2a10** was prepared following a procedure analogous to that of **4.2a1** in 95% yield (3.7 g) as a tan solid. **$^{1}$H-NMR** (300 MHz; $CDCl_3$): δ 7.41-7.32 (m, 5H), 7.28 (d, *J* = 8.6 Hz, 2H), 7.20 (d, *J* = 6.7 Hz, 2H), 7.02 (s, 1H), 6.88 (d, *J* = 8.6 Hz, 2H), 6.58 (d, *J* = 8.8 Hz, 2H), 5.17 (s, 2H), 4.22 (s, 2H), 3.99 (s, 1H), 3.80 (s, 3H). **$^{13}$C-NMR** (75 MHz; $CDCl_3$): δ 158.8, 154.0, 144.88, 144.86, 136.5, 131.4, 128.8, 128.5, 128.26, 128.17, 121.2, 114.0, 113.3, 66.7, 55.3, 48.1 **HRMS** (ESI-TOF) Calc. for $[C_{22}H_{22}N_2O_3Na]^+$= 385.1523, Found = 385.1526.

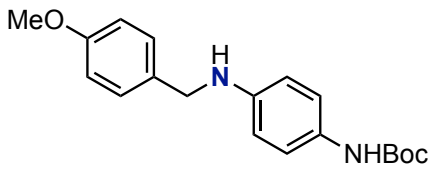


**4.2a11** was prepared by first installing a Boc group at one end of 1,4-phenylenediamine following a reported procedure.[30] From this intermediate, **4.2a11** was prepared following a procedure analogous to that of **4.2a1** in 42% yield (600 mg) as a white solid. **$^{1}$H-NMR** (300 MHz; $CDCl_3$): δ 7.30 (d, *J* = 7.6 Hz, 2H), 7.16 (d, *J* = 8.3 Hz, 2H), 6.89 (d, *J* = 8.7 Hz, 2H), 6.61 (d, *J* = 8.8 Hz, 2H), 6.30 (s, 1H), 4.24 (s, 2H), 3.82 (s, 3H), 1.52 (s, 9H). **$^{13}$C-NMR** (75 MHz; $CDCl_3$): δ 158.8, 153.5, 144.5, 131.3, 128.8, 121.3, 115.6, 114.0, 113.4, 80.0, 55.3, 48.2, 28.4 **HRMS** (ESI-TOF) Calc. for $[C_{19}H_{25}N_2O_3]^+$ = 339.1021, Found = 339.1017.

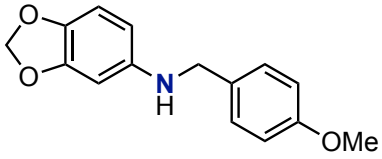


**4.2a12** was prepared analogously to compound **4.2a1** in 72% yield (2.3 g). Physical and spectral data was in accordance with the literature.[31]

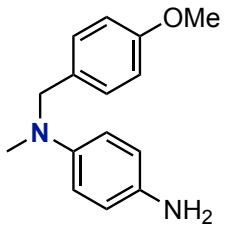


**4.2a13** was prepared by dissolving compound **4.2a3** in a 3:1 mixture of MeCN:AcOH at room temperature. To this mixture was added 1 equivalent of formaldehyde (37 wt% solution in water) followed by $NaCNBH_3$ (1.5 equiv). The reaction was allowed to stir at room temperature for an additional 2 hours, at which time water was added and the mixture was extracted with EtOAc. The organic fractions were then collected, dried over sodium sulfate, and evaporated under reduced pressure. To this crude methylated product was added a 3:1 mixture of water and ethanol (0.2 M). KOH was then added (5 equiv) and the reaction was heated to reflux for 16 hours. The reaction was then allowed to cool to room temperature, water was added, and the solid that precipitated was filtered to give **x** as a dark solid in 92% yield (3.3 g). **$^1$H-NMR** (300 MHz; $CDCl_3$): δ 7.19 (d, $J$ = 8.8 Hz, 2H), 6.86 (d, $J$ = 8.7 Hz, 2H), 6.76 (d, $J$ = 8.9 Hz, 2H), 6.67 (d, $J$ = 9.0 Hz, 2H), 4.33 (s, 2H), 3.81 (s, 3H), 2.86 (s, 3H). **$^{13}$C-NMR** (75 MHz; $CDCl_3$): δ 158.6, 144.0, 137.3, 131.3, 128.7, 116.8, 115.2, 113.9, 58.0, 55.36, 39.0 **HRMS** (ESI-TOF) Calc. for $[C_{15}H_{18}N_2O]^+$ = 242.144, Found = 242.1413.

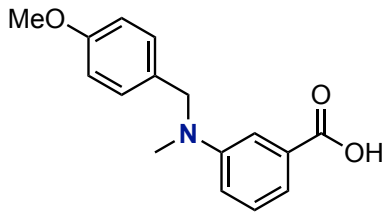


**4.2a14** was prepared by dissolving 3-(*N*-p-methoxybenzyl)benzoic acid in a 3:1 mixture of MeCN:AcOH at room temperature. To this mixture was added 1 equivalent of formaldehyde (37 wt% solution in water) followed by $NaCNBH_3$ (1.5 equiv). The reaction was allowed to stir at room temperature for an additional 2 hours, at which time water was added and the solid that precipitated was foltered and washed witth water to give compound **4.2a14** in 95% yield (1.0 g) as a white solid. **$^1$H-NMR** (400 MHz; DMSO-$d_6$): δ 7.21 (s, 2H), 7.17 (t, *J* = 6.7 Hz, 1H), 7.07 (d, *J* = 8.3 Hz, 2H), 6.91 (d, *J* = 7.6 Hz, 1H), 6.82 (d, *J* = 8.4 Hz, 2H), 4.48 (s, 2H), 3.66 (s, 3H), 2.97 (s, 3H). **$^{13}$C-NMR** (100 MHz; DMSO-$d_6$): δ 168.4, 158.7, 149.5, 131.9, 130.8, 129.6, 128.4, 117.3, 116.9, 114.4, 112.9, 55.5, 55.2, 39.0. **HRMS** (ESI-TOF) Calc. for $[C_{16}H_{16}NO_3]^-$ = 270.1136, Found = 270.1137.

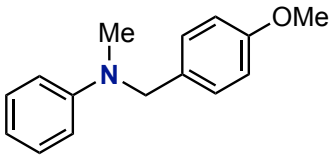


**4.2a15** was prepared as previously reported using p-methoxybenzyl bromide in lieu of the chloride. Physical and spectral data was in accordance with the literature.[32]

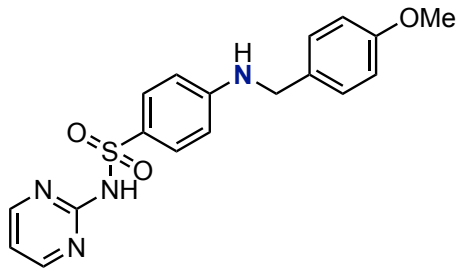


**4.2a16** was prepared analogously to compound **4.2a1** in 27% yield (1.0 g) as a white solid. **$^1$H-NMR** (300 MHz; DMSO-$d_6$): δ 11.30 (s, 1H), 8.48 (d, *J* = 4.8 Hz, 2H), 7.66 (d, *J* = 8.8 Hz, 2H), 7.25 (d, *J* = 8.6 Hz, 2H), 7.05 (dt, *J* = 25.7, 5.3 Hz, 2H), 6.89 (d, *J* = 8.6 Hz, 2H), 6.63 (d, *J* = 8.9 Hz, 2H), 4.24-4.22 (m, 2H), 3.72 (s, 3H). **$^{13}$C-NMR** (75 MHz; DMSO-$d_6$): δ 158.7, 157.7, 152.6, 131.3, 130.0, 129.0, 125.6, 116.0, 114.3, 111.2, 55.5, 45.8 **HRMS** (ESI-TOF) Calc. for $[C_{18}H_{18}N4O_3SNa]^+$= 393.0992, Found = 393.0988.

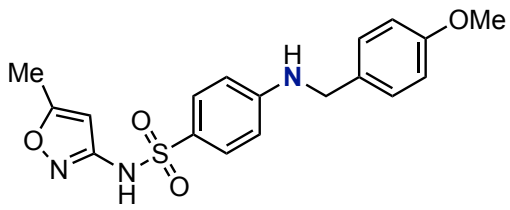


**4.2a17** was prepared analogously to **4.2a1** in 52% yield (2.4 g). **4.2a17** was purified by recrystallization from hexanes/ethyl acetate to give an off-white solid. **$^1$H-NMR** (300 MHz; DMSO-$d_6$): δ 10.97 (s, 1H), 7.50 (d, *J* = 8.9 Hz, 2H), 7.26 (d, *J* = 8.7 Hz, 2H), 7.17 (t, *J* = 5.8 Hz, 1H), 6.90 (d, *J* = 8.7 Hz, 2H), 6.64 (d, *J* = 8.9 Hz, 2H), 6.10 (d, *J* = 0.9 Hz, 1H), 4.24 (d, *J* = 5.8 Hz, 2H), 3.72 (s, 3H), 2.28 (s, 3H). **$^{13}$C-NMR** (75 MHz; DMSO-$d_6$): δ 170.3, 158.8, 158.4, 152.8, 131.2, 129.06, 128.97, 124.9, 114.3, 111.7, 95.8, 55.5, 45.7, 12.5. **HRMS** (ESI-TOF) Calc. for $[C_{18}H_{19}N_3O_4SNa]^+$ = 396.0988, Found = 396.0985.

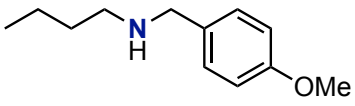


**4.2a18** was prepared as previously reported. Physical and spectral data was in accordance with the literature.[33]

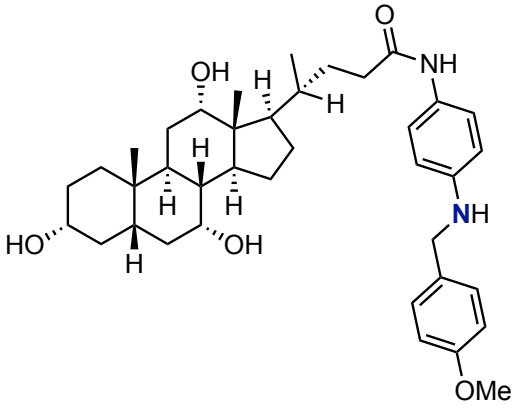


**4.2a19** was prepared by first coupling cholic acid and 1,4-phenylenediamine using a reported procedure.[34] This compound was then used to prepare **4.2a19** using an analogous procedure to that of **4.2a1** in 10% yield over two steps (100 mg as a pale red solid. **$^{1}$H-NMR** (300 MHz; $CDCl_3$): δ 8.06 (s, 1H), 7.35 (d, *J* = 8.9 Hz, 2H), 7.28 (d, *J* = 8.7 Hz, 3H), 6.88 (d, *J* = 8.7 Hz, 2H), 6.58 (d, *J* = 8.9 Hz, 2H), 4.22 (s, 2H), 3.98 (s, 1H), 3.85 (s, 1H), 3.81 (s, 3H), 3.49-3.45 (m, 1H), 2.34-0.99 (m, 28H), 0.89 (s, 3H), 0.69 (s, 3H). **$^{13}$C-NMR** (75 MHz; DMSO-$d_6$): δ 171.2, 158.5, 145.0, 132.5, 129.3, 128.9, 121.2, 114.1, 112.8, 71.5, 70.9, 66.7, 55.5, 46.81, 46.63, 46.2, 42.00, 41.84, 35.77, 35.68, 35.4, 34.9, 33.8, 32.2, 30.9, 29.0, 27.8, 26.7, 23.29, 23.09, 17.6, 12.8. **HRMS** (ESI-TOF) Calc. for $[C_{38}H_{55}N_2O_5]^+$= 619.4105, Found = 619.4108.

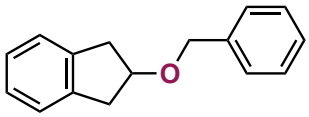


**4.2a20** was prepared analogously to **4.2a22** using benzyl bromide in lieu of 4-methoxy benzyl bromide in 42% yield (700 mg). Physical and spectral data was in accordance with the literature.[35]

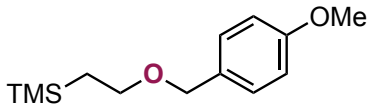


**4.2a21** was prepared analogously to **4.2a22** in 81% yield (2.0 g). Physical and spectral data was in accordance with the literature.[36]

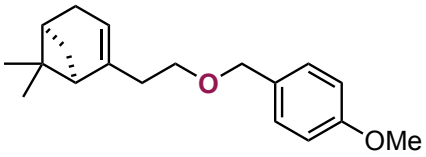


**4.2a22** was prepared as previously reported using 4-methoxy benzyl bromide in lieu of the chloride in 23% yield (700 mg).[37] This same procedure (and in some case, with slight modification when noted) was used to prepare many of the other PMB- and Bn-protected alcohols below. Physical and spectral data was in accordance with the literature.[37]

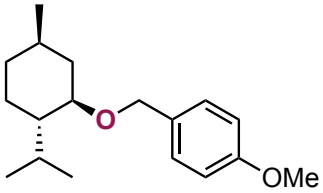


**4.2a23** was prepared analogously to **4.2a22** in 14% yield (400 mg). Physical and spectral data was in accordance with the literature.[38]

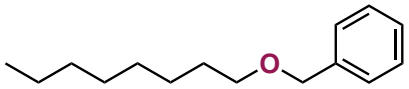

**4.2a24** was prepared analogously to **4.2a22** using benzyl bromide in lieu of 4-methoxy benzyl bromide in 38% yield (800 mg). Physical and spectral data was in accordance with the literature.[39]

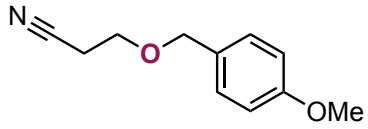

**4.2a25** was prepared as previously reported. Physical and spectral data was in accordance with the literature.[40]

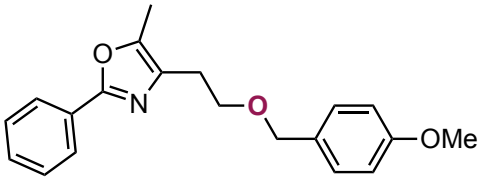

**4.2a26** was prepared analogously to **4.2a22** in 76% yield (1.7 g) as an orange oil. **$^{1}$H-NMR** (300 MHz; $CDCl_3$): δ 8.00 (d, $J$ = 8.1 Hz, 2H), 7.47-7.41 (m, 3H), 7.26 (d, $J$ = 8.7 Hz, 2H), 6.87 (d, $J$ = 8.7 Hz, 2H), 4.49 (s, 2H), 3.80 (s, 3H), 3.76 (t, $J$ = 7.0 Hz, 2H), 2.83 (t, $J$ = 6.9 Hz, 2H), 2.35 (s, 3H). **$^{13}$C-NMR** (75 MHz; $CDCl_3$): 159.30, 159.11, 144.6, 133.3, 130.6, 129.7, 129.2, 128.6, 127.9, 125.9, 113.7, 72.7, 68.9, 55.2, 26.9, 10.2 **HRMS** (ESI-TOF) Calc. for $[C_{20}H_{22}NO_3]^+$= 324.1594, Found = 324.1594.

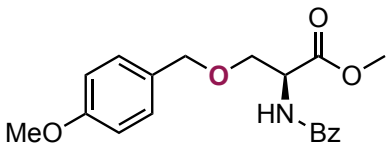


**4.2a27** was prepared as previously reported. Physical and spectral data was in accordance with the literature.[41]

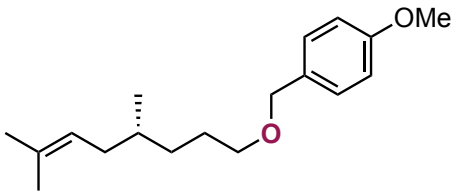


**4.2a28** was prepared as previously reported. Physical and spectral data was in accordance with the literature.[42]

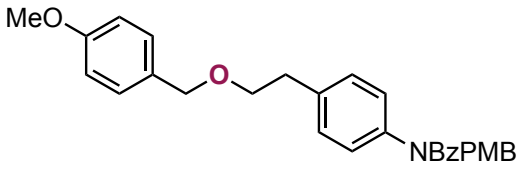


**4.2a29** was prepared starting from substrate **4.2a9.** To a solution of compound **4.2a9** in DCM (0.2 M) was added benzoyl chloride (1.1 equiv) and TEA (1.5 equiv). the reaction mixture was allowed to stir at room temperature for 12 hours, after which the water was added and the organic layer was separated, dried over sodium sulfate, and evaporated under reducted pressure. To this crude product, THF was added (0.5 M) followed by TBAF (3 equiv, 1.0 M solution in THF) at room temperature. The reaction was allowed to stir for 30 minutes, after which water was added and the mixture was extracted three times with EtOAc. The organic fractions were collected, dried over sodium sulfate, and evaporated under reduced presure. Finally, the crude product mixture was subjected to p-methoxy benzylation conditions analogous to those used for compound **4.2a22** to yield compound **4.2a29** in 64% yield over 3 steps (1.1g) as a thick, colorless oil. **$^{1}$H-NMR** (300 MHz; $CDCl_3$): δ 7.34-6.82 (m, 18H), 5.07 (s, 2H), 4.41 (s, 2H), 3.82 (s, 3H), 3.80 (s, 4H), 3.60 (t, *J* = 6.9 Hz, 2H), 2.82 (t, *J* = 6.9 Hz, 2H). **$^{13}$C-NMR** (75 MHz; $CDCl_3$): δ 170.4, 159.2, 158.9, 141.5, 137.7, 136.2, 130.3, 129.86, 129.83, 129.50, 129.44, 129.2, 128.8, 127.68, 127.65, 113.8, 72.7, 70.4, 55.28, 55.21, 53.3, 35.8 **HRMS** (ESI-TOF) Calc. for $[C_{31}H_{32}NO_4]^+$= 482.2326, Found = 482.2322.

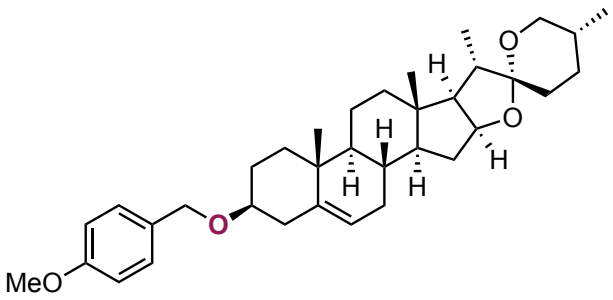


**4.2a30** was prepared analogously to **4.2a22** in 38% yield as an off white solid (1.4 g). **$^{1}$H-NMR** (300 MHz; $CDCl_3$): δ 7.28 (d, *J* = 8.1 Hz, 2H), 6.88 (d, *J* = 8.1 Hz, 2H), 5.36 (s, 1H), 4.50 (s, 2H), 4.43-4.41 (m, 1H), 3.81 (s, 3H), 3.36-3.26 (m, 3H), 2.45-2.42 (m, 1H), 2.32-2.24 (m, 1H), 1.99-1.50 (m, 17H), 1.04-0.81 (m, 17H). **$^{13}$C-NMR** (75 MHz; $CDCl_3$): δ 159.0, 141.0, 131.1, 129.1, 121.2, 113.8, 109.2, 80.8, 78.2, 69.6, 66.8, 62.1, 56.5, 55.3, 50.1, 41.6, 40.3, 39.8, 39.2, 37.24, 37.05, 32.1, 31.9, 31.46, 31.42, 30.3, 28.8, 28.5, 20.9, 19.4, 17.2, 16.3, 14.6 **HRMS** (ESI-TOF) Calc. for $[C_{35}H_{51}O_4]^+$ = 535.3782, Found = 535.3778.

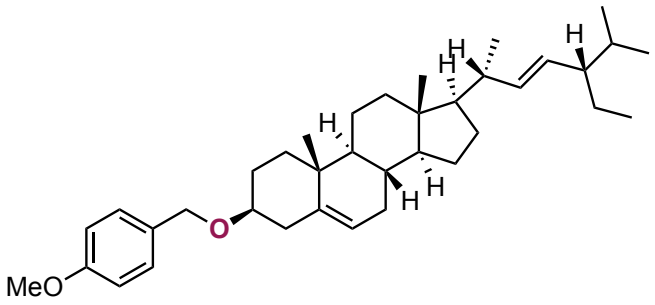


**4.2a31** prepared analogously to compound **4.2a22** in 39% yield (500 mg) as an off white solid. **$^1$H-NMR** (300 MHz; $CDCl_3$): δ 7.31 (d, *J* = 8.6 Hz, 2H), 6.90 (d, *J* = 8.6 Hz, 2H), 5.39-5.37 (m, 1H), 5.23-5.01 (m, 2H), 4.52 (s, 2H), 3.82 (s, 3H), 3.30 (tt, *J* = 11.1, 4.5 Hz, 1H), 2.45 (dd, *J* = 13.2, 2.8 Hz, 1H), 2.35-2.26 (m, 1H), 2.09-1.17 (m, 21H), 1.06 (d, *J* = 7.2 Hz, 8H), 0.85 (t, *J* = 7.6 Hz, 9H), 0.74 (s, 3H). **$^{13}$C-NMR** (75 MHz; $CDCl_3$): δ 159.1, 141.0, 138.4, 131.2, 129.28, 129.13, 121.5, 113.8, 78.3, 71.5, 69.6, 56.9, 56.0, 55.3, 51.3, 50.3, 42.2, 40.5, 39.7, 39.2, 37.3, 36.9, 31.97, 31.92, 29.0, 28.5, 25.5, 24.4, 21.27, 21.14, 21.10, 19.4, 19.0, 12.3, 12.1 **HRMS** (ESI-TOF) Calc. for $[C_{37}H_{57}O_2]^+$ = 533.4353, Found = 533.4355.

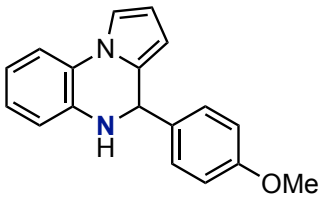


**4.2a32** was prepared as previously reported.[43] Physical and spectral data was in accordance with the literature.[44]

### 4.5.3 General Debenzylation Procedures

****Caution: while no problems were encountered in this work, alkylhydroperoxides can undergo spontaneous and rapid exothermic decomposition and appropriate care should be taken in their handling****

**General Debenzylation Procedure:** To a 1-dram vial charged with a magnetic stir bar was added the respective PMB- or Bn-protected substrate (0.2 mmol), AIBN (0.05 equivalents), pentafluorothiophenol (0.1 equivalents) and chlorobenzene (0.2 mL). The vial was capped and heated to 80 °C. The reaction progress was then monitored every 60 minutes by crude H-NMR to determine whether or not all of the starting material had been consumed. If starting material had been consumed, the reaction was allowed to cool to room temperature, the respective workup procedure was performed, and the desired product was isolated. If starting material had not been consumed as judged by H-NMR, an additional 0.05 equivalents of AIBN and 0.1 equivalents of pentafluorthiophenol was added. This process was repeated every 60 minutes until complete consumption of the starting material was observed.

**General Workup Procedure A (N-protected substrates):** Upon completion of the reaction as determined by crude H-NMR, the reaction mixture was allowed to cool to room temperature and several drops of 5 M aqueous HCl was added to the reaction. The mixture was then gently shaken by hand for approximately 30 seconds. The mixture was then diluted with a small amount of water (about 1 mL) and then extracted 4 times with EtOAc (2 mL). The aqueous fraction was then evaporated under reduced pressure to yield the desired deprotected amine product as its hydrochloride salt.

**General Workup Procedure B (N-protected substrates):** Upon completion of the reaction as determined by crude H-NMR, the reaction mixture was allowed to cool to room temperature and several drops of 5 M aqueous HCl was added to the reaction. The mixture was then gently shaken by hand for approximately 30 seconds. The mixture was then basified with 5 M aqueous NaOH and extracted 4 times with EtOAc (2 mL). The organic fractions were then collected and evaporated under reduced pressure. 2 mL of methanol followed by 5 mL of saturated

$NaHSO_3$[45] was then added to the crude material, the reaction was shaken by hand for several seconds, and then diluted with water. The mixture was then extracted with EtOAc, the organic fractions were collected, and evaporated under reduced pressure. The desired product was then isolated by flash column chromatography (5-100% EtOAc in hexanes).

**General Workup Procedure C (N-protected substrates):** Upon completion of the reaction as determined by crude H-NMR, the reaction mixture was allowed to cool to room temperature and 1 mL of methanol followed by 10 equivalents of hydrazine monohydrate was added. The reaction was then allowed to stir at 80 °C for 5 minutes, after which the mixture was allowed to cool to room temperature and the solvent was removed under reduced pressure. The desired product was then isolated by flash column chromatography (5-100% EtOAc in hexanes).

**General Workup Procedure D (N-protected substrates):** Upon completion of the reaction as determined by crude HNMR, the reaction mixture was allowed to cool to room temperature and 1 mL of a 1:1 mixture of THF:water followed by 10 equivalents of hydroxylamine hydrochloride[46] was added. The reaction was then allowed to stir at 80 °C for 10 minutes, after which the mixture was allowed to cool to room temperature, the organic layer was separated, and the solvent was removed under reduced pressure. The desired product was then isolated by recrystallization from EtOAc.

**General Workup Procedure E (O-protected substrates):** Upon completion of the reaction as determined by crude HNMR, the mixture was allowed to cool to room temperature and the solvent was removed under reduced pressure. The desired product was then isolated by flash column chromatography (0-25% EtOAc in hexanes).

### 4.5.4 Characterization of Products

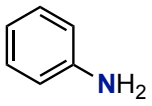

Compound **4.2c1** was prepared according to the general debenzylation procedure A (3 total additions of 10% PFTP and 5% AIBN) from its PMB-protected congener in 100% yield (27 mg) as a pale yellow oil. Physical and spectral data was in accordance with that of an authentic sample purchased and used for the synthesis of the protected starting material (CAS: 62-53-3).

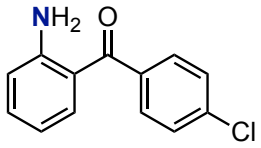

Compound **4.2c2** was prepared according to the general debenzylation procedure B from its PMB-protected congener in 86% yield (40 mg) as a bright yellow solid. Physical and spectral data was in accordance with that of an authentic sample purchased and used for the synthesis of the protected starting material (CAS: 2894-51-1).

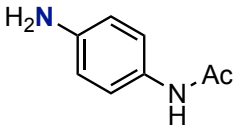

Compound **4.2c3** was prepared according to the general debenzylation procedure C (3 total additions of 10% PFTP and 5% AIBN) from its PMB-protected congener in 100% yield (31 mg) as an off white solid. Physical and spectral data was in accordance with that of an authentic sample purchased and used for the synthesis of the protected starting material (CAS: 122-80-5).

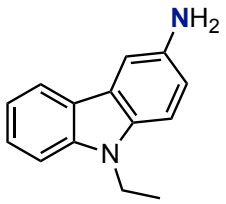

Compound **4.2c4** was prepared according to the general debenzylation procedure C (3 total additions of 10% PFTP and 5% AIBN) from its PMB-protected congener in 83% yield (35 mg) as an off white solid. Physical and spectral data was in accordance with that of an authentic sample purchased and used for the synthesis of the protected starting material (CAS: 132-32-1).

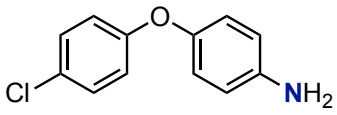

Compound **4.2c5** was prepared according to the general debenzylation procedure C (3 total additions of 10% PFTP and 5% AIBN) from its PMB-protected congener in 86% yield (37 mg) as a pale yellow oil. Physical and spectral data was in accordance with that of an authentic sample purchased and used for the synthesis of the protected starting material (CAS: 1072-98-6).

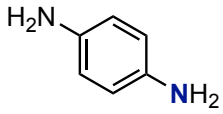

Compound **4.2c7** was prepared according to the general debenzylation procedure C (3 total additions of 10% PFTP and 5% AIBN) from its PMB-protected congener in 100% yield (23 mg) as a red solid. Physical and spectral data was in accordance with the literature.[47]

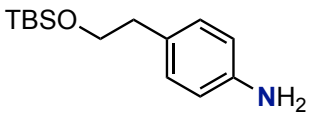


Compound **4.2c8** was prepared according to the general debenzylation procedure C (3 total additions of 10% PFTP and 5% AIBN) from its PMB-protected congener in 60% yield (30 mg) as a pale yellow oil. Physical and spectral data was in accordance with the literature.[48]

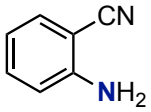


Compound **4.2c6** was prepared according to the general debenzylation procedure C (3 total additions of 10% PFTP and 5% AIBN) from its PMB-protected congener in 68% yield (16 mg) as a pale yellow oil. Physical and spectral data was in accordance with the literature.[49]

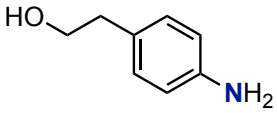


Compound **4.2c9** was prepared according to the general debenzylation procedure C (3 total additions of 10% PFTP and 5% AIBN) from its PMB-protected congener in 66% yield (18 mg) as a pale yellow oil Physical and spectral data was in accordance with that of an authentic sample purchased and used for the synthesis of the protected starting material (CAS: 104-10-9).

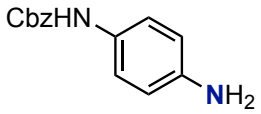


Compound **4.2c10** was prepared according to the general debenzylation procedure D (3 Total additions of 10% PFTP and 5% AIBN) from its PMB-protected congener in 72% yield (35 mg) as a pale yellow solid. Physical and spectral data was in accordance with the literature.[50]

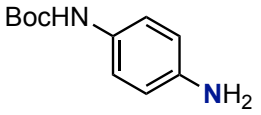


Compound **4.2c11** was prepared according to the general debenzylation procedure D (3 total additions of 10% PFTP and 5% AIBN) from its PMB-protected congener in 20% yield (7 mg) as a pale red solid. Physical and spectral data was in accordance with the literature.[51]

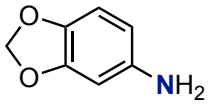


Compound **4.2c12** was prepared according to the general debenzylation procedure C (3 total additions of 10% PFTP and 5% AIBN) from its PMB-protected congener in 43% yield (15 mg) as a pale yellow oil. Physical and spectral data was in accordance with that of an authentic sample purchased and used for the synthesis of the protected starting material (CAS: 14268-66-7).

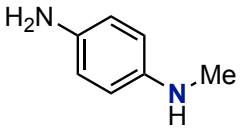

Compound **4.2c13** was prepared according to the general debenzylation procedure C (6 total additions of 10% PFTP and 5% AIBN) from its PMB-protected congener in 30% yield (7 mg) as an off white solid. Physical and spectral data was in accordance with the literature.[52]

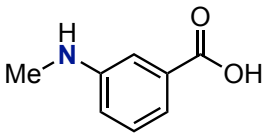

Compound **4.2c14** was prepared according to the general debenzylation procedure C (6 total additions of 10% PFTP and 5% AIBN) from its PMB-protected congener in 33% yield (10 mg) as an off white solid. Physical and spectral data was in accordance with the literature.[53]

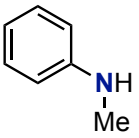

Compound **4.2c15** was prepared according to the general debenzylation procedure A (3 total additions of 10% PFTP and 5% AIBN) from its Bn-protected congener in 70% yield (20 mg) as a pale yellow oil. Physical and spectral data was in accordance with that of an authentic sample purchased and used for the synthesis of **x** the protected starting material (CAS: 100-61-8).

Compound **4.2c16** was prepared according to the general debenzylation procedure C (6 total additions of 10% PFTP and 5% AIBN) from its PMB-protected congener in 36% yield (42 mg) as an off white solid. Physical and spectral data was in accordance with that of an authentic sample purchased and used for the synthesis of the protected starting material (CAS: 68-35-9).

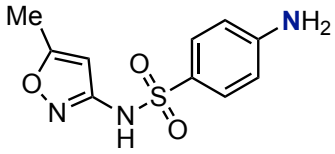

Compound **4.2c17** was prepared according to the general debenzylation procedure D (3 total additions of 10% PFTP and 5% AIBN) from its PMB-protected congener in 49% yield (25 mg) as an off white solid. Physical and spectral data was in accordance with that of an authentic sample purchased and used for the synthesis of the protected starting material (CAS: 723-46-6).

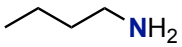

Compound **4.2c18** was prepared according to the general debenzylation procedure C (3 total additions of 10% PFTP and 5% AIBN) from its Bn-protected congener in 46% yield (10 mg) as a pale yellow oil. Physical and spectral data was in accordance with that of an authentic sample purchased and used for the synthesis of the protected starting material (CAS: 109-73-9).

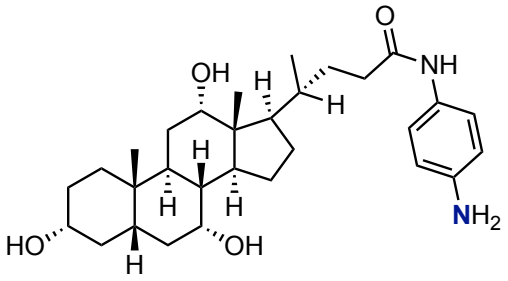


Compound **4.2c19** was prepared according to the general debenzylation procedure C (2 total additions of 10% PFTP and 5% AIBN) from its PMB-protected congener in 36% yield (15 mg) as an off white solid. Physical and spectral data was in accordance with the literature.[34]

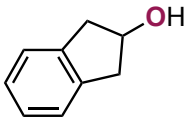


Compound **4.2c20** was prepared according to the general debenzylation procedure E (3 total additions of 10% PFTP and 5% AIBN) from its Bn-protected congener in 20% yield (6 mg) as a white solid (64% NMR yield using dibromomethane as an internal standard). Physical and spectral data was in accordance with that of an authentic sample purchased and used for the synthesis of the protected starting material (CAS: 4254-29-9).

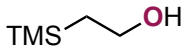


Compound **4.2c21** was prepared according to the general debenzylation procedure (3 total additions of 10% PFTP and 5% AIBN) from its PMB-protected congener in 81% yield. Spectral data was in accordance with that of an authentic sample purchased and used for the synthesis of the protected starting material (CAS: 28351-78-2). The yield of this compound is represented by a H-NMR because of difficulties encountered separating the desired product from the aldehyde byproduct of the reaction.

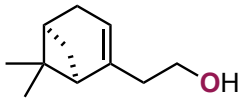


Compound **4.2c22** was prepared according to the general debenzylation procedure (3 total additions of 10% PFTP and 5% AIBN) from its PMB-protected congener in 44% H-NMR yield. Spectral data was in accordance with that of an authentic sample purchased and used for the synthesis of the protected starting material (CAS: 35836-73-8). The yield of this compound is represented by a H-NMR because of difficulties encountered separating the desired product from the aldehyde byproduct of the reaction.

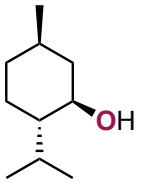


Compound **4.2c23** was prepared according to the general debenzylation procedure (3 total additions of 10% PFTP and 5% AIBN) from its PMB-protected congener in 85% H-NMR yield. Spectral data was in accordance with that of an authentic sample purchased and used for the synthesis of the protected starting material (CAS: 89-78-1). The yield of this compound is represented by a H-NMR because of difficulties encountered separating the desired product from the aldehyde byproduct of the reaction.

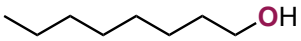


Compound **4.2c24** was prepared according to the general debenzylation procedure (3 total additions of 10% PFTP and 5% AIBN) from its Bn-protected congener in 45% yield. Spectral data was in accordance with that of an authentic sample purchased and used for the synthesis of the protected starting material (CAS: 111-87-5). The yield of this compound is represented by a H-NMR because of difficulties encountered separating the desired product from the aldehyde byproduct of the reaction.

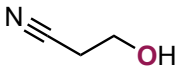


Compound **4.2c25** was prepared according to the general debenzylation procedure (6 total additions of 10% PFTP and 5% AIBN) from its PMB-protected congener in 81% H-NMR yield. Spectral data was in accordance with the literature.[54] The yield of this compound is represented by a H-NMR because of difficulties encountered separating the desired product from the aldehyde byproduct of the reaction.

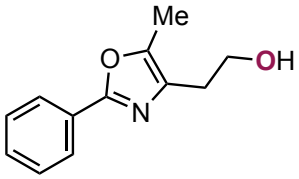


Compound **4.2c26** was prepared according to the general debenzylation procedure E (6 total additions of 10% PFTP and 5% AIBN) from its PMB-protected congener in 47% yield (19 mg) as a white solid. Physical and spectral data was in accordance with that of an authentic sample purchased and used for the synthesis of the protected starting material (CAS: 103788-65-4).

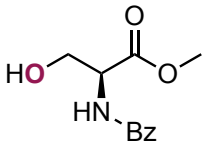


Compound **4.2c27** was prepared according to the general debenzylation procedure E (6 total additions of 10% PFTP and 5% AIBN) but using MeCN in lieu of chlorobenzene from its PMB-protected congener in 67% yield (30 mg) as a clear oil. Physical and spectral data was in accordance with the literature.[55]

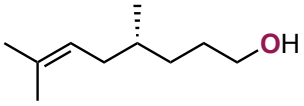


Compound **x** was prepared according to the general debenzylation procedure (3 total additions of 10% PFTP and 5% AIBN) from its PMB-protected congener in 36% yield. Spectral data was in accordance with that of an authentic sample purchased and used for the synthesis of the protected starting material (CAS: 7540-51-4). The yield of this compound is represented by a H-NMR because of difficulties encountered separating the desired product from the aldehyde byproduct of the reaction.

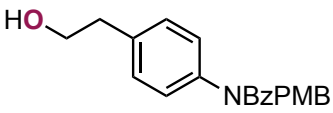


Compound **4.2c29** was prepared according to the general debenzylation procedure E (6 total additions of 10% PFTP and 5% AIBN) from its PMB-protected congener in 46% yield (33 mg) as a clear oil. **$^{1}$H-NMR** (300 MHz; $CDCl_3$): δ 7.32 (d, *J* = 6.7 Hz, 2H), 7.25-7.12 (m, 5H), 6.99 (d, *J* = 8.3 Hz, 2H), 6.85-6.80 (m, 4H), 5.05 (s, 2H), 3.78 (s, 3H), 3.74 (t, *J* = 6.7 Hz, 2H), 2.74 (t, *J* = 6.7 Hz, 2H). **$^{13}$C-NMR** (75 MHz; $CDCl_3$): δ 170.6, 158.9, 141.7, 137.2, 136.1, 129.77, 129.73, 129.55, 129.51, 128.7, 127.86, 127.69, 113.8, 63.2, 55.2, 53.3, 38.5. **HRMS** (ESI-TOF) Calc. for $[C_{23}H_{24}NO_3]^+$= 362.1751, Found = 362.1752.

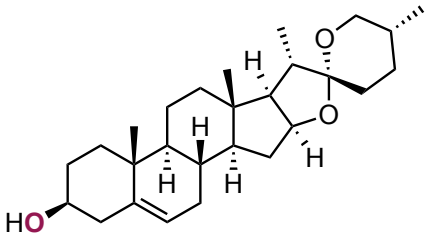


Compound**4.2c30** was prepared according to the general debenzylation procedure E (6 total additions of 10% PFTP and 5% AIBN) from its PMB-protected congener in 25% yield (21 mg) as a white solid. Physical and spectral data was in accordance with that of an authentic sample purchased and used for the synthesis of the protected starting material (CAS: 512-04-9).

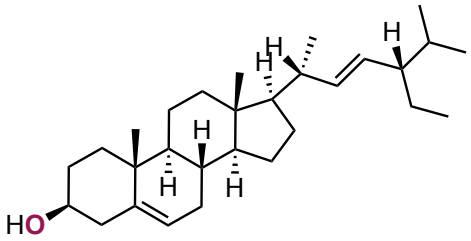


Compound **4.2c31** was prepared according to the general debenzylation procedure E (3 total additions of 10% PFTP and 5% AIBN) from its PMB-protected congener in 68% yield (56 mg) as a light brown solid. Physical and spectral data was in accordance with that of an authentic sample purchased and used for the synthesis of the protected starting material (CAS: 83-48-7).

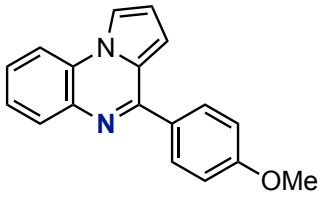


Compound **4.2b32** was prepared according to the general debenzylation procedure C (2 total additions of 10% PFTP and 5% AIBN) from compound **4.2a32** in 53% yield (29 mg) as an off white solid (quantitative H-NMR yield). Physical and spectral data was in accordance with the literature.[56]

### 4.5.5 Computational Details

All calculations were performed using Gaussian 16, Revision B.01.[57] Molecular structures were visualized using Avogadro version 1.2.0.[58]

The S-H bond dissociation enthalpies of pentafluorothiophenol and methyl thioglycolate were calculated according to the method presented by Dilman in: Ranferova, L. I.; Zubov, M. O.; Kokorekin, V. A.; Levin, V. V.; Dilman, A. D. Using The Thiyl Radical for Aliphatic Hydrogen Atom Transfer: Thiolation of Unactivated C-H Bonds. *Angew Chem.* **2021**, 2885-2890.

The S-H bond dissociation enthalpy of thiophenol was taken from: Borges dos Santosm R. M.; Muralha, V. S. F.; Correia, C. F.; Guedes, R. C.; Costa Cabral, B. J.; Martinho Simões, J. A. S-H Bond Dissociation Enthalpies in thiophenols: A Time Resolved Photoacoustic Calorimetry and Quantum Chemistry Study. *J. Phys. Chem. A* **2002**, 9883-9889.

The electron affinity of the methyl thioglycolate, thiophenol, and pentafluorothiophenol derived thiyl radicals were calculated according to the method presented in: Chandra, A. K.; Nam, P.-C.; Nguyen. The S-H Bond Dissociation Enthalpies and Acidities of Para and Meta Substituted Thiophenols: A Quantum Chemical Study. *J. Phys. Chem. A* **2003**, 9182-9188.

**Structures for BDE calculations:**

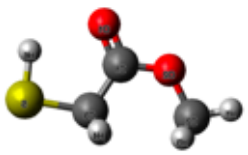

**Methyl thioglycolate, B3LYP/6-311G(d,p)**

| | | | |
|---|---|---|---|
| C | -0.4582280000 | 0.5857750000 | 0.0050570000 |
| O | -0.0036890000 | 1.6961230000 | 0.0014460000 |
| O | -1.8027380000 | 0.4297720000 | -0.0058150000 |
| C | -2.4240530000 | -0.8620260000 | -0.0118740000 |
| H | -3.4935810000 | -0.6637940000 | 0.0004670000 |
| H | -2.1757040000 | -1.4244990000 | -0.9154280000 |
| H | -2.1583450000 | -1.4435710000 | 0.8743770000 |
| C | 0.3811050000 | -0.6893150000 | 0.0337910000 |
| H | 0.1378130000 | -1.2482390000 | 0.9405160000 |
| H | 0.1112200000 | -1.3172340000 | -0.8175070000 |
| S | 2.1866200000 | -0.3799740000 | -0.0148070000 |
| H | 2.0511490000 | 0.9631470000 | 0.0275930000 |

Zero-point correction= 0.088911 (Hartree/Particle)

Thermal correction to Energy= 0.096461

Thermal correction to Enthalpy= 0.097405

Thermal correction to Gibbs Free Energy= 0.055502

Sum of electronic and zero-point Energies= -666.573520

Sum of electronic and thermal Energies= -666.565969

Sum of electronic and thermal Enthalpies= -666.565025

Sum of electronic and thermal Free Energies= -666.606928

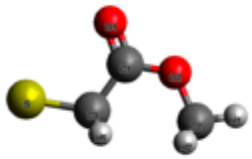

**Methyl thioglycolate thiyl radical, B3LYP/6-311G(d,p)**

| | | | |
|---|---|---|---|
| C | 0.4405100000 | 0.6191550000 | 0.0000270000 |
| O | 0.0395680000 | 1.7435750000 | 0.0000780000 |
| O | 1.7836570000 | 0.3937430000 | -0.0000040000 |
| C | 2.3465160000 | -0.9232470000 | -0.0000440000 |
| H | 3.4243830000 | -0.7741060000 | -0.0000580000 |
| H | 2.0678780000 | -1.4864140000 | 0.8947860000 |
| H | 2.0678520000 | -1.4863690000 | -0.8948950000 |
| C | -0.4533080000 | -0.6273740000 | 0.0001360000 |
| H | -0.2256870000 | -1.2556930000 | -0.8682070000 |
| H | -0.2257200000 | -1.2555190000 | 0.8686070000 |
| S | -2.2310510000 | -0.3282280000 | -0.0000960000 |

Zero-point correction= 0.077573 (Hartree/Particle)

Thermal correction to Energy= 0.084427

Thermal correction to Enthalpy= 0.085372

Thermal correction to Gibbs Free Energy= 0.045029

Sum of electronic and zero-point Energies= -665.937143

Sum of electronic and thermal Energies= -665.930288

Sum of electronic and thermal Enthalpies= -665.929344

Sum of electronic and thermal Free Energies= -665.969687

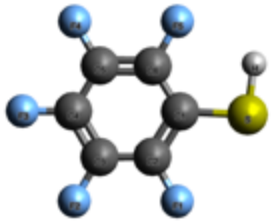

**Pentafluorothiophenol, B3LYP/6-311G(d,p)**

| | | | |
|---|---|---|---|
| C | 1.1141290000 | -0.0044240000 | 0.0000160000 |
| C | 0.3861850000 | -1.1934540000 | -0.0000670000 |
| F | 1.0395760000 | -2.3639090000 | -0.0000660000 |
| C | -1.0018000000 | -1.2007290000 | 0.0000700000 |
| F | -1.6692490000 | -2.3568790000 | 0.0001030000 |
| C | -1.6971760000 | 0.0030360000 | 0.0000000000 |
| F | -3.0317100000 | 0.0075940000 | -0.0000620000 |
| C | -0.9949790000 | 1.2025740000 | 0.0000180000 |
| F | -1.6567950000 | 2.3625670000 | -0.0000770000 |
| C | 0.3933010000 | 1.1892910000 | 0.0001060000 |
| F | 1.0441480000 | 2.3654920000 | 0.0000370000 |
| S | 2.8878300000 | -0.0850910000 | -0.0000520000 |
| H | 3.0630460000 | 1.2499140000 | 0.0005580000 |

Zero-point correction= 0.058597 (Hartree/Particle)

Thermal correction to Energy= 0.069222

Thermal correction to Enthalpy= 0.070166

Thermal correction to Gibbs Free Energy= 0.022173

Sum of electronic and zero-point Energies= -1126.745428

Sum of electronic and thermal Energies= -1126.734803

Sum of electronic and thermal Enthalpies= -1126.733859

Sum of electronic and thermal Free Energies= -1126.781852

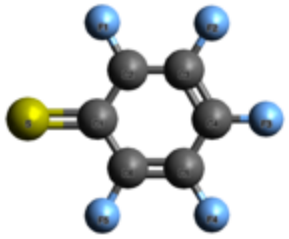

**Pentafluorothiophenol thiyl radical, B3LYP/6-311G(d,p)**

| | | | |
|---|---|---|---|
| S | -2.8897210000 | 0.0000000000 | 0.0000380000 |
| C | -1.1774240000 | 0.0000000000 | -0.0000190000 |
| C | -0.4301230000 | 1.2076060000 | -0.0000140000 |
| F | -1.0569100000 | 2.3771570000 | -0.0000440000 |
| C | 0.9522520000 | 1.2116020000 | 0.0000060000 |
| F | 1.6367100000 | 2.3568010000 | 0.0000140000 |
| C | 1.6442770000 | 0.0000000000 | 0.0000070000 |
| F | 2.9702780000 | 0.0000000000 | 0.0000140000 |
| C | 0.9522510000 | -1.2116020000 | 0.0000020000 |
| F | 1.6367090000 | -2.3568010000 | 0.0000070000 |
| C | -0.4301240000 | -1.2076050000 | -0.0000200000 |
| F | -1.0569110000 | -2.3771570000 | -0.0000340000 |

Zero-point correction= 0.049689 (Hartree/Particle)

Thermal correction to Energy= 0.059641

Thermal correction to Enthalpy= 0.060586

Thermal correction to Gibbs Free Energy= 0.013062

Sum of electronic and zero-point Energies= -1126.121683

Sum of electronic and thermal Energies= -1126.111731

Sum of electronic and thermal Enthalpies= -1126.110786

Sum of electronic and thermal Free Energies= -1126.158310

**Structures for electron affinity calculations:**

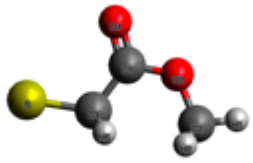

**Methyl thioglycolate thiolate anion, wb97xd/6-311++g(d,p) scrf=(iefpcm,solvent=benzene)**

| | | | |
|---|---|---|---|
| C | 0.4431300000 | 0.6141610000 | -0.0000670000 |
| O | 0.1254180000 | 1.7701310000 | -0.0000850000 |
| O | 1.7941410000 | 0.3616890000 | -0.0000460000 |
| C | 2.3134900000 | -0.9585050000 | -0.0000210000 |
| H | 3.3977500000 | -0.8482600000 | -0.0001540000 |
| H | 2.0115340000 | -1.5148660000 | 0.8914620000 |
| H | 2.0113250000 | -1.5149760000 | -0.8913660000 |
| C | -0.4669160000 | -0.5981230000 | -0.0000060000 |
| H | -0.1688580000 | -1.1952390000 | -0.8712210000 |
| H | -0.1687410000 | -1.1953350000 | 0.8710960000 |
| S | -2.2611070000 | -0.3206930000 | 0.0001120000 |

Zero-point correction= 0.080139 (Hartree/Particle)

Thermal correction to Energy= 0.087069

Thermal correction to Enthalpy= 0.088013

Thermal correction to Gibbs Free Energy= 0.047227

Sum of electronic and zero-point Energies= -665.972974

Sum of electronic and thermal Energies= -665.966044

Sum of electronic and thermal Enthalpies= -665.965100

Sum of electronic and thermal Free Energies= -666.005886

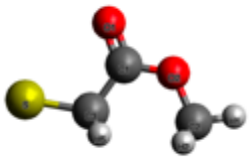

**Methyl thioglycolate thiyl radical, wb97xd/6-311++g(d,p) scrf=(iefpcm,solvent=benzene)**

| | | | |
|---|---|---|---|
| C | 0.4418020000 | 0.6118220000 | -0.0000860000 |
| O | 0.0380560000 | 1.7378350000 | -0.0000160000 |
| O | 1.7687060000 | 0.3942430000 | -0.0000690000 |
| C | 2.3267040000 | -0.9197570000 | -0.0000520000 |
| H | 3.4043760000 | -0.7748300000 | -0.0000270000 |
| H | 2.0417640000 | -1.4756580000 | 0.8959340000 |
| H | 2.0418090000 | -1.4756620000 | -0.8960510000 |
| C | -0.4503110000 | -0.6277250000 | 0.0000170000 |
| H | -0.2190970000 | -1.2537920000 | -0.8689020000 |
| H | -0.2189970000 | -1.2537180000 | 0.8689620000 |
| S | -2.2133200000 | -0.3255630000 | 0.0000940000 |

Zero-point correction= 0.079863 (Hartree/Particle)

Thermal correction to Energy= 0.086930

Thermal correction to Enthalpy= 0.087874

Thermal correction to Gibbs Free Energy= 0.046390

Sum of electronic and zero-point Energies= -665.837741

Sum of electronic and thermal Energies= -665.830674

Sum of electronic and thermal Enthalpies= -665.829730

Sum of electronic and thermal Free Energies= -665.871214

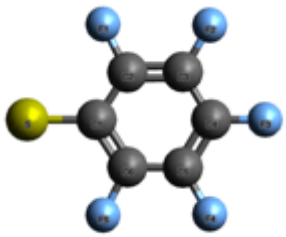

**Pentafluorothiophenol thiolate anion, wb97xd/6-311++g(d,p) scrf=(iefpcm,solvent=benzene)**

| | | | |
|---|---|---|---|
| S | -2.9283790000 | 0.0000010000 | 0.0000140000 |
| C | -1.1958770000 | 0.0000010000 | -0.0000120000 |
| C | -0.4275910000 | 1.1792060000 | -0.0000050000 |
| F | -1.0349760000 | 2.3756060000 | -0.0000170000 |
| C | 0.9559600000 | 1.1897300000 | 0.0000020000 |
| F | 1.6269210000 | 2.3508660000 | 0.0000080000 |
| C | 1.6638850000 | 0.0000000000 | 0.0000010000 |
| F | 3.0056240000 | -0.0000010000 | 0.0000050000 |
| C | 0.9559590000 | -1.1897300000 | -0.0000010000 |
| F | 1.6269200000 | -2.3508660000 | 0.0000010000 |
| C | -0.4275920000 | -1.1792060000 | -0.0000060000 |
| F | -1.0349770000 | -2.3756070000 | -0.0000080000 |

Zero-point correction= 0.049964 (Hartree/Particle)

Thermal correction to Energy= 0.059858

Thermal correction to Enthalpy= 0.060802

Thermal correction to Gibbs Free Energy= 0.014163

Sum of electronic and zero-point Energies= -1126.057190

Sum of electronic and thermal Energies= -1126.047295

Sum of electronic and thermal Enthalpies= -1126.046351

Sum of electronic and thermal Free Energies= -1126.092990

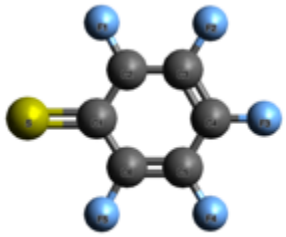

**Pentafluorothiophenol thiyl radical, wb97xd/6-311++g(d,p) scrf=(iefpcm,solvent=benzene)**

| | | | |
|---|---|---|---|
| S | -2.8790890000 | 0.0000000000 | 0.0000130000 |
| C | -1.1741990000 | 0.0000000000 | 0.0000010000 |
| C | -0.4286620000 | 1.2021560000 | -0.0000080000 |
| F | -1.0521810000 | 2.3660820000 | -0.0000200000 |
| C | 0.9506880000 | 1.2074200000 | 0.0000030000 |
| F | 1.6281090000 | 2.3474010000 | 0.0000110000 |
| C | 1.6413370000 | 0.0000000000 | 0.0000030000 |
| F | 2.9590620000 | 0.0000000000 | 0.0000030000 |
| C | 0.9506880000 | -1.2074200000 | -0.0000030000 |
| F | 1.6281090000 | -2.3474010000 | 0.0000010000 |
| C | -0.4286620000 | -1.2021550000 | -0.0000140000 |
| F | -1.0521810000 | -2.3660830000 | -0.0000060000 |

Zero-point correction= 0.050495 (Hartree/Particle)

Thermal correction to Energy= 0.060325

Thermal correction to Enthalpy= 0.061269

Thermal correction to Gibbs Free Energy= 0.014008

Sum of electronic and zero-point Energies= -1125.902089

Sum of electronic and thermal Energies= -1125.892259

Sum of electronic and thermal Enthalpies= -1125.891314

Sum of electronic and thermal Free Energies= -1125.938575

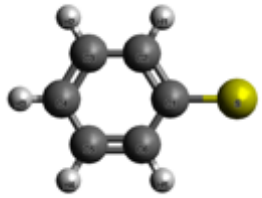

**Thiophenol thiolate anion, wb97xd/6-311++g(d,p) scrf=(iefpcm,solvent=benzene)**

| | | | |
|---|---|---|---|
| S | 2.3390560000 | 0.0000000000 | 0.0000130000 |
| C | 0.5845400000 | 0.0000000000 | -0.0000420000 |
| C | -0.1626260000 | 1.1965160000 | -0.0000060000 |
| H | 0.3766350000 | 2.1382380000 | -0.0000290000 |
| C | -1.5516050000 | 1.1962420000 | 0.0000050000 |
| H | -2.0831050000 | 2.1443360000 | 0.0000030000 |
| C | -2.2662070000 | 0.0000010000 | 0.0000130000 |
| H | -3.3511800000 | 0.0000010000 | 0.0000210000 |
| C | -1.5516050000 | -1.1962410000 | 0.0000050000 |
| H | -2.0831060000 | -2.1443350000 | 0.0000020000 |
| C | -0.1626260000 | -1.1965170000 | -0.0000060000 |
| H | 0.3766320000 | -2.1382410000 | -0.0000280000 |

Zero-point correction= 0.090631 (Hartree/Particle)

Thermal correction to Energy= 0.096139

Thermal correction to Enthalpy= 0.097083

Thermal correction to Gibbs Free Energy= 0.060847

Sum of electronic and zero-point Energies= -629.826359

Sum of electronic and thermal Energies= -629.820852

Sum of electronic and thermal Enthalpies= -629.819907

Sum of electronic and thermal Free Energies= -629.856143

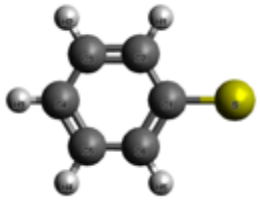

**Thiophenol thiyl radical, wb97xd/6-311++g(d,p) scrf=(iefpcm,solvent=benzene)**

| | | | |
|---|---|---|---|
| S | 2.3138410000 | 0.0000000000 | -0.0000160000 |
| C | 0.5528370000 | -0.0000020000 | 0.0000580000 |
| C | -0.1477580000 | 1.2084240000 | 0.0000010000 |
| H | 0.3872880000 | 2.1518550000 | 0.0000370000 |
| C | -1.5372910000 | 1.2007090000 | -0.0000070000 |
| H | -2.0715170000 | 2.1443560000 | 0.0000010000 |
| C | -2.2379300000 | 0.0000010000 | -0.0000150000 |
| H | -3.3218030000 | 0.0000020000 | -0.0000140000 |
| C | -1.5372940000 | -1.2007070000 | -0.0000070000 |
| H | -2.0715230000 | -2.1443520000 | 0.0000020000 |
| C | -0.1477600000 | -1.2084260000 | 0.0000010000 |
| H | 0.3872780000 | -2.1518600000 | 0.0000380000 |

Zero-point correction= 0.091173 (Hartree/Particle)

Thermal correction to Energy= 0.096711

Thermal correction to Enthalpy= 0.097655

Thermal correction to Gibbs Free Energy= 0.060730

Sum of electronic and zero-point Energies= -629.680361

Sum of electronic and thermal Energies= -629.674823

Sum of electronic and thermal Enthalpies= -629.673878

Sum of electronic and thermal Free Energies= -629.710804

### 4.5.6 $^{1}H$, $^{13}C$, and 2-D NMR Spectra

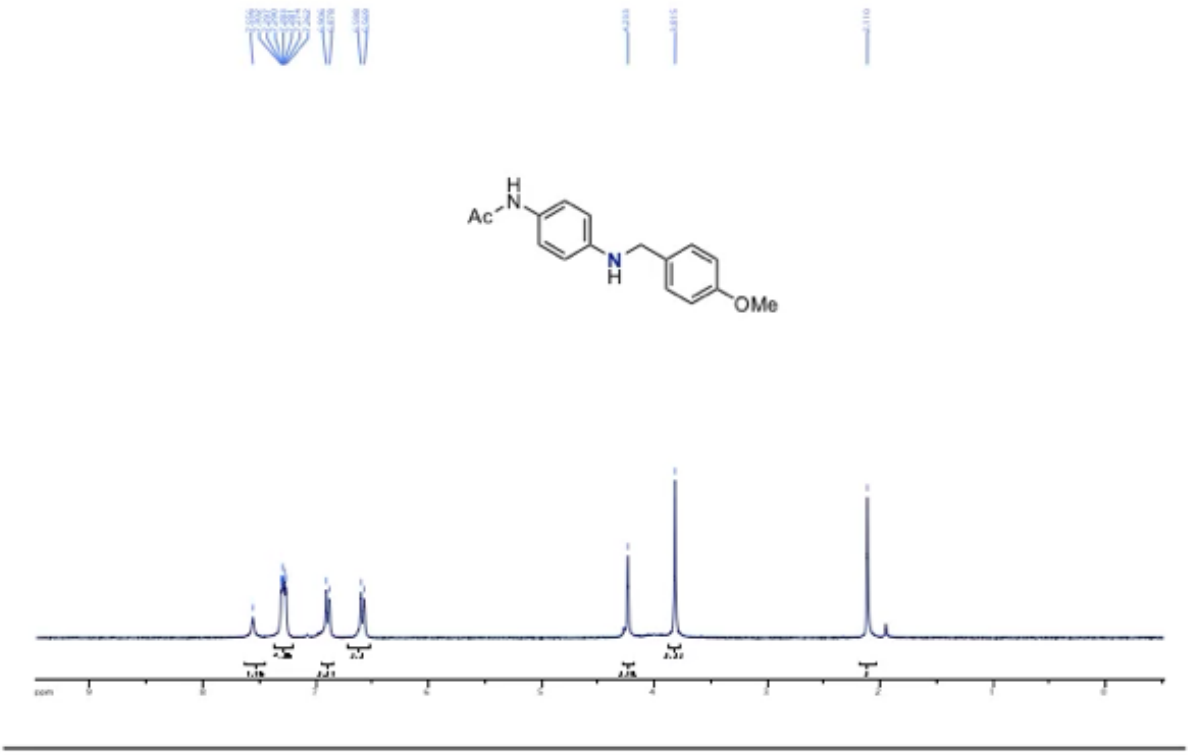
Ac
H
N
N
H
OMe

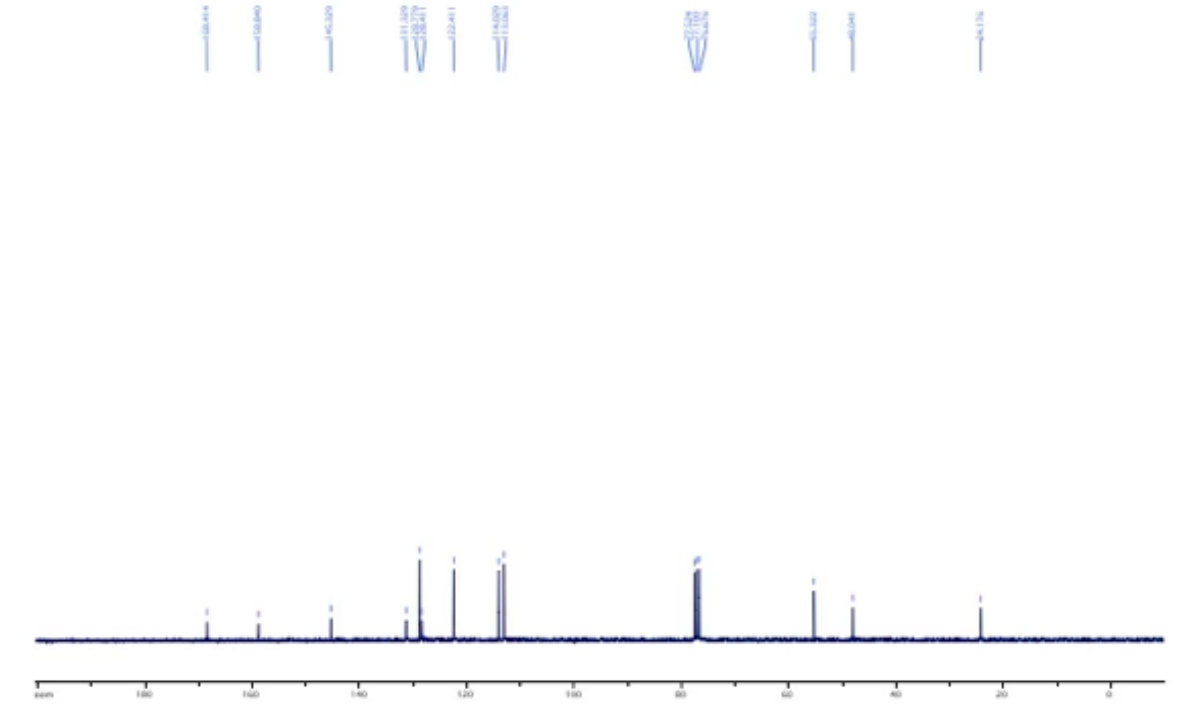

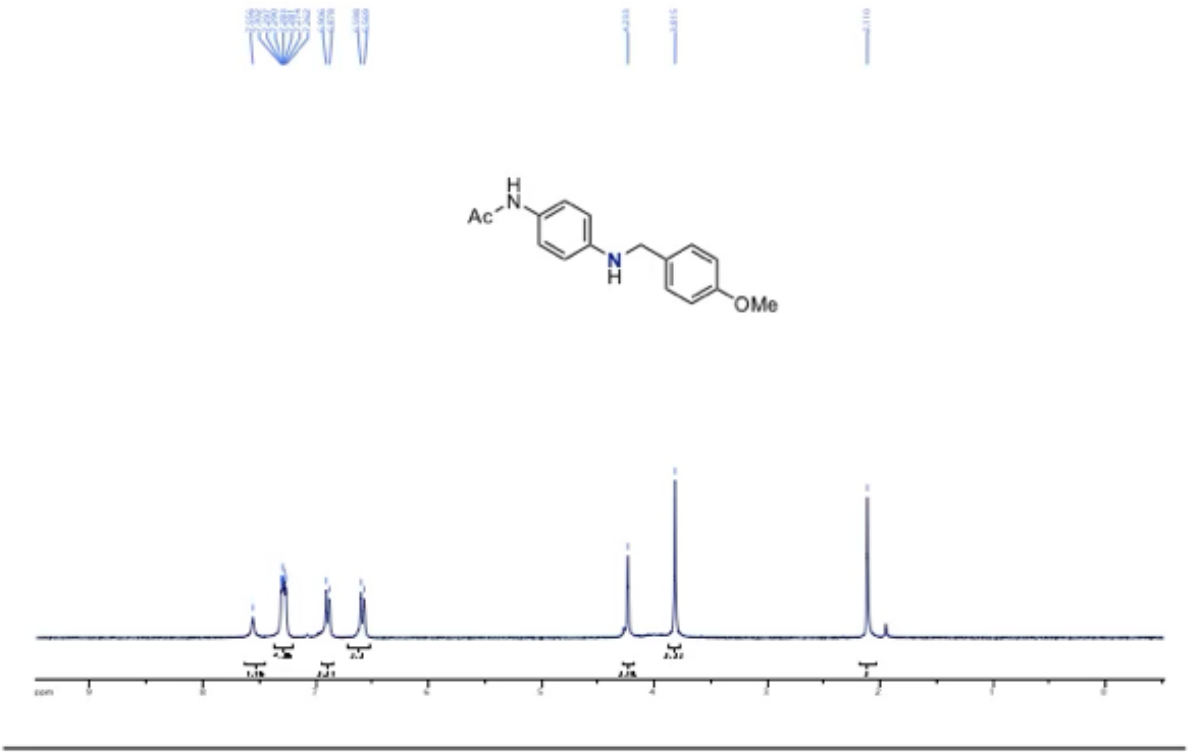
Ac
H
N
N
H
OMe

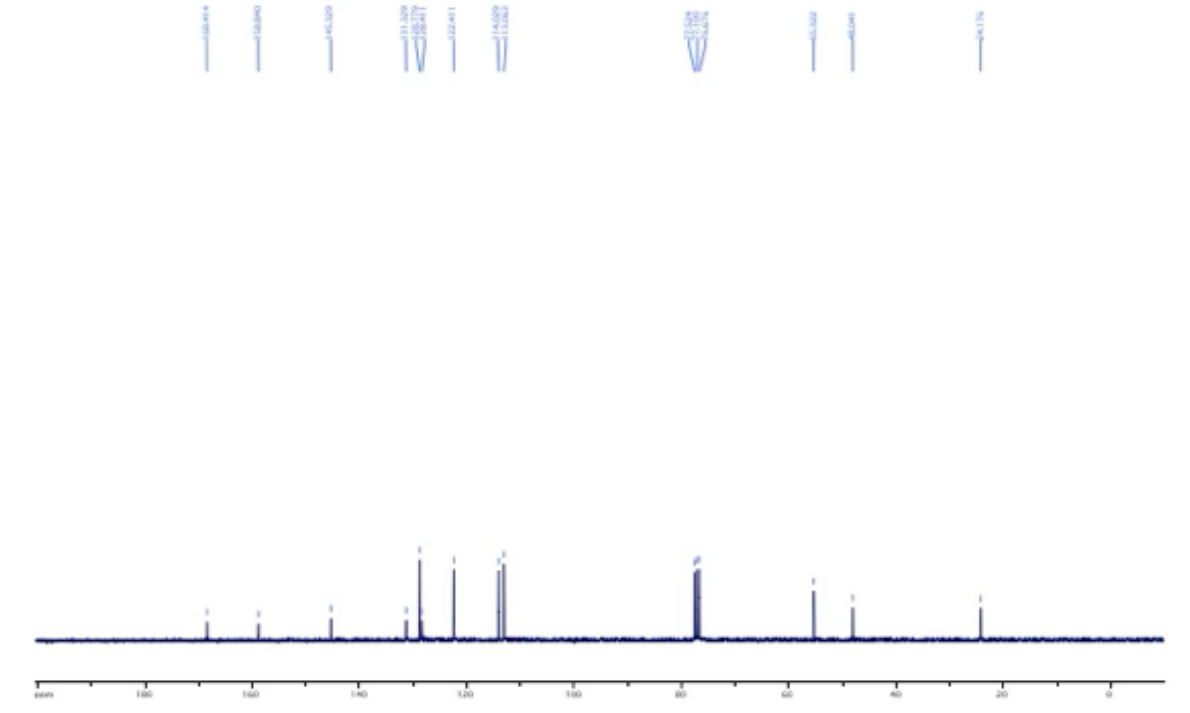

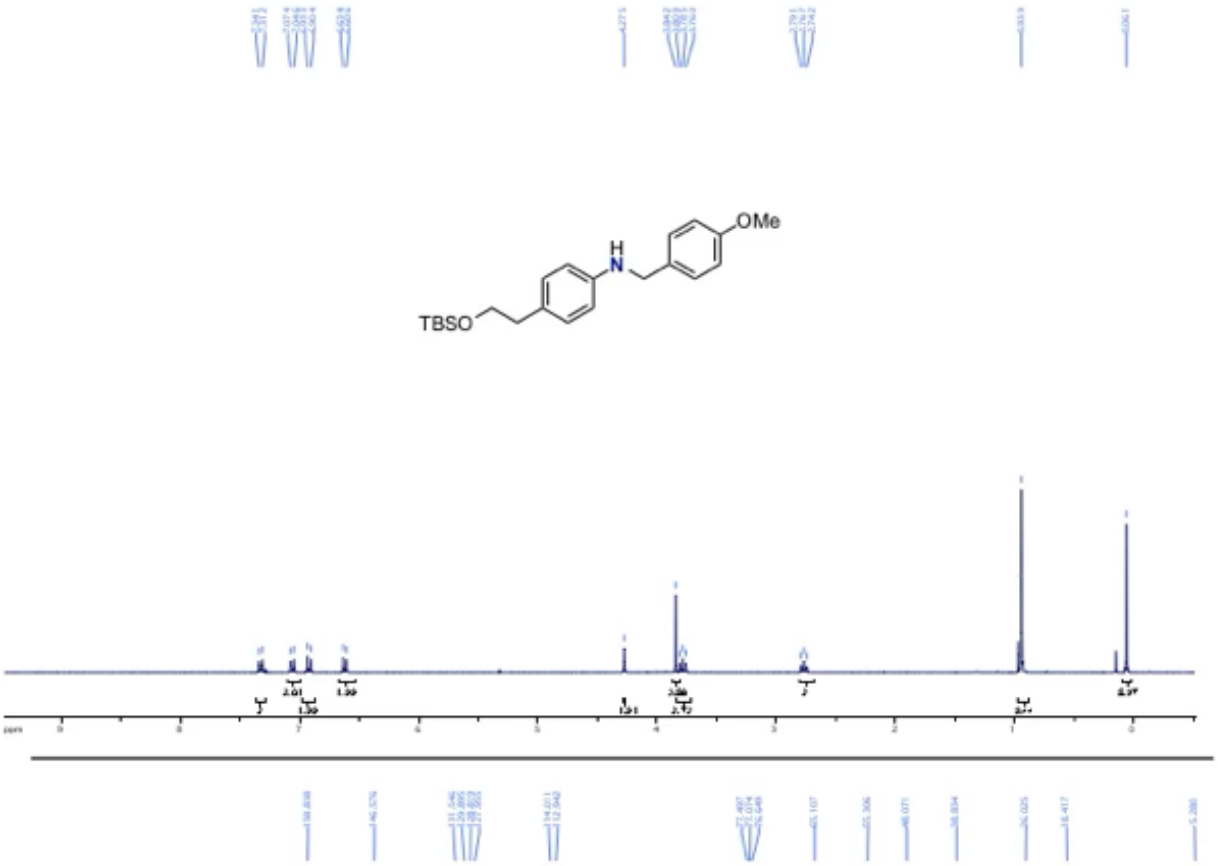
OMe
H
N
TBSO





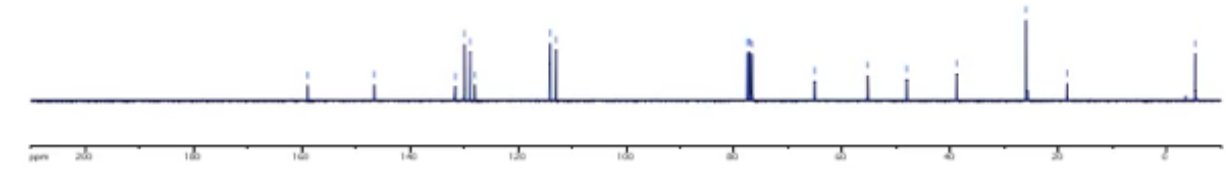

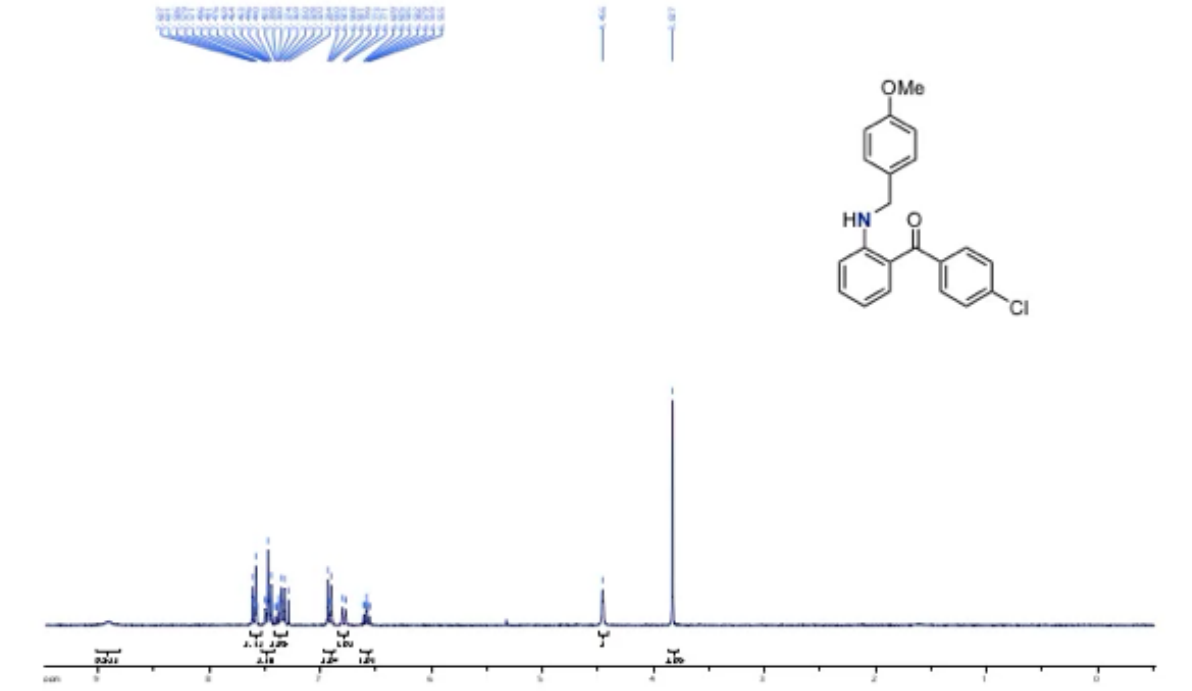
OMe
HN
O
Cl

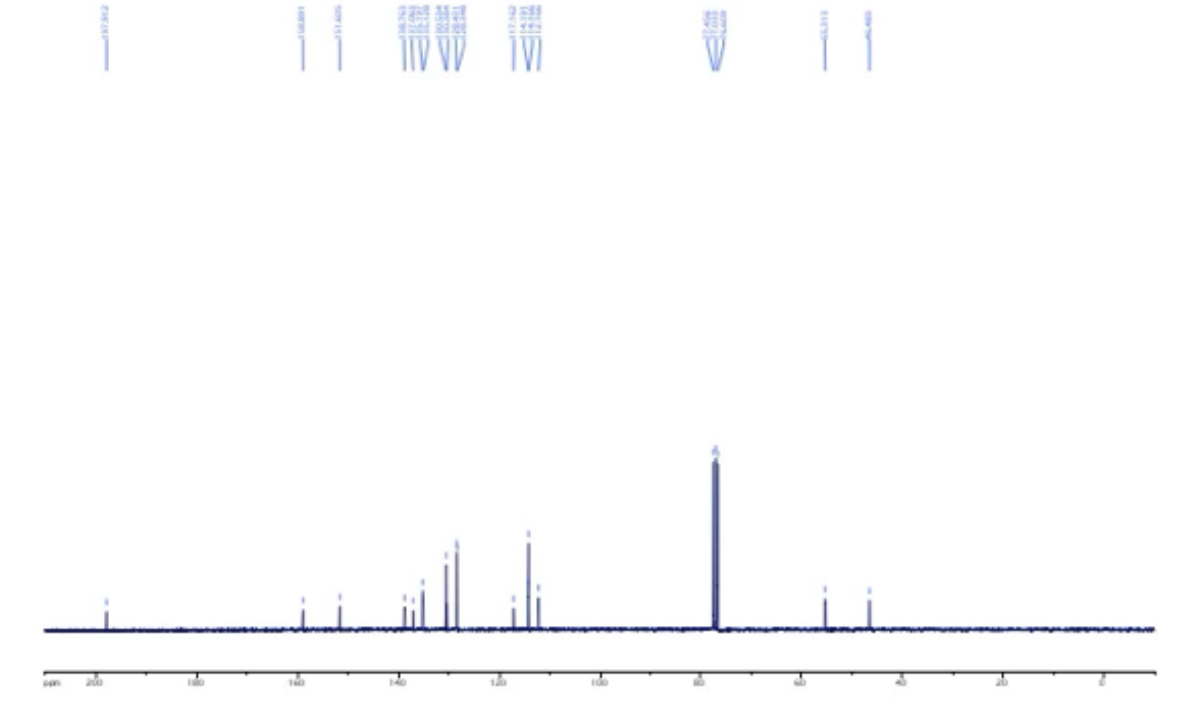

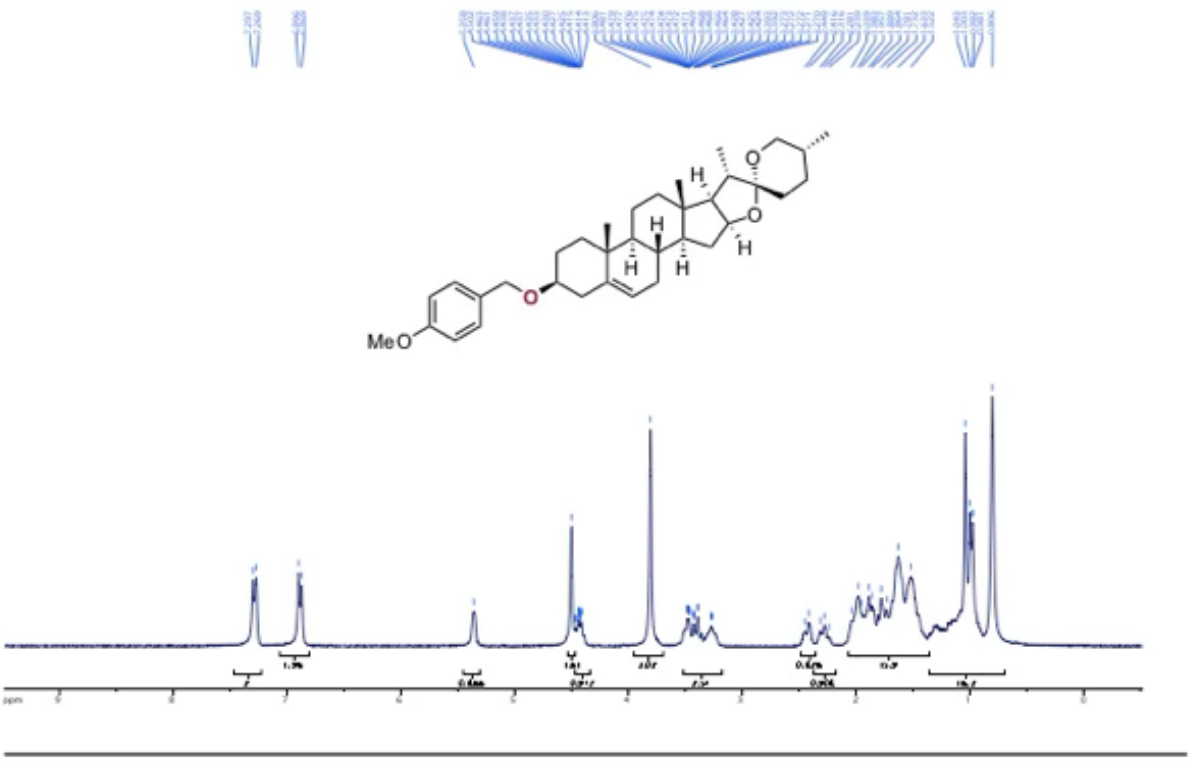
MeO
O
H
H
H
H
O
O
H

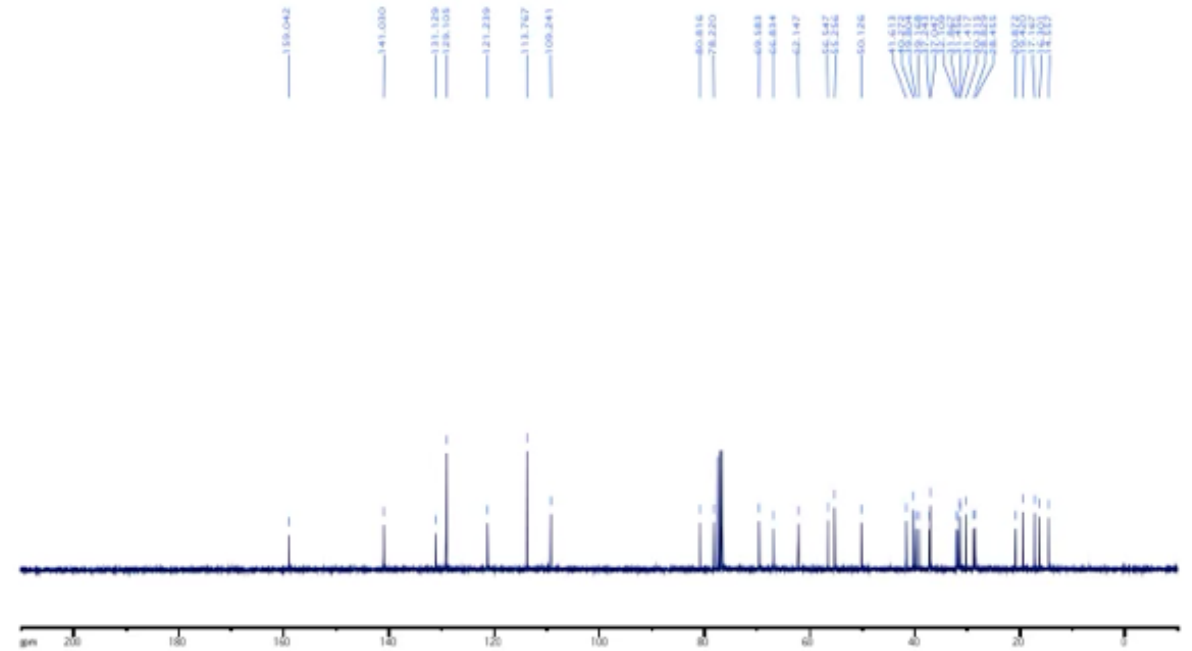

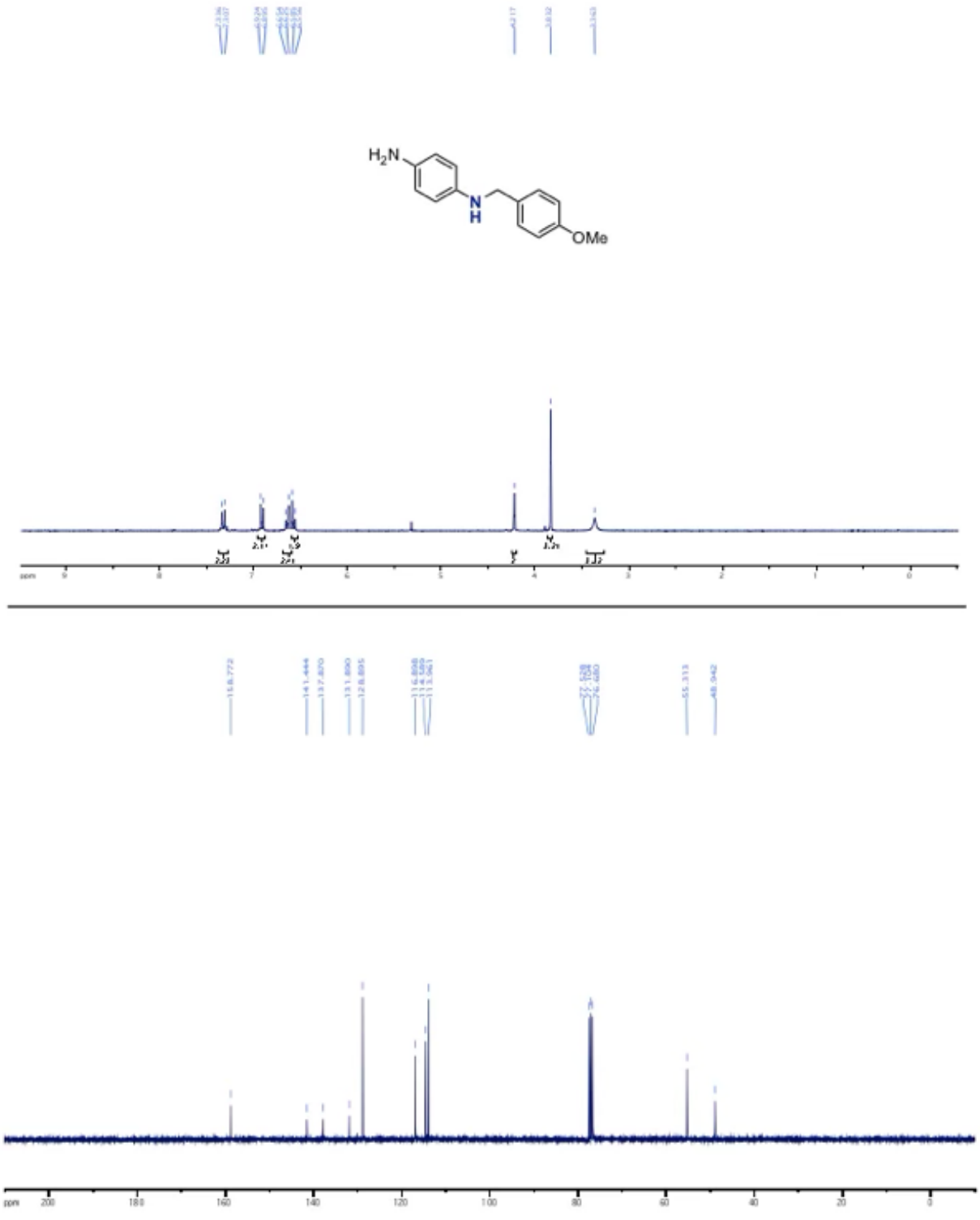
H2N
N
H
OMe

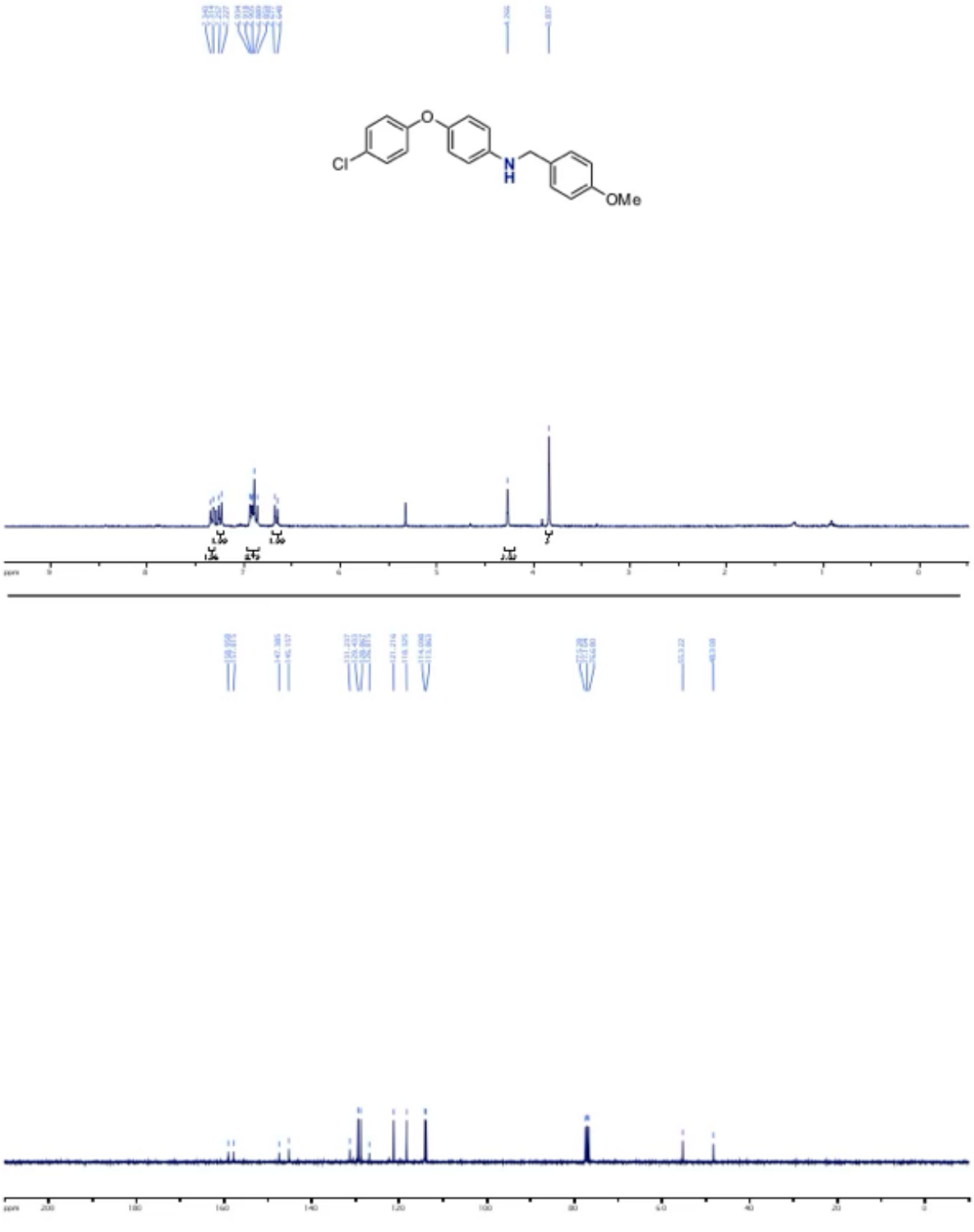
Cl
O
N
H
OMe

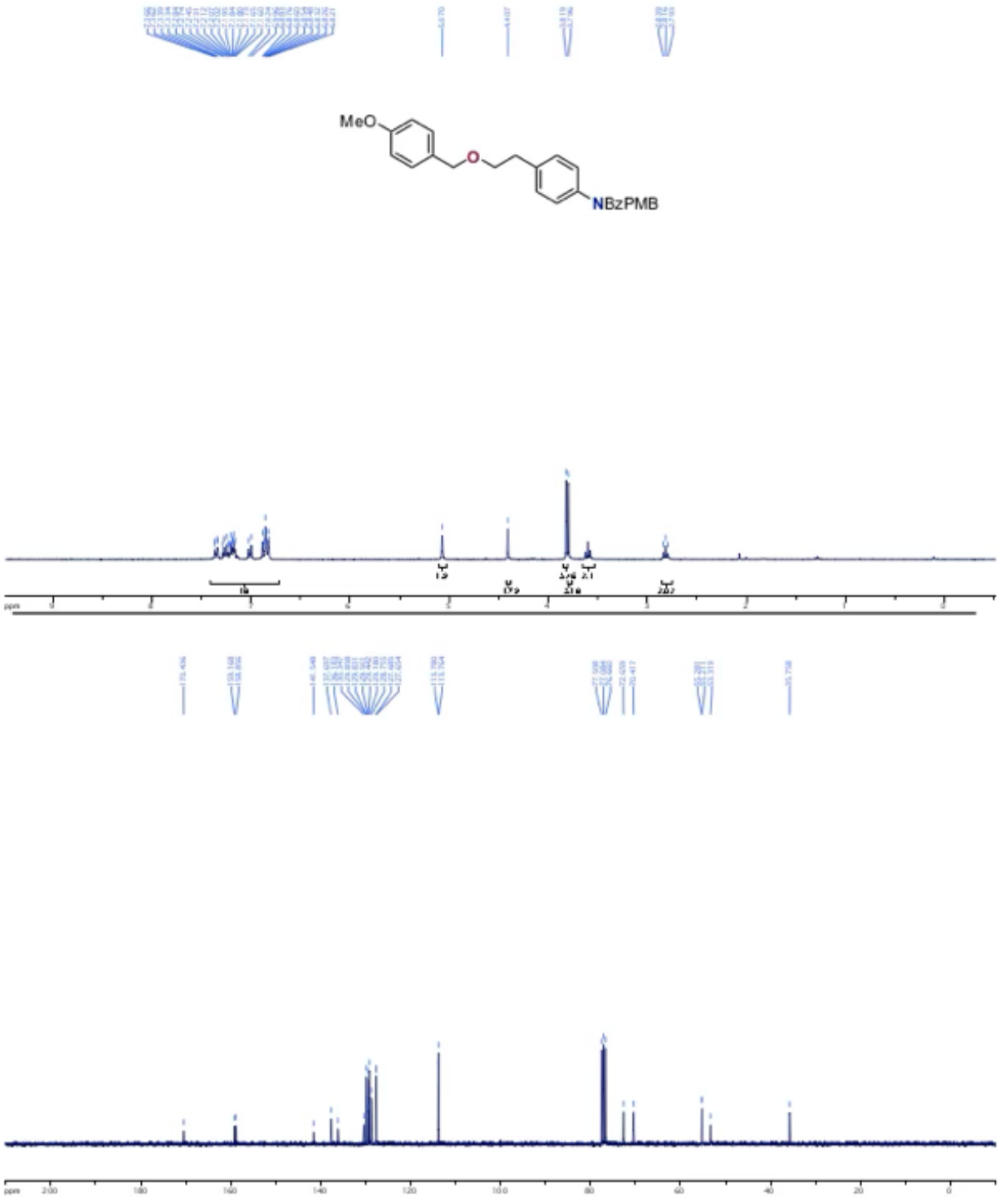
MeO
O
NBzPMB

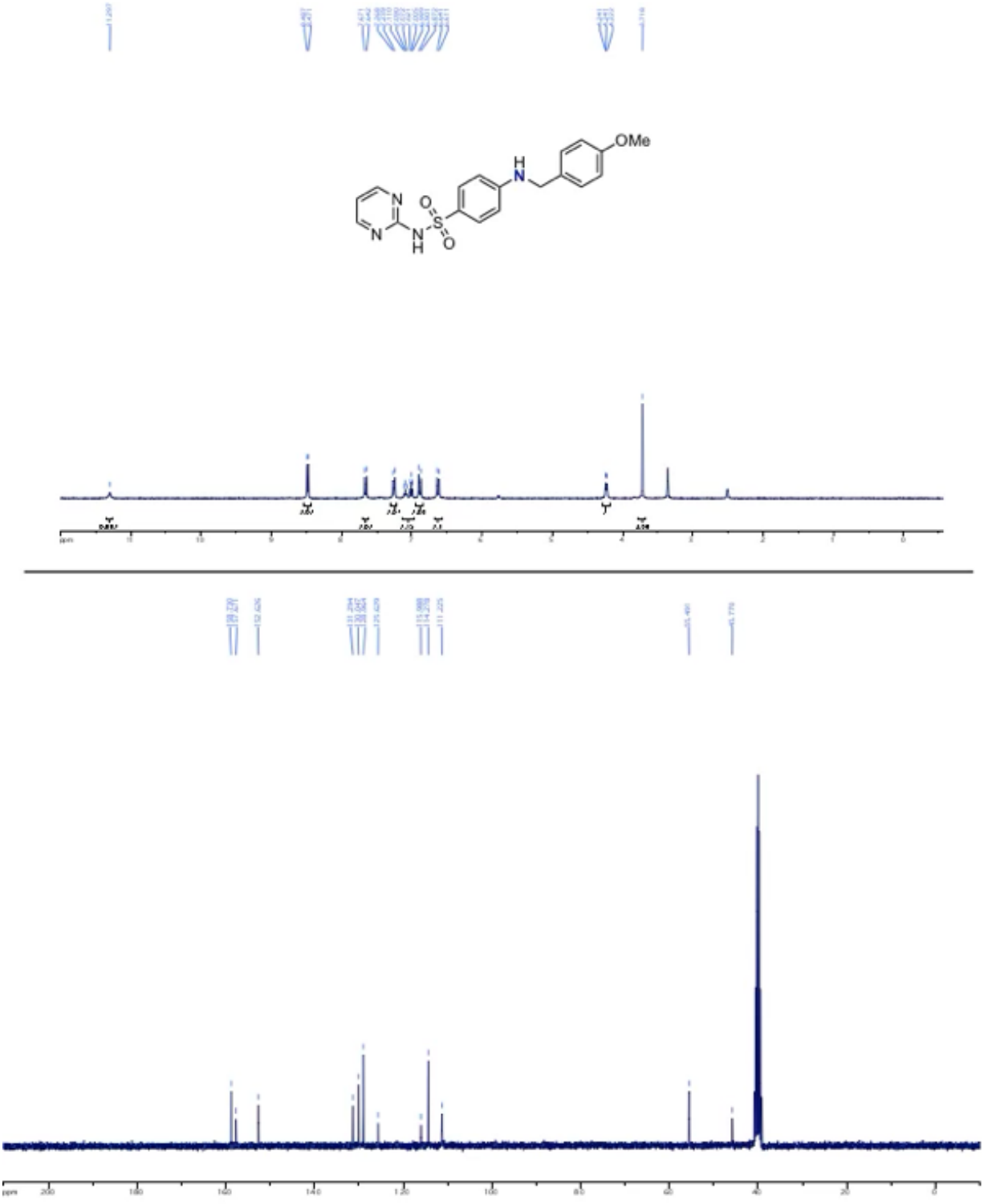
OMe
H
N
N
N
O
S
O
H
N

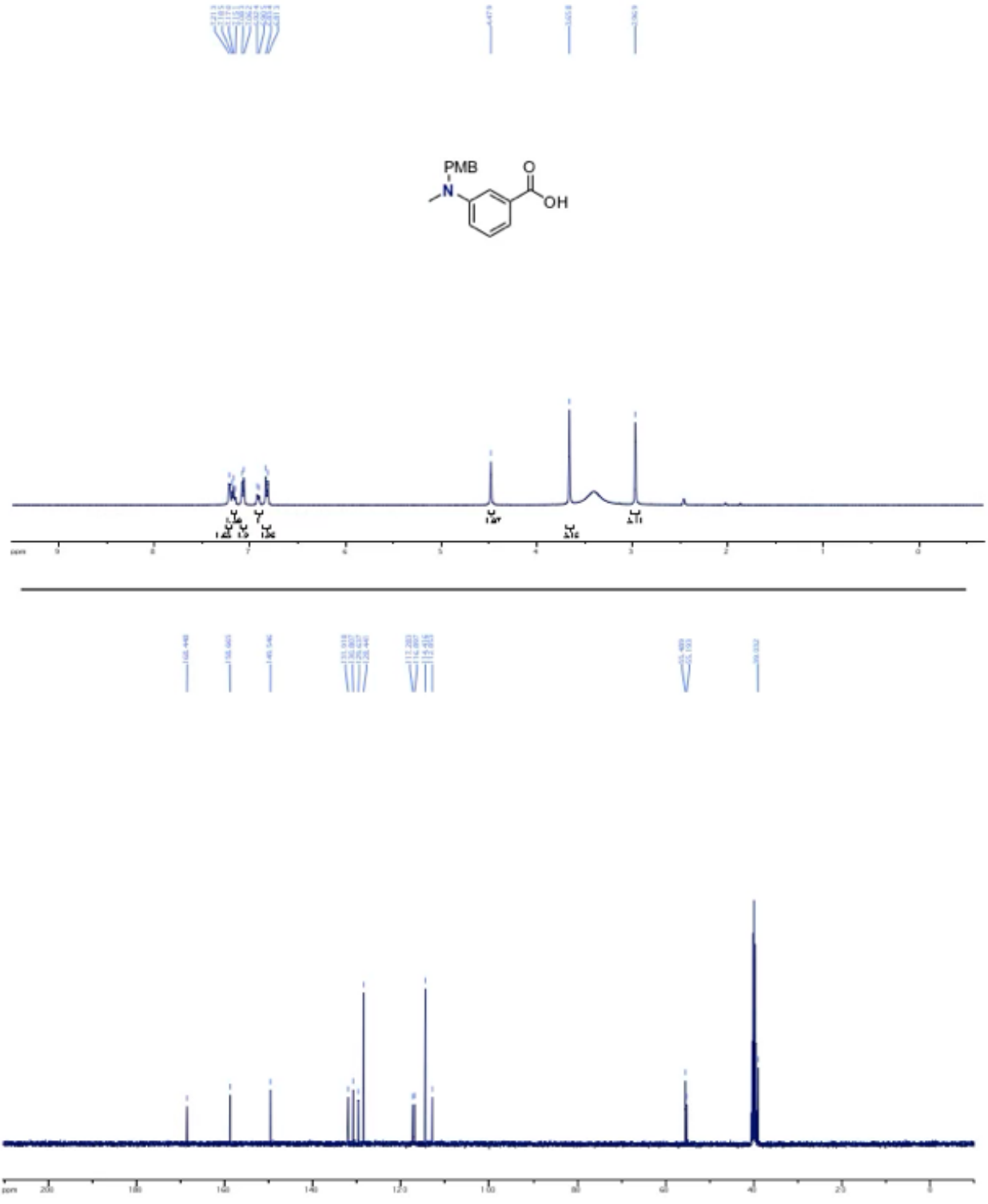
PMB
N
O
OH

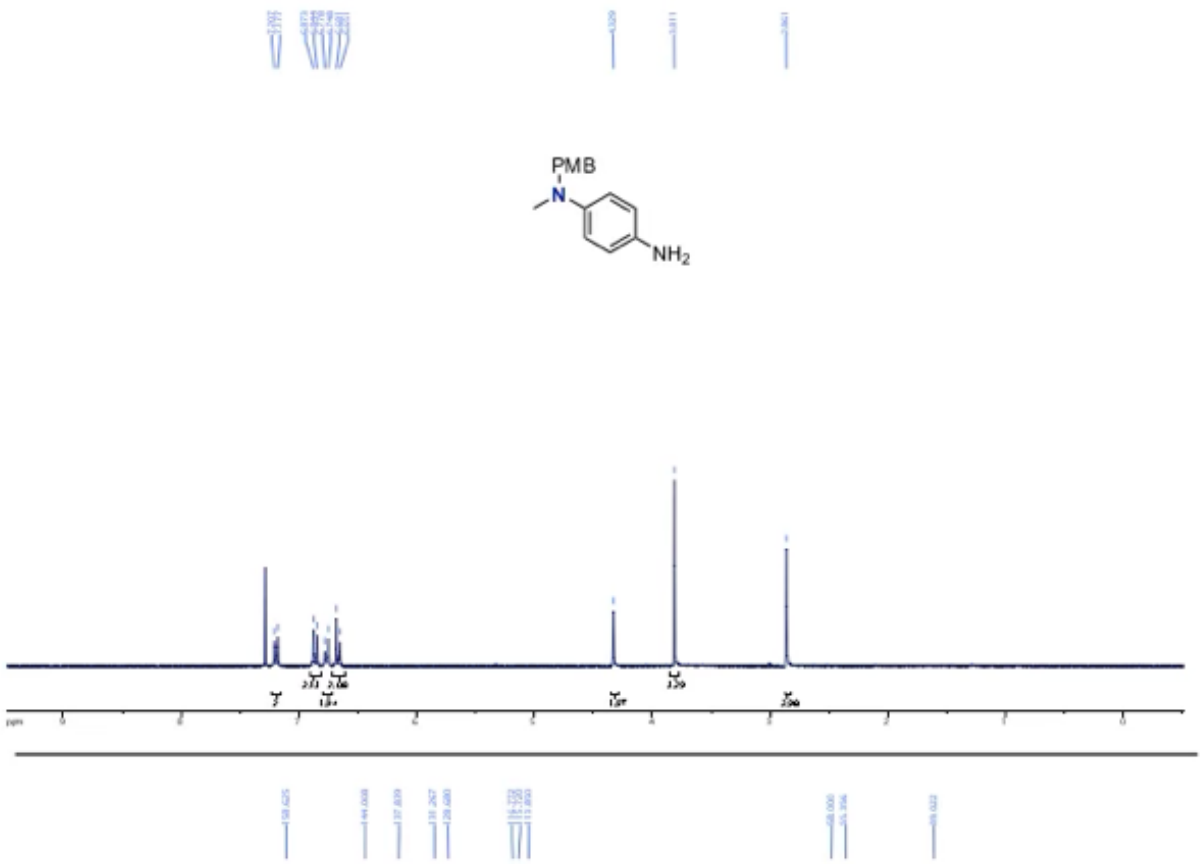
PMB
N
NH2





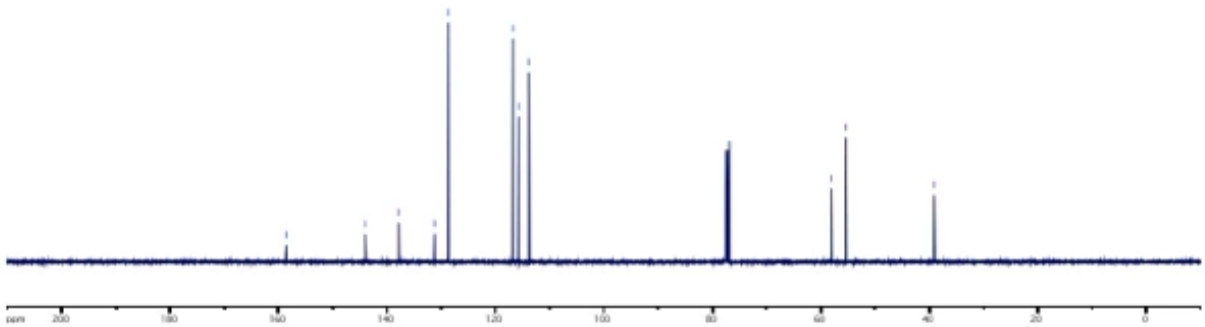

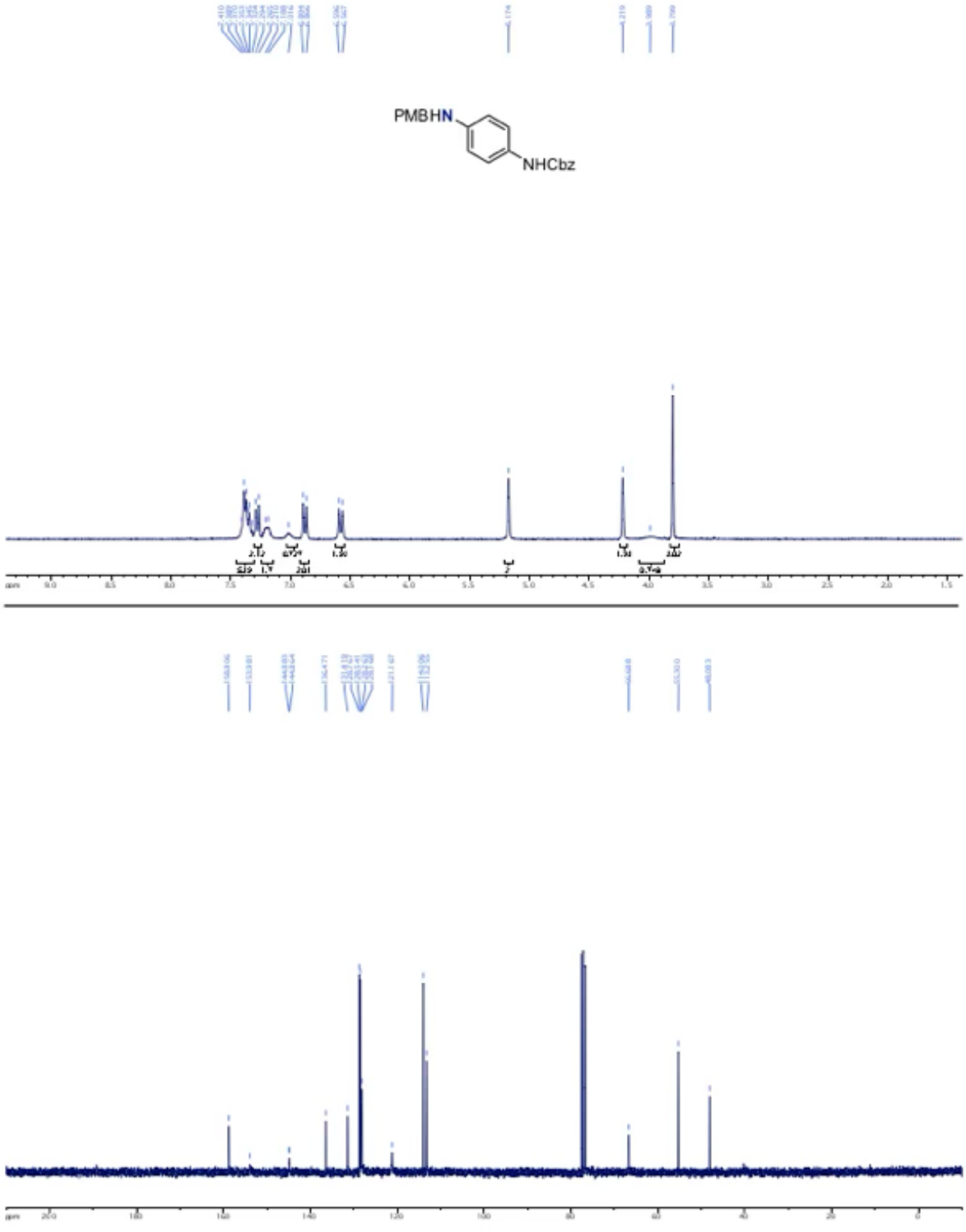
PMBHN
NHCbz

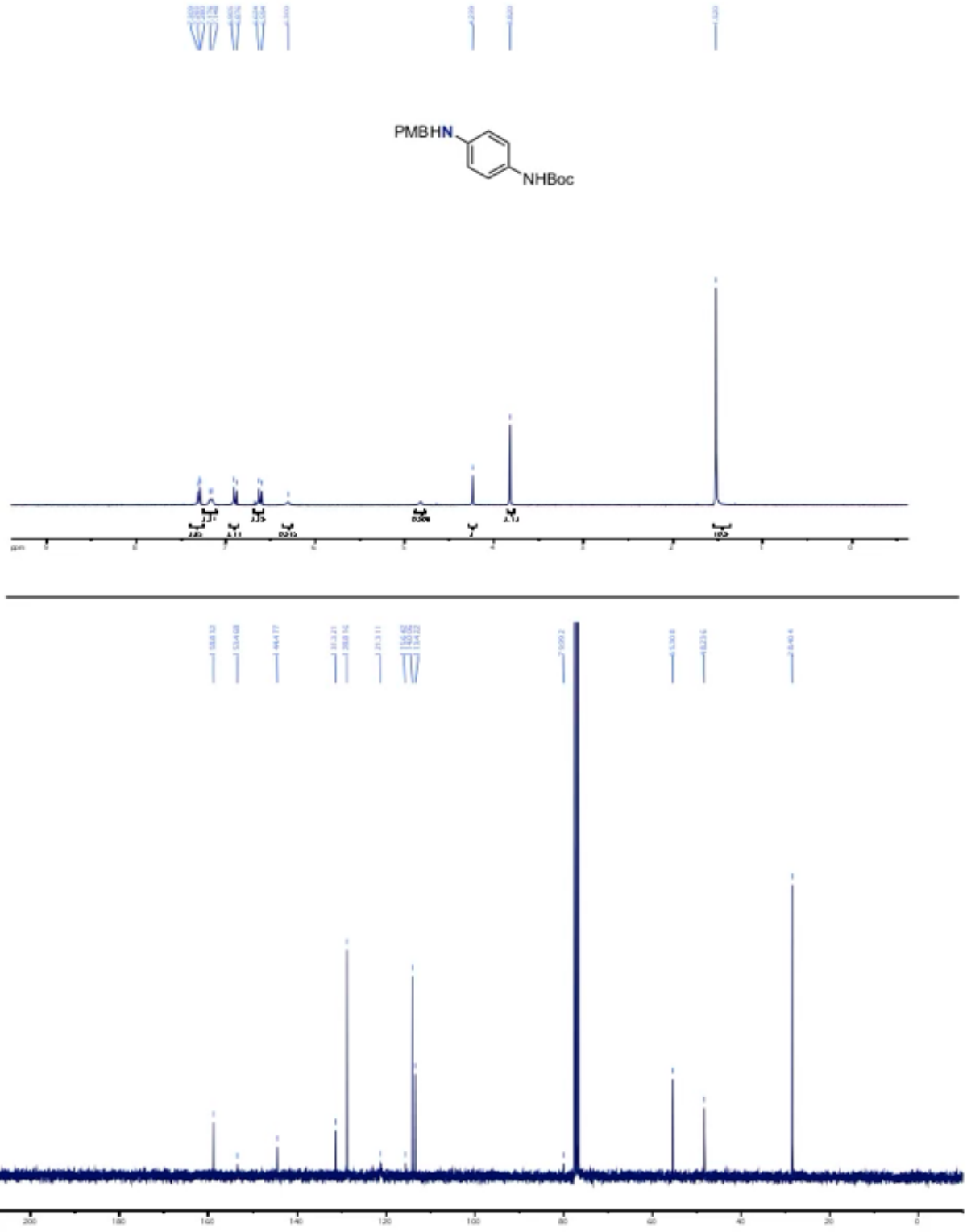
PMBHN
NHBoc

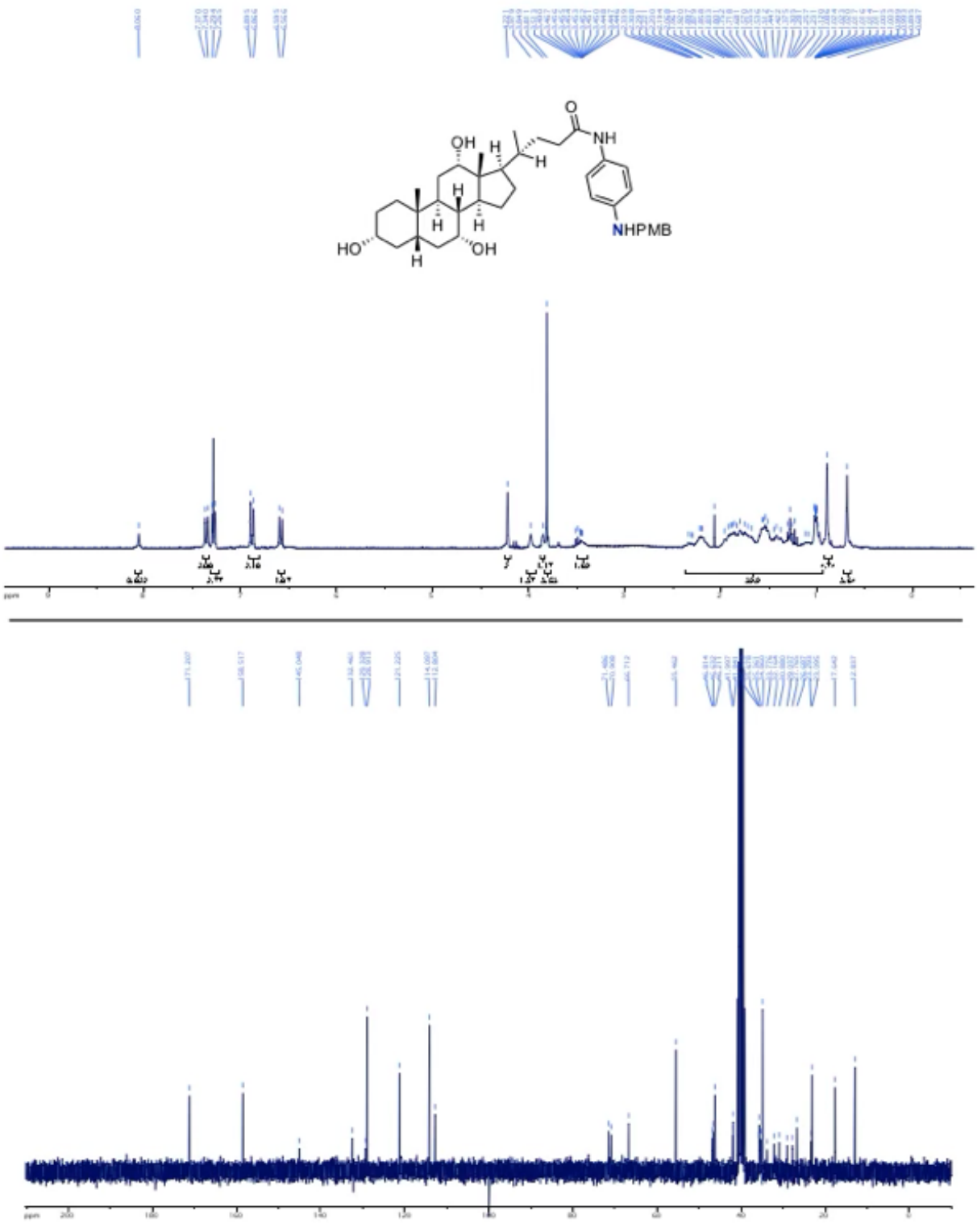
O
NH
OH
H
H
H
H
H
H
HO
OH
NHPMB

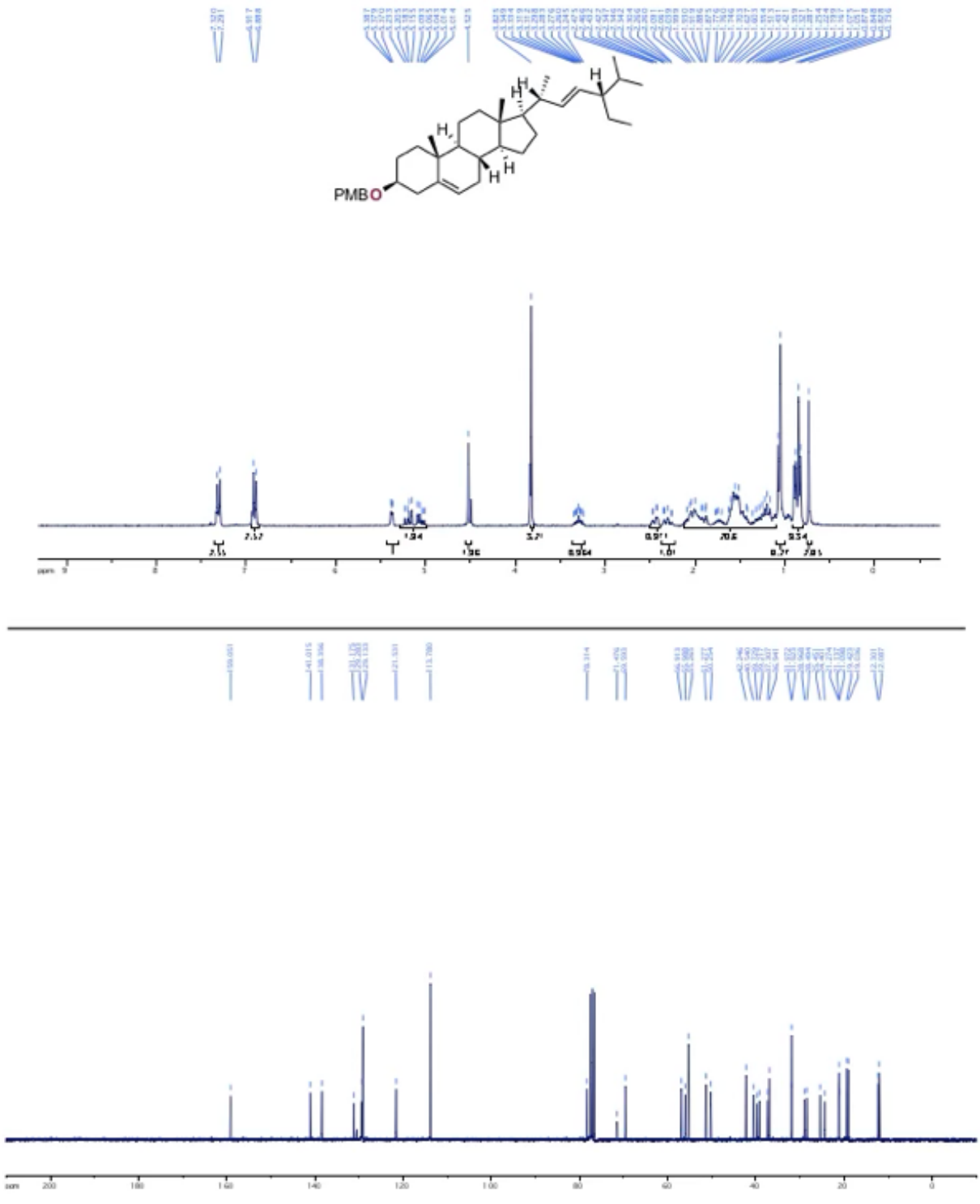
PMBO
H
H
H
H
H

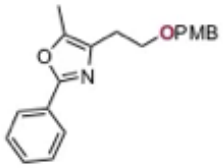
OPMB
O
N

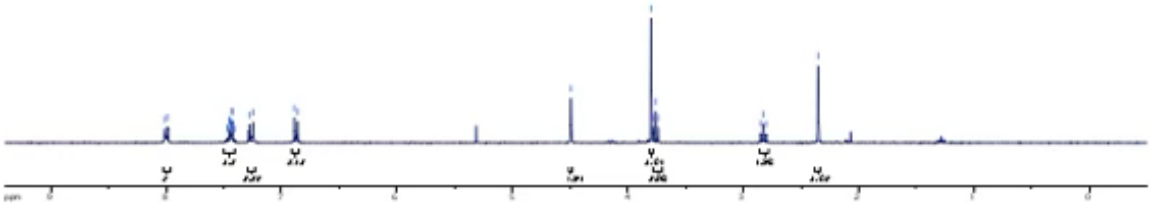

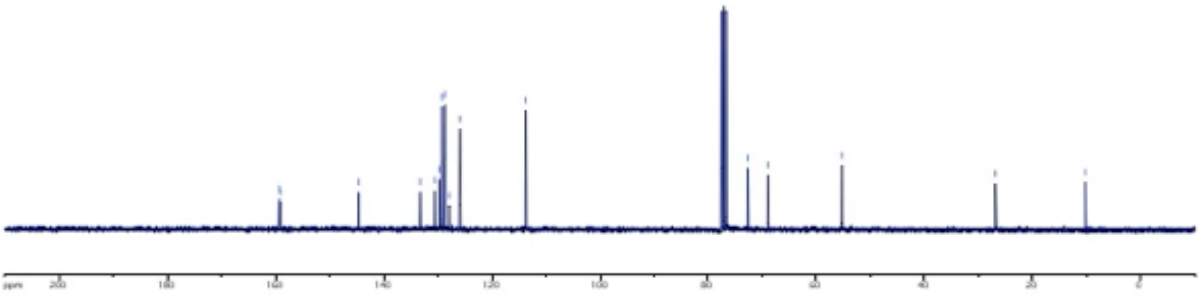

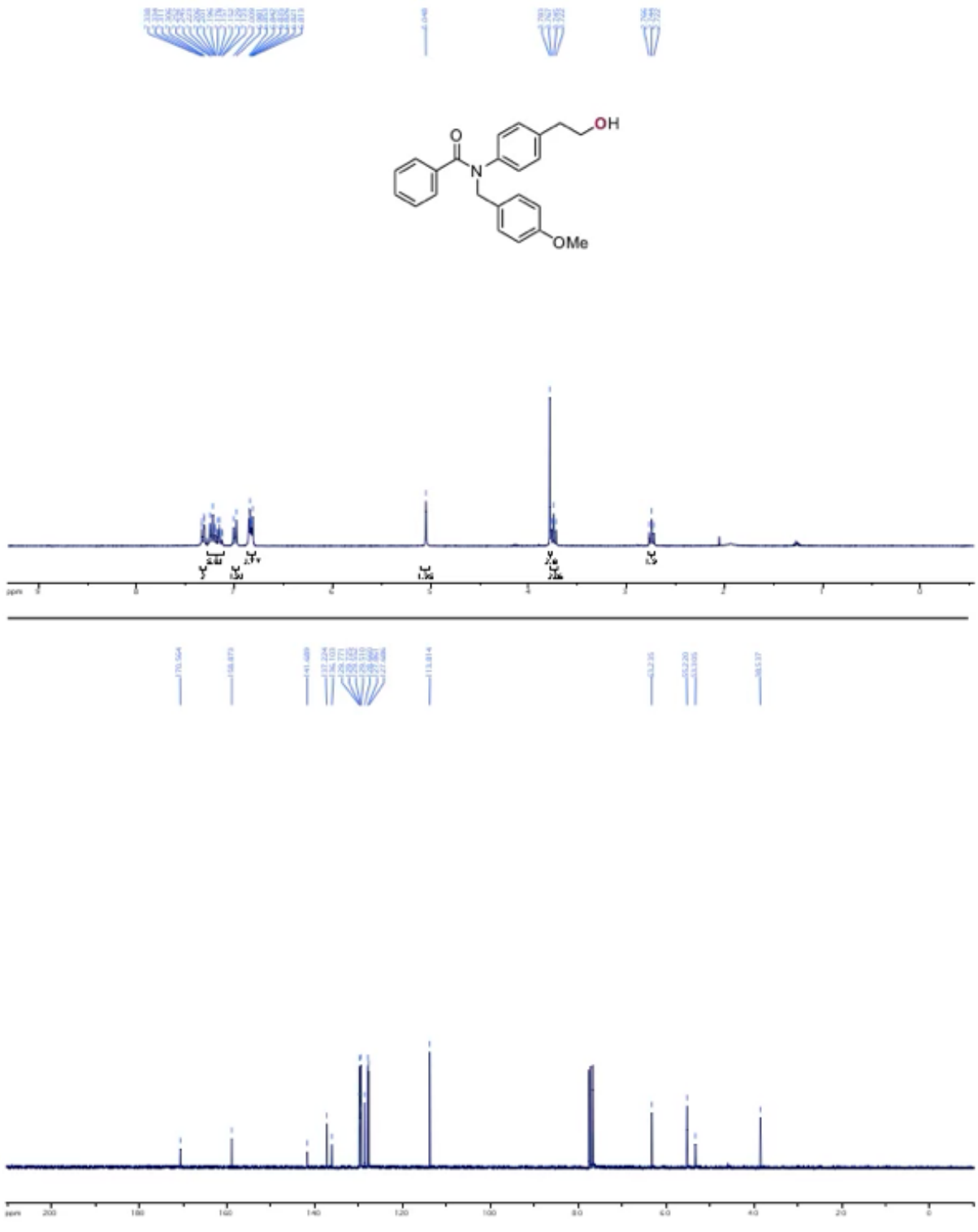
OH
O
N
OMe

## 4.6 References

[1] Denes, F.; Pichowicz, M.; Povie, G.; Renaud, P. Thiyl Radicals in Organic Synthesis. *Chem. Rev.* **2014***,* 2587-2693.

[2] (a) For a seminal report of thiols acting as hydrogen atom abstractors from silanes, please see: Dang, H.-S.; Roberts, B. P. Polarity-Reversal Catalysis by Thiols of Radical-Chain Hydrosilylation of Alkenes. *Tet. Lett.* **1995**, 2875-2878. (b) for an early review on radical polarity reversal catalysis, please see: Roberts, B. P. Polarity-Reversal Catalysis of Hydrogen-Atom Abstraction Reactions: Concepts and Applications in Organic Chemistry. *Chem. Soc. Rev*. **1999**, 25-35.

[3] Pan, X.; Lacôte, E.; Lalevée, J.; Curran, D. P. Polarity Reversal Catalysis in Radical Reductions of Halides by N-Heterocyclic Carbene Boranes. *J. Am. Chem. Soc.* **2012**, 5669-5674.

[4] (a) Harris, E. F. P.; Waters, W. A. Thiol Catalysis of the Homolytic Decompisition of Aldehydes. *Nature*, **1952**, 212-213. (b) Dang, H.-S.; Roberts, B. P. Radical-Chain Addition of Aldehyes to Alkenes Catalysed by Thiols. *J. Chem. Soc., Perkin Trans. 1* **1998**, 67-75.

[5] (a) Dang, H.-S.; Franchi, P.; Roberts, B. P. Radical-Chain Deoxygenation of Tertiary Alcohols, Protected as Their Methoxymethyl (MOM) Ethers, using Thiols as Polarity-Reversal Catalysts. *Chem. Commun.* **2000**, 499-500. (b) Dang, H.-S.; Roberts, B. P. Radical-Chain Cyclisation of Unsaturated Acetals and Thioacetals in the Presence of Thiols as Polarity-Reversal Catalysts. *Tet. Lett.* **1999**, 8929-8933. (c) Dang, H.-S.; Roberts, B. P. Deoxygenation of Tertiary and Secondary Alcohols ROH by Thiol-Catalysed Radical-Chain Redox Decomposition of Derivatives $ROCH_2X$ to Give RH and XCHO. *J. Chem. Soc., Perkin Trans. 1*, **2002**, 1161-1170.

[6] Ranferova, L. I.; Zubov, M. O.; Kokorekin, V. A.; Levin, V. V.; Dilman, A. D. Using h Thiyl Radical for Aliphatic HydrogenAtom Transfer: Thiolation of Unactivated C-H Bonds.

[7] Wuts, P. G. M.; Greene, T. W. *Greene's Protective Groups in Organic Synthesis*, 4th ed.; Wiley: Hoboken, 2007; pp 748-761 and pp 41-45.

[8] Bergmann, M.; Zervas, L. About a General Method of Peptide Synthesis. *Ber.* **1932**, 1192-1201.

[9] Hungerhoff, B.; Samanta, S. S.; Roels, J.; Metz, P. Chemoselective Oxidative Debenzylation of N,N-Dibenzylamines. *Synlett*, **2000**, 77-79.

[10] Baker, S. R.; Parsons, A. F.; Wilson, M. A Radical Approach to Debenzylation of Amides. *Tet. Lett.* **1998**, 331-332.

[11] Moriyama, K.; Nakamura, Y.; Togo, H. Oxidative Debenzylation of N-Benzyl Amides and O-benzyl Ethers Using Alkali Metal Bromide. *Org. Lett.* **2014**, 3812-3815.

[12] For a recent example of an amine-debenzylation using oxygen as an oxidant, please see: Martínez-Montero, L.; Díaz-Rodriguez, A.; Gotor, V.; Gotor-Fernández, V.; Lavandera, I. Broadening the Scope of Laccases: Selective Deprotection of N-Benzyl Groups. *Green Chem.*

**2015**, 2794-2798. For a recent example of a method for the oxidation of benzylamine to imines using oxygen as the oxidant, please see: Kumar, R.; Gleibner, E. H.; Tiu, E. G. T.; Yamakoshi, Y. $C_{70}$ as a Photocatalyst for Oxidation of Secondary Benzylamines to Imines. *Org. Lett.* **2016**, 184-187. For an example of a method for the deprotection of PMP-protected alcohols using air and ammonium persulfate as the terminal oxidant, please see: Ahn, D. K.; Kang, Y. W.; Woo, S. K. Oxidative Deprotection of p-Methoxybenzyl Ethers via Metal-Free Photoredox Catalysis. *J. Org. Chem.* **2019**, 3612-3623.

[13] Jung, M. E.; Koch, P. Mild, Selective Deprotection of PMB Etheres with Triflic Acid/1,3-dimethoxybenzene. *Tet. Lett.* **2011**, 6051-6054.

[14] Sinha, A. K.; Equbal, D. Thiol- Ene Reaction: Synthetic Aspects and Mechanistic Studeis of an Anti-Markovnikov-Selective Hydrothiolation of Olefins. *Asian J. Org. Chem.* **2019**, 32-47.

[15] Wang, C.; Li, Y.; Zhao, J.; Cheng, B.; Wang, H.; Zhai, H. An Environmentally Friendly Approach to Pyrrolo[1,2-a]quinoxalines Using Oxygen as the Oxidant. *Tett. Lett.* **2016**, 3908-3911.

[16] Preetam, A.; Nath, M. An Eco-Friendly Pictet-Spengler, approach to Pyrrolo- and Indolo[1,2-a]quinoxalines using p-dodecylbenzenesulfonic Acid as an Efficient Bronsted Acid Catalyst. *RSC Adv.* **2015**, 21843-21853.

[17] The thiyl radical generated from pentafluorothiophenol has been shown to abstract benzylic postions in previous work. Please see the work of Roberts in reference 5c.

[18] (a) Wayner, D. D. M.; McPhee, D. J.; Griller, D. Oxidation and Reduction Potentials of Transient Free Radicals. *J. Am. Chem. Soc.* **1988**, 132-137. (b) Fu, Y.; Liu, L.; Yu, H.-Z.; Wang, Y.-M.; Guo, Q.-X. Quantum-Chemical Predictions of Absolute Standard Redox Potentials of Diverse Organic Molecules and Free Radicals in Acetonitrile. *J. Am. Chem. Soc.* **2005**, 7227-7234.

[19] Fenter, F. F.; Noziere, B.; Caralp, F.; Lesclaux, R. Study of the Kinetics and Equilibrium of the Benzyl-Radical Association Reaction with Molecular Oxygen. *Int. J. Chem. Kinet.* **1994**, 171-189.

[20] In the first possible pathway where a single electron oxidation takes place, the carbocation that is formed will likely be trapped by the concomitantly formed superoxide radical, which will produce the benzylic-peroxy-radical species shared by both pathways. For a recent review on the possible reaction pathways between molecular oxygen and carbon radicals, please see: Tang, C.; Qiu, X.; Cheng, Z.; Jiao, N. Molecular Oxygen-Mediated Oxygenation Reactions Involving Radicals. *Chem. Soc. Rev.* **2021**, Advance Article.

[21] The S-H bond dissociation enthalpies of pentafluorothiophenol and methylthioglycolate were calculated according to the method presented by Dilman in reference 6. The BDE for thiophenol was taken from Borges dos Santosm R. M.; Muralha, V. S. F.; Correia, C. F.; Guedes, R. C.; Costa Cabral, B. J.; Martinho Simões, J. A. S-H Bond Dissociation Enthalpies in thiophenols: A Time Resolved Photoacoustic Calorimetry and Quantum Chemistry Study. *J. Phys. Chem. A* **2002**, 9883-9889.

[22] The electron affinity of the methythioglycolate, thiophenol, and pentafluorothiophenol derived thiyl radicals were calculated according to the method presented in: Chandra, A. K.; Nam, P.-C.; Nguyen. The S-H Bond Dissociation Enthalpies and Acidities of Para and Meta Substituted Thiophenols: A Quantum Chemical Study. *J. Phys. Chem. A* **2003**, 9182-9188.

[23] Experimentally determined S-H BDE of thiophenol in benzene solution taken from: Borges dos Santos, R. M.; Muralha, V. S. F.; Correira, C. F.; Guedes, R. C.; Cabral, B. J. C.; Simões, J. A. M. S-H Bond Dissociation Enthalipes in Thiophenols: A Time-Resolved Photoacoustic Calorimetry and Quantum Chemistry Study. *J. Phys. Chem. A* **2002**, 9883-9889.

[24] We use electron affinity as an approximation for absolute electronegativity for two reasons: (1) electron affinity is directly correlated to absolute electronegativity as described by Mulliken in Mulliken, R. S. A New Elecroaffinity Scale; Together with Data on Valence States and on Valence Ionization Potentials and Electron Affinites. *J. Chem. Phys. 2* **1934**, 782-793. And (2) to the best of our ability, the heat of formation of the methylthioglycolate cation could not be calculated due to the propensity for the molecule to fracture generating thioformaldehye and oxonium methyl ester cation ($^{+}$OCOMe). This value is necessary to determine the ionization potential for the methylthioglycolate thiyl radical, which is in turn necessary to determine absolute electronegativity. The absolute electronegativity of the thiophenol and pentafluorothiophenol thiyl radicals were found to be 123 and 138 kcal/mol, respectively.

[25] Jafari, M. R.; Yu, H.; Wickware, J. M.; Lin. Y.-S.; Derda, R. *Org. Biomol. Chem.* **2018**, 7588-7594.

[26] Gaddam, V.; Nagarajan, R. *Tet. Lett.* **2009**, 1243-1248.

[27] Chen, C.-y.; He, F.; Tang, G.; Yuan, H.; Li, N.; Wang, J,; Faessler, R. *J. Org. Chem.* **2018**, 2395-2401.

[28] Landge, V. G.; Mondal, A.; Kumar, V.; Nandakumar, A.; Balaraman, E. *Org. Biomol. Chem.* **2018**, 8175-8180.

[29] Hasserodt, J.; Janda, K. D.; *Tetrahedron*, **1997**, 11237-11256.

[30] Chu-Farseeva, Y.-y.; Mustafa, N.; Poulsen, A.; Tan, E. C.; Yen, J. J. Y.; Chng, W. J.; Dymock, B. W. *Eur. J. Med. Chem.* **2018**, 593-619.

[31] Zhang, C.; Zhan, Z.; Lei, M.; Hu, L. *Tetrahedron*, **2014**, 8817-8821.

[32] Leng, L.; Fu, Y.; Liu, P.; Ready, J. P. *J. Am. Chem. Soc.* **2020**, 11972-11977.

[33] Hu, B.; Li, Y.; Dong, W.; Ren, K.; Xie, X.; Wan, J.; Zhang, Z. *Chem. Commun.* **2016**, 3709-3712.

[34] Alves, dos Santos, J.; Polonin I, H. C.; Suzuki, E. Y.; Raposo, N. R. B.; David da Silva, A. *Steroids*, **2015**, 114.
[35] Kirmse, W.; Kund, K. *J. Am. Chem. Soc.* **1989**, 1465-1473.

[36] Fujita, H.; Terasaki, H.; Kakuyama, S.; Hioki, K.; Kunishima, M. *Org. Lett.* **2019**, 3093-3097.

[37] Adams, H.; Bell, R.; Cheung, Y.-Y.; Jones, D. N.; Tomkinson, N. C. O. *Tetrahedron: Asymmetry*, **1999**, 4129-4142.

[38] Ahn, D. K.; Kang, Y. W.; Woo, S. K. *J. Org. Chem.* **2019**, 3612-3623.

[39] Kern, N.; Dombray, T.; Blanc, A.; Weibel, J.-M.; Pale, P. *J. Org. Chem.* **2012**, 9227-9235.

[40] Lee, A.; Betori, R. C.; Crane, E. A.; Scheidt, K. A. *J. Am. Chem. Soc.* **2018**, 6212-6216.

[41] Cini, N.; Machetti, F.; Menchi, G.; Occhiato, E. G.; Guarna, A. *Eur. Chem. J. Org. Chem.* **2002**, 873-880.

[42] Callejo, R.; Corr., M. J.; Yang, M.; Wang, M.; Cordes, D. B.; Slawin, A. M. Z.; O'Haggan, D. *Chem. Eur. J.* **2016**, 8137-8151.

[43] Szabó, G. et al. *Biorg. Med. Chem. Lett.* **2009**, 3471-3475.

[44] Huo, H.-R.; Tang, X.-Y.; Gong, Y.-F. *Synthesis*, **2018**, 2727-2740.

[45] Boucher, M. M.; Furigay, M. H.; Quach, P. K.; Brindle, C. S. *Org. Process Res. Dev.* **2017**, 1394-1403.

[46] Bindschädler, P.; Lialer, L. O.; Seeberger, P. H. *Journal of Carbohydrate Chemistry,* **2009**, 395-420.

[47] Liao, B.-S.; Liu, S.-T. *J. Org. Chem.* **2012**, 6653-6656.

[48] Zhao, H.-B.; Hou, Z.-W.; Liu, Z.-J.; Zhou, Z.-F.; Song, J.; Xu, H.-C. *Angew. Chem. Int. ed.* **2017**, 587-590.

[49] Shen, T.; Wang, T.; Qin, C.; Jiao, N. *Angew. Chem. Int. Ed.* **2013**, 6677-6680.

[50] Afanasyev, O, I.; Tsygankov, A. A.; Usanov, D. L.; Chusov, D. *Org. Lett.* **2016**, 5968-5970.

[51] Kollarigowda, R. H.; Braun, P. V. *J. Org. Chem.* **2021**, 4391-4397

[52] Wang, D.; Kuang, D.; Zhang, F.; Yang, C.; Zhu, X. *Adv. Synth. Catal.* **2015**, 714-718.

[53] Saaverda, J. E. et. al. *J. Med. Chem.* **2006**, 1157-1164.

[54] Barthelemy, A.-L.; Tuccio, B.; Magnier, E.; Dagousset, G. *Angew. Chem. Int. Ed.* **2018**, 13790-13794.
[55] Glöckner, S.; Tran, d. N.; Ingham, r. J.; Fenner, S.; Wilson, Z. E.; Battilocchio, C.; Ley, S. V. *Org. Biomol. Chem.* **2015**, 207-214.

[56] Wang, C.; Li, Y.; Zhao, J.; Cheng, B.; Wang, H.; Zhai, H.; *Tetrahedron Letters* **2016**, 3908-3911.

[57] Gaussian 16, Revision B.01, Frisch, M. J.; Trucks, G. W.; Schlegel, H. B.; Scuseria, G. E.; Robb, M. A.; Cheeseman, J. R.; Scalmani, G.; Barone, V.; Petersson, G. A.; Nakatsuji, H.; Li, X.; Caricato, M.; Marenich, A. V.; Bloino, J.; Janesko, B. G.; Gomperts, R.; Mennucci, B.; Hratchian, H. P.; Ortiz, J. V.; Izmaylov, A. F.; Sonnenberg, J. L.; Williams-Young, D.; Ding, F.; Lipparini, F.; Egidi, F.; Goings, J.; Peng, B.; Petrone, A.; Henderson, T.; Ranasinghe, D.; Zakrzewski, V. G.; Gao, J.; Rega, N.; Zheng, G.; Liang, W.; Hada, M.; Ehara, M.; Toyota, K.; Fukuda, R.; Hasegawa, J.; Ishida, M.; Nakajima, T.; Honda, Y.; Kitao, O.; Nakai, H.; Vreven, T.; Throssell, K.; Montgomery, J. A., Jr.; Peralta, J. E.; Ogliaro, F.; Bearpark, M. J.; Heyd, J. J.; Brothers, E. N.; Kudin, K. N.; Staroverov, V. N.; Keith, T. A.; Kobayashi, R.; Normand, J.; Raghavachari, K.; Rendell, A. P.; Burant, J. C.; Iyengar, S. S.; Tomasi, J.; Cossi, M.; Millam, J. M.; Klene, M.; Adamo, C.; Cammi, R.; Ochterski, J. W.; Martin, R. L.; Morokuma, K.; Farkas, O.; Foresman, J. B.; Fox, D. J. Gaussian, Inc., Wallingford CT, 2016.

[58] Hanwell, M. D.; Curtis, D. E.; Lonie, D. C.; Vandermeersch, T.; Zurek, E.; Hutchinson, G. R. Avogadro: An Advanced Semantic Chemical Editor, Visualization, and Analysis Platform. *Journal of Cheminformatics*, **2012**, 4:17.

# Chapter 5: Conclusions

Over the past several decades, the development of radical mediated synthetic transformations has seen an impressive resurgence. The ability for open-shell process to tolerate otherwise reactive polar functionalities makes them particularly attractive. Within our own efforts, we found that hydroxylamine-containing compounds could serve as highly reactive N-centered radical precursors in the presence of trivalent phosphorus. In the seminal work presented herein, we discovered that N-hydroxyphthalimide could serve as a source of phthalimidyl radical toward the highly regioselective hydroamination of alkenes.

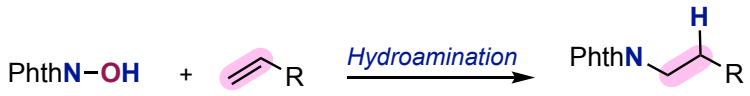


Scheme 5.1. Intermolecular hydroamination of alkenes using NHPI.

Further mechanistic inquiry revealed that our hydroamination protocol was occurring through an ATRA type pathway in which N-hydroxyphthalimide was providing both the N-atom and H-atom for the overall transformation. With this realization, we were able to extend the scope of this reactivity to the difunctionalization of alkenes using ally-oxyphthalimides derivatives of NHPI through a GTRA pathway. This unique reactivity provided further mechanistic evidnce in agreement with an ATRA mechanism for our hydroamination protocol, and served as an excellent example of the guiding effects of radical polarities.

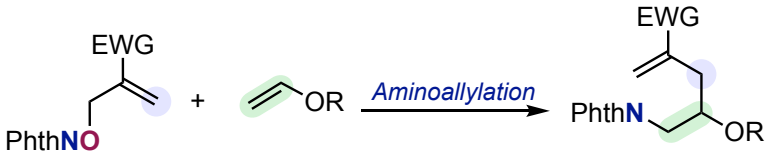


Scheme 5.2. Intermolecular aminoallylation of alkenes using allyl-oxyphthalimides.

Staying on the same theme of trivalent phosphorus-mediated deoxygention of hydroxylamines, we extended the reactivity observed for NHPI and allyl-oxyphthalimide derivatives to include hydroxamic acids toward the synthesis of aromatic amines. Through the

facile construction of an intermediary hydroxamic acid scaffold starting from phenols, we were able to perform the formal conversion of phenols to anilines via a radical-type Smiles rearrangement. Intramolecular substitution at the ipso-carbon of the phenol-derived hydroxamic acid by an amidyl radical lead to the formation of a new aromatic C-N bond in exchange for the cleavage of the phenolic C-O bond.

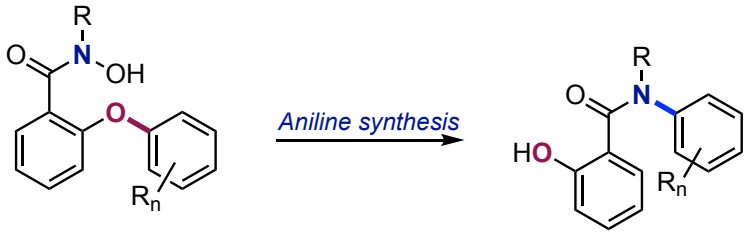


Scheme 5.3. Formal aniline synthesis from phenols.

In a separate vein, we explored the capability of thiols to serve as site-selective H-atom abstraction reagents toward the debenzylation of alcohols and amines. By carefully evaluating the electronic properties of a host of thiyl radicals, we discovered that pentafluorothiophenol would be the ideal catalyst to invoke this transformation due to exceptionally high electron affinity and low S-H bond dissociation enthalpy. Our theoretical investigation was corroborated by our experimental success in deprotecting a host of Bn- and PMB- protected alcohols and amines.

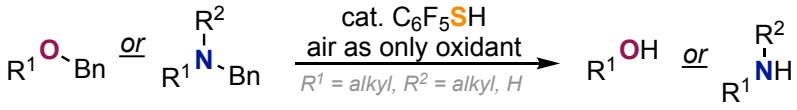


Scheme 5.4. Thiol catalyzed debenzylation of alcohols and amines.

## 5.1 Future Directions

Ever since the first carbon-centered radical was identified, isolated, and characterized in the year 1900, radical mediated synthetic methods have become widely popular and the rate of development for these processes continues to increase. In the past, radical chemistry has been given somewhat of a bad reputation due to the use of hazardous reagents and unpredictable

reactivity in certain cases. But as the field of radical chemistry has aged and progressed, newer methods have been able to demonstrate the employment of easily handled reagents toward the development of highly chemo- and regio-selective chemical processes that achieve amazing transformations where two-electron, polar pathways otherwise may have not. Presented here, benchtop stable hydroxylamines have been found to be highly effective N-centered radical precursors, and simple thiols have shown their efficiency in radical-mediated deprotection strategies. These examples serve as but a sliver of evidence toward the idea that radical chemistry is capable of achieving fantastic transformations, and that the development of future methods is of great importance to organic synthesis as a whole.